

Springer Tracts in Additive Manufacturing

M. Adam Khan
J. T. Winowlin Jappes *Editors*

Innovations in Additive Manufacturing



Springer Tracts in Additive Manufacturing

Series Editor

Henrique de Amorim Almeida, Polytechnic Institute of Leiria, Leiria, Portugal

The book series aims to recognise the innovative nature of additive manufacturing and all its related processes and materials and applications to present current and future developments. The book series will cover a wide scope, comprising new technologies, processes, methods, materials, hardware and software systems, and applications within the field of additive manufacturing and related topics ranging from data processing (design tools, data formats, numerical simulations), materials and multi-materials, new processes or combination of processes, new testing methods for AM parts, process monitoring, standardization, combination of digital and physical fabrication technologies and direct digital fabrication.

More information about this series at <https://link.springer.com/bookseries/16694>

M. Adam Khan · J. T. Winowlin Jappes
Editors

Innovations in Additive Manufacturing

Editors

M. Adam Khan
School of Automotive and Mechanical
Engineering
Kalasalingam Academy of Research
and Education
Virudhunagar, India

J. T. Winowlin Jappes
School of Automotive and Mechanical
Engineering
Kalasalingam Academy of Research
and Education
Virudhunagar, India

ISSN 2730-9576

ISSN 2730-9584 (electronic)

Springer Tracts in Additive Manufacturing

ISBN 978-3-030-89400-9

ISBN 978-3-030-89401-6 (eBook)

<https://doi.org/10.1007/978-3-030-89401-6>

© The Editor(s) (if applicable) and The Author(s), under exclusive license to Springer Nature Switzerland AG 2022

This work is subject to copyright. All rights are solely and exclusively licensed by the Publisher, whether the whole or part of the material is concerned, specifically the rights of translation, reprinting, reuse of illustrations, recitation, broadcasting, reproduction on microfilms or in any other physical way, and transmission or information storage and retrieval, electronic adaptation, computer software, or by similar or dissimilar methodology now known or hereafter developed.

The use of general descriptive names, registered names, trademarks, service marks, etc. in this publication does not imply, even in the absence of a specific statement, that such names are exempt from the relevant protective laws and regulations and therefore free for general use.

The publisher, the authors and the editors are safe to assume that the advice and information in this book are believed to be true and accurate at the date of publication. Neither the publisher nor the authors or the editors give a warranty, expressed or implied, with respect to the material contained herein or for any errors or omissions that may have been made. The publisher remains neutral with regard to jurisdictional claims in published maps and institutional affiliations.

This Springer imprint is published by the registered company Springer Nature Switzerland AG
The registered company address is: Gewerbestrasse 11, 6330 Cham, Switzerland

Thanks to ALMIGHTY

*Editors would like to dedicate this book to the
Management and Administration Team of
Kalasalingam Academy of Research and
Education.*

Dr. M. Adam Khan

Dr. J. T. Winowlin Jappes

Preface

Recently, advances in additive manufacturing and its related work are thriving many researchers to get involved in effective/innovative findings for the past few years. This book entitled *Innovations in Additive Manufacturing* discusses on the history, fundamentals, process development, applications, post-processing and many more experimental results on additive manufacturing techniques. Many engineering applications have started to employ additive manufacturing techniques for component development. Some Industries are using additive manufacturing widely for developing high-end toys and drones for play station. Beyond the research, the additive manufacturing has placed records in developing bio-implants and biomedical instruments. Opportunities have been evolved in post-processing and finish machining of additive manufacturing components. Contents such as surface treatments, modification and engineering such advancements in heat treatment, mechanical hardening and coating, etc., the science of their effects on properties and its characteristics of parts made by them are also covered. Further, simulation, modelling, and optimization of material processing and surface engineering techniques are also focused.

The scope of this book is:

- Fundamental knowledge and research advances in additive manufacturing.
- Covering recent developments and advancements in additive manufacturing.
- Case studies, experimental research, and optimization studies in the current field.
- Unique combination of advanced materials processing and surface sciences.

This book consist of three main parts such as (1) Introduction to Additive Manufacturing; (2) Additive Manufacturing and Materials Development; and (3) Post-Processing and Investigations on 3D Built Materials. Authors of this book are from different countries, and they have made their contribution on research findings and experiences through full length chapters. In Part I, two chapters have been written to cover the history of additive manufacturing along with the basic application and fundamentals. In Part II, there are five chapters to cover the developments of additive manufacturing for metals and non-metals including plastics/polymers. Also, the role of additive manufacturing in biomedical engineering is covered in this part. The post-processing and investigations on additive manufacturing is

discussed in Part III. This part covers various aspects on heat treatment, machining, surface finish, surface coatings, electrochemical corrosion, and challenges in additive manufacturing standards.

We appreciate all the contributors for submitting their innovative content extracted from their experience and learnings on additive manufacturing. We would also like to express our sincere gratitude to Springer Team, for their professional support and patronage towards the successful completion of the book on *Innovation in Additive Manufacturing*.

Virudhunagar, India
July 2021

Dr. M. Adam Khan
Dr. J. T. Winowlin Jappes

Introduction

This series supports with the information on additive manufacturing process on all aspects of history, applications, development metals, non-metals, biomedical components, heat treatment processing, machining, coating, corrosion and surface science studies. The chapters in this book were reviewed and verified to disseminate the valuable technical content to young researchers, professionals, students, and all interested aspirants on the innovations and latest developments in additive manufacturing for the current scenario.

Contents

Part I Introduction to Additive Manufacturing

- | | |
|---|-----------|
| 1 Metal Additive Manufacturing: From History to Applications | 3 |
| Amritbir Singh and Harpreet Singh | |
| 2 Development in Additive Manufacturing Techniques | 33 |
| K. Arunprasath, V. Arumugaprabu, P. Amuthakkannan,
R. Deepak Joel Johnson, and S. Vigneshwaran | |

Part II Additive Manufacturing and Materials Development

- | | |
|---|------------|
| 3 Challenges in Additive Manufacturing for Metals and Alloys | 57 |
| Monsuru Ramoni, Ragavanantham Shanmugam,
N. Thangapandian, and M. Vishnuvarthanan | |
| 4 Laser Additive Manufacturing of Aluminium Matrix
Composites | 73 |
| P. S. Samuel Ratna Kumar and P. M. Mashinini | |
| 5 Additive Manufacturing of Non-ferrous Metals | 91 |
| Temel Varol, Onur Güler, Fatih Yıldız, and S. Suresh Kumar | |
| 6 Development and Optimization Study of Poly-Lactic Acid
Blended Carbon Particles by Fused Deposition Modelling
Method | 121 |
| S. P. Jani, A. Senthil Kumar, B. Anushraj, P. M. Mashinini,
and Sudhakar Uppalapati | |
| 7 Role of Additive Manufacturing in Biomedical Engineering | 139 |
| R. Ruban, V. S. Rajashekhar, B. Nivedha, H. Mohit, M. R. Sanjay,
and Suchart Siengchin | |

Part III Post-Processing and Investigations on 3D Built Materials

- 8 Surface Finishing Post-treatments for Additive Manufactured Metallic Components** 161
T. S. N. Sankara Narayanan and Hyung Wook Park
- 9 Surface Treatments and Surface Modification Techniques for 3D Built Materials** 189
P. Vijaya Kumar and C. Velmurugan
- 10 Surface Coatings and Surface Modification Techniques for Additive Manufacturing** 221
P. Kumaravelu, S. Arulvel, and Jayakrishna Kandasamy
- 11 Mechanical Testing of Additive Manufacturing Materials** 239
I. Akilan and C. Velmurugan
- 12 Electrochemical Corrosion Behavior of Heat Treated Inconel 718 Superalloy Manufactured by Direct Metal Laser Sintering (DMLS) in 3.5% NaCl Solution** 279
B. Anushraj, N. C. Brintha, D. Chella Ganesh, and A. Ajithram
- 13 Machinability of 3D Printed Materials** 297
Şenol Bayraktar and Erhan Şentürk
- 14 Challenges Involved in Framing Additive Manufacturing Standards** 321
V. S. Rajashekhar and R. Ruban

Editors and Contributors

About the Editors



Dr. M. Adam Khan is working as Associate Professor in the School of Automotive and Mechanical Engineering and heading the Centre for Surface Engineering at Kalasalingam Academy of Research and Education, Virudhunagar, India. He completed his Post-Doctoral Research from the University of Johannesburg, Doornfontein Campus, Johannesburg, South Africa. He received his Doctoral Degree from National Institute of Technology, Tiruchirappalli, India, and his Undergraduate and Postgraduate Degrees from Anna University, Chennai, India. His research focus is on material development for different engineering applications. He has developed nickel-based superalloys through direct laser sintering process for high temperatures. Further, the material has been investigated for different property studies including mechanical strength, surface qualities, corrosion, and oxidation behaviour. Beyond his research, he is serving as Reviewer for more than 30 journals. He is also acting as Guest Lead Editor for the Special Issue on 'Influence of Bio- Laser- and Mechanical Attrition in Tribology' in the journal *Advances in Materials Science and Engineering*. He has published sixty-five research articles in the journal of international repute. He handles class for undergraduate and postgraduate for the core courses on materials science, manufacturing, design, and modelling. He has good knowledge on teaching learning process (outcome-based education)

evaluation. Under his supervision, two research scholars have been awarded doctoral degree. e-mail: adamkhan.m@klu.ac.in



Dr. J. T. Winowlin Jappes is working as Senior Professor and Dean in the School of Automotive and Mechanical Engineering and heading the Centre for Surface Engineering at Kalasalingam Academy of Research and Education (KARE), Virudhunagar, India. He completed his Ph.D. from Indian Institute of Technology Madras (IITM), Chennai, India. His research focus includes surface modifications, composites, and advanced manufacturing. He has contributed majorly towards the development of ‘Centre for Composite Materials’ and ‘Centre for Surface Engineering’ at Kalasalingam Academy of Research and Education. He has seven ongoing and completed projects from different funding agencies, namely DST, DRDO, and AICTE. He has published more than 100 research projects in journals. Under his supervision, ten research scholars have been awarded their doctoral degree. He has organized many international- and national-level conferences and workshops.

Apart from his teaching to UG-, PG- and Ph.D.-level candidates, he is also mentoring many institutions towards implementing outcome-based accreditations (NBA and NAAC). e-mail: winowlin@klu.ac.in

Contributors

A. Ajithram Department of Mechanical Engineering and Centre for Surface Engineering, Kalasalingam Academy of Research and Education, Virudhunagar, Tamilnadu, India

I. Akilan Department of Mechanical Engineering, Indian Institute of Information Technology Tiruchirappalli, Tiruchirapalli, Tamil Nadu, India

P. Amuthakkannan Department of Mechanical Engineering, PSR Engineering College, Sivakasi, Tamil Nadu, India

B. Anushraj Department of Mechanical Engineering and Centre for Surface Engineering, Kalasalingam Academy of Research and Education, Virudhunagar, Tamilnadu, India;

School of Automotive and Mechanical Engineering, Kalasalingam Academy of Research and Education, Krishnankoil, Tamil Nadu, India

S. Arulvel School of Mechanical Engineering, Vellore Institute of Technology, Vellore, Tamil Nadu, India

V. Arumugaprabu Department of Mechanical Engineering, Kalasalingam Academy of Research and Education, Krishnankoil, Tamil Nadu, India

K. Arunprasath Department of Mechanical Engineering, PSN College of Engineering And Technology, Tirunelveli, Tamil Nadu, India

Şenol Bayraktar Faculty of Engineering and Architecture, Department of Mechanical Engineering, Recep Tayyip Erdoğan University, Rize, Turkey

N. C. Brintha Department of Computer Science and Engineering, Kalasalingam Academy of Research and Education, Virudhunagar, Tamilnadu, India

D. Chella Ganesh Department of Mechanical Engineering and Centre for Surface Engineering, Kalasalingam Academy of Research and Education, Virudhunagar, Tamilnadu, India

R. Deepak Joel Johnson Department of Mechanical Engineering, Saveetha School of Engineering, Saveetha Institute of Medical and Technical Sciences, Chennai, Tamil Nadu, India

Onur Güler Department of Metallurgical and Materials Engineering, Engineering Faculty, Karadeniz Technical University, Trabzon, Turkey

S. P. Jani Department of Mechanical Engineering, Marri Laxman Reddy Institute of Technology and Management, Hyderabad, India

Jayakrishna Kandasamy School of Mechanical Engineering, Vellore Institute of Technology, Vellore, Tamil Nadu, India

A. Senthil Kumar Department of Mechanical Engineering, Sethu Institute of Technology, Virudhunagar, India

P. Kumaravelu School of Mechanical Engineering, Vellore Institute of Technology, Vellore, Tamil Nadu, India

P. M. Mashinini Department of Mechanical and Industrial Engineering Technology, University of Johannesburg, Johannesburg, South Africa

H. Mohit Natural Composites Research Group Lab, Department of Materials and Production Engineering, The Siridhorn International Thai-German Graduate School of Engineering, King Mongkut's University of Technology, North Bangkok (KMUTNB), Bangkok, Thailand

B. Nivedha Department of Physics, National Institute of Technology, Tiruchirappalli, India

Hyung Wook Park Department of Mechanical Engineering, Ulsan National Institute of Science and Technology (UNIST), UNIST-Gil 50, Ulsan, Republic of Korea

V. S. Rajashekhar Department of Aerospace Engineering, Indian Institute of Science, Bangalore, Karnataka, India

Monsuru Ramoni School of Engineering, Math and Technology, Navajo Technical University, Crownpoint, NM, USA

R. Ruban Department of Mechanical Engineering, National Institute of Technology, Tiruchirappalli, India

P. S. Samuel Ratna Kumar Department of Mechanical and Industrial Engineering Technology, University of Johannesburg, Johannesburg, South Africa

M. R. Sanjay Natural Composites Research Group Lab, Department of Materials and Production Engineering, The Siridhorn International Thai-German Graduate School of Engineering, King Mongkut's University of Technology, North Bangkok (KMUTNB), Bangkok, Thailand

T. S. N. Sankara Narayanan Department of Mechanical Engineering, Ulsan National Institute of Science and Technology (UNIST), UNIST-Gil 50, Ulsan, Republic of Korea;

Department of Analytical Chemistry, University of Madras, Chennai, India

Erhan Şentürk Faculty of Engineering and Architecture, Department of Mechanical Engineering, Recep Tayyip Erdoğan University, Rize, Turkey

Ragavanantham Shanmugam School of Engineering, Math and Technology, Navajo Technical University, Crownpoint, NM, USA

Suchart Siengchin Natural Composites Research Group Lab, Department of Materials and Production Engineering, The Siridhorn International Thai-German Graduate School of Engineering, King Mongkut's University of Technology, North Bangkok (KMUTNB), Bangkok, Thailand

Amritbir Singh Department of Mechanical Engineering, Indian Institute of Technology Jammu, Jammu, India

Harpreet Singh Department of Mechanical Engineering, Indian Institute of Technology Ropar, Rupnagar, India

S. Suresh Kumar Department of Mechanical Engineering, Kalasalingam University, Srivilliputhur, Tamil Nadu, India

N. Thangapandian Department of Mechanical Engineering, St. Joseph's Institute of Technology, Chennai, India

Sudhakar Uppalapati Department of Mechanical Engineering, Marri Laxman Reddy Institute of Technology and Management, Hyderabad, India

Temel Varol Department of Metallurgical and Materials Engineering, Engineering Faculty, Karadeniz Technical University, Trabzon, Turkey

C. Velmurugan Department of Mechanical Engineering, Indian Institute of Information Technology, Tiruchirappalli, Tamil Nadu, India

S. Vigneshwaran Department of Mechanical Engineering, Saveetha School of Engineering, Saveetha Institute of Medical and Technical Sciences, Chennai, Tamil Nadu, India

P. Vijaya Kumar Department of Mechanical Engineering, Indian Institute of Information Technology, Tiruchirappalli, Tamil Nadu, India

M. Vishnuvarthan Department of Printing Technology, College of Engineering Guindy, Anna University, Chennai, India

Fatih Yıldız Department of Mechanical Engineering, Engineering Faculty, Erzurum Technical University, Erzurum, Turkey

Abbreviations

3DP	Three-dimensional printing
4DP	Four-dimensional printing
ABS	Acrylonitrile butadiene styrene
AM	Additive manufacturing
BJT	Binder jetting technology
CDLP	Continuous direct light processing
DED	Directed energy deposition
DfAM	Design for additive manufacturing
DLP	Direct light processing
DMLM	Direct metal laser melting
DMLS	Direct metal laser sintering
DMP	Direct metal printing
DOD	Drop-on-demand
EBAM	Electron beam additive manufacture
EBM	Electron beam melting
FDM	Fused deposition modelling
HAGB	High angle grain boundary
LAM	Laser additive manufacturing
LED	Linear energy density
LENS	Laser engineered net shaping
LMF	Laser metal fusion
LOM	Laminated object manufacturing
LPBF	Laser powder bed fusion
MJF	Multi-jet fusion
PBF	Powder bed fusion
PEO	Plasma electrolytic oxidation
PLA	Polylactic acid
SLA	Stereolithography
SLM	Selective laser melting
SLS	Selective laser sintering
STEM	Science technology engineering mathematics

WAAM	Wire arc additive manufacturing
WLAM	Wire laser additive manufacturing
YAG	Yttrium aluminium garnet

Part I

Introduction to Additive Manufacturing

Chapter 1

Metal Additive Manufacturing: From History to Applications



Amritbir Singh and Harpreet Singh

1.1 History

In the last 25 years, the additive manufacturing (AM) industry has taken a giant leap of success in the technical world. Earlier, being used only for restricted and few scientific purposes (like prototyping), AM has evolved in terms of material and application flexibility. The technology was first patented and commercialized by Chuck Hull (co-founder of 3d Systems) in 1984 and 1987 respectively [1]. Within four years after the first commercial processing machine, fused deposition modelling (FDM) by Stratasys [2] and STEREOS 400 by EOS [3] contributed to the expansion of the additive technology arena. However, the erstwhile machines, limited to lightweight materials, have prompted some researchers to focus on improving their material versatility. Consequently, the EOS company introduced the first metal processed AM machine (EOSINT M160) to the market based on direct metal laser sintering (DMLS) [3]. The blend of powders was used as feedstock in which low melting point constituent acted like glue to join high melting temperature particles (liquid phase sintering). The chronological order of various firms taking dip into this technology is shown in Fig. 1.1.

Post three years, with an intent to carry out titanium alloy processing, a new firm named AeroMet came into existence. The organization developed a technique entitled laser additive manufacturing (LAM) or directed energy deposition (DED), which uses a high-performance laser to fulfil the purpose as aspired [4]. The material

A. Singh (✉)

Department of Mechanical Engineering, Indian Institute of Technology Jammu, Jammu 181221, India

e-mail: 2021rme1032@iitjammu.ac.in

H. Singh

Department of Mechanical Engineering, Indian Institute of Technology Ropar, Rupnagar 140001, India

e-mail: harpreatsingh@iitrpr.ac.in

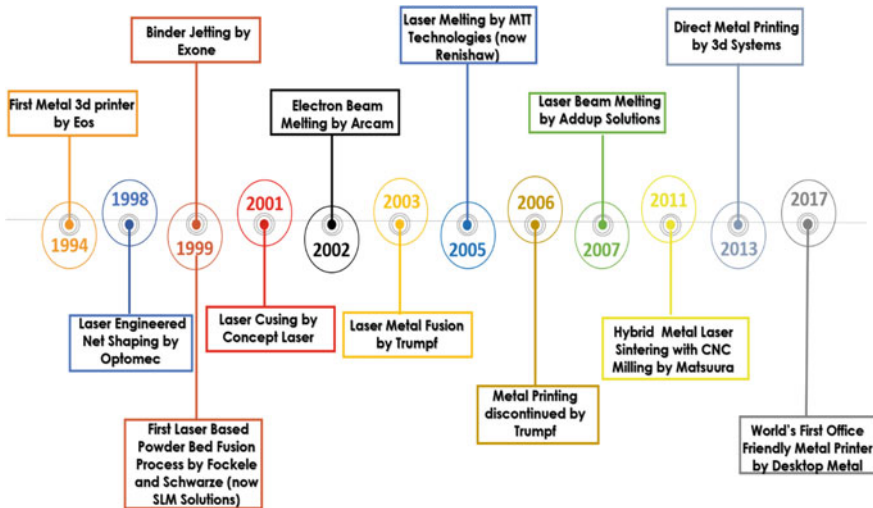


Fig. 1.1 Chronological order of entry of several firms with their respective proprietary names of AM technique in the market of metal 3D printers

processed includes Ti-6Al-4 V, Ti-5Al-2.5Sn, Ti-6Al-2Sn-4Zr-2Mo-0.1Si, and Ti-6Al-2Sn-2Zr-2Cr-2Mo-0.25Si. As the titanium alloy holds its usage in the aviation industry, they produced components for them until it was shut in the year 2005. In 1998, soon after AeroMet, a Mexican company, OPTOMECH at Sandia national labs commercialized the metal printer known as laser engineered net shaping (LENS) worked on the same concept of DED [5]. Moreover, roughly the same year, they achieved a milestone by winning the award for the “top 25 technologies of the year”. The following year, ExOne grabs the market attention by introducing the first-ever inkjet-based metal 3d printer, pronounced as binder jetting technology (BJT) [6]. This invention resulted from hard work put up by a group of scientists at the Massachusetts Institute of Technology (MIT) and was first stationed in Motorola. The old type of BJT was soon evolved into an advanced version involving certain technical improvements. These requisite upgrades were made according to the feedback of the consumer. Moreover, in 2000, Frank and Kerstin Herzog established Concept Laser GmbH [7]. They introduced laser cusing (LC) also known as direct metal laser melting (DMLM) at EuroMold in Frankfurt in 2001. In their method, localized melting of stainless steel powder was accomplished layer by layer using yttrium-aluminium-garnet (YAG) laser.

With the growth of metal AM from 1994–2001, it was understood that laser was the backbone for the majority of the production techniques because it was extensively deployed in that timeframe as a driving force for particle consolidation. However, in 2002, Arcam, a Swedish firm, developed a freeform part utilizing an electron beam instead of a laser. Hence, they launched their first production model under the name of electron beam melting (EBM) S12 at EuroMold-2002 [8]. Although the processing

of conductive material by electron beam was copyrighted in the year 1993, still it took nine years to get commercialized. Owing to its ability to produce components quickly and cost-effectively, the orthopaedic and aerospace industries acclaimed the EBM and found its utilisation worthwhile. A year after, Trumpf, a German company, introduced laser metal fusion (LMF) machines (TrumaForm LF and TrumaForm DMD) in the market [9]. They manoeuvred laser of 250 watts as heat source plus fibre optics to focus onto pure metal for particle coalescence. Akin to the other machines, their process solely relied on the basic principles of powder bed fusion (PBF). Howbeit, in contrast to other commercialized techniques, it varies in terms of build volume shape (cylindrical). Furthermore, metal 3d printing being a cynosure in the manufacturing field during that period, caught the interest of several other firms. Consequently, on account of the popularity gained by 3d printing in regard to metal AM, these companies from various regions took a step forward to develop their own technique. In particular, laser melting (LM) by MTT technologies in 2005 (presently known as Renishaw) [10], selective laser melting (SLM) by ReaLizer in 2005 (now called DMG Mori) [11], laser beam melting (LBM) by Addup solutions in 2007 [12], SLM by SLM solutions in 2011 [13], Lumex Avance-25 by Matsuura in 2011 [14], direct metal printing (DMP) by 3d Systems in 2013 [15], MetalOne by Sharebot in 2013 [16], LMF by Sisma in 2014 [17], Laser PBF by Aconity3d in 2014 [18] etc. were some of the firms that took a dip into AM processing.

With the addition of the competitive players in the market, the upsurge of innovation in the technology becomes evident. To put it another way, the upgradation of the existing technologies is of considerable significance to meet the customer demands and compete with the rivals. As an example, EOS undergoes various re-developments in their machine to cope up with the present scenario. Likewise, other companies like 3d Systems, SLM solutions, Renishaw, GE Additives etc., did investigation to increase the reliability of the operation by reducing output lead times, expanding build volume etc. Besides, several hybrid systems were developed by integrating AM with subtractive manufacturing, such as CNC machines. The Optomec, Matsuura were some of the companies that contributed to such modernized machines [19]. The firm named Velo^{3d}, facilitated manufacturers to tackle a complex design challenge by providing the scope of support less manufacturing [20]. Further, in an attempt to make metal 3d printers affordable to universities or smallscale industries, Xact Metal constructed a system (XM200C) with the ability to produce diminutive parts [21]. Such a system was capable of performing a task related to direct tooling, prototyping etc. Furthermore, the substantial development of metal printers has captured the market's attention.

Therefore, as a manufacturing engineer, it becomes critical to have an acquaintance regarding the process working. So, the requisite procedural steps of action for achieving 3d printing via discussed commercialized systems are mentioned in the following Sect. 1.2.

1.2 Fundamentals of Additive Manufacturing

The top of the line in metal AM has changed over the last years as it has shifted from developing prototypes to forming end products in industries. Besides, the AM evolved radically in terms of versatility concerning process capabilities and feedstock material. However, to accomplish the building up of mentioned materials, product creation is usually carried out by performing a series of fundamental steps. Regardless of the type of machine employed, these general steps are essential to build the end product and remain consistent with all metal printing techniques. The process series would be broken down into seven main stages (Fig. 1.2) and explained as follows.

1.2.1 Preparation of CAD File and Saving to STL Format

In any event, either the prototype or the part to be built for end-use, the need for a CAD file for AM machine is indispensable. Moreover, if it weren't for 3d design, the birth of AM techniques would not have been feasible. We could only evolve technologies to mechanically replicate solid structures after learning how to interpret them in computers using the software. The very first step in the AM processing for product creation is to envision the appearance of the product. Initially, the component outline will take the form of rough drawings with a blurred indication of dimensions. Once the idea is transformed into appropriate sketching and measurements, it is considered fit for its conversion to digital form via various softwares [22]. Under the

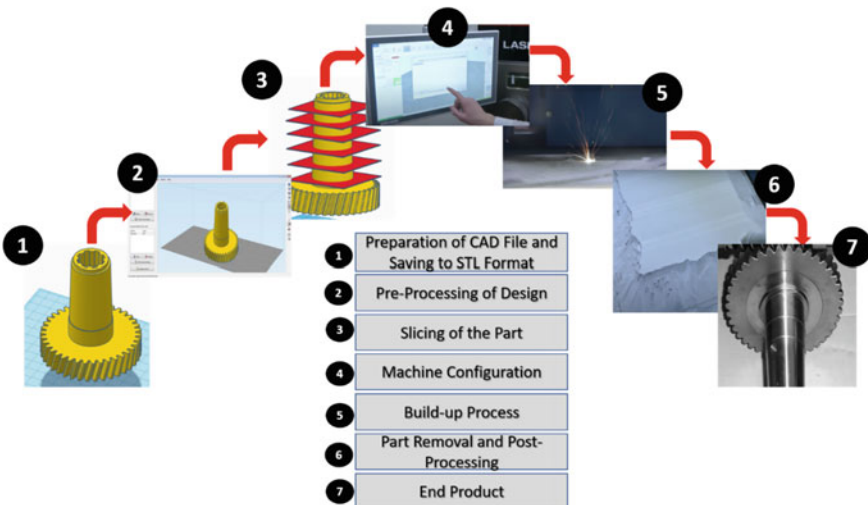


Fig. 1.2 The common sequential steps involved to carry out metal 3d printing using any of the AM techniques

broader umbrella of CAD software packages, SOLIDWORKS, CATIA, FUSION 360°, CREO, AUTOCAD, etc., are widely expended. An open-source application such as TINKERCAD, on the other hand, is readily available as an online platform and deemed easy to use for newcomers [23]. Another option for creating a digital file is to 3d scan an already existed physical part. 3D scanners and photogrammetry tools are the most effective means of assisting the designer in the recreation process [24]. Developing digital models via CAD software or by 3d scanning for AM is only practical if the data is stored in a specific format. This standardized format was created by 3D Systems named STL in the United States and was the first corporation to publicize it in AM technology [25]. This format being copyright, has been rendered a public domain for all CAD providers to conveniently access and hopefully incorporate it into their AM processes. Primarily, this format is explicitly known to describe a design surface as a triangular mesh and therefore referred to as Standard Triangle Language (STL). For several freeform shapes, STL most often prepares accurate and reliable models. However, concerning the presence of unnecessary data and its laborious fixation of inaccurate details are ascribed as its disadvantages [26].

1.2.2 Pre-Processing of Design

After the creation of the STL file and before sending the same to the associated AM machine, a range of measures are required prior to the printing. This pre-processing comes under the subject of utmost importance, regarded as Design for Additive Manufacturing (DfAM). Hence, to make use of this subject, various software solutions are provided by numerous firms. For instance, AMPHYON by ADDITIVE WORKS, 3DXPERT by 3DSYSTEMS, INSPIRE PRINT3D by ALTAIR ENGINEERING, EOSPRINT by EOS, SIMUFACT by MSC etc. are employed widely in this particular field [27]. So, in this step of AM, the part to be printed is virtually positioned and oriented (if required) in the confined space, known as build volume (Fig. 1.3a). With the employment of orientation to the component at a certain angle, support structures become inevitable (Fig. 1.3b). These structures, indeed expended in the majority of the metal AM processes, are also added virtually utilizing the software alluded earlier. The purpose of their inclusion is to stave off the part distortion owing to the residual stresses, printability of overhang features and ensures appropriate thermal conduction. However, their use is often perceived as problematic in terms of part's economics and appearance. Moreover, in regard to the flexibility of software, the designer has the freedom to virtually place the number of parts to be printed at once within the build volume (Fig. 1.3c). Besides, these packages are incorporated in order to get the component printed in the efficient way possible. The efficiency here basically describes the superior properties, cost and time cutting by optimizing the process parameters. The reduction in the aforementioned parameters is relied on the support structure minimization and making an optimal decision on part orientation [28].

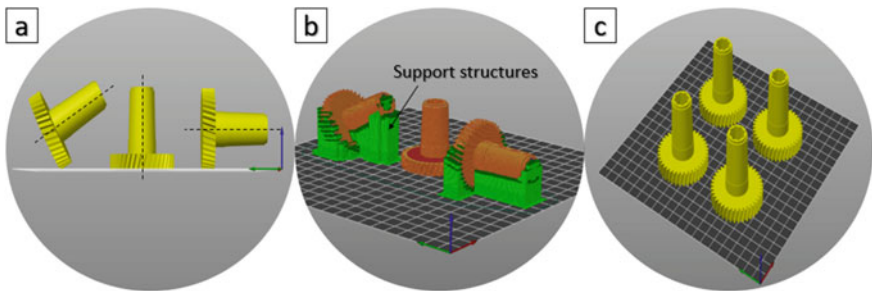


Fig. 1.3 The functions of software provided typically for the subject of DfAM includes **a** part orientation, **b** addition of support structures, **c** ability to fabricate more than one part on a build platform

1.2.3 *Slicing of the Part*

After pre-processing procedures have been implemented, the following step is to slice the component into the number of 2d cross-sections using previously mentioned software. The slicing partitions the object into several layers to accomplish this process. In essence, it provides ample detail with respect to the path to be followed by the tool in each layer. Such information originates in the form of G-codes and is thus understandable by the AM machine. In other words, slicing a 3d model essentially means the design can be read and printed by a 3D printer [29].

1.2.4 *Machine Configuration*

All AM machines have specific setup parameters added and exclusive to that system or operation. These parameters, in particular when it comes to metal AM, determine the quality of the component produced for the end application. Therefore, ideal parameters selection of specific material is predominant in the decision making concerning part superiority. In some instances, a component can be built despite an erroneous setup parameter. However, the final outcome in terms of the quality of that component can be unacceptably low. Besides, it is relevant to mention that these machine parameters are introduced in the AM software cited previously. Further, following the loading of the STL file into the AM machine, there are still several necessary system initialization measures to follow. These measures primarily involve the preparation of AM machine for the physical building of part. The manufacturer must ensure that adequate feedstock is laden into the system to accomplish the construction process. Since most of the metal AM machinery uses powder, it is generally filtered prior to the loading by the operator. Although machine setup is not only limited to the material loading but the oxygen content inside the build volume

must also be preserved at permissible amounts. Owing to the propensity of the feed-stock or molten-pool to oxidize, the necessity of an inert gas environment becomes justifiable. Helium, nitrogen, argon or their mixtures can be expended to minimize the oxidation effects. Consequently, the gas cylinders pressure is to be checked before the process initiates. Howbeit, for the electron based metal AM process, employing these gases can be catastrophic. Thus, for such systems, a vacuum is to be created in an enclosed chamber [29].

1.2.5 Build-Up Process

The machines utilized for creating the component is primarily an automated system and competent enough to perform the vital task. Hence, it can proceed the majority of the time without monitoring. However, from time to time, an inspection of material quantity, power supply, or any other errors is still necessary to ensure proper operational processes.

1.2.6 Part Removal and Post-Processing

After the consummation of the build-up process, the corresponding step is to remove the part from the build plate. Although the part is known to be present inside a cake of powder (particularly for PBF), therefore, prior to the withdrawal, either brush or vacuum system are expended for part cleaning. Following the excess powder elimination, the subsequent course of action is the support removal via hand tools or machines such as wire-electric discharge machining for precision cutting. Consequently, the part face attached to the support lacks surface quality [30]. Owing to this repercussion, post-processing becomes evident. Such processing comprises finishing operations, mainly polishing, sandpapering, coating, etc. [31]. Moreover, AM parts are fabricated to meet the implementation demands. So, most of the time, the part in an as-formed (directly from the machine) state is not considered fit for use and requires further processing like thermal treatment. Several articles have been published in the literature that describes the impact of post-heat treatment on different materials [32–34]. Besides, it is worth mentioning that the type of post-treatment essential on AM part is mainly application-specific.

1.2.7 End Product

After following the requisite action plan, the part printed is ready to go in for practical usage. The application area covers many industries, including medical, automobile,

aeronautical etc., and their in-depth discussion is outside the reach of this segment and will be addressed in Sect. 1.5 of this chapter.

1.3 Material Compatibility in Metal Additive Manufacturing

The type of material used for consolidation solely depends upon the laser/electron beam interaction with feedstock. On account of this perfect interrelation, commercialized processing machines, addressed in the Sect. 1.1, are technically sound to form part out of several materials like stainless steels (316L, 304L, 17-4PH), titanium (CP, Ti-6Al-4 V), aluminum and nickel alloys [35]. Even though there exist some alloys from the same family that are not processed effectively owing to its incapability to provide sufficient properties desired for AM feedstock. Accordingly, the study of their physical properties to understand their process feasibility and corresponding formation of molten-pool is of paramount importance. So, some of the significant parameters necessary for the material processing in metal AM systems are as follows.

1.3.1 Melting Point

When it comes to process spontaneity of AM, the melting property of the metal feedstock are crucial. Basically, it's the melting point that decides the material selection in a particular type of AM systems. As already discussed, with the evolution of metal AM, the researchers played a vital role in improving the process capabilities. For instance, a paradigm shift from inefficient thermal sources to high power sources opens up the path for processing high melting point material [36]. So, in a nutshell, the maximum heat source power available governs the type of AM material that can be easily processed. Moreover, most of the material expended in the metal AM is the alloys of iron, nickel, titanium, aluminum etc. In addition, it is well known that these alloys change their state from solid to liquid in a specific temperature range, unlike metals. However, phase depends upon energy density (also known as Andrew's number) produced owing to the heat source at the area of interest. The energy density can either be sufficient to produce the full melting or even low enough to result only in solid state fusion of parts. Besides, the existence of two phases (solid and liquid) can be attributed to the moderate energy density levels [37]. Numerous experimental and numerical validations are presented in the past studies exploring the temperature distribution of heat source over the build platform [38, 39]. In one of the study [40] with Ti6Al4V feedstock, the temperature variation over the powder bed in the PBF process was analyzed. The ability to obtain full and the partial melting region, solid state sintering region, explains the feasibility of Ti6Al4V as AM feedstock. However,

materials like tantalum, tungsten or others from ceramic family, owing to its high melting point, require extreme thermal power to get processed. Therefore, AM of such feedstock is non-viable in its purest state, instead needs a secondary material to make them fuse [41]. Moreover, the above concept makes us realize that the low melting point material must be highly utilized as AM feedstock, but that is not the case. In particular, even with a low melting point, copper is as challenging to process as high melting point material [42]. This can be attributed to the fact that the other properties like absorption, transmission etc., are also of considerable weightage in affecting the compatibility of material as AM feedstock.

1.3.2 Optical Interactions

As a visible light of a specific wavelength travels from one media to the next, a well-known pertinent phenomenon transpires. Such occurrence is associated with the optical interactions at the interface of gas and solid medium. As far as metal AM is concerned, one of the main facets is the light interaction with the powder (for the PBF process) over the build platform. This light interaction is nothing but the heat source employed for 3d printing purpose. Moreover, the concerned relation of feedstock at the build surface is quantified in terms of absorptivity, transmissivity and reflectivity [43]. So, to examine the material compatibility with the heat source, there are some questions that require a thorough investigation. It includes how well the material absorbs the spectrum of light used, how much extent the transmission of light occurred in the solid media, and what losses incurred due to the reflectivity at the interface? Fig. 1.4 shows the schematic interaction of the heat source with the

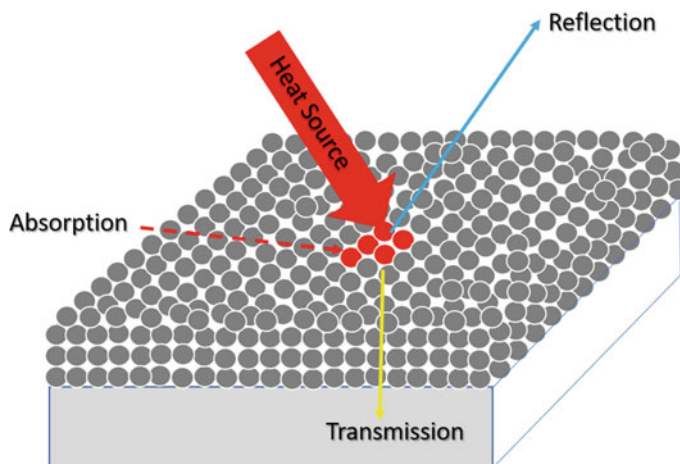


Fig. 1.4 Schematic representation of material interaction with the focused heat source in terms of its optical parameters like absorption, transmission and reflection during the process working

build platform of the PBF process.

The relation between the optical characteristics is given by [44]:

$$A + T + R = 1$$

where A is absorptivity, T is transmissivity and R is reflectivity. A is the ratio of the intensity of radiation absorbed to the total intensity of incident radiation. Likewise, T and R is the radiation intensity transmitted and reflected to the total amount respectively.

Particularly in the PBF process, the thermal source beam is guided over the powder bed with sufficiently high velocity. The process is considered successful only if the heat source–material interaction is adequate enough to melt the powder on the surface to form a melt-pool (relates to absorptivity of material) and to the depth that two corresponding layers should fuse properly (relates to transmissivity characteristic) [44]. Moreover, suppose the powder is comprised of both properties to enough values with the least reflectivity, in that case, the fusion of powder and corresponding layers to requisite depth is achievable, as shown in Fig. 1.5a. On the other hand, the material with better absorption and poor transmission will not form a melt-pool of suitable depth and consequently results in poor adhesion of the adjacent layer (Fig. 1.5b). Further, it was mentioned in the previous Sect. 3.1 that the utilization of copper

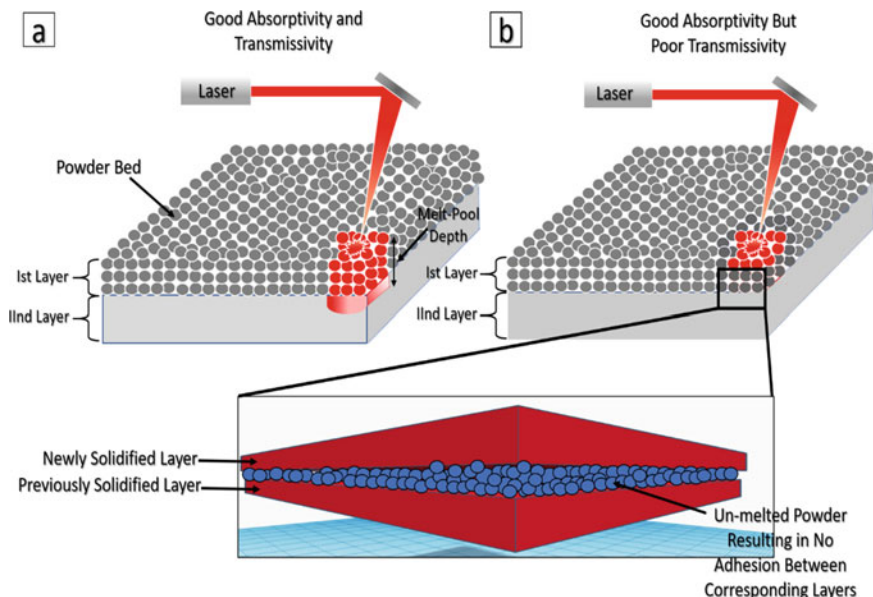


Fig. 1.5 The schematic depiction and effect of material with **a** good absorptivity and transmissivity and **b** good absorptivity but poor transmissivity on the depth of melt-pool or adhesion of corresponding layers in the PBF process

Table 1.1 The list of feasible materials with indispensable properties utilized in the commercialized metal AM systems for energy based processing [35]

Aluminum Alloys	1. Al-7Si-0.6 Mg 2. Al-10Si-Mg 3. Al-12Si
Steel Alloys	1. 316L 2. 17-4PH 3. M300
Nickel Alloy	1. Ni625 2. Ni718
Cobalt-Chrome Alloy	1. CoCrMo 2. CoCrF75
Titanium Alloy	1. CpTi Grade 1 2. CpTi Grade 2 3. Ti-6Al-4 V Grade 5 4. Ti-6Al-4 V Grade 23 5. Ti-6Al-2Sn-4Zr-2Mo 6. Ti-5Al-5 V-5Mo-3Cr 7. Ti-48Al-2Cr-2Nb

feedstock in the PBF process was considered burdensome despite its relatively low melting point than commercially processed materials. This can ascribe to its high optical reflectance and greater thermal conductivity equivalent to 400 W/mK [45]. Although it is relevant to mention that the processing is possible but obtaining defect free copper part is seldom. However, to ease the processing of such materials, different additives are blended with the parent feedstock to enhance their absorptivity and making the process feasible [46].

Besides, considering these compatibility aspects, different firms provided several processable feedstocks utilized widespread in metal AM are shown in Table 1.1

1.4 Processing Techniques for Metal Additive Manufacturing

Metal AM, also known as metal 3D printing, has the ability to significantly alter part with change in design requirements without any difficulty. However, such alterations of product design are considered cumbersome and cost inefficient while processing through traditional methods. Therefore, the customization of parts is an unchallenging task for metal AM and provides enough freedom to perform specific jobs in the industries effortlessly. Moreover, seeking these pros, numerous market players got the attention of this technology in the late 90's. Presently, the market of metal additive production methods is now widespread and currently available in various forms of technologies. These technologies are classified as shown in Fig. 1.6.

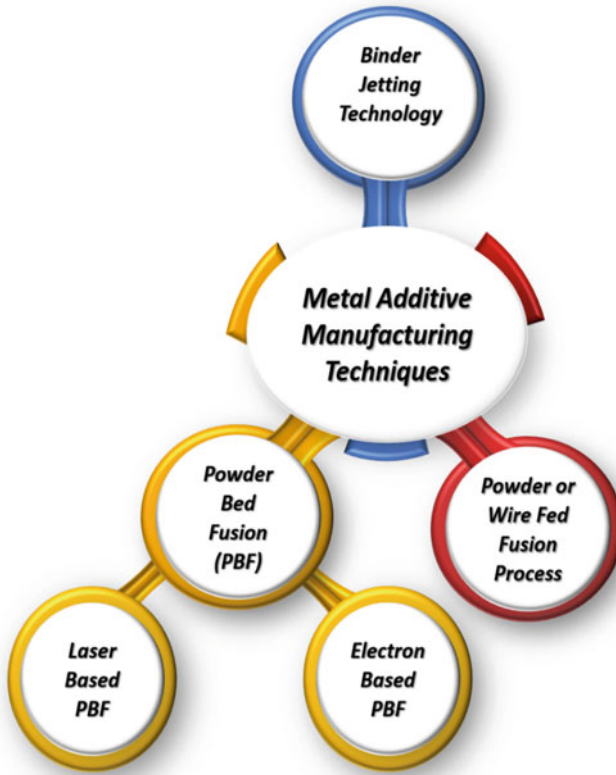


Fig. 1.6 The picture illustrates the types of metal AM processing techniques currently employed as a commercialized system by numerous firms under their respective proprietary names

1.4.1 Powder Bed Fusion (PBF) Process

The PBF was one of the first commercialized systems that found their way into the metal AM technology. This technology came into existence on account of efforts put up by researchers at the University of Texas in the 1980s [47]. All other PBF processes alter this simple method in one or more respects to improve machine efficiency, allow for processing various products, and prevent special proprietary features. Nevertheless, the fundamental set of attributes associated with multiple PBF processes is almost common, and their respective schematics are shown in the upcoming sub-sections. Its primary mechanism of action is depicted in the form of points. This includes,

- the movement of build platform either up or down by prescribed amount,

- the formation of powder bed over build platform with the aid of certain physical spreader (roller or doctors blade),
- the scanning of the selective region over powder bed using a heat source to consolidate,
- and the cycle continues till part is completed.

Type of Heat Source

The kind of heat source utilized plays a vital role in fulfilling the sole purpose of AM for different materials. Laser, electron beam and infrared heaters as driving sources are widespread in certain systems and provide the possible consolidation. By dint of mentioned sources of coalescence, the PBF is subdivided into categories shown in Fig. 1.6.

Laser Based PBF

It is regarded as the most popular thermal source than any other available in the market. Different names are given by several firms (as discussed in Sect. 1.1) to such laser based systems under the title of DMLS [3], DMLM [7], SLM [13], direct metal printing DMP [15] etc. Although the name being different, the basic approach of 3d printing behind each system is analogous. All these systems opted for laser owing to its ability to provide ample concentrated energy to form melt-pool in the selective region. As per the slice information, the galvanometers are accountable to direct the laser light over the region of interest in a particular layer (Fig. 1.7). The laser beam focused has the wavelength of 1070–1080 nm and the power of 700–1000 W for metal processed PBF processes [36]. Besides, this concentrated beam tends to form the molten pool, is highly susceptible to the surrounding gases. The mixing up of such gases can either causes oxidation or several gas defects [48]. Such course of action is considered disruptive for the printed part. Hence, the need for shielding gas in a closed chamber becomes evident to shun this reactivity. So, nitrogen, helium, argon etc., are some of the widespread gases used to fulfil such objectives. Also, the level of oxygen required for the satisfactorily process completion inside the enclosed chamber is around a few ppm [47].

Moreover, the laser technology employed has progressed over time in terms of power competencies and this can be attributed to the paradigm shift of gas laser, particularly CO₂, to fiber lasers. The need for such development was considered imperative as former lasers were inefficient enough to convert the majority of input power to useful power. Mathematically, near about 20% of what is converted into desired power and the rest is vanished in the form of heat. Howbeit, the introduction of fiber laser increased the conversion mark up to 80% and reduced the losses by a greater extent [49]. Presently, all firms related to the concerned technique utilize fiber lasers to amalgamate the feedstock. Almost majority of the commercial laser based PBF machines employ single fiber lasers for processing. The utilization of one

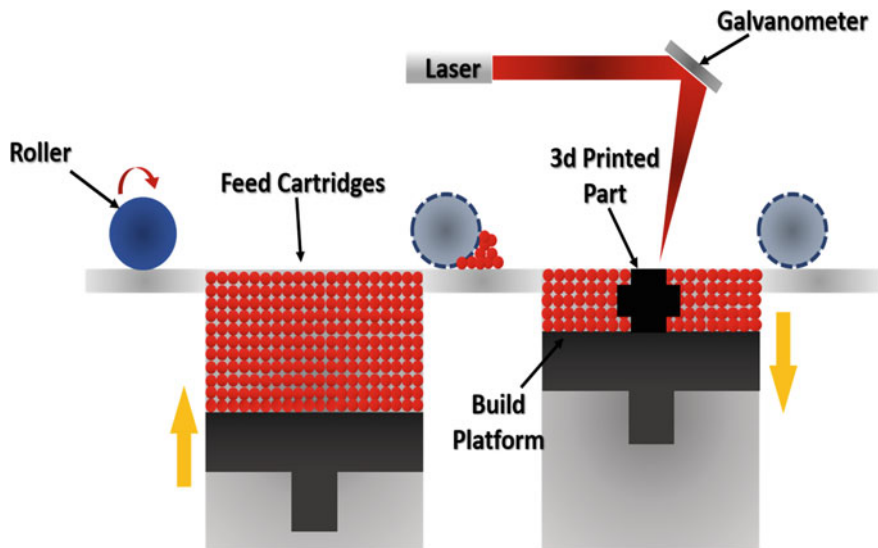


Fig. 1.7 The schematic illustration of laser based PBF process expended for 3d printing metal components

laser beam is considered time-consuming and therefore needed attention to solve the speed issues. However, to expedite the same process, the use of a multi-laser becomes evident (Fig. 1.8). With its ability to scan different regions simultaneously, productivity is improved at the cost of reduced lead times [50].

Electron Based PBF

This system drives the process by virtue of a high velocity electron beam focused over the particular region (Fig. 1.9). It is commonly pronounced as electron beam melting (EBM). The first commercialized system was manufactured by a firm named Arcam in 2002 [8]. It has high process efficiency (electron beam power to the input power) in comparison to other systems. The vital heat energy for powder consolidation is produced on account of the high kinetic energy of the electron. However, the same developed in laser PBF is regarded to the process of photon absorption. Moreover, there are several other differences in both laser and electron based PBF that are inherent. For instance, owing to the propensity of electrons to get deflected with the interaction to atoms, the printing operation is exercised in the requisite vacuum environment. Furthermore, the motion of the electron beam is controlled using magnetic coils. These coils have the potential to react to altering input conditions almost instantaneously. On account of this, an electron beam may be scanned gradually or very quickly. In essence, the electron quick scan represents its ability to create a complete component in a relatively shorter period of time. Thus, less

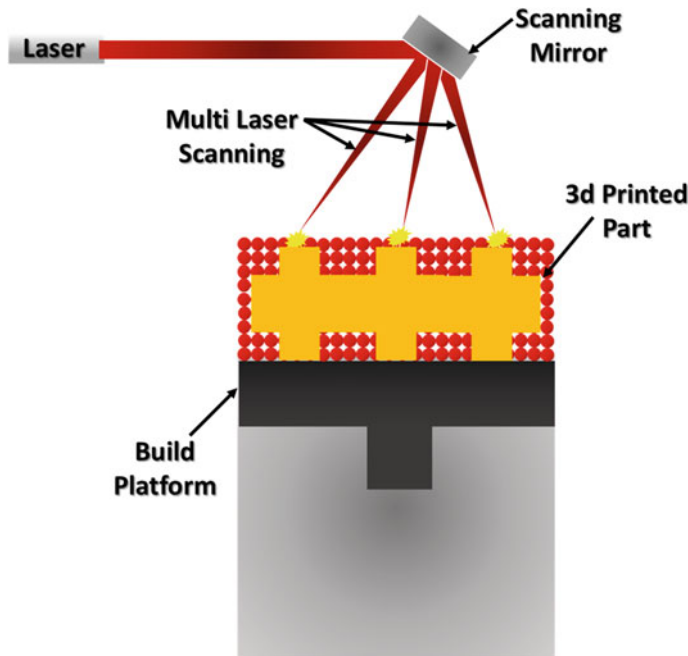


Fig. 1.8 The schematic showing the PBF process that utilizes multi-laser scanning approach for 3d printing metal components

lead time signifies the high productivity and low cost for each component which is a significant attribute of EBM [49].

Although we know that nothing is perfect, the same applies to the EBM process. Along with various process capabilities, there is some system incompetence as well. The main drawback is its inability to process non-conductive materials [51]. There are several reasons for it explained in Fig. 1.10. In non-conductive material, negative charge accumulation over a certain area is evident and inevitable. This charge deposition is the root cause of the problems like beam deflection and rapid expulsion. Owing to such difficulties, the conductive material is best suited for the electron based PBF process.

Bonding Mechanisms

With the advent of the metal PBF process, every modern inventor of this technology has developed conflicting terms to characterize the fusion mechanism, with the most common versions of “sintering” and “melting.” However, using a single term to explain the feedstock consolidation process is potentially controversial due to the possibility of several mechanisms. Hence, three distinct bonding processes relevant

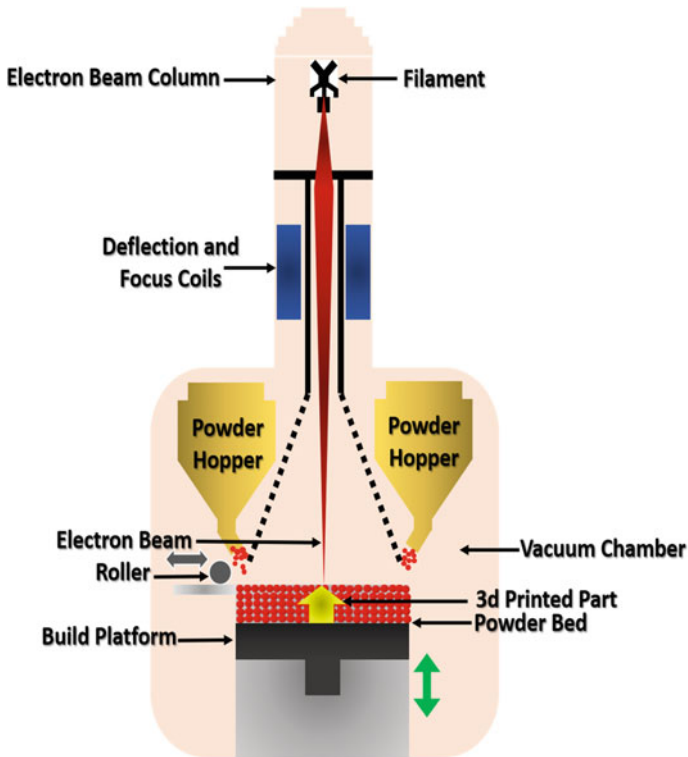


Fig. 1.9 The schematic representation of electron based PBF process expended for 3d printing metal components

to metal fusion can transpire, controlled by laser power and powder relationship. These are comprised of solid state sintering, liquid phase sintering and full melting.

Solid State Sintering

It is among the most possible fusion processes involving particle diffusion in a solid state [52]. Also, sintering, in its traditional context, refers to the bonding without melting at an extreme temperature below the melting point of the feedstock. Now the issue emerges related to how and what factors led the powder to consolidate by this bonding mechanism. So, to answer this, we need to understand the basic process of sintering in the concerned technique. In the PBF method, as we are aware, a powder layer is produced in the form of a bed over a building platform. This bed is composed of particles of either shape and particle size distribution having a high surface area to volume ratio. Therefore, owing to the existence of this, the powder bed is highly unstable and is susceptible to achieve its state of stability. This desired state is accomplished by virtue of raising the temperature, a consequence of which

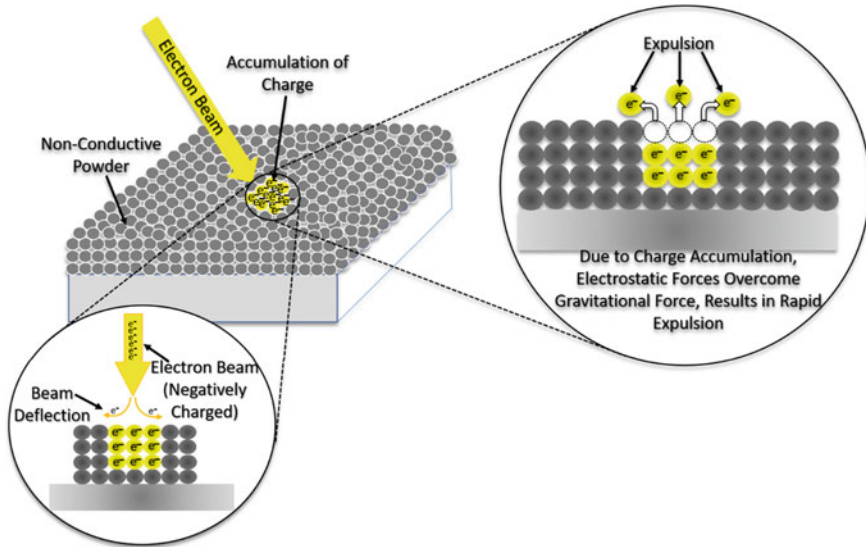


Fig. 1.10 The schematic representation of repercussions that occurred while processing non-conductive powder utilizing electron beam as an energy source in the EBM process

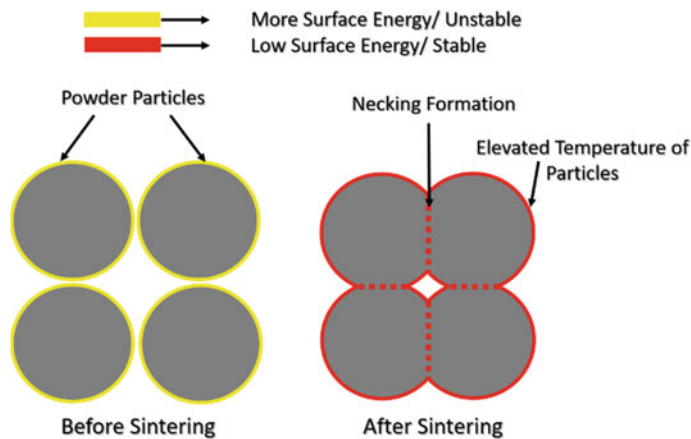


Fig. 1.11 The schematic depiction of solid state sintering mechanism of powder particles in PBF process

triggers the formation of a solid state bond and thereby reduces the free surface area (Fig. 1.11). The free surface is related to the surface energy in the direct sense and hence, the governing force for the sintering mechanism is the reduction of the surface energy of the powder particles [53].

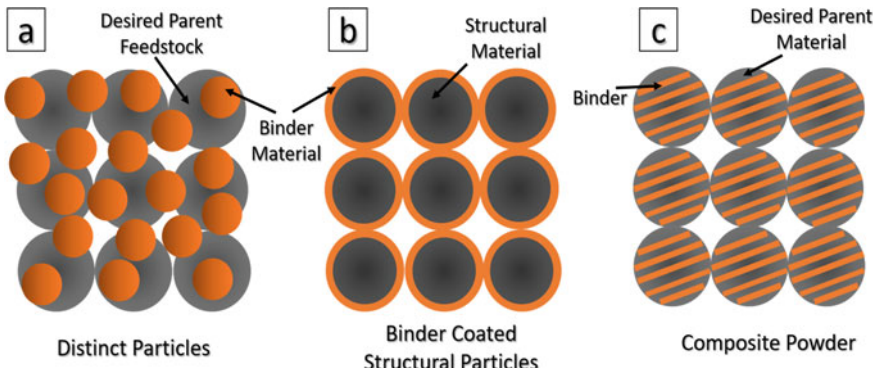


Fig. 1.12 Diagram illustrating the kinds of feedstock mixture **a** distinct particles, **b** binder coated structural particles and **c** composite powder that can be utilized during liquid phase sintering type of mechanism in PBF process

Liquid Phase Sintering

Liquid phase sintering [54], on the other hand, is a concept widely expanded in the concerned area of AM where heat source power available for fusion is insufficient to undergo metal 3d printing of desired material. Thus, the finest way out in such a scenario is to blend two powders (one of which is desired structural feedstock) with different melting point temperature. The other constituent ought to have low melting points, capable of melting and acting as a glue to the parent powder when exposed to the appropriate heat source. Therefore, the part fabricated by dint of this method is primarily a composite and even requires post-processing for part densification [49]. Such process of fusion can use any of the following types of feedstock:

- Mixing of high with low melting point powder (Fig. 1.12a),
- Coating high with low melting constituent (Fig. 1.12b),
- Using a composite material containing one with low melting temperature (Fig. 1.12c).

Full Melting

It is the mechanism that is most often utilized with the metal PBF production process and considered a highly desirable bonding phenomenon for superior part properties. In this fusion approach, the heap of powder is selectively melted over the suitable region utilizing an impinging heat source to a depth greater than the layer thickness. Consequently, the re-melting of the formerly solidified layer occurs owing to the heat source and is considered exceptionally constructive in building the well bonded layered component. Hence, the part with immensely great adhesion strength is expected in such bonding mechanisms [55].

Moreover, it is pertinent to state that any of the aforementioned bonding approaches is possible despite the type of commercial systems available in the market [49].

1.4.2 *Binder Jetting Technology (BJT)*

It came into force in 1999 by ExOne [6], primarily function on the principle of consolidation via adhesives at definite region acquired from slicing cross section. This coalescence of powder is managed by a binder material, regarded as the process initiator. Followed by powder layer formation at the outset, the binder is poured selectively onto the bed using a printhead (Fig. 1.13). Subsequently, the same is subjected to warmth via an external infrared heater such that the adhesive is partly healed in the binder-saturated areas and the minimal mechanical properties can be established. After heating, a fresh layer is again added with the aid of rollers from feed cartridges and the cycle repeats itself until the whole desired part is formed. However, the properties of the actual part formed are inferior for its use as end product, thus necessitating post-processing measures like sintering, infiltration, finishing, etc. Furthermore, it is quite interesting to note in the context of manufacturing lead time that the majority of it is spent during post processing and least is consumed while printing [56].

Except for the binder and type of thermal source, the entire process is akin to the laser and electron based PBF. Besides, BJT exhibits significant benefits over them, for instance, its ability to process extensive material types, exclusion of heat related problems owing to the inadequacy of thermal input, non-usage of exorbitant priced lasers or electron beams makes this technique economical [57]. Also, the need for

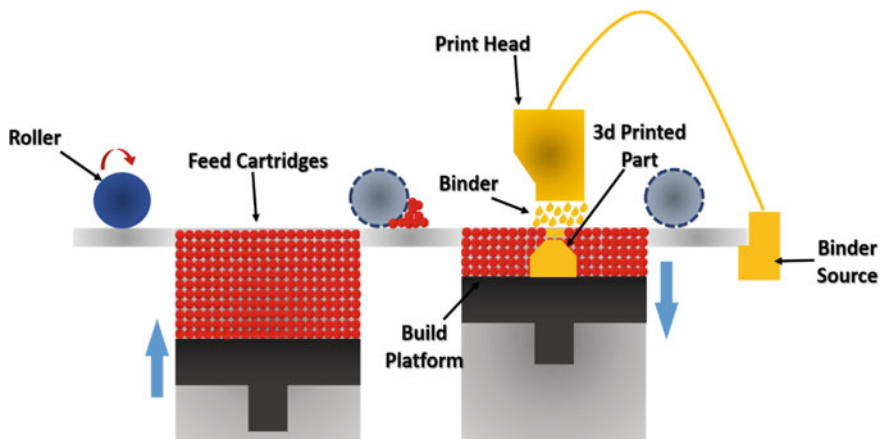


Fig. 1.13 The schematic illustration of the process of BJT utilized for 3d printing metal components

support structures is inessential because the loose and leftover feedstock delivers ample hold up to solidified part along with the overhangs. Despite these positives, BJT also incorporates a unique feature of forming coloured objects. Its spontaneity can be attributed to the coloured binder utilization that imparts such characteristics to the part [56].

After the birth of BJT in the late 1990s, it has undergone numerous technological advancements. Over the past few years, a slew of new firms has joined the fray, most with their unique perspective on this technology. Out of them, ExOne is regarded as a pioneer in the BJT [6]. They have introduced four systems throughout its existence, each one the modification of last. For instance, in 2018, ExOne launched the Innovent+, an improvement of M-Flex 3d [58]. Although the new machine time consumption for part fabrication is slightly more, it still incorporates two significant enhancements. First of all, it is fitted with an ultra-sonic recoater, designed to enhance material flowability and second is the ease of feedstock change. In addition, other firm like 3DEO invented the hybrid technology involving the integration of BJT and CNC milling machine into one [59]. This combinational approach helps 3DEO produce very detailed metal parts with more than 99.5% density after post-processing. Several industries acknowledged the possible breakthrough in BJT and are already striving hard to take advantage of its prospects. In the end, this would allow the BJT to develop a significant portion of the entire production industry.

1.4.3 Powder or Wire Fed Fusion Process

Also known as DED, encompasses a variety of nomenclature, for instance, LENS [5], DMD [9], electron beam additive manufacturing (EBAM) [60], wire arc additive manufacturing (WAAM) [61] etc. It was often expended for restoring or adding new materials to existing parts and is now utilized for freeform fabrication as well. The production of parts is accomplished on account of focused thermal source like a laser, electron beam, electric arc etc. However, the only heat source employment is not adequate for process operation rather, simultaneous addition of material is highly relevant. Akin to PBF, the whole process transpires over build plate having the freedom to move up or down by a specific amount. The procedure is usually carried out in an enclosed environment containing inert gas or vacuum to maintain tight control over the material's properties and shield it from oxidation [62]. The PBF based process consolidates because of different bonding approaches, but in DED, the powder or wire supplied to the concentrated region fully melts to form coalescence. Owing to the full melting, the part primarily produced are often dense [47].

DED innovation has already been in operation for many years and provides several distinct advantages compared to other competitive technologies. For instance, in contrast to PBF, no feedstock bed is formed, but external inclusion via feeders is attained. Besides, due to the addition of material alongside heat source, a need for a large amount of feedstock is avoided. Further, in numerous applications, the crack formation owing to fatigue or some other related defect on component deteriorates



Fig. 1.14 The advantages and disadvantages of the DED process over PBF utilized to 3d print metal components

the structural integrity and thus requires replacement. However, DED offers a crucial advantage to restore the same part by material deposition over the requisite region, thus saving enormous capital [62]. The other related positives and negatives of the concerned process are shown in Fig. 1.14.

Further, the DED can be classified based on the type of energy source (heat or kinetic energy) and type of material (wire or powder form) employed.

On the Basis of Feedstock Material

As far as material based categorization of DED is concerned, the powder used systems (Fig. 1.15a) has been widely reviewed in the past and is a frequently employed method [11]. Moreover, several systems also utilize the material in the form of wire (Fig. 1.15b) to fulfil the printing process [63]. Both type of feedstock primarily uses either heat source (laser or electron beam or electric arc) for material consolidation.

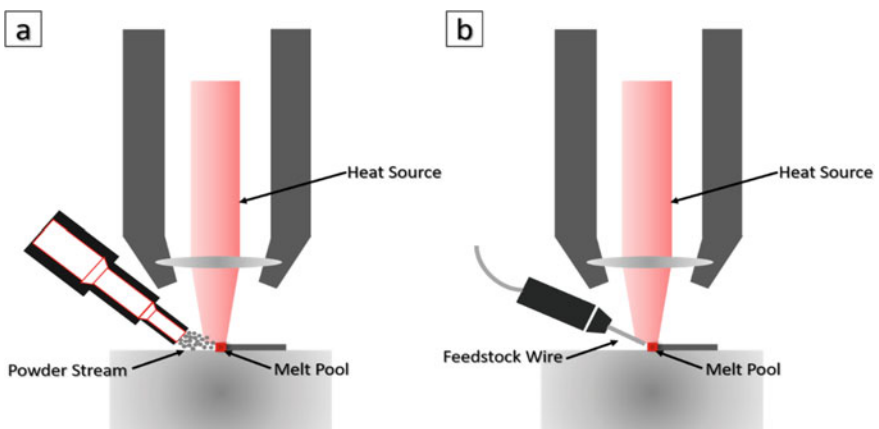


Fig. 1.15 The alteration in the DED process on the basis of type of feedstock material, for instance, **a** powder based and **b** wire based systems used to 3d print metal components over the substrate material

The respective forms of material in DED have their advantages and disadvantages. For instance, the wire has typically a diameter of 1–3 mm and on the other hand, powder size is equivalent to 50–150 microns. Therefore, the smaller size of powder based systems proves its ability to form near-net shape part with high resolution. However, the greater size of wire systems represents its limitation of not fabricating such parts [64]. On the other hand, unlike the wire, the powder feeder method is quite expensive and requires comparatively more significant time for process completion. Besides, it also leads to less efficiency of deposition relative to metal wires because only a bit of overall powder is melted and consolidated to the build plate or corresponding solidified layer. On the other hand, wire based DED is deployed when higher deposition rates and large size components are expected [65].

On the Basis of Energy Source

The driving force employed for consolidation can be classified in terms of thermal and kinetic energy. Thermal energy can be either be in the form of an electron or laser beam [66]. In the laser beam DED (Fig. 1.16a), the beam diameter is comparatively smaller, enabling the development of intricate features. Such a process is performed in an inert environment to avoid oxidation of melt-pool. Conversely, rather than using an enclosed chamber filled with protective gas, a covering that is adequate to secure the metal from contamination can be created by inert gas around the molten pool. Besides, the electron beam DED (Fig. 1.16b) process works in a vacuum environment with a relatively large spot diameter to avoid charge accumulation. Consequently, the printing time is less in electron based systems and, therefore, dominates the other techniques in high productivity [47]. However, the use of these high temperature processes is deemed to be inappropriate for temperature sensitive materials like aluminum, magnesium etc. Therefore, kinetic energy based methods are considered ideal for processing these materials [67]. The cold spray is one of the most commonly employed kinetic energy type methods that usually work at a comparatively lower temperature. It is also referred to as a solid state technique that achieves material consolidation on account of the high velocity of powder walloped over the substrate. The high kinetic energy of the particle is achieved with the aid of pressurized and pre-heated carrier gas expanded in a de-laval nozzle [68]. The whole process working is shown in Fig. 1.16c. The adhesion mechanism in this technique is attributed to the severe plastic deformation with high strain rates at the interfaces [69]. Despite processing thermally sensitive materials, this process offers additional advantages over others. For instance, retaining the feedstock properties, no phase change, high deposition rates etc., are some of the paramount benefits [67].

DED provides various advantages for industries requiring the production or effective maintenance of high-end devices and unique metal components, in particular large parts. Owing to the groundbreaking trend of hybrid technology, it can be anticipated that the ambit of applications of DED will broaden. Therefore, in future, DED's incorporation with the traditional manufacturing system has the ability to advance companies in search of advanced and cost-effective manufacturing possibilities.

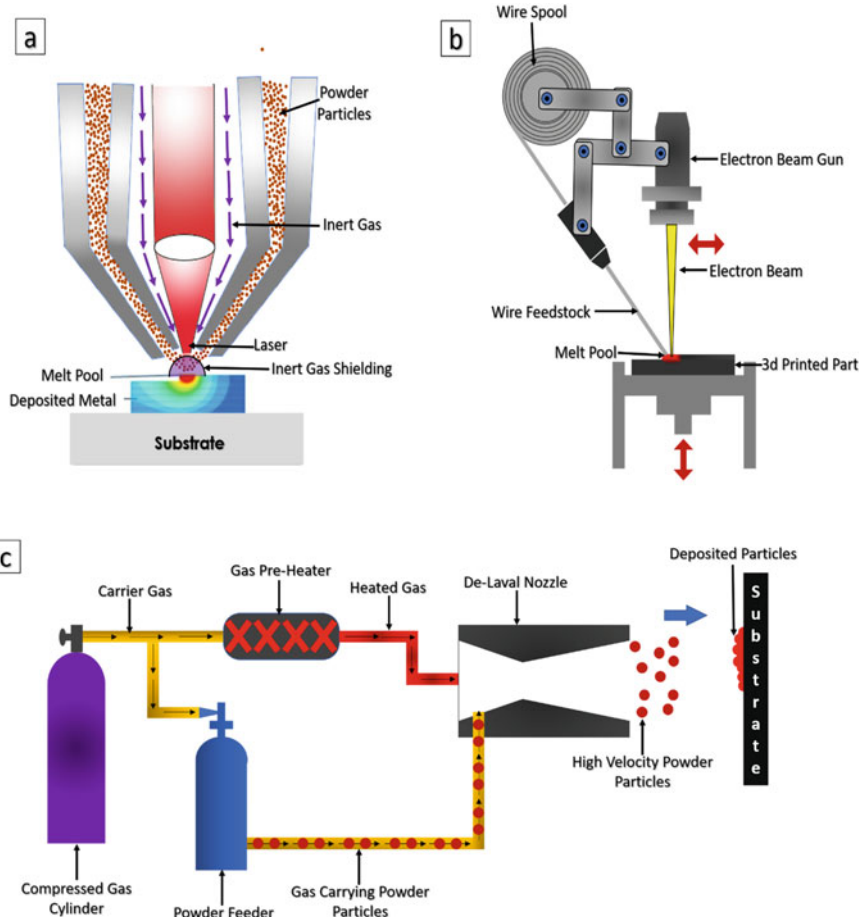


Fig. 1.16 The kinds of DED process differs on the basis of energy source employed like **a** laser based, **b** electron beam based and **c** kinetic energy based techniques utilized for the consolidation of feedstock to obtain a 3d printed metal part

1.5 Applications of Metal Additive Manufacturing

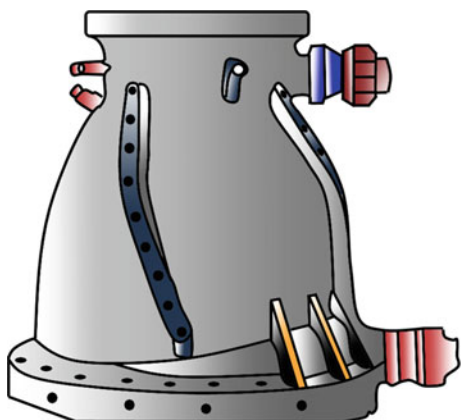
Initially envisioned as a method for prototype modelling, AM has grown in popularity during the last few years to incorporate applications of almost every aspect. The plethora of applications of metal AM results from its competency to perform the requisite task with greater ease. This section will explore the existing state of metal AM in several markets and the implementation of technology throughout industries like aeronautical, automobile and biomedical.

1.5.1 Aeronautical Industry

Metal AM has been initially established as a production technology to fix defective components in aerospace and thereby save enormous expenditure [70]. However, with the evolution in technology, aerospace extends the usage of AM from repair technology to standalone part manufacturing. With this expansion of application, the AM offered numerous advantages. For instance, reduction in the number of components in an assembly results in cost depreciation in terms of tooling and inspection etc. [71]. GE Aviation registered a decline from 855 parts made utilizing traditional production into a few components using AM techniques [72]. This component consolidation, therefore, reduces weight and enhances component efficiency. Besides, the method enables developers to invent and produce rocket components in a shorter period of time. In particular, the ArianeGroup build injector system made of nickel based alloy using EOS M 400–4 metal 3d printer [73]. The same part manufactured with casting and machining previously took more than three months but AM shortened the processing period to 35 h. There is a slew of other critical aerospace related applications such as the production of chopper's combustion chamber (aerospace applications book), restoration of the airfoil, rapid tooling to build Aircraft A320 mechanical door hinges etc. [74]. The recent progress in regard to aerospace applications is made by Masten Space Systems [75]. They designed a lightweight, long lasting rocket engine in support of NASA's goal of making several journeys to the moon in quick succession with little gap between launches. It was pronounced as a "Broadsword" engine manufactured expending powder bed fusion technique, in particular, DMLS by EOS. Besides, AM led to the emergence of complex air cooled channels present within the bulk of the combustion chamber of Broadsword and the integration of the engine's components into only three main parts (Fig. 1.17).

Moreover, with the expectation to achieve production demands in future, metal AM needs to tackle some obstacles. Among these are validation of AM components,

Fig. 1.17 The design of 3d printed Broadsword engine fabricated by Masten Space Systems with the aid of the DMLS technique for aerospace applications

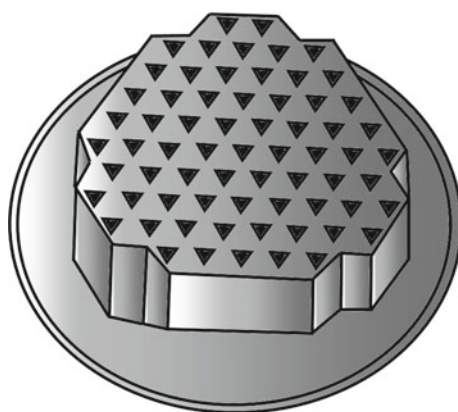


improved process reproducibility and security. Nonetheless, with significant investment now made in developing and certifying AM technologies and feedstock, the future of AM in the aeronautical industries seems to be very promising.

1.5.2 *Biomedical Industry*

AM developments have revolutionized the biomedical industry over the last decade by offering a groundbreaking platform for the growth of the latest healthcare techniques (for instance, tissue engineering, orthopaedic applications) [65]. Moreover, as we know, AM is adept at customization, the development of patient-specific parts is deemed very feasible and achieved within the requisite time. For example, acetabular cup, human osteoblasts, knee and dental implants, screws, bio-sensors, etc., are some of the widespread things fabricated utilizing AM techniques [76]. Amid the covid-19 pandemic, the AM played a vital role in solving the issues pertaining to N-95 masks in particular [77]. It is well known that such masks are required to dispose of after a single use owing to the presence of a chunk of impurities in the utilized filter. On account of the intention to replace disposable N-95 masks, the corporation named ExOne in 2020 started exploring BJT usage to create reusable filters made out of copper. Although, ExOne in reality was aimed at developing the copper filters for water, nonetheless, ended up with innovation pertaining to the same for corona virus [78]. As alluded to in the Sect. 1.3, the processing of copper to obtain a high density component is quite onerous because of its undesirable optical properties. However, such a disadvantage was considered advantageous to develop a copper filter with high and controlled porosity. These porosities are minute in size and have an indefinite path in bulk. Moreover, its use as the filter is considered suitable attributed to its ability to trap the virus in these pores and ultimately kill them (Fig. 1.18).

Fig. 1.18 The design of 3d printed reusable copper filter for N-95 masks fabricated by ExOne amid the covid-19 pandemic with the aid of BJT for biomedical applications



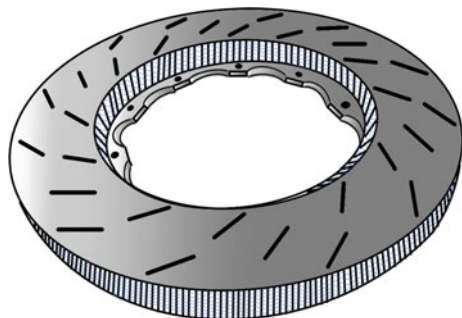
As AM technology progresses, not only can we predict a drop in the price of equipment, but we can also anticipate the development of innovative and unique technologies that will enhance its applications. Moreover, at the moment, the biomedical sectors are expected to account for 11% of the total AM industry. With the advantages offered like complex parts fabrications, patient-specific components, etc., it's thrilling to speculate about what the foreseeable future can bring in the concerned medical field [79].

1.5.3 Automobile Industry

Automobile manufacturers are boosting the deployment of AM technology to remain pertinent in the era of industry 4.0. Currently, AM is employed throughout different stages of the automotive sector, from the prototype and tool production to end products, allowing automakers to remain agile and inventive. Moreover, auto-manufacturers successfully create better parts with complicated designs and structures with the aid of metal AM. Parts pertained to powertrain, body panels, suspension springs, seat frames, cooling systems in exhaust etc., [80] are widespread manufactured in the automobile sector using AM. Besides the component manufacturing, AM is also considered competent to produce the whole 3d printed car for end use. However, such practice was made possible utilizing lightweight material in one of AM process named fused deposition modelling by Stratasys [81]. Since our chapter is concerned with metal AM, it also has a slew of applications in industries. For instance, one of the famous industries named Bugatti 3d printed titanium brake callipers to deaccelerate the car from 261 mph to the rest [82]. However, the use of traditionally made callipers was heavy and, therefore, significantly affects the handling. So, without compromising the handling characteristics, Bugatti developed the callipers utilizing metal AM that was responsible for the 40% reduction in weight than the conventionally made part. Furthermore, metal AM's potential to produce the internal lattice structure has made the automobile industries to avoid the wastage of material and money. Also, owing to the production of such parts, weight reduction becomes evident and considered accountable for increased energy efficiency. As an example, the firm named Ceramic Disc Technologies (CDT) developed the brake rotors (made of aluminum and ceramic composite) for Dodge Challenger with the same mentioned idea of lattice structure and consequently saved a significant amount of material for its development [83] as shown in Fig. 1.19. However, this AM fabricated part offers considerable variation in terms of weight reduction. Moreover, the presence of lattice structure enables the proper flow of air and hence results in superior heat transfer.

AM has made automotive pertained organizations more versatile and allowed them to build better car components that were otherwise unachievable using conventional techniques. However, along with process advantages, there too exists some inherent limitation. The primary disadvantage is the inability of the equipment to manufacture automotive components in huge quantities. So, the future of AM in an automobile is its working as mass manufacturing of components to deal with public demands.

Fig. 1.19 The design of 3d printed brake rotors made of aluminum and ceramic composites for Dodge Challenger Hellcat fabricated by Ceramic Disc Technologies to reduce weight and enhance energy efficiency



References

1. Hull, C.W.: Apparatus for production of three-dimensonal objects by stereolithography, US Patent 4,575,330
2. Stratasys: The history of stratasys. <https://www.stratasys.co.in/>. Accessed 20 Apr. 2021
3. EOS GmbH: The eos story. <https://www.eos.info/en/about-us/history>. Accessed 20 Apr. 2021
4. Arcella, F.G., Froes, F.H.: Producing titanium aerospace components from powder using laser forming. *Jom.* **52**, 28–30 (2000). <https://doi.org/10.1007/s11837-000-0028-x>
5. Optomec: Milestones. <https://optomec.com/milestones/>. Accessed 21 Apr. 2021
6. ExOne: Our story. <https://www.exone.com/en-US/About/Our-Story>. Accessed 21 Apr. 2021
7. GE Additive: Milestones. <https://www.ge.com/additive/who-we-are/concept-laser>. Accessed 22 Apr. 2021
8. GE Additive: Arcam ebm. <https://www.ge.com/additive/who-we-are/about-arcam>. Accessed 22 Apr. 2021
9. Trumpf: Additive production systems. https://www.trumpf.com/en_IN/products/machines-systems/additive-production-systems/. Accessed 22 Apr. 2021
10. Renishaw: A brief history. <https://www.renishaw.com/en/heritage--32458>. Accessed 23 Apr. 2021
11. DMG Mori: Additive manufacturing. <https://in.dmgmori.com/products/machines/additive-manufacturing>. Accessed 23 Apr. 2021
12. AddUp Solutions: The history of addup group. <https://addupsolutions.com/>. Accessed 23 Apr. 2021
13. SLM Solutions: Welcome to slm solutions. <https://www.slm-solutions.com/>. Accessed 23 Apr. 2021
14. Matsuura: Lumex avance-25. <https://www.matsuura.co.uk/additive-manufacturing/lumex-avance-25/>. Accessed 24 Apr. 2021
15. 3d Systems: Our story. <https://www.3dsystems.com/our-story>. Accessed 24 Apr. 2021
16. Sharebot: Metal 3d printer. <https://www.sharebot.it/en/sharebot-metalone-dmls/>. Accessed 24 Apr. 2021
17. Sisma: Additive manufacturing. <https://www.sisma.com/en/professional-3d-printers/>. Accessed 24 Apr. 2021
18. Aconity Systems: Laser powder bed fusion. <https://aconity3d.com/machines>. Accessed 24 Apr. 2021
19. Gornet, T.: History of additive manufacturing. (2017)
20. Velo3d: Support-free metal AM printing. <https://www.velo3d.com/about-us/>. Accessed 25 Apr. 2021
21. Xact Metal: XM200C printer. <https://xactmetal.com/xm200c/>. Accessed 25 Apr. 2021
22. Frazier, W.E.: Metal additive manufacturing: A review. *J. Mater. Eng. Perform.* **23**, 1917–1928 (2014)

23. Autodesk: Tinkercad. <https://www.tinkercad.com/>. Accessed 25 Apr. 2021
24. Goyanes, A., Det-Amornrat, U., Wang, J., Basit, A.W., Gaisford, S.: 3D scanning and 3D printing as innovative technologies for fabricating personalized topical drug delivery systems. *J. Control. Release.* **234**, 41–48 (2016)
25. 3d Systems: An Invitation to Share a Special Moment at AMUG 2018. <https://www.3dsystems.com/blog/2018/2018-03/invitation-share-special-moment-amug-2018>. Accessed 27 Apr. 2021
26. Qin, Y., Qi, Q., Scott, P.J., Jiang, X.: Status, comparison, and future of the representations of additive manufacturing data. *Comput. Des.* **111**, 44–64 (2019)
27. Wiberg, A., Persson, J., Ölvander, J.: Design for additive manufacturing – a review of available design methods and software. *Rapid Prototyp. J.* **25**, 1080–1094 (2019)
28. Morgan, D., Agba, E., Hill, C.: Support structure development and initial results for metal powder bed fusion additive manufacturing. *Procedia Manuf.* **10**, 819–830 (2017)
29. Gibson, D.W.R. and B.S.: Generalized additive manufacturing process chain. In: *Additive Manufacturing Technologies*, pp. 43–61. Springer US (2015)
30. Jiang, J., Xu, X., Stringer, J.: Support structures for additive manufacturing: a review. *J. Manuf. Mater. Process.* **2**, 64 (2018)
31. AMFG: Post-Processing for Industrial 3D Printing. <https://amfg.ai/2019/12/11/post-processing-for-industrial-3d-printing-trends/>. Accessed 30 Apr. 2021
32. Yin, S., Yan, X., Jenkins, R., Chen, C., Kazasidis, M., Liu, M., Kuang, M., Lupoi, R.: Hybrid additive manufacture of 316L stainless steel with cold spray and selective laser melting: microstructure and mechanical properties. *J. Mater. Process. Technol.* **273**, (2019)
33. Maskery, I., Aboulkhair, N.T., Corfield, M.R., Tuck, C., Clare, A.T., Leach, R.K., Wildman, R.D., Ashcroft, I.A., Hague, R.J.M.: Quantification and characterisation of porosity in selectively laser melted Al-Si10-Mg using x-ray computed tomography. *Mater. Charact.* **111**, 193–204 (2016)
34. Salman, O.O., Gammer, C., Chaubey, A.K., Eckert, J., Scudino, S.: Effect of heat treatment on microstructure and mechanical properties of 316l steel synthesized by selective laser melting. *Mater. Sci. Eng. A.* **748**, 205–212 (2019)
35. Shi, Y., Yan, C., Zhou, Y., Wu, J., Wang, Y., Yu, S., Chen, Y.: Metal materials for additive manufacturing. In: *Materials for Additive Manufacturing*. pp. 403–595. Academic Press (2021)
36. Lee, H., Huat, C., Lim, J., Low, M.J., Tham, N.: Lasers in additive manufacturing : a review. *Int. J. Precis. Eng. Manuf. Technol.* (2017)
37. Prashanth, K.G., Scudino, S., Maity, T., Das, J., Eckert, J.: Is the energy density a reliable parameter for materials synthesis by selective laser melting ? *Mater. Res. Lett.* **5**, 386–390 (2017)
38. Criales, L.E., Öznel, T.: Temperature profile and melt depth in laser powder bed fusion of Ti-6Al-4V titanium alloy. *Prog. Addit. Manuf.* **2**, 169–177 (2017)
39. Hooper, P.A.: Melt pool temperature and cooling rates in laser powder bed fusion. *Addit. Manuf.* **22**, 548–559 (2018)
40. Ansari, M.J., Nguyen, D.S., Park, H.S.: Investigation of SLM process in terms of temperature distribution and melting pool size: modeling and experimental approaches. *Materials (Basel).* **12**, (2019)
41. Huber, F., Rasch, M., Schmidt, M.: Laser powder bed fusion (Pbf-lb/m) process strategies for in-situ alloy formation with high-melting elements. *Metals (Basel).* **11**, 1–15 (2021)
42. Lassègue, P., Salvan, C., De Vito, E., Soulard, R., Herbin, M., Hemberg, A., Godfroid, T., Baffie, T., Roux, G.: Laser powder bed fusion (L-PBF) of Cu and CuCrZr parts: influence of an absorptive physical vapor deposition (PVD) coating on the printing process. *Addit. Manuf.* **39**, 101888 (2021)
43. Milewski, J.O.: Understanding metal for additive manufacturing. In: *Additive Manufacturing of Metals*. pp. 49–83 (2017)
44. Schmid, M.: LS materials: polymer properties. In: *Laser Sintering with Plastics*. pp. 65–99 (2018)

45. Lindström, V., Liashenko, O., Zweiacker, K., Derevianko, S., Morozovych, V., Lyashenko, Y., Leinenbach, C.: Laser powder bed fusion of metal coated copper powders. *Mater.* (Basel, Switzerland). **13**, 3493 (2020)
46. Jadhav, S.D., Dhekne, P.P., Brodu, E., Van Hooreweder, B., Dadbakhsh, S., Kruth, J.-P., Van Humbeeck, J., Vanmeensel, K.: Laser powder bed fusion additive manufacturing of highly conductive parts made of optically absorptive carburized CuCr1 powder. *Mater. Des.* **198**, 109369 (2021)
47. Diegel, O., Nordin, A., Motte, D.: *Additive Manufacturing Technologies*. (2019)
48. Gordon, J. V., Narra, S.P., Cunningham, R.W., Liu, H., Chen, H., Suter, R.M., Beuth, J.L., Rollett, A.D.: Defect structure process maps for laser powder bed fusion additive manufacturing. *Addit. Manuf.* **36**, 101552 (2020)
49. Gibson, I., Rosen, D.W., Stucker, B.: Powder bed fusion processes. In: *Additive Manufacturing Technologies: Rapid Prototyping to Direct Digital Manufacturing*. pp. 120–159. Springer US, Boston, MA (2010)
50. EOS GmbH: EOS M 400-4. <https://www.eos.info/en/additive-manufacturing/3d-printing-metal/eos-metal-systems/eos-m-400-4>. Accessed 1 May 2021
51. Murr, L.E., Gaytan, S.M.: Electron beam melting. In: *Comprehensive Materials Processing*. pp. 135–161. Elsevier, Oxford (2014)
52. Johnson, D.L.: Solid-state sintering. In: BROOK, R.J. (ed.) *Concise Encyclopedia of Advanced Ceramic Materials*. pp. 454–458. Pergamon, Oxford (1991)
53. Moya, J.S., Baudín, C., Miranzo, P.: Sintering. In: Meyers, R.A. (ed.) *Encyclopedia of Physical Science and Technology* (Third Edition), pp. 865–878. Academic Press, New York (2003)
54. German, R.M., Suri, P., Park, S.J.: Review: liquid phase sintering. *J. Mater. Sci.* **44**, 1–39 (2009)
55. Kruth, J., Mercelis, P., Van Vaerenbergh, J., Froyen, L., Rombouts, M.: Binding mechanisms in selective laser sintering and selective laser melting. *Rapid Prototyp. J.* **11**, 26–36 (2005)
56. Miyanaji, H.: Binder jetting additive manufacturing process fundamentals and the resultant influences on part quality, 2018
57. Leary, M.: Binder jetting. In: Leary, M. (ed.) *Design for Additive Manufacturing*. pp. 335–339. Elsevier (2020)
58. ExOne: Innovent+. <https://www.exone.com/en-US/3D-printing-systems/metal-3d-printers/Innovent>. Accessed 12 May 2021
59. 3deo: Metal additive manufacturing (AM) processes—binder jetting. 3deo.co/metal-3d-printing/metal-additive-manufacturing-am-processes-binder-jetting/. Accessed 14 May 2021
60. Sciaky: Electron beam additive manufacturing. <https://www.sciaky.com/additive-manufacturing/electron-beam-additive-manufacturing-technology>. Accessed 14 May 2021
61. Jafari, D., Vaneker, T.H.J., Gibson, I.: Wire and arc additive manufacturing: Opportunities and challenges to control the quality and accuracy of manufactured parts. *Mater. Des.* **202**, 109471 (2021)
62. Ahn, D.-G.: Directed energy deposition (DED) process: state of the art. *Int. J. Precis. Eng. Manuf. Technol.* **8**, 703–742 (2021)
63. WAAM: Wire arc additive manufacturing. <https://waammat.com/about/waam>. Accessed 16 May 2021
64. DigitalAlloys: Directed energy deposition. <https://www.digitalalloys.com/blog/directed-energy-deposition/>. Accessed 16 May 2021
65. Sing, S.L., Tey, C.F., Tan, J.H.K., Huang, S., Yeong, W.Y.: 3D printing of metals in rapid prototyping of biomaterials: techniques in additive manufacturing. In: Narayan, R. (ed.) *Rapid Prototyping of Biomaterials* (Second Edition). pp. 17–40. Woodhead Publishing (2020)
66. Ehmsen, S., Yi, L., Aurich, J.C.: Process chain analysis of directed energy deposition: energy flows and their influencing factors. *Procedia CIRP* **98**, 607–612 (2021)
67. Karthikeyan, J.: The advantages and disadvantages of the cold spray coating process. In: Champagne, V.K. (ed.) *The Cold Spray Materials Deposition Process*. pp. 62–71. Woodhead Publishing (2007)
68. Arbegast Materials Processing and Joining Lab: Cold spray - a guide to best practice. (2012)

69. Schmidt, T., Gärtnert, F., Assadi, H., Kreye, H.: Development of a generalized parameter window for cold spray deposition. *Acta Mater.* **54**, 729–742 (2006)
70. Liu, R., Wang, Z., Sparks, T., Liou, F., Newkirk, J.: Aerospace applications of laser additive manufacturing. In: Brandt, M. (ed.) *Laser Additive Manufacturing*. pp. 351–371. Woodhead Publishing (2017)
71. Duda, T., Raghavan, L.V.: 3D metal printing technology. *IFAC-PapersOnLine.* **49**, 103–110 (2016)
72. GE aviation: Fired up: GE successfully tested its advanced turboprop engine with 3d-printed parts. <https://www.ge.com/news/reports/ge-fired-its-3d-printed-advanced-turboprop-engine>. Accessed 22 May 2021
73. ArianeGroup: Future ariane propulsion module simplified. <https://www.eos.info/en/3d-printing-examples-applications/all-3d-printing-applications/aerospace-additive-manufacturing-for-ariane-injection-nozzles>. Accessed 22 May 2021
74. Najmon, J.C., Raeisi, S., Tovar, A.: Review of additive manufacturing technologies and applications in the aerospace industry. In: *Additive Manufacturing for the Aerospace Industry*. pp. 7–31. Elsevier Inc. (2019)
75. Additive manufacturing: Lightweight combustion chamber for 3d printed rocket engine: the cool parts show. <https://www.additivemanufacturing.media/articles/lightweight-combustion-chamber-for-3d-printed-rocket-engine-the-cool-parts-show-30>. Accessed 23 May 2021
76. Aimar, A., Palermo, A., Innocenti, B.: The role of 3d printing in medical applications: a state of the art. *J. Healthc. Eng.* **2019**, 5340616 (2019)
77. Elisheva, R.: Adverse effects of prolonged mask use among healthcare professionals during covid-19. *J. Infect. Dis. Epidemiol.* **6**, 6–10 (2020)
78. Additive manufacturing: Reusable, 3d printed copper filter: the cool parts show. <https://www.additivemanufacturing.media/articles/reusable-3d-printed-copper-filter-the-cool-parts-show-28>. Accessed 23 May 2021
79. AMFG: Industrial applications of 3d printing: the ultimate guide. <https://amfg.ai/industrial-applications-of-3d-printing-the-ultimate-guide/>. Accessed 24 May 2021
80. Javid, I., Christmann, S.: Additive manufacturing in the automotive industry. (2020)
81. Stratasys: The first fuel-efficient 3d printed car is back on the map. <https://www.stratasysdirect.com/industries/transportation/3d-printed-car-fuel-efficient-fdm-urbee-2>. Accessed 26 May 2021
82. Bugatti: World premier—brake caliper from 3d printer. <https://www.bugatti.com/media/news/2018/world-premiere-brake-caliper-from-3-d-printer/>. Accessed 26 May 2021
83. Additive manufacturing: Lighter, better-performing brake rotor from 3d printing: the cool parts show. <https://www.additivemanufacturing.media/articles/lighter-better-performing-brake-rotor-from-3d-printing-the-cool-parts-show-27>. Accessed 26 May 2021

Chapter 2

Development in Additive Manufacturing Techniques



**K. Arunprasath, V. Arumugaprabu, P. Amuthakkannan,
R. Deepak Joel Johnson, and S. Vigneshwaran**

2.1 Evolutions in Additive Manufacturing

2.1.1 *History of Additive Manufacturing*

The development of manufacturing techniques produces a different orientation towards greater weight reduction with a fine look. After the introduction of AM technique, the quality and strength of the products are very good than the conventional methodologies. However, additive manufacturing has some disadvantages, the output achieved from this technology is excellent in all the fields of engineering and medicine. AM technique is also improved the mechanical strength of the products by controlling the printing microstructure [1].

The history of additive manufacturing techniques started from the year 1987 with stereolithography (SLA). Japanese doctor Hideo Kodama from Municipal Industrial Research Institute at Nagoya, Japan introduced this solid 3D printed model using SLA. The initial materials they have chosen were polymeric materials for the layer-by-layer formation. Laser and UV-light sources are used to solidifies the forming

K. Arunprasath (✉)

Department of Mechanical Engineering, PSN College of Engineering And Technology,
Tirunelveli, Tamil Nadu, India

V. Arumugaprabu

Department of Mechanical Engineering, Kalasalingam Academy of Research and Education,
Krishnankoil, Tamil Nadu 626126, India

P. Amuthakkannan

Department of Mechanical Engineering, PSR Engineering College, Sivakasi, Tamil Nadu 626140,
India

R. Deepak Joel Johnson · S. Vigneshwaran

Department of Mechanical Engineering, Saveetha School of Engineering, Saveetha Institute of
Medical and Technical Sciences, Chennai, Tamil Nadu 602105, India

layer, later there is an introduction of many materials were processed through this technique. After the introduction of 3D printing technology, it is very easy to produce complex dimensions in all applications [2].

The conventional metallurgical theory proposes that numerous alloying components in an alloy could bring about the arrangement of new intermetallic stages with complex microstructures. Since the advancement of many materials, the exploration in the field of 3D printing (3DP) technology is speeding up, because of the fascinating properties of new material introductions. They have essentially higher blending entropies than those in conventional alloys [3].

The utilization of polymeric materials ruled the AM technology with the help of 3DP. Owing to the need for metals in all the areas, the introduction of metal-based AM techniques enters the commercial markets. In those metals like aluminium, titanium, gold, copper, silver is seen as a product in markets. Solidification is one of the problems initially noted for metal-based manufacturing, later it is overcome by the introduction of the laser, ultra-violet (UV), the electron beam in the manufacturing process. Machining results of these 3D printed products also very good with microstructural packings to withstand the strength [4].

Moreover, the mechanical output is good, AM has not been appropriate for the high-volume creation of large scope projects. Notwithstanding, with signs of progress in materials, measure controls, and mechanical technology, the field of AM technique, keep on advancing towards turning into a practical alternative for maximum scope for large volume production industries. This is an illustration of such change in the execution of polymer big area additive manufacturing (BAAM) using AM techniques [5]. Figure 2.1 illustrates the history of AM technique.

Powder-based AM products show very good strength and compatibility with molecular arrangements. The manufacturing of complex shapers is very easy through powdered materials. Among powder AM techniques, direct energy deposition (DED) is more profitable than powder bed fusion (PBF) for assembling producing parts because of its higher deposition rate. Wire arc additive manufacturing (WAAM), which is a DED strategy of manufacturing cyclic process that includes the softening of the provided wire utilizing a circular segment as the warmth source, and is a bead-based AM method with a quick statement rate. Contrasted with powder-based strategies, it causes fewer deformities, like pores, empowering the acknowledgment of greater products [6].

The development of advanced AM technology day by day is an innovation, it has been getting expanding the research towards mechanical, bone implants, and medical considerations in the new year's. With this quick turn, the significance of the value of checking in AM measurement has been perceived, which altogether influences the property of the producing parts. Since the conventional products made highlights for quality distinguishing proof for the most part exorbitant, tedious and delicate to commotions, the smart information-driven programmed measure observing strategies are getting increasingly more famous as of now [7].

Additive manufacturing producing creates essentially less waste than customary assembling strategies. For instance, a processing machine works by eliminating material from a square that is greater than the actual item will be. Along these lines, added

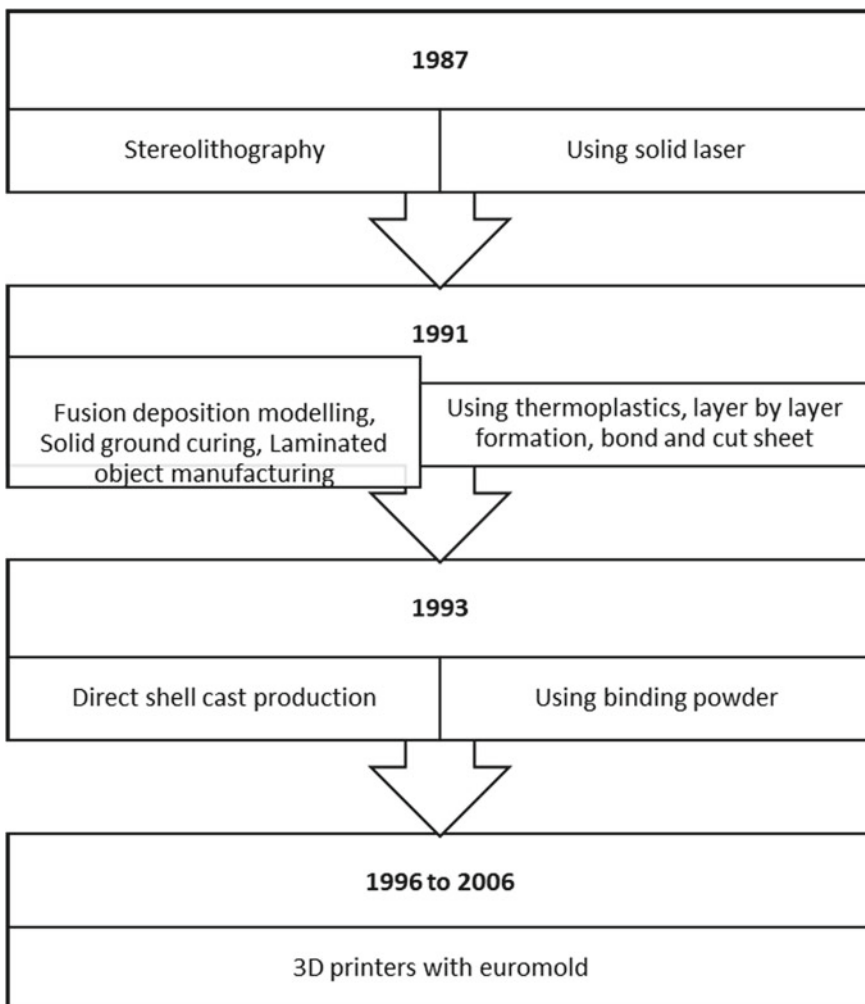


Fig. 2.1 History of AM technique

substance assembling can decrease material expenses and waste by as much as 90%. cost of entry is becoming more affordable, it is easy to change or revise versions of a product, training programs are becoming readily available at all levels, it reduces waste production, it saves on energy costs, and demand continues to rise.

2.1.2 Types of Additive Manufacturing with Materials

Additive manufacturing is one of the realizations of complex 3D transformation into real products. This additive manufacturing is classified by the method of binding since it is a layer-by-layer formation process. Based on the basic principle of binding AM is classified into seven categories. Through, these manufacturing technologies plastics, wax, gypsum or sand metals, and resin-based products were manufactured for different applications.

In the past years, the development of AM technique which is the incorporation of stereolithography (SLA) combined with fused deposition modelling (FDM), selective laser sintering (SLS), laminated object manufacturing (LOM), and 3D printing (3DP). In any case, major difficulties stay to be settled, for example, AM technique selection is dependent on basic AM technique, material determination, the part direction which is to limit the stair-stepping effect, residual stresses, and selection of suitable tolerance in the product is responsible for the very good surface finish of the final products [8]. In this discussion vat photo polymerization, powder bed fusion, material extrusion, material jetting, binder jetting, direct energy deposition, and its technologies. Figure 2.2 represents the Additive manufacturing technologies.

Vat Photopolymerization

Vat polymerization is one of the polymer material filling processes with the use of UV light for the curing of the products which is manufactured through 3D printing. This reaction mostly happens for materials like styrene, polyamides, ceramics, graphene, and super polymeric elastomers. In this technique, ultraviolet (UV) light initiates the polymerization reaction and allows to complete of the polymeric structure. Figure 2.3 shows the vat photo polymerization and its 3DP technologies. By using this principle, Stereolithography (SLA), Direct Light Processing (DLP), Continuous DLP (CDLP) are worked. Flexible and transparent jewels and polymeric brittle products are manufactured through this technique.

Powder Bed Fusion (PBF)

The material powder is melted and bind together with the heat source. The heat source may be a laser beam or an electron beam. The mechanism starts with smoothing of thin layers of powder on the part which is exposed to the different light source make the desired products. This technique is suitable for the materials such as metals, and polymer powders. Automotive parts, tire moulds, and implants are some of the products seen from powder bed fusion technology. Figure 2.4 demonstrates the Powder Bed Fusion and its 3DP technologies. Selective Laser Sintering (SLS), Selective Laser Melting (SLM) and Direct Metal Laser Sintering (DMLS), Electron

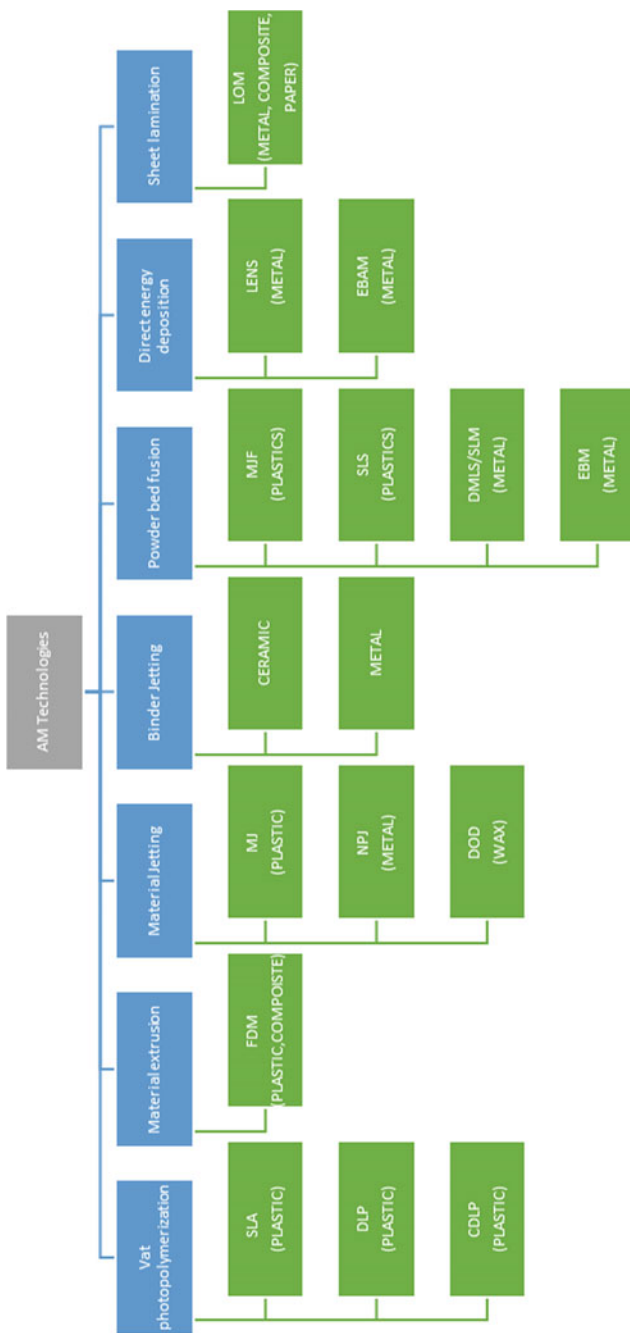


Fig. 2.2 Additive manufacturing technologies

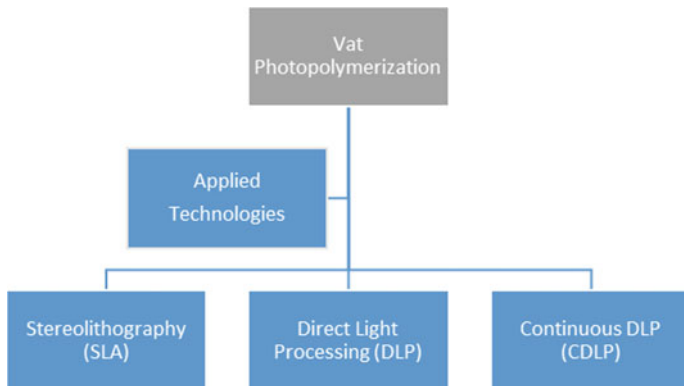


Fig. 2.3 Vat photopolymerization and its 3DP technologies

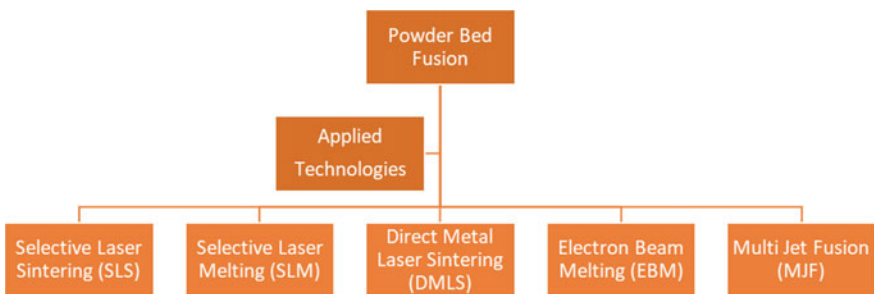


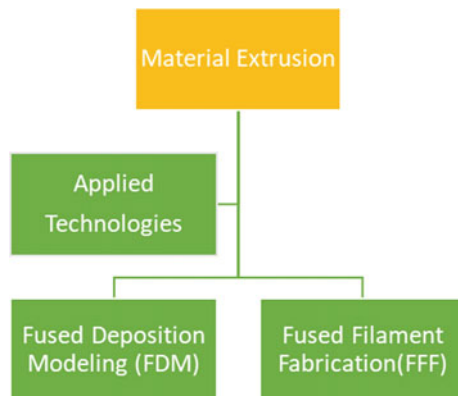
Fig. 2.4 Powder bed fusion and its 3DP technologies

Beam Melting (EBM), Multi Jet Fusion (MJF) are some of the applications of PBF technology in AM.

Material Extrusion

Material extrusion is one of the chosen technologies for 3D printing in which the materials are dispensed through a nozzle. The diameter of the nozzle decided the meshing and size of the print on the build plate. All types of thermoplastic materials are well suitable for this technology. The major application of this technology is to produce plastic prototypes with very good accuracy and it is one of the cost-effective methods of additive manufacturing technology. Figure 5 material extrusion and its 3DP technologies.

Fig. 2.5 Material extrusion and its 3DP technologies



Material Jetting

Material jetting is regularly contrasted with the 2D ink-jetting cycle. Photopolymers, metals, or wax that fix or solidify when presented to UV light or raised temperatures can be utilized to assemble parts each layer by time. The idea of the material streaming cycle takes into account multi-material printing by layer. This capacity is regularly used to print support from various materials during the build stage. Materials in Jetting, Nanoparticle jetting, Drop-On-Demand (DOD) are some of the application technologies of AM technique. Acrylic, ABS, multi-color printing rubber are some of the materials used to produce medical and bio-medical products. Figure 2.6 explains material jetting in 3DP technologies.

Fig. 2.6 Material jetting and its 3DP technologies

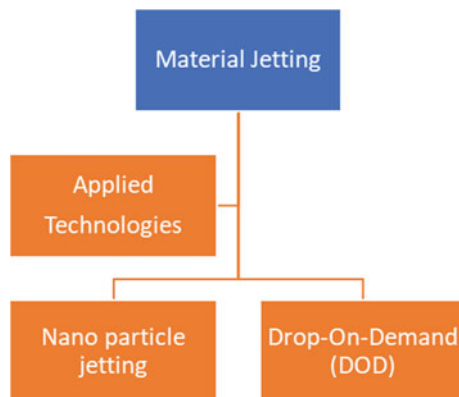
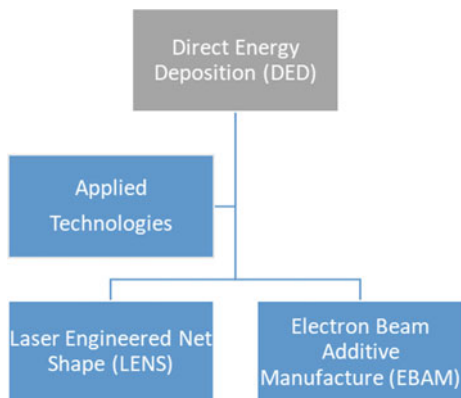


Fig. 2.7 Direct energy deposition (DED) and its 3DP technologies



Binder Jetting

This is one of the technologies in which powder materials and ceramics are printed for specific mechanical parts. Binder Jetting is an AM technique measure in which a mechanical print head specifically stores a fluid restricting specialist onto a liquid layer of powder particles either metal, sand, ceramics, or composites to assemble in the tooling system. It can be utilized to print a variety of materials including metals, sands, and ceramics. These layers bind to each other to frame a strong product.

Direct Energy Deposition

Directed Energy Deposition (DED) is a 3D printing strategy that utilizes an engaged fuel source, for example, a plasma arc, laser, or electron beam to soften a material that is at the same time stored by a nozzle. Direct Energy Deposition (DED) makes parts by dissolving powder material as it is deposited on the product. Technologies such as Laser Engineered Net Shape (LENS), and Electron Beam Additive Manufacture (EBAM) are followed this principle for printing the products. Titanium, stainless-steel, aluminum, and copper are some of the materials used to produce desired products for various applications. Figure 2.7 DED and its 3DP technologies.

Materials

The additive manufacturing process has many forms of dimensions to print the product from the digital file. However, 3D printed objects are used for many applications, the role of selection of material determines the quality and durability of the products. The materials are in different ranges using applying temperature and its processing. And, these materials are stronger, cheaper, and lighter added with some new properties also.

There are a lot of materials that can react with 3D printed products. That plastics, metals, resins are some of the materials which are predominantly used to produce more products for different applications. AM process helps to understand the development of temperature beyond the top surface. Simulation of the model utilizes the temperature results from warm models to anticipate microstructure on changing length scales.

As AM technique includes building layer upon layer, the liquefy tracks experience various remelting. Experimental information can just give the grain structure after the whole form, while recreation gives simulation to the development of the grain structure all through the interaction, all these functional changes are purely depending on the selection of the material [9]. Increasing the demand for energy protection led to the need for lightweight parts in functional applications. In the Aerospace industry, the decline in the weight of the parts reduces the fuel consumption and its costs. As in the Automotive industry, 10% decrease in weight of the parts can decrease up to 6–8% of fuel utilization. It is observed that grid structures of the materials are the better answers to achieve these goals [10]. Figure 2.8 illustrates materials used in 3D printing technologies.

2.1.3 Developments in Additive Manufacturing

Current scenario of manufacturing focuses on stronger, cheaper and lightweight material for all the type of applications. Additive manufacturing provides a solution and satisfied the needs of industrial and commercial customers. In these AM technologies, some of the techniques involved with more accuracy in the product generation and supports for mass production. The main advantage of AM technology is now a day, it is more suitable for metal-based production to produce high performed metallic parts. With more cost-effective and this technology development towards next level optimization for further better studies [11].

AM-based Design for Manufacturability (DFM) considers the abilities to assemble which measures with plan limitations to recognize fabricating issues with points of diminishing the lead times, burned through in the product development just to improving a product characteristic. As advancement in product development with AM is as yet newer, the development of sharable and organized plan rule information is prescribed to give rules to DFMAAM dynamic exercises to achieve better designs [12]. Additive manufacturing producing is mentioned as an assembling technique where intricacy or customization is free. Nonetheless, this requires checking and following the various parts contrasted with large-scale manufacturing of similar sort of parts. Figure 2.9 represents the developments in additive manufacturing technology.

When looking at AM against ordinary manufacturing, it has a lot higher potential for customization and complex calculations. AM technique is typically less expensive if the calculation is intended for large-scale manufacturing, but the assembling cost

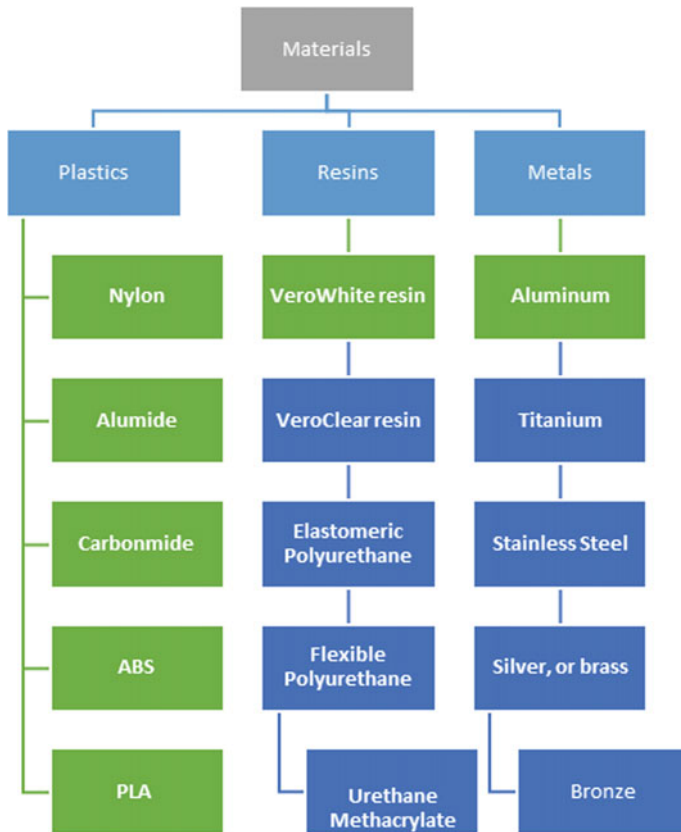


Fig. 2.8 Materials used in 3D printing technologies

is determined. It would do the trick to emphasize the design of the entire product and take a gander at the financial matters over the whole product lifecycle [13].

Jingchao Jiang [14] discussed the topology optimization for AM has gotten perhaps the main branches in DFAM, as topology optimization can completely misuse the critical advantages given by the expanded manufacturing opportunity offered by AM. As conventional component-based calculations like strong isotropic material with penalization (SIMP), level-headed material with penalization (RAMP), and bi-directional transformative underlying advancement (BESO) will shape non-smooth limits, post-procession or with upgrade techniques must be utilized to get precise limit data for engineering applications.

The manufacturing complex design and geometry the information available in the form of three-dimensional (3D) computer-aided plan (CAD) is more enough. The process comprises successive printing layers of material storing one layer over another. Different materials also produce through 3D printing for various applications such as bioprinting, polymers, bioceramics, metals. Materials used for 3D printing

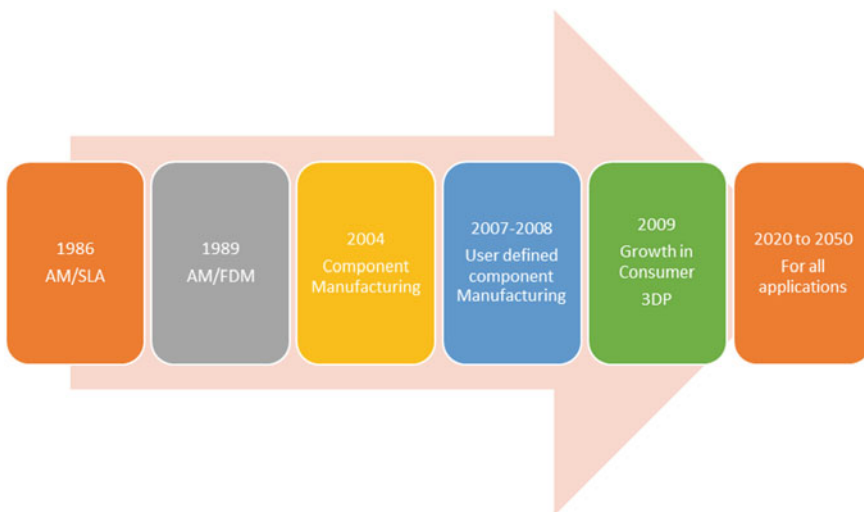


Fig. 2.9 Developments in additive manufacturing technology

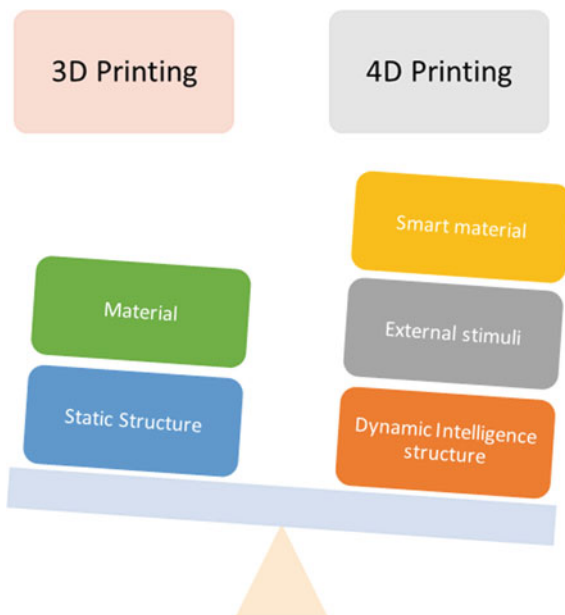
should have been painstakingly picked dependent on the proposed application of the product development [15].

The powder manufacturing process is decided by the powder qualities. Atomization is the most well-known manufacturing process for powder used in additive manufacturing. While water-atomized metallic powders are more normal and practical in customary press and sintering procedures, gas-atomized powders have lower oxygen content, round shape, and better flow ability. Thus, gas-atomized powders are all the more regularly utilized in additive manufacturing [16]. The extrusion-based AM technique is produced from thermoplastics such as acrylonitrile butadiene styrene (ABS), high-impact polystyrene (HIPS), polylactic acid (PLA), polyurethane (TPU), aliphatic polyamides. These materials are expelled from the print spout and afterward situated on the stage. The stage moves as one layer height down after completing each layer manufacture, until the entire product is finished [17].

Laser powder bed fusion (L-PBF), which is usually known as specific laser melting (SLM) or direct metal laser melting (DMLM), encourages close to net shape producing with precision. The layer thickness of these slices is considered as one of the process parameters. The L-PBF measure incorporates powder deposition onto a substrate plate handled layers, specifically melting of the powder particles with a high energy laser beam as per each profile cut, bringing down the stage by predetermined layer thickness and afterward recoating another layer of powder produces an effective design [18].

Laser-based powder bed fusion added substance producing offers the adaptability to fuse standard and user-defined characterized examine methodologies in a layer or the middle of the layers for the manufacturing of metallic parts. The prospects of using different scanning techniques through the PBF-AM strategies can produce energizing

Fig. 2.10 Difference between traditional 3D printing and novel 4D printing



roads for the microstructure and surface texturing study of metallic material parts [18]. Figure 2.10 shows the difference between traditional 3D printing and novel 4D printing.

Another strategy being concentrated to produce a more prominent assortment of feedstock materials and improved mechanical execution is through the execution of composite materials. The composites manufactured for 3D printing can shift from lignocellulosic materials to carbon-based materials and even inorganic filers. The combination of composites in printing materials can help with the age of the materials, and 3D printing innovation can grow towards 4-dimensional (4D) printing to showcase and create novel products [19]. The acquaintance of the fourth dimension with the 3D printing innovation is named as 4D Printing. With this new measurement, 3D printed objects have the capacity to change its shape without help from anyone else over the impact of outer upgrades, like light, heat, power, attractive field. 4D printing enables 3D printed objects to change their shape over the long haul. The expression 4D printing alludes to this extra fourth measurement: time. The arising innovation consolidates 3D printing procedures with undeniable level material science, designing and programming. 4D printing has the imminent to work on the plan and assembling of various items and has the immense potential to make parts that self-impel to respond to their current circumstance. Utilizations of 4D printing are in regions like biomedical gadgets, security, manufacture of designed surfaces for optics and constructions with multi directional properties. Figure 2.11 represents the functional evolution of 4D printing.

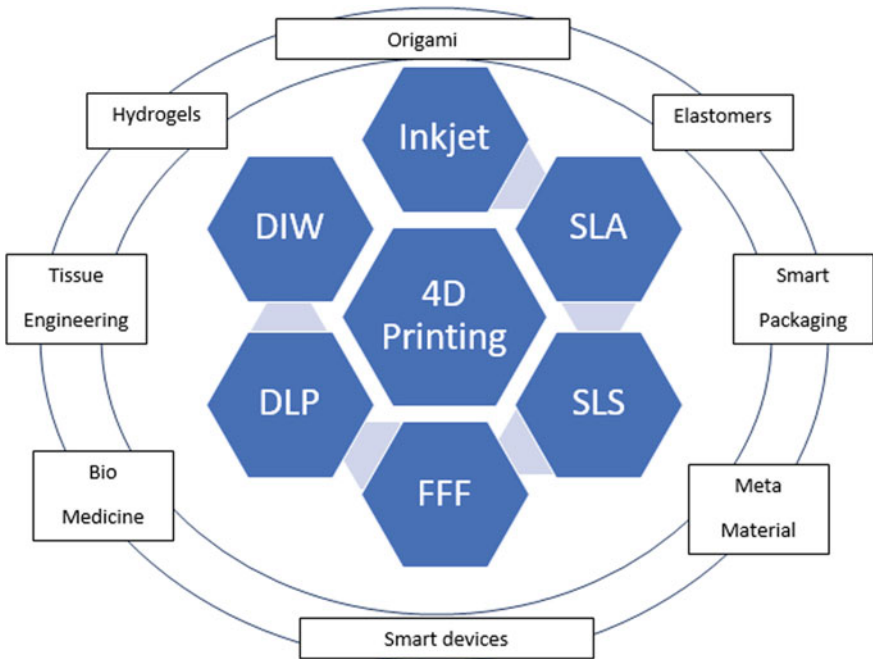


Fig. 2.11 Functional evolution of 4D printing

2.1.4 Applications

The development of 3D printing technology for the past decades was very higher in reach. While 3D printing has been around for quite a long time, it gets popular and uses lately. New 3D printing applications are continually being grown yet the applications point by point beneath have as of late ascended in popularity.

A large part of the justification for the new rise in 3D printing use is that it is a straightforward innovation that can be utilized in applications in a wide range of fields. In the initial years, 3D printing was introduced with high entry costs. 3D printer models and materials were costly. Lately, with enhancements and varieties in the advancements of both the machines and materials utilized in them, costs have been reduced, making 3D printing applications more available and cost-effective, across the industries and educational training centers. The fields which using 3D printing technology (3DPT) emerge the world into the next direction. In that consideration, the most five important of AM (3DPT) application was discussed in this portion. Figure 2.12 shows the applications of 3D printing.



Fig. 2.12 3D printing applications

Education

Consistently, more schools are fusing 3D printing techniques into their educational programs. The advantages of 3D printing for schooling are that it betters plan schoolings for their future by permitting undergraduates to make models without the requirement for costly tooling requirements. Undergraduates find out about 3D printing applications by planning and creating models they can a better hold for students.

3D printing overcomes any issues from thoughts and pictures on a page or screen, taking into account the making of those thoughts/pictures in the physical 3-dimensional world. 3D printers are presently normally found in homerooms and public libraries. Colleges have 3D printers accessible for undergraduates to use in classes and undertakings.

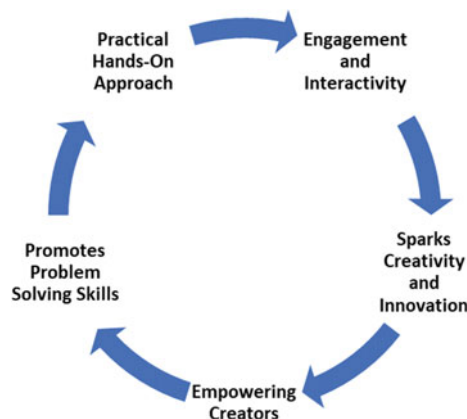
3D printing instruments are additionally changing STEM (Science Technology Engineering Mathematics) schooling by offering the capacity for ease fast prototyping by undergraduates in the study hall just as creating minimal effort excellent scientific designs from open hardware plans. In basic levels, 3DPT helps to find out about an assortment of 3D printing applications by investigating configuration, designing, and engineering standards. They can copy gallery things like fossils and verifiable ancient rarities to concentrate in the homeroom without the chance of harming sensitive assortments. They can acquire another, 3-dimensional viewpoint on geological symbols and maps.

Visual design for undergraduates can undoubtedly develop models with complex working parts. Undergraduates in the sciences can make and study cross-areas of organs in the human body just as other natural examples. Science undergraduates can make 3D models of molecules and chemical compounds. Also, solve problem-solving with creative design for all the possible concepts of practical education. Figure 2.13 represents the educational approaches of 3DPT.

Prototyping and Component Making

3D printing was first evolved as a method for quick prototyping. With a customary infusion formed model, it may cost a huge number of dollars and require a long time to create a solitary shape in the business. That is exceptionally unfeasible on the off chance that you are attempting to develop a plan with each new emphasis. 3D printing innovation incredibly decreases the lead times needed in conventional

Fig. 2.13 Education approaches of 3DPT



assembling, permitting a model to be created in hours, not weeks, and for a portion of the expense. The automobile and aerospace businesses are only two industries that are engaged with assembling exploiting progress in 3D printing technology in advancement.

Customary assembling is the most financial considerations everywhere in volumes. In this circumstance, where a product won't be mass-created, is the ideal as it takes into account the generally cheap creation of a product in more modest volumes or dependent upon the situation. In this equivalent vein, propels in rapid prototyping (RP) innovation has likewise brought about the improvement of materials and cycles, like Selective Laser Sintering (SLS) and Direct Metal Laser Sintering (DMLS) that are appropriate for the assembling of the latest form of a product, not simply it's a model. 3D printing advancements have made what is called 'fast tooling'. This is the place where tooling utilized in assembling cycles, for example, hydro-forming, stepping, and infusion forming is planned by particular methods, empowering speedy prototyping and reactions to tooling and installation needs.

Medical

3DP technology allows the medical representatives to provide a three-dimensional view of the field. The 3D-printing innovation permits to give the specialist an actual 3D model of the ideal patient life structures that could be utilized to precisely design the careful methodology alongside cross-sectional imaging or, then again, demonstrating custom prosthetics (or careful instrument) in light of patient-explicit life systems.

The strategy has been applied to (and used by) various businesses, including clinical innovation. Frequently clinical imaging techniques, for example, X-rays, computerized tomography (CT) examines, magnetic resonance imaging (MRI) outputs, and ultrasounds are utilized to create the first advanced model, which is consequently taken care of into the 3D printer. This tissue develops or organoids can

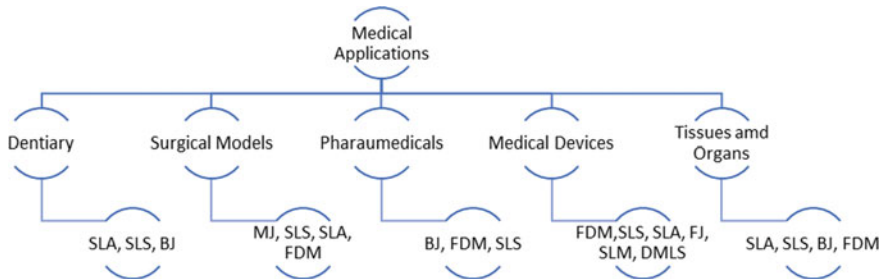


Fig. 2.15 Medical applications of 3DP technology

be utilized for medical exploration as they mirror organs on a smaller than usual scale. They are likewise being tested as less expensive options in contrast to human organ transfers.

Another use of 3D imprinting in the medical field is making patient-explicit organ reproductions that specialists can be used to rehearse on before performing complicated operations. This strategy has been demonstrated to accelerate strategies and trauma injury for patients. Sterile surgical instruments, like forceps, haemostats, surgical blade handles, and braces, can be created manufactured through 3D printers.

3D printing likewise permits the patient to design a prosthetic that is directly utilized to their requirements. For example, body labs have made a framework that permits patients to join their prosthetic on their limb with appropriate design. Additionally, the skincare packages, plastic surgery are some of the applications of 3DP in the medical field. Figure 2.15 Medical applications of 3DP technology.

Construction

In the construction industry 3DP technology permits to print the entire building, this construction may be faster with more accurate output in the design. In the development business, 3D printing can be utilized to make development parts or to ‘print’ whole structures. Development is appropriate to 3D printing as a large part of the data important to make a thing will exist because of the design process, and the business is as of now knowledgeable about computer-supported assembling.

The new rise of building information modelling (BIM) specifically may work with more utilization of 3D printing. Development of 3D printing may permit, quicker and more precise development of unpredictable or complex things just as bringing down the labour costs and delivering less product waste. It may likewise empower development to be attempted dangerous conditions not reasonable for a human labour force, for example, in space.

Concrete 3D printing in the development business helps save time, exertion, and material contrasted with traditional development strategies. It is imperative to note, however, that 3D printers are not yet fit for making a completely practical house. This may happen in the future with some updated design and printing considerations.

Commercial Purposes

The commercial usage of 3D printed products is more, which can be utilized as several applications. While discussing the commercial availability of 3DP products areas like jewellery making, medicine is predominantly ruled by 3DPT. The combination of multiple active medicinal drugs in a single ingredient. This is one of the customized form drugs which can be utilized for multiple purposes. Now a day most of the pharmaceutical industries are using 3DPT for manufacturing drugs. The first commercial 3D printed tablet is levetiracetam which is commercialized in the year 2015 by Aprecia Pharmaceuticals from the USA.

To meet the technological demand, customization is needed for the products, with the attribute of high productivity, 3D printers could help manufacturers make fast reaction to the interest of customer's customization and hold onto the high of the line market, like jewellery customization.

The production of jeweller parts emerged, since 3D printing innovation increasingly more typically applied for amazing jewellery design items started to arise unendingly, for example, 3D printed jewellery, showed up in a few worldwide design weeks, which impressed the individuals extraordinarily and brings more design through 3PDT in this brilliant world with marvellous components made from gold, silver, platinum-based materials in various forms such as earrings, rings, bangles, and anklets.

2.1.5 Advancement in 3D Printing Technology

The advancement of 3D printing technology has facilitated the use of low-cost 3D printing machines; it should be noted that 3D printers are now found in educational institutions and homes. This enabled the development of 3D printed parts in various combinations, shapes, and sizes to analyze the properties and performance. The ultimate goal of 3D printing technology is to provide high-strength 3D printed parts and components. It should be noted that the mechanical strength of 3D printed materials is determined not only by material properties but also by the performance of 3D printing machines. As a result, optimizing the properties of 3D printing parameters became more important. In this vein, a few researchers have recently investigated the influence of printing properties and parameters on part performance. For example, Ferro et al. [20] investigated the effect of process parameters in the selective laser melting process on the formation of porosity in the printed AlSi10Mg-based aluminum alloy. The authors examined the effect of two important printing parameters, namely laser power and exposure time. The other printing parameters in the selective laser melting process were kept constant. Lower porous was found on parts printed with a lower laser power and exposure time. Similarly, Zvonek et al. [21] investigated the influence of selective laser melting process parameters on the formation of porosity and weld track in AlSi7Mg aluminum alloy. When working at constant laser power, this investigation found that increasing the scanning speed could result in a decrease in

weld depth and width. Thus, various studies in 3D printing have been conducted to improve 3D printing performance and printability.

For instance, In the case of polymers, filament deposition modelling (FDM) has emerged as a popular technique. Various printing factors influence the part performance of FDM printed material. The material and printing parameters influence the performance of FDM printed parts. The printing parameters have been found to have a significant impact on the mechanical strength and performance of the printed part [22–24]. Wang et al. [25] studied the effect of FDM process parameters on the development of PLA-based polymer materials. The effect of process parameters such as printing angle, layer thickness, fill rate, and nozzle temperature on elastic modulus, tensile strength, elongation at break, storage modulus, loss modulus, and loss factor were studied. It was found that the printing angle affects the fracture of the material. This investigation recommended the use of thinner layer thicknesses. The smaller layer thickness leads to the strength of the polymer and also restricted the movement of polymer chains. The increase in the fill rate leads to the reduction of air gap corresponding to increased layer bonding. These notable results could lead to the possible printing of high-strength polymers. Rarani et al. [26] investigated the effect of FDM printing parameters (infill density, printing speed, and layer thickness) on the tensile strength of the PLA polymer in another study. According to the findings, and infill density of 80%, a printing speed of 40 mm/s, and a layer thickness of 0.1 mm were effective in achieving the optimum tensile strength of the FDM printed component. A similar investigation has been carried by several researchers to analyze the process parameters of different 3D printing methods and their influence.

Further another important development in 3D printing is the development of composites. Both metal-based composites and polymer-based composites have been in recent years. This made it possible to print high-strength 3D printed parts. For instance, Enrique et al. [27] developed Inconel 625 based metal composite reinforced with the carbide. In another work, Levy et al. [28] developed TiC/steel composites through binder jet 3Dprinting. In comparison to polymer-based composites, only a small amount of work has been done on metal-based composites. Because of the flexibility of 3D printing polymers, nanocomposites, short fiber composites, continuous fiber composites, and nanocomposites have been developed [29–32]. Recycled polymers have also been used in polymer printing technology in recent years; for example, Vigneshwaran et al.[33] reported the FDM process as a tool for developing a circular economy in additive manufacturing technology. As a result, the use of recycled polymers in additive manufacturing could reduce polymer-based waste and create a more sustainable environment. The establishment of biomimicry is another significant advancement in the field of 3D printing technology. 3D printing allows for the development of complex designs inspired by nature. The bio-inspired design adaption could provide enhancement in the strength and other properties of the 3D printed materials. Jia and Wang et al. [34] reported enhanced fracture toughness in the 3D printed biomimicry-based composites.

The greatest difficulties throughout the long term and all through the enterprises looking in the space of 3D printing are as per the following in our pick list, including

equipment costs, limited materials accessible, post-preparing necessities, manufacturing costs, lack of in-house added substance fabricating assets, lack of aptitude and additionally preparing among, labor force/representatives, limited repeatability, lack of formal principles, lack of demonstrated documentation of added substance assembling abilities, software improvement and capacities, longer creation courses of events restricted recyclability, risk of suit/lawful ramifications, and data storage prerequisites [36–41].

2.2 Summary

This chapter of the book gives a deep discussion on innovative ideas and technological development in the field of additive manufacturing. In the addition, this chapter discusses the evolutions in additive manufacturing, in this section, the origin of AM technologies and the history of AM technological development were discussed. The major types of additive manufacturing technologies like SLA, SLS, LOM, and fusion deposition modelling with the materials used for the fabrication are also discussed. The basic principles of AM fabrication like vat photopolymerization, powder bed fusion, material jetting, and other techniques with the stage-by-stage development of AM technologies are discussed. Applications with recent 4D advancements in AM techniques are also included in this chapter. This information helps, the researchers to work in the AM field, by understanding the basic concepts and procedures to create further development in the field of engineering and technology using additive manufacturing.

References

1. Cooke, S., Ahmadi, K., Willerth, S., Herring, R.: Metal additive manufacturing technology, metallurgy and modelling. *J. Manuf. Process.* **57**, 978–1003 (2020)
2. Ahmed, M., Pasha, M., Nan, W., Ghadiri, M.: A simple method for assessing powder spread ability for additive manufacturing. *Powder Technol.* **12**, 12–18 (2020)
3. Karimi, J., Ma, P., Jia, Y.D., Prashanth, K.G.: Linear patterning of high entropy alloy by additive manufacturing. *Manufact. Lett.* **24**, 9–13 (2020)
4. Alonso, U., Veiga, F., Suárez, A., Artaza, T.: Experimental investigation of the influence of wire arc additive manufacturing on the machinability of titanium parts. *Metals*. **10**(1), 24 (2020)
5. Hassen, A.A., Noakes, M., Nandwana, P., Kim, S., Kunc, V., Vaidya, U., Love, L., Nyocz, A.: Scaling Up metal additive manufacturing process to fabricate molds for composite manufacturing. *Addit. Manufact.* **32**, 101093 (2020)
6. Lee, S.H.: CMT-based wire arc additive manufacturing using 316L stainless steel effect of heat accumulation on the multi-layer deposits. *Metals* **10**(2), 278 (2020)
7. Li, X., Jia, X., Yang, Q., Lee, J.: Quality analysis in metal additive manufacturing with deep learning. *J. Intell. Manuf.* **31**(8), 2003–2017 (2020)
8. Elhoone, H., Zhang, T., Anwar, M. and Desai, S.: Cyber-based design for additive manufacturing using artificial neural networks for Industry 4.0. *Int. J. Prod. Res.* **58**(9), 2841–2861

9. Tan, J.H.K., Sing, S.L., Yeong, W.Y.: Microstructure modelling for metallic additive manufacturing: a review. *Virt. Phys. Prototyping.* **15**(1), 87–105 (2020)
10. Nagesha, B.K., Dhinakaran, V., Shree, M.V., Kumar, K.M., Chalawadi, D., Sathish, T.: Review on characterization and impacts of the lattice structure in additive manufacturing. *Mater. Today Proceed.* **21**, 916–919. Elsevier, Netherlands (2020)
11. Ning, J., Sievers, D.E., Garmestani, H., Liang, S.Y.: Analytical modeling of part porosity in metal additive manufacturing. *Int. J. Mech. Sci.* **172**, 105428 (2020)
12. Wang, Y., Zheng, P., Peng, T., Yang, H., Zou, J.: Smart additive manufacturing: current artificial intelligence-enabled methods and future perspectives. *Sci. China Technol. Sci.* **63**, 1600–1611 (2020)
13. Motaman, S.A.H., Kies, F., Köhnen, P., Létang, M., Lin, M., Molotnikov, A., Haase, C.: Optimal design for metal additive manufacturing: an integrated computational materials engineering (ICME) approach. *JOM.* **72**(3), 1092–1104 (2020)
14. Jiang, J.: A novel fabrication strategy for additive manufacturing processes. *J. Cleaner Prod.* **272**, 122916 (2020)
15. Jiang, F., Drummer, D.: Curing kinetic analysis of acrylate photopolymer for additive manufacturing by Photo-DSC. *Polymers* **12**(5), 1080 (2020)
16. Nadammal, N., Mishurova, T., Fritsch, T., Serrano-Munoz, I., Kromm, A., Haberland, C., Portella, P.D., Bruno, G.: Critical role of scan strategies on the development of microstructure, texture, and residual stresses during laser powder bed fusion additive manufacturing. *Add. Manuf.* **38**, 101792 (2021)
17. Salmi, M.: Additive manufacturing processes in medical applications. *Materials* **14**(1), 191 (2021)
18. Picard, M., Mohanty, A.K., Misra, M.: Recent advances in additive manufacturing of engineering thermoplastics: challenges and opportunities. *RSC Adv.* **10**(59), 36058–36089 (2020)
19. Ferro, P., Meneghelli, R., Razavi, S.M.J., Berto, F., Savio, G.: Porosity inducing process parameters in selective laser melted AlSi10Mg aluminium alloy. *Phys. Mesomech.* **23**, 256–262 (2020). <https://doi.org/10.1134/S1029959920030108>
20. Zvoníček, J., Koutný, D., Pantlejov, L., Paloušek, D.: Development of process parameters for SLM processing of AlSi7Mg aluminum alloy. In: *Lecture Notes in Mechanical Engineering*, pp. 515–524. Springer (2020)
21. Vigneshwaran, S., Uthayakumar, M., Arumugaprabu, V.: A review on erosion studies of fiber-reinforced polymer composites (2017). <https://doi.org/10.1177/0731684417699711>
22. Babu, K., Das, O., Shanmugam, V., Mensah, R.A., Försth, M., Sas, G., Restás, Á., Berto, F.: Fire behavior of 3D-printed polymeric composites. *J. Mater. Eng. Perform.* 1–11 (2021). <https://doi.org/10.1007/s11665-021-05627-1>
23. Shanmugam, V., Johnson, D.J., Babu, K., Rajendran, S., Veerasimman, A., Marimuthu, U., Singh, S., Das, O., Neisiany, R.E., Hedenqvist, M.S., Berto, F., Ramakrishna, S.: The mechanical testing and performance analysis of polymer-fibre composites prepared through the additive manufacturing. *Polymer Test.* **106925** (2020). <https://doi.org/10.1016/j.polymertesting.2020.106925>
24. Wang, S., Ma, Y., Deng, Z., Zhang, S., Cai, J.: Effects of fused deposition modeling process parameters on tensile, dynamic mechanical properties of 3D printed polylactic acid materials. *Polym. Test.* **86**, 106483 (2020). <https://doi.org/10.1016/j.polymertesting.2020.106483>
25. Heidari-Rarani, M., Ezati, N., Sadeghi, P., Badrossamay, M.R.: Optimization of FDM process parameters for tensile properties of polylactic acid specimens using Taguchi design of experiment method. *J. Thermoplast. Compos. Mater.* (2020). <https://doi.org/10.1177/0892705720964560>
26. Enrique, P.D., Mahmoodkhani, Y., Marzbanrad, E., Toyserkani, E., Zhou, N.Y.: In situ formation of metal matrix composites using binder jet additive manufacturing (3D printing). *Mater. Lett.* **232**, 179–182 (2018). <https://doi.org/10.1016/j.matlet.2018.08.117>
27. Levy, A., Miriyev, A., Elliott, A., Babu, S.S., Frage, N.: Additive manufacturing of complex-shaped graded TiC/steel composites. *Mater. Des.* **118**, 198–203 (2017). <https://doi.org/10.1016/j.matdes.2017.01.024>

28. Sedlacek, F., Lasova, V.: Additive manufacturing of PA6 with short carbon fibre reinforcement using fused deposition modelling. In: Materials Science Forum, pp. 26–31. Trans Tech Publications Ltd (2018)
29. Justo, J., Távara, L., García-Guzmán, L., París, F.: Characterization of 3D printed long fibre reinforced composites. *Compos. Struct.* **185**, 537–548 (2018). <https://doi.org/10.1016/j.compositstruct.2017.11.052>
30. Prasath, K.A., Arumugaprabu, V., Amuthakkannan, P., Naresh, K., Muthugopal, M.S., Jeganathan, M., Pragadeesh, R.: Quasi static and flexural mechanical property evaluation of basalt/flax reinforced composites. *Mater. Phys. Mech.* **46**, 32–138 (2020)
31. Gebhardt, A., Höller, J.-S.: Additive manufacturing 3D printing for prototyping and manufacturing. Carl Hanser Verlag GmbH Co KG (2018)
32. Prashantha, K., Roger, F.: Multifunctional properties of 3D printed poly(lactic acid)/graphene nanocomposites by fused deposition modeling. *J. Macromol. Sci. Part A Pure Appl. Chem.* **54**, 24–29 (2017). <https://doi.org/10.1080/10601325.2017.1250311>
33. Shanmugam, V., Das, O., Neisiany, R.E., Babu, K., Singh, S., Hedenqvist, M.S., Berto, F., Ramakrishna, S.: Polymer recycling in additive manufacturing: an opportunity for the circular economy. *Mater Circular Economy*. **2**, 11 (2020). <https://doi.org/10.1007/s42824-020-00012-0>
34. Jia, Z., Wang, L.: 3D printing of biomimetic composites with improved fracture toughness. *Acta Mater.* **173**, 61–73 (2019). <https://doi.org/10.1016/j.actamat.2019.04.052>
35. Tiismus, H., Kallaste, A., Belahcen, A., Tarraste, M., Vaimann, T., Rassõlkin, A., Asad, B., Shams Ghahfarokhi, P.: AC Magnetic Loss reduction of SLM processed Fe-Si for additive manufacturing of electrical machines. *Energies* **14**(5), 1241 (2021)
36. Ko, H., Witherell, P., Lu, Y., Kim, S., Rosen, D.W.: Machine learning and knowledge graph-based design rule construction for additive manufacturing. *Addit. Manuf.* **37**, 101620 (2021)
37. Fu, Y.F., Ghabraie, K., Rolfe, B., Wang, Y., Chiu, L.N.: Smooth design of 3D self-supporting topologies using additive manufacturing filter and SEMDOT. *Appl. Sci.* **11**(1), 238 (2021)
38. Ariz, A., Tasneem, I., Bharti, D., Vaish, A., Haleem, A., Javaid, M.: Is additive manufacturing of patient-specific implant is beneficial for orthopedics. *Apollo Med.* **18**(1), 33 (2021)
39. Mirzababaei, S., Paul, B.K., Pasebani, S.: Metal powder recyclability in binder jet additive manufacturing. *JOM* **72**(9), 3070–3079 (2020)
40. Jiang, J., Xu, X., Xiong, Y., Tang, Y., Dong, G., Kim, S.: A novel strategy for multi-part production in additive manufacturing. *Int J Adv Manuf Technol.* **109**(5), 1237–1248 (2020)
41. Sing, S.L., Yeong, W.Y.: Laser powder bed fusion for metal additive manufacturing: perspectives on recent developments. *Virt. Phys. Prototyping*. **15**(3), 359–370 (2020)

Part II

**Additive Manufacturing and Materials
Development**

Chapter 3

Challenges in Additive Manufacturing for Metals and Alloys



**Monsuru Ramoni, Ragavanantham Shanmugam, N. Thangapandian,
and M. Vishnuvarthan**

3.1 Introduction

Additive Manufacturing is a 3D printing technique which commands huge popularity by manufacturing complex and larger structures with less lead time for design and fabrication. Additive Manufacturing allows the material design from various 3D design models for manufacturing rapid prototyping. It has become one of the most promising technologies and is represented as an industrial era [1]. AM is widely used due to optimized manufacturing techniques that offer highly realistic results from computer-generated design and are primed to utilize the parts that consists of even more intricate shape and structures. As shown in Fig. 3.1, the AM landscape is huge and gets bigger every year as new processes are developed for 3D printing of engineering materials such as metal, ceramic, polymer and composites [2]. Metal AM is a process of fabricating parts of a product by successive cross-sectional layering of an object beginning with 3D solid modelling. Metal AM parts are complex in structure and minimum in production but offer the following advantages (Fig. 3.2).

M. Ramoni (✉) · R. Shanmugam (✉)

School of Engineering, Math and Technology, Navajo Technical University, Crownpoint, NM 87313, USA

e-mail: mramoni@navajotech.edu

R. Shanmugam

e-mail: rags@navajotech.edu

N. Thangapandian

Department of Mechanical Engineering, St. Joseph's Institute of Technology, Chennai 600119, India

M. Vishnuvarthan

Department of Printing Technology, College of Engineering Guindy, Anna University, Chennai 600025, India

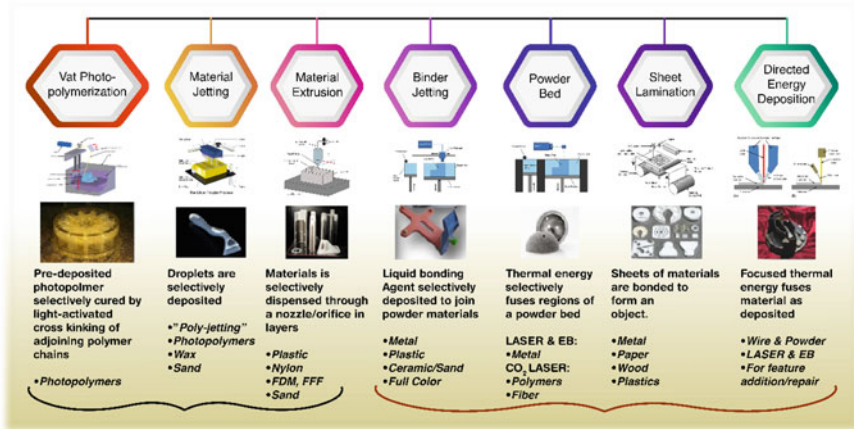


Fig. 3.1 Types of additive manufacturing process



Fig. 3.2 Benefits of additive manufacturing in aerospace and defense industries

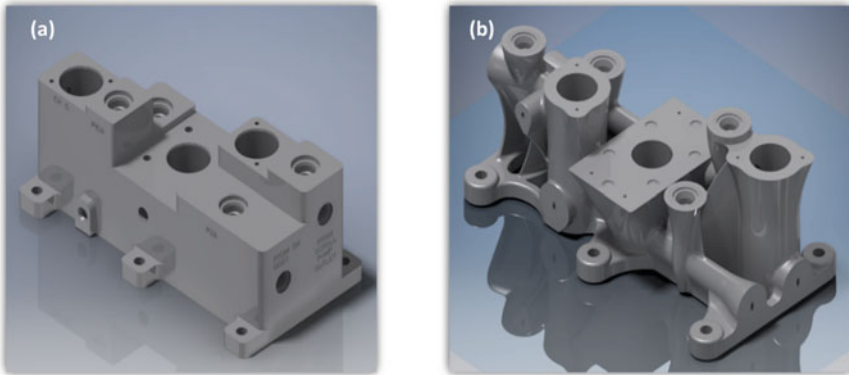


Fig. 3.3 Weight saving in metal additive manufacturing **a** Existing design; **b** Design for AM

Design flexibility which has the ability to design a complex geometry shapes, reduced costs of geometric complexity due to minimal wastage of prototyping material, Efficiency of production timing and production cost, features that could not be fabricated by other, near net-shape complex geometry, product properties are better than casting process, 10–15% below wrought. As shown in Fig. 3.3, alternative Purge Pump Manifold was re-designed to be lighter. Printed in Titanium with a reduction of 12–6.7 lbs, 35% of weight savings.

Despite these potentials of metal AM, it is generally limited to weldable alloys and also hindered by the following issues; limits in size, minimum size of the hole, surface overhanging, imperfect surface roughness, postprocessing of built microstructure, generation of waste, failed parts and more cost than conventional manufacturing process [1, 2].

3.2 Comparison of Metal Additive Manufacturing Processes

AM processes are classified in terms of material feeding system, types of energy source, product volume, etc., The manufacturing systems are classified into three major types such as (1) Powder Feed System, (2) Powder Bed System and (3) Wire Feed System based on the feed system. Selection of suitable AM process from the different processes as mentioned above depends on the cost of production, surface quality and the place of application. These different processes are compared in the terms of feature of the build and printing rate as shown in Fig. 3.4.

Among the metal AM methods, the most used are Directed Energy Deposition (DED) and Laser Powder Bed Fusion (LPBF) process. The both processes are change in various features such as the conditions of processing, rate of deposition, part

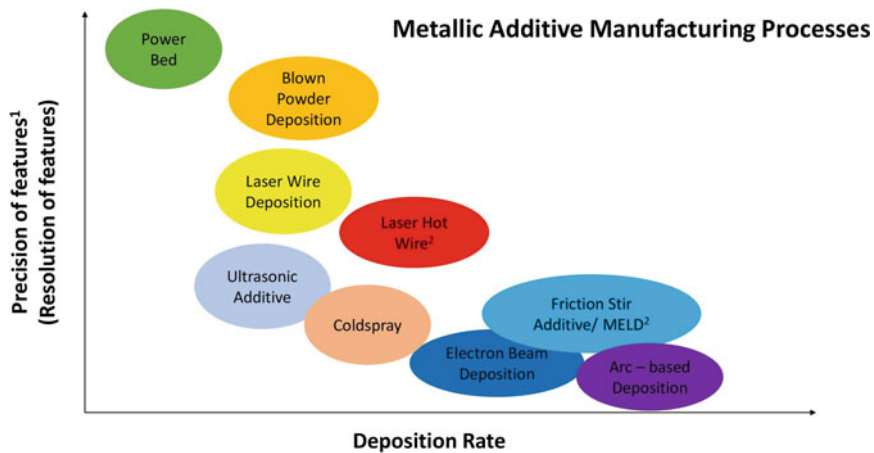


Fig. 3.4 Comparison of metallic additive manufacturing processes

outputs and part resolution. The material deposition approach for the above techniques is important for various computational treatments and also for modeling. In powder bed fusion, the process presents a powder layer on the earlier deposited material [3]. But in DED, the input material interconnect with heat source before the physical contact. This difference makes the powder bed fusion process more complex and it is very important to alter the properties of material in its powder form itself. On the other side, the DED processes uses a gas to transmit the metallic powder which is a great challenge. Even though, in DED, the deposited material melts directly on the substrate. Hardware scale, material complexity, process speed, cost, properties of materials, availability, geometry of material are some of the issues related to metal additive manufacturing process [4] (Fig. 3.5).

3.3 Printable Metals and Alloys for Metal AM

Printability is commonly used in AM processing of metals and alloys which has the ability to convert the material feedstock into a bulk material by deposition to meet the required functional performance for a specific application [5]. It is totally depending on the metals, alloy properties and printing processes. The printability of the materials differs with materials properties and various thermal and processing conditions of the specific AM processes. Below are some of the materials that have shown printability for metal additive manufacturing (Fig. 3.6).

Laser Powder Bed Fusion (L - PBF)		Directed Energy Deposition (DED)
Features Resolution / Complexity	High resolution of features Wall Thickness and holes <0.010"	+ Medium resolution of features Walls>0.040" and limited holes
Deposition Rate	Low build rates <0.3 lb/hr	+ High Build rates lbs per hour (some systems>20lb/hr)
Multi-alloys / Gradient Materials	Monolithic materials in single build	Option for multi-alloys or gradients within single build
Materials Available	High number of materials available and being developed	+ High number of materials available and being developed
Production Rates	High volume with several parts in a single build	+ Generally limited to single builds: longer programming/setup time
Scale / Size of components	Limited to existing build volumes <15.6" dia or 16"x24"x19"	+ Scale is limited to gantry or robot size
Added Features / Repair	No (limited) ability to add material to existing part	+ Can add materials or features to an existing part

Fig. 3.5 Metallic additive manufacturing process

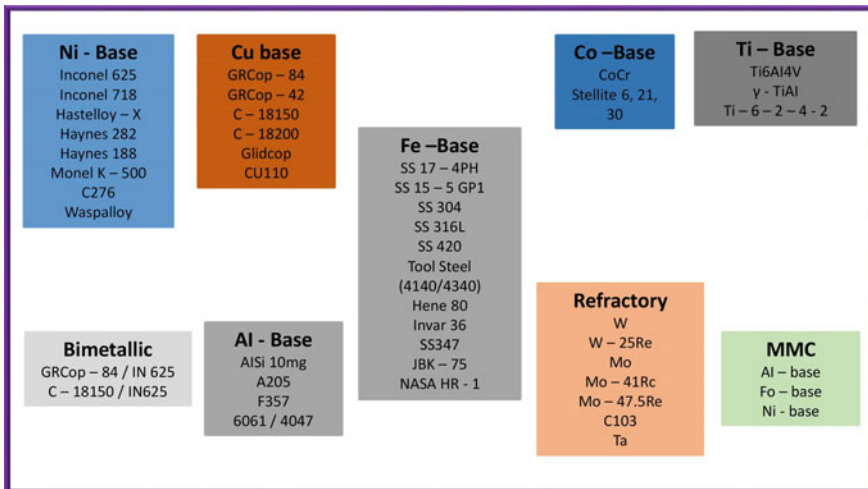


Fig. 3.6 Metals for additive manufacturing process

3.4 Challenges of Metal Additive Manufacturing

There are different issues that are hindering the widespread adoption of metal AM. The issues categorized into three folds- scientific, technological, and economic (Fig. 3.7).

For the paper, the focus will be on the issues related science of AM technology. It affects their performance in applications use. Thermal history (Fig. 3.8) is central to issues affecting additive manufactured parts, ranging from physics-based process optimization, monitoring and control, and prediction of part functional properties.

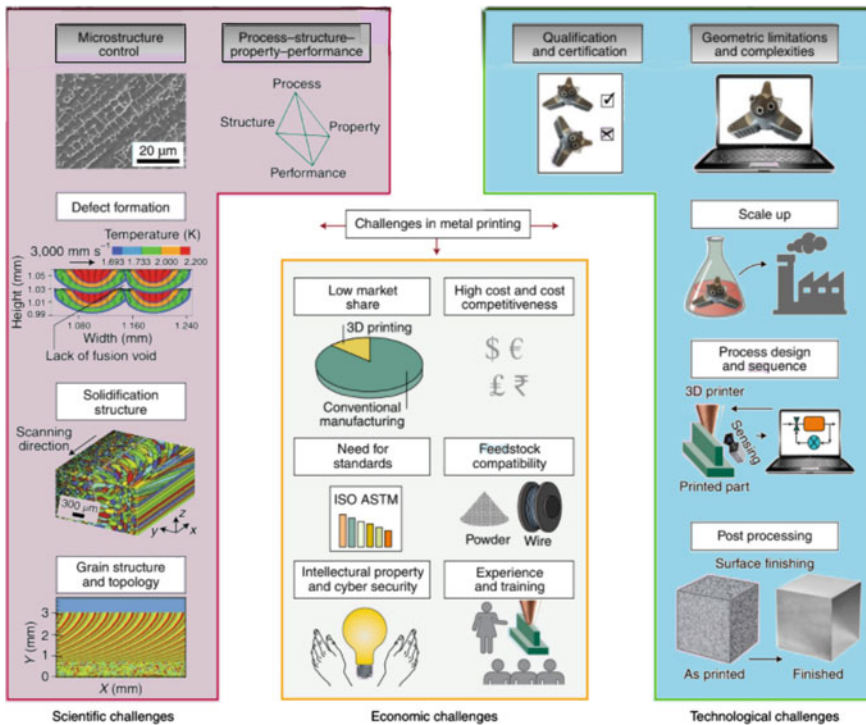


Fig. 3.7 Challenges of additive manufacturing process

As compared to the casting quick cooling of product and contiguous gradients of temperature provide to the product intricacy of microstructures [6]. The parts printed by metals and alloys frequently shows element segregation, high dislocation density, smooth solidification structures and grain elongation. To achieve the proper microstructure and properties of the printed part, it is necessary to understand the basic parameters for controlling the evolution of microstructures [7].

3.4.1 Anisotropic Behavior and Mechanical Properties

Anisotropic behavior is the biggest challenge in the additive manufacturing. Due to the printing method of layer by layer, the microstructure of individual layer's internal material at the boundary between the layers and anisotropic behavior leads to differences [9]. Compare the mechanical properties of AM parts, it is good in horizontal direction. In the AM of metals and alloys, the process by hot metal (Selective Laser Sintering or Selective Laser Melting) and the inclusion of following layers will reheat the already deposited prior layers. It leads to different grain microstructures and anisotropic behavior. Thermal gradient is important that the laser beam heat

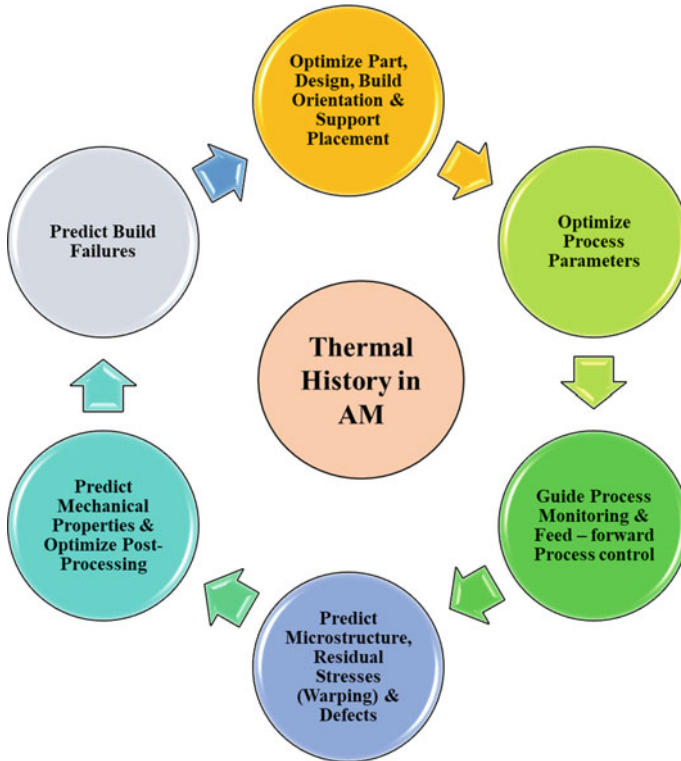


Fig. 3.8 Thermal history in metal additive manufacturing, processes and microstructure [8]

penetrates each layer. These are the factors control the sintering process and also limit the material anisotropic behavior [10]. During the metal parts AM process, the alloys face multi heating, material melting, solidification of material and the part cooling.

The eternal distortion in various places of the product may takes place and it totally depends on the part rigidity, thermo physical properties of materials and temporary temperature area [11]. For metal additive manufacturing process, it is necessary to understand the process of printing, alloy capability to endure distortion, absence of fusion flaws and change of composition [12]. There is very limited knowledge of defects in Metal AM. The insufficient diffusion of upper layer molten pool into the substrate or to the prior layer cause the defect of lack of fusion. It also creates the voids in the final part which have the diameter greater than $10 \mu\text{m}$. The gas entrapment during powder particles atomization and the deposit shape also created the voids [13]. As compared to lens shape, the omega shaped deposit generates more inter layer porosity. The oxidation of materials, dissolved gases and absorption of surface moisture are also responsible for the macro and micro pores. The depth of penetration depends on the various physical properties of alloy and metal powder. It

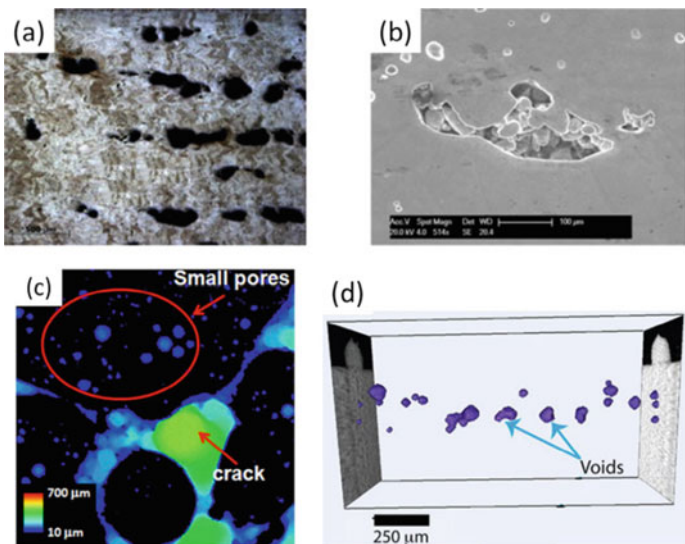


Fig. 3.9 Metal additive manufacturing defects—porosity and lack of fusion

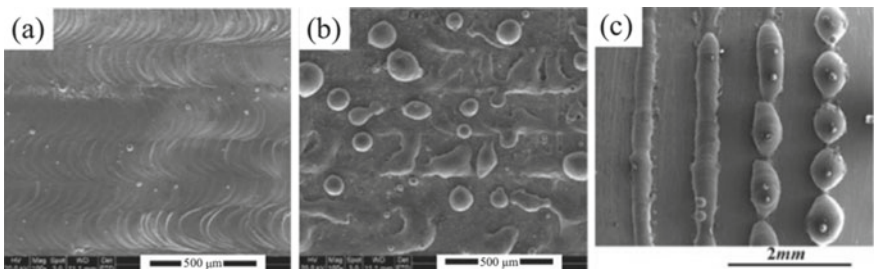


Fig. 3.10 Balling phenomenon defect in metal AM resulting **a** Oxygen **b** Thickness of layer **c** Speed of scanning

also depends on the speed of scanning, power of laser and method of deposition [14]. However, the penetration depth is varied for various alloys in AM process (Figs. 3.9 and 3.10; Table 3.1).

3.4.2 Material Heterogeneity and Structural Reliability

Material heterogeneity is known as the quality or state of consisting of dissimilar or diverse elements in which structural reliability is the capability of a structure to operate without failure when put into service. Consumer goods are made by various materials which have different behaviors and functions and material selection. The

Table 3.1 Defects in metal AM at different scales

Compositional scale	Micro	Macro
Evaporative loss	Grain size	Un melted material Lack of fusion
Interstitial getting	Precipitates	Hot tearing
Reduced partitioning		Porosity Residual stress Texture

function of additive manufacturing system is very limited. Product generation troubles of advanced AM system anisotropic mechanical properties are caused by inter-layer bonding effects [15]. In addition, most additive manufacturing systems process only one material once. Multi-material additive manufacturing systems make functional graded materials continue to emerge in polymers and metals. Due to uncertainty, the adoption of these systems is restricted along with the behavior of the physical interface and lack of design software support. Furthermore, existing commercial software packages cannot make it easy for designers to model or analyze the geometry of multiple materials and their concomitant anisotropy [16].

3.4.3 ***Void Formation***

Void formation is a formation of pores that remain unfilled with polymer and fibers in a composite material. The main problem of AM is the void formation between the printed layers. It leads to the porosity problem which can decrease the mechanical properties because of reduced interface bonding between the layers [17]. The void formation degree is totally depending on the method of printing and the printing source material. The void formation is very frequent defect in AM part caused the poorer mechanical properties and anisotropic behavior.

3.4.4 ***Difficulty in Powder Preparation, Powder Splash, Crack Formation, Porosity***

The biodegradable metallic materials used in biomedical applications especially in orthopedic areas have drawn attention due to their exceptional combination properties of mechanical and biodegradability [18]. In the biodegradable metallic materials, Magnesium (Mg) and its alloys have been extensively investigated and explored clinically [19]. The preparation of magnesium powder is very dangerous because of its high tendency to explode. Mechanical crushing, molten metal atomization, evaporation, condensation, and electrolysis are the basic methods for the magnesium

powder preparation [19]. This powder is prepared by gas atomization process because the size of powder used for bio implants are in the range of 20–70 μm [20]. The additive manufacturing of implants made of magnesium and alloys presents some challenges because decrease in vapor temperature, increase in vapor pressure and oxidation. In the magnesium and alloy AM process, the powder splash problem is noted. This reduces the stability of Mg alloys production. During the process some of the magnesium powders and are eliminated by vapor at the time of scanning and imperfections are generated during the scanning path. To solve this issue, an add-on powder strategy must be applied. Reducing the Mg powder vapor trend is also another solution [21].

The formation of cracks during the additive manufacturing process happens occasionally. Still there is no solid evidence for the formation of cracks but it could possibly be due to the powder splash and the presence of porosity. The crack formation reduces with a reduction in powder splash under the input of low energy. In the processing of aluminum alloys, the cracking was classified into solidification cracking and liquation. Solidification cracking occurs at the final stage caused by inadequate flow of liquid [22]. The liquation is caused in the selective melting processed parts as heat is applied.

The most common defect in the additive manufacturing of alloy is porosity mostly in the laser process. The gas pores, shrinkage pores and fusion errors are the pore types. The main aspects related to the formation of porosity are hot cracking, speed of scanning, scanning technology and the gas used for protection [23]. The common pores formed in SLM process are metallurgical and keyhole pores. The gas bubbles trapped under the surface of part after the scan. The fast laser scanning speeds are responsible for keyhole pores and the slow laser scanning speeds are responsible for metallurgical pores [24]. Improper adhesion between printed layers and the incomplete melting of alloy powders can cause other types of pores [25]. The higher porosity in AM part can be eliminated by following ways: The control of porosity is the biggest advantage in the area of scaffold design in tissue engineering. Utilizing the reason for the void formation in AM process is because it introduces higher pores into the structure of lattice at higher level and the microstructure in the foam yarn created by the bubbles [26]. The increase in moisture absorption caused the higher porosity in the AM of bio composites. The thermal distortion in AM parts created the dimensional inaccuracy because of improper expansion and reduction in various places of the part due to temperature change [27]. Thermal variation during the AM process depends on the properties of alloy, input temperature, time of deposition, dimension of the part, geometry of the part, difference in time between layer deposition and other parameters [28].

3.4.5 Stair Stepping, Dimensional Inaccuracy, Generation of Balling, Evaporation of Volatile Elements

The presence of staircase effect in the printed parts is also the biggest challenge in additive manufacturing process. The staircase effect is commonly appearing and is not important for the fabrication of internal surfaces. But the staircase problem totally affects the property and quality of external surfaces. It can be overcome by possible post processing methods like sand sintering, but it increases the overall process cost and time [29]. The evaporation of volatile elements from alloy composition is one of the major challenges in additive manufacturing process. Most of the alloys contain some amounts of volatile elements. It may vaporize at high temperature during the AM process. However, some alloys are having chances to vaporize which cause the change in chemical composition [30].

When high power density is applied in alloy composition, the evaporation of elements in alloys may occur and it is due to the lower melting points of those elements as compared to base metal. The changes in alloy compositions can change the mechanical properties and corrosion resistance [31]. When the difference in surface tension occurs in additive manufacturing process, the liquid metal may shrink into spherical geometry and the contact with substrate is not good. The formation of sphere is termed as balling [32]. Because of the poor surface contact, rough surfaces in the part can occurred on the layers after solidification. This leads to the poor quality of part. Balling problem is commonly related to melting and sintering. Powder splashing and low wettability can also cause balling. Balling is to be suppressed by maintaining the sufficient melting level in the lower melt pool.

3.5 Wear Failure in AM Products

Though AM processes have advantages, cost of production, defects and wear failure cause a second-thought in implementing this process in industries. Numerous researchers have attempted to analyze the structure vs strength relationship in the different additive manufacturing process, but a very meagre amount of research have been attempted on the wear properties. This is due to the restrictions in AM product size and the place of application which are not the same as conventional manufacturing process. Comparing the tribological behavior of the developed products via AM process with the conventional manufacturing processes is essential for the efficient usage of AM process for particular applications.

The particles discharged due to wear acts as the lubricants in the application of smaller loads, since the wear rate is low in AM samples. It can be distinguished that the increasing load adversely affects the surface. The worn-out particles pile up in the wear track and cause severe damage to the surface. But when compared to the conventionally cold rolled SS 316 L, additive manufactured sample exhibits superior tribological properties [33] (Fig. 3.11).

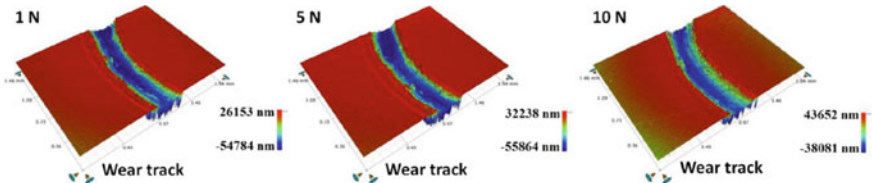


Fig. 3.11 Worn Out Surface of SS 316L Produced by L-PBF at Different Loads [33]

The wear performance of the electron beam based additively manufactured product was superior to that of the laser beam AM products. Since, Electron beam AM samples do not need any stress relieving techniques, since it works in a vacuum environment. Preheating of samples occurs before the melting phase in Electron beam AM processes, which reduces the thermal gradient [34]. Moreover, the High Angle Grain boundary (HAGB) fraction is dominant in the Electron beam AM samples, due to the dislocation annihilation and increase in secondary phase particles. The materials with higher HAGB fraction effectively resist the applied wear, due to the dislocation pile-up. However, the electron-based systems are expensive when compared to others.

The different AM processes produces almost same micro structured samples, whereas the processing parameters and initial powder/particle properties decides the mechanical properties. The porosity can be decided by selecting the laser power supply. Both the powder based additively manufactured products properties are affected by the particle's properties such as sphericity, size, density, composition and melting point. For example, the sphericity of the particle is very essential for the improved strength of the final product. Moreover, the porosity can also be reduced with the usage of spherical powders [35].

The hip stem of Ti-6Al-4 V with different % of porosity has been fabricated with LENS and is shown in Fig. 3.9 [36]. The porosity will help in extending the life of implants by reducing wear induced bone loss and good adherence between the implants and tissues (Fig. 3.12).

Interestingly, the formation oxidization layer and its effects on the wear improvement have been discussed in the surface and wear property comparison of wrought Ti-6Al-4 V and LENS process Ti-6Al-4 V [37]. The increase in hardness is due to the rapid cooling is the main reason for improved wear resistant. Among the three AM (L-PBF, WAAM and LENS) processes, the SLM or L-PBF process has the lowest Linear Energy Density (LED). The wear resistance and the final microstructure can be related. Due to this and because of the finer and uniform microstructure, SLM process showed improved wear resistant properties than the other two processes [38].

Relating the AM process under one canopy is quite difficult, since the usage of AM processes depends on the application and material used. Still, a comparison was attempted with respect to the wear properties of the different metal Additive Manufacturing processes. This comparison will be helpful in understanding the process parameters such as laser power and laser speed with respect to the wear characteristics. Most of the AM processes have been used for the wear resistant applications

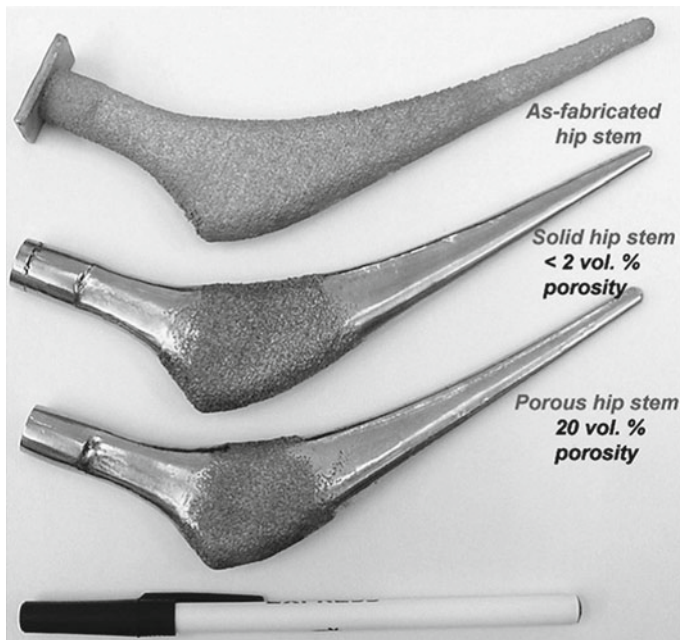


Fig. 3.12 Hip stems with tailored porosity for improved wear resistant by LENS [36]

such as bio-implants, aerospace and defense. Understanding the wear characteristics of the different AM processes will be a real challenge for the researchers. The proper selection of the suitable processes and process parameters results in better wear resistance.

3.6 Conclusion

The advantages of additive manufacturing techniques are design freedom, mass customization, minimum waste, material savings. These attributes make the usage of AM in automobile, aerospace, biomedical, construction and other engineering industries a sheer necessity. A complete analysis of additive manufacturing process methods, materials and progress in various applications was discussed. The main challenges related to the AM process of metals and alloys were also discussed.

There are few challenges in additive manufacturing of metals and alloys that need more research and development to use this technology without any flaws. Formation of voids between the layers results in further formation of porosity which reduces the mechanical properties due to the decrease in interfacial bonding between printed layers. Anisotropic behavior is also the challenge in additive manufacturing which gives dissimilar mechanical and other properties. The powder preparation for various

metals and alloy implants are very difficult because of decrease in vapor temperature and increase in vapor pressure. The alloys powder stability is reduced because of powder splash and it can be avoided by reducing the vapor trend of powder. The transferring of design model into printed part frequently leads to the defects, particularly on part bent surfaces because of CAD tessellation concept. The formation of cracks could be avoided by proper solidification process. Improper adhesion, fast scanning and gas trapping are the main causes of pore formation in the AM product. The layer-by-layer appearance in applications is not a good choice. The stair stepping can be avoided by sand sintering and the printing of small volume of scaled parts should be avoided. The evaporation of volatile elements is the biggest challenge in the process of alloys, and it can be minimized by proper basic understanding of materials used in alloys. The generation of balling and satellite is due to the difference in surface tension and trapping of particles in the surface. Illegal usage should be restricted, and safety standards are to be followed with rules and regulations. Therefore, further research and development is needed in the additive manufacturing on metals and alloys to reach defect free printed parts.

References

1. Abdulhameed, O., Al-ahmari, A., Ameen, W., Mian, S.H.: Additive manufacturing: challenges, trends applications **11**, 1–27 (2019). <https://doi.org/10.1177/1687814018822880>
2. Alt, S.C., Yardley, V.A., Shi, Z., Lin, J.: Challenges in additive manufacturing of high-strength aluminium alloys and current developments in hybrid additive manufacturing **4** (2021). <https://doi.org/10.1016/j.ijlamm.2020.12.004>
3. Arcos, PDe, Birkelandsvei, R.: ScienceDirect Structural ScienceDirect - Loading of and Additively Environmental Manufactured effects on Structural Inconel Integrity 718 Fatigue Behaviour Produced Selective Manufactured Laser Melting. Fatigue Behaviour of by Additively Pr. Procedia Struct. Integr. **13**, 1762–1767 (2018). <https://doi.org/10.1016/j.prostr.2018.12.371>
4. Bala, M., Klob, D., Pambaguiyan, L., Conradi, M., Kocijan, A.: Materials Characterization Hybrid additive manufacturing of Inconel 718 for future space applications **172** (2021). <https://doi.org/10.1016/j.matchar.2020.110842>
5. Brinksmeier, E., Karpuschewski, B., Yan, J., Sch, L.: CIRP annals—manufacturing technology manufacturing of multiscale structured surfaces **69** (2020). <https://doi.org/10.1016/j.cirp.2020.06.001>
6. Javidani, M., Arreguin-Zavala, J., Danovitch, J., Tian, Y., Brochu, M.: Additive manufacturing of alsi10mg alloy using direct energy deposition: microstructure and hardness characterization. J. Therm. Spray Technol. **26**, 587–597 (2016). <https://doi.org/10.1007/s11666-016-0495-4>
7. Cruzado, A., Gan, B., Jiménez, M., Barba, D., Ostolaza, K., Linaza, A., Molina-aldareguia, J.M., Llorca, J., Segurado, J.: Acta Materialia Multiscale modeling of the mechanical behavior of IN718 superalloy based on micropillar compression and computational homogenization Carbides γ' phases δ phases 20 μm . ACTA Mater. **98**, 242–253 (2015). <https://doi.org/10.1016/j.actamat.2015.07.006>
8. Reza Yavari, M., Williams, R.J., Cole, K.D., Hooper, P.A., Rao, P.: Thermal modeling in metal additive manufacturing using graph theory: experimental validation with laser powder bed fusion using in situ infrared thermography data. J. Manuf. Sci Eng. **142**, 12 (2020)

9. Elkhatib, M.G., Shin, Y.C.: Analysis of the effects of microstructure heterogeneity on the mechanical behavior of additively manufactured Ti6Al4V using mechanics of structure genome. *Mater. Des.* **204**, 109643 (2021). <https://doi.org/10.1016/j.matdes.2021.109643>
10. Ford, S.: Additive manufacturing and sustainability: an exploratory study of the advantages and challenges **137** (2016). <https://doi.org/10.1016/j.jclepro.2016.04.150>
11. Gao, J., Chen, S., Liu, T., Ye, J., Liu, J.: Additive manufacture of low melting point metal porous materials: Capabilities, potential applications and challenges. *Mater. Today*. xxx, 1–30 (2021). <https://doi.org/10.1016/j.mattod.2021.03.019>
12. Gu, D., Ma, C., Xia, M., Dai, D., Shi, Q.: A Multiscale understanding of the thermodynamic and kinetic mechanisms of laser additive manufacturing. *Engineering* **3**, 675–684 (2017). <https://doi.org/10.1016/J.ENG.2017.05.011>
13. Guessasma, S., Zhang, W., Zhu, J., Belhabib, S., Nouri, H.: Challenges of additive manufacturing technologies from an optimisation perspective. (2016). <https://doi.org/10.1051/smdo/2016001>
14. Kumar, M.B., Sathiya, P.: Thin-walled structures methods and materials for additive manufacturing: a critical review on advancements and challenges. *Thin-Walled Struct.* **159**, 107228 (2021). <https://doi.org/10.1016/j.tws.2020.107228>
15. Ngo, T.D., Kashani, A., Imbalzano, G., Nguyen, K.T.Q., Hui, D.: Additive manufacturing (3D printing): a review of materials, methods, applications and challenges. *Compos. Part B*. (2018). <https://doi.org/10.1016/j.compositesb.2018.02.012>
16. Picard, M., Misra, M.: Engineering thermoplastics: challenges and. *Royal Soc. Chem.* (2020)
17. Tiismus, H., Kallaste, A., Belahcen, A., Member, S., Rassölklin, A., Vaimann, T.: Challenges of additive manufacturing of electrical machines, 44–48 (2019)
18. Staiger, M.P., Pietak, A.M., Huadmai, J., Dias, G.: Magnesium and its alloys as orthopedic biomaterials: a review. *Biomaterials* **27**, 1728–1734 (2006). <https://doi.org/10.1016/j.biomaterials.2005.10.003>
19. Ding, D., Shen, C., Pan, Z., Cuiuri, D., Li, H., Larkin, N., Van Duin, S.: Towards an automated robotic arc-welding-based additive manufacturing system from CAD to finished part. *CAD Comput. Aided Des.* **73**, 66–75 (2016). <https://doi.org/10.1016/j.cad.2015.12.003>
20. Zumnick, N.A., Jauer, L., Kersting, L.C., Kutz, T.N., Schleifenbaum, J.H., Zander, D.: Additive manufactured WE43 magnesium: a comparative study of the microstructure and mechanical properties with those of powder extruded and as-cast WE43. *Mater. Charact.* **147**, 384–397 (2019). <https://doi.org/10.1016/j.matchar.2018.11.011>
21. A.M., Koumoulos, E.P., Bandyopadhyay, A., Bose, S., Donoghue, L.O., Charitidis, C.: Additive manufacturing : scientific and technological challenges , market uptake and opportunities. *Biochem. Pharmacol.* **00**, 1–16 (2017). <https://doi.org/10.1016/j.mattod.2017.07.001>
22. Wang, Y., Fu, P., Wang, N., Peng, L., Kang, B., Zeng, H., Yuan, G., Ding, W.: Challenges and solutions for the additive manufacturing of biodegradable magnesium implants. *Engineering* **6**, 1267–1275 (2020). <https://doi.org/10.1016/j.eng.2020.02.015>
23. Xiao, K., Zardawi, F., Van Noort, R., Yates, J.M.: Developing a 3D colour image reproduction system for additive manufacturing of facial prostheses. *Int. J. Adv. Manuf. Technol.* **70**, 2043–2049 (2014). <https://doi.org/10.1007/s00170-013-5448-1>
24. Gu, D.D., Meiners, W., Wissenbach, K., Poprawe, R.: Laser additive manufacturing of metallic components: materials, processes and mechanisms. *Int. Mater. Rev.* **57**, 133–164 (2012). <https://doi.org/10.1179/1743280411Y.0000000014>
25. Kaufmann, N., Imran, M., Wischeropp, T.M., Emmelmann, C., Siddique, S., Walther, F.: Influence of process parameters on the quality of aluminium alloy en AW 7075 using selective laser melting (SLM). *Phys. Procedia*. **83**, 918–926 (2016). <https://doi.org/10.1016/j.phpro.2016.08.096>
26. Wei, H.L., Mukherjee, T., Zhang, W., Zuback, J.S., Knapp, G.L., De, A.: Progress in materials science mechanistic models for additive manufacturing of metallic components **116** (2021). <https://doi.org/10.1016/j.pmatsci.2020.100703>
27. Oropallo, W., Piegl, L.A.: Ten challenges in 3D printing. *Eng. Comput.* **32**, 135–148 (2016). <https://doi.org/10.1007/s00366-015-0407-0>

28. Govdeli, Y., Wong, Z.W., Kayacan, E.: Additive manufacturing of unmanned aerial vehicles: current status, recent advances, and future perspectives. *Proc. Int. Conf. Prog. Addit. Manuf. Part F129095*, 39–48 (2016)
29. Horgar, A., Fostervoll, H., Nyhus, B., Ren, X., Eriksson, M., Akselsen, O.M.: Additive manufacturing using WAAM with AA5183 wire. *J. Mater. Process. Technol.* **259**, 68–74 (2018). <https://doi.org/10.1016/j.jmatprotec.2018.04.014>
30. Gu, D., Wang, H., Chang, F., Dai, D., Yuan, P., Hagedorn, Y.C., Meiners, W.: Selective laser melting additive manufacturing of TiC/AlSi10Mg bulk-form nanocomposites with tailored microstructures and properties. *Phys. Procedia* **56**, 108–116 (2014). <https://doi.org/10.1016/j.phpro.2014.08.153>
31. Wu, D., Liu, D., Niu, F., Miao, Q., Zhao, K., Tang, B., Bi, G., Ma, G.: Al–Cu alloy fabricated by novel laser-tungsten inert gas hybrid additive manufacturing. *Addit. Manuf.* **32**, 100954 (2020). <https://doi.org/10.1016/j.addma.2019.100954>
32. Yadroitsev, I., Krakhmalev, P., Yadroitsava, I., Johansson, S., Smurov, I.: Energy input effect on morphology and microstructure of selective laser melting single track from metallic powder. *J. Mater. Process. Technol.* **213**, 606–613 (2013). <https://doi.org/10.1016/j.jmatprotec.2012.11.014>
33. Upadhyay, R.K., Kumar, A.: Scratch and wear resistance of additive manufactured 316L stainless steel sample fabricated by laser powder bed fusion technique, *Wear* 458–459, 1–17
34. Galati, M., Iuliano, L.: A literature review of powder-based electron beam melting focusing on numerical simulations. *Add. Manuf.* **19**, 1–20 (2018)
35. Niu, H.J., Chang, I.T.H.: Selective laser sintering of gas and water atomized high speed steel powders. *Scripta Mater.* **41**(1), 25–30 (1999)
36. Espana, F.A., Balla, V.K., Bose, S., Bandyopadhyay, A.: Design and fabrication of CoCrMo alloy based novel structures for load bearing implants using laser engineered net shaping. *Mater. Sci. & Engg. C* **30**(1), 50–57 (2010)
37. Azarniya, A., Colera, X.G., Mirzaali, M.J., Sovizi, S., Bartolomeu, F., Wits, W.W., Yap, C.Y., Ahn, J., Miranda, G., Silva, F.S. and Hosseini, H.R.M.: Additive manufacturing of Ti–6Al–4V parts through laser metal deposition (LMD): process, microstructure, and mechanical properties. *J. Alloys Compounds* **804** 163–191 (2019)
38. Attar, H., Birmingham, M.J., Ehtemam-Haghighe, S., Dehghan-Manshadi, A., Kenta, D., Dargusch, M.S.: Evaluation of the mechanical and wear properties of titanium produced by three different additive manufacturing methods for biomedical application. *Mater. Sci. Engg. A* **760**, 339–345 (2019)
39. Marianne, M., King, E., Jon, N., Allan, C., Neil, N., Kyle, C., Scot, T., John, W., Wiel, V., Alan, S., Jean, A., William, M.: Modeling of additive manufacturing processes for metals: challenges and opportunities disclaimer: modeling of additive manufacturing processes for metals: challenges and opportunities. *Curr. Opin. Solid State Mater. Sci.* 24513 (2017). <https://doi.org/10.1016/j.cossms.2016.12.001>

Chapter 4

Laser Additive Manufacturing of Aluminium Matrix Composites



P. S. Samuel Ratna Kumar and P. M. Mashinini

4.1 Introduction

Aluminium alloys are used in aerospace, automotive, and military applications due to their low density, high specific strength, and corrosion resistance [1–3]. Aluminium alloys, on the other hand, have drawbacks including weak electrical conductivity, a high thermal expansion coefficient, and low resistance to wear [4–6]. Aluminium metal matrix composites (AMMC) are a revolutionary aluminium alloy alternative that exhibits excellent basic stiffness, exceptional wear resistance, structural stability, and physical characteristics, attracting the interest of researchers in a variety of industries [6–10]. Particle reinforced aluminium composites, which combine good strength, thermal properties, durability, and isotropy, are developed in a number of different ways and are widely used on the structural parts. In the literature, different variants of reinforcements and matrix materials have been identified, with the emphasis on aluminium metal matrix composites and the most commonly used reinforcement materials such as carbides, oxides and nitrides [11–14]. AMMC have immense potential in both basic research and commercial product developments [15].

Conventional manufacturing processes are usually multistage, with the first phase associated with rough component production and subsequent phases associated with material removal processes. It may not be cost-effective to make a rough metallic component out of the raw material and then remove the majority of its volume eventually. Furthermore, different phases of production are often carried out in different places, causing logistical problems and increased energy usage. Additive manufacturing (AM) techniques, from the other hand, can create fully functioning components in a single process with minimal material wastage. AM techniques also offer design engineers wider flexibility in developing geometrically complex concepts without

P. S. Samuel Ratna Kumar (✉) · P. M. Mashinini
Department of Mechanical and Industrial Engineering Technology, University of Johannesburg,
Doornfontein Campus, Johannesburg, South Africa

needing to worry about manufacturing process. According to the Wohlers study in 2019 [16], metal-based AM revenues has been growing at a rate of more than 40% per year for the previous five years. It also predicts that perhaps the total AM industry economy will grow to \$23.9 billion by 2022 and \$35.6 billion by 2024. Manufacturing sector has become more conscious of such advantages of using additive manufacturing processes to create metal components. Laser based AM technologies have received a lot of interest from academic and industrial researchers in the last three decades. These have become recognized as more relevant manufacturing techniques with expanding application niches. A standard laser-based AM technique uses laser beam to fabricate a component layer-by-layer blending metal powders depending on sliced 3D digital information comprising the geometric model [16]. Several different terms have been used (as per ASTM Standard F2792) for quite common additive manufacturing techniques due to the business practices of different companies in the additive manufacturing industry. Directed energy deposition (DED) is the primary type, that whatever materials are fused using targeted thermal energy starting to melt the materials when they are deposited. Laser engineered net shaping (LENS) and laser metal deposition (LMD) are two names for DED. The benefits of DED-type additive manufacturing include a rapid production rate, adaptable powder pattern, as well as the capabilities to deposit on curvatures, among others. Powder bed fusion (PBF) is the secondary method, which the heat energy is used to randomly fuse powder type material in a bed. SLS (selective laser sintering), DMLS (direct metal laser sintering), and SLM (selective laser melting) these are the examples of PBF [17]. Accuracy rate, dimensional stability, and mostly excellent mechanical strength are among the key benefits of PBF. These benefits are widely due to the limited laser focus zone as well as the fine surface morphology and high resolution that results [18].

Laser additive manufacturing (LAM) can achieve quick closest shapes and complete densification of high-performance metal components, thanks to its high energy output, increased processing efficiency, short processing period, and tailored output [19]. AMMC materials developed by LAM are being collected in a short span of time with optimum conditions precision and easily controlled physical characteristics by combining the benefits of aluminium alloy, metal matrix composite materials, additive manufacturing techniques and laser. In addition, novel functional material for various sectors can be created, by altering the form of aluminium alloy, the sort of reinforced material, as well as the energy density of laser. The surface morphology of AMMC is entirely optimized using aggressive fusion of materials, and the resulting parts have incredibly fine grains and mechanical characteristics that are substantially greater than those of LAM processed aluminium alloy and AMMC prepared using conventional methods. Laser processing of aluminium nanocomposite materials (ANC) deposits aluminium reinforced by coarse dispersed nanomaterials layers of material, increasing laser absorption by nearly one order of magnitude over pure aluminium powders. A higher concentration of well-dispersed nanomaterials, better interfacial interaction between nanomaterials and aluminium matrix material, and ultra-fine grain boundaries are responsible for the high efficiency [20]. This Chapter is focusing on the existing research condition and production of LAM

processed AMMC and ANC. To gain a better understanding of AMMC and ANC LAM technologies using PBF method, mechanical properties and its strengthening mechanisms are discussed.

4.2 Methods for Preparing AMMC

The perfect metal matrix composite powder particles have a homogeneous distribution of elements and good fluidity. Ball-milling, electrostatic self-assembly and in-situ process formulation have all been used to prepare composite materials in powder form. The most popular method of mixing composite material is ball-milling as shown in Fig. 4.1. Inside a ball-milling container, blended powders and strong mixing metal balls are placed. The metal powders in between hard balls are fused

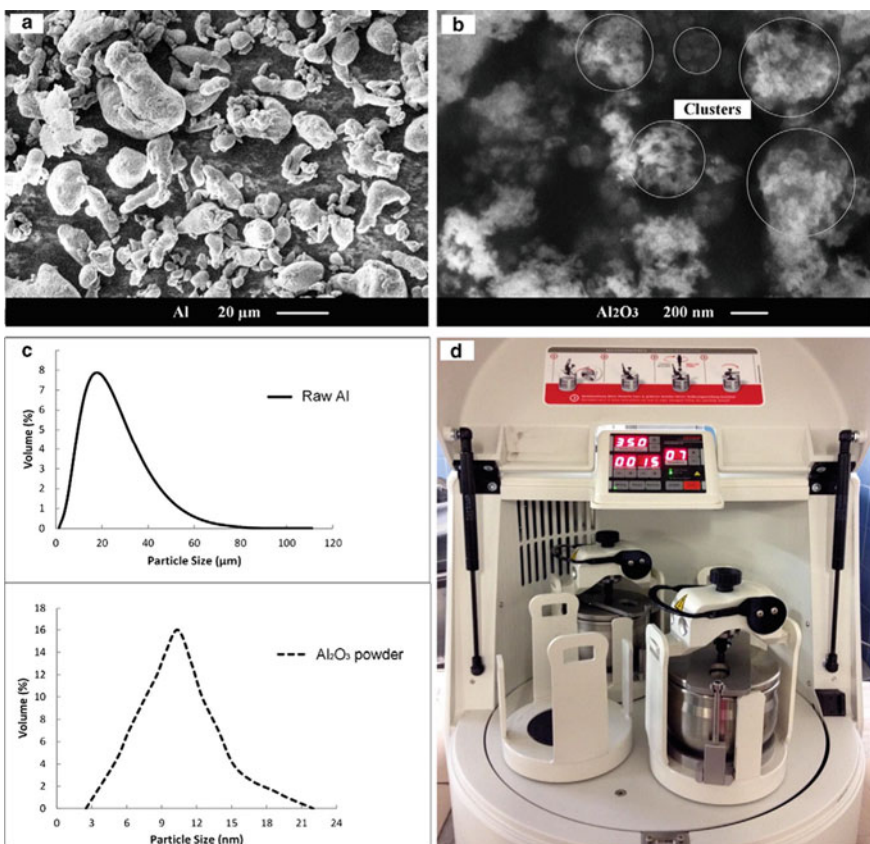


Fig. 4.1 Image of Ball-milling process and material size distribution data [21]

during the mixing process when the balls interact. By changing the ball-milling process parameters, it can achieve a variety of mixing results [21, 22].

Moreover, the spherical powder mobility is decreased, and the aluminium powder surface is susceptible to oxidation, influencing the processability of LAM samples. The powder electrostatic self-assembly method involves making the dual powders contain opposite charges. So that they can be combined equally under electrostatic interaction, essentially preventing the issues associated with ball-milling process. However, there are few issues, such as time-consuming fabrication method, worst preparation quality and a poor bonding impact for powder that is difficult to charge [23].

The reinforcement particles are mixed with the liquid state aluminium alloy for a timeframe in the in-situ activation process and the composite material is formed by powder atomizer. In the powdered aluminium alloy, the reinforced materials are evenly dispersed. Although the synthesised composite powder are perfect composite materials with homogeneous composition and good mobility, the production process is extremely difficult and expensive [24].

4.3 LAM Processed Aluminium Composites

After utilizing low or high carbon and various types of steel, aluminium (Al) based materials seem to be the next commonly utilized engineering material category [25]. Aluminium metal matrix composites (AMMC) are composites made from aluminium alloys with macro or micro or nano reinforcements added. The reinforcements will enhance the matrix materials properties such as mechanical strength, thermal stability, thermal conductivity, resistance to wear, and dimensional stability among other properties. These advancements have a wide range of applications in aviation, automobile, electronic components, and other domains. Many researchers have published lots of research on Al and its alloy-based metal matrix composites, with oxide, carbon and nitride particles serving as the primary reinforcing material [26]. The majority of latest research on the use of laser based additive manufacturing technique to manufacture AMMC use additional later phases oxide or carbide particles as reinforcements since they are cost-effective. In specific, outward later phases particles provide some strengthening but even at the risk of reducing the material ductility and so on. Carbon based nanomaterials, like graphene or carbon nanotubes and its types, from the other end, might substantially improve mechanical properties due to its superior load carrying effect in nano size [27]. Nevertheless, successful structural stability preserving of carbon-based materials is a major struggle because of the carbon particles or elements react with any matrix to produce carbide formation, particularly in laser influenced high-temperature molten material [28]. The direct metal laser sintering (DMLS) approach as shown in Fig. 4.2 was used to make AA 2-series matrix composite material reinforced with SiC reinforcement. The bond of SiC particles to the matrix material is soft and crack-free as shown in Fig. 4.3. The tribology characteristics of DMLS prepared AMMC are also analysed

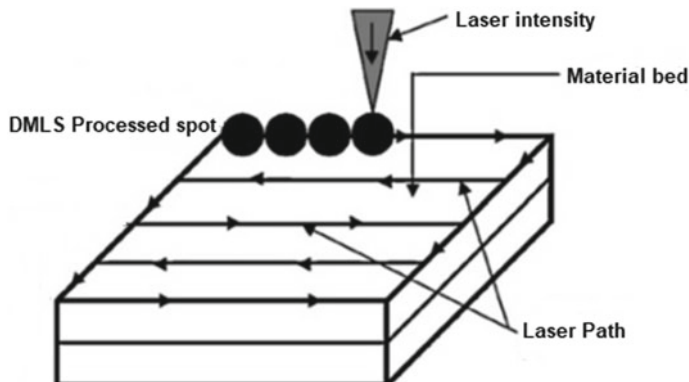
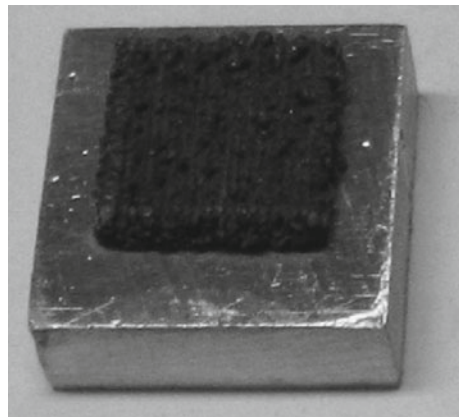


Fig. 4.2 Direct metal laser sintering (DMLS) method [29]

Fig. 4.3 Direct metal laser sintering (DMLS) sintered AMMC sample [29]



for different combinations of SiC volume fraction and particle size. When the particle size of reinforced material increases, the resistance to wear of produced materials decreases, and fracture intensity due to thermally induced stress of contracting stress increases, when the volume fraction of reinforcement exceeds 15% [29].

During the laser sintering phase, the densifying rate of AA 6-series-SiC reinforced composite obeys 1st order kinetic model and is influenced significantly by SiC volume %. An intermetallic bond Al_4SiC_4 is also generated by the interaction of aluminium melt with SiC particles [30]. Correspondingly, two separate ceramic-based reinforcement materials were included in the DMLS method for AA 6-series, respectively with 10% of SiC and 1% of nano-sized MgAl_2O_4 in weight fraction. The findings indicate that when SiC particle added in AMMC, the dispersion of SiC reinforcement is homogeneous and fully interact with aluminium matrix material. This interaction forms an intermetallic bond (aluminium carbide) and increases the hardness of the AMMC by 70% [31]. When the nano sized MgAl_2O_4 were added

into the matrix material, hardness of the AMMC reduced by 11% due to the non-homogenous dispersion pattern of nanoparticle inside the matrix material and high porosity in ANC [32].

When AA 6-series alloy is added with nano sized TiC, its microhardness of ANC material have increased by 30% compared to its matrix material when the selective laser melting (SLM) process criteria have been met correctly. The TiC reinforcement particles are observed to agglomerate in the dendrites of the crystal regions. The agglomeration of dendrites causes the nanomaterials to develop a ring like formation whenever the laser intensity per unit length is increased [33]. In the meantime, inter-metallic bonds are formed when TiC reinforcement material interact with base material. In SLM developed nano size TiC added ANC drastically reduces the wear rate and coefficient of friction (COF), due to the presence of nano sized TiC reinforcement particle [34].

Other ceramic particles were being used to strengthen aluminium metal matrix composites. Due to the presence of strong oxide bonds produced among solid materials during the SLM method (as shown in Fig. 4.4), investigators reported that hot isostatic pressing does not adequately densify the laser processed aluminium with 15% in weight fraction of Fe_2O_3 particle. The recrystallization impact on the developed material surface morphology causes the hardness decrease after hot isostatic pressing. By adding 4% volume fraction of Al_2O_3 to aluminium during SLM process

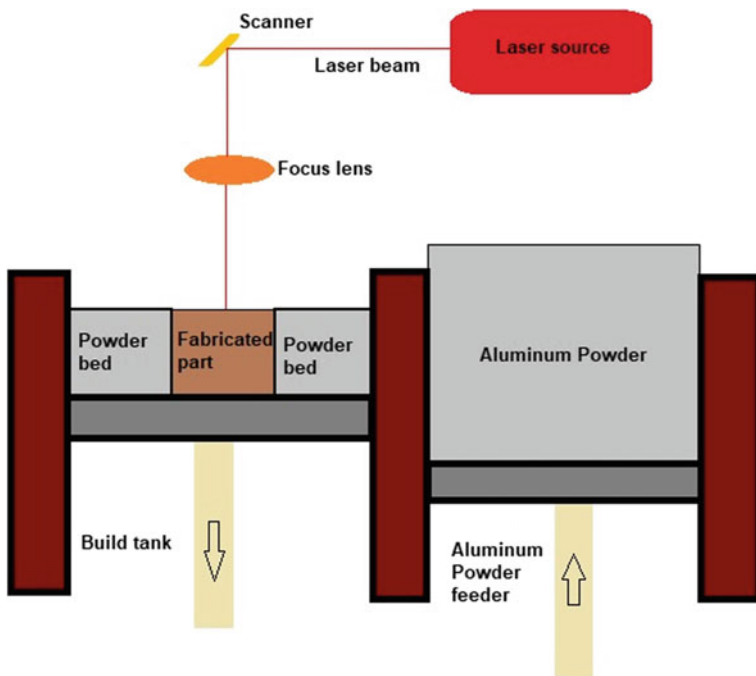


Fig. 4.4 Schematic diagram of selective laser melting (SLM)

increases yield strength about 36%, stiffness by 18%, and ductility by over 100% [35, 36]. The fabrication of an aluminium alloy executes using the SLS process, which then get debound and infused with a different aluminium alloy. Inside this SLS phase, aluminium powders are partially transformed into a percolating AlN form when reacting through nitrogen to develop the proposed frame. However, during infiltration level it gives a structural foundation [37].

Carbon based nano size materials have gained popularity as a means of strengthening by reinforcing the aluminium and its alloys. Due to aluminium's poor operating temperature ability, ensures carbon based reinforcing materials maintain a structure balancing. Carbon nanotubes (CNT) and graphene are recent aluminium alloy reinforcements. The intermetallic bonding (aluminium carbide) Al_4C_3 were formed between the aluminium and carbon-based reinforcement during the laser process, which strengthens interfacial connections and uniformly distributed inside the matrix material, increasing the mechanical properties of the matrix material. As a result, the Al_4C_3 formation process and dispersion characteristics have received lot of interest. When the lasers energy intensity is absorbed mostly by the CNT and graphene, the system architecture is damaged while the graphene and CNT are relatively decomposed [38, 39]. Thus, in situ transformation occurs at the interfacial reaction between the matrix and reinforcement material, resulting in carbide formation. Also, the CNT and graphene are highly reactive to temperature above ~ 400 °C [40]. Aluminium carbide separated just at molten metal pool's edges and relocated somewhere along in the structural path, according to selective laser additive manufacturing techniques were used to make 2% in weight fraction CNT/Al samples to develop an aluminium nanocomposite (ANC) [41]. Similarly, researchers used same technology to develop a AMMC by reinforcing graphene oxide into the aluminium (99.1 wt%). The laser energy intensity influenced, aluminium and graphene oxide in the molten state which fully transformed into aluminium carbide nanorods [42].

The matrix/micro or nano reinforcement material, procedures, and process parameters of laser additive manufactured aluminium based metal matrix composites are summarised in Table 4.1.

4.4 Mechanical Behaviour of Aluminium Composites

The aluminium (99.1 wt%) samples were made and compared to see how the addition of Al_2O_3 reinforcing material modified the tensile strength of the matrix material. The tensile strength test reports of aluminium (99.1 wt%) samples and its corresponding composite samples under various conditions are shown in Fig. 4.5. In comparison to a aluminium specimen developed under the same conditions, yield strength of the reinforced material specimen improved by 36.3% under optimized process specifications. The AMMC and aluminium specimens' maximum tensile strength were found to be increase by 46%. The tensile value of the as-developed composite specimens fabricated at 100 mm/s is also shown in Fig. 4.5a, with a 106 MPa maximum

Table 4.1 Research work on laser additive fabrication of Aluminium metal matrix composites

Researchers	Material used	Parameter selection	Observation
Ghosh [29]	AA 2-series matrix and SiC, 10–30% volume fraction of SiC	Pulse energy: 9 (J) Layer thickness: ~390–405 (μm) Scanning space: ~450 (μm)	The density of SiC particles is higher The amount of SiC particle present in a matrix material increases its microhardness With the inclusion of SiC reinforcement Particle above 25%, microhardness improves from 2 to 4 GPa
Simchi [30]	AA 6-series + 5–20% volume fraction of SiC	Intensity: 8.6 (W/mm^2) Thickness: ~90–105 (μm) Scanning space: 300 (μm)	Al_4SiC_4 is identified in situ The densifying rate of AA 6-series alloy is increased by adding 5% volume fraction of SiC SiC reinforcement particle improves surface quality while increasing stability
Manfredi [31]	AA 6-series + 10% weight fraction of SiC	Power: 170–200 (W) Scanning speed: 450–750 (mm/s) Scanning space: 170 (μm)	Residual porosity ranges from 4.4 to 5% SiC particle nearly vanishes, and Al_4C_3 intermetallic bond is developed By using DMLS technique, the AMMC seems to have a 70% higher hardness value than matrix material
Gu [33]	AA 6-series + 3% weight fraction of nano size TiC	Power: 70–150 (W) Scanning speed: 180–210 (mm/s) Thickness: ~45–60 (μm) Scanning space: 50 (μm)	Ultimate tensile strength rises about 490 MPa in composite from 399 MPa of matrix material, with a 10.8% of elongation The microhardness climbs from 144.8 to 187.6 HV0.1 in composite material

(continued)

Table 4.1 (continued)

Researchers	Material used	Parameter selection	Observation
Dadbakhsh [35]	Aluminium (99%) + 5–15% weight fraction Fe ₂ O ₃	Power: 60–80 (W) Scanning speed: 0.20–0.30 (m/s) Thickness: ~40–55 (μm) Scanning space: 50 (μm)	The mechanical and microstructure efficiency of the product are altered by HIP treatment The materials treated with HIP removes unstable phase transformation from the aluminium matrix composite Microhardness of the composite increases as Fe ₂ O ₃ content rises upon HIP treatment
Sercombe [37]	AA 6-series + 2% Mg and 4% nylon in weight fraction	Power: 25–30 (W)	While infiltration, the developed AlN framework enhances dimensional accuracy
Jiang [38]	AA 6-series + 1% CNT in weight fraction	Power: 350–400 (W) Scanning speed: 800–2000 (mm/s) Scanning space: 105 (μm) Thickness: ~20–40 (μm)	Al ₄ C ₃ intermetallic bond is formed when certain CNT react with aluminium matrix material Compared to matrix material, the strength and hardness of the composite material increases due to the interfacial bonding between the matrix and reinforcement material
Zhao [39]	AA 6-series + 0.5% MWCNT weight fraction	Power: 220–380 (W) Scanning speed: 500–800 (mm/s) Scanning space: 80 (μm) Thickness: ~20–40 (μm)	The substance has a greater porosity owing to fluid contained by CNT Decomposition of carbon nanotubes. There is no evidence of Al ₄ C ₃ carbide formation CNT dispersion improves the hardness of the material. It is possible to achieve a major decrease in electrical properties

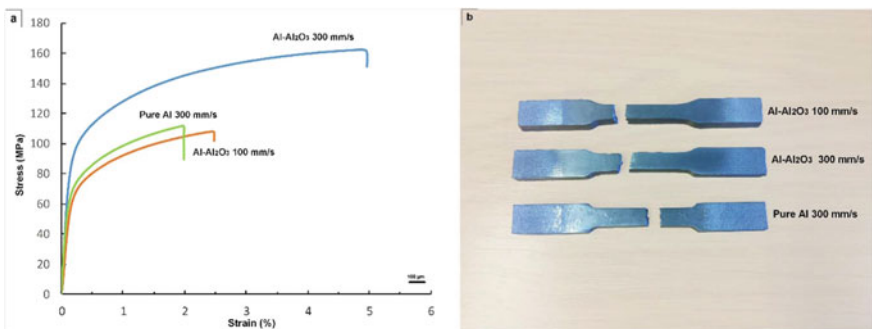


Fig. 4.5 Maximum tensile strength graph of aluminium (99.1 wt%) and AMMC specimens; **b** fractured image of the tensile specimens [43]

tensile strength and 2.4% elongation. Figure 4.5b shows the tensile specimens used to understand the maximum strength of the material developed [43].

Nanocomposites have ultra-smooth grains and distributed in secondary nanophases, potentially lengthening grain boundary layer and preventing plastic deformation. The insoluble particles were evenly dispersed in the ANC, which helps to enhance dispersion and enhance physical mechanical characteristics. Researchers used LMD technique to process 3% in weight fraction TiB₂ (500 nm)/AA 2-series specimens, which had a tensile stress of 284 MPa, microhardness of 108.5 HV with an impressive elongation property of 19%, all of which were higher than those of as-processed AA 2-series matrix material as shown in Fig. 4.6 [44]. Similar material developed by SLM techniques also possess good tensile stress, microhardness and elongation property. Nevertheless, a large quantity of nano sized reinforced particles can affect micro structural hardening and leads to brittle fracture over small crystallite cracking, resulting in reduced tensile stress. CNT is an outstanding reinforcement material for metal matrix composites (MMC) with greater modulus value

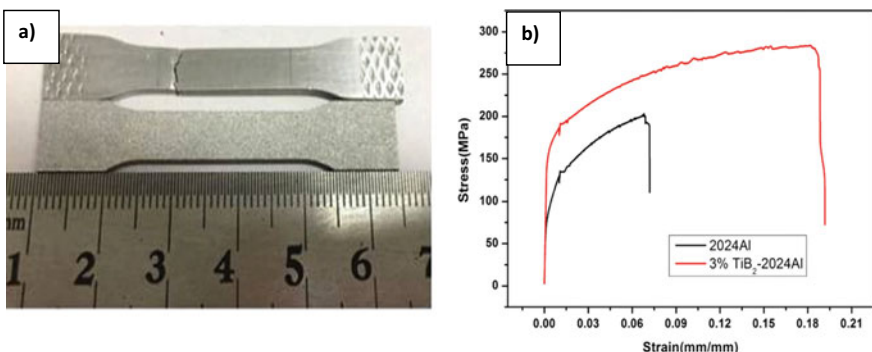


Fig. 4.6 **a** Tensile sample of AA 2-series and composite material; **b** maximum tensile strength graph of AA 2-series and composite material [44]

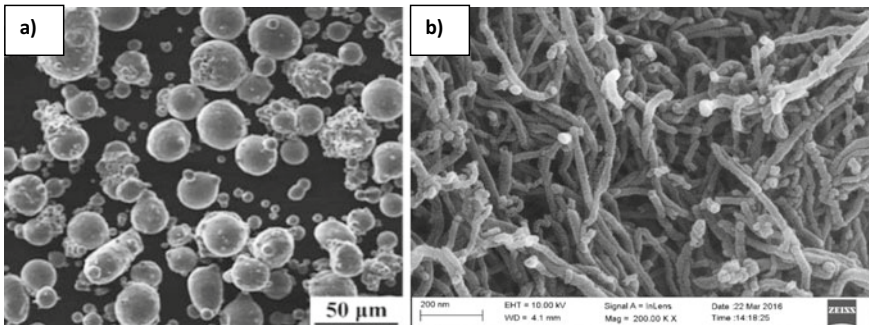


Fig. 4.7 **a** SEM analysis of AA 6-series powder [48]; **b** FESEM analysis of MWCNT [49]

of 1 TPa [45, 46]. Few CNT lose their shape in ANC, and thus the product formed is nano-Al₄C₃ does have a similar impact to nanotubes. When ANC are exposed to lateral load, the unbreakable CNT with a parallel direction to load direction reliably resist external factors, reduce the stress on the matrix grains, and increase tensile stress significantly. Many studies have found adding carbon nanotubes into aluminium alloys will enhance mechanical characteristics [47]. Figure 4.7 shows the SEM/FESEM analysis of AA 6-series powder material and Multiwalled Carbon Nanotubes (MWCNT). Due to the MWCNT retaining its tube structure and taking the lead role in the loading, the MWCNT/AA 6-series metal matrix composite material developed by SLM technique have achieved the mechanical strength of low carbon steel [38]. Graphene, as a 2-D carbon based nanosized material, inhibits ANC grain development and produces nano Al₄C₃ intermetallic bond with aluminium. Moreover, the graphene particles that has been weakened will become a major weakness that has a significant impact on tensile strength and only enhances the resistance to wear and hardness property.

The surface fractures of the developed composite specimens fabricated at 100 mm/s and 300 mm/s respectively, are depicted in Fig. 4.8. The surface fracture of the specimens were fabricated at 100 mm/s had some visible cracks, this led to a brittle failure with small elastic deformation, which became compatible with the tensile output as shown in Fig. 4.5. The existing fractures were verified by Energy Dispersive X-ray Spectroscopy (EDS) image as shown in Fig. 4.8b to be caused by metal oxide from the actual feedstock or created at the time of SLM operation. The surface fracture of the developed composite specimens at 300 mm/s is shown in Figure 4.8d-f. When subjected to tensile specimens manufactured at 100 mm/s, the surface fracture has more fine dimple formations and less cracks, indicating a ductility fracture. Some few shallow craters were produced at the surface fracture, which were accompanied by very small indentation formations, implying that the morphology at the transverse surface was not very homogeneous due to grain development.

The tensile specimens manufactured at 100 mm/s had some crack propagation along the surface. EDS analysis image verified that these damages were due to oxide formation (Fig. 4.8a, b). The fine oxide layer used in this investigation unable to

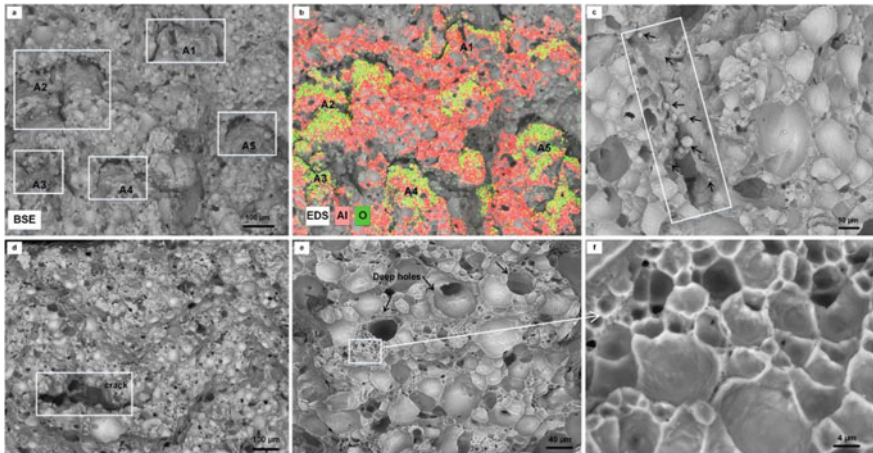


Fig. 4.8 SEM and EDS analysis shows the fracture surface morphology of developed composite specimens as-fabricated for varying process parameters **a–c** 100 mm/s and **d–f** 300 mm/s [43]

sufficiently wet the underlying materials in powder form, resulting in poor bonding between the matrix and reinforcement due to microcracks and holes. When laying the second layer powder, most of the powdered material may have been caught in the low bonding locations and create pores. Extensive cracks formed in the failure specimens as a result of these faults, as illustrated in Fig. 4.8c.

The surface fractures of the tensile investigated samples of AA 2-series matrix material and TiB_2 reinforced composites images are shown in Fig. 4.9. As illustrated in Fig. 4.9a, tabular grain characteristics develop on the surface fracture, and damaged regions are located at grain boundary. The pits may be seen in Fig. 4.9b, revealing a ductility fracture (indicated in red). There are few lacks at integration zones and voids, as highlighted in yellow and blue color. The shortage of integration zones and voids in the fractured surface could result in the formation and progression of the cracks. As a result, it is the primary cause of AA 2-series matrix material exhibits poor ductility and tensile strength. Microstructures of TiB_2 material reinforced with AA 2-series are shown in Fig. 4.9c, d, and tabular grain characteristics are not visible. This is in line with the surface morphology observations. Additionally, pits and certain precipitating phase in pits were seen, indicating ductility breakage.

The following are the major strengthening mechanism of the laser additive manufactured samples of AMMC and ANC. Although the coefficient of thermal expansion of aluminium is greater than one of ceramic reinforcing material, highly dense deformations aggregate in the grain boundaries as a result of ductile fracture due to thermal expansion, leading to an improvement grain deformation resistance and exceptional mechanical strength which is due to dislocation strengthening mechanism. This mechanism is most effective in AMMC/ANC where the reinforcement's coefficient of thermal expansion differs significantly from that of the aluminium alloy, like Al_2O_3 , TiB_2 , CNT, SiC, and so forth. The inclusion of reinforcement

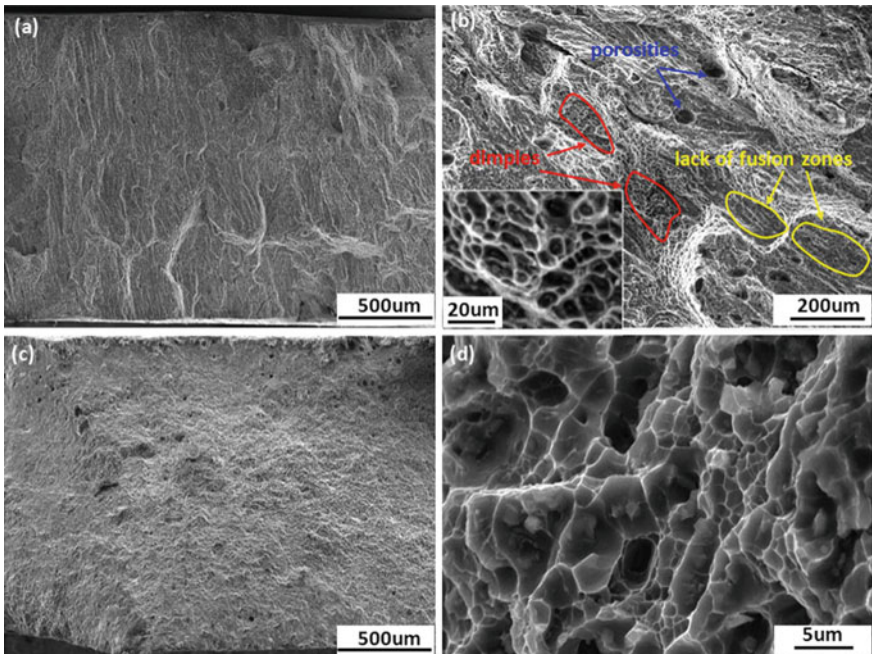


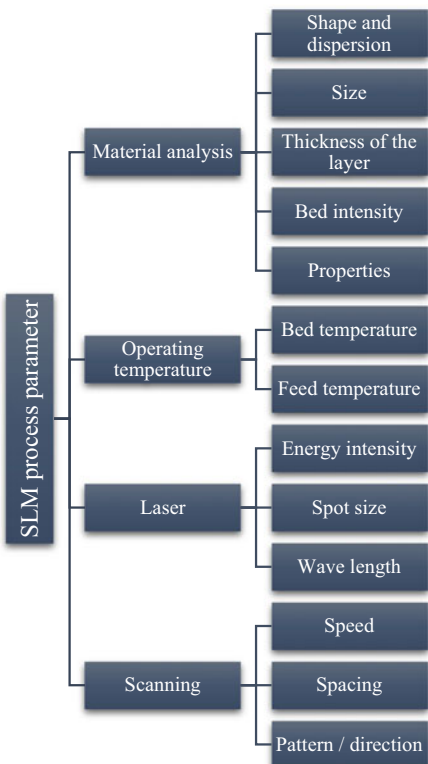
Fig. 4.9 SEM analysis shows fracture surface morphology of developed AA 2-series and composite material specimens [44]

significantly shows the volume of rigid secondary phases inclusions in the samples, preventing dislocation movement and interface relocation. The disorientation line passes across secondary phase molecules during the disorientation slip process, generating dislocation loops and increasing the dislocation density, which improves the resist-deformation capacity and mechanical strength. Furthermore, for reinforcement particles that are smaller than $\sim 0.9 \mu\text{m}$, the Orowan strengthening mechanism remains important. In ANC, the process has a number of benefits [50, 51]. At the interface region, combined diffusion and dissolution between some of the reinforcing material and the melted aluminium occur, creating in the in-situ process by converting the mechanical to chemical relationship, that secures the reinforcement material in the proper position [52]. The interfacial bonding significantly improves the AMMC/ANC mechanical strength. The inclusion of reinforcement particles as well as a higher cooling time are advantageous in the LAM method for obtaining a finer crystal structure of AMMC/ANC.

4.5 Challenges in Metal Additive Manufacturing

Additive manufacturing (AM) technique, that has gotten a lot of attention over the last few years. In spite of the benefits from aluminium additive manufacturing technique, there are obstacles that must be overcome even before true capacity of AM could be realized. These concerns arise at many stages, from preliminary concept to full manufacture phase, which include a diverse range of concerns like base material quality, process parameters, quality and industry standards [53, 54]. In reality, just a few materials communicate appropriately with high intensity of laser beams. This seems to be a major concern in the LAM. The strong refraction of the laser beam, the strong oxidizing rate, and the good thermal conductivity of aluminium, which pose major challenges for AM of aluminium alloys [55]. Fortunately, since the SLM process scope is seriously complex due to various process variables like process complexity, which may be a limiting factor as shown in Fig. 4.10. A high penetrating laser intensity is needed to melt as well as conquer quick heat transfer during diffusion, while quick heat transfer is much more typical for solid phase than for aluminium powders. Furthermore, Aluminium and its alloy are sensitive to oxidation, low wettability and porous in nature, posing difficult obstacles during SLM

Fig. 4.10 Flow chart of the SLM process parameter



process. The complexity of ensuring a homogeneous dispersion of the reinforcement material, particularly if nano size reinforcing particulates were being used, is the major technical challenge of developing AMMC using LAM technique [25, 56]. Several researchers have discovered that clustering of reinforcement particle restricts the efficiency of final AMMC components. As a result, more effective particle distribution techniques in LAM processes were intended to lower the clustering of nano size reinforcement particles.

4.6 Conclusion

For both materials and design scientist, aluminium matrix composites provide a lot of possibilities and opportunities. Aluminium matrix composites are expected to be used more frequently in present and future manufacturing advancements. As a result of new and evolving technological innovations. Laser additive manufacturing techniques for AMMC/ANC development are indeed a promising field for both industry and academia. Considerable attempts were made in recent years to acquire different AMMC/ANC using the powder bed fusion (PBF) processes. The addition of reinforcement into the matrix material using the LAM processed AMMC/ANC is challenging, due to the cluster formation of micro or nano reinforced particle. Physical characteristics of carbon based reinforced AMMC/ANC samples developed by LAM need to be investigated further. The mechanical properties of nano size reinforced composite materials possess better properties than micro reinforced particle. Hence, the research on aluminium composites using varied laser based additive manufacturing needs to be formulated.

References

1. Rometsch, P.A., Zhang, Y., Knight, S.: Heat treatment of 7xxx series aluminum alloys—some recent developments. *Trans. Nonferrous Met. Soc. China*. **24**, 2003–2017 (2014). [https://doi.org/10.1016/S1003-6326\(14\)63306-9](https://doi.org/10.1016/S1003-6326(14)63306-9)
2. Harrison, T.J., Crawford, B.R., Janardhana, M., Clarka, G.: Differing microstructural properties of 7075-T6 sheet and 7075-T651 extruded aluminium alloy. *Proce Eng.* **10**, 3117–3121 (2011). <https://doi.org/10.1016/j.proeng.2011.04.516>
3. Sairam, V., Kishor Kanna, S., Samuel Ratna Kumar, P.S.: Analysis of low-velocity impact response in Aa5083 plate. *IOP Conf. Ser. Mater. Sci. Eng.* **1123**, 012040 (2021). <https://doi.org/10.1088/1757-899X/1123/1/012040>
4. Mazahery, A., Shabani, M.O.: A356 reinforced with nano particles: numerical analysis of mechanical properties. *JOM* **64**, 323–329 (2012). <https://doi.org/10.1007/s11837-012-0245-0>
5. Singh, J.: Fabrication characteristics and tribological behavior of Al/SiC/Gr hybrid aluminum matrix composites: a review. *Friction* **4**, 191–207 (2016). <https://doi.org/10.1007/s40544-016-0116-8>
6. Chi, Y., Gu, G., Yu, H.: Laser surface alloying on aluminum and its alloys: a review. *J. Opt. Lasers Eng.* **100**, 23–37 (2018). <https://doi.org/10.1016/j.optlaseng.2017.07.006>

7. Samuel Ratna Kumar, P.S., Mashinini P.M.: Investigation on tribological behaviour of aluminosilicate reinforced AA7075 composites for aviation application. *Trans. Indian Inst. Met.* **74**, 79–88 (2021). <https://doi.org/10.1007/s12666-020-02112-6>.
8. Kumar, P.S.S.R., Mashinini, P.M.: Dry sliding wear behaviour of AA7075—Al₂SiO₅ layered nanoparticle material at different temperature condition. *SILICON* (2020). <https://doi.org/10.1007/s12633-020-00728-3>
9. Borgonovo, C., Apelian, D.: Manufacture of aluminum nanocomposites: a critical review. *Mater. Sci. Forum.* **678**, 1–22 (2011). <https://doi.org/10.4028/www.scientific.net/MSF.678.1>
10. Kumar, S., Balasubramanian, V.: Effect of reinforcement size and volume fraction on the abrasive wear behaviour of AA7075 Al/SiC_p P/M composites—a statistical analysis. *Tribol. Int.* **43**, 414–422 (2010). <https://doi.org/10.1016/j.triboint.2009.07.003>
11. Yilmaz, O., Buytoz, S.: Abrasive wear of Al₂O₃-reinforced aluminium-based MMCs. *Compos. Sci. Technol.* **61**, 2381–2392 (2001). [https://doi.org/10.1016/S0266-3538\(01\)00131-2](https://doi.org/10.1016/S0266-3538(01)00131-2)
12. Pradeep, P., Kumar, P.S.S.R., Lawrence, I.D., Jayabal, S.: Characterization of Particulate reinforced aluminium 7075/TiB₂ Composites. *Int. J. Civil Eng. Technol.* **8**, 178–190 (2017). <http://www.iaeme.com/ijciet/issues.asp?JType=IJCIE&VType=8&IType=9>
13. Qu, X.H., Zhang, L., Wu, M., Bin, R.S.: Review of metal matrix composites with high thermal conductivity for thermal management applications. *Prog. Nat. Sci. Mater. Int.* **21**, 189–197 (2011). [https://doi.org/10.1016/S1002-0071\(12\)60029-X](https://doi.org/10.1016/S1002-0071(12)60029-X)
14. Sidduesh Kumar, N.G., Suresh, R., Shiva Shankar, G.S.: High temperature wear behavior of Al2219/n-B4C/MoS₂ hybrid metal matrix composites. *Compo. Commun.* **19**, 61–73. <https://doi.org/10.1016/j.coco.2020.02.011>
15. Rohatgi, P.K.: Use of lightweight metal-matrix composites for transportation applications in India. *SAE Technical Paper.* 2004-28-0070 (2004). <https://doi.org/10.4271/2004-28-0070>
16. Shi, J., Wang, Y.: Development of metal matrix composites by laser-assisted additive manufacturing technologies: a review. *J Mater Sci* **55**, 9883–9917 (2020). <https://doi.org/10.1007/s10853-020-04730-3>
17. Standard, A.: F2792-12a: Standard Terminology for Additive Manufacturing Technologies. ASTM International, West Conshohocken, PA, 2012 (2013)
18. Bhavar, V., Kattire, P., Patil V.: A review on powder bed fusion technology of metal additive manufacturing. In: *Additive Manufacturing Handbook*, pp. 251–253. CRC Press, Boca Raton (2017)
19. Pinkerton, A.J.: Lasers in additive manufacturing. *J. Opt. Laser Technol.* **78**, 25–32 (2016). <https://doi.org/10.1016/j.optlastec.2015.09.025>
20. Bo, C., Xin, X., Caiwang, T., Xiaoguo, S.: Recent progress in laser additive manufacturing of aluminum matrix composites. *Curr. Opin. Chem. Eng.* **28**, 28–35 (2020). <https://doi.org/10.1016/j.coche.2020.01.005>
21. Han, Q., Setchi, R., Evans, S.L.: Synthesis and characterisation of advanced ball-milled Al-Al₂O₃ nanocomposites for selective laser melting. *Powder Technol.* **297**, 183–192 (2016). <https://doi.org/10.1016/j.powtec.2016.04.015>
22. Jiang, B., Lei, Z., Chen, X.: Microstructure and mechanical properties of TiB₂-reinforced 7075 aluminum matrix composites fabricated by laser melting deposition. *Ceram. Int.* **45**, 5680–5692 (2019). <https://doi.org/10.1016/j.ceramint.2018.12.033>
23. Martin, J.H., Yahata, B.D., Hundley, J.M.: 3D printing of high strength aluminium alloys. *Nature* **549**, 365–369 (2017). <https://doi.org/10.1038/nature23894>
24. Li, X., Ji, G., Chen, Z.: Selective laser melting of nano-TiB₂, decorated AlSi10Mg alloy with high fracture strength and ductility. *Acta Mater.* **129**, 183–193 (2017). <https://doi.org/10.1016/j.actamat.2017.02.062>
25. Sercombe, T.B., Li, X.: Selective laser melting of aluminium and aluminium metal matrix composites. *Mater. Technol.* **31**, 77–85 (2016). <https://doi.org/10.1179/175355715Y.0000000078>
26. Song, B., Dong, S., Coddet, P.: Microstructure and tensile behavior of hybrid nano-micro SiC reinforced iron matrix composites produced by selective laser melting. *J. Alloys Compd.* **579**, 415–421 (2013). <https://doi.org/10.1016/j.jallcom.2013.06.087>

27. Prashantha Kumar, H.G., Xavior, M.A.: Graphene reinforced metal matrix composite (GRMMC): a review. *Proced. Eng.* **97**, 1033–1040 (2014). <https://doi.org/10.1016/j.proeng.2014.12.381>
28. Jiang, J., He, X., Du, J.: In-situ fabrication of graphene-nickel matrix composites. *Mater. Lett.* **220**, 178–181 (2018). <https://doi.org/10.1016/j.matlet.2018.03.039>
29. Ghosh, S.K., Saha, P., Kishore, S.: Influence of size and volume fraction of SiC particulates on properties of ex situ reinforced Al–4.5Cu–3 Mg metal matrix composite prepared by direct metal laser sintering process. *Mater. Sci. Eng. A* **527**, 4694–4701 (2010). <https://doi.org/10.1016/j.msea.2010.03.108>
30. Simchi, A., Godlinski, D.: Effect of SiC particles on the laser sintering of Al–7Si–0.3 Mg alloy. *Ser. Mater.* **59**, 199–202 (2008). <https://doi.org/10.1016/j.scriptamat.2008.03.007>
31. Manfredi, D., Calignano, F., Krishnan, M.: Additive manufacturing of Al alloys and aluminium matrix composites (AMCs). *Light Met. Alloy. Appl.* **11**, 3–34 (2014). <https://doi.org/10.5772/57069>
32. Gu, D., Chang, F., Dai, D.: Selective laser melting additive manufacturing of novel aluminum based composites with multiple reinforcing phases. *J. Manuf. Sci. Eng.* **137**(021010), 1–11 (2015). <https://doi.org/10.1115/1.4028925>
33. Gu, D., Wang, H., Dai, D.: Rapid fabrication of Al based bulk-form nanocomposites with novel reinforcement and enhanced performance by selective laser melting. *Scr. Mater.* **96**, 25–28 (2015). <https://doi.org/10.1016/j.scriptamat.2014.10.011>
34. Gu, D., Wang, H., Dai, D.: Densification behavior, microstructure evolution, and wear property of TiC nanoparticle reinforced AlSi10Mg bulk-form nanocomposites prepared by selective laser melting. *J. Laser Appl.* **27**, S17003 (2015). <https://doi.org/10.2351/1.4870877>
35. Dadbakhsh, S., Hao, L.: Effect of hot isostatic pressing (HIP) on Al composite parts made from laser consolidated Al/Fe₂O₃ powder mixtures. *J. Mater. Process Technol.* **212**, 2474–2483 (2012). <https://doi.org/10.1016/j.jmatprotec.2012.06.016>
36. Han, Q., Setchi, R., Lacan, F., Gu, D., Evans, S.L.: Selective laser melting of advanced Al-Al₂O₃ nanocomposites: Simulation, microstructure and mechanical properties. *Mater. Sci. Eng. A* **698**, 162–173 (2017)
37. Sercombe, T.B., Schaffer, G.B.: On the role of tin in the infiltration of aluminium by aluminium for rapid prototyping applications. *Scr. Mater.* **51**, 905–908 (2004). <https://doi.org/10.1016/j.scriptamat.2004.06.032>
38. Jiang, L.Y., Liu, T.T., Zhang, C.D.: Preparation and mechanical properties of CNTs-AlSi10Mg composite fabricated via selective laser melting. *Mater. Sci. Eng. A* **734**, 171–177 (2018). <https://doi.org/10.1016/j.msea.2018.07.092>
39. Zhao, X., Song, B., Fan, W.: Selective laser melting of carbon/AlSi10Mg composites: microstructure, mechanical and electronical properties. *J. Alloys Compd.* **665**, 271–281 (2016). <https://doi.org/10.1016/j.jallcom.2015.12.126>
40. Chen, B., Shen, J.: Solid-state interfacial reaction and load transfer efficiency in carbon nanotubes (CNTs)-reinforced aluminum matrix composites. *Carbon* **114**, 198–208 (2017). <https://doi.org/10.1016/j.carbon.2016.12.013>
41. Aboulkhair, N., Simonelli, M., Salama, E.: Evolution of carbon nanotubes and their metallurgical reactions in Al-based composites in response to laser irradiation during selective laser melting. *J. Mater. Sci. Eng. A* **765**, 138307 (2019). <https://doi.org/10.1016/j.msea.2019.138307>
42. Zhou, W., Dong, M., Zhou, Z.: In situ formation of uniformly dispersed Al₄C₃ nanorods during additive manufacturing of graphene oxide/al mixed powders. *Carbon* **141**, 67–75 (2019). <https://doi.org/10.1016/j.carbon.2018.09.057>
43. Han, Q., Setchi, R., Lacan, F.: Selective laser melting of advanced Al-Al₂O₃ nanocomposites: simulation, microstructure and mechanical properties. *Mater. Sci. Eng. A* **698**, 162–173 (2017). <https://doi.org/10.1016/j.msea.2017.05.061>
44. Wen, X., Wang, Q., Mu, Q.: Laser solid forming additive manufacturing TiB₂ reinforced 2024Al composite: microstructure and mechanical properties. *J. Mater. Sci. Eng. A* **745**, 319–325 (2019). <https://doi.org/10.1016/j.msea.2018.12.072>

45. Batista, L.A., Felisberto, M.D.V., Silva, L.S.: Influence of multiwalled carbon nanotubes reinforcements on hardness and abrasion behaviour of porous Al-matrix composite processed by cold pressing and sintering. *J. Alloys Compd.* **791**, 96–99 (2019). <https://doi.org/10.1016/j.jallcom.2019.03.265>
46. Liu, X., Li, C., Eckert, J.: Microstructure evolution and mechanical properties of carbon nanotubes reinforced Al matrix composites. *J. Mater. Charact.* **133**, 122–132 (2017). <https://doi.org/10.1016/j.matchar.2017.09.036>
47. Rikhtegar, F., Shabestari, S.G., Saghaian, H.: Microstructural evaluation and mechanical properties of Al-CNT nanocomposites produced by different processing methods. *J. Alloys Compd.* **723**, 633–641 (2017). <https://doi.org/10.1016/j.jallcom.2017.06.222>
48. Xiao, Y.K., Bian, Z.Y., Wu, Y.: Effect of nano-TiB₂ particles on the anisotropy in an AlSi10Mg alloy processed by selective laser melting. *J. Alloys Compd.* **798**, 644–655 (2019). <https://doi.org/10.1016/j.jallcom.2019.05.279>
49. Nekilesh, Boobathi, S., Jyothi, S., Kumar, P.S.S.R., Sudhagar, P.E.: A study on corrosion behavior of AA5083—MWCNT reinforced composite. *Mater. Today Proceed.* **22**, 2725–2731 (2020). <https://doi.org/10.1016/j.matpr.2020.03.403>
50. Chen, B., Shen, J., Ye, X.: Length effect of carbon nanotubes on the strengthening mechanisms in metal matrix composites. *Acta Mater.* **140**, 317–325 (2017). <https://doi.org/10.1016/j.actamat.2017.08.048>
51. Li, J., Nie, J., Xu, Q.: Enhanced mechanical properties of a novel heat resistant Al-based composite reinforced by the combination of nano-aluminides and submicron TiN particles. *Mater. Sci. Eng. A* **770**, 138488 (2020). <https://doi.org/10.1016/j.msea.2019.138488>
52. Chen, L., Xu, J., Choi, H.: Processing and properties of magnesium containing a dense uniform dispersion of nanoparticles. *Nature* **528**, 539–543 (2015). <https://doi.org/10.1038/nature16445>
53. Li, C., Liu, Z.Y., Fang, X.Y., Guo, Y.B.: Residual stress in metal additive manufacturing. *Procedia CIRP* **71**, 348–353 (2018). <https://doi.org/10.1016/j.procir.2018.05.039>
54. Megahed, M., Mindt, H.W., N'Dri, N.: Metal additive-manufacturing process and residual stress modeling. *Integr. Mater. Manuf. Innov.* **5**, 61–93 (2016). <https://doi.org/10.1186/s40192-016-0047-2>
55. Han, Q., Setchi, R., Karihaloo, B.: Challenges and Opportunities in the additive layer manufacturing of Al-Al₂O₃ nanocomposites. *Sustain. Design Manuf.* 389–399 (2015). <http://orca.cf.ac.uk/id/eprint/84193>
56. Bartkowiak, K., Ullrich, S., Frick, T., Schmidt, M.: New developments of laser processing aluminium alloys via additive manufacturing technique. *Phys. Procedia* **12**, 393–401 (2011). <https://doi.org/10.1016/j.phpro.2011.03.050>

Chapter 5

Additive Manufacturing of Non-ferrous Metals



Temel Varol , Onur Güler, Fatih Yıldız, and S. Suresh Kumar

5.1 Introduction

It is possible to classify metals and alloys in two groups. These are ferrous metals (FMs) and non-ferrous metals (NMs). While ferrous metals and their alloys are defined as metals and alloys containing the element iron, non-ferrous metals and their alloys include all other elements and alloys that do not contain iron (Fe) [38]. FMs and their alloys, which are known to have high tensile strength and durability, are also known for their inadequate corrosion resistance. Although corrosion resistance can be increased with the addition of chromium, it is a disadvantage that it is heavy compared to NMs and their alloys. In this context, FMs and alloys are preferred in areas where extreme strength is important, while NMs and their alloys are preferred in areas requiring flexibility, lightness, conductivity and corrosion resistance [63]. The most important factors in the use of NMs and their alloys in industry are excellent corrosion resistance, machinability by methods such as casting, welding, machining, rolling and high thermal and electrical conductivity, lightness and attractive colors

T. Varol (✉) · O. Güler
Department of Metallurgical and Materials Engineering, Engineering Faculty, Karadeniz
Technical University, Trabzon, Turkey
e-mail: tvarol@ktu.edu.tr

O. Güler
e-mail: onurguler@ktu.edu.tr

F. Yıldız
Department of Mechanical Engineering, Engineering Faculty, Erzurum Technical University,
Erzurum, Turkey
e-mail: fatih.yildiz@erzurum.edu.tr

S. Suresh Kumar
Department of Mechanical Engineering, Kalasalingam University, Srivilliputhur, Tamil Nadu,
India
e-mail: ssureshkumar@klu.ac.in

[35]. Electronics, batteries, construction and energy industries are the most important areas where these materials and alloys are the most preferred.

Considering the use of aluminum and its alloys (AAs) in the group of NMs, it is known that they are the most used materials after steels. Having almost 3 times less density than steels, being economical and having a ductile structure make these materials attractive. In addition, thanks to the natural protective oxide film formed on the surfaces of AAs', its corrosion resistance is excellent [14]. Usage areas of AAs have been reported in recent years as shown in Fig. 5.1.

Another excellent corrosion resistance NMs are titanium and their alloys (TAs). It is used more frequently in aerospace and defense industry areas thanks to its features such as high strength, low density and high fatigue resistance, and working up to 700 °C. Thanks to its high specific strength, for example, up to 30% of the aircraft structure can be composed of TAs in fighter aircraft manufacturing. Especially in the aviation industry, the fact that low weight is one of the crucial features encourages the production of TAs with SLM method [23]. The most frequently used areas of TAs, which are increasingly used in the world industry, are given in Fig. 5.2.

Nickel metal and its alloys (NAs), which are another common area of use, is harder than iron and exhibits magnetic properties at temperatures below 360 °C. Being ductile, malleable and corrosion resistant also increases their usage areas.

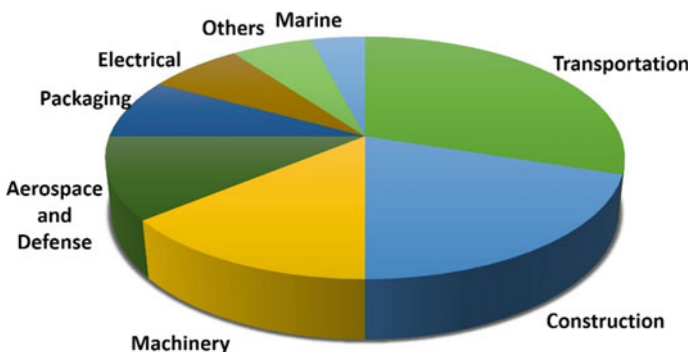
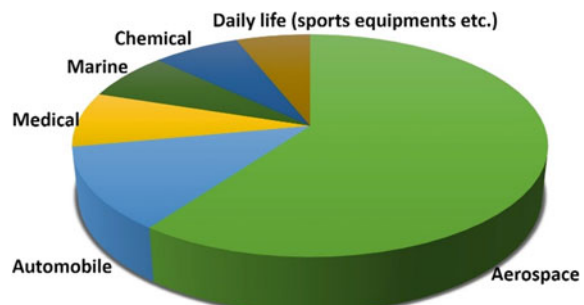


Fig. 5.1 AAs (end-use) market in the world [78]

Fig. 5.2 TAs (end-use) market in the world [2]



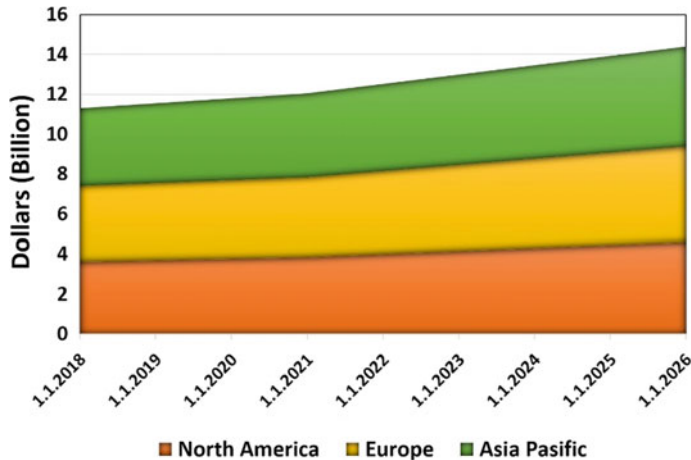


Fig. 5.3 Prediction of global NAs market [79]

These alloys are very suitable for production with SLM due to their properties such as obtaining cellular structure and optimizing the surface topography [43, 83]. Until 2026, it is estimated that the spending on the global NAs market will gradually increase and is graphically given in Fig. 5.3.

Another element frequently used in modern industry is the element cobalt, which is found in the periodic table between iron and nickel. Cobalt exhibits very similar properties to those of iron and nickel. In particular, its ferromagnetic and high melting point (1495 °C) enables this metal to be used in gas and jet turbines. The most crucial feature is the need for cobalt metal in obtaining clean energy. It is reported that each electric vehicle should provide about 9.4 kg cobalt content [47, 72]. With the development of the electric vehicle industry, the demand for cobalt for use in vehicle batteries is expected to increase over the years, as shown in Fig. 5.4.

Another NM that can be encountered in every aspect of our daily life are copper and their alloys (CAs). The fact that copper metal has the highest electrical and thermal conductivity after silver in nature makes CAs indispensable in the electrical and electronics industry. In addition to these properties of copper, its easy formability, solderability and weldability features further expand its usage areas with the production by SLM method [77]. As can be seen in Fig. 5.5, according to the forecasts until 2100, the infrastructure use of CAs will gradually increase.

Traditional methods such as casting and powder metallurgy are frequently used in the production of the aforementioned NMs. However, long work time and problems such as scrap materials and production difficulties of very complex parts that occur in traditional methods such as casting, machining, powder metallurgy encourage researchers to develop new production methods. Additive manufacturing (AM) and also known as rapid prototyping (RP) are generally based on the fusion of selective powder or wire regions by melting with high energy laser according to computer-aided design data (CAD). The huge interest in this material production method in

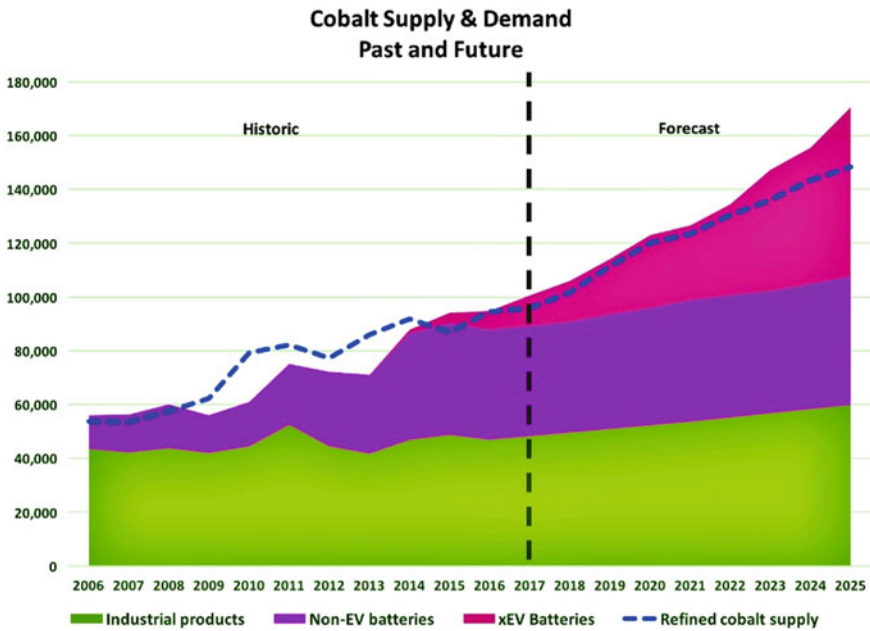


Fig. 5.4 Cobalt demand change and forecast over years [69]

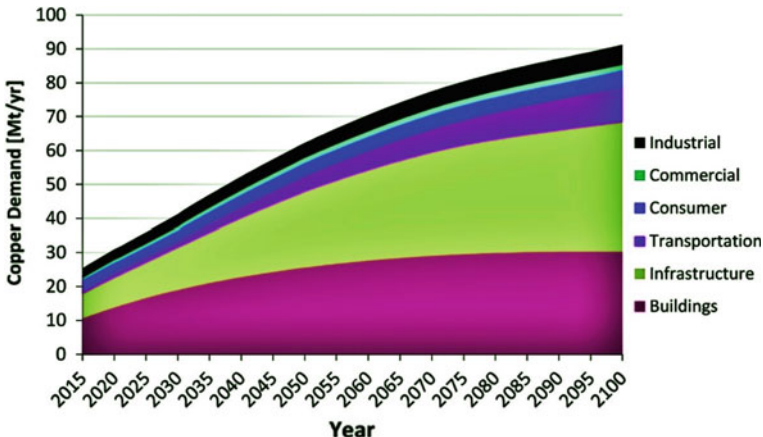


Fig. 5.5 CAs demand forecast until 2100 [86]

the last 15 years is due to the fact that it provides unrivaled design shaped materials and the delivery in a short time. Considering the rapid increase in demand for the aforementioned NMs and the advantages of the AM method, it is doubtless that the interest in the fabrication of these NMs by AM methods will increase significantly [33]. This technique especially for the fabrication of non-ferrous metals, still has

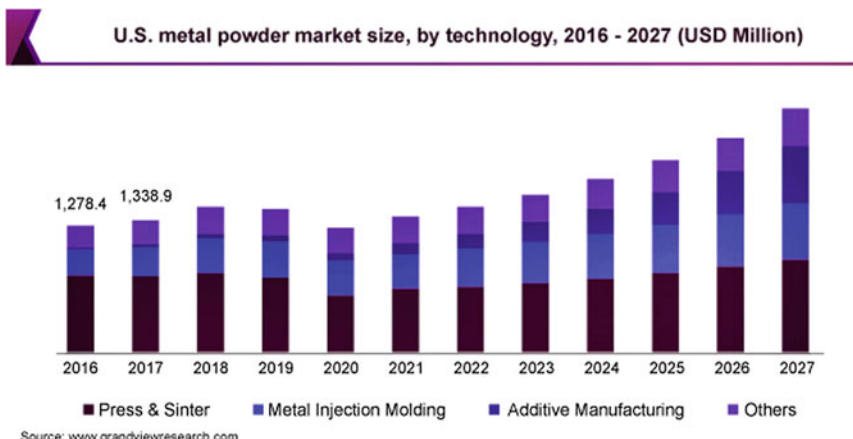


Fig. 5.6 AM demand until 2027 in US [27]

some difficulties and disadvantages. The difficulty of integrating the system well, having too many process parameters, including scanning motion and speed, creates difficulties in providing dimensional controls and obtaining high material density [95]. Figure 5.6 provides estimates of the demand for metal powders used in several traditional and AM methods in the US up to 2027. It is clear that with the development of AM methods, the amount of metal powder demanded to be used in these methods has been increasing over the years.

In particular, the SLM method can provide the production of smart NM (NiTi shape memory alloy) quickly, with unlimited complex shapes, at affordable costs, in a multi-layered manner that does not require processing [22]. It is an indispensable method in the manufacture of porous implants (titanium, titanium alloys, CoCr alloys) made of NM and in the production of parts with better surface quality [12]. Parameters changed in SLM for different areas of NM parts allow the microstructure to be modified as desired. Moreover, NM (Ti-22Al-25Nb) with different microstructure properties can be easily produced in a single material structure [70].

However, today, there are still difficulties in the production of high quality and fast materials with the SLM technique in the NM industry, as it is a new technique. Therefore, considering the difficulties encountered in the light of all these advantages and disadvantages of AM, the research of the precautions and the things to be done in the production of the aforementioned NM with SLM method which is one of AM techniques will be discussed in this book section.

5.2 Fabrication of NMs with SLM

5.2.1 Properties of SLMed Ti and Ti Alloys with Challenges

The structural and mechanical properties of the parts produced by SLM method that is one of AM methods are greatly affected by the parameters / strategies used in production and post processes to be applied after production. Therefore, it is extremely important to know / control the effects of the parameters to be used in production and post-production post processes on the mechanical properties of the material and to determine the optimum production conditions. Some of the factors that cause the change of chemical, morphological and microstructural properties of the product created by SLM method are given in Fig. 5.7 [81].

In the SLM method, the major laser manufacturing parameters are laser power (P), layer thickness (t), laser scanning speed (V), hatch spacing (h) and laser energy density (E) controlled by changing top four parameters. All these variables affect the energy density required for melt formation, and this energy has a direct effect on the mechanical and surface properties of the manufactured geometry [29, 50]. Porosity, microstructure, and surface condition can be altered by modifying the sub-parameters while the energy density is constant [52]. Therefore, the optimization of the laser production parameters/strategies is necessary to determine the most suitable conditions resulting in the desired microstructure and mechanical properties. The applied parameters affect each layer of the product and eventually the properties of these layers directly affect the basic mechanical properties of the final product such as hardness, porosity, ductility, and strength [105].

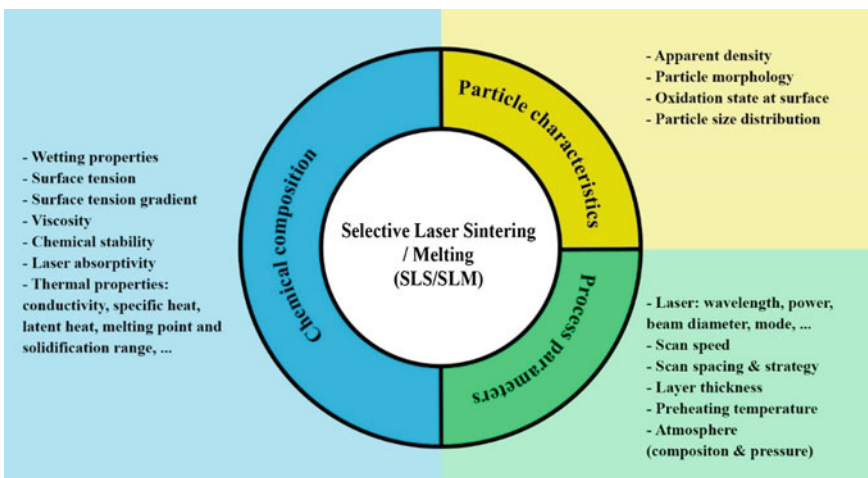


Fig. 5.7 Parameters affecting the selective laser melting process [81]

Titanium and its alloys are the most suitable materials for many implant applications because of its high strength according to its density, high corrosion resistance and biocompatibility. In addition, Ti and its alloys are widely used in areas such as aviation, defense and automotive industry due to their high specific strength. For that reason, the SLM studies of titanium and its alloys have recently received great deal of attention and are still developing [41].

The influence of the different process parameters, such as layer thickness, hatch spacing, scan strategy, laser power, scan speed and build orientation on the microstructure, mechanical and morphological properties of Ti alloys such as the density and surface quality have been investigated to achieve optimal building conditions [21, 29, 98]. Studies in the literature have mainly focused on Ti6Al4V alloy, which is widely used in biomedical, aerospace and automotive fields.

As shown in many previous studies [15, 29, 40], the microstructure of Ti6Al4V processed by SLM consists of a fine acicular martensite called the α' phase. Mechanical properties of these SLM parts are a high yield stress (about 1 GPa), a high ultimate tensile strength but a relatively low ductility (less than 10%) [98]. To improve the ductility of Ti6Al4V products manufactured by SLM, and to achieve a variety of desired mechanical properties for particular applications, suitable post-production heat treatments must be elaborated. Furthermore, these treatments allow the reduction of thermal stresses that have been built up during the process.

In a study by Zhou et al. [114], they performed a comparison between nearly β titanium, α titanium and $\alpha + \beta$ titanium alloys were additively manufactured by selective laser melting. The characteristic microstructures of SLM-processed Ti alloys samples are shown in Fig. 5.8 [56]. Fine martensite grains which can be identified as hcp α' phases were evident in the microstructure of Ti alloys in the top view. When viewing the front section, the β grain cannot be seen in Fig. 5.8c. The β grains oriented along the build-up direction with the lengths over to layer thickness (Fig. 5.8e). Ti alloy exhibited a different structure in which the laser scanning tracks

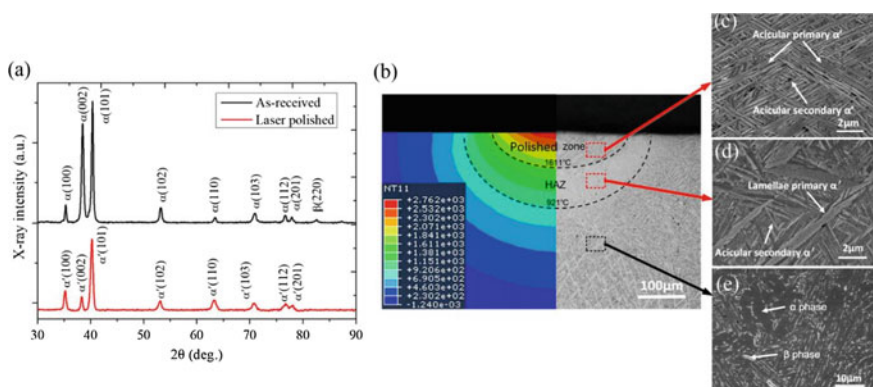


Fig. 5.8 The XRD **a**, simulation, **b** and SEM microstructure images **(c-e)** of SLM-processed Ti alloys [56]

and melt pools are clearly seen in the sections after etched. The microstructure of SLM-processed Ti alloy revealed extremely fine primary α' martensite in the β matrix (Fig. 5.8c and d).

In a study by Hacısalıhoğlu et al. [29], they described the evaluation of the melt pool of selective laser melted Ti6Al4V alloy with 100 W laser power and different scan speeds. When the laser energy causes the vaporization of the material, the melt pool shape is observed to have a keyhole shape with deep melt penetration rather than a bowl shape. It was obtained that the keyhole form replaced the bowl form with increasing scanning speed. The homogeneous of the thermal input was achieved by obtaining approximately the same pool dimensions in lateral and cross-sectional depth with the 100 W laser power and 1400 mm/s scanning speed. Thus, it was also observed that the thermal gradient effect arising from the nature of SLM method will provided a more balanced distribution [29]. The effect of different hatch spacing values on relative density of the samples produced with 100 W laser power, 1400 mm/s scanning speed and 25 μm layer thickness was investigated. These process parameters were chosen due to adequate melting, integration and high production speed. While there was no significant change in the relative density up to 67.5 μm hatch spacing value, it was observed that the hatch spacing above this value the density decreased significantly. As a result of increasing the hatch spacing, the inadequate integration defects between the adjacent laser tracks that could not come into contact with each other and insufficient melting zones in the microstructure accelerated the decrease of relative density values. In another study, with power of 400 W and layer thickness of 200 μm , the optimum scanning speed was determined to be 40–80 mm/s (Fig. 5.9). Balling (Fig. 5.9d) and inappropriate melting pool formation were observed at scanning speeds above 80 mm/s. The hatch spacing effect is also clearly seen in Fig. 5.10 (top right) according to the results obtained in another study [45].

The mechanical properties of different Ti and its alloys produced by additive manufacturing technique have been investigated in many studies in the literature. The tensile properties of different Ti and its alloys produced by additive manufacturing and conventional methods are comparatively given in Table 5.1. The main deficiency known in the additive manufacturing process was the low elongation values resulting from insufficient joints and rapid cooling [29]. The significantly improved ultimate tensile strength can be explained by the grain refinement and the formation of α' martensitic structure. The α' martensite with a higher density of dislocations in comparison with α phase [114] could result in a more effective barrier against dislocation movement during deformation, leading to the strengthening of alloys.

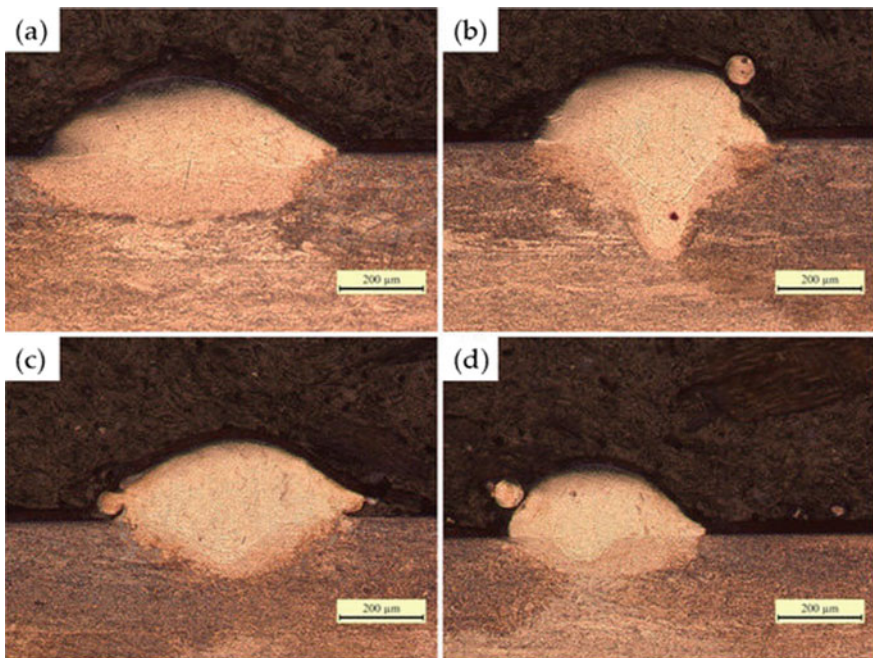


Fig. 5.9 Scan tracks with the increase of scanning speeds for Ti6Al4V alloys; **a** 80 mm/s, **b** 120 mm/s, **c** 160 mm/s and **d** 200 mm/s [87]

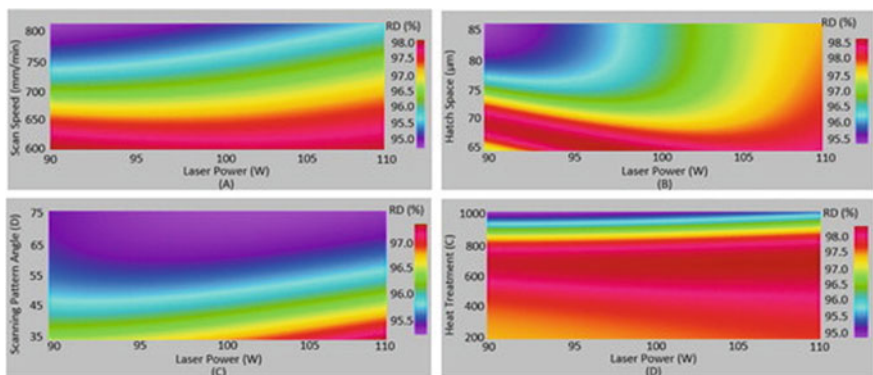


Fig. 5.10 Relative density values depending on the hatch spacing with different parameters [45]

5.2.2 Properties of SLMed Ni and Ni Alloys with Challenges

Shape Memory Alloys (SMAs) is a new class of materials which becomes inevitable material group in earthquake resilient construction, satellite, medical and biomedical fields. NiTi is renowned SMA group having better mechanical behavior with

Table 5.1 Tensile mechanical properties of Ti and Ti Alloys processed by different technologies

Tensile properties					
	Condition	σ_{uts} (MPa)	$\sigma_{0.2}$ (MPa)	ϵ_f (%)	References
Ti	SLM	990 ± 10	792 ± 5	6.086 ± 1	[114]
	SLM	757 ± 12.5	555 ± 3	19.5 ± 1.8	[4]
	Sheet forming	345	280	20	[8]
	Full annealed	561	432	14.7	[7]
	Arc-melting	641 ± 52	527 ± 46	19.7 ± 1.3	[57]
Ti-6Al-4 V	SLM	1334 ± 15	1110 ± 5	6.351 ± 0.5	[114]
	SLM	1190 ± 10	850 ± 25	9 ± 0.5	[29]
	EBM	1100 ± 20	900 ± 10	10 ± 0.5	[112]
	Arc-melting	1137 ± 17	846 ± 67	7.1 ± 1.9	[57]
Ti-13Nb-13Zr	SLM	1020 ± 13	794 ± 15	5 ± 0.3	[114]
	Powder Metallurgy	750	/	10.4	[32]
	Arc-melting	945 ± 14	656 ± 22	17.3 ± 1.3	[57]

resilience properties, lightweight with high damping behavior [44]. This uniqueness of SMA made it suitable for vibration control, drive, sensing and structural reworking, exclusively in medical applications [101]. The processability of these material through conventional route is ineffective and in other hand SLM method end with close geometrical tolerance and good surface finish.

SMA materials such as NiTi alloy used for medical implants are potentially fabricated through SLM process [108]. As it has been used in implant applications, the shape and size of the component prepared is important consideration. Developing the component to the near net shape through SLM is possible and also obligatory. SLM is extensively employed for producing complex and fully functional NiTi parts. Based on the parametric consideration, the behavior of the component will be changed. The NiTi based component with varying transition temperature is produced by the proper selection of SLM parameters. The properties and microstructure of the produced components are influenced by the factors namely scan speed, power, and thickness of powder layer, scan path and focus size.

It is observed that higher laser power with cooling rate leads to non-equilibrium solidification process and also influence the microstructure of the materials [10]. Bormann et al. reported the increased martensite transformation temperature at higher laser power densities [10]. The phase transition temperature of SMA is affected highly by the concentration of Ni content in the alloy and higher the Ni will decrease the temperature [25]. The SLM process influences the change in the Ni content in the alloy and hence temperature may change. During the SLM process, Ni content from the alloy is removed by evaporation as time elapsed for exposure of laser is increased. Louvis et al. [61] have revealed that depletion of Ni is encumbered because of the oxide layer formation. The investigation also reports that the depletion near melt pool area is partially recompensed by diffusion route.

While process through SLM, the better bonding between the layers is achieved by the proper parameter selection. The higher laser input with slower scanning speed ensuring the good bonding across the SLM processed layers which influencing the properties of the components made [107]. In addition, the size of the laser beam also prompting the quality of SLM parts. On the other hand, the laser beam focusing position also affecting the surface quality of the material. The influence of focus diameter of laser beam at varying focus position of $61\text{ }\mu\text{m}$ and $128\text{ }\mu\text{m}$ on two varying Ni50.2Ti samples are investigated by Habijan et al. [28]. The result revealed that the position of $61\text{ }\mu\text{m}$ has resulted in the reduced particle adherence and Fig. 5.11 shows the microscopic image of SLM processed parts.

Table 5.2 detailing the findings of various researchers depicting the effects of laser parameters on grain size of NiTi alloy fabricated through SLM and LENS process. The grain morphology of the particle with varying exposure time and laser power are determined and presented as Fig. 5.12.

The presence of Ti elements and their effect on properties are investigated by the researchers. The average micro hardness of NiTi alloy tends to increase with the higher Ti element as it leads to the formation of NiTi_2 [89]. According to Shishkovsky et al. 1.5–2 times increased microhardness was observed on NiTi alloy prepared through SLM pressed than conventional cast process route [88]. It is understood that the temperature and phase transition duration affect the hardness of NiTi alloys. Interestingly, Saedi et al. investigated the Ni rich NiTi alloy sample processed through SLM route and determined the effect of post heat treatment on hardness. Figure 5.13

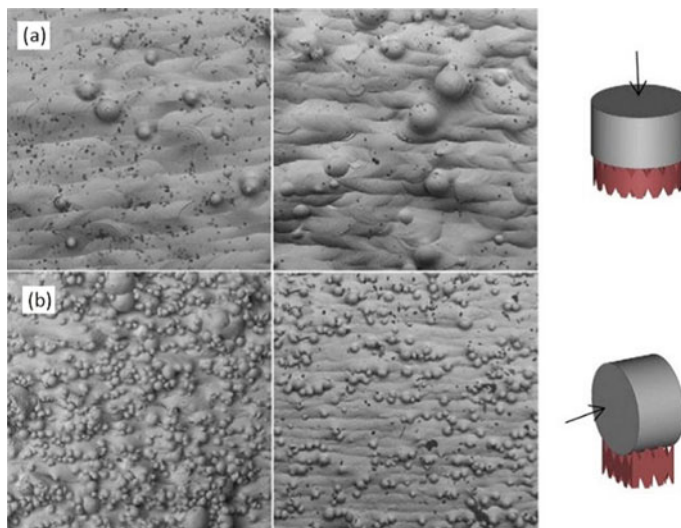
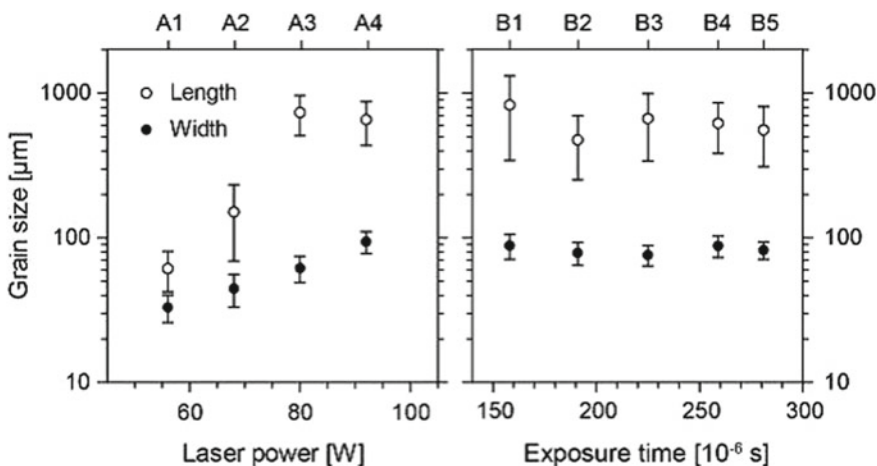


Fig. 5.11 SEM micrographs showing the effect of two different beam diameters of $128\text{ }\mu\text{m}$ (left) and $61\text{ }\mu\text{m}$ (right) on the level of adherent particles as well as the top surface quality of SLM NiTi: **a** vertically fabricated; **b** horizontally fabricated [28]

Table 5.2 Laser parameters versus Grain size

Methods	Size of the particles (μm)	Scanning speed (mm/s)	Laser power (W)	Length of grain (μm)	Width of grain (μm)
SLM [9]	35–180	133	56–100	61–655	33–90
		107–190	80	145–172	185–190
LENS [64]	50–150	20	200–400	–	8.5–15.2
		10–20	200	–	8.5–9.5
		10–20	400	–	11.5–15.2
LENS [49]	50–150	15	300–500	–	3.7–6.7
		10–15	300	–	3.2–3.7
		10–15	500	–	6.3–6.7

**Fig. 5.12** The variation of grain size with SLM Process parameters [9]

shows the optical micrographs of the initial ingot, and as-fabricated and solutionized SLM Ni50.8Ti49.2 alloys [85].

Zhao et al. [111] have fabricated near eutectic Ni–Sn alloy by blending the powders using SLM process. The microstructure of the samples are investigated and due to thermal stress induced during the process, defects such as cracks and pores are formed. Moreover, it is understood that the chemical homogeneity is observed on the sample processed at lower scanning speed and power. Also reported that post annealing of elemental powder blends is the better solution to form two phase bulk material of near-eutectic composition.

Over all way, it is big task to produce SMA like NiTi alloy as it is high reactive owing to higher Ti presence. The traditional route are not effective and hence process like SLM is needed. SLM badges developing patient-specific implants captivating benefit of three-dimensional anthropometric and medical data for tissue engineering.

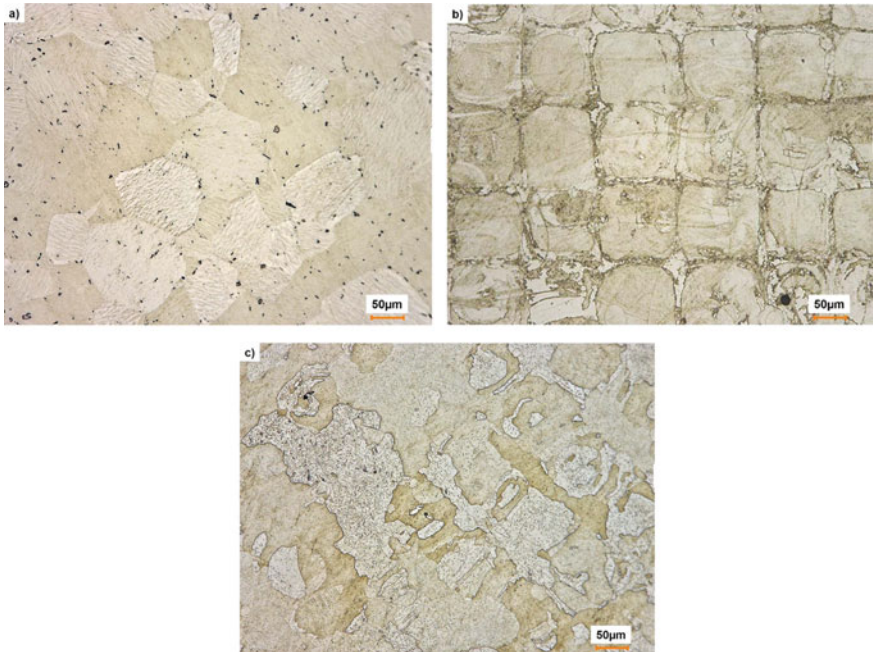


Fig. 5.13 Optical micrographs **a** the initial ingot, **b** the as-fabricated, and **c** the solutionized Ni50.8Ti49.2 alloys [84]

Finally defects formation on parts are still need to be investigated by the proper selection of parameters and it is again a great challenge.

5.2.3 Properties of SLMed Co and Co Alloys with Challenges

One of the most commonly used cobalt-based biomaterials is CoCrMo alloy (Fig. 5.14). CoCrMo (CCM) alloys have been widely used for removable partial dentures, metal frames, porcelain-fused-to-metal crowns in dentistry and hip joint, knee joint, spinal fixation, coronary artery stents in orthopedics [16, 26, 30, 93, 100], ascribed to their excellent mechanical properties, superior corrosion and wear resistance, good biocompatibility and long service duration [26, 110]. The vast majority of orthopedic implants produced using this alloy are cast products. However, casting alloys have some disadvantages such as large grain size, dendritic structure, potential for casting defects such as tensile gaps, and relatively low tensile and fatigue strengths to wrought alloys. These disadvantages have been tried to be eliminated as a result of the production of surgical implants from forged CoCrMo alloys. The cobalt-based alloy group is generally resistant to abrasion, corrosion and high temperatures. The solid-state effect of chromium, tungsten and molybdenum in cobalt-based alloys, the

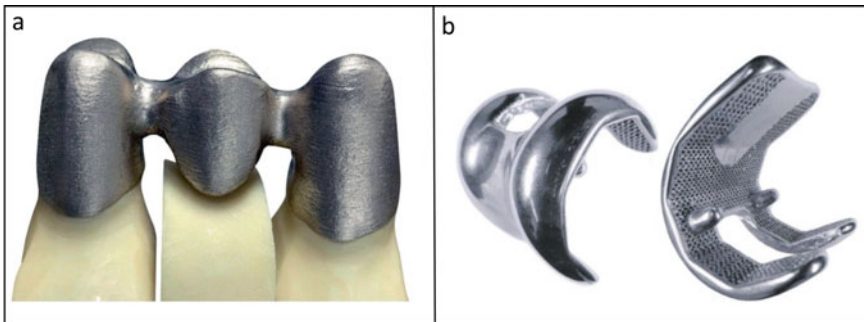


Fig. 5.14 CoCr alloy produced by additive manufacturing **a** Dental bridge [20], **b** Knee joint [67]

formation of metal carbides and the corrosion resistance of chromium originate from the crystallographic nature of cobalt [13].

The cobalt-based alloys used today are generally derived from CoCrW and CoCrMo ternary alloys. Co-Cr binary alloy is high-strength and stainless, and the subsequent addition of tungsten and molybdenum to the Co-Cr system are strength-giving factors. While these alloys were used in elements such as turbine blades where durability at high temperatures were used in the years they started to be used, today they are mostly preferred for wear resistance. These alloys are known with trade names such as Stellite, Haynes, Vitallium, Biodur and are a wide range of alloy types [18]. The main structures that can be encountered in cobalt chrome based alloys are YMK structured σ ($\text{Co}0.4\text{Cr}0.6$), SPH structured σ , YMK structured cobalt phase α (or γ) and SPH structured cobalt phase σ . Along with these, different phases may also exist depending on other alloying elements [74].

Due to the low workability of Cobalt-Chromium alloy, some complex components, such as dentures and hip joint, are difficult to be fabricated by the conventional wrought method, while the near net shape forming techniques especially the additive manufacturing (AM) become more and more attractive [26]. Selective laser melting (SLM) and electron beam melting (EBM) are the most commonly used AM techniques for metals. The SLM method provides superiority compared to systems using EBM, with relatively low maintenance costs and ease of processing, since it does not require a vacuum environment during laser melting of the powdered material.

There have been many studies in the literature investigating the structural and mechanical properties of CrCo alloys produced with SLM, depending on the production parameters. In a study where CoCrMo alloy was produced by Direct Laser Metal Sintering process and 200 W laser power, 7 m/s scanning speed and 20 μm layer thickness parameters were used, the sintered sample consisted of only γ (fcc) cobalt phase in powder form, while the sintered sample was both (fcc) and It also includes ε (hcp) phases. As a result of rapid cooling in the laser process, it has been determined that the cobalt-based alloy undergoes $\text{fcc} \leftrightarrow \text{hcp}$ martensitic transformation [6].

In a study by Takaichi et al., the microstructural and mechanical properties of Co-29Cr-6Mo alloy produced by SLM technique using different production parameters

were compared with the alloy produced by casting [93]. In the study, microstructure images obtained from samples produced with SLM using 200 W laser power and 0.1 mm hatch spacing values and produced by traditional casting method. Circular arch-shaped boundaries and numerous fine particles were observed in the OM image taken from the transverse cross section normal to the building direction. A SEM observation revealed that the latter included cellular dendrites with a diameter of about 2.7 mm. In the transverse cross section parallel to the building direction, gradual arch-shaped boundaries were observed almost normal to the building direction. The boundary spacing almost agreed with the stacking thickness of the powders (0.05 mm). Therefore, the boundaries may correspond to the fusion boundaries, which were formed by laser scans. In addition, fine lamellae elongated to the building direction were observed in the vertical cross section. This indicates that the cellular dendrites were grown along the building direction. These microscopic features were different from those of the as-cast alloy, which consisted of coarse dendrites with large particles [93].

Song et al. investigated (Morphology and properties of CoCrMo parts fabricated by selective laser melting) the effects of heat treatment as a post-process on CoCrMo alloy produced by SLM technique on the mechanical properties of the alloy [91]. The optimized parameters are using a laser power of 195 W, scan speed of 500 mm/s, scanning space of 0.08 mm/s and layer thickness of 0.025 mm. Heat treatment conditions were heating for 2 h at 1200 °C at a high temperature furnace under a nitrogen-protected atmosphere, followed by furnace cooling. The mean tensile strength of the parts fabricated by SLM was 1070 MPa, and 1210 MPa for the heat treated parts, both values being substantially higher than the 655 MPa for the standard cast alloy. Heat treatment resulted insubstantial increase in tensile strength. The yield strength declined to 662 MPa after heat treatment, but this was still higher than that of the standard as-cast state. The mean elongation of the parts fabricated directly by SLM at 7.2% was lower than the ASTM F75 standard (8%), but it almost doubled after heat treatment to 14.3%. It was evident that the hardness of the parts fabricated by SLM before and after heat processing was greater than that of the ASTM F75 standard, although, heat treatment did result in small decrease [91]. In addition, it was determined that the heat treatment of composites or alloys containing Co after SLM treatment considerably increased the wear resistance of the materials. In this context, as seen in Fig. 5.15, it has been understood that the wear resistance of Co-WC parts can be increased almost 15 times by heat treatment [11].

Additionally, CoCr alloys, especially used in dentistry, are popular materials with excellent corrosion resistance. However, it is very difficult to process due to its high hardness. For this reason, the production of CoCr materials is made with SLM today. In this method, in which complex shaped parts can be produced easily, no machining is required. However, it has been emphasized in the literature that post-production heat treatment with SLM is required to increase the mechanical properties of the materials [48].

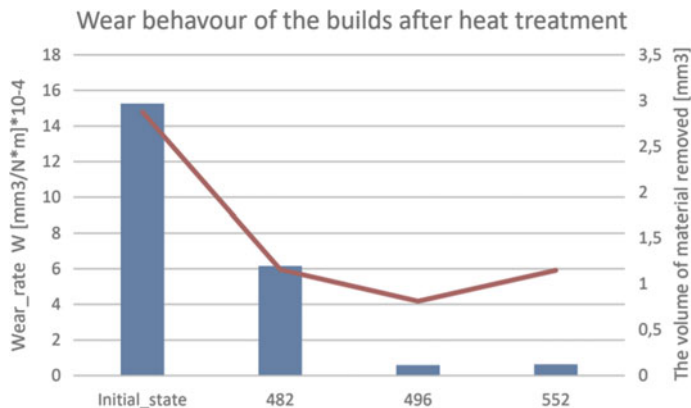


Fig. 5.15 Comparison of the tribological properties of WC–Co parts fabricated by SLM with heat treatment [11]

5.2.4 Properties of SLMed Al and Al Alloys with Challenges

Next to the steel and iron, aluminum and its alloys (AAs) are mostly used materials for structural purpose in the various engineering fields like automobile, aviation, defense, naval and power electronics applications. Thanks to their superior behaviors for example high strength to weight ratio, lower density, excellent corrosion resistance, easy processing and also the admirable thermal and electrical conductivity [31, 66, 104]. Currently, conventional methods such as casting, welding, extrusion, and powder metallurgy are used to produce AA based structural elements. Despite the widespread use of AAs products produced using these conventional methods, still issues are existing regarding their processing and applications. Table 5.3 shows the deficiencies of casting process of AAs which results in the reduced mechanical properties.

On the other hand, preparation through forming process of high performance AAs based components pushing towards long chain process with restricted adaptability. Further, the needs of modern industrial world progress towards developing AAs components having high performance and well-structured materials. For example, aerospace vehicle engines often employ a lattice or cellular structure to meet engineering necessities for high thermal conductivity, light weight, and high load carrying capacity. Integral forming process not only minimizing the cost and time for making

Table 5.3 Deficiencies in casting of AAs [39, 75, 94]

Causes	Behavioral Effect	Defects	Properties changes
Low cooling rate	Coarse microstructure	Slag inclusion, offset, defects, shrinkage porosity, element segregation	Lower mechanical properties

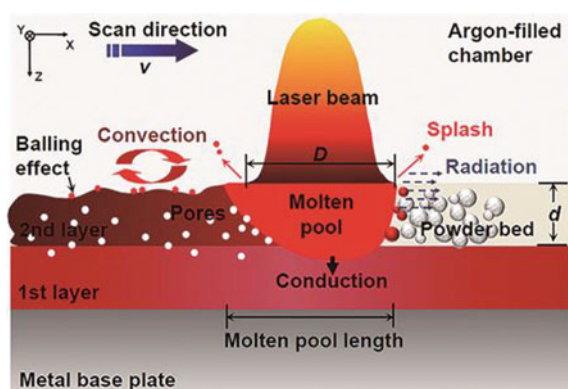
and assembly of small and medium scaled geometry employed for making complex structured elements. But also influencing to lower the weight and stress concentration commonly establish during the forming operations [54, 65, 68]. In this case, fabricating AAs parts with varying microstructure for the required applications and also with dimensional accuracy will be a challenging task for the researchers in the coming decades.

SLM is a suggested processing techniques which exploits laser beam to completely melt powders in appropriate environment and followed by solidification of molten metal [60]. Due to the faster cooling rate, grain growth and segregation of alloying element is entertained. In addition to the stirring action, uniform and fine microstructure is produced which results in the improved strength and toughness. Conversely, the necessity from the industrial standards is not able to meet by the products made through SLM process. So as to overcome this snag, post treatment, surface modification and machining are required, which consumes more production time. Cyclic processing of laser beam resulting in the changes in the microstructure of the materials and hence it becomes anisotropic [90]. Consequently, the selection of process parameters namely, laser power, scanning speed, layer thickness etc. affect the quality of SLMed components. In contrast, these parameter selections are impacted by material behavior, size and shape of the particles, type of laser and fluidity of powder [17, 92].

As laser come into contact with metal powders during the process, a series of portents will occur as a part of heating and solidification process. The changes happening in the powders are depicted in Fig. 5.16. The various process parameters influencing the cooling and solidification process which also leads to the changes in microstructure of the materials. The size and microstructure depend on the cooling rate and solidification rate and sometimes morphology becomes cellular from dendritic. Hence the different form of grain structures is existing in SLMed parts. It is understood that the higher rate of cooling resulting in the formation of fine grain structured materials.

The higher power of laser and slow scanning speed increases the density of laser energy and interaction time. This leads to the formation of coarse microstructure due

Fig. 5.16 Interaction between powders and laser source [113]



to the induced lower temperature gradient and cooling rate [109]. On other hand, the faster scanning speed with lower power hinders grain growth. The thermal effect and distribution of heat sources in the material leads to residual stresses. As consequences, various defects specifically cracking, delamination are induced in and around the pool region owing to its high thermal conductivity and high thermal expansion [34]. When the induced stress surpasses its yield strength, crack, deformation and distortion is happening. AAs having varying solidification temperature range depends on their alloying elements, whereas 5XXX series having lower cracking tendency than other series.

Still more research work needs to be done in order to facilitate the SLM process for the fabrication of non-ferrous metals. There are few challenges are existing towards SLM of aluminum alloys compared to other metals. The poor fluidity, higher laser reflectivity, strong moisture absorption, higher thermal expansion and solidification range hinders the processing of AAs through SLM process. So far the research work on SLM of AAs are fabricating AlSi10Mg and Al-Si12 alloys only. As it has lower melting point and near-eutectic alloys with less shrinkage porosity, it is appropriate for SLM processing [3, 80]. The physical and mechanical properties of SLM processed Al-Si alloys were determined by the various researchers and presented in Table 5.4 and Table 5.5.

Li et al. [55] reported that the heat treatment affecting the microstructure and properties of the materials. The coarse particle of Si in the Al matrix is evident with the long heat treatment process. Moreover, it is understood that decrease in yield strength and ultimate tensile strength is observed after the heat treatment. The increases ductility in the vertical direction is noted and it is unfailing through analysis. In addition, high performance alloys can be produced by adding more soluble elements to Al alloys, since the SLM method provides faster solidification than traditional methods [82].

5.2.5 Properties of SLMed Cu and Cu Alloys with Challenges

Due to the high thermal and electrical conductivity of CAs, they are frequently preferred materials in electrical engineering fields. They are seen as an indispensable metal especially in the manufacture of cooling elements. CAs, which are obtained by the application of alloying that can provide precipitation hardening, can be produced with high strength in addition to their high thermal and electrical conductivity in heating and cooling systems [19, 62]. As it is known, the fact that the cooling elements have very complex structures encourages the fabrication of CAs with AM and thus mass production is inevitable. However, the very high thermal conductivity of CAs reduces the melting efficiency by reducing the absorption of the laser that occurs in AM. In this case, melting the powder material creates a huge energy input requirement. This negative situation of CAs with AM methods especially with selective laser melting (SLM) as stated by Jadhav et al. [36], causes the formation of highly

Table 5.4 Physical and mechanical properties of AlSi10Mg alloy

Condition	Ultimate tensile strength (MPa)	Yield strength (MPa)	Elongation (%)	Hardness (HV)
SLM processed [76]	~375	~270	~4	–
SLM processed [42]	~396	–	~3.5	136
SLM processed [103]	~360	–	~6	139–146
SLM processed [53]	~434	~322	~5.3	~133
SLM+solution at 450°C [53]	~282	~196	~13.4	~90
SLM+solution at 550 °C [53]	~168	~90	~23.7	~60
SLM+T6 [53]	~187	–	~19.5	~78
SLM processed [1]	~333	~268	~1.4	125
SLM+T6 [1]	~292	~239	~3.9	~103
SLM processed [99]	~391	~311	~7.2	–
SLM processed [99]	~455	~300	~5.4	–
SLM processed [24]	~377	~255	~1.2	–
SLM+annealing [24]	~256	~158	~9.9	–
SLM+T6 [24]	~284	~210	~4.9	–

Table 5.5 Physical and Mechanical Properties of Al-Si alloy

Materials	Condition	Ultimate tensile strength (MPa)	Yield strength (MPa)	Elongation (%)	Hardness
AlSi12 [55]	SLM+Solution	–	~110	~190	~25
AlSiMg0.75 [5]	SLM processed	~ 150	354.9	427.7	2.54
	SLM+annealing	~ 110	275.4	360.2	4.57
AlSi9Mg [73]	SLM processed	–	328	379	~8.1
AlSi12 [73]	SLM processed	–	~260	~380	~3
	SLM+annealing	–	~95	~140	~15
AlSi7Mg0.3 [46]	SLM processed	–	~200	~400	12–17

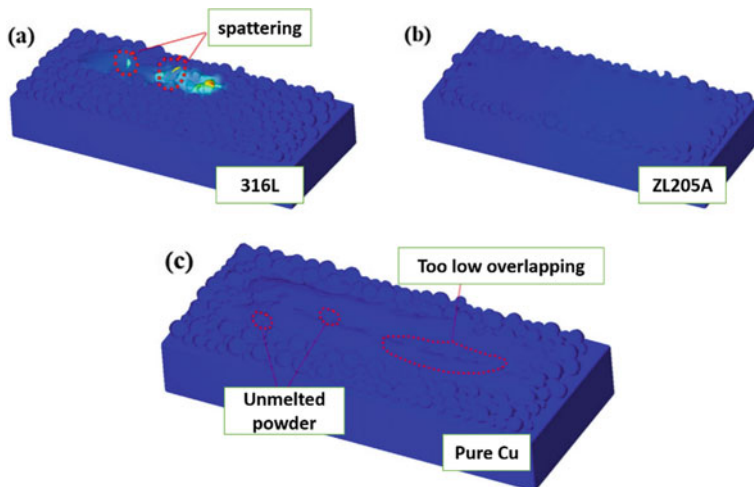


Fig. 5.17 Selective laser melted (SLMed) materials in **a** 316L, **b** ZL205A and **c** Pure copper [59]

porous structures like obtained in another study in comparison with some other metals (Fig. 5.17).

Moreover, we were determined in the previous study [97] that SLM process parameters also play a critical role in the production of SLM and such materials silver coated copper with high electrical and thermal conductivity. In the mentioned study, the effect of the scanning speed on the porosity on the internal structure is clearly noticed as can be seen in Fig. 5.18.

However, the result obtained in changing the process parameters was not satisfactory. During the production of high thermal conductivity materials such as copper and silver with SLM, the negative effect on laser behavior causes damage to the final products. In this context, Popovich et al. [71] applied heat treatment to the parts produced after producing Cu-Cr-Zr-Ti alloys by selective laser melting (SLM) method, which is an AM method, and stated that higher strength can be obtained by applying hot isostatic pressing of the final products obtained with SLM. During the production of CAs by AM methods, the high thermal conductivity of copper metal causes the final



Fig. 5.18 SLMed Cu-Ag core–shell particles with different scanning speeds; **a** 250 mm/s, **b** 300 mm/s and **c** 400 mm/s [97]

products to contain porosity, stratification, and regional thermal gradients. Therefore, it is clear that different tactics should be tried in the production of non-ferrous metals with high thermal conductivity coefficient such as CAs with AM. In order to overcome this problem caused by high thermal conductivity, in recent years, the laser absorption can be increased by coating the surfaces of CA powders with metals such as electroless tin (Sn) and nickel (Ni) [58]. Thanks to the metal coatings surrounding the CAs powders, the laser absorption will increase on the surfaces, the heat input will continuously increase and the melt pool will expand. This process will continue until the coating layer is distributed homogeneously in the CA matrix, and the region will continue to warm with secondary reflections from the melt pool (Fig. 5.19).

In this way, the porosity that will be experienced in uncoated CAs due to energy loss will be absorbed and structures with minimum porosity will be obtained. An example of porosities seen in finished products produced with AM from uncoated and Sn, Ni plated CAs powders is given in Fig. 5.20.

In addition, the copper metal's affinity for oxygen suggests that an oxide film layer can always form on the surface of CAs powders. Therefore, it can be ensured that the oxidation treatment of CAs materials before their production with AM methods

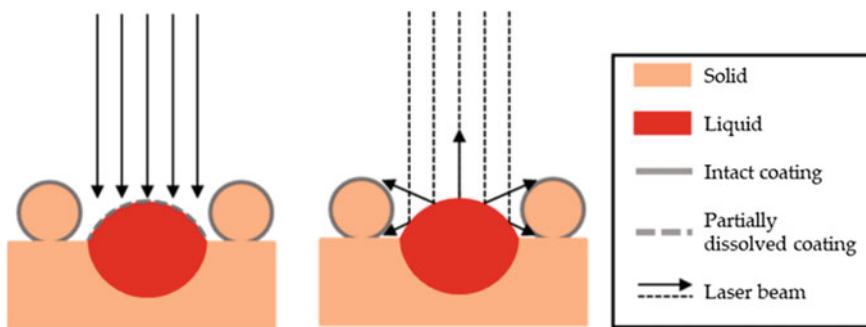


Fig. 5.19 Reflection mechanism in coated Cu powders during AM production [58]

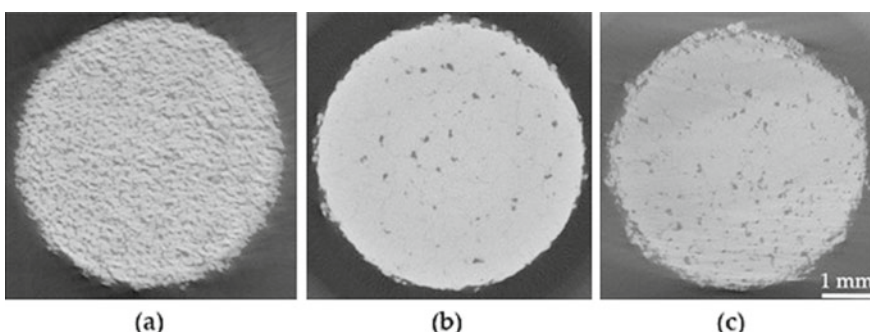


Fig. 5.20 Additive manufactured samples; **a** Cu, **b** Sn coated Cu, **c** Ni coated Cu (obtained from [58])

and their coating with a thin oxide-inhibiting polymeric film have a great effect on the direct increase of the final product density. In this context, Ledford et al. ensured that the initial copper powders were reduced in H₂ environment and covered with a polydimethylsiloxane (PDMS) polymeric film. Later, they stated that the final products produced by the AM method from these powders were denser and of low porosity [51]. In addition, Chao et al. [102] detected the presence of non-melting zones in the structure due to the low laser absorption of the copper metal during the production of copper-containing functional graded materials (FGMs) by the SLM method. Therefore, they emphasized that SLM parameters should be determined separately for each transition metal with modeling methods such as Taguchi. The low laser absorption property of CAs forces the use of high energy lasers during SLM processes. However, in this case, since evaporation may occur in some melting regions, the gas outlets cause porosity formation rapidly. Therefore, Yan et al. [106] have succeeded in producing copper parts with a density of more than 99% with SLM at high scanning speeds and low energy laser use. In this context, they produced a laser with 300 W power, which is not sufficient for CAs under normal conditions, but obtained the best density value when they used the scanning speed as 600 mm/s.

Jadhav et al. [37] studied on different parameters and process environment in SLM processing of surface oxidized copper particles. While they observed that sufficient density could not be achieved in the case of energy density of 300 and 400 W, they obtained more dense material when the working medium was nitrogen than when the working medium was argon. The relevant phenomenon is given in Fig. 5.21. In the production of parts made of copper and copper alloys by the AM methods, the removal of the produced parts can be difficult due to the high ductility of copper in addition to the production parameters. In addition, copper may require special handling and storage due to its low oxidation resistance [96].

5.3 Conclusions

Depending on the developing technology day by day, rapidity and quality material production in mass production gains great importance. Accordingly, in recent years, serial and superior material production with the use of metal powders has been carried out by AM methods. There are still many issues to be developed about new AM methods that provide superior advantages over powder metallurgy, casting, machining methods. Production of each metal and metal alloy with AM has different difficulties and appropriate Am methods are used. Especially in SLM method of AM methods, which are indispensable methods in the production of complex shaped parts, engineering parts are made by layering on the layer and layers are formed by the use of powder or wire selectively melted by a laser source followed by cooling. In this book chapter study, the advantages of the SLM method over other traditional methods in the production of Al, Ti, Ni, Co and Cu metals and their alloys were investigated and presented with examples. It has been reported that the biggest factor in the materials produced with SLM is the production process parameters. It is obvious that

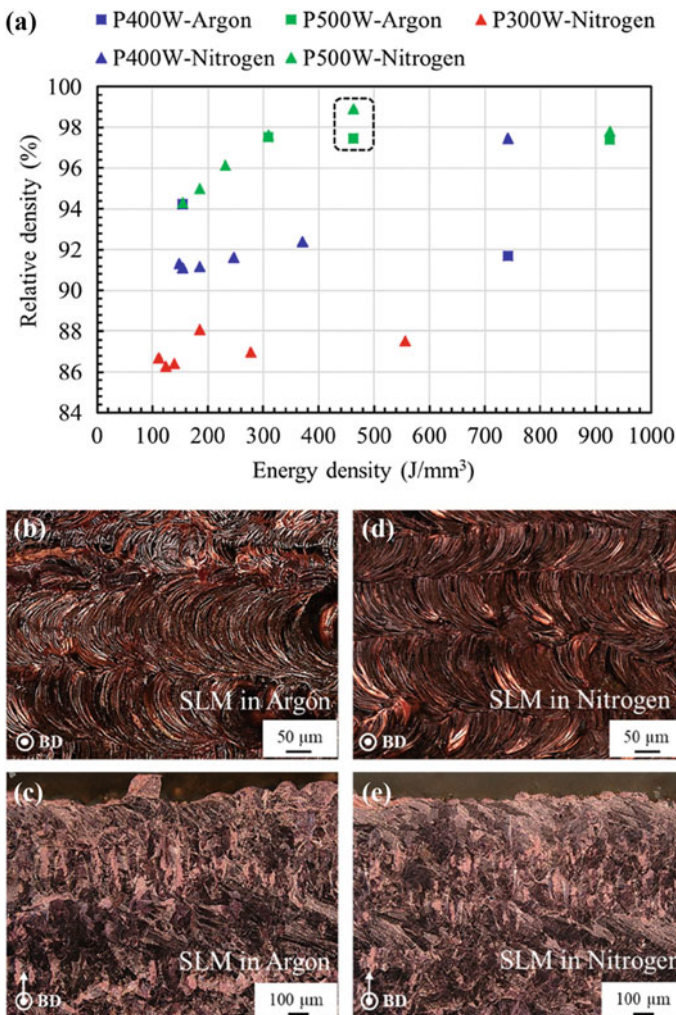


Fig. 5.21 The variation on (a) relative density and energy density of Cu samples fabricated by SLM and the top-cross section image in (b–c) argon and (d–e) nitrogen [37]

the materials can be produced at almost 100% density as a result of post-processing processes such as post-production rolling and with appropriate process parameters. For example, it has been determined that materials with high thermal conductivity, such as copper and silver, absorb the laser effect and require high laser power, while an unbalanced internal structure is formed in materials produced at high laser powers. Therefore, it is a critical point to adjust the process parameters according to the properties of the material to be produced. In the production of materials with high thermal conductivity, coating the powders with materials such as nickel before production and including them in the production can prevent laser absorption. In addition, post

processes such as rolling are applied to prevent the porosity created by the materials containing the non-melting regions due to laser absorption.

Acknowledgements The authors thank Scientific and Technological Research Council of Turkey (TÜBİTAK) for the financial support on this study with the project numbered 119M398.

References

1. Aboulkhair, N.T., Maskery, I., Tuck, C., Ashcroft, I., Everitt, N.M.: The microstructure and mechanical properties of selectively laser melted AlSi10Mg: the effect of a conventional T6-like heat treatment. *Mater. Sci. Eng. A.* **667**, 139–146 (2016). <https://doi.org/10.1016/j.msea.2016.04.092>
2. Advanced refractory metals: 6 major uses of titanium | refractory metals and alloys, <https://www.refractorymetal.org/uses-of-titanium/>
3. Arvie, C., Galy, C., Le Guen, E., Lacoste, E.: Relative density of SLM-produced aluminum alloy parts: interpretation of results. *J. Manuf. Mater. Process.* **4**, 83 (2020). <https://doi.org/10.3390/JMMP4030083>
4. Attar, H., Calin, M., Zhang, L.C., Scudino, S., Eckert, J.: Manufacture by selective laser melting and mechanical behavior of commercially pure titanium. *Mater. Sci. Eng. A.* **593**, 170–177 (2014). <https://doi.org/10.1016/j.msea.2013.11.038>
5. Bai, Y., Yang, Y., Xiao, Z., Zhang, M., Wang, D.: Process optimization and mechanical property evolution of AlSiMg0.75 by selective laser melting. *Mater. Des.* **140**, 257–266 (2018). <https://doi.org/10.1016/j.matdes.2017.11.045>
6. Barucca, G., Santecchia, E., Majni, G., Girardin, E., Bassoli, E., Denti, L., Gatto, A., Iuliano, L., Moskalewicz, T., Mengucci, P.: Structural characterization of biomedical Co-Cr-Mo components produced by direct metal laser sintering. *Mater. Sci. Eng. C.* **48**, 263–269 (2015). <https://doi.org/10.1016/j.msec.2014.12.009>
7. Bathini, U., Srivatsan, T.S., Patnaik, A., Quick, T.: A study of the tensile deformation and fracture behavior of commercially pure titanium and titanium alloy: Influence of orientation and microstructure. *J. Mater. Eng. Perform.* **19**, 1172–1182 (2010). <https://doi.org/10.1007/s11665-010-9613-5>
8. Beal, J.D., Boyer, R., Sanders, D.: Forming of titanium and titanium alloys. In: Metalworking: Sheet Forming. pp. 656–669. ASM International (2018)
9. Bormann, T., Müller, B., Schinhammer, M., Kessler, A., Thalmann, P., De Wild, M.: Microstructure of selective laser melted nickel-titanium. *Mater. Charact.* **94**, 189–202 (2014). <https://doi.org/10.1016/j.matchar.2014.05.017>
10. Bormann, T., Schumacher, R., Müller, B., Mertmann, M., De Wild, M.: Tailoring selective laser melting process parameters for nitinol implants. *J. Mater. Eng. Perform.* **21**, 2519–2524 (2012). <https://doi.org/10.1007/s11665-012-0318-9>
11. Bricín, D., Jansa, Z., Somr, J., Elmanová, A., Kříž, A.: Influence of heat treatment on properties of SD251-PH1 composite produced by additive SLM technology. In: IOP Conference Series: Materials Science and Engineering. p. 012003. Institute of Physics Publishing (2020)
12. Buj-Corral, I., Tejo-Otero, A., Fenollosa-Artés, F.: Development of am technologies for metals in the sector of medical implants. *Metals (Basel).* **10**, 686 (2020). <https://doi.org/10.3390/met10050686>
13. Çelik, A., Bayrak, Ö., Alsaran, A., Kaymaz, I., Yetim, A.F.: Effects of plasma nitriding on mechanical and tribological properties of CoCrMo alloy. *Surf. Coatings Technol.* **202**, 2433–2438 (2008). <https://doi.org/10.1016/j.surco.2007.08.030>
14. Chen, H., Zhang, C., Jia, D., Wellmann, D., Liu, W.: Corrosion behaviors of selective laser melted aluminum alloys: A review. *Metals (Basel).* **10**, 102 (2020). <https://doi.org/10.3390/met10010102>

15. Chen, S., Zhang, Y., Wu, Q., Gao, H., Gao, Z., Li, X.: Effect of solid-state phase transformation on residual stress of selective laser melting Ti6Al4V. *Mater. Sci. Eng. A.* **819**, 141299 (2021). <https://doi.org/10.1016/j.msea.2021.141299>
16. Chen, Y., Li, Y., Koizumi, Y., Haider, H., Chiba, A.: Effects of carbon addition on wear mechanisms of CoCrMo metal-on-metal hip joint bearings. *Mater. Sci. Eng. C.* **76**, 997–1004 (2017). <https://doi.org/10.1016/j.msec.2017.03.211>
17. Clare, A.T., Chalker, P.R., Davies, S., Sutcliffe, C.J., Tsopanos, S.: Selective laser melting of high aspect ratio 3D nickel-titanium structures two way trained for MEMS applications. *Int. J. Mech. Mater. Des.* **4**, 181–187 (2008). <https://doi.org/10.1007/s10999-007-9032-4>
18. Cramer, D.S., Covino, S.B. (eds): Corrosion of cobalt and cobalt-base alloys. In: *Corrosion: Materials*. pp. 164–176. ASM International (2018)
19. DeGroh, H.C., Ellis, D.L., Loewenthal, W.S.: Comparison of GRCop-84 to other Cu alloys with high thermal conductivities. *J. Mater. Eng. Perform.* **17**, 594–606 (2008). <https://doi.org/10.1007/s11665-007-9175-3>
20. EOS: 3D printing of dental restorations. *Met. Powder Rep.* **68**, 32–33 (2013). [https://doi.org/10.1016/S0026-0657\(13\)70062-6](https://doi.org/10.1016/S0026-0657(13)70062-6)
21. Facchini, L., Magalini, E., Robotti, P., Molinari, A., Höges, S., Wissenbach, K.: Ductility of a Ti-6Al-4V alloy produced by selective laser melting of prealloyed powders. *Rapid Prototyp. J.* **16**, 450–459 (2010). <https://doi.org/10.1108/13552541011083371>
22. Farber, E., Zhu, J.N., Popovich, A., Popovich, V.: A review of NiTi shape memory alloy as a smart material produced by additive manufacturing. In: *Materials Today: Proceedings*. pp. 761–767. Elsevier Ltd (2019)
23. Fereiduni, E., Ghasemi, A., Elbestawi, M.: Selective laser melting of aluminum and titanium matrix composites: recent progress and potential applications in the aerospace industry. *Aerospace* **7**, 77 (2020). <https://doi.org/10.3390/AEROSPACE7060077>
24. Fousová, M., Dvorský, D., Michalcová, A., Vojtěch, D.: Changes in the microstructure and mechanical properties of additively manufactured AlSi10Mg alloy after exposure to elevated temperatures. *Mater. Charact.* **137**, 119–126 (2018). <https://doi.org/10.1016/j.matchar.2018.01.028>
25. Frenzel, J., George, E.P., Dlouhy, A., Somsen, C., Wagner, M.F.X., Eggeler, G.: Influence of Ni on martensitic phase transformations in NiTi shape memory alloys. *Acta Mater.* **58**, 3444–3458 (2010). <https://doi.org/10.1016/j.actamat.2010.02.019>
26. Gong, X., Li, Y., Nie, Y., Huang, Z., Liu, F., Huang, L., Jiang, L., Mei, H.: Corrosion behaviour of CoCrMo alloy fabricated by electron beam melting. *Corros. Sci.* **139**, 68–75 (2018). <https://doi.org/10.1016/j.corsci.2018.04.033>
27. Grand view research: metal powder market size analysis report, 2020–2027, <https://www.grandviewresearch.com/industry-analysis/metal-powder-market>
28. Habijan, T., Haberland, C., Meier, H., Frenzel, J., Wittsiepe, J., Wuwer, C., Greulich, C., Schildhauer, T.A., Köller, M.: The biocompatibility of dense and porous Nickel-Titanium produced by selective laser melting. *Mater. Sci. Eng. C.* **33**, 419–426 (2013). <https://doi.org/10.1016/j.msec.2012.09.008>
29. Hacisalihoğlu, I., Yıldız, F., Çelik, A.: The effects of build orientation and hatch spacing on mechanical properties of medical Ti–6Al–4V alloy manufactured by selective laser melting. *Mater. Sci. Eng. A.* **802**, 140649 (2021). <https://doi.org/10.1016/j.msea.2020.140649>
30. Hedberg, Y.S., Qian, B., Shen, Z., Virtanen, S., Odnevall Wallinder, I.: In vitro biocompatibility of CoCrMo dental alloys fabricated by selective laser melting. *Dent. Mater.* **30**, 525–534 (2014). <https://doi.org/10.1016/j.dental.2014.02.008>
31. Heinz, A., Haszler, A., Keidel, C., Moldenhauer, S., Benedictus, R., Miller, W.S.: Recent development in aluminium alloys for aerospace applications. *Mater. Sci. Eng. A.* **280**, 102–107 (2000). [https://doi.org/10.1016/S0921-5093\(99\)00674-7](https://doi.org/10.1016/S0921-5093(99)00674-7)
32. Henriques, V.A.R., Galvani, E.T., Petroni, S.L.G., Paula, M.S.M., Lemos, T.G.: Production of Ti-13Nb-13Zr alloy for surgical implants by powder metallurgy. *J. Mater. Sci.* **45**, 5844–5850 (2010). <https://doi.org/10.1007/s10853-010-4660-8>

33. Herzog, D., Seyda, V., Wycisk, E., Emmelmann, C.: Additive manufacturing of metals. *Acta Mater.* **117**, 371–392 (2016). <https://doi.org/10.1016/j.actamat.2016.07.019>
34. Hussein, A., Hao, L., Yan, C., Everson, R.: Finite element simulation of the temperature and stress fields in single layers built without-support in selective laser melting. *Mater. Des.* **52**, 638–647 (2013). <https://doi.org/10.1016/j.matdes.2013.05.070>
35. ikbooks: ferrous materials and non-ferrous metals and alloys, https://www.ikbooks.com/home/samplechapter?filename=150_Sample-Chapter.pdf
36. Jadhav, S.D., Dadbakhsh, S., Goossens, L., Kruth, J.P., Van Humbeeck, J., Vanmeensel, K.: Influence of selective laser melting process parameters on texture evolution in pure copper. *J. Mater. Process. Technol.* **270**, 47–58 (2019). <https://doi.org/10.1016/j.jmatprotec.2019.02.022>
37. Jadhav, S.D., Vleugels, J., Kruth, J.P., Van Humbeeck, J., Vanmeensel, K.: Mechanical and electrical properties of selective laser-melted parts produced from surface-oxidized copper powder. *Mater. Des. Process. Commun.* **2**, (2020). <https://doi.org/10.1002/mdp2.94>
38. John, V.: Non-ferrous metals and alloys. In: *Introduction to Engineering Materials*. pp. 195–220. Palgrave Macmillan UK, London (1992)
39. Kang, J., Huang, T., Radhakrishnan, P., Wang, W., Yi-ming, R.: Modeling and simulation of heat transfer in loaded continuous heat treatment furnace. In: 14th International Federation for Heat Treatment and Surface Engineering Congress. pp. 69–72. , Shanghai (2004)
40. Karimi, J., Suryanarayana, C., Okulov, I., Prashanth, K.G.: Selective laser melting of Ti6Al4V: effect of laser re-melting. *Mater. Sci. Eng. A.* **805**, 140558 (2021).<https://doi.org/10.1016/j.msea.2020.140558>
41. Kaya, G., Yıldız, F., Hacisalihoglu, İ.: Characterization of the structural and tribological properties of medical Ti6Al4V alloy produced in different production parameters using selective laser melting. *3D Print. Addit. Manuf.* **6**, 253–261 (2019). <https://doi.org/10.1089/3dp.2019.0017>
42. Kempen, K., Thijs, L., Humbeeck, J.V., Kruth, J.P.: Processing AlSi10Mg by selective laser melting: Parameter optimisation and material characterisation. *Mater. Sci. Technol. (United Kingdom)* **31**, 917–923 (2015). <https://doi.org/10.1179/1743284714Y.00000000702>
43. Khomutov, M., Potapkin, P., Cheverikin, V., Petrovskiy, P., Travyanov, A., Logachev, I., Sova, A., Smurov, I.: Effect of hot isostatic pressing on structure and properties of intermetallic NiAl–Cr–Mo alloy produced by selective laser melting. *Intermetallics.* **120**, 106766 (2020).<https://doi.org/10.1016/j.intermet.2020.106766>
44. Khoo, Z.X., Liu, Y., Low, Z.H., An, J., Chua, C.K., Leong, K.F.: Fabrication of SLM NiTi Shape memory alloy via repetitive laser scanning. *Shape Mem. Superelasticity.* **4**, 112–120 (2018). <https://doi.org/10.1007/s40830-017-0139-7>
45. Khorasani, A.M., Gibson, I., Ghasemi, A.H., Ghaderi, A.: A comprehensive study on variability of relative density in selective laser melting of Ti-6Al-4V. *Virtual Phys. Prototyp.* **14**, 349–359 (2019). <https://doi.org/10.1080/17452759.2019.1614198>
46. Kimura, T., Nakamoto, T.: Microstructures and mechanical properties of A356 (AlSi7Mg0.3) aluminum alloy fabricated by selective laser melting. *Mater. Des.* **89**, 1294–1301 (2016). <https://doi.org/10.1016/j.matdes.2015.10.065>
47. Klarstrom, D., Crook, P., Sharif, A.: Cobalt Alloys: Alloying and Thermomechanical Processing. In: *Reference Module in Materials Science and Materials Engineering*. Elsevier (2017)
48. Konieczny, B., Szczesio-Włodarczyk, A., Sokolowski, J., Bociong, K.: Challenges of co-cr alloy additive manufacturing methods in dentistry-the current state of knowledge (Systematic review), www.mdpi.com/journal/materials, (2020)
49. Krishna, B.V., Bose, S., Bandyopadhyay, A.: Laser processing of net-shape NiTi shape memory alloy. *Metall. Mater. Trans. A Phys. Metall. Mater. Sci.* **38**, 1096–1103 (2007). <https://doi.org/10.1007/s11661-007-9127-4>
50. Kusuma, C., Ahmed, S.H., Mian, A., Srinivasan, R.: Effect of laser power and scan speed on melt pool characteristics of commercially pure titanium (CP-Ti). *J. Mater. Eng. Perform.* **26**, 3560–3568 (2017). <https://doi.org/10.1007/s11665-017-2768-6>

51. Ledford, C., Rock, C., Carriere, P., Frigola, P., Gamzina, D., Horn, T.: Characteristics and processing of hydrogen-treated copper powders for EB-PBF additive manufacturing. *Appl. Sci.* **9**, 3993 (2019). <https://doi.org/10.3390/app9193993>
52. Li, R., Liu, J., Shi, Y., Wang, L., Jiang, W.: Balling behavior of stainless steel and nickel powder during selective laser melting process. *Int. J. Adv. Manuf. Technol.* **59**, 1025–1035 (2012). <https://doi.org/10.1007/s00170-011-3566-1>
53. Li, W., Li, S., Liu, J., Zhang, A., Zhou, Y., Wei, Q., Yan, C., Shi, Y.: Effect of heat treatment on AlSi10Mg alloy fabricated by selective laser melting: Microstructure evolution, mechanical properties and fracture mechanism. *Mater. Sci. Eng. A* **663**, 116–125 (2016). <https://doi.org/10.1016/j.msea.2016.03.088>
54. Li, W., Yang, K., Yin, S., Yang, X., Xu, Y., Lupoi, R.: Solid-state additive manufacturing and repairing by cold spraying: A review. *J. Mater. Sci. Technol.* **34**, 440–457 (2018). <https://doi.org/10.1016/j.jmst.2017.09.015>
55. Li, X.P., Wang, X.J., Saunders, M., Suvorova, A., Zhang, L.C., Liu, Y.J., Fang, M.H., Huang, Z.H., Sercombe, T.B.: A selective laser melting and solution heat treatment refined Al-12Si alloy with a controllable ultrafine eutectic microstructure and 25% tensile ductility. *Acta Mater.* **95**, 74–82 (2015). <https://doi.org/10.1016/j.actamat.2015.05.017>
56. Li, Y.H., Wang, B., Ma, C.P., Fang, Z.H., Chen, L.F., Guan, Y.C., Yang, S.F.: Material characterization, thermal analysis, and mechanical performance of a laser-polished Ti Alloy prepared by selective laser melting. *Metals (Basel.)* **9**, 112 (2019). <https://doi.org/10.3390/met9020112>
57. Lin, C.W., Ju, C.P., Chern Lin, J.H.: A comparison of the fatigue behavior of cast Ti-7.5Mo with c.p. titanium, Ti-6Al-4V and Ti-13Nb-13Zr alloys. *Biomaterials* **26**, 2899–2907 (2005). <https://doi.org/10.1016/j.biomaterials.2004.09.007>
58. Lindström, V., Liashenko, O., Zweicker, K., Derevianko, S., Morozovych, V., Lyashenko, Y., Leinenbach, C.: Laser powder bed fusion of metal coated copper powders. *Materials (Basel.)* **13**, 3493 (2020). <https://doi.org/10.3390/ma13163493>
59. Lingqin, X., Guang, C., Luyu, Z., Pan, L.: Explore the feasibility of fabricating pure copper parts with low-laser energy by selective laser melting. *Mater. Res. Express.* **7**, 106509 (2020). <https://doi.org/10.1088/2053-1591/abbd08>
60. Liu, Y., Yang, Y., Mai, S., Wang, D., Song, C.: Investigation into spatter behavior during selective laser melting of AISI 316L stainless steel powder. *Mater. Des.* **87**, 797–806 (2015). <https://doi.org/10.1016/j.matdes.2015.08.086>
61. Louvis, E., Fox, P., Sutcliffe, C.J.: Selective laser melting of aluminium components. *J. Mater. Process. Technol.* **211**, 275–284 (2011). <https://doi.org/10.1016/j.jmatprotec.2010.09.019>
62. Lu, L., Shen, Y., Chen, X., Qian, L., Lu, K.: Ultrahigh strength and high electrical conductivity in copper. *Science* (80-.). **304**, 422–426 (2004). <https://doi.org/10.1126/science.1092905>
63. Mahmoodian, M.: Introduction. In: *Reliability and Maintainability of In-Service Pipelines*. pp. 1–48. Elsevier (2018)
64. Marattukalam, J.J., Singh, A.K., Datta, S., Das, M., Balla, V.K., Bontha, S., Kalpathy, S.K.: Microstructure and corrosion behavior of laser processed NiTi alloy. *Mater. Sci. Eng. C* **57**, 309–313 (2015). <https://doi.org/10.1016/j.msec.2015.07.067>
65. Mishra, R.S., Ma, Z.Y.: *Friction stir welding and processing*, (2005)
66. Mohyaldeen, H., Williams, J.C., Starke, E.A.: Progress in structural materials for aerospace systems. *Acta Mater.* **51**, 5775–5799 (2003). <https://doi.org/10.1016/j.actamat.2003.08.023>
67. Murr, L.E., Gaytan, S.M., Martinez, E., Medina, F., Wicker, R.B.: Next generation orthopaedic implants by additive manufacturing using electron beam melting. *Int. J. Biomater.* (2012). <https://doi.org/10.1155/2012/245727>
68. Nie, F., Dong, H., Chen, S., Li, P., Wang, L., Zhao, Z., Li, X., Zhang, H.: Microstructure and mechanical properties of pulse MIG welded 6061/A356 aluminum alloy dissimilar butt joints. *J. Mater. Sci. Technol.* **34**, 551–560 (2018). <https://doi.org/10.1016/j.jmst.2016.11.004>
69. Petersen, J.: Morgan Stanley's cobalt report mirrors my analysis of tesla's supply chain risks (NASDAQ:TSLA) | Seeking Alpha. <https://seekingalpha.com/article/4106081-morgan-stanleys-cobalt-report-mirrors-analysis-of-teslas-supply-chain-risks>

70. Polozov, I., Sufiarov, V., Kantukov, A., Masaylo, D., Popovich, A.: Tailoring microstructure and properties of graded Ti-22Al-25Nb/SiC and Ti-22Al-25Nb/Ti-6Al-4V alloys by in-situ synthesis during selective laser melting. In: Materials Today: Proceedings. pp. 672–678. Elsevier Ltd (2019)
71. Popovich, A., Sufiarov, V., Polozov, I., Borisov, E., Masaylo, D., Orlov, A.: Microstructure and mechanical properties of additive manufactured copper alloy. Mater. Lett. **179**, 38–41 (2016). <https://doi.org/10.1016/j.matlet.2016.05.064>
72. Pourret, O., Faucon, M.-P.: Cobalt. In: White, W.M. (ed.) Encyclopedia of Geochemistry, pp. 1–3. Springer, Cham (2016)
73. Prashanth, K.G., Scudino, S., Klauss, H.J., Surreddi, K.B., Löber, L., Wang, Z., Chaubey, A.K., Kühn, U., Eckert, J.: Microstructure and mechanical properties of Al-12Si produced by selective laser melting: Effect of heat treatment. Mater. Sci. Eng. A. **590**, 153–160 (2014). <https://doi.org/10.1016/j.msea.2013.10.023>
74. Rajan, K.: Thermodynamic assessment of heat treatments for a Co-Cr-Mo alloy. J. Mater. Sci. **18**, 257–264 (1983). <https://doi.org/10.1007/BF00543833>
75. Ranganath, S.: Review on particulate-reinforced titanium matrix composites. J. Mater. Sci. **32**, 1–16 (1997)
76. Read, N., Wang, W., Essa, K., Attallah, M.M.: Selective laser melting of AlSi10Mg alloy: Process optimisation and mechanical properties development. Mater. Des. **65**, 417–424 (2015). <https://doi.org/10.1016/j.matdes.2014.09.044>
77. Ren, Z., Zhang, D.Z., Fu, G., Jiang, J., Zhao, M.: High-fidelity modelling of selective laser melting copper alloy: Laser reflection behavior and thermal-fluid dynamics. Mater. Des. **207**, 109857 (2021).<https://doi.org/10.1016/j.matdes.2021.109857>
78. Reports and Data: aluminum alloys market size, Demand, 2017–2027 | Global Report
79. Reports and Data: Nickel alloys market share, analysis | global industry report, 2019–2026. (2018)
80. Romanova, V., Balokhonov, R., Zinovieva, O., Emelianova, E., Dymnich, E., Pisarev, M., Zinoviev, A.: Micromechanical simulations of additively manufactured aluminum alloys. Comput. Struct. **244**, 106412 (2021).<https://doi.org/10.1016/j.compstruc.2020.106412>
81. Rombouts, M.: Selective laser sintering/melting of iron-based powders (Selectief laser sinteren/smelen van ijzergebaseerde poeders), <https://lirias.kuleuven.be/1751565>, (2006)
82. Rometsch, P., Jia, Q., V. Yang, K., Wu, X.: Aluminum alloys for selective laser melting - towards improved performance. In: Additive Manufacturing for the Aerospace Industry. pp. 301–325. Elsevier Inc. (2019)
83. Saadlaoui, Y., Milan, J.L., Rossi, J.M., Chabrand, P.: Topology optimization and additive manufacturing: comparison of conception methods using industrial codes, (2017)
84. Saedi, S., Turabi, A.S., Andani, M.T., Haberland, C., Elahinia, M., Karaca, H.: Thermomechanical characterization of Ni-rich NiTi fabricated by selective laser melting. Smart Mater. Struct. **25**, 035005 (2016).<https://doi.org/10.1088/0964-1726/25/3/035005>
85. Saedi, S., Turabi, A.S., Andani, M.T., Moghaddam, N.S., Elahinia, M., Karaca, H.E.: Texture, aging, and superelasticity of selective laser melting fabricated Ni-rich NiTi alloys. Mater. Sci. Eng. A. **686**, 1–10 (2017). <https://doi.org/10.1016/j.msea.2017.01.008>
86. Schipper, B.W., Lin, H.C., Meloni, M.A., Wansleeben, K., Heijungs, R., van der Voet, E.: Estimating global copper demand until 2100 with regression and stock dynamics. Resour. Conserv. Recycl. **132**, 28–36 (2018). <https://doi.org/10.1016/j.resconrec.2018.01.004>
87. Shi, X., Ma, S., Liu, C., Chen, C., Wu, Q., Chen, X., Lu, J.: Performance of high layer thickness in selective laser melting of Ti6Al4V. Materials (Basel) **9**, 975 (2016). <https://doi.org/10.3390/ma9120975>
88. Shishkovsky, I., Yadroitsev, I., Smurov, I.: Direct selective laser melting of nitinol powder. In: Physics Procedia. pp. 447–454. Elsevier B.V. (2012)
89. Shiva, S., Palani, I.A., Mishra, S.K., Paul, C.P., Kukreja, L.M.: Investigations on the influence of composition in the development of Ni-Ti shape memory alloy using laser based additive manufacturing. Opt. Laser Technol. **69**, 44–51 (2015). <https://doi.org/10.1016/j.optlastec.2014.12.014>

90. Song, B., Dong, S., Coddet, P., Liao, H., Coddet, C.: Fabrication of NiCr alloy parts by selective laser melting: Columnar microstructure and anisotropic mechanical behavior. *Mater. Des.* **53**, 1–7 (2014). <https://doi.org/10.1016/j.matdes.2013.07.010>
91. Song, C., Zhang, M., Yang, Y., Wang, D., Jia-kuo, Y.: Morphology and properties of CoCrMo parts fabricated by selective laser melting. *Mater. Sci. Eng. A.* **713**, 206–213 (2018). <https://doi.org/10.1016/j.msea.2017.12.035>
92. Spierings, A.B., Herres, N., Levy, G.: Influence of the particle size distribution on surface quality and mechanical properties in AM steel parts. *Rapid Prototyp. J.* **17**, 195–202 (2011). <https://doi.org/10.1108/1355254111124770>
93. Takaichi, A., Suyalatu, Nakamoto, T., Joko, N., Nomura, N., Tsutsumi, Y., Migita, S., Doi, H., Kurosu, S., Chiba, A., Wakabayashi, N., Igarashi, Y., Hanawa, T.: Microstructures and mechanical properties of Co-29Cr-6Mo alloy fabricated by selective laser melting process for dental applications. *J. Mech. Behav. Biomed. Mater.* **21**, 67–76 (2013). <https://doi.org/10.1016/j.jmbbm.2013.01.021>
94. Tjong, S.C., Ma, Z.Y.: Microstructural and mechanical characteristics of in situ metal matrix composites. *Mater. Sci. Eng. R Reports* **29**, 49–113 (2000). [https://doi.org/10.1016/S0927-796X\(00\)00024-3](https://doi.org/10.1016/S0927-796X(00)00024-3)
95. Tofail, S.A.M., Koumoulos, E.P., Bandyopadhyay, A., Bose, S., O'Donoghue, L., Charitidis, C.: Additive manufacturing: scientific and technological challenges, market uptake and opportunities. (2018). <https://doi.org/10.1016/j.mattod.2017.07.001>
96. Tran, T.Q., Chinnappan, A., Lee, J.K.Y., Loc, N.H., Tran, L.T., Wang, G., Kumar, V.V., Jayathilaka, W.A.D.M., Ji, D., Doddamani, M., Ramakrishna, S.: 3D printing of highly pure copper. *Metals (Basel.)* **9**, 756 (2019). <https://doi.org/10.3390/met9070756>
97. Varol, T., Hacısalihoğlu, I., Kaya, G., Güler, O., Yıldız, F., Aksa, H.C., Akçay, S.B.: The effect of selective laser melting process on the microstructure, density, and electrical conductivity of silver-coated copper cores. *J. Mater. Eng. Perform.* 1–11 (2021). <https://doi.org/10.1007/s11665-021-05712-5>
98. Vrancken, B., Thijs, L., Kruth, J.P., Van Humbeeck, J.: Heat treatment of Ti6Al4V produced by Selective Laser Melting: Microstructure and mechanical properties. *J. Alloys Compd.* **541**, 177–185 (2012). <https://doi.org/10.1016/j.jallcom.2012.07.022>
99. Wang, L., Jiang, X., Guo, M., Zhu, X., Yan, B.: Characterisation of structural properties for AlSi10Mg alloys fabricated by selective laser melting. *Mater. Sci. Technol. (United Kingdom)* **33**, 2274–2282 (2017). <https://doi.org/10.1080/02670836.2017.1398513>
100. Wang, X., Li, Y., Hou, Y., Bian, H., Koizumi, Y., Chiba, A.: Effects of surface friction treatment on the in vitro release of constituent metals from the biomedical Co-29Cr-6Mo-0.16N alloy. *Mater. Sci. Eng. C* **64**, 260–268 (2016). <https://doi.org/10.1016/j.msec.2016.03.050>
101. Wang, X., Yu, J., Liu, J., Chen, L., Yang, Q., Wei, H., Sun, J., Wang, Z., Zhang, Z., Zhao, G., Van Humbeeck, J.: Effect of process parameters on the phase transformation behavior and tensile properties of NiTi shape memory alloys fabricated by selective laser melting. *Addit. Manuf.* **36**, 101545 (2020). <https://doi.org/10.1016/j.addma.2020.101545>
102. Wei, C., Sun, Z., Chen, Q., Liu, Z., Li, L.: Additive manufacturing of horizontal and 3D functionally graded 316L/Cu10Sn components via multiple material selective laser melting. *J. Manuf. Sci. Eng. Trans. ASME* **141**, (2019). <https://doi.org/10.1115/1.4043983>
103. Wei, P., Wei, Z., Chen, Z., Du, J., He, Y., Li, J., Zhou, Y.: The AlSi10Mg samples produced by selective laser melting: single track, densification, microstructure and mechanical behavior. *Appl. Surf. Sci.* **408**, 38–50 (2017). <https://doi.org/10.1016/j.apsusc.2017.02.215>
104. Xu, W., Luo, Y., Zhang, W., Fu, M.: Comparative study on local and global mechanical properties of bobbin tool and conventional friction stir welded 7085–T7452 aluminum thick plate. *J. Mater. Sci. Technol.* **34**, 173–184 (2018). <https://doi.org/10.1016/j.jmst.2017.05.015>
105. Yadroitsev, I., Bertrand, P., Smurov, I.: Parametric analysis of the selective laser melting process. *Appl. Surf. Sci.* **253**, 8064–8069 (2007). <https://doi.org/10.1016/j.apsusc.2007.02.088>
106. Yan, X., Chang, C., Dong, D., Gao, S., Ma, W., Liu, M., Liao, H., Yin, S.: Microstructure and mechanical properties of pure copper manufactured by selective laser melting. *Mater. Sci. Eng. A* **789**, 139615 (2020). <https://doi.org/10.1016/j.msea.2020.139615>

107. Yang, Y., Huang, Y., Wu, W.: One-step shaping of NiTi biomaterial by selective laser melting. In: Lasers in Material Processing and Manufacturing III. p. 68250C. SPIE (2007)
108. Yu, Z., Xu, Z., Guo, Y., Xin, R., Liu, R., Jiang, C., Li, L., Zhang, Z., Ren, L.: Study on properties of SLM-NiTi shape memory alloy under the same energy density. *J. Mater. Res. Technol.* **13**, 241–250 (2021). <https://doi.org/10.1016/j.jmrt.2021.04.058>
109. Zhang, Q., Xue, H., Tang, Q., Pan, S., Rettenmayr, M., Zhu, M.: Microstructural evolution during temperature gradient zone melting: Cellular automaton simulation and experiment. *Comput. Mater. Sci.* **146**, 204–212 (2018). <https://doi.org/10.1016/j.commatsci.2018.01.032>
110. Zhang, X., Li, Y., Tang, N., Onodera, E., Chiba, A.: Corrosion behaviour of CoCrMo alloys in 2 wt% sulphuric acid solution. *Electrochim. Acta* **125**, 543–555 (2014). <https://doi.org/10.1016/j.electacta.2014.01.143>
111. Zhao, R., Gao, J., Liao, H., Fenineche, N., Coddet, C.: Selective laser melting of elemental powder blends for fabrication of homogeneous bulk material of near-eutectic Ni-Sn composition. *Addit. Manuf.* **34**, 101261 (2020) <https://doi.org/10.1016/j.addma.2020.101261>
112. Zhao, X., Li, S., Zhang, M., Liu, Y., Sercombe, T.B., Wang, S., Hao, Y., Yang, R., Murr, L.E.: Comparison of the microstructures and mechanical properties of Ti-6Al-4V fabricated by selective laser melting and electron beam melting. *Mater. Des.* **95**, 21–31 (2016). <https://doi.org/10.1016/j.matdes.2015.12.135>
113. Zheng, L., Zhang, Q., Cao, H., Wu, W., Ma, H., Ding, X., Yang, J., Duan, X., Fan, S.: Melt pool boundary extraction and its width prediction from infrared images in selective laser melting. *Mater. Des.* **183**, 108110 (2019) <https://doi.org/10.1016/j.matdes.2019.108110>
114. Zhou, L., Yuan, T., Tang, J., He, J., Li, R.: Mechanical and corrosion behavior of titanium alloys additively manufactured by selective laser melting—a comparison between nearly β titanium, α titanium and $\alpha + \beta$ titanium. *Opt. Laser Technol.* **119**, 105625 (2019) <https://doi.org/10.1016/j.optlastec.2019.105625>

Chapter 6

Development and Optimization Study of Poly-Lactic Acid Blended Carbon Particles by Fused Deposition Modelling Method



S. P. Jani, A. Senthil Kumar, B. Anushraj, P. M. Mashinini,
and Sudhakar Uppalapati

6.1 Introduction

In present scenario manufacturing industries are looking forward to low production cost, increased life cycle of product, better consistency and also product dependability in today's dynamic environment. The increasing demand for specialized things in various fields such as plastic, automotive, jewel, high speed automobile, bio medical, aircraft, complicated geometry and nuance characteristics of vehicles has contributed to a growth in the use of layering technology [1–4]. This technology has confirmed to be a successful solution for factories to manufacture complicated products at a faster production rate with less manual labour, thus effectively eliminating the need for instant tooling and Architecture for Manufacturing (DfM)-related constraints. In the current situation, among the various layering technologies available, Because of its exact properties, such as the capacity to create multifaceted structures in a additive manufacturing process beginning from a Computer Assisted Design file and the ability to use different types of materials in the manufacturing industries,

S. P. Jani (✉) · S. Uppalapati

Department of Mechanical Engineering, Marri Laxman Reddy Institute of Technology and Management, Hyderabad 500043, India

A. S. Kumar

Department of Mechanical Engineering, Sethu Institute of Technology, Virudhunagar, India

B. Anushraj

School of Automotive and Mechanical Engineering, Kalasalingam Academy of Research and Education, Krishnankoil, Tamil Nadu, India

P. M. Mashinini

Department of Mechanical and Industrial Engineering Technology, University of Johannesburg, Doornfontein Campus, Johannesburg, South Africa

Fused Deposition Modelling (FDM) was selected as the focus field [5]. The affordability and viability of remote control of the process for the manufacture of personalized consumer products made this revolutionary technique a favorable means of manufacturing through different industries [6].

Tale et al. stated the most part interfacing bar are made utilizing carbon steel however lately aluminum composites are discovering its application in associating pole. In this work associating pole material is supplanted by aluminum based composite material fortified with silicon carbide and fly debris. What's more, it portrays the demonstrating, examination and 3d printing of interfacing bar. Contrasted with previous material to the new material found to have less weight [7].

Enrique Cuan-Urquiza et al. reported the increment in openness of melded fiber manufacture (FFF) machines has roused mainstream researchers to pursue the comprehension of the underlying presentation of parts created with this innovation. Different activities were defined in the writing to represent and evaluate the mechanical and physical characteristics of designs manufactured with FFF. Test representations of 3D printed segments have been widely published. In any event, hardly any tasks were developed to predict the properties of printed structures with computational models and to work significantly less with logical approximations [8].

Zhuo et al. utilizing 3D printing procedure in assembling ceaseless fiber strengthened composites was proposed and the upsides of utilizing this cycle in composite designs fabricating were examined. 3 point bowing examples were printed out utilizing a business composites 3D printer. The flexural strength and modulus were acquired, just as voids content, to assess the nature of the printed example. A work area Fusion Deposition Modeling (FDM) printer was changed for nonstop fiber fortified composites printing. Unusual fiber designs were planned and printed out. A composite carry structure with curvilinear fiber design was fabricated utilizing the ceaseless fiber 3D printing strategy [9].

The effects of two different kinds of impact modifiers, such as center shell elastic and aliphatic polyester, on the mechanical and warm 3D printing properties of polylactide (PLA) fibers have been discovered [10]. To begin with, PLA/sway modifier mixes were set up by dissolve mixing in a co-turning twin screw extruder with different groupings of impact modifiers and test examples by infusion formation [11]. Ductile and twisting tests, Dynamic Mechanical Investigation (DMA) and Charpy sudden impact test have examined the mechanical and warm properties of mixes. It was found that Charpy toughness resistance at loadings above 5 wt% was incredibly enhanced by center shell elastic (up to 74.6%). As demonstrated by DMA, the PLA/10 wt present center shell elastic mix displayed better damping execution when contrasted with slick PLA over the entire inspected recurrence range [12].

Mst Faujiya Afrose et al. investigated A FDM printer was utilized to print PLA canine bone test examples in three (X, Y and 45) diverse form directions. These canine bone parts depended on ASTM D638 standard and were consistently tried at 80, 70, 60 and 50% ostensible estimations of a definitive pliable pressure by utilizing a Zwick Z010 widespread testing machine [13].

The effect of layer thickness, deposition angle and infill on the overall flexural force in FDM specimens made from PLA was discussed by Luzanin et al. [14].

Recently some researcher studied, the functional relationship between the FDM parameters such as part orientations and raster angles analyzed from this analysis specimen strength, surface roughness and production cost [7, 8, 15].

The main objective of the present work is to find influenced process parameters of Fused Deposition Modelling (FDM) for carbon nano particles blended biodegradable Polylactic Acid (PLA) components. A Design of Experiment (DoE) of three factors and three levels (L9 orthogonal array) was taken to this study and the influenced processing parameters effect on the mechanical strength such as tensile strength, compressive strength, bending strength and shore hardness, as input variable infill rate, layer thickness, and print nozzle speed.

6.2 Fused Deposition Modelling

Fused Deposition Modelling (FDM) is a type of layer manufacturing that may be used to make components with complex interior geometry. An FDM printer is simply a CNC gantry machine with one or two extrusion nozzles heads. One nozzle is for the primary (modeling) material, while the next can be for secondary (support) material that is either quickly brittle or soluble in OH (alkaline) solutions in double-nozzle systems. Parts are made using the FFF technology by melting and extruding polymeric filament in a predefined pattern on to a base plate using a heated nozzle. The thermoplastic filament cools to chamber temperature, hardens, and fuses with the adjacent material as it is deposited. The base plate or the print head slides down or up after one layer of patterning and depositing when the next layer begins. Because the process is totally automated and requires little human, it is increasingly being used to create personalized products in a variety of industries. The capacity to build objects with functionally graded qualities is a key feature of the FFF process (porosity, density, and mechanical properties). With advancements in materials and technology, FFF is transitioning from prototyping to manufacturing finished goods. To completely develop FFF into a production tool rather than just a prototyping machine, the mechanical qualities of the parts generated must be enhanced so that the produced components' performance is kept during service. Aside from that, the polymers that can be employed in FDM technology should be more diverse. Figure 6.1 shows schematic view of FDM process.

6.3 Materials and Methodology

All specimens used in this study were fabricated with Flashforge Guider II FDM machine, it is a modern evaluation 3D printer intended for the outrageous specialist or prosumer at the top of the priority list. This is the highest point of the level FFF 3D printer from Flashforge, intended to give the most extreme dependability and

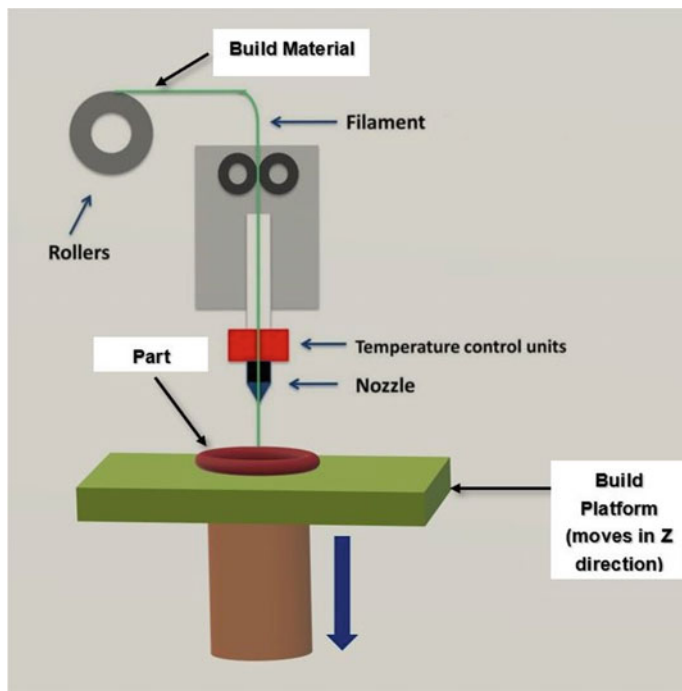


Fig. 6.1 Schematic of the fused deposition modelling

toughness when printing your plans, the specification of machine is listed in Table 6.1 and image show in Fig. 6.2.

PLA antibacterial material and carbon nano particles purchased from local market. PLA antibacterial material is prepared by adding 2%wt. carbon nano particles and further the material is extruded from the extrusion machine with diameter of 1.75 mm. The same developed material is tested for antibacterial activity and further optimization of process parameters like nozzle speed, infill rate and layer

Table 6.1 Specification of FDM machine

Elements	Range
Device size (without cover)	549 × 490 x 561 mm
Build volume	280 × 250 x 300 mm
Printing precision	± 0.1–0.2 mm
Printing software	Flash print
AC input	100 V-240 V ~ , 500 W
Input support	USB stick/USB Cable/WIFI/Ethernet

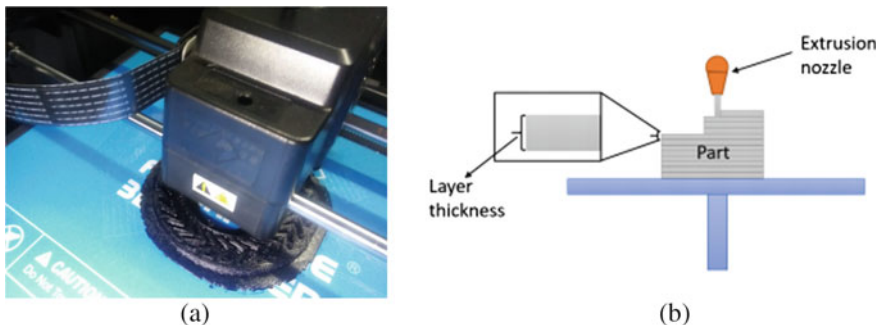


Fig. 6.2 FDM **a** Printing process image **b** Schematic view of layer thickness

height. ASTM standard specimens are prepared out of developed antibacterial Material for improving mechanical properties such as tensile strength, flexural strength, compression strength and shore hardness D scale.

Tensile properties of the carbon filled PLA specimens were tested with the universal testing machine (UTM) by ASTM D638 standard test method and the cross-head speed is 3 mm/min. The 3d design, ASTM standard and printed tensile specimens are show in Fig. 6.3.

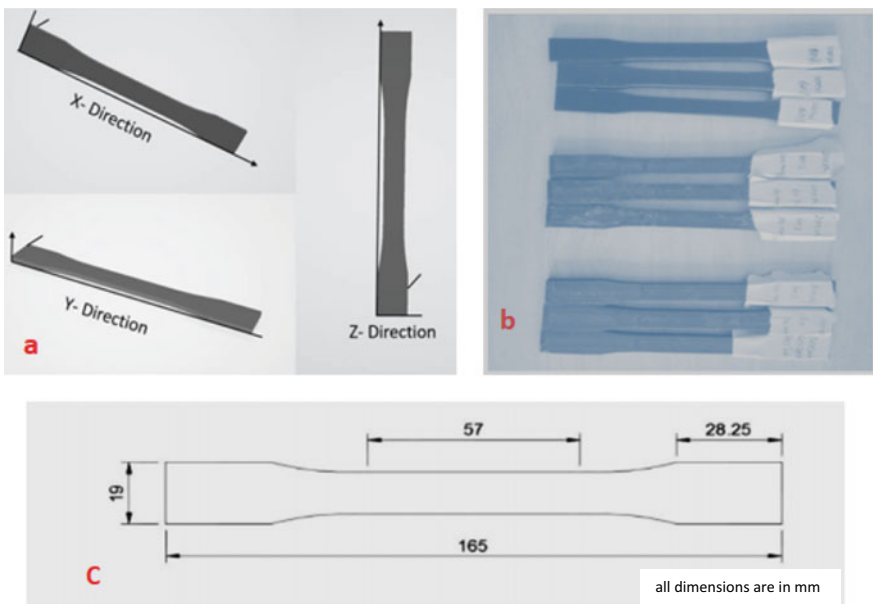


Fig. 6.3 Tensile specimen **a** 3D design view **b** printed specimen **c** ASTM D638 size

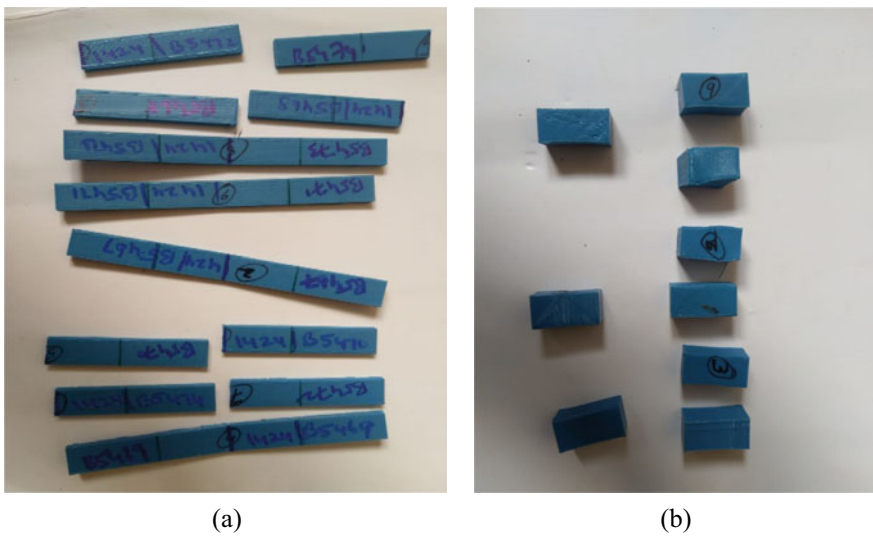


Fig. 6.4 **a** Flexural test specimens (after test) **b** Compressive test specimens (after test)

The bending and compression strength of the carbon filled PLA specimens were tested with the universal testing machine (UTM) by ASTM D790 and ASTM D695 standard Test Method. The printed specimens are show in Fig. 6.4.

Shore hardness is a proportion of the obstruction in a material to distinguish. The shore hardness scales enemy estimating the hardness of the various materials (delicate, elastic, strands, unbending plates, and overly delicate gels, are the models). The scales were imagined to individuals to have the normal perspective. In this the higher number on the scale shows a more prominent protection from space and consequently harder materials. Lower numbers demonstrate less opposition and delicate materials. The term is likewise used to depict a material rating on the scale as in an item having Shore durometer of 90'. The 3d designed, ASTM D2240 standard printed specimens are show in Fig. 6.5.

6.4 Design of Experiment (DoE)

It states to the process of planning and conducting the experiment so that appropriate data can be collected and analyzed by statistical methods, resulting in valid and objective conclusions and to signify the relationship between input variables and output responses. The statistical approach to experimental design is necessary to draw meaningful conclusions from the data and to estimate the present or predict the future with respect to the present.

The response values are to be noted for each experimental run or condition for the effect analysis. The statistical significance of the factors is evaluated by conducting

Fig. 6.5 Hardness test specimens



the analysis of variance (ANOVA). The ANOVA is performed to find the contribution of each factor for attaining the desired process outcome that may maximum tensile strength. Three process parameters considered for optimization of the study are; rotational speed, tilt angle and feed. Table 6.2 shows the Taguchi orthogonal array (OA) selector which shows the orthogonal array for the considered parameters and their levels. For three parameters which are at three levels L9 orthogonal array is selected from the array selector. Table 6.2 given below is the process parameters and their 3 levels. Table 6.3 describes the experimental design as per the Taguchi L9 approach used for the experiment [16].

Table 6.2 Process parameters and their 3 levels

Process parameters	Level 1 (-1)	Level 2 (0)	Level 3 (+1)
Infill rate (%)	65	75	85
Layer height (microns)	100	200	300
Nozzle speed (mm/sec)	60	80	100

Table 6.3 Experimental design using L9 orthogonal array

Specimen Id	Levels		
	Infill rate (%)	Layer height (Microns)	Print speed (mm/sec)
SP1	65	100	60
SP2	65	200	80
SP3	65	300	100
SP4	75	100	80
SP5	75	200	100
SP6	75	300	60
SP7	85	100	100
SP8	85	200	60
SP9	85	300	80

6.5 Results and Discussion

6.5.1 Compressive Property Analysis

The compressive strength of the PLA deposited by FDM is shown in Fig. 6.6. The maximum compressive strength is 41.23 N/mm² for SP9 sample and the minimum compressive stress is obtained is 20.89 N/mm² for SP3 sample. The compressive stress is influenced by the infill rate. The infill rate is directly proportional to the

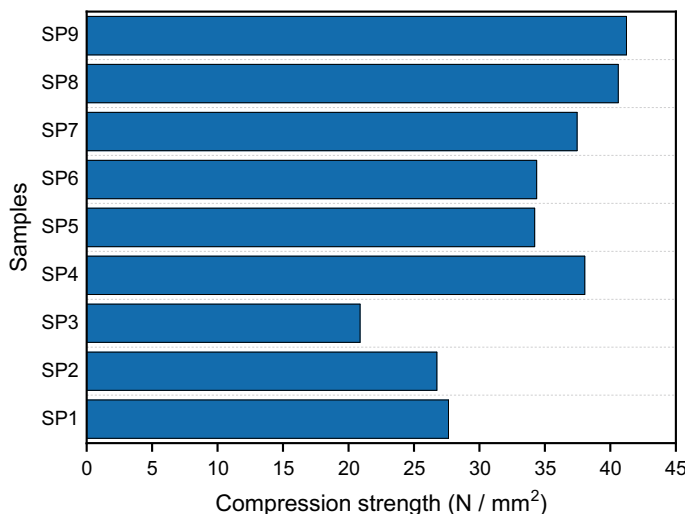


Fig. 6.6 Compressive strength of the PLA deposited by FDM

compressive strength. The print speed also reduces the compressive strength of the material.

6.5.2 Tensile Property Analysis

From Fig. 6.8, With the increase of the infill rate of the PLA sample the tensile strength is increased. The tensile strength is maximum for the 85%-infill rate and very low for 65% infill rates. The layer height and print speed also affect the tensile strength of the PLA sample. For the minimum layer height, the tensile strength is high. The optimum combination to produce high tensile strength is 85 infill rates, 300 microns layer heights and 80 print speeds. The 65 and 75 infill rate and low layer height produce maximum tensile strength and for 85 infill rate the higher layer height produce the greatest tensile strength. Figure 6.7 illustrate tensile load versus displacement curve of all 9 tested specimens.

6.5.3 Flexural Property Analysis

The flexural strength is also directly proportional to infill rate and print speed. The flexural strength is lower when for the minimum infill rate and print speed and it is gradually increasing with the increase of infill rate and print speed. The layer heights of the PLA sample not affect the flexural strength. If the print speed is very low the filament of the PLA is uneven and the bonding of fusion is very not easy. The maximum flexural strength is obtained for SP5 and the flexural strength is low for the sample SP1. Figure 6.9 shows flexural strength comparison of specimens.

6.5.4 Shore Hardness Analysis

The increase in the infill rate of the PLA samples the shore hardness is increased. At the layer thickness 200 microns the shore hardness is high when compared to layer thickness 100 and 300 microns. The print speed is not influencing the shore hardness of the PLA sample. The shore hardness is high for the PLA sample SP5 and very low for the PLA sample SP1. Figure 6.10 shows hardness comparison of specimens. Table 6.4 shows all test results.

6.5.5 Taguchi Analysis for Obtained Responses

As per the Taguchi L9 experimental design, nine 3D printed samples are prepared. Statistical software named as Minitab is used to draw the experimental conditions.

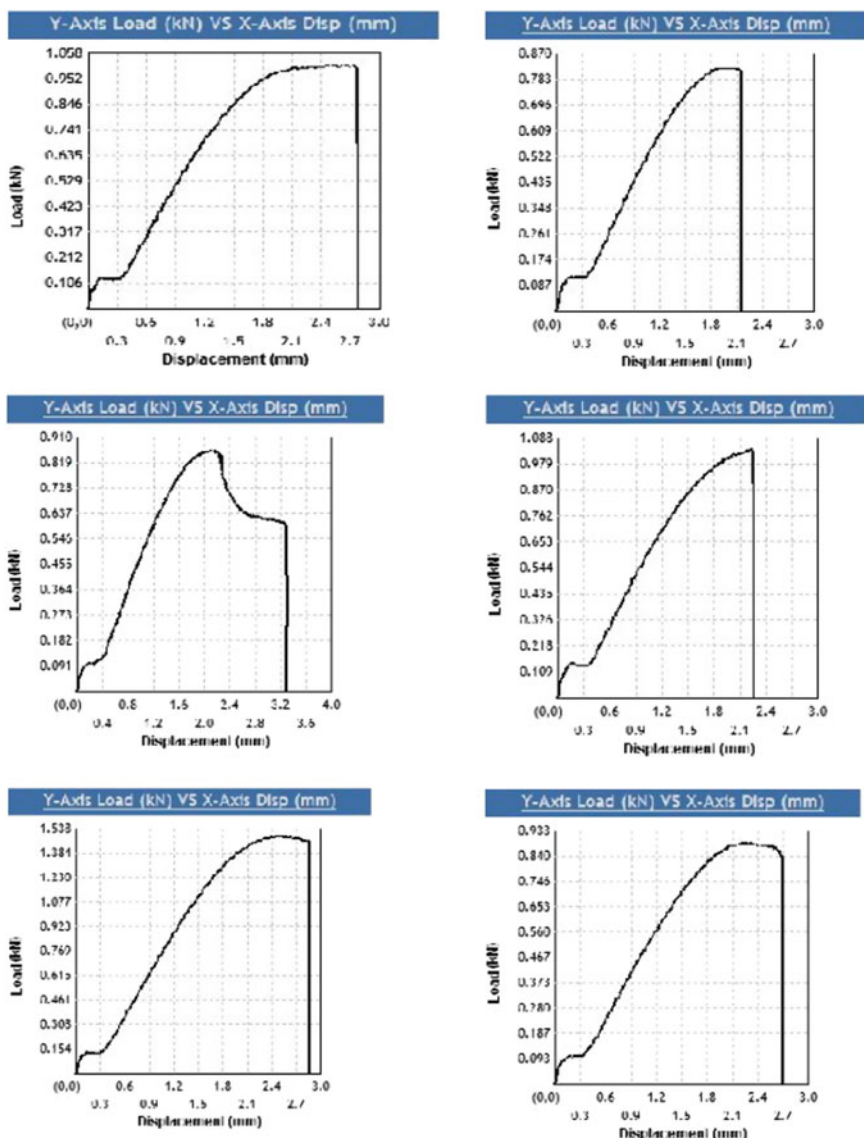


Fig. 6.7 Tensile load versus displacement curve of all 9 specimens

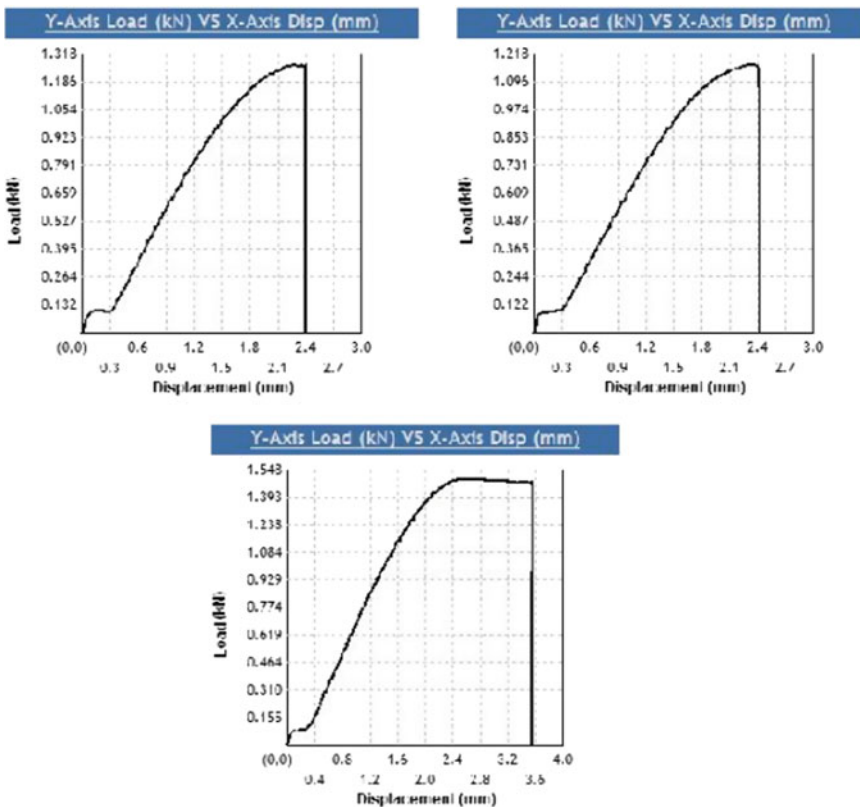


Fig. 6.7 (continued)

The adequacy of the developed relationship is evaluated using the Analysis of Variance Technique (ANOVA). ANOVA helps to identify the effect of each factor versus the objective function and it also determines the total variation present in the model. From the investigational study, the results and response over defined printing process parameters has been estimate for variance analysis using signal to noise (S/N) ratio. The total experiment performance is depending on tensile strength, flexural strength, compressive strength and shore hardness. Hence, the smaller is better (SB) ratio was selected than nominal is best and larger is best (LB) condition. The mean values of process parameters show in Fig. 6.11. The experiential equation used to calculate the S/N (SB) ratio is as follows:

$$S/N_{(LB)} = -10 \log \left(\sum_{i=0}^n \frac{y_i^2}{n} \right) \quad (6.1)$$

where: y_i = response on process parameter and n = number of trials repeated.

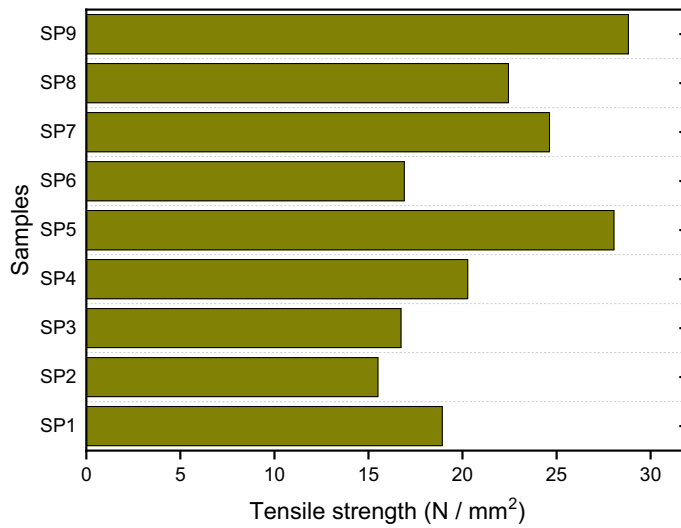


Fig. 6.8 Tensile strength of the PLA deposited by FDM

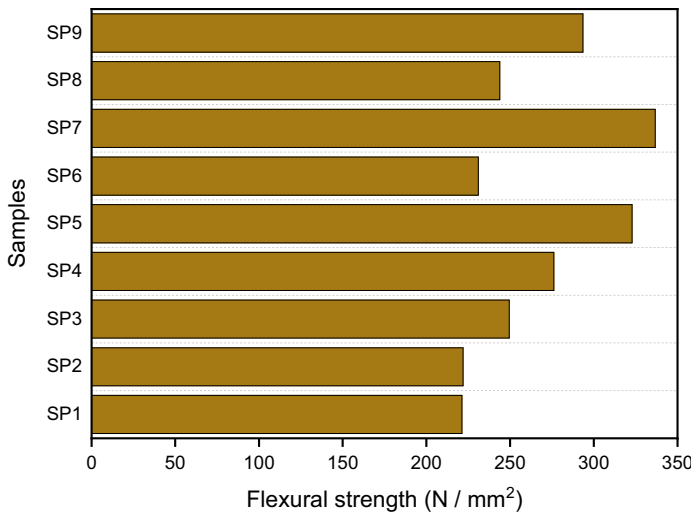
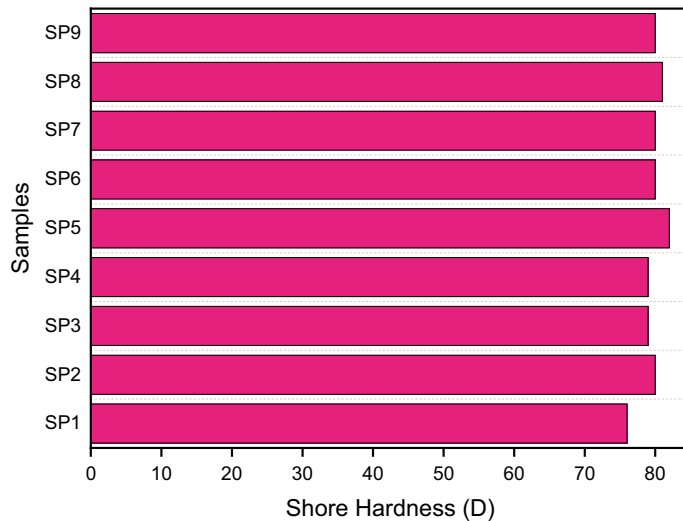


Fig. 6.9 Flexural strength of the PLA deposited by FDM

The impact of the process parameter has been designed and plotted in Fig. 6.12. From the above Table 6.5 the infill rate and print speed are plays major important role in all selected output parameters (tensile, flexural and compressive strength). These two process parameters are most influencing process parameters than layer thickness for the proposed investigational design. In shore hardness layer thickness and infill rate are most influencing process parameter. A recent article on fused deposition

**Fig. 6.10** Shore hardness of the PLA deposited by FDM**Table 6.4** Experiments with the test results

S. no	Infill rate (%)	Layer height (microns)	Print speed (mm/sec)	Tensile strength (N/mm ²)	Compression strength (N/mm ²)	Flexural strength (N/mm ²)	Shore hardness (D)
SP1	65	100	60	18.92	27.64	221.24	76
SP2	65	200	80	15.50	26.74	221.95	80
SP3	65	300	100	16.73	20.89	249.53	79
SP4	75	100	80	20.27	38.04	276.12	79
SP5	75	200	100	28.05	34.22	322.86	82
SP6	75	300	60	16.91	34.36	231.04	80
SP7	85	100	100	24.62	37.46	336.73	80
SP8	85	200	60	22.44	40.61	243.84	81
SP9	85	300	80	28.82	41.23	293.51	80

modeling (FDM) has described and suggested that the infill rate is playing a major role in process parameters. This is because the material filling rate in the nozzle convergence and divergence in all output parameters varies. At a high filling rate, more material is deposited and it gives more strength to the printed materials. However, print speed is the second level influencing parameter in the printed material. Because nozzle moving time is less at high speed, so contact area is reduced during printing. The next level influenced process parameter is layer thickness. This parameter is too low and too high-level parameters extract poor mechanical properties.

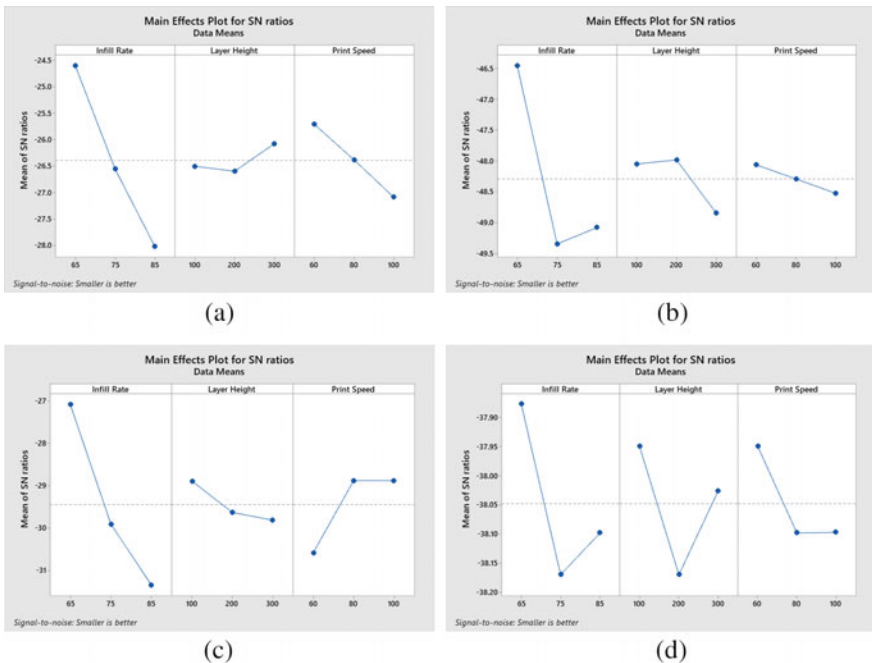


Fig. 6.11 Mean of S/N ratio **a** Tensile **b** Flexural **c** Compressive strength **d** Shore hardness

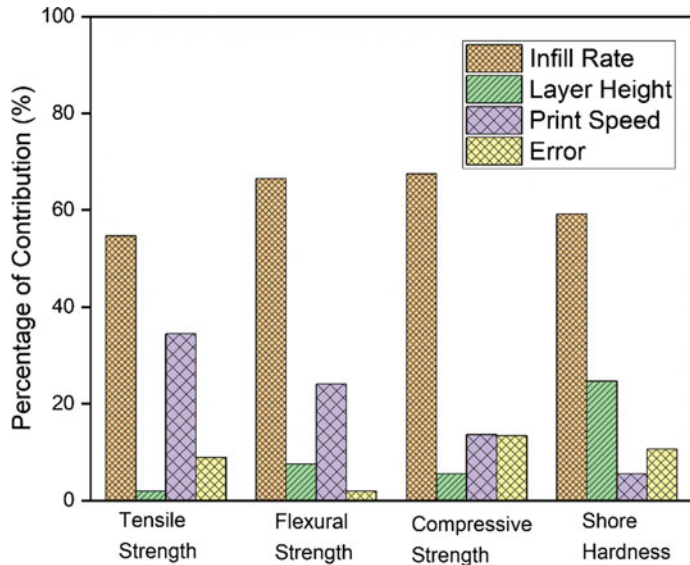


Fig. 6.12 Process parameter contribution in output parameters

Table 6.5 Influenced process parameters from S/N (SB) ratio analysis

Sl.no	Output parameter	Infill rate	Layer height	Print speed
1	Tensile strength	1	3	2
2	Flexural strength	1	3	2
3	Compressive strength	1	3	2
4	Shore hardness	1	2	3

6.5.6 Regression Analysis

Continuous predicted standardization method was used to make the nonlinear regression analysis. These models were settled at 95% confidence level for tensile, flexural, compressive and shore hardness by MINITAB 19 statistical software using the investigational data (un-coded units) from Tables 6.6, 6.7, 6.8 and 6.9. The nonlinear regression equations for the objectives are presented in equations (6.2–6.5). The fitness plots of residuals [Figs. 6.13a–d] depict normal distribution of errors; and closeness of residuals to the fitness lines. It exposes that the projected models are significant and adequate.

$$\begin{aligned} \text{Tensile Strength} &= -16.5 + 0.412 \text{ Infill Rate} - 0.0023 \\ \text{Layer Height} &+ 0.0927 \text{ Print Speed} \end{aligned} \quad (6.2)$$

$$\text{Compression Strength} = -16.2 + 0.722 \text{ Infill Rate}$$

Table 6.6 ANOVA for tensile strength

Symbol	Cutting parameter	D.O.F	S.S	M.S	F	Contribution
1	Infill rate	2	0.425	0.213	6.184	54.694
2	Layer height	2	0.015	0.008	0.223	1.976
3	Print speed	2	0.268	0.134	3.899	34.486
Error		2	0.069	0.034		8.844
Total			0.778	0.389		100.000

Table 6.7 ANOVA for flexural strength

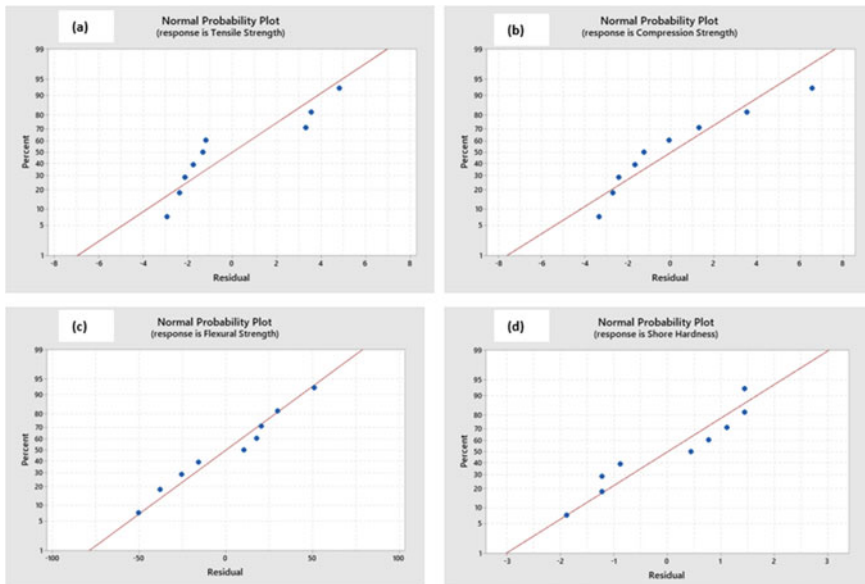
Symbol	Cutting parameter	D.O.F	S.S	M.S	F	Contribution
1	Infill rate	2	51.000	25.500	34.313	66.504
2	Layer height	2	5.754	2.877	3.871	7.503
3	Print speed	2	18.447	9.223	12.411	24.055
Error		2	1.486	0.743		1.938
Total			76.687	38.343		100.000

Table 6.8 ANOVA for compression strength

Symbol	Cutting parameter	D.O.F	S.S	M.S	F	Contribution
1	Infill rate	2	0.062	0.031	5.591	59.224
2	Layer height	2	0.026	0.013	2.326	24.644
3	Print speed	2	0.006	0.003	0.523	5.538
Error		2	0.011	0.006		10.593
Total			0.105	0.053		100.000

Table 6.9 ANOVA for shore hardness

Symbol	Cutting parameter	D.O.F	S.S	M.S	F	Contribution
1	Infill rate	2	1.283	0.641	5.032	67.466
2	Layer height	2	0.105	0.053	0.413	5.533
3	Print speed	2	0.258	0.129	1.014	13.593
Error		2	0.255	0.127		13.408
Total			1.902	0.951		100.000

**Fig. 6.13** Fitness graphs of **a** Tensile **b** Compressive **c** Flexural **d** Shore hardness

$$+ 0.0214 \text{ Layer Height} - 0.1458 \text{ Print Speed} \quad (6.3)$$

$$\text{Flexural Strength} = -83 + 3.82 \text{ Infill Rate}$$

$$+ 0.142 \text{ Layer Height} + 0.398 \text{ Print Speed} \quad (6.4)$$

$$\begin{aligned} \text{Shore Hardness} = & 69.06 + 0.1000 \text{ Infill Rate} \\ & + 0.00333 \text{ Layer Height} + 0.0333 \text{ Print Speed} \end{aligned} \quad (6.5)$$

6.6 Conclusion

The effect of FDM processing parameters on the mechanical properties such as tensile, flexural, compression and shore hardness of PLA material was successfully investigated in this study. From the experimental investigation and response on processing parameters performed following conclusions are drawn:

- The maximum compressive strength is 41.23 N/mm^2 and the minimum compressive stress is obtained is 20.89 N/mm^2 . The compressive stress is influenced by the infill rate and print speed also reduces the compressive strength of the material. The tensile strength is maximum for the 85%-infill rate and very low for 65% infill rates. The layer height and print speed also affect the tensile strength of the PLA sample. For the minimum layer height, the tensile strength is high. The layer heights of the PLA sample not affect the flexural strength. If the print speed is very low the filament of the PLA is uneven and the bonding of fusion is very not easy. At the layer thickness 200 microns the shore hardness is high when compared to layer thickness 100 and 300 microns. The print speed is not influencing the shore hardness of the PLA sample.
- Results of ANOVA revealed that infill rate is most significant parameter process parameter for all mechanical property (tensile, flexural, compression and shore hardness) analysis. Almost 60% contribution for all output parameters. Print speed is second level significant parameter for tensile, flexural and shore hardness excluding compression strength. Layer thickness is not significant parameter. Similarly, for compression strength layer hight is second level significant parameter (24.64% contribution) but print speed is not significant.
- Continuous predicted standardization method was used to made the nonlinear regression analysis. These models were settled at 95% confidence level for tensile, flexural, compressive and shore hardness. Their adequacies were verified through normal fitness probability plots of residuals.

References

1. Zindani, D., Kumar, K.: An insight into additive manufacturing of fiber reinforced polymer composite. *Int. J. Lightweight Mater. Manuf.* **2**, 267–278 (2019)
2. Barone, S., Neri, P., Orsi, S., Paoli, A., Razionale, A., Tamburrino, F.: Two coatings that enhance mechanical properties of fused filament-fabricated carbon-fiber reinforced composites. *Addit. Manuf.* **32**, 101105 (2020)
3. Eltes, P., Kiss, L., Bartos, M., Gyorgy, Z., Csakany, T., Bereczki, F., Lesko, V., Puhl, M., Varga, P., Lazary, A.: Geometrical accuracy evaluation of an affordable 3D printing technology for spine physical models. *J. Clin. Neurosci.* **72**, 438–446 (2020)
4. Dutra, T., Ferreira, R., Resende, H., Blinzler, B., Larsson, R.: Expanding Puck and Schürmann inter fiber fracture criterion for fiber reinforced thermoplastic 3D-printed composite materials. *Materials* **13**, 1653 (2020)
5. Arastouei, M., Khodaei, M., Atyabi, S., Jafari Nodoushan, M.: Poly lactic acid-akermanite composite scaffolds prepared by fused filament fabrication for bone tissue engineering. *J. Market. Res.* **9**, 14540–14548 (2020)
6. Deng, X., Zeng, Z., Peng, B., Yan, S., Ke, W.: Mechanical properties optimization of poly-ether-ether-ketone via fused deposition modeling. *Materials* **11**, 216 (2018)
7. Tale, A., Shingane, A., Shinghane, P., Thakare, S., Wasekar, M.: Review on comparison of connecting rod made by 3D printing method. *Int. J. Res. Eng. Sci. Managem.* **2**, 658–663 (2019)
8. Cuan-Urquiza, E., Barocio, E., Tejada-Ortigoza, V., Pipes, R., Rodriguez, C., Roman-Flores, A.: Characterization of the mechanical properties of FFF structures and materials: a review on the experimental. *Computat. Theoret. Approaches. Mater.* **12**, 895 (2019)
9. Yang, C., Tian, X., Liu, T., Cao, Y., Li, D.: 3D printing for continuous fiber reinforced thermoplastic composites: mechanism and performance. *Rapid Prototyping J.* **23**, 209–215 (2017)
10. Xu, Z., Ha, C., Kadam, R., Lindahl, J., Kim, S., Wu, H., Kunc, V., Zheng, X.: Additive manufacturing of two-phase lightweight, stiff and high damping carbon fiber reinforced polymer microlattices. *Addit. Manuf.* **32**, 101106 (2020)
11. Ravi, P., Shiakolas, P., Welch, T.: Poly-l-lactic acid: Pellets to fiber to fused filament fabricated scaffolds, and scaffold weight loss study. *Addit. Manuf.* **16**, 167–176 (2017)
12. Slapnik, J., Bobovnik, R., Mešl, M., Bolka, S.: Modified polylactide filaments for 3D printing with improved mechanical properties. *Contemporary Mater.* **7**(2), 142–150 (2016)
13. Afrose, M., Masood, S., Iovenitti, P., Nikzad, M., Sbarski, I.: Effects of part build orientations on fatigue behaviour of FDM-processed PLA material. *Progress in Additive Manuf.* **1**, 21–28 (2015)
14. Luzanin, O., Guduric, V., Ristic, I., Muhic, S.: Investigating impact of five build parameters on the maximum flexural force in FDM specimens—a definitive screening design approach. *Rapid Prototyping J.* **23**, 1088–1098 (2017)
15. Liu, S., Qin, S., He, M., Zhou, D., Qin, Q., Wang, H.: Current applications of poly (lactic acid) composites in tissue engineering and drug delivery. *Compos. Part B Eng.* **199**, 108238 (2020)
16. Jani, S., Kumar, A., Khan, M., Kumar, M.: Machinability of hybrid natural fiber composite with and without filler as reinforcement. *Mater. Manuf. Processes* **31**, 1393–1399 (2015)

Chapter 7

Role of Additive Manufacturing in Biomedical Engineering



**R. Ruban, V. S. Rajashekhar, B. Nivedha, H. Mohit, M. R. Sanjay,
and Suchart Siengchin**

7.1 Introduction to Additive Manufacturing

Additive manufacturing (AM), often known as fast prototyping or desktop manufacturing, is a collection of manufacturing techniques used to turn a three-dimensional CAD model into a three-dimensional realistic thing. The technology works by layering one material upon another utilizing fast prototyping software and a 3D CAD model [1]. The introduction of additive manufacturing in the 1980s changed the course of manufacturing history. When compared to traditional manufacturing, additive manufacturing has more advantages, such as the elimination of waste products and the ability to produce complicated geometry items. As a result, additive manufacturing is becoming increasingly important in a variety of disciplines, particularly in the medical field. In biomedical applications, AM methods have been used in a variety of ways. It was immediately put to use in the field of medical engineering to meet the demands of patients and clinicians when it was developed. Furthermore, AM can be used to make medical devices such as orthoses and prostheses, as well as diagnostic and surgical instruments. AM also has advantages, such as the ability to create anatomical models for surgery planning and procedural training, particularly in uncommon diseases where device and process customization is crucial.

R. Ruban (✉)

Department of Mechanical Engineering, National Institute of Technology, Tiruchirappalli, India

V. S. Rajashekhar

Department of Aerospace Engineering, Indian Institute of Science, Bengaluru, India

B. Nivedha

Department of Physics, National Institute of Technology, Tiruchirappalli, India

H. Mohit · M. R. Sanjay · S. Siengchin

Natural Composites Research Group Lab, Department of Materials and Production Engineering, The Siridhorn International Thai-German Graduate School of Engineering, King Mongkut's University of Technology, North Bangkok (KMUTNB), Bangkok 10800, Thailand

AM is also useful in the manufacture of drug delivery systems, medicinal implants, and medical devices on both a large and small scale in clinical settings [2, 3]. AM can also be used to create personalized medical devices, allowing final goods to be tailored to the patient's needs while also being produced at a lesser cost. The design and printing personalized implants and prosthesis has become the gold standard procedure for many patients who require specialized structures based on their desired issue recent times. The customization, personalisation of medical items, biocompatibility, cost effectiveness, better productivity, accessibility, quick production time, simple assembly, collaboration, and democratization are some of the benefits of additive manufacturing [4–10]. The application of additive manufacturing in the medical area has a number of advantages, including medical product customisation and personalization, biocompatibility, cost effectiveness, and increased productivity. The applications of AM in the biomedical fields of pharmaceuticals, clinical implants, medical devices, and tissue regeneration scaffold fabrication are described in the following sections from these perspectives. In this chapter, developments of rapid prototyping (RP) in the fabrication of medical implants, medical instruments, and scaffold for tissue regeneration so far are reviewed and discussed.

7.2 Additive Manufacturing Techniques

There are distinct additive manufacturing technologies such as Stereolithography (SLA), Digital Light processing (DLP), Selective laser sintering (SLS), Electron beam melting (EBM), Fusion deposition modelling (FDM), Multiset/Polyjet 3D printing, Selective laser melting (SLM) and laminated object manufacturing. The broad classification of rapid prototyping technologies are shown in Fig. 7.1 [11]. These technologies can fabricate any complex 3D component of any shape by utilizing only 3D CAD model data unlikely with the case of traditional manufacturing processes. In the medical field, however, 2D radiographic images such as computed tomography, magnetic resonance imaging, and X-rays can be transformed to three-dimensional digital print files, allowing the production of personalized anatomical, complex, and medicinal structures [11, 12].

7.3 Application of Additive Manufacturing in Medical Field

The development of additive manufacturing may be traced back to the 1980s, when Charles Hull invented stereolithography while working in a manufacturing company. When photopolymers (acrylic-based substances) are exposed to UV light, they become tougher, according to him. Then he built a device that used ultraviolet light to engrave acrylic films into shapes and then piled the layers together to create an object. SLA technique of rapid prototyping interprets data in a computer-aided design file

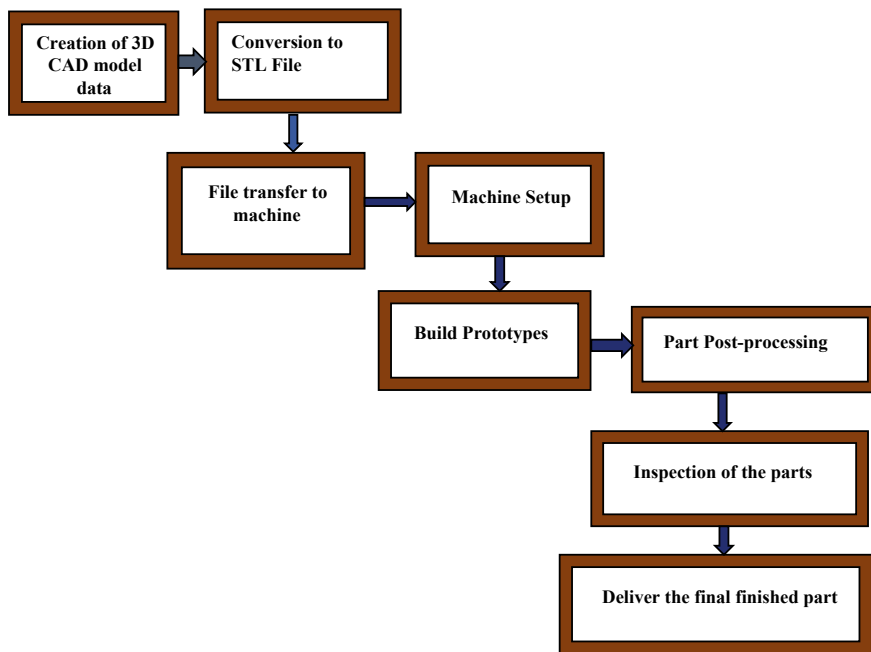


Fig. 7.1 Steps involved in fabrication using RP processes [11]

and sends instructions to a three-dimensional printer using a standard triangulation language file format. This is the existence for 3D printer for additive manufacturing.

Additive manufacturing was first used in medical applications in the 1990s. Finally, scientists created organs from patient cells and supported them with a three-dimensional printed scaffold. To support them, scientists created the first three-dimensional printed scaffold in 2008. A manufacturing company created a three-dimensional printed jaw using layer by layer technique in Holland in 2012. With technological advancements, 3D printing machines have become more affordable, and they are now commonly used in hospitals to generate human organs.

The demand for additive manufacturing is expanding due to the necessity to customize medical parts [13].

7.3.1 *Biomedical Materials, Mechanical Properties and Their Applications*

The utility/properties required in the manufacture of the final part or AM model, such as personalized implants, surgical tools, prosthetic limbs, tissue scaffolds, and many more, are the primary considerations in material selection. Rapid prototyping is employed in medical applications where durability, flexibility, and strength are

required. In this case, nylon and acrylonitrile butadiene styrene (ABS), polylactic acid is a good choice for biodegradable material in the medical field. The classification of biomaterials used in rapid prototyping to fabricate medical parts are shown in Fig. 7.2. Biomaterials should have features such as being easy to print, biocompatible, morphologically mimicking biological tissue, nontoxic and so on. Metals and alloys are utilized in orthopaedic implants, plates, screws, and other applications that require significant strength. Ceramics are a good material for bioactive orthopaedic implants. Table 7.1 lists the numerous research articles that have been published on the usage of several types of biomaterials for 3D printing to fabricate medical implants. Because of its superior mechanical qualities, composite is employed for porous orthopaedic implants. In the medical field, polymers, on the other hand, are the most commonly used substance. Polymer-based materials are the most commonly utilized biomaterials (86%).

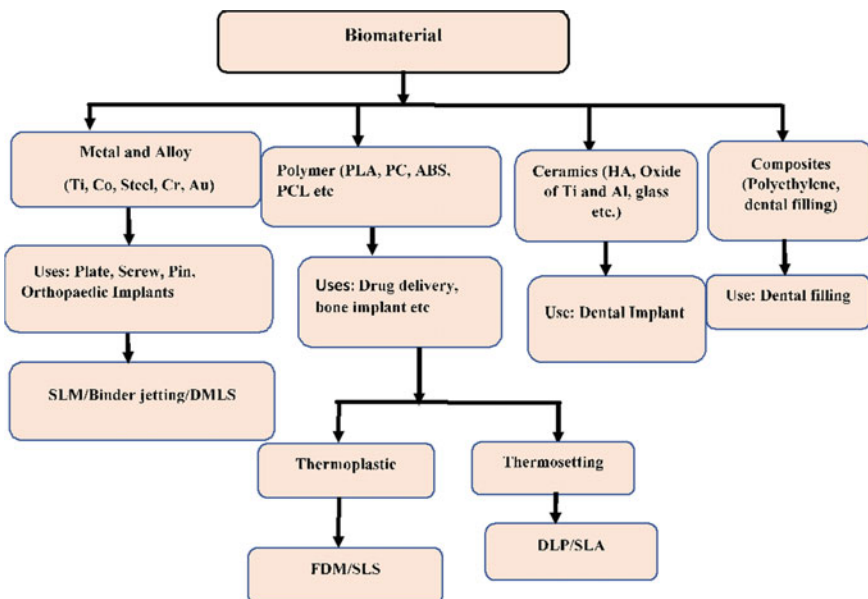


Fig. 7.2 Classification of AM material [11]

Table 7.1 Rapid prototyping materials for distinct applications

Types of metal	Application	Reference
Polyglycolic acid	Internal fixation	[14]
	Graft material	[15]
	Scaffold	[16]
	Interference screw	[17]
Poly lactic glycolic acid	Scaffolds, microspheres and carries for BMP, composite	[18, 19]
Hydroxyapatite (HA)	Composites, scaffolds, bone fillers, pastes, coatings, drug delivery	[20–22]
Magnesium	Implants, osteosynthesis devices, plates, screws, ligatures and wires	[23–27]
Tricalcium phosphate	Bone fillers, injectable pastes, cements	[28–31]
Titanium Alloy	Orthognathic surgery, mid-facial fracture treatment	[32–34]
Bioglass	Bone defect fillers	[35]

7.4 Rapid Prototyping Techniques for Additive Manufacturing Applications

7.4.1 Fused Deposition Modelling

Fused deposition modelling (FDM), also known as extrusion-based fast prototyping, fabricates the component by extruding the material on the substrate in layers with the use of a nozzle. The nozzle melts the material more quickly and extrudes the liquid in accordance with the scan path strategy defined by the user in the computer. To begin with, the liquid substance hardens quickly and serves as a solid-state substrate for the subsequent fresh layer. As a result, the manufacturing temperature should be controlled below the material's melting point [36] to ensure that the interlayer has high adhesion ability. Thermoplastic filaments are the most common material utilized in this application. The technique involved in inkjet printing is shooting out liquid to solid compound on the substrate and forming a layer by layer on the substrate with intermediate deposition of liquid powder material deposits over the completed region, resulting in a 3D volume of the object [37]. These approaches use polymer latex and silica colloid as binders, and powder materials such as metallic, ceramic, and composites.

7.4.2 Selective Laser Sintering

In this technique, the powder is dispersed over the substrate plate and then sintered by a laser spot, which is also known as the layer wise mechanism. A computer is in charge of the scanning. A specific location on the powder bed is linked together

to create a whole portion. When the component is complete, the loose powder in the chamber can be collected and recycled for future production. SLS may use a wider range of materials than other AM processes, including polymers, metals, and composites [38].

7.4.3 Sintered Laser Melting

It is an AM technique that utilizes a high-energy source to make a nearly full-density component. SLM, like SLS, is a layer-by-layer manufacturing technology that uses a computer to control the manufacturing of components based on a 3D CAD model [39]. The SLM systems employ laser energy as the input energy to totally melt the powder material; the computer controls the laser beam via a mirror deflection system and then focuses it on the powder bed. During the production process, the processing chamber is filled with a protective environment, typically argon gas, to prevent oxidation of the components. Metals, polymers, and ceramics are the materials employed in the RP processes.

7.4.4 Electron Beam Melting

The powder is melted by an electron beam spot in EBM. Before the component is manufactured, the building chamber is evacuated to free up space. To reduce residual tension between the substrate plate and the component produced, the plate must be warmed to 700 degrees Celsius. EBM techniques are used to create a variety of biological applications, including knee, hip joint, and jaw replacements [40, 41]. Table 7.2 shows how rapid prototyping biomodels require different additive manufacturing techniques to meet their strict application requirements.

7.5 Developments in Additive Manufacturing for Clinical Applications

Rapid prototyping is beneficial in the fabrication of 3D biomodels for preoperative planning in terms of assessing, diagnosing, and designing for the surgery of a patient. The patient-specific implants are designed and manufactured using computerized tomography (CT)/magnetic resonance imaging (MRI) scanned images, which are then imported into modeling software, converted to IGES (Inner graphics exchange script) file format, and then converted to STL (standard tessellation language) format. STL format which is acceptable in the fast prototyping machine, error correction in

Table 7.2 Typical implants fabricated by various additive manufacturing techniques [42]

Additive manufacturing techniques	Materials	Targeted clinical cases	Comments	References
FDM	Heterogenous hydrogel	3D heterogenous hydrogel model	Promoted the repair of osteochondral defects	[43]
FDM	Polyether ether ketone	Facial implant	Three dimensionally printed implants were suitable for the complex bone structure	[44]
FDM	Ti-6Al-4 V	Rat implants	Porosity played an important role in tissue growth	[45]
SLM	Ti-24Nb-4Zr-8Sn	Acetabular cup	The implant has high relative density and good mechanical properties	[46]
EBM	Ti-6Al-4 V	Human fetal osteoblasts	Very rough surface reduced cell proliferation	[47]
EBM	Ti-6Al-4 V	Pig skull	Scaffolds were suitable for bone ingrowth	[48]

MIMICS software, a program for defect correction in CAD models, and lastly the product fabrication.

Rapid prototyping aids in pre-surgical planning, which reduces surgery time and increases surgical success. A vast number of research have shown that 3D printed models can help with orthopaedic surgery success [49–52]. The numerous researches have found that 3D-printed components promote tissue regeneration in vitro and in vivo trials. In the case of patient-specific 3D implant models, particular guidance and templates are used. The 3D printed screw guide proposed approach, for example, advantages interoperative pedicle fixation of screws, which is a routine practice of spinal instrumentation in the thoracic spine shown in Fig. 7.3 [52]. It decreases operating time and radiation exposure during surgery.

Furthermore, for use in knee arthroplasty, patient-specific disposable surgical saw guides/cutting blocks can be created. Prior to surgery, different cuts of bone resections, as well as the size and part of each implant, are planned using imaging and planning software. This lessens the number of issues to be addressed before the procedure may commence. This can reduce tissue loss and improve the location of implants, extending the life of implant prosthesis [53].

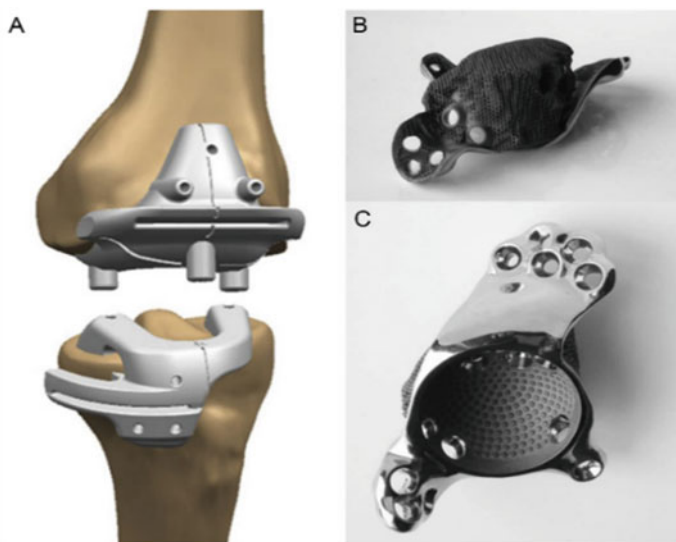


Fig. 7.3 Knee arthroplasty [52]

Rapid prototyping also assists in the understanding of the anatomy of complicated body parts like the heart, which has numerous arteries, veins, and tissues. It provides definitive information on heart structures. In difficult cardiac surgeries and interventional treatments, this method enhances safety and cuts down on time. Another significant benefit is that patients are informed about the surgical or interventional method prior to operation. A portion of human heart that was manufactured via rapid prototyping is shown in Fig. 7.4 [54]. Similarly, there are plenty of benefits in using additive manufacturing to create 3D prototype models for medical students and patients. AM technologies have long been regarded as unrivaled in terms of productivity. Indeed, anatomical models can be made to order depending on their intended



Fig. 7.4 Prototype of “Heart” using rapid prototyping [54]

use such as color models for identifying anatomical bone subregions, multimaterials for increased realism, particularly in the case of bones and muscles [55].

Rapid prototyping is now widely recognized as an important instrument in the educational system that complements traditional instruction. Nowadays, patients are passive recipients of care who are interested in learning about the diagnosis process, treatment options, and consequences from a reliable source such as physicians, medical personnel, and medical authorities.

As a result, AM enhances patient consent, compliance, and satisfaction, resulting in a better patient-doctor relationship. Currently, bone diseases are assessed using image modalities that result in 2D (e.g. radiography) or 3D virtual models (e.g. computed tomography scan) that aid in conveying anatomical information with patients, but not on a fully suited scale. As a result, physical patient-specific 3D models are the useful pedagogic tools for explaining bone diseases and other treatment alternatives [56]. In the case of cranial surgery, fast prototyping plays a vital role during the surgery of critical parts, when preoperative operative planning of reconstructive surgery is very necessary [57]. As each patient's anatomy structure is different, as determined by CT scan images, it takes a lot of experience for a surgeon to perform surgical operations. However, 3D fast prototyping of anatomical models is now possible using scanned images generated from CT/MRI scans.

Rapid prototyping is used to address a patient's skull bone deformities as follows:

- (1) Spiral CT was used to examine the patient, and data was exported in the form of Digital imaging and communications in medicine (DICOM).
- (2) The CT data was reconstructed and imported into the Mimics software, where it was evaluated and processed.
- (3) The part was transferred to the RP equipment and manufactured.
- (4) The doctor integrated titanium mesh onto the created bio-model.
- (5) Finally, the bio-model implanted in the patient's body was artificially transferred.

The rising frequency of traffic accidents and high-energy injuries adds to the complexity of trauma and wounds, resulting in a variety of tissue defects, including lengthy segmental bone deformities. As a result, tissue engineering is becoming a popular focus that blends basic life science principles with engineering techniques.

7.6 Role of Rapid Prototyping in Tissue Engineering

Tissue Engineering has shown promising outcomes in the treatment and replacement of damaged tissues and organs, such as skin, heart, and kidney tissues, as well as treating some concerns with bone abnormalities. Three-dimensional prototyping methodologies aimed at solving various muscoskeletal tissue pathologies are still being developed, and in-vitro studies are being conducted. This approach is used in tissue engineering for bone and cartilage regeneration, as well as meniscus, tendon, ligament, and muscle regeneration. Rapid prototyping technologies have

been used to create 3D scaffolds (tricalcium phosphate (TCP)/alginate) with regulated structure and orientation in the case of bone regeneration [58]. In recent years, 3D bioprinting has received a lot of attention in the biomedical field since it solves problems like biocompatibility. The art of life science and 3D printing are combined in 3D bioprinting, which is a layer-by-layer deposition of bio-inks along with living cells and supporting components to print the substrate, as opposed to 3D printing, which uses cell-free scaffolds and seeds cells on the substrate after the product is created [59, 60]. 3D bioprinting allows for more precise control of cell distribution and the microenvironment of the ECM (extracellular matrix). The selection of materials, cell types, growth and differentiation factors, sensitivity to living cells (for example, mammalian cells are sensitive to shear forces), and tissue building are all concerns related with 3D bioprinting. The Natural (gelatin, collagen, and chitosan, for example) or synthetic materials are utilized in 3D bioprinting (alginate or fibrin). In comparison to synthetic 3D biomaterials, natural 3D biomaterials exhibit biocompatibility and extracellular matrix-like behaviour [61].

In the case of 3D bioprinting, the approach is divided into three steps: (i) pre-processing, (ii) processing, and (iii) post-processing [62] shown in Fig. 7.5. The pre-processing is comparable in similar to 3D printing in that it incorporates imaging of the organ or tissue utilizing CT scans, MRI scans, X-rays, or ultrasound techniques. The 3D model obtained from the imaging software are converted into STL format (Standard tessellation language), a language for 3D bioprinters that is widely accepted, followed by slicing methods. The harvesting primary cells from patients, cultivating, and growing them ex-vivo for the bioprinting process were the first steps in the procedure. The post processing involves bioprinted tissue/organ is kept in a bioprinter so that the cells can be increased via cell culture and, in the case of stem cells, differentiated to generate specific functions and cell morphologies. It also entails keeping the bioprinted tissue/organ in a bioprinter for maturation before implanting it into the patient's body. The proper bioinks with qualities must be chosen carefully in relation to the target tissue to be printed. The bio printed material may include a variety of biologics, such as cells, medium, serum, genes, proteins, and so on. The printability, degradation, and biocompatibility in nature are the material factors to consider for bioink in 3D bioprinting. The selection of various printing processes for the manufacturing of rapid prototyping products affects the creation of bioink. The most difficult aspect is embedding cells in the bioink. To generate the solid structure, an ideal bioink should have no pre- or post-printing processing such as physical, chemical, or photo crosslinking. The bioink should be homogeneously mixed with the other components and encapsulation time should be short. The cell density, cytotoxicity, and bioprintability are all elements to consider when making the bioink, as well as the bio ink's rheological characteristics, gelation kinetics, and surface tension.

Fusion of hydrogels, deformation owing to gravity, non-uniform droplet size or extrusion, and crosslinker concentration are all process characteristics to consider while making bioink, non-uniform droplet size or extrusion, concentration of crosslinker and solidification. The property of shear thinning should be used in the

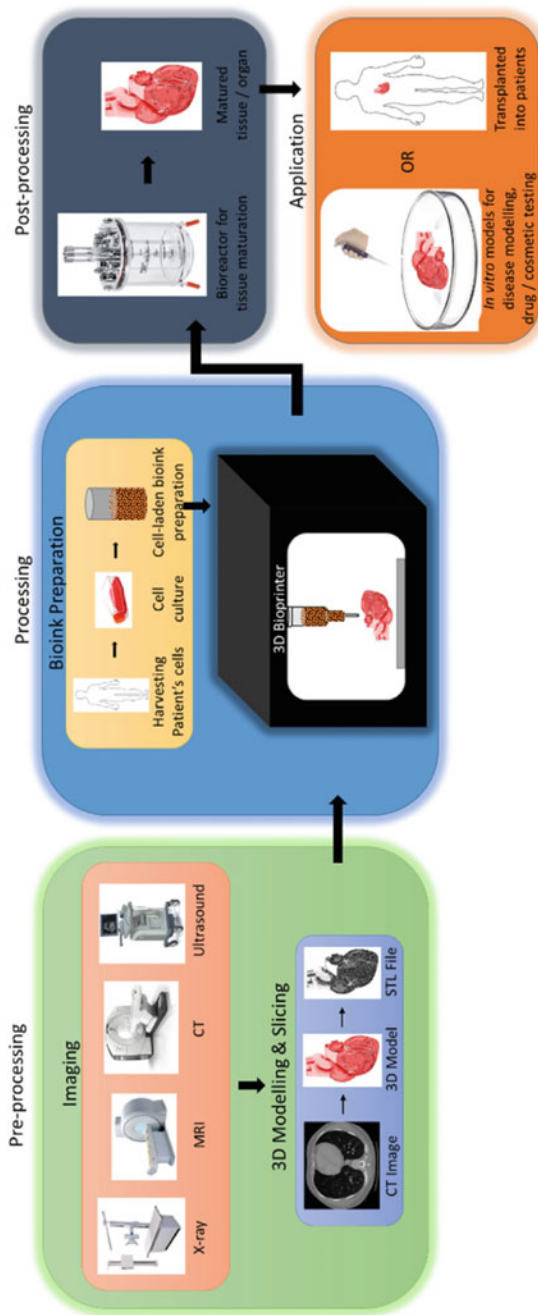


Fig. 7.5 Workflow of 3D bioprinting [62]

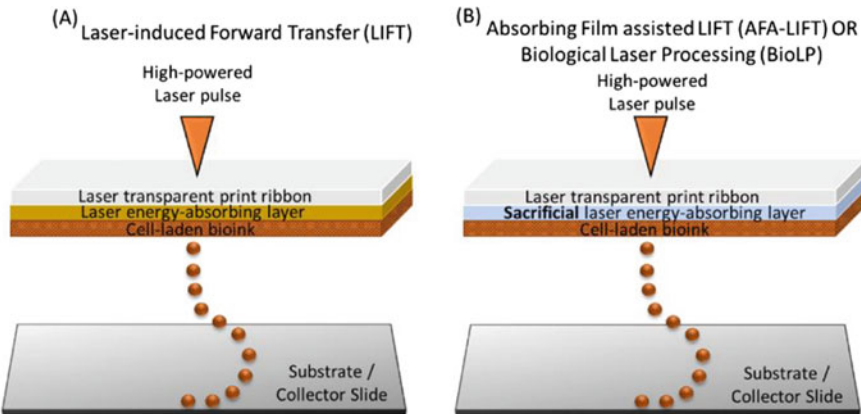


Fig. 7.6 Laser based bioprinting techniques [62]

bioink preparation to ensure a smooth flow during printing and a return to a higher viscosity after printing.

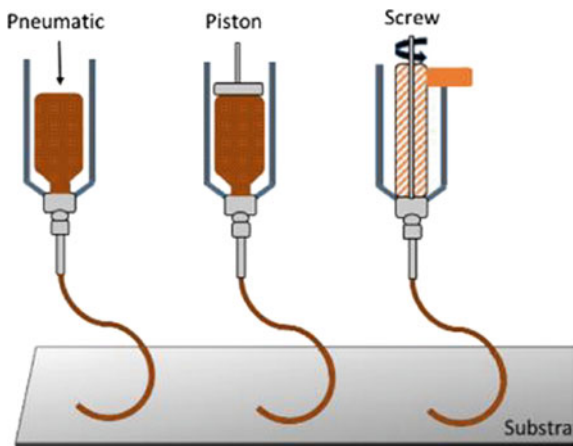
The type of bioink to use is determined by the sort of 3D bioprinting machines that will be used to create the 3D product. The laser-based bioprinting and extrusion-based bioprinting are the two most common types of 3D bioprinting processes.

The laser energy is used to pattern cell-laden bioinks in laser-based bioprinting is shown in Fig. 7.6. In laser-based bio printing, there are two sorts of approaches. The laser induced forward transfer technique (LIFT) and the absorbent film assisted LIFT technique are two types of LIFT techniques. LIFT (laser induced forward transfer) is the most prevalent approach. This increases the pressure on the bioink, allowing a droplet of cell-laden bioink to be propelled towards the substrate. In the case of the absorbing film assisted LIFT approach, the LTPR is coated with a thick sacrificial metal layer. This approach works well with cell-laden bioinks because it limits the contact of the bioinks with the laser radiation. The Droplet-based bioprinting is a method of 3D bioprinting in which cell-laden bioinks are expelled from a nozzle onto a substrate in the shape of droplets. The bioinks are extruded here using pneumatic pressure or mechanical force, as seen in Fig. 7.7, through a piston or screw. In recent years, 3D bioprinting has been used to create skin, bone, vascular grafts, tracheal splints, heart tissue, and cartilage. It is also used to create tissue models for research, medication development, and toxicology [62].

7.7 3D Printing for Personalised Protective Equipments Despite During COVID-19

The world is currently afflicted with a terrible disease (CORONA, a second mutation of the SARS-2 virus). Many international and national health service

Fig. 7.7 Extrusion based bioprinting [62]

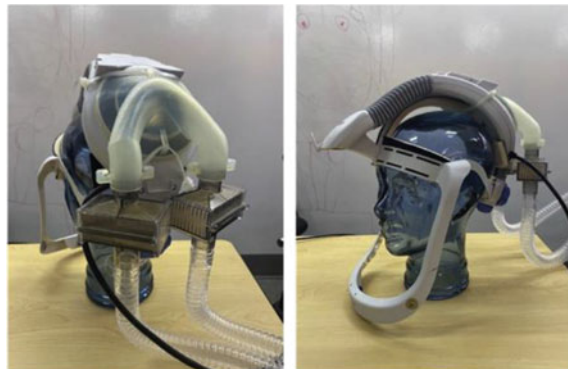


authorities/organizations recommend wearing PPE (Personal Protective Equipment) for respiratory, eye/mouth/face, body, and hand protection when interacting with COVID-19 patients to avoid or minimize any possible contact, droplet, and airborne transmission. During this COVID-19 crisis, health care institutions have become the most dangerous locations for health care personnel who care for and provide services to sick patients. Due to the lockdown imposed by the corona virus (COVID-19) pandemic, the worldwide supply chain has been severely disrupted, including crucial medical supplies such as face shields and ventilator valves. According to reports, 35% of firms believe the COVID-19 situation has disrupted their supply chain [63]. 3D printing technology is actively engaging in the production of some of the most important PPE components, such as face shields, masks, and ventilator valves, with the support of scientists and researchers.

7.7.1 Face Shields and Masks

The 3D printing technology was able to mitigate some of the problems by printing and supplying such items to the hospitals and frontline workers. The 3D printing can be done with the various approaches for the medical equipments. The medical safety is an important factor while during the production of PPE. In the case of SLS/SLA, the use of resin or petroleum-based plastic powders to build the product necessitates the addition of an extra layer to avoid skin contact issues. As a result, if filaments are used to fabricate the product, the usage of FDM method for PPE manufacturing plays a key role. Typically, a 3D printed face mask is made up of two parts: a strap and a filter membrane support, with the filter being replaceable after a long time of use. The shielding functions which is used as a barrier to aerosols, lowering the danger of contamination. Typically, ABS (Acrylic butadiene styrene) filaments are commonly used in FDM to create robust face shields [64–67]. Amin et al. [68] effectively

Fig. 7.8. 3D printed helmet with attached accessories such as manifold and secured anaesthesia tubings [70]



build 3D print face shields for an average cost of 7.30 \$ utilizing polylactic acid as filament material. These headlight face shield adapters are manufactured with printers utilizing readily available materials like PLA (Polylactic acid) [69]. In order to protect surgical workers from infectious blood splashes/debris, Ericsson et al. [70] created a surgical helmet for arthroplasty surgeons. Most arthroplasty surgeons currently wear surgical helmets, which have been delayed due to the COVID-19 pandemic and helmet systems being unused to be used as PPEs using 3D printing technology. Figure 7.8 shows the 3D printed design of the manufactured helmet attached to the manifold and secured with extra air filters and necessary anaesthetic tubing attached with the adaptor.

HP created the P2 Half Mask (see Fig. 7.9a), which was successfully tested against EN1827. It was created with BASF Ultrasint TPU01 and HP Jet Fusion 5200 3D. Materialise has created and manufactured a 3D-printed medically certified Oxygen PPE mask (Fig. 7.9b) to address the ventilator shortage.

Prusa Research, a leading FDM 3D Printer manufacturer, responded to the scarcity of PPE for medical workers by mass-producing 3D printed protective face shields (Fig. 7.9c, d) and donating over 200,000 face shields to Czech medical professionals. Our disease-prevention gadget is a simple addition to our hospital's conventional door handles. Taipei Veterans General Hospital developed a new 3D printed door handle shown in Fig. 7.10 [72]. It adds an extension to the door, allowing passers-by to open it with their forearms rather than their hands. Based on three factors, a door extension was designed that allows a person's forearm to control the door. First, because most of the people grab the door handles with their hands, we needed a device that could be manipulated with a body component that was as close to the hand as feasible. Second, because forearms are rarely used to contact their mouths, noses, or eyes, they are an excellent body part to operate. Third, it is safe for users to use this device.

Similarly, notwithstanding example of COVID-19, numerous devices such as door hooks, hand-free openers, and button pushers are manufactured at industrial institutions utilizing 3D prototyping [73]. As a result, rapid prototyping is useful for producing various personal protective equipment (PPE) for humans to combat the covid 19.



Fig. 7.9 **a** P2 half mask. **b** Oxygen PPE mask. **c** Face shields by Prusa. **d** Oxyframe attached to PPE [71]

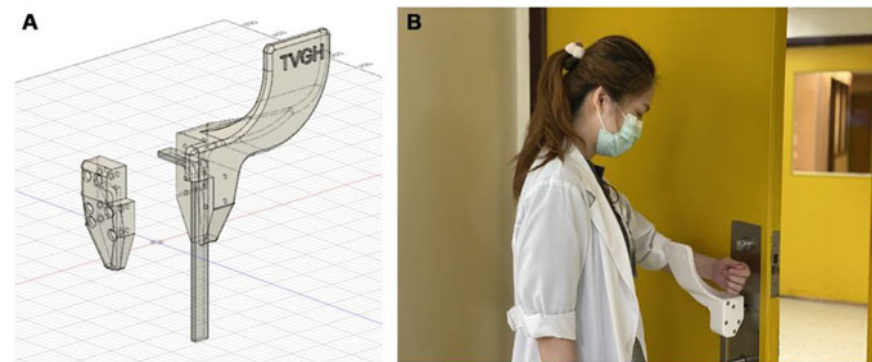


Fig. 7.10 Door opening through forearm using 3D rapid prototyping [72]

7.8 Conclusions

The application of rapid prototyping in biomedical fields and the challenges and researches are reviewed in this chapter. The role of rapid prototyping in biomedical engineering and medicine are greatly expanding. The distinct applications of rapid prototyping requires the importance in selecting the materials in fabricating the rapid prototyping product. Rapid prototyping finds its very useful advantages in fabricating the various implant prosthesis and scaffolds in tissue engineering. The scaffolds produced by 3D printing which is cell free substrate are not effective in showing good biocompatibility, where the drawback can be made by printing cell along with the ink to produce the product called bioprinting. The procedures carried out in fabricating the biomodel in 3D bioprinting are discussed here. The rapid prototyping plays a vital role in fabricating the personalised protective equipments such as face shields, masks, door openers, door hooks to the people in the present today's amidst COVID-19.

References

1. Sames, W.J., List, F.A., Pannala, S., Dehoff, R.R., Babu, S.S.: The metallurgy and processing science of metal additive manufacturing. *Int. Mater. Rev.* **61**(5), 315–360 (2016)
2. Chen, R.K., Jin, Y.A., Wensman, J., Shih, A.: Additive manufacturing of custom orthoses and prostheses—a review. *Addit. Manuf.* **12**, 77–89 (2016)
3. Cuellar, J.S., Smit, G., Zadpoor, A.A., Breedveld, P.: Ten guidelines for the design of non-assembley mechanisms: the case of 3D-printed prosthetic hands. *Proc. Inst. Mech. Eng. [H]* **232**(9), 962–971 (2018)
4. Banks, J.: Adding value in additive manufacturing: researchers in the United Kingdom and Europe look to 3D printing for customization. *IEEE Pulse* **4**(6), 22–26 (2013)
5. Mertz, L.: Dream it, design it, print it in 3-D: What can 3-D printing do for you? *IEEE Pulse* **4**(6), 15–21 (2013)
6. Ibrahim, A.M., Jose, R.R., Rabie, A.N., Gerstle, T.L., Lee, B.T., Lin, S.J.: Three-dimensional printing in developing countries. *Plast Re-constr. Surg. Glob. Open.* **3**(7), e443 (2015)
7. Rankin, T.M., Giovinco, N.A., Cucher, D.J., Watts, G., Hurwitz, B., Armstrong, D.G.: Three-dimensional printing surgical instruments: are we there yet? *J. Surg. Res.* **189**(2), 193–197 (2014)
8. Ursan, I.D., Chiu, L., Pierce, A.: Three-dimensional drug printing: a structured review. *J. Am. Pharm. Assoc.* **53**(2), 136–144 (2013)
9. Cui, X., Boland, T., DD'Lima, D.K., Lotz, M.: Thermal inkjet printing in tissue engineering and regenerative medicine. *Recent Pat. Drug Deliv. Formulation* **6**(2), 149–55 (2012)
10. Gross, B.C., Erkal, J.L., Lockwood, S.Y., Chen, C., Spence, D.M.: Evaluation of 3D printing and its potential impact on biotechnology and the chemical sciences (2014)
11. Kumar, R., Kumar, M., Chohan, J.S.: The role of additive manufacturing for biomedical applications: a critical review. *J. Manuf. Process.* **64**, 828–850 (2021)
12. Javaid, M., Haleem, A.: Additive manufacturing applications in medical cases: a literature-based review. *Alexandria J. Med.* **54**, 411–422 (2018)
13. Culmone, C., Smit, G., Breedveld, P.: Additive manufacturing of medical instruments: a start of the art review. *Addit. Manuf.* **27** (2019)
14. Törmälä, P.: Biodegradable self-reinforced composite materials; manufacturing structure and mechanical properties. *Clin. Mater.* **10**(1–2), 29–34 (1992)

15. Christel, P.: Biodegradable composites for internal fixation. *Biomaterials* **1**, 271–280 (1980)
16. Linhart, W., Peters, F., Lehmann, W., Schwarz, K., Schilling, A.F., Amling, M., Rueger, J.M., Epple, M.: Biologically and chemically optimized composites of carbonated apatite and polyglycolide as bone substitution materials. *J. Biomed. Mater. Res.: Official J. Soc. Biomater. Jpn. Soc. Biomater.* **54**(2), 162–171 (2001)
17. Ji, Y., Ping Xu, G., Peng Zhang, Z., Jun Xia, J., Long Yan, J., Ha Pan, S.: BMP-2/PLGA delayed-release microspheres composite graft, selection of bone particulate , and prevention of aseptic inflammation for bone tissue engineering. *Annals Biomed. Eng.* **38**(3), 632–9 (2010)
18. Gavenis, K., Schneider, U., Groll, J., Schmidt-Rohlfing, B.: BMP-7-loaded PGLA microspheres as a new delivery system for the cultivation of human chondrocytes in a collagen type I gel: the common nude mouse model. *Int. J. Artif. Organs* **33**(1), 45–53 (2010)
19. Fei, Z., Hu, Y., Wu, D., Wu, H., Lu, R., Bai, J., Song, H.: Preparation and property of a novel bone graft composite consisting of rhBMP-2 loaded PLGA microspheres and calcium phosphate cement. *J. Mater. Sci.—Mater. Med.* **19**(3), 1109–1116 (2008)
20. Balçık, C., Tokdemir, T., Şenköylü, A., Koç, N., Timuçin, M., Akin, S., Korkusuz, P., Korkusuz, F.: Early weight bearing of porous HA/TCP (60/40) ceramics in vivo: a longitudinal study in a segmental bone defect model of rabbit. *Acta Biomater. IA* **3**(6), 985–996 (2007)
21. Bedi, T.S., Kumar, S., Kumar, R.: Corrosion performance of hydroxyapatite and hydroxyapatite/titania bond coating for biomedical applications. *Mater. Res. Expr.* **7**(1), 015402 (2019)
22. Mardziah, C.M., Sopyan, I., Ramesh, S.: Strontium-doped hydroxyapatite nano powder via sol-gel method: effect of strontium concentration and calcination temperature on phase behavior. *Trends Biomater. Artif. Organs.* **23**(2), 105–113 (2009)
23. Staiger, M.P., Pietak, A.M., Huadmai, J., Dias, G.: Magnesium and its alloys as orthopedic biomaterials: a review. *Biomaterials* **27**(9), 1728–1734 (2006)
24. Wong, H.M., Yeung, K.W., Lam, K.O., Tam, V., Chu, P.K., Luk, K.D., Cheung, K.M.: A biodegradable polymer-based coating to control the performance of magnesium alloy orthopaedic implants. *Biomaterials* **31**(8), 2084–2096 (2010)
25. Zeng, R., Dietzel, W., Witte, F., Hort, N., Blawert, C.: Progress and challenge for magnesium alloys as biomaterials. *Adv. Eng. Mater.* **10**(8), B3–B14 (2008)
26. Waizy, H., Seitz, J.M., Reifenrath, J., Weizbauer, A., Bach, F.W., Meyer-Lindenberg, A., Denkena, B., Windhagen, H.: Biodegradable magnesium implants for orthopedic applications. *J. Mater. Sci.* **48**(1), 39–50 (2013)
27. Gu, X.N., Zheng, Y.F.: A review on magnesium alloys as biodegradable materials. *Front. Mater. Sci. Chin.* **4**(2), 111–115 (2010)
28. Ghosh, S.K., Nandi, S.K., Kundu, B., Datta, S., De, D.K., Roy, S.K., Basu, D.: In vivo response of porous hydroxyapatite and β -tricalcium phosphate prepared by aqueous solution combustion method and comparison with bioglass scaffolds. *J. Biomed. Mater. Res. B Appl. Biomater.* **86**(1), 217–227 (2008)
29. Cutright, D.E., Bhaskar, S.N., Brady, J.M., Getter, L., Posey, W.R.: Reaction of bone to tricalcium phosphate ceramic pellets. *Oral Surg., Oral Med., Oral Pathol.* **33**(5), 850–856 (1972)
30. Bohner, M.: Physical and chemical aspects of calcium phosphates used in spinal surgery. *Eur. Spine J.* **10**(2), S114–S121 (2001)
31. Peter, S.J., Kim, P., Yasko, A.W., Yaszemski, M.J., Mikos, A.G.: Crosslinking characteristics of an injectable poly (propylene fumarate)/ β -tricalcium phosphate paste and mechanical properties of the crosslinked composite for use as a biodegradable bone cement. *J. Biomed. Mater. Res.: Official J. Soc. Biomater. Jpn. Soc. Biomater., Australian Soc. Biomater.* **44**(3), 314–321 (1999)
32. Kang, I.G., Jung, J.H., Kim, S.T., Choi, J.Y., Sykes, J.M.: Comparison of titanium and biodegradable plates for treating midfacial fractures. *J. Oral Maxillofac. Surg.* **72**(4), 762–e1 (2014)
33. Mazzoni, S., Bianchi, A., Schiariti, G., Badiali, G., Marchetti, C.: Computer-aided design and computer-aided manufacturing cutting guides and customized titanium plates are useful in upper maxilla waferless repositioning. *J. Oral Maxillofac. Surg.* **73**(4), 701–707 (2015)

34. Paeng, J.Y., Hong, J., Kim, C.S., Kim, M.J.: Comparative study of skeletal stability between biocritical resorbable and titanium screw fixation after sagittal split ramus osteotomy for mandibular prognathism. *J. Cranio-Maxillofacial Surg.* **40**(8), 660–664 (2012)
35. Fiorilli, S., Baino, F., Cauda, V., Crepaldi, M., Vitale-Brovarone, C., Demarchi, D., Onida, B.: Electrophoretic deposition of mesoporous bioactive glass on glass–ceramic foam scaffolds for bone tissue engineering. *J. Mater. Sci.—Mater. Med.* **26**(1), 21 (2015)
36. Bártoło, P.J., Almeida, H.A., Rezende, R.A., Laoui, T., Bidanda, B.: Advanced processes to fabricate scaffolds for tissue engineering. In: Virtual prototyping & bio manufacturing in medical applications, pp. 149–170. Springer, Boston, MA (2008)
37. Liu, X., Shen, Y., Yang, R., Zou, S., Ji, X., Shi, L., Zhang, Y., Liu, D., Xiao, L., Zheng, X., Li, S.: Inkjet printing assisted synthesis of multicomponent mesoporous metal oxides for ultrafast catalyst exploration. *Nano. Lett.* **12**(11), 5733–5739 (2012)
38. Mazzoli, A.: Selective laser sintering in biomedical engineering. *Med. Biol. Eng. Comput.* **51**(3), 245–256 (2013)
39. Attar, H., Bönisch, M., Calin, M., Zhang, L.C., Scudino, S., Eckert, J.: Selective laser melting of in situ titanium–titanium boride composites: processing, microstructure and mechanical properties. *Acta Mater.* **76**, 13–22 (2014)
40. Cronskär, M., Bäckström, M., Rännar, L.E.: Production of customized hip stem prostheses—a comparison between conventional machining and electron beam melting (EBM). *Rapid Prototyping J.* (2013)
41. Mazzoli, A., Germani, M., Raffaeli, R.: Direct fabrication through electron beam melting technology of custom cranial implants designed in a PHANTOM-based haptic environment. *Mater. Des.* **30**(8), 3186–3192 (2009)
42. Liu, Y., Wang, W., Zhang, L.C.: Additive manufacturing techniques and their biomedical applications. *Fam. Med. Commun. Health.* **5**(4), 286–298 (2017)
43. Fedorovich, N.E., Schuurman, W., Wijnberg, H.M., Prins, H.J., Van Weeren, P.R., Malda, J., Alblas, J., Dhert, W.J.: Biofabrication of osteochondral tissue equivalents by printing topologically defined, cell-laden hydrogel scaffolds. *Tissue Eng. Part C Methods* **18**(1), 33–44 (2012)
44. Gerbino, G., Zavattiero, E., Zenga, F., Bianchi, F.A., Garzino-Demo, P., Berrone, S.: Primary and secondary reconstruction of complex craniofacial defects using polyetheretherketone custom-made implants. *J. Cranio-Maxillofacial Surg.* **43**(8), 1356–1363 (2015)
45. Bandyopadhyay, A., Espana, F., Balla, V.K., Bose, S., Ohgami, Y., Davies, N.M.: Influence of porosity on mechanical properties and in vivo response of Ti6Al4V implants. *Acta Biomater.* **6**(4), 1640–1648 (2010)
46. Zhang, L.C., Klemm, D., Eckert, J., Hao, Y.L., Sercombe, T.B.: Manufacture by selective laser melting and mechanical behavior of a biomedical Ti–24Nb–4Zr–8Sn alloy. *Scripta Mater.* **65**(1), 21–24 (2011)
47. Ponader, S., Vairaktaris, E., Heinl, P., Wilmowsky, C.V., Rottmair, A., Körner, C., Singer, R.F., Holst, S., Schlegel, K.A., Neukam, F.W., Nkenke, E.: Effects of topographical surface modifications of electron beam melted Ti-6Al-4V titanium on human fetal osteoblasts. *J. Biomed. Mater. Res. Part A: An Official J. Soc. Biomater. Jpn. Soc. Biomater. Australian Soc. Biomater. Korean Soc. Biomater.* **84**(4), 1111–1119 (2008)
48. Ponader, S., Von Wilmowsky, C., Widemayer, M., Lutz, R., Heinl, P., Körner, C., Singer, R.F., Nkenke, E., Neukam, F.W., Schlegel, K.A.: In vivo performance of selective electron beam-melted Ti-6Al-4V structures. *J. Biomed. Mater. Res. Part A: Official J. Soc. Biomater. Jpn. Soc. Biomater. Australian Soc. Biomater. Korean Soc. Biomater.* **92**(1), 56–62 (2010)
49. Wixted, C.M., Peterson, J.R., Kadakia, R.J., Adams, S.B.: Three-dimensional printing in orthopaedic surgery: current applications and future developments. *JAAOS Glob. Res. Rev.* **5**(4) (2021)
50. Eltorai, A.E., Nguyen, E., Daniels, A.H.: Three-dimensional printing in orthopaedic surgery. *Orthopaedics.* **38**(11), 684–687 (2015)
51. Spirig, J.M., Golshani, S., Farshad-Amacker, N.A., Farshad, M.: Patient-specific template-guided versus standard freehand lumbar pedicle screw implantation: a randomized controlled trial. *J. Neurosurg.: Spine* **1**(aop), 1–7 (2021)

52. Mok, S.W., Nizak, R., Fu, S.C., Ho, K.W., Qin, L., Saris, D.B., Chan, K.M., Malda, J.: From the printer: potential of three-dimensional printing for orthopaedic applications. *J. Orthop. Transl.* **6**, 42–49 (2016)
53. Noble, J.W., Jr., Moore, C.A., Liu, N.: The value of patient-matched instrumentation in total knee arthroplasty. *J. Arthroplasty* **27**(1), 153–155 (2012)
54. Mishra, S.: Application of 3D printing in medicine. *Indian Heart J.* **68**(1), 108 (2016)
55. Li, K.H., Kui, C., Lee, E.K., Ho, C.S., Sunny Hei, S.H., Wu, W., Wong, W.T., Voll, J., Li, G., Liu, T., Yan, B.: The role of 3D printing in anatomy education and surgical training: a narrative review. *MedEdPublish.* **6**(2) (2017)
56. Nikitichev, D.I., Patel, P., Avery, J., Robertson, L.J., Bucking, T.M., Aristovich, K.Y., Maneas, E., Desjardins, A.E., Vercauteren, T.: Patient-specific 3D printed models for education, research and surgical simulation. *3D Print.* **10**, 115 (2018)
57. Wu, W., Zhang, Y., Li, H., Wang, W.: Fabrication of repairing skull bone defects based on the rapid prototyping. *J. Bioact. Compatible Polym.* **24**(1_suppl), 125–36 (2009)
58. Fradique, R., Correia, T.R., Miguel, S.P., De Sa, K.D., Figueira, D.R., Mendonça, A.G., Correia, I.J.: Production of new 3D scaffolds for bone tissue regeneration by rapid prototyping. *J. Mater. Sci.—Mater. Med.* **27**(4), 69 (2016)
59. Vanaei, S., Parizi, M.S., Salemizadehparizi, F., Vanaei, H.R.: An overview on materials and techniques in 3d bioprinting toward biomedical application. *Eng. Regeneration.* **2**, 1–8 (2021)
60. Ozbolat, I.T., Moncal, K.K., Gudapati, H.: Evaluation of bioprinter technologies. *Addit. Manuf.* **13**, 149–200 (2017)
61. Jeong, H.J., Nam, H., Jang, J., Lee, S.J.: 3D bioprinting strategies for the regeneration of functional tubular tissues and organs. *Bioengineering* **7**(2), 32 (2020)
62. Vijayaventakaraman, S., Yan, W.C., Lu, W.F., Wang, C.H., Fuh, J.Y.: 3D bioprinting of tissues and organs for regenerative medicine. *Adv. Drug Deliv. Rev.* **132**, 296–332 (2018)
63. Bartik, A.W., Bertrand, M., Cullen, Z., Glaeser, E.L., Luca, M., Stanton, C.: The impact of COVID-19 on small business outcomes and expectations. *Proc. Natl. Acad. Sci.* **117**(30), 17656–17666 (2020)
64. Shokrani, A., Loukaides, E.G., Elias, E., Lunt, A.J.: Exploration of alternative supply chains and distributed manufacturing in response to COVID-19; a case study of medical face shields. *Mater. Des.* **192**, 108749 (2020)
65. Banerjee, S.S., Burbine, S., Kodihalli Shivaprakash, N., Mead, J.: 3D-printable PP/SEBS thermoplastic elastomeric blends: Preparation and properties. *Polymers* **11**(2), 347 (2019)
66. Ishack, S., Lipner, S.R.: Applications of 3D printing technology to address COVID-19-related supply shortages. *Am. J. Med.* **133**(7), 771–773 (2020)
67. Meglioli, M., Toffoli, A., Macaluso, G.M., Catros, S.: 3D printing workflows for printing individualized personal protective equipment: an overview. *Trans. Add. Manuf. Meets Med.* **2**(1) (2020)
68. Amin, D., Nguyen, N., Roser, S.M., Abramowicz, S.: 3D printing of face shields during COVID-19 pandemic: a technical note. *J. Oral Maxillofacial Surg.* (2020)
69. Viera-Artiles, J., Valdiande, J.J.: 3D-printable headlight face shield adapter. Personal protective equipment in the COVID-19 era. *Am. J. Otolaryngol.* **41**(5), 102576 (2020)
70. Erickson, M.M., Richardson, E.S., Hernandez, N.M., Bobbert, D.W., II., Gall, K., Fearis, P.: Helmet modification to PPE with 3D printing during the COVID-19 pandemic at Duke University Medical Center: a novel technique. *J. Arthroplasty* **35**(7), S23–S27 (2020)
71. Jafferson, J.M., Pattanasethi, S.: Use of 3D printing in production of personal protective equipment (PPE)-a review. *Mater. Today: Proc.* (2021)
72. Chen, K.L., Wang, S.J., Chuang, C., Huang, L.Y., Chiu, F.Y., Wang, F.D., Lin, Y.T., Chen, W.M.: Novel design for door handle—a potential technology to reduce hand contamination in the COVID-19 pandemic
73. François, P.M., Bonnet, X., Kosior, J., Adam, J., Khonsari, R.H.: 3D-printed contact-free devices designed and dispatched against the COVID-19 pandemic: the 3D COVID initiative. *J. Stomatology, oral Maxillofac. Surg.* (2020)

Part III

**Post-Processing and Investigations on 3D
Built Materials**

Chapter 8

Surface Finishing Post-treatments for Additive Manufactured Metallic Components



T. S. N. Sankara Narayanan and Hyung Wook Park

8.1 Introduction

Additive manufacturing (AM) involves fabrication of numerous components by a layer-by-layer approach. AM processes assume significance due to their ability to fabricate thin lattice structures, struts and scaffolds with high material utility. Selective laser melting (SLM) and electron beam melting (EBM) are commonly employed for the fabrication of metallic components. One of the major limitations of components built by SLM and EBM is their higher surface roughness. Adherence of the partially melted particles, balling effect and stair case effect are the major reasons for the higher surface roughness [12, 43]. Many components involve complex shapes. Parts built away from the centre point of the build plate exhibit a higher surface roughness. Down-skin surfaces have a higher surface roughness than up-skin surfaces [12]. A higher surface roughness of the as-built AM part could deleteriously influence the mechanical properties, fatigue strength and corrosion resistance. The higher surface roughness of the AM parts restricts their use for the intended purpose and warrants suitable surface finishing post-treatments. Hence, the most important purpose of surface finishing post treatments is to reduce the surface roughness and to remove the partially melted particles present in the as-built AM parts. Surface finishing of AM components with a simple design can be easily accomplished. However, AM

T. S. N. Sankara Narayanan (✉) · H. W. Park

Department of Mechanical Engineering, Ulsan National Institute of Science and Technology (UNIST), UNIST-Gil 50, Eonyang-eup, Ulsan 689-798, Republic of Korea

H. W. Park

e-mail: hwpark@unist.ac.kr

Present Address:

T. S. N. Sankara Narayanan

Department of Analytical Chemistry, University of Madras, Guindy Campus, Chennai 600 025, India

parts with a complex design, internal surfaces, thin lattice structures, struts and scaffolds pose a tough challenge [52, 70]. A variety of surface finishing post-treatments are explored to decrease the surface roughness of AM parts [40, 41, 48, 56]. They can be broadly classified as (i) mechanical surface finishing methods; (ii) abrasive finishing methods; (iii) chemical and electrochemical processes; and (iv) laser and electron beam irradiation processes. This chapter aims to provide an outline of the ability of various surface finishing post-treatments to improve the surface finish of AM parts. The principle and mechanism of the treatment method, the beneficial effects induced by the treatment and the major limitations are highlighted.

8.2 Mechanical Surface Finishing Methods

8.2.1 *Tumble/barrel Finishing*

Tumble finishing (TF) or barrel finishing (BF) is a mechanical surface treatment process to improve surface finishing of metallic components. It involves tumbling or rotation of a barrel in which the parts to be treated and abrasive particles dispersed in a media are placed together. The friction between the surface being treated and the abrasive particles is responsible for the reduction in surface roughness. The extent of decrease in surface roughness is rather limited since the abrasive particles mainly remove the peaks while they have very little influence on the deep valleys. Boschetto et al. [9] have ascertained the suitability of BF for treating complex AM parts using a Ti6Al4V alloy impeller and an Inconel 718 alloy automotive exhaust manifold. The availability of limited space for the movement of the abrasive particles delays the speed of BF of the blades of the Ti6Al4V alloy impeller (Fig. 8.1a, b). The limited access for the abrasive particles on the angled internal surface limits the extent of surface finishing of the Inconel 718 alloy automotive exhaust manifold (Fig. 8.1c, d). Although BF has the advantage of treating many parts at the same time, the requirement of longer processing time (~48 h), wastage of the abrasive media, and problems in disposal are the major limitations in using them.

8.2.2 *Finish Machining*

Finish machining (FM) has been shown to decrease the surface roughness of SLM Inconel 718 alloy and 316L SS part by 90–96%. The extent of deformation induced by FM is very high, which enables grain refinement. In addition, the deformation helps to reduce the surface and sub-surface porosities. The strain hardening induced by FM increased the hardness and wear resistance and, decreased the risk of fatigue failure [37–39]. FM is not considered to be suitable for AM parts with complex shapes [38]. The depth of material removal during FM assumes significance as it

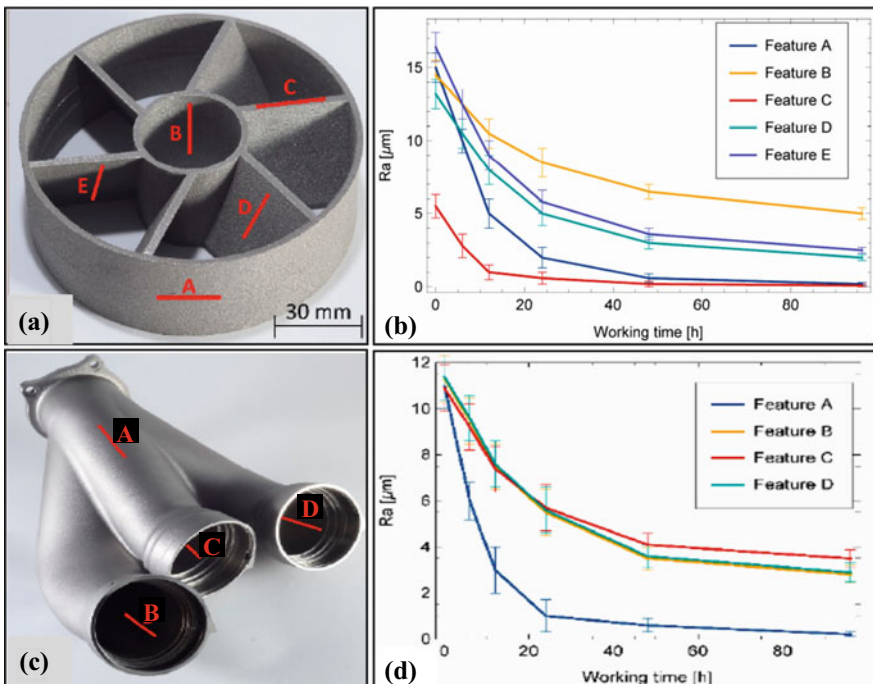


Fig. 8.1 Photographic images of SLM **a** Ti6Al4V impeller and **c** Inconel 718 alloy automotive exhaust manifold showing the regions at which the surface roughness was measured after BF; **b**, **d** Decrease in average surface roughness of these components after BF, measured as a function of time (Reprinted from, Boschetto et al. [9], under Creative Commons Attribution License)

could expose porosities and other defects from sub-surfaces. FM of EBM Ti6Al4V alloy parts to a depth of 1.00 mm bring out lack of fusion (LOF) defects to the top surface while those machined to a depth of 0.50 mm was free of such defects (Fig. 8.2). Although FM to a higher depth could offer considerable improvement in fatigue life by removing most of the pores and defects, such approach defeats the main principles of AM in terms of material utility with minimal wastage [17].

8.2.3 Blasting

Blasting involves propelling of abrasive particles (quartz sand, glass bead, alumina) on the surface to be treated under high pressure. Air pressure, stand-off distance, size and shape of the abrasive particles, angle of impingement and time are the main process variables. Blasting reduces the surface roughness, improves the surface integrity, increases the hardness and induces compressive residual stress. Micro-forming of the surface during blasting is responsible for smoothening of the surface.

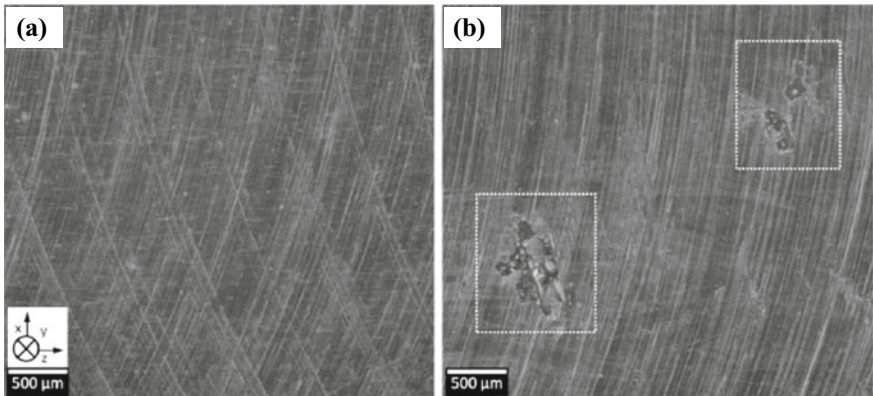


Fig. 8.2 Confocal microscopy images acquired at the surface of EBM Ti6Al4V specimens after FM to a depth of **a** 0.50 mm and; **b** 1.00 mm; dotted squares in (b) highlight defects (Reprinted from, T. Cilderhouse et al. [17], with permission from Elsevier)

The extent of decrease in roughness, however, is rather limited (~44–50%). In spite of its ability to remove partially melted powder particles from the surface of the as-built AM part, the impingement of sharp-edged abrasive particles could again cause roughening of the surface. Incorporation of the abrasive particles on the treated surface is a matter of concern. Blasting is considered to be suitable for thick AM parts and it should be used with caution while treating thin lattice structures as impingement of the abrasive particles might damage the part. Zhang [78] have suggested microblasting, which is capable of removing partially melted particles without damaging the part, as a suitable alternative for post-processing of thin lattice structures.

8.2.4 *Shot Peening, Cavitation Peening and Laser Shock Peening*

Shot peening (SP) involves impingement of a stream of shots on the surface being treated using compressed air. Multiple impingement of the shots enable plastic deformation of the surface and sub-surface, eliminate the surface defects, refine the grains, induce strain hardening, impart compressive residual stress and increase the fatigue resistance [50]. SP facilitated shrinkage of pores and reduced the porosity of SLM AlSi10Mg alloy part by 0.1–0.3%. In addition, SP increased the sphericity of larger pores [18]. SP has been envisioned as a game changer to improve the performance of AM lightweight alloy parts [4]. Unlike SP, cavitation peening (CP) is a shot-less method in which the peening effect is generated by collapsing cavitation bubbles. Similar to SP, CP is also capable of reducing the surface roughness, inducing compressive residual stress and improving the fatigue strength [60].

In laser shock peening (LSP), the shock waves generated by the laser beam induce surface severe plastic deformation (S²PD), leading to strain hardening, resulting in an increase in hardness along with the formation of a thick hardened layer (~700–900 μm) (Fig. 8.3a) and refines the grain size [16, 31]. LSP changes the tensile residual stress, which is prevalent in LSM metal parts to compressive residual stress (Fig. 8.3b). The choice of a smaller spot size and higher overlap rate (~80%) increase the magnitude of compressive residual stress and the depth to which it is imparted (~900 μm) [35]. The ability of LSP to induce compressive residual stress and to refine the grain size of the α phase helps to reduce the pre-existing crack size, suppress the crack initiation and increase the threshold for fatigue fracture of EBM Ti6Al4V alloy [31]. LSP facilitates a decrease in surface roughness. However, the extent of decrease in roughness of SLM and EBM Ti6Al4V alloy part is relatively less for LSP than SP [33]. Tong et al. [69] have shown that LSP is effective in closing the surface pores (Fig. 8.4) and promoting the formation of a gradient layer structure on DED CoCrFeMnNi high-entropy alloy. According to them, the strength and ductility of the CoCrFeMnNi high-entropy alloy are increased after LSP. The fracture mechanism of CoCrFeMnNi high-entropy alloy and Ti6Al4V alloy is changed to ductile from a mixture of ductile and brittle for as-fabricated part [44, 69].

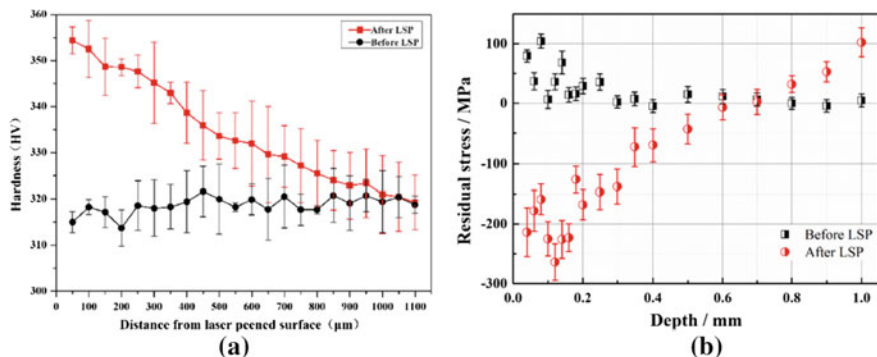


Fig. 8.3 **a** Hardness profile of EBM Ti6Al4V alloy after LSP as a function of depth; and **b** Residual stress of Ti6Al4V alloy as a function of depth before and after LSP (Reprinted from **a** X. Jin et al. [31]; **b** W. Guo et al. [25], with permission from Elsevier)

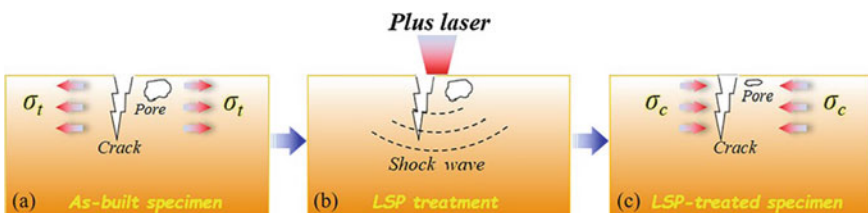


Fig. 8.4 Schematic illustration of closure of surface pores in DED CoCrFeMnNi high-entropy alloy by LSP (Reprinted from Z. Tong et al. [69], with permission from Elsevier)

SLM Ti6Al4V alloy part consists of α' -martensite phase. During SLM, tensile residual stress is induced at the surface of the part. The hardness, YS and UTS of the as-built Ti6Al4V alloy part are higher while it lacks the elongation. Post heat-treatment transformed the α' -martensite phase to $\alpha + \beta$ phases, decreased the hardness, increased the elongation, released the tensile residual stress, but decreased the YS and UTS. Also, heat-treatment increased the impact toughness, but decreased the corrosion and wear resistance. Yeo et al. [77] have shown that LSP of the heat-treated Ti6Al4V alloy sample has recovered the hardness and wear resistance by about 92% and decreased the corrosion rate by 64%. The ability of LSP to refine the grain size, to increase the magnitude and depth of hardness and, to induce compressive residual stress has enabled an increase in hardness, wear resistance and corrosion resistance of heat-treated SLM Ti6Al4V alloy sample.

Soyama and Takeo [63] have compared the effect of SP, CP and LSP on the extent of decrease in roughness, compressive residual stress induced during peening and increase in fatigue strength of SLM and EBM Ti6Al4V alloy samples. Irrespective of the method of fabrication, the extent of decrease in R_a and R_z by these methods of peening follows the order: SP > CP > LSP while the compressive residual stress induced during peening follows the order: CP > SP > LSP. The increase in fatigue strength after these methods of peening follows the order: CP > CP = LSP for SLM Ti6Al4V alloy and SP > LSP > CP for EBM Ti6Al4V alloy. In terms of fatigue strength, surface roughness exerts a negative influence while compressive residual stress has a positive effect. Sato et al. [60] have shown that the magnitude of compressive residual stress induced during CP of as-built EBM Ti6Al4V alloy is much higher (194 ± 34 MPa) than those induced by SP (127 ± 30 MPa), which is also reflected in the fatigue life. CP has been shown to reduce the microstrain while SP increased the microstrain, which could be the origin of crack initiation. LSP is more expensive when compared to SP and CP [26].

8.2.5 Surface Mechanical Attrition Treatment

Surface mechanical attrition treatment (SMAT) is used as a post-treatment to improve the surface finish of AM metal parts. SMAT is a S^2PD method. The repeated multi-directional impingement of spherical balls on the surface being treated enables plastic deformation, resulting in surface nanocrystallization [7] (Fig. 8.5). During SMAT, plastic deformation of the rough peaks and partially melted particles and subsequent filling of the valleys by the deformed material is responsible for smoothing of the surface [64]. Since plastic deformation is the governing mechanism, the extent of decrease in roughness is dependent on the ductility of the material. SMAT increased the hardness and the strain hardening effect could be realized in the sub-surface region also. SMAT increased the mechanical properties and wear resistance [64]. The compressive residual stress induced by SMAT improves the fatigue performance. Since tensile residual stress dominates on the surface of AM parts, SMAT

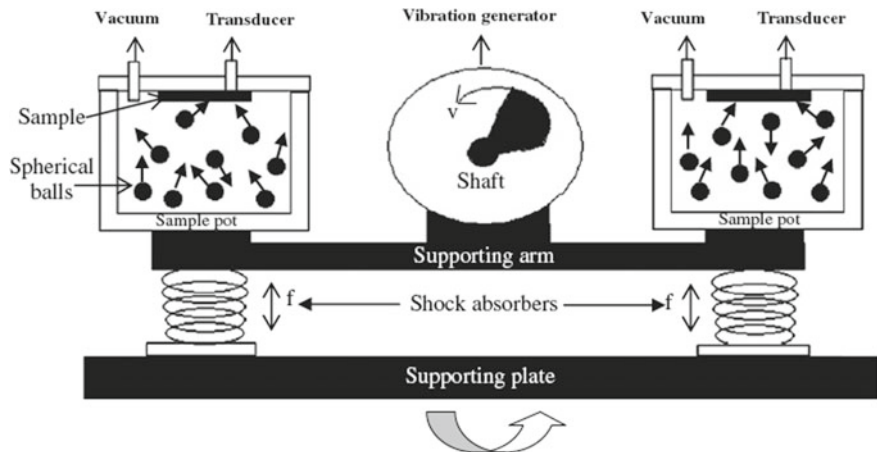


Fig. 8.5 Schematic of the surface mechanical attrition treatment (SMAT) set-up (Reprinted from T. Balusamy et al. [6], with permission from Elsevier)

will be useful to convert it to compressive residual stress [22]. However, SMAT is not amenable for treating AM parts with complex design and internal channels.

8.2.6 Ultrasonic Nanocrystal Surface Modification

Like SMAT, ultrasonic nanocrystal surface modification (UNSM) is also a S²PD method. UNSM involves repetitive bombardment of a WC tip on the surface being treated at ultrasonic frequencies under a controlled static load (Fig. 8.6a). UNSM

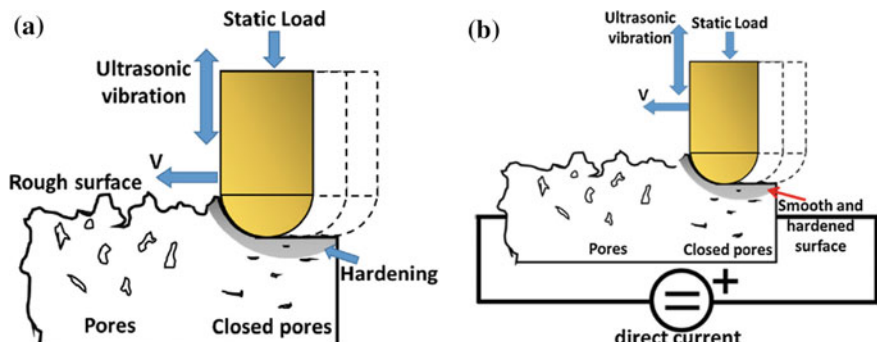


Fig. 8.6 Schematic representation of (a) ultrasonic nanocrystal surface modification (UNSM); and (b) electrically assisted ultrasonic nanocrystal surface modification (EA-UNSM) processes (Reprinted from (a) C. Ma et al. [47]; and (b) H. Zhang et al., [80] with permission from Elsevier)

decreased the surface roughness, improved the surface finish along with the formation of a uniform dimple-like features, decreased the sub-surface porosity, refined the grain size, increased the hardness, converted tensile residual stress to compressive residual stress, improved the fatigue life and increased the corrosion and wear resistance of Ti6Al4V alloy and Ni–Ti alloy [79, 47]. The extent of plastic deformation of SLM 316L SS becomes much higher during UNSM at 400 °C than at 27 °C, which helps to increase the hardness and wear resistance [1]. By an appropriate choice of temperature UNSM can be used to tailor the microstructure of Co-Cr-Mo alloy with a gradient nanostructure (at 25 °C) and a harmonic structure (at 500 °C) [2]. The extent of decrease in surface roughness of AM parts by UNSM is limited. UNSM reduced the elongation of SLM 316L SS from 40 to 24% [1].

Zhang et al. [80] have explored electrically assisted ultrasonic nanocrystal surface modification (EA-UNSM) (Fig. 8.6b) as a post-treatment for 3D printed Ti6Al4V alloy part. When compared to UNSM, the extent of decrease in surface roughness, improvements in surface finish and reduction in surface/sub-surface pores and hardness are much higher in EA-UNSM. The R_a of as-printed Ti6Al4V alloy and those subjected to post-treatment using UNSM and EA-UNSM is 10.6 μm , 7.1 μm and 1.3 μm , respectively. The porosity of the as-printed Ti6Al4V alloy is ~ 1.74%, which is decreased to 1.16% and 0.82% after UNSM and EA-UNSM. The surface hardness of as-printed Ti6Al4V alloy and those subjected to post-treatment using UNSM and EA-UNSM is 359.5 ± 17.3 HV, 437.8 ± 14.2 HV and 484.5 ± 11.9 HV, respectively. Refinement in grain size and strain-hardening are considered responsible for the increase in surface hardness and this effect is much pronounced after EA-UNSM. By an appropriate choice of current density, the temperature can be increased to ~ 425 °C, which enabled a higher extent of plastic deformation. During EA-UNSM, the synergistic mechanical and thermal effect helped to close the surface and sub-surface pores. Materials with plasticity are hard-to-deform. UNSM using a low force is not sufficient to cause plastic deformation while use of a very high force could lead to cracking of the surface/subsurface. On the contrary, the resistive heating during EA-UNSM enables an increase in temperature, which increases the plasticity and facilitates deformation. The easy flow of the rough peak following deformation could offer a better surface finish than those obtained by UNSM.

8.3 Abrasive Finishing Methods

8.3.1 Abrasive Flow Machining

Abrasive flow machining (AFM) was developed by Extrude Hone Corporation to improve the surface finish of internal channels. A viscoelastic medium consisting of abrasive particles pumped at 220 bar enables removal of partially melted particles by micro-cutting and micro-ploughing mechanisms. AFM of SLM Ti6Al4V alloy coupons using a mixture of 60% B₄C, 37% borosiloxane polymer, 2.5% lubricating

grease, and 0.5% oleic acid has reduced the surface roughness from 26 to $0.74 \mu\text{m}$ [10]. The ability of AFM to reduce both the upskin and downskin surface roughness has been established by [55]. AFM reduced the surface roughness of SLM conformal cooling maraging steel internal channels [27] (Fig. 8.7). In addition, AFM induced compressive residual stress and increased the fatigue strength by 26%. Since the abrasive particles could have limited access in deep valleys, the extent of improvement in fatigue strength becomes limited [27]. Lack of uniform surface finish, particularly at complex bends of internal channels, contamination of the surface with abrasive particles and damage of thin-walled structures at excessive pressures are the major limitations of AFM.

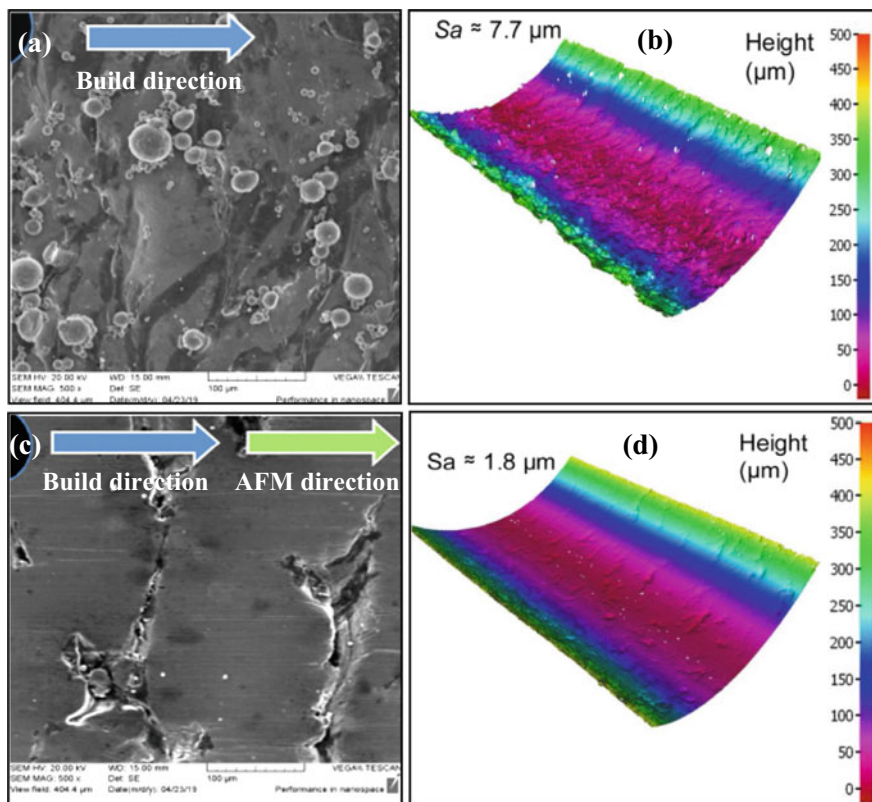


Fig. 8.7 Surface morphology **a, c** and 3D surface profile **b, d** of SLM conformal cooling maraging steel internal channel: **a, b** as-built; **c, d** after AFM (Reprinted from S. Han et al. [27], with permission from Elsevier)

8.3.2 Magnetic Field Assisted Abrasive Finish Machining

The difficulty encountered in controlling the cutting force of the abrasive particles in AFM has led to the development of magnetic field assisted abrasive finish machining (MF-AFM) and magnetorheological abrasive flow machining (MR-AFM). The movement of a mixture consisting of abrasive slurry and magnetic particles using an external magnet (NdFeB magnet) enables control of the cutting force of the abrasive particles and limit excessive material removal. Both MF-AFM and MR-AFM can be effectively used to reduce the surface roughness of internal structures of AM parts. Karakurt et al. [34] have shown that MF-AFM using slurries containing SiC and Al_2O_3 is effective in reducing the surface roughness of the external surface of EBM Cu sample from 35 to 4 μm . MF-AFM has been shown to effectively remove all the partially melted particles and balling effect and offer a 76% decrease in surface roughness for SLM 316L SS [81]. MF-AFM performed in three different stages using coarse, medium and fine particles for 120 min decreased the R_z of SLM 316L SS from 100 to 0.1 μm . However, it involves a material loss of ~ 164 mg with a corresponding decrease in layer thickness by ~ 40 μm .

8.3.3 Abrasive Fluidized Bed Machining

Abrasive fluidized bed machining (A-FBM) is based on fluidized bed hydrodynamics in which the hydrodynamic effect created by the air bubbles helps the abrasive particles to impact on the surface of the sample placed inside the fluidized bed [41]. Rotation of the sample inside the fluidized bed promotes interaction between the sample surface and abrasive particles, increases the speed of impingement of abrasive particles and the extent of material removal and thereby improving the process efficiency [21]. Microplooughing or microcutting by the abrasive particles is the main mechanism of removal of the partially molten particles. Spherical shaped abrasive particles remove the partially molten particles mainly by microplooughing mechanism while both microplooughing and microcutting is found to be operative with the use of angular shaped abrasive particles [3]. The cost-effectiveness, ease of automation and sustainability of the process, are the major advantages of A-FBM. Contamination of the surface with abrasive particles, lack of improvement in the surface finish at complex bends of the internal channels are some of the major limitations of A-FBM [41].

8.3.4 Ultrasonic and Hydrodynamic Cavitation Abrasive Finishing

Two types of cavitation abrasive finishing based on ultrasonic and hydrodynamic principles were explored to improve the surface finish of AM parts. Ultrasonic cavitation abrasive finishing (UCAF) involves two different mechanisms: (i) collapse of bubbles on the surface by cavitation; and (ii) impingement of the abrasive particles on the surface. The combined action of both of them offers a decrease in surface roughness. The cavitation bubbles nucleate and grow at the crevices present on the rough as-built AM part subsequently collapse on the surface [65, 66]. Repeated collapse of these bubbles on the surface removes the partially melted powders. Impingement of the abrasive particles accelerated by the cavitation action removes larger-size balls and flattens rough peaks. Use of 1200 grit size micro-abrasive particles is recommended to achieve a good surface finish [65].

In hydrodynamic cavitation abrasive finishing (HCAF), the cavitation bubbles are generated based on hydrodynamic flow principles in which abrasive particles are freely suspended. The partially melted particles present on the surface of the AM part are removed by hydrodynamic cavitation while large-sized balls and rough peaks are removed by the impingement of the abrasive particles accelerated by cavitation [53] (Fig. 8.8).

The bubble-particle interaction that creates a synergistic effect on surface finishing is the unique advantage of HCAF. Due to the synergistic action, HCAF requires only 1% of the abrasive particles as opposed to > 50% of abrasive particles in traditional abrasive finishing methods [53]. The combination of hydrodynamic flow and the use of lower amount of abrasive particles eliminate damage of the corners/edges, thus

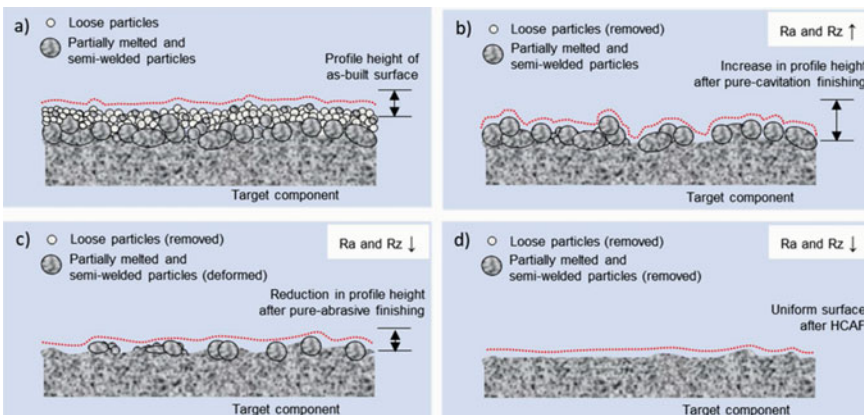


Fig. 8.8 Schematic representation of improvement in surface finishing by HCAF process: **a** as-built AM component surface; **b** after pure-cavitation finishing; **c** after pure-abrasive finishing; and **d** after combined hydrodynamic cavitation abrasive finishing (Reprinted from A.P. Nagalingam, et al. [53], with permission from Elsevier)

preserving the dimensional integrity of the AM part (Fig. 8.9). HCAF is effective in improving the surface finish of internal channels and preserving the circularity of internal contours [52]. HCAF increases the hardness, improves the wetting characteristics, induces compressive residual stress and increases the fatigue life. Erosion of the pump valves with time will be a major concern in HCAF.

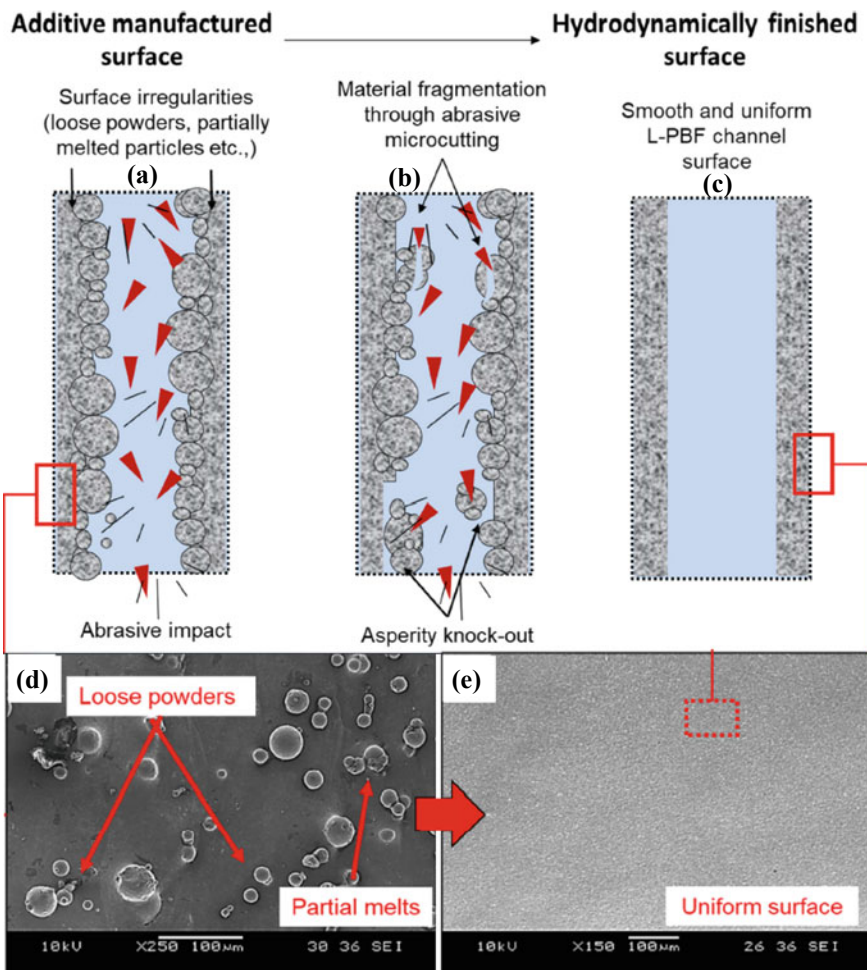


Fig. 8.9 Mechanism of removal of surface irregularities in SLM Inconel 625 alloy internal channels by multi-jet hydrodynamic finishing: **a–c** schematics showing the various stages of material removal and surface smoothening; **d, e** surface morphology: **d** as-built internal channel with surface irregularities; and **e** smooth and uniform texture after surface finishing (Reprinted from A.P. Nagalingam and S.H. Yeo, [52] with permission from Elsevier)

8.4 Chemical and Electrochemical Processes

8.4.1 Chemical Etching

Chemical etching (CE) of AM parts involves removal of partially melted particles using acid mixtures. CE of SLM and HIP treated Ti6Al4V alloy part using HF-HNO₃-H₂O mixture in 1:2:3 ratios for 10 min has enabled a complete removal of partially melted particles, reduced the surface roughness from 12.2 to 6.6 μm , increased the fatigue life, improved the biocompatibility and promoted cellular activity [30]. However, CE decreased the relative density of EBM Ti6Al4V alloy lattice structures following the reduction in strut diameter during CE [19]. SLM CoCr F75 scaffolds become more fragile after CE [73]. Hence, appropriate allowances for the strut thickness and scaffolds should be provided during the design stage itself.

8.4.2 Chemical Polishing

Chemical polishing (CP) involves removal of partially melted powder particles by dissolution using acid mixtures without the requirement for any tools [75]. The difference in rate of dissolution between the peaks and valleys in the AM part enables smoothing of the surface. The gas bubbles formed on the surface keep the dissolution process active without any stagnation. The acid mixtures used for CP is selected based on the type of material. Appropriate dilution of the acid mixtures with longer processing time offers much control during CP while stirring of the polishing solution provides good stability [46]. Unlike mechanical post-treatments, CP concurrently improves the surface finish of both the outer and inner surfaces [70]. CP can be applied to AM parts with complex geometries as well as for thin porous lattice structures and scaffolds (Fig. 8.10). CP is capable of removing irregularities present in AM

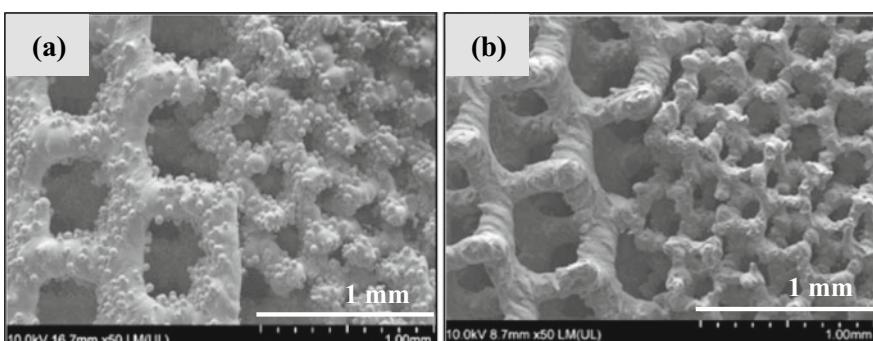


Fig. 8.10 SEM images of the surface of Ti scaffolds: **a** before, **b** after chemical polishing (Reprinted from B. Wysocki et al. [75], with permission from Elsevier)

parts and smoothing of the surface without any change in chemical composition. CP Ti scaffold fails to show any negative effect on the proliferation and growth of MG63 cells, rather it helped to improve colonization [75]. Since the mechanism of eliminating the surface irregularities is by dissolution, mass loss is inevitable during CP. Hence, dimensional integrity of the part after CP is a matter of concern. CP has been shown to decrease the Young's modulus (~ 70%) and compressive strength (~ 30%) [75]. CP is not considered as a suitable choice for post-treating scaffolds with smaller pores.

8.4.3 Combined Chemical and Abrasive Flow Polishing

Mohammadian et al. [51] have shown that the combined chemical abrasive flow polishing using 40 vol. % HF + 40 vol. % HNO₃ + 20 vol. % H₂O dispersed with 420 μm Al₂O₃ particles at a flow velocity of 3 m/s is effective in improving the partially melted particles on the inner surfaces of tubular part made of IN625 alloy, reducing its surface roughness and improving its surface texture. During chemical flow polishing, formation of a passive oxide layer could reduce the rate of polishing. Abrasive flow polishing requires a higher fluid velocity. In combined chemical abrasive flow polishing, the passive oxide layer formed on the surface is continuously removed by the impingement of the abrasive particles.

8.4.4 Electropolishing

Electropolishing (EP) is based on the electrochemically assisted dissolution of the anode under the influence of an applied current and it can be effectively used to improve the surface finish of AM metal parts. Current density is the major factor in determining the efficiency of the EP process. During the initial stages of EP, the residual powders, which protrude outside the surface of the AM part, are removed. Subsequently, polishing of the completed melted layer occurs until the entire surface of the part is uniformly polished (Fig. 8.11). Random dissolution of crystallographic planes during EP is considered responsible for the observed improvement in surface finish [58]. An increase in current density, temperature, treatment time, flow rate, and narrowing the inter-electrode distance would increase the rate of polishing and efficiency. EP is suitable for polishing AM parts with complex shapes, internal channels and thin walled structures, which are usually fragile [71]. EP reduced the contact angle of SLM 316L SS part to 45°, thus making the surface of the part more hydrophilic [70]. The level of surface finish accomplished by EP is much better than those achieved by CP and it is possible to achieve a reduction in surface roughness as high as 92% [71]. Since the average surface roughness (R_a) of SLM Ti6Al4V alloy parts built at different build angles varies from 4 μm (0°) to 23 μm (135°), it is imperative to provide suitable allowance for the current density and time during

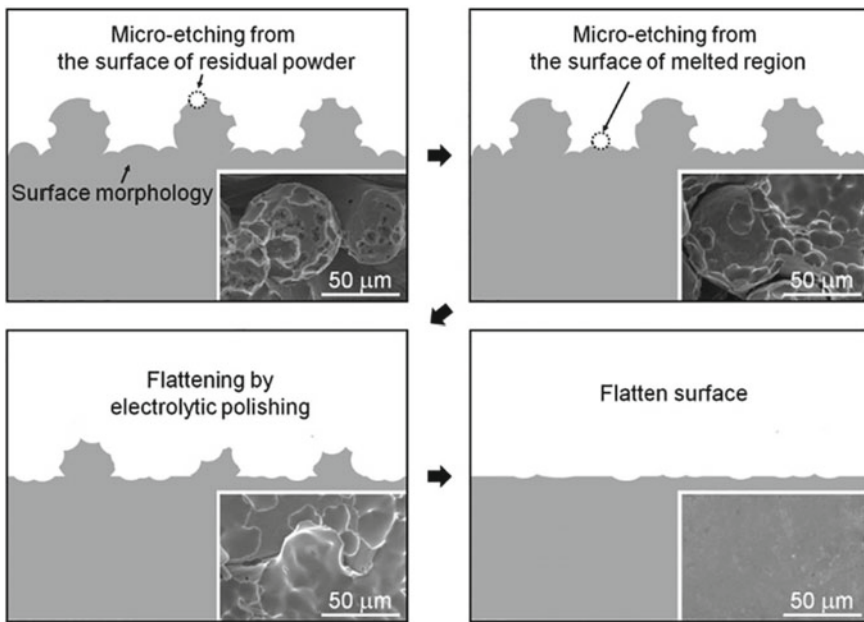


Fig. 8.11 Schematic diagram depicting the mechanism of flattening of surface during EP (Inset: higher magnification images) (Reprinted from J.-H. Jung et al. [32], with permission from Elsevier)

EP to achieve uniform surface finish [71]. The formation of a dense and compact passive oxide layer with fewer defects after EP has increased the corrosion resistance of EMB Ti6Al4V alloy part [74].

The reduction in surface roughness by EP is accompanied a reduction in thickness; the higher the current density, the greater is the extent of polishing and greater is the thickness reduction. For highly rough surfaces, the thickness reduction during EP can be as high as 80 μm , which challenges the dimensional integrity of the AM part [71]. In spite of its ability, the difficulty in placing the cathode within the confined space of internal channels limits the use of EP [70]. EP has been shown to be ineffective in removing holes or cracks or slag present on the surface of the AM part. The presence of an underlying pore in the AM part could promote crack nucleation or crack growth during EP [5, 40]. EP is not effective when the AM part contains non-conducive phases [58]. EP encounters difficulty in polishing multi-phase alloys due to the difference in reactivity of the phases during the electrochemical dissolution process, resulting in an uneven surface finish. The presence of a passive oxide layer such as TiO_2 on the surface of Ti and its alloys poses difficulty during EP and warrants the use of hazardous perchloric (HClO_4) and hydrofluoric (HF) acid based electrolytes to remove the passive TiO_2 layer. An increase in duration of EP has been shown to decrease the hardness by 35% and Young's modulus by 45% of SLM Inconel 718 alloy part [5]. Retention of microscopic cavities is a major limitation of EP [70]. Use of an excessive current density for EP has led to the formation of tiny

dots on the surface of EBM Ti6Al4V alloy part, which deleteriously influenced its corrosion resistance in simulated body fluid [74].

8.4.5 Jet Electrochemical Machining

Cheng et al. [15] have suggested jet electrochemical machining (JECM) as a post-treatment method for SLM 316L SS coupons. During JECM, the SLM 316L SS coupon was made as the anode and a nozzle which sprays 10% NaCl was made as the cathode. During JECM, the resistance between the anode and cathode is determined by the electrolyte layer thickness. The higher the thickness, the greater is the resistance. Since the as-built SLM 316L SS coupon is rough, the thickness of the electrolyte layer between the rough peaks (anode) and the nozzle (cathode) is less, which facilitates an easy dissolution of the peaks (Fig. 8.12). During EP as well as in JECM, these peaks assume high current density, which enforces dissolution. Obviously, the rate of metal dissolution will be less at the valleys as the electrolyte layer thickness and the resistance is relatively higher. The surface of SLM 316L SS coupon becomes defect free along with the formation of a microporous structure after JECM at 120 mA/cm² for 10 min. The difference in the rate of dissolution at different locations has lead to the development of surface roughness during JECM, resulting in a decrease in roughness only by 53%.

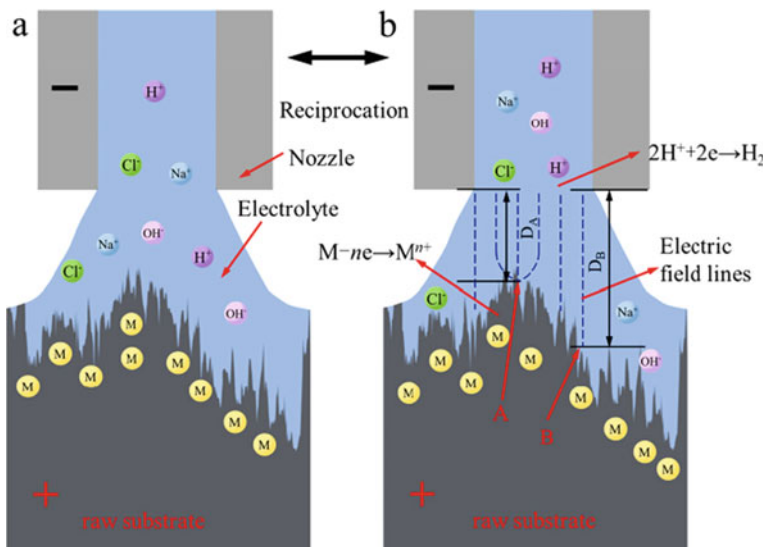


Fig. 8.12 Schematic representation of the JECM: **a** Before JECM; and **b** during JECM (Reprinted from H. Cheng et al. [15], with permission from Elsevier)

8.5 Laser and Electron Beam Processes

8.5.1 Laser Polishing

Laser polishing (LP) involves melting of a thin surface layer and re-distributing the molten layer from the peaks and valleys using the surface tension of the melt, signifying no material removal and only relocation of the molten layer [49, 68] (Fig. 8.13). Hence, dimensional integrity of the component is preserved. The laser energy density, scanning speed, pulse overlap and number of passes are the major factors influencing the process [13, 28]. LP is effective in eliminating the partially melted particles and asperities present in as-built AM part and reconstruct the surface with a smooth finish [13, 14, 42].

The extent of decrease in roughness achieved after LP can be as high as 90–96%. The extent of decrease in surface roughness depends on melt pool velocity. It is imperative to optimize the conditions to achieve a low melt pool velocity which increases the melt pool width rather than the depth [49]. LP refines the grain size, increase the hardness, tensile strength, ductility, fatigue strength, wear resistance and corrosion resistance [13, 14]. LP makes the surface hydrophilic. Repeatability of the process, high speed and ability to polish a selective area are some of the highlights of the process. LP induces tensile residual stress [42, 68]. Crack formation during LP is a major concern [54]. LP is not amenable for surface finishing of internal channels [41]. The choice of a higher laser energy density, insufficient overlap and number of laser passes beyond a threshold has led to an increase in surface roughness [28]. LP promotes surface oxidation in the absence of vacuum or an inert atmosphere [49, 54]. An increase in exposure time during LP extends the HAZ. LP under pulsed mode leads to the formation of porous, cracked surface with an uneven surface oxide layer [23].

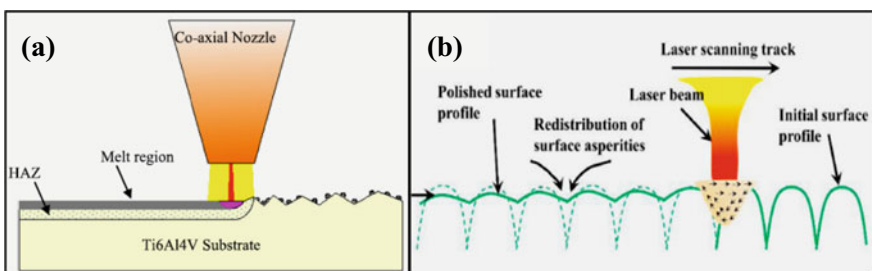


Fig. 8.13 Schematic representation of **a** laser polishing; and **b** how the initial surface profile is changed after laser polishing with redistribution of surface asperities (Reprinted from **a** S. Marimuthu et al. [49]; **b** L. Chen et al. [13], with permission from Elsevier)

8.5.2 Laser Re-Melting

Laser remelting improves the surface finish, eliminates the lack of fusion (LOF) pores, decreases the size of the metallurgical pores, increases the density of the part and decreases the residual stress (Fig. 8.14). The rapid solidification after laser remelting refines the grain size. The elimination of pores, decrease in grain size and decrease in residual stress helps to increase the hardness and UTS [36]. The change in surface chemical composition and the thickness of the oxide layer after laser remelting of SLM Ti6Al4V alloy part raises concern on the corrosion resistance and biocompatibility of such parts [72]. The higher cost, decrease in ductility and formation of a thick oxide layer are the major limitations in employing in situ laser remelting.

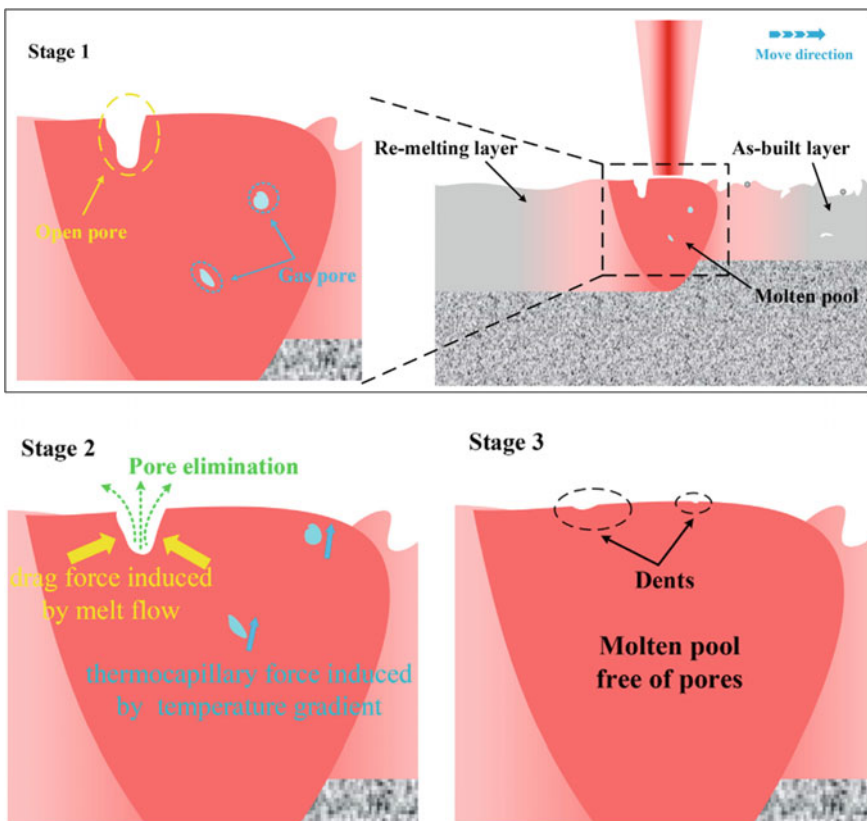


Fig. 8.14 Schematic representation of pore elimination mechanism during laser re-melting process (Reprinted from F. Lv et al. [45], with permission from Elsevier)

8.5.3 Large Pulsed Electron-Beam Irradiation

Large pulsed electron-beam (LPEB) irradiation is similar to LP. Both of them involve melting of the thin surface layer and redistribution of the molten metal pool between the peaks and valleys, resulting in a smooth surface. LPEB irradiation is effective in removing partially melted particles, spatters, cavities, and improving the surface finish [59, 62]. The level of surface finish accomplished after LPEB irradiation is ~75% and the treated surfaces are free of microcracks (Fig. 8.15) [59]. LPEB irradiation induces tensile residual stress and involves the formation of a heat affected zone. LPEB irradiation is not suitable for surface finishing of internal channels.

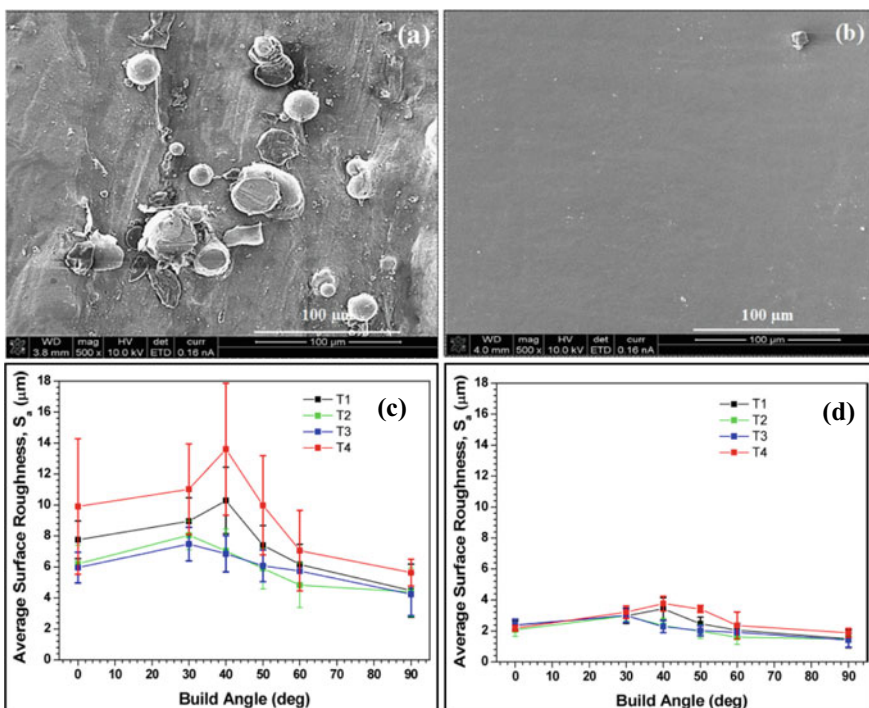


Fig. 8.15 **a, b** Surface morphology of the uppermost layer of SLM maraging steel samples; and **c, d** arithmetical mean height (S_a) of SLM maraging steel samples as a function of build angles: **a, c** As-built; and **b, d** after large pulsed electron-beam (LPEB) irradiation; (Reprinted from T.S.N. Sankara Narayanan et al. [59], with permission from Elsevier)

8.6 Hybrid Additive/subtractive Manufacturing

TF could reduce the surface roughness of SLM Ti6Al4V alloy part whereas TF alone could not offer an improvement in fatigue life. SP could induce compressive residual stress and increase the fatigue life. A hybrid treatment of TF and SP has reduced the surface roughness, induced compressive residual stress and increased the fatigue life of SLM.

Ti6Al4V alloy part [20]. The choice of prolonged time duration for TF to decrease the surface roughness and subsequent SP would be cost-effective.

Teng et al. [67] have explored a hybrid treatment involving grinding process (GP) and MAF to decrease the surface roughness of SLM AlSi10Mg alloy. The GP using 160–200 μm sized Al_2O_3 abrasive particles reduced the surface roughness of the as-built AlSi10Mg alloy sample from 7 to 0.6 μm , leaving behind the scratches and pores. The subsequent MAF using spherical SiC W7 magnetic abrasives has reduced the surface roughness from 0.6 to 0.155 μm with a smooth surface finish. The GP induces strain hardening and increased the surface hardness, which is decreased after MAF.

Guo et al. [24] have explored a hybrid treatment of precision grinding (PG) and EP to improve the surface finish of EBM Ti6Al4V alloy part. The R_a as-built part varies from 23–32 μm . EP decreased the R_a to 21–28 μm . PG reduced the R_a to 2 μm , induced compressive residual stress and increased the hardness but it leaves tool marks on the surface. A hybrid treatment of PG followed by EP reduced the R_a to < 1 μm and removed the tool marks. The R_a is decreased further to 0.65 μm when the EP time is increased to 40 min. However, EP released the compressive residual stress induced during PG. Since both PG and EP involves thickness/mass loss, adequate compensation should be provided for the part during the initial design stage.

E-blasting, which combines the unique features of blasting and EP, has been suggested as a hybrid treatment to improve the surface finish of SLM Ti6Al4V alloy part [23]. During E-blasting, the Ti6Al4V alloy part is subjected to EP using a mixture of 700 ml/L of ethyl alcohol + 300 ml/L isopropyl alcohol + 60 g/L AlCl_3 + 250 g/L of ZnCl_2 and simultaneously blasted using 40–70 μm sized spherical glass beads at a pressure of 5.5 MPa. E-blasting has enabled a clean, smooth and bright surface finish without any defects. Most importantly, the finished surface after E-blasting was free from the blasting media, which is a serious concern in conventional blasting treatment. The level of surface finishing obtained by E-blasting is as high as 92%. E-blasting is effective in reducing the surface roughness of internal cavities.

A hybrid treatment of chemical etching (CE) and electropolishing (EP) using HF based solution has been shown to offer a good reduction in surface roughness of 3D printed Ti6Al4V alloy open porous structure with controlled strut morphology [57]. CE using a mixture of 0.5 ml of 48% HF + 50 g H_2O for 10 min removed the partially melted powders attached to the strut surface. EP using a mixture of 55 ml CH_3COOH + 30 ml H_2SO_4 + 15 ml HF at 1.2 mA/mm² for 8 min removed the unevenness and provides a smooth surface finish. However, this hybrid treatment

has increased the internal porosity, decreased the strut thickness and decreased the mechanical properties.

Seo et al. [61] have suggested a hybrid treatment approach of blasting and plasma electrolytic polishing (PEP) to improve the surface finishing of SLM CoCr alloy part. Blasting of the part using stainless steel balls at 7.5 bar reduced the R_a from 13 μm to 3 μm . PEP of the blasted surface using 0.3 M $(\text{NH}_4)_2\text{SO}_4$ (pH: 5.30; temperature: 75 °C) at 450 V for 8 min has reduced the R_a to 20 nm. The formation of an oxide film on the surface of CoCr alloy after this hybrid treatment has offered an excellent corrosion resistance in 3.5% NaCl.

In situ laser remelting (LR) during fabrication of the part by SLM is a well-known hybrid treatment approach. The SLM-LR hybrid treatment has been shown to eliminate irregular pores and LOF defects, decrease the surface roughness and increase the density of SLM parts [76]. However, this would be possible only with the choice of an appropriate laser power and scanning speed that enables sufficient spreading of the molten material. The choice of a higher laser power for LR provides sufficient time for spreading of the molten material, which reduces the porosity and surface roughness of the top surface. However, the side surface roughness is increased. Although LR at higher laser power reduces the residual stress, it also facilitates the formation of a thick oxide layer, which could affect the mechanical properties of the AM part [8]. During LR at higher laser power, new pores could also be introduced [29]. The choice of a higher scanning speed for LR fails to eliminate the pores whereas a lower scanning speed introduces new pores [45]. LR of each layer after solidification provides a good platform for deposition of the subsequent layer by SLM. The molten layer generated by LR properly wet the underlying solid metal and offer a relatively smooth surface finish [8]. LR decreased the amount of partially melted Ta particles, increased the homogeneity, YS and elastic modulus of the SLM Ti25Ta alloy. However, LR has led to a slight increase in porosity, increased the residual stress, increased the dislocation density, reduced the ductility, decreased the fatigue strength and increased the crack propagation rate of the SLM Ti25Ta alloy. Hence, it is imperative to optimize the conditions employed for LR during the hybrid treatment processes to impart the desired characteristics in the AM part [11].

8.7 Concluding Remarks

A variety of surface finishing post-treatments have been explored to improve the surface finishing of AM metallic components. Each one of them has its own advantages and limitations. The suitability of these methods is ascertained in terms of: (i) Extent of decrease in surface roughness; (ii) thickness/mass loss; (iii) amenability to treat complex design, internal channels and thin lattice structures; (iv) beneficial attributes; (v) problems due to the post-treatment; (vi) process merits in terms of

design aspects, treatment time, selectivity, ability to treat different type of surfaces, wastage and disposal problems and (vii) cost-effectiveness.

(i) Extent of decrease in roughness

The extent of decrease in surface roughness is limited for many mechanical finishing methods. FM could reduce the roughness by 90–96%. Blasting and CE could provide a 50% reduction in roughness. Based on the ability to decrease the surface roughness, peening methods can be ranked as follows: SP > CP > LSP. The level of surface finish accomplished by EP is much better than CP. The reduction in surface roughness can be as high as 92% for EP. Although both CP and EP are capable of treating the internal surfaces of AM parts, CP has an edge over EP due to the difficulty in placing the counter electrode in the latter case. The extent of decrease in roughness achieved after LP can be as high as 90–96% while LPEB irradiation offers ~ 75% reduction in surface roughness.

(ii) Thickness/mass loss

Mechanical surface finishing methods obviously involve thickness/mass loss. The extent of thickness/mass loss is much higher in CP and EP. The thickness reduction during EP can be as high as 80 μm . Hence, dimensional integrity of the AM part after CP and EP is a matter of concern. LP and LPEB irradiation involve no material removal and the molten material is redistributed between the peaks and valleys, resulting in a smooth surface. Hence, dimensional integrity of the AM component is preserved.

(iii) Amenability to treat complex design, internal channels and thin lattice structures

TF/BF is amenable for treating AM parts with complex shapes with limited improvement in surface finish. Blasting is considered to be suitable for treating thick AM parts. Internal channels can be treated with limited success. However, impingement of the abrasive particles might damage thin lattice structures. Abrasive finishing methods are effective in treating internal channels. CP and EP are suitable for treating AM parts with complex geometries, internal channels and fragile thin walled structures. FM, LP, LPEB irradiation, SMAT and UNSM are not amenable for treating AM parts with complex shapes and internal channels.

(iv) Beneficial attributes

SP, CP, LSP, SMAT and UNSM reduce the surface roughness by plastic deformation. The compressive residual stress induced during these methods helps to increase the fatigue strength of the AM part. CP, EP and LP provide a highly polished surface, decrease the contact angle and make the finished surface more hydrophilic. Such surfaces could increase the biocompatibility and promote cell proliferation and growth. Repeatability, high speed and ability to polish a selective area are some of the highlights of LP.

(v) Problems imposed by the post-treatment methods

Blasting leads to incorporation of abrasive particles on the treated surface. CE reduced the strut diameter and decreased the relative density of lattice structures. Moreover, CE makes the scaffolds fragile. Prolonged use of SP is not effective in reducing the surface roughness. CP decreased the Young's modulus and compressive strength of AM part. EP decreased the hardness and Young's modulus. Both CP and EP retain microscopic cavities. Use of an excessive current density for EP induced pitting on the surface and deleteriously influenced the corrosion resistance. LP induces tensile residual stress. Crack formation during LP is a major concern. LP promotes surface oxidation when performed in the absence of vacuum or an inert atmosphere. An increase in exposure time during LP extends the HAZ. LP under pulsed mode results in the formation of a porous, cracked surface with an uneven surface oxide layer. LPEB irradiation induces tensile residual stress and involves the formation of a heat affected zone.

(vi) Process merits in terms of design aspects, treatment time, selectivity, ability to treat different type of surfaces, wastage and disposal problems

Many mechanical methods such as TF/BF, DF, VSF, etc. require a longer processing time to decrease the surface roughness. On the contrary, FM, SP, LP and EP could reduce the surface roughness at a shorter duration of time. Wastage of the abrasive media and problems in disposing them are the major limitations in TF/BF as well as in abrasive finishing methods. CE, CP, EP involves immersion of the whole AM part in the electrolyte, pointing out the lack of selectivity. Disposal of spent acids is a serious concern in CE, CP and EP. Designing cathodes according to the geometry of the AM and the difficulty in placing the cathode within a confined space of internal channels are other major process limitations in EP. The difficulty encountered in treating AM parts with multi-phase alloys, non-conductive phases and slags is yet another challenge in EP. The choice of a higher laser energy density, insufficient overlap and number of laser passes beyond a threshold has increased the surface roughness in LP.

(vii) Cost-effectiveness

Mechanical surface finishing methods are cost-effective. Abrasive finishing methods and chemical and electrochemical methods involve a moderate cost. Laser based processes such as LP and LSP as well as LPEB irradiation are expensive.

Regarding the choice of post-treatment for AM part, “one solution for all” is not possible. The appropriate method should be chosen based on the type of AM part, its complexity, thickness, fragility, type of phase present and the end use of the part. If fatigue strength of the part is important, then peening methods might be a good choice. For treating internal channels, abrasive finishing methods are the most appropriate choice. Many hybrid treatment methods are also being explored. For many parts, a suitable combination of two or three methods of surface post-treatment under optimized conditions would offer a good surface finish. The quest for a better surface finishing post-treatment for AM parts continues.

8.8 Future Perspectives

The role of surface finishing post-treatments to improve the surface finish of metals and alloys are addressed in this chapter. Many hybrid treatments are emerging, which extends the window of opportunity of achieving a better surface finish for metals and alloys. Recently, the realm of AM extends beyond metals and alloys. Bimetallic materials, composites and functionally graded materials are fabricated by AM. In addition, AM of components with multi-materials such as metal–metal, metal–ceramic and metal–polymeric are being explored for numerous applications. The surface finishing post-treatment methods and conditions employed for metals and alloys cannot be used as such for the emerging bimetallic materials, composites, functionally graded materials and multi-material systems. To realize the fullest potential of AM of emerging materials, suitable modifications have to be proposed in the surface finishing methods to accommodate the emerging materials. The functionally graded materials and multi-material systems warrant the development of new methods of surface finishing. Much remains to be explored in this area. Surface engineering/modification research will again assume significance as many new developments are made in AM.

References

1. Amanov, A.: Effect of local treatment temperature of ultrasonic nanocrystalline surface modification on tribological behavior and corrosion resistance of stainless steel 316L produced by selective laser melting. *Surf. Coat. Technol.* **398**, 126080 (2020a)
2. Amanov, A.: A promising post-additive manufacturing surface modification for tailoring gradient nanostructure and harmonic structure in Co-Cr-Mo alloy. *Vacuum* **182**, 109702 (2020b)
3. Atzeni, E., Barletta, M., Calignano, F., Iuliano, L., Rubino, G., Tagliaferri, V.: Abrasive fluidized bed (AFB) finishing of AlSi10Mg substrates manufactured by direct metal laser sintering (DMLS). *Addit. Manuf.* **10**, 15–23 (2016)
4. Bagherifard, S.: Enhancing the structural performance of lightweight metals by shot peening. *Adv. Eng. Mater.* **21**, 1801140 (2019)
5. Baicheng, Z., Xiaohua, L., Jiaming, B., Junfeng, G., Pan, W., Chen-nan, S., Muiling, N., Guojun, Q., Jun, W.: Study of selective laser melting (SLM) Inconel 718 part surface improvement by electrochemical polishing. *Mater. Des.* **116**, 531–537 (2017)
6. Balusamy, T., Kumar, S., Sankara Narayanan, T.S.N.: Effect of surface nanocrystallization on the corrosion behaviour of AISI 409 stainless steel. *Corros. Sci.* **52**(11), 3826–3834 (2010)
7. Balusamy, T., Sankara Narayanan, T.S.N. and Park, H.Y.: Surface Nanostructuring of Metallic Materials for Implant Applications. In: Santra, T.S. Mohan, L. (Eds.) *Nanomaterials and Their Biomedical Applications*, pp. 465–511. Springer, Singapore (2021)
8. Bayati, P., Safaei, K., Nematollahi, M., Jahadakbar, A., Yadollahi, A., Mahtabi, M., Elahinia, M.: Toward understanding the effect of remelting on the additively manufactured NiTi. *Int. J. Adv. Manuf. Technol.* **112**, 347–360 (2021)
9. Boschetto, A., Bottini, L., Macera, L., Veniali, F.: Post-processing of complex SLM parts by Barrel Finishing. *Appl. Sci.* **10**, 1382 (2020)
10. Boulard, C., Urlea, V., Beaubier, K., Samoilenko, M., Brailovski, V.: Abrasive flow machining of laser powder bed-fused parts: Numerical modeling and experimental validation. *J. Mater. Process. Technol.* **273**, 116262 (2019)

11. Brodie, E.G., Richter, J., Wegener, T., Niendorf, T., Molotnikov, A.: Low-cycle fatigue performance of remelted laser powder bed fusion (L-PBF) biomedical Ti25Ta. *Mater. Sci. Eng. A* **798**, 140228 (2020)
12. Chen, Z., Wu, X., Tomus, D., Davies, C.H.J.: Surface roughness of selective laser melted Ti-6Al-4V alloy components. *Addit. Manuf.* **21**, 91–103 (2018)
13. Chen, L., Richter, B., Zhang, X., Ren, X., Pfefferkorn, F.E.: Modification of surface characteristics and electrochemical corrosion behavior of laser powder bed fused stainless-steel 316L after laser polishing. *Addit. Manuf.* **32**, 101013 (2020)
14. Chen, L., Richter, B., Zhang, X., Bertsch, K.B., Thoma, D.J., Pfefferkorn, F.E.: Effect of laser polishing on the microstructure and mechanical properties of stainless steel 316L fabricated by laser powder bed fusion. *Mater. Sci. Eng. A* **802**, 140579 (2021)
15. Cheng, H., Xu, B., Xie, D., Yang, Y., Shen, L., Qiu, M., Chen, Y., Lou, G., Zhao, J., Tian, Z.: Improvement of selective laser melting substrate surface performance via combined processing of jet electrochemical machining and jet electrodeposition. *Surf. Coat. Technol.* **412**, 127028 (2021)
16. Chi, J., Cai, Z., Zhang, H., Zhang, H., Guo, W., Wan, Z., Han, G., Peng, P., Zeng, Z.: Combining manufacturing of titanium alloy through direct energy deposition and laser shock peening processes. *Mater. Des.* **203**, 109626 (2021)
17. Childerhouse, T., Hernandez-Nava, E., M'Saoubi, R., Tapoglou, N., Jackson, M.: Surface and sub-surface integrity of Ti-6Al-4V components produced by selective electron beam melting with post-build finish machining. *Procedia CIRP* **87**, 309–314 (2020)
18. Damon, J., Dietrich, S., Vollert, F., Gibmeier, J., Schulze, V.: Process dependent porosity and the influence of shot peening on porosity morphology regarding selective laser melted AlSi10Mg parts. *Addit. Manuf.* **20**, 77–89 (2018)
19. de Formanoir, C., Suard, M., Dendievre, R., Martin, G., Godet, S.: Improving the mechanical efficiency of electron beam melted titanium lattice structures by chemical etching. *Addit. Manuf.* **11**, 71–76 (2016)
20. Denti, L., Bassoli, E., Gatto, A., Santecchia, E., Mengucci, P.: Fatigue life and microstructure of additive manufactured Ti6Al4V after different finishing processes. *Mater. Sci. Eng. A* **755**, 1–9 (2019)
21. El Hassinan, A., Troiano, M., Scherillo, F., Silvestri, A.T., Contaldi, V., Solimene, R., Scala, F., Squillace, A., Salatino, P.: Rotation-assisted abrasive fluidised bed machining of AlSi10Mg parts made through selective laser melting technology. *Procedia Manuf.* **47**, 1043–1049 (2020)
22. Eyzat, Y., Chemkhi, M., Portella, Q., Gardan, J., Remond, J., Retraint, D.: Characterization and mechanical properties of as-built SLM Ti-6Al-4V subjected to surface mechanical post-treatment. *Procedia CIRP* **81**, 1225–1229 (2019)
23. García-Blanco, M.B., Díaz-Fuentes, M., Espinosa, E., Mancisidor, A.M., Vara, G.: Comparative study of different surface treatments applied to Ti6Al4V parts produced by Selective Laser Melting. *Trans. Inst. Met. Finish.* (2021). <https://doi.org/10.1080/00202967.2021.1898171>
24. Guo, J., Goh, M.H., Wang, P., Huang, R., Lee, X., Wang, B., Nai, S.M.L., Wei, J.: Investigation on surface integrity of electron beam melted Ti-6Al-4V by precision grinding and electropolishing. *Chinese J. Aeronaut.* Available online 2 Sept 2020. <https://doi.org/10.1016/j.cja.2020.08.014>
25. Guo, W., Sun, R., Song, B., Zhu, Y., Li, F., Che, Z., Li, B., Peng, P.: Laser shock peening of laser additive manufactured Ti6Al4V titanium alloy. *Surf. Coat. Technol.* **349**, 503–510 (2018)
26. Hackel, L., Rankin, J.R., Rubenchik, A., King, W.E., Matthews, M.: Laser peening: A tool for additive manufacturing post-processing. *Addit. Manuf.* **24**, 67–75 (2018)
27. Han, S., Salvatore, F., Rech, J., Bajolet, J., Courbon, J.: Effect of abrasive flow machining (AFM) finish of selective laser melting (SLM) internal channels on fatigue performance. *J. Manuf. Process.* **59**, 248–257 (2020)
28. Hofele, M., Schanz, J., Roth, A., Harrison, D.K., De Silva, A.K.M., Riegel, H.: Process parameter dependencies of continuous and pulsed laser modes on surface polishing of additive manufactured aluminium AlSi10Mg parts. *Mater. Sci. Eng. Technol. (Materialwiss. Werkstofftech)* **52**(4), 409–432 (2021)

29. Hu, Z., Nagarajan, B., Song, X., Huang, R., Zhai, W., Wei, J.: Tailoring surface roughness of micro selective laser melted SS316L by In-Situ Laser Remelting. In: Itoh, S., Shukla, S. (eds.) INCASE 2019, LNME, pp. 337–343, Springer, Singapore Pte Ltd. (2020)
30. Jamshidi, P., Aristizabal, M., Kong, W., Villapun, V., Cox, S.C., Grover, L.M., Attallah, M.M.: Selective laser melting of Ti-6Al-4V: The impact of post-processing on the Tensile, Fatigue and biological properties for medical implant applications. *Materials* **13**(12), 2813 (2020)
31. Jin, X., Lan, L., Gao, S., He, B., Rong, Y.: Effects of laser shock peening on microstructure and fatigue behavior of Ti-6Al-4V alloy fabricated via electron beam melting. *Mater. Sci. Eng. A* **780**, 139199 (2020)
32. Jung, J.-H., Park, H.-K., Lee, B.S., Choi, J., Seo, B., Kim, H.K., Kim, H.G., Kim, H.G.: Study on surface shape control of pure Ti fabricated by electron beam melting using electrolytic polishing. *Surf. Coat. Technol.* **324**, 106–110 (2017)
33. Kahlin, M., Ansell, H., Kerwin, A., Smith, B., Moverare, J.: Variable amplitude loading of additively manufactured Ti6Al4V subjected to surface post processes. *Int. J. Fatigue* **142**, 105945 (2021)
34. Karakurt, I., Ho, K.Y., Ledford, C., Gamzina, D., Horn, T., Luhmann, N.C., Lin, L.: Development of a magnetically driven abrasive polishing process for additively manufactured copper structures. *Procedia Manuf.* **26**, 798–805 (2018)
35. Kalentics, N., Boillat, E., Peyre, P., Gorny, C., Kenel, C., Leinenbach, C., Jhabval, J., Logé, R.E.: 3D Laser shock peening—A new method for the 3D control of residual stresses in Selective Laser Melting. *Mater. Des.* **130**, 350–356 (2017)
36. Karimi, J., Suryanarayana, C., Okulov, I., Prashanth, K.G.: Selective laser melting of Ti6Al4V: Effect of laser re-melting. *Mater. Sci. Eng. A* **805**, 140558 (2020)
37. Kaynak, Y., Kitay, O.: Porosity, surface quality, microhardness and microstructure of selective laser melted 316L stainless steel resulting from finish machining. *J. Manuf. Mater. Process.* **2**(2), 36 (2018)
38. Kaynak, Y., Kitay, O.: The effect of post-processing operations on surface characteristics of 316L stainless steel produced by selective laser melting. *Addit. Manuf.* **26**, 84–93 (2019)
39. Kaynak, Y., Tascioglu, E.: Post-processing effects on the surface characteristics of Inconel 718 alloy fabricated by selective laser melting additive manufacturing. *Prog. Addit. Manuf.* **5**, 221–234 (2020)
40. Khan, H.M., Karabulut, Y., Kitay, O., Kaynak, Y., Jawahir, I.S.: Influence of the post-processing operations on surface integrity of metal components produced by laser powder bed fusion additive manufacturing: A review. *Mach. Sci. Technol.* **25**(1), 118–176 (2021)
41. Lee, J.-Y., Nagalingam, A.P., Yeo, S.H.: A review on the state-of-the-art of surface finishing processes and related ISO/ASTM standards for metal additive manufactured components. *Virtual Phys. Prototyp.* **16**(1), 68–96 (2021)
42. Lee, S., Ahmadi, Z., Pegues, J.W., Mahjouri-Samani, M., Shamsaei, N.: Laser polishing for improving fatigue performance of additive manufactured Ti-6Al-4V parts, *Opt. Laser Technol.* **134**, 106639 (2021b)
43. Liu, S., Shin, Y.C.: Additive manufacturing of Ti6Al4V alloy: A review. *Mater. Des.* **164**, 107552 (2019)
44. Lu, J., Lu, H., Xu, X., Yao, J., Cai, J., Luo, K.: High-performance integrated additive manufacturing with laser shock peening induced microstructural evolution and improvement in mechanical properties of Ti6Al4V alloy components. *Int. J. Mach. Tools Manuf.* **148**, 103475 (2019)
45. Lv, F., Liang, H., Xie, D., Mao, Y., Wang, C., Shen, L., Tian, Z.: On the role of laser in situ re-melting into pore elimination of Ti6Al4V components fabricated by selective laser melting. *J. Alloys Compd.* **854**, 156866 (2021)
46. Łyczkowska, E., Szymczyk, P., Dybała, B., Chlebus, E.: Chemical polishing of scaffolds made of Ti-6Al-7Nb alloy by additive manufacturing. *Arch. Civ. Mech. Eng.* **14**, 586–594 (2014)
47. Ma, C., Andani, M.T., Qin, H., Moghaddam, N.S., Ibrahim, H., Jahadakbar, A., Amerinatanzi, A., Ren, Z., Zhang, H., Doll, G.L., Dong, Y., Elahinia, M., Ye, C.: Improving surface finish and wear resistance of additive manufactured nickel-titanium by ultrasonic nano-crystal surface modification. *J. Mater. Process. Technol.* **249**, 433–440 (2017)

48. Maleki, E., Bagherifard, S., Bandini, M., Guagliano, M.: Surface post-treatments for metal additive manufacturing: Progress, challenges, and opportunities. *Addit. Manuf.* **37**, 101619 (2021)
49. Marimuthu, S., Triantaphyllou, A., Antar, M., Wimpenny, D., Morton, H., Beard, M.: Laser polishing of selective laser melted components. *Int. J. Mach. Tools Manuf.* **95**, 97–104 (2015)
50. Maamoun, A., Elbestawi, M., Veldhuis, S.: Influence of shot peening on AlSi10Mg parts fabricated by additive manufacturing. *J. Manuf. Mater. Process.* **2**(3), 40 (2018)
51. Mohammadian, N., Turenne, S., Brailovski, V.: Surface finish control of additively-manufactured Inconel 625 components using combined chemical-abrasive flow polishing. *J. Mater. Process. Technol.* **252**, 728–738 (2018)
52. Nagalingam, A.P., Yeo, S.H.: Surface finishing of additively manufactured Inconel 625 complex internal channels: A case study using a multi-jet hydrodynamic approach. *Addit. Manuf.* **36**, 101428 (2020)
53. Nagalingam, A.P., Yuvaraj, H.K., Yeo, S.H.: Synergistic effects in hydrodynamic cavitation abrasive finishing for internal surface-finish enhancement of additive-manufactured components. *Addit. Manuf.* **33**, 101110 (2020)
54. Nesli, S., Yilmaz, O.: Surface characteristics of laser polished Ti-6Al-4V parts produced by electron beam melting additive manufacturing process. *Int. J. Adv. Manuf. Technol.* **114**, 271–289 (2021)
55. Peng, C., Fu, Y., Wei, H., Li, S., Wang, X., Gao, H.: Study on improvement of surface roughness and induced residual stress for additively manufactured metal parts by abrasive flow machining. *Procedia CIRP* **71**, 386–389 (2018)
56. Peng, X., Kong, L., Fuh, J.Y.H., Wang, H.: A review of post-processing technologies in additive manufacturing. *J. Manuf. Mater. Process.* **5**(2), 38 (2021)
57. Pyka, G., Burakowski, A., Kerckhofs, G., Moesen, M., Van Bael, S., Schrooten, J., Wevers, M.: Surface modification of Ti6Al4V open porous structures produced by additive manufacturing. *Adv. Eng. Mater.* **14**(6), 363–370 (2012)
58. Rotty, C., Doche, M.-L., Mandroyan, A., Hihn, J.-Y., Montavon, G., Moutarlier, V.: Comparison of electropolishing behaviours of TSC, ALM and cast 316L stainless steel in H_3PO_4/H_2SO_4 . *Surf. Interfaces* **6**, 170–176 (2017)
59. Sankara Narayanan, T.S.N., Kim, J., Jeong, H.E., Park, H.W.: Enhancement of the surface properties of selective laser melted maraging steel by large pulsed electron-beam irradiation. *Addit. Manuf.* **33**, 101125 (2020)
60. Sato, M., Takakuwa, O., Nakai, M., Niinomi, M., Takeo, F., Soyama, H.: Using cavitation peening to improve the fatigue life of titanium alloy Ti-6Al-4V manufactured by electron beam melting. *Mater. Sci. Appl.* **7**, 181–191 (2016)
61. Seo, B., Park, H.-K., Kim, H. G., Kim, W. R., Park, K.: Corrosion behavior of additive manufactured CoCr parts polished with plasma electrolytic polishing. *Surf. Coat. Technol.* **406**, 126640 (2021)
62. Shinonaga, T., Yamaguchi, A., Okamoto, Y., Okada(1), A.: Surface smoothing and repairing of additively manufactured metal products by large-area electron beam irradiation, CIRP Annals, IN Press, Available online 13 May 2021 (2021). <https://doi.org/10.1016/j.cirp.2021.04.063>
63. Soyama, H., Takeo, F.: Effect of various peening methods on the fatigue properties of titanium alloy Ti6Al4V manufactured by direct metal laser sintering and electron beam melting. *Materials* **13**, 2216 (2020)
64. Sun, Y., Bailey, R., Moroz, A.: Surface finish and properties enhancement of selective laser melted 316L stainless steel by surface mechanical attrition treatment. *Surf. Coat. Technol.* **378**, 124993 (2019)
65. Tan, K.L., Yeo, S.H.: Surface modification of additive manufactured components by ultrasonic cavitation abrasive finishing. *Wear* **378–379**, 90–95 (2017)
66. Tan, K.L., Yeo, S.H.: Surface finishing on IN625 additively manufactured surfaces by combined ultrasonic cavitation and abrasion. *Addit. Manuf.* **31**, 100938 (2020)
67. Teng, X., Zhang, G., Zhao, Y., Cui, Y., Li, L., Jiang, L.: Study on magnetic abrasive finishing of AlSi10Mg alloy prepared by selective laser melting. *Int. J. Adv. Manuf. Technol.* **105**, 2513–2521 (2019)

68. Tian, Y., Gora, W.S., Cabo, A.P., Parimi, L.L., Hand, D.P., Tammas-Williams, S., Prangnell, P.B.: Material interactions in laser polishing powder bed additive manufactured Ti6Al4V components. *Addit. Manuf.* **20**, 11–22 (2018)
69. Tong, Z., Liu, H., Jiao, J., Zhou, W., Yang, Y., Ren, X.: Improving the strength and ductility of laser directed energy deposited CrMnFeCoNi high-entropy alloy by laser shock peening. *Addit. Manuf.* **35**, 101417 (2020)
70. Tyagi, P., Goulet, T., Riso, C., Stephenson, R., Chuenprateep, N., Schlitzer, J., Benton, C., Garcia-Moreno, F.: Reducing the roughness of internal surface of an additive manufacturing produced 316 steel component by chempolishing and electropolishing. *Addit. Manuf.* **25**, 32–38 (2019)
71. Urlea, V., Brailovski, V.: Electropolishing and electropolishing-related allowances for powder bed selectively laser-melted Ti-6Al-4V alloy components. *J. Mater. Process. Technol.* **242**, 1–11 (2017)
72. Vaithilingam, J., Goodridge, R.D., Hague, R.J.M., Christie, S.D.R., Edmondson, S.: The effect of laser remelting on the surface chemistry of Ti6Al4V components fabricated by selective laser melting. *J. Mater. Process. Technol.* **232**, 1–8 (2016)
73. van Hooreweder, B., Lietaert, K., Neirinck, B., Lippiatt, N., Wevers, M.: CoCr F75 scaffolds produced by additive manufacturing: influence of chemical etching on powder removal and mechanical performance. *J. Mech. Behav. Biomed. Mater.* **70**, 60–67 (2017)
74. Wu, Y.-C., Kuo, C.-N., Chung, Y.-C., Ng, C.-H., Huang, J.C.: Effects of electropolishing on mechanical properties and bio-corrosion of Ti6Al4V fabricated by electron beam melting additive manufacturing. *Materials* **12**(9), 1466 (2019)
75. Wysocki, B., Idaszek, J., Buhagiar, J., Szlązak, K., Brynk, T., Kurzydłowski, K.J., Świeżkowski, W.: The influence of chemical polishing of titanium scaffolds on their mechanical strength and in-vitro cell response. *Mater. Sci. Eng. C* **95**, 428–439 (2019)
76. Yasa, E., Deckers, J., Kruth, J.: The investigation of the influence of laser re-melting on density, surface quality and microstructure of selective laser melting parts. *Rapid Prototyp. J.* **17**(5), 312–327 (2011)
77. Yeo, I., Bae, S., Amanov, A., Jeong, S.: Effect of laser shock peening on properties of heat-treated Ti-6Al-4V manufactured by laser powder bed fusion. *Int. J. Precis. Eng. Manuf.-Green Tech.* (2020). <https://doi.org/10.1007/s40684-020-00234-2>
78. Zhang, J.: Micro-blasting of 316L tubular lattice manufactured by laser powder bed fusion. In: Proceedings of the 19th International Conference of the European Society For Precision Engineering and Nanotechnology EUSPEN 2019, Bilbao, Spain, 3–7 June 2019
79. Zhang, H., Chiang, R., Qin, H., Ren, Z., Hou, X., Lin, D., Doll, G.L., Vasudevan, V.K., Dong, Y., Ye, C.: The effects of ultrasonic nanocrystal surface modification on the fatigue performance of 3D-printed Ti64. *Int. J. Fatigue* **103**, 136–146 (2017)
80. Zhang, H., Zhao, J., Liu, J., Qin, H., Ren, Z., Doll, G.L., Dong, Y., Ye, C.: The effects of electrically-assisted ultrasonic nanocrystal surface modification on 3D-printed Ti-6Al-4V alloy. *Addit. Manuf.* **22**, 60–68 (2018)
81. Zhang, J., Chaudhari, A., Wang, H.: Surface quality and material removal in magnetic abrasive finishing of selective laser melted 316L stainless steel. *J. Manuf. Process.* **45**, 710–719 (2019)

Chapter 9

Surface Treatments and Surface Modification Techniques for 3D Built Materials



P. Vijaya Kumar and C. Velmurugan

9.1 Introduction

Additive Manufacturing (AM) is the unavoidable manufacturing technology in the present world to manufacture the products in various applications. These AM technologies are used in different fields such as research and development, prototyping, Jigs, fixtures and tooling, bridge production, mechanical components, repair and maintenance. Especially in R&D field, the AM techniques are vital role to develop and implement the new concepts [1]. Generally the AM processing stages are classified into three types, they are (i) Pre-processing stage (ii) Intermediate processing stage (iii) Post-processing stage. Initially, the pre-processing stage includes design and modeling of the planned part, material selection and optimal process selection. Thereafter, the required components can be printed using any one AM technique by collecting details from the previous step. Finally, the post-processing stage is done depending on the properties of printed parts [2]. After completing these stages the end part will be allowed for testing and quality assurance. Further, the tested components are implemented in the required applications. Hence, the post processing is an essential step to improve the properties of the printed parts. The common defects such as dimensional accuracy, poor surface finish due to removal support structure, curling, cracks, warping, inclusion, porosity, residual stresses and anisotropic properties occurred in AM products. Hence, these defects can be avoided by selecting proper post processing technique for AM technology [3].

Generally two types of processes such as powder bed fusion (PBF) and direct energy deposition (DED) are used in metal based additive manufacturing techniques. Both processes are working based on thermal energy source by fusion and deposition

P. Vijaya Kumar · C. Velmurugan (✉)

Department of Mechanical Engineering, Indian Institute of Information Technology,
Tiruchirappalli, Tamil Nadu 620012, India

e-mail: velmuruganc@iiit.ac.in

respectively. Figure 9.1 shows the working principle and details of DED and PBF based AM processes. Obviously, the metal parts are directly fabricated using any of these mentioned processes rather than the Vat photo polymerization, Material jetting and Material extrusion process [4]. Table 9.1 reveals further classification of the metal based AM processes. The powder materials are melted uniformly and deposited on the bed to fabricate the parts with PBF technique where the heat sources such as laser and electron beam are involved. Similarly, either powder or wire material is laid upon the bed to build the part in the DED technique. Among these two techniques, PBF is the best one due to accuracy, features and rapid speed for metal deposition [2]. Table 9.1 clearly detailed the working environment, material usage, heating source, feedstock type and parameter of various PBF and DED techniques.

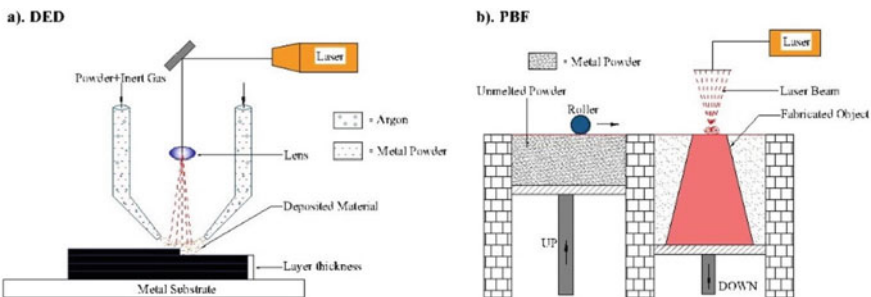
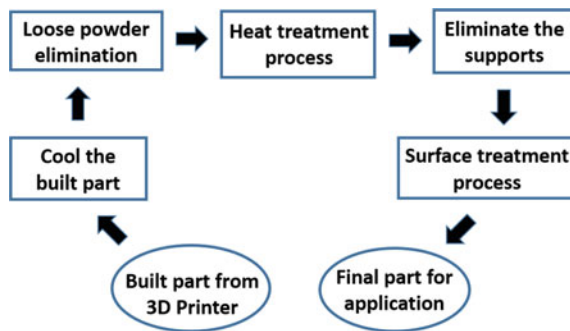


Fig. 9.1 Metal additive manufacturing techniques **a** DED and **b** PBF

Table 9.1 Metal based AM technology details

Powder bed fusion (PBF)			Direct energy deposition (DED)	
Selective laser sintering (SLS)	Selective laser melting (SLM)	Electron beam melting (EBM)	Laser engineered net shaping (LENS)	Electron beam AM (EBAM)
Fused with laser	Fused with laser	Fused with electron beam	Fused with laser	Fused with electron beam
Feedstock: powder	Feedstock: powder	Feedstock: powder	Feedstock: powder, wire	Feedstock: wire, powder
Heat source: laser	Heat source: laser	Heat source: electron beam	Heat source: laser	Heat source: electron beam
Material used: polymer, fiber	Material used: polymer, fiber	Material used: metals	Material used: metals, polymer, ceramic	Material used: metals, polymer, ceramic
Atmosphere: inert gas	Atmosphere: inert gas	Atmosphere: vacuum	Atmosphere: inert gas	Atmosphere: vacuum

Fig. 9.2 Flow diagram of AM stages in post process



9.1.1 Post Processing Works in AM

In Additive Manufacturing, post processing works are given an important characteristics and make challenges to finish the physical product. It frequently requires post processes of specimen to assurance mechanical, physical and other material properties for a convinced process [5]. The post processing stages are listed in Fig. 9.2: (i) cool the built part for set and cure the object (ii) loose powder elimination for cleaning the exterior surface of the part (iii) heat treatment for the microstructure/stress relieving of the part (iv) eliminate the support structures in the part due to required shape and (v) surface treatment applied on the part surface to achieve the needed properties. The built part curing and removal of loose powder stages are common to all 3D printing systems. But some other systems go for the next level, especially fused deposition modelling (FDM) and material jetting (MJ) due to elimination of the voids and overhanging structures that meet the support structure removal [6].

9.1.2 Importance of Post Processes in AM

After the fabrication of 3D objects, there needs to be conducted some finishing works for satisfaction its applications, it is called as post processing. Its takes a major role in AM after the products are released from 3D printers. It can include any or all of these points like excess material removal, support removal, surface finish processes, curing/heat treatment, machining, colouring and inspection [7]. The post processing is consideration of overall cost per part and anything up to 60% of total cost depending on the applications. Skilled workers are need to remove support structure of post processing action, due to the consumption of time and cost. Moreover, there is a requirement to develop the end part peculiarity in favor of its performances [8]. The better surface finish and improving surface roughness lead a vital role in post processing of any AM systems, it also gives the material properties and functionality of the object.

9.2 Post Processing Stages in AM

To get final part for the required application, some post processing stages are to be followed in Additive Manufacturing technology. Figure 9.2 shows the various stages of AM process which includes the post processing operation.

9.2.1 *Cool the Built Part*

After the three dimensional part is built from 3D printer, allow it to cool the part for solidification condition, it helps to set permanently [9].

9.2.2 *Loose Powder Elimination*

The loose powder elimination is a manual process and it depends on the part identification. The shockwave cleaning or dry-ice blasting methods are mostly used to eliminate the loose powder and these methods are demanded to grant some priority of 3D built part [10].

9.2.3 *Heat Treatment Process*

Generally high temperature and low temperature type processes are used in heat treatments, to achieve the mechanical properties, increasing fatigue resistance and ductility while it heal pores by more relevant microstructures and hot isostatic pressing (HIP) respectively on a high temperature process [11]. Similarly, a low temperature process is used to eliminate the deformations when the finished part is removed from build plate so as to relieve the stresses.

9.2.4 *Eliminate the Supports*

After building the 3D part, allow to solidify then remove it from the build plate by hand and it is noted in the beginning when design of the part. The part might have the support structures, so it should be removed by using any one post processing method to get the required shape and it also designed properly [12] to decrease the part weight and material wastage by using self-supporting structures. The supports create the problem when the real parts function, that's why these supports must be

removed either manually or automatically with the help of any suitable modification technique [13].

9.2.5 Surface Treatment Process

The surface treatment is applied on the build part when the support structure is removed from that part. This process gives the required surface finish in desired specific application reducing the course roughness. Some polishing techniques are applied to get the final smooth surface of the end part. Also these treatments are used to develop the desired properties and improve the surface quality of 3D built part [14].

9.3 Surface Modification Methods

Several surface modification methods are popularly known and they come under the post processing techniques in AM process. These methods are used to achieve the required quality of the 3D part surface. Figure 9.3 illustrates the details about recent surface modification methods in AM. It is mostly dependent on the geometry of the part and application of the part [1]. There are six major surface modification methods and these are briefly discussed in this chapter, they are Mechanical, Physical, Chemical, Thermal, Electrochemical and Laser methods. Every method has some techniques to apply on the 3D part to complete the post processing stage for utilizing

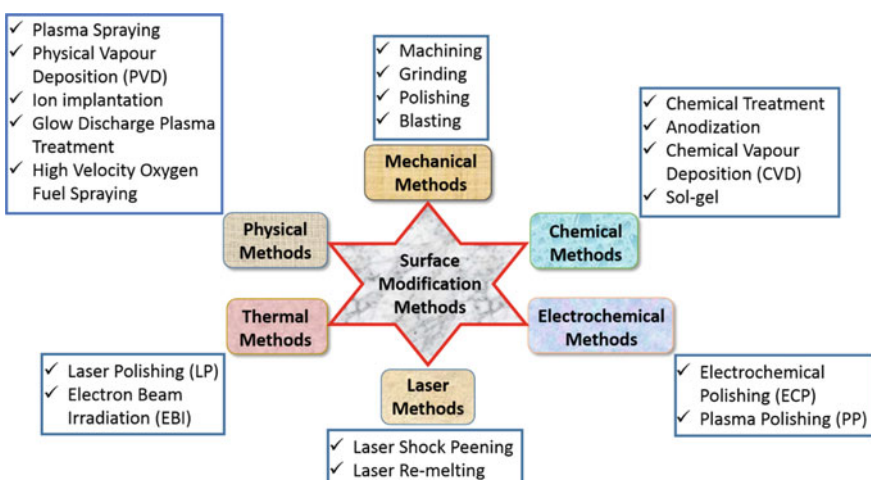


Fig. 9.3 Surface modification methods using in AM

its particular application. By using the surface modification methods to overcome the inflammation and allergic reactions in biomaterials which is implant into the human body and also improve the different properties [4].

9.3.1 Mechanical Methods

Ease any simple conventional type process conducted in mechanical methods to improve the surface finishing of 3D built part. This method is applicable to only flat surface objects not for complex geometries. The common methods like machining, grinding, polishing and blasting further explained with the schematic diagram shown in Fig. 9.4. Table 9.2 reveals that the mechanical type surface modification methods advantages, limitations and applications.

Machining

Machining is a standard method used in post processing of metal AM in which improvement of the roughness on parts surface is done. This method is done with limited amount of material only removed with the help of cutting tools and power driven machine on the 3D part. It mainly considers the motion, cutting tool type and surface finish quality to achieve the levelled finishing surface [16].

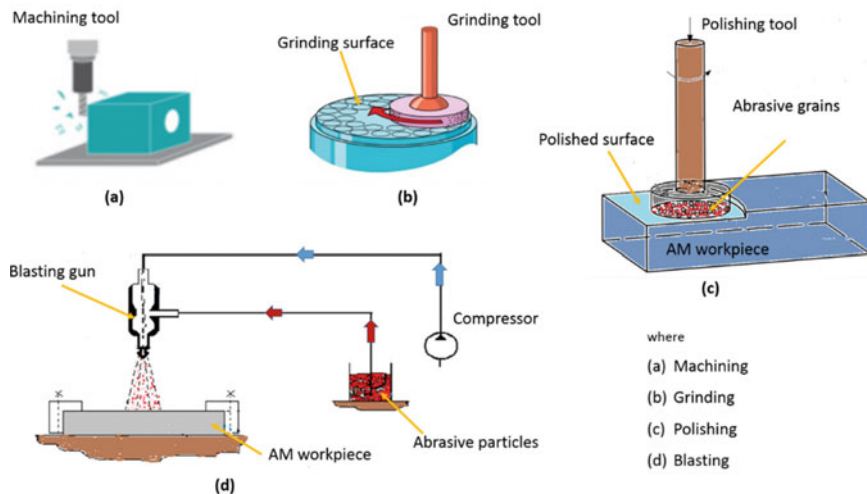


Fig. 9.4 Schematic diagrams of the mechanical surface modification methods

Table 9.2 Mechanical surface modification methods detail

Mechanical methods	Advantages	Limitations	Applications	Refs.
Machining	To get good surface roughness, $R_a = 0.4 \mu\text{m}$, good dimensional accuracy and specific tolerance is possible	Complex geometry is not possible, needs line of sight, can involve complex programming	Flat structures (external surface)	[2, 15]
Grinding	To get very good surface roughness, $R_a = 0.34 \mu\text{m}$, eliminate partially melted powders	Complex geometry is not possible, metal removal rate is very less. It consumes more time	Flat structures (external surface)	[2, 15]
Polishing	To get normal surface roughness, $R_a = 1.25 \mu\text{m}$	Complex geometry is not possible	Flat structures (external surface)	[15]
Blasting	To get moderate surface roughness, $R_a = 3.87 \mu\text{m}$	To eliminate unsintered powders only, complex geometry is not possible	Flat structures (external surface)	[2, 15]

Grinding

Grinding is the vital role to improve the surface finishing of 3D part in mechanical method and it gives the smoother surface roughness than blasting method. But it is only feasible to flat surfaces, not suitable for curved or complex shape parts [4].

Polishing

Polishing is used to make a 3D part surface which is highly polished and it is developing the surface quality of mechanical type surface modification method. Moreover, this polishing improves the fatigue behaviour of that part. This polishing also gives a more efficient surface roughness reduction compared with mechanical machining [16].

Blasting

Blasting specifically means the Sand/Bead blasting (SB/BB) means the target surface capturing the sand or ceramic beads type abrasive material and compressed air directly hit with high pressure. It is also one of the common method to apply on the various fields to achieve precision finishing, shaping and removing the oxides or contaminants in built part surface for improve the surface roughness [17]. This

sand blasting method is highly convenient to increase the fatigue strength when compared with machining and grinding. It also improves the built metal parts mechanical properties like surface hardness, yield strength, fracture strength and percentage of elongation [5].

9.3.2 Physical Methods

This is one of the most economic method in which preparation and working procedures are very simple but it may be unsuitable for the complex parts due to the weak bonding force [18]. To change the surface topography or morphology by the dry transformation technique to improve medical implants [19]. Further the paper discusses the physical modification methods include Plasma spraying, Physical Vapour Technique (PVD), Ion-implantation, Glow Discharge Plasma Treatment, High Velocity Oxygen Fuel Spraying, etc., Table 9.3 discussed about physical type surface modifications method details.

Table 9.3 Physical surface modification methods detail

Physical methods	Advantages	Limitations	Applications	Refs.
Plasma spraying	It able to coat large areas, high deposition rate	Thermal stress and crystallinity of coating affected by temperature and gas atmosphere	Small and special shaped workpiece	[20, 21]
Physical vapour deposition	Used to improve corrosion, wear and fatigue properties	Difficult to coat undercuts, deposition rate is low	Large area and low substrate temperature	[21, 22]
Ion-implantation	No sharp interface between material layer and substrate, it increases corrosion and wear resistance	Vacuum is much needed, energy of ions deep penetration is possible into inner substrate	Titanium implants, metallic substrates	[20, 21]
Glow discharge plasma treatment	To remove surface contamination and increase surface energy	Need expensive vacuum systems, low deposition rate	Clean, oxide surface	[23, 24]
High velocity oxygen fuel spraying	Better wear protection and corrosion resistance, denser and smoother coating is possible	Need skilled operators, internal surfaces of small cylindrical components are not suitable	Hard metal, ceramic, polymer, cermet and composite surface	[25, 26]

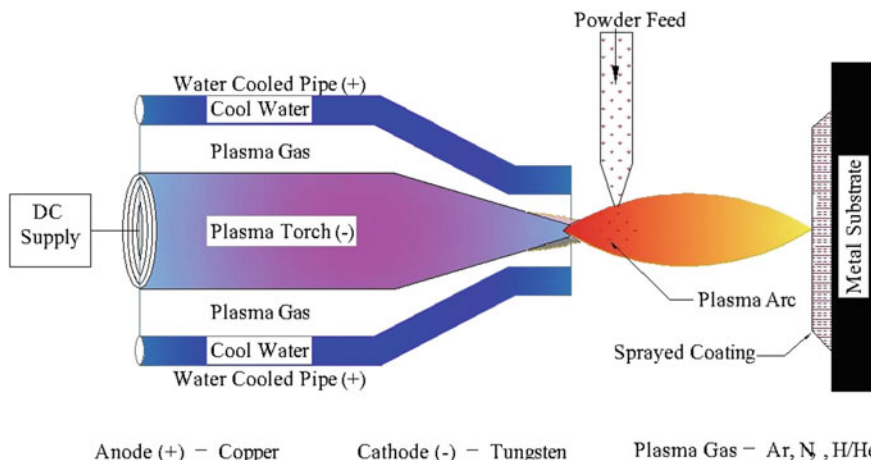


Fig. 9.5 Working principle of plasma spraying

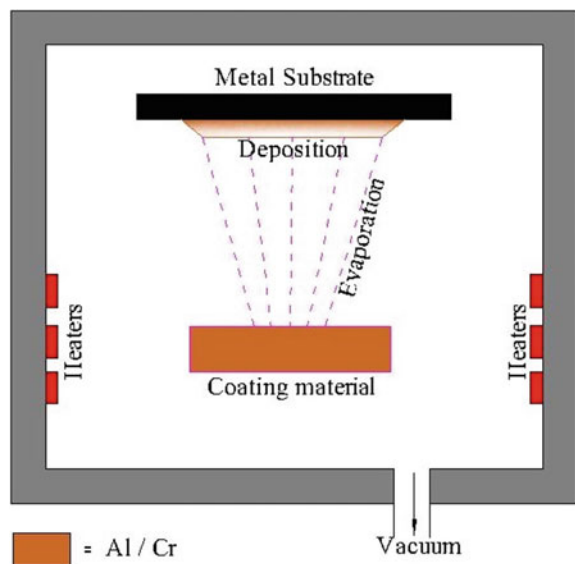
Plasma Spraying

Plasma spraying method comes under thermal spraying technique, it helps to produce a plasma arc heat source when apply the coating on part surface. It gives the better mechanical, physical and chemical properties in various application [27]. The materials are melted by the temperature nearly 1000 °C comes under vacuum through plasma torch with low pressure formation to deposit onto a surface and allow rapid solidification. Figure 9.5 shown the schematic diagram of plasma spraying with its working condition. This plasma spraying method makes a coating thickness range varied from nanometer to millimeter and it is a safe method, also provides cost effective and positive approach to develop a coating on the part surface [28]. The high temperature and gas atmosphere (Argon and Nitrogen gas) will disturb the thermal stress and high degree crystallinity respectively. Some parameters are involved and affected the factors such as microstructure, porosity and coating properties when carry out the surface quality. Obviously to attain the best quality of the coatings, it is required to limit the plasma gas temperature to decrease microcracks [17, 29].

Physical Vapour Deposition (PVD)

PVD method commonly popular and it is working in both conventional and AM processes to develop the surface quality and its properties. This method is applied on the metallic surface, it involves the vacuum condition in which the solid metal evaporated then deposit onto a metal built part surface. It includes the major methods such as vacuum evaporation, sputter coating and ion plating, etc. Figure 9.6 shown the setup of physical vapour deposition process. This method established the good surface topography and tribological properties while comfortably adhere the layer

Fig. 9.6 Physical vapour deposition setup



of materials. The weakening of bonding force is the main drawback when thermal expansion occurs on the surface area of the part and coating due to the mismatch issue [22]. In the medical engineering field, in order to raise the resistance opposing abrasion, coating materials like Titanium (Ti) and Titanium Nitride (TiN) are used periodically. These coating materials are given the mechanical properties alike wear resistance, thermal stability and less friction coefficient [30]. Mostly, in orthopedic and dental applications, sputtering deposition technique is used and ion bombardment reject the unwanted ions from required surface and maintain space for coating when during the process. All inorganic and few organic type materials are able to access the PVD method, addition to the coating surface has strong adhesive aspects [31].

Ion-Implantation

Depends on metal materials, to get the mechanical and electrochemical properties in biomedical applications captured by Ion implantation process. This method improves the coating strength on substrate which is do not disturb the actual characteristics of that materials. It also add to increase the hardness, corrosion and wear resistance properties at that time it prohibit infection and enhance the implant Osseointegration (OI) for biomedical systems. This surface modification method is more beneficial, controllable and flexible to the titanium materials. In addition to the titanium alloys upgrade antimicrobial ability [32]. Ion implantation method works in vacuum condition with committing the bombardment of ions into the substrate layer surface. Figure 9.7 shows the schematic diagram of ion implantation setup. It can be producing

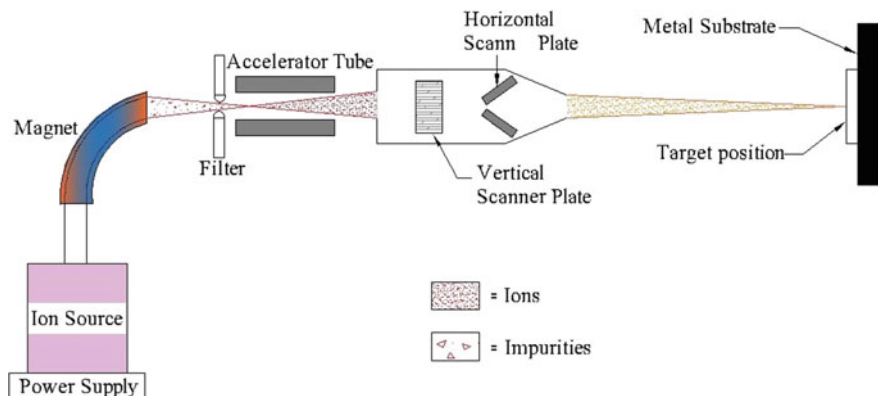


Fig. 9.7 Schematic diagram of ion implantation setup

the layers are able to control with concentration and allowed depth on impurity distribution to get more purity and accuracy. This method is conducted less than critical temperature, to modify the material surface mechanical properties. It have not any sharp interface between the substrate and material layer due to unavailability of the adhesion issues. Moreover this method is used to increase the resistance of corrosion and wear parameters [33].

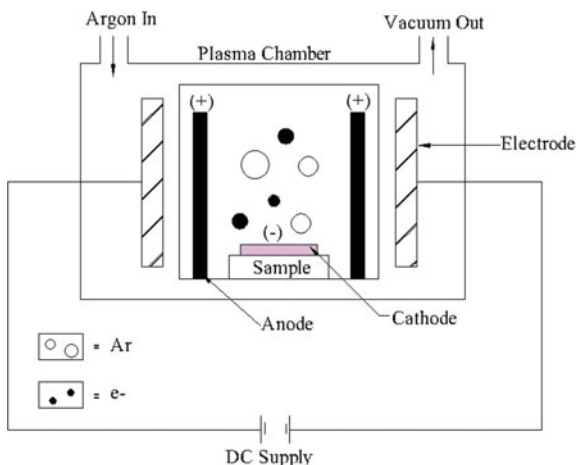
Glow Discharge Plasma Treatment

The physical type glow discharge plasma treatment method is most suitable for titanium and its alloys, but it is not worthy to stainless steel 316L due to reduction of corrosion resistance. Obviously it increases the surface layer structure wear resistance property and microhardness of the materials. The thickness of oxide layer gives a chance to increase the oxidation temperature, it is a major reason to develop the hardness. This treatment is fully conducted in vacuum environment. The main advantages of this method is that it has low gas consumption (air and pure oxygen), less processing time and environment impact [23, 34]. In surface, the tensile strength of films are increased depends on etch and crosslinking when these treatment were finished. The interaction of plasma and film surface was established by longer plasma in surface modification of the concern process [24]. Figure 9.8 illustrates the diagram for glow discharge plasma treatment process with its working conditions.

High Velocity Oxygen Fuel Spraying (HVOF)

This method is a thermal spray coating which comes under physical surface modification technique, used to improve 3D part surface properties such as wear resistance, erosion and corrosion protection. In HVOF method the applied coating material is

Fig. 9.8 Working principle of glow discharge plasma treatment



cemented carbides, more heat energy transferred to the part surface [35]. That's why the prevention of coating defects are controlled by special cooling or discontinuous spraying process. In addition, this method is not suggested to coating of refractory or ceramic materials [36]. The fuel and oxygen are intermixed in high pressure and temperature with powder maintaining inside the combustion chamber, then the substrate capturing high speed particles from chamber to hit the target. So the HVOF coatings are compared with anodized surface getting decreased surface roughness depends on high speed particles are suddenly attacking the surface [26]. HVOF spraying diagram shown in Fig. 9.9.

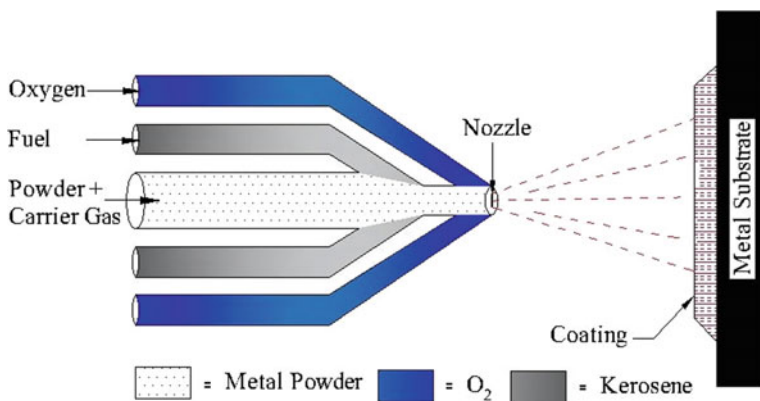


Fig. 9.9 Schematic diagram of high velocity oxygen fuel spraying

9.3.3 Chemical Methods

The chemical methods are related with simple and comparison of any spraying process; however, the coating material thickness have lesser adhesion. Additionally, these methods can be enforced to a broad range of metal substrate like stainless steel, titanium alloys, magnesium alloys, etc., [25]. It is convenient, when the metal acts as cathode and preventing oxidation to electrolyte passed on its rough surface. The advantages of these methods are less cost, low process temperature and possible to produce the coatings like nanoporous [37]. In biomedical field the minor changes applied on implant surface by using some chemical based reactions such as oxidation and nitridation [33]. The chemicals have improved mechanical properties alike compressive strength, ductility and flexural strength but decreasing the tensile strength due to different reaction rate or surface pattern of parts [38]. In this section some advanced chemical methods including Chemical treatment, Sol-gel, Anodization, chemical vapour deposition (CVD) and Biochemical treatment are explained further clearly. Table 9.4 detailed the advantages, limitations and applications of the chemical type surface modifications method.

Table 9.4 Chemical surface modification methods detail

Chemical methods	Advantages	Limitations	Applications	Refs.
Chemical treatment	Used to remove oxide scales and contamination	It can enhance wear by abrasion of opposing surface	Internal complex surfaces	[15, 39]
Sol-gel	Used at low temperature, produce very fine powders in compositions	Large volume shrinkage and cracking during drying, chemicals cost is high	Powder materials coating and thin films are possible	[39, 40]
Anodization	Increased corrosion resistance and durability	It increased grain formation and roughness	Lattice and cellular structures	[39, 40]
Chemical vapour deposition	Corrosion and wear resistance improved	Toxic or flammable source materials, it requires high temperature	Complex geometries, coating on inside hole	[15, 39, 40]

Chemical Treatment

The chemical treatment method is a common strategic approach to achieve the surface quality of metal based 3D built parts. It also offers the possibility to surface any irregular complex parts alike lattice and cellular structures. Mainly this method used to maintain the surface area, after trim the support structure marks or signs in AM parts [41]. Actually the common stages of this categories are noted as purely chemical based etching, machining, brightening and polishing. The drawback of this treatment is may be affect the metallic surface depth due to the part submerged in chemical solution. Moreover some other chemical treatments were applied to metals aimed at increasing the surface finishing and induce the surface characteristics of its application. By using the chemical reactions, nano features and surface chemistry structure are created due to the surface treatments [42].

Sol–Gel

Sol–gel is an important chemical method that has been matured recently to increase the material properties. It can produce magnificent coating with less processing temperature and cost effective preparation. This method is also connected with different coating methods by selecting the relevant conditions [18]. Figure 9.10 shows the flow of sol–gel process working steps to coating on metallic surface. The annealing temperature was controlled in so the sol–gel coating then improves mechanical properties and bonding strength [15]. Sol–gel method is an attractive way to adjust the implants surface. To combination of changes in coating preparation and add some functional components then obtain the various functional coatings [4]. Ease fabrication nature, feasible consuming equipment, more uniformity films and various substrates size are the main advantages of this method. Unfortunately these method was disturbed by pH value, time, precursor interface, chemical equilibrium, etc. This method greatly strengthen the corrosion protection and also decrease the prosthesis rejection [5]. It form an oxide/solid compound with the use of thermal

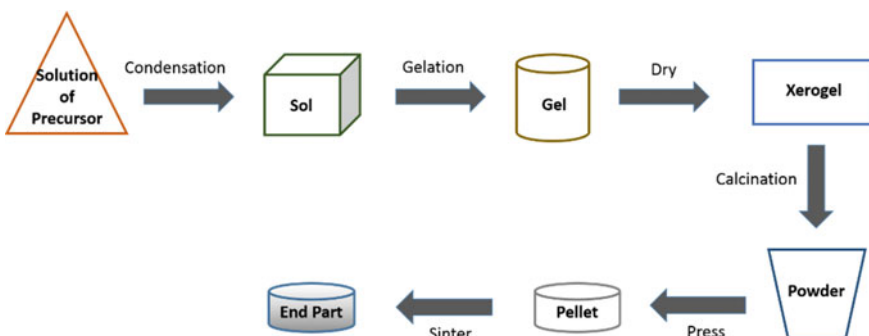
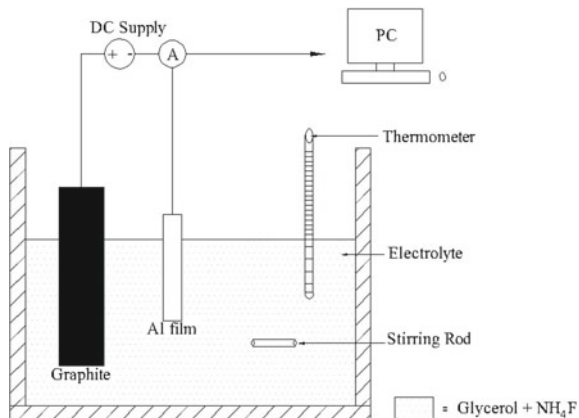


Fig. 9.10 Flow diagram of sol–gel process

Fig. 9.11 Process of anodization setup



based treatment and sol–gel method. The organic or inorganic compounds changed into “sol” then it is turned into “gel” and balance liquid is evaporated by drying process. The thermal treatment is utilized to further poly condensation and boost the mechanical properties [33, 43].

Anodization

Anodic oxidation is the other name of Anodization. It is also one of the chemical process, during the oxide film spread in anode (+ve) metal substrate surface while inserted into electrolyte solution. Anodization is used to improving the corrosion resistance of material and develop the bioactivity Osseointegration (OI) in Titanium screw implants of biomedical application [39]. Figure 9.11 shown the process of Anodization setup. This method developed the grain formation, roughness, and hydrophilicity. The combination of Anodization and sandblasting is to rework the Titanium surface and validate the stability of early-stage OI [33].

Chemical Vapour Deposition (CVD)

CVD is a coating method on the substrate surface and is fully occupied by a thin film layer using chemical reaction of single or more vapour elements or compounds. It is used to develop the inorganic materials such as graphene, TiO₂, carbon nanotube, etc., [44]. In this method high temperature reaction points out low deposition rate same as this coating source reflect exhaust gas have toxic which is harmful to the consecutive implantation process. The CVD equipment has high cost, also more film forming temperature which affects the substrate structure [5]. This method deposited the coating with chemical bonding while generate a heat source on to the substrate. Figure 9.12 illustrates the schematic diagram of CVD method with its working process.

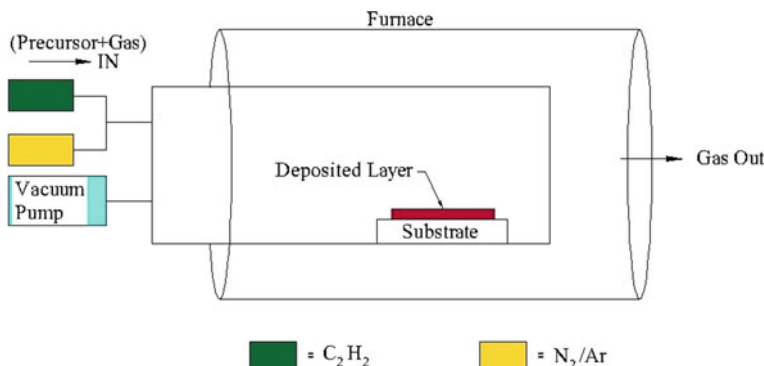


Fig. 9.12 Schematic diagram of chemical vapour deposition

9.3.4 Electrochemical Methods

The electrochemical methods need less cooling compared with abrasive machining. In this method the Anode (workpiece) and Cathode (electrode) both are sink in covered electrolytic solution. Direct Current supply is given to cathode material for conducting electrochemical polishing and also the voltage is controlled during finishing process [45]. The electrolyte should be stirred continuously to manage homogeneity. The redox reaction occurred in electrodes which gradually remove the material from the target surface. These methods are most suitable for different complex geometries. Mainly in this method electrochemical polishing and plasma polishing techniques were used to develop the surface quality and its properties [46]. The advantages, limitations and applications of electrochemical methods are discussed clearly in Table 9.5.

Table 9.5 Electrochemical surface modification methods detail

Electrochemical methods	Advantages	Limitations	Applications	Refs.
Electrochemical polishing (ECP)	To get smooth surface features when adhesion particles are pre-removed	Internal finishing is not uniformity	Fit to free form and complex shapes	[2, 15]
Plasma polishing (PP)	Less volatile chemicals and more aggressive finishing than ECP	High elevated temperature, not fit for thin features	Fit to free form shapes	[2, 15]

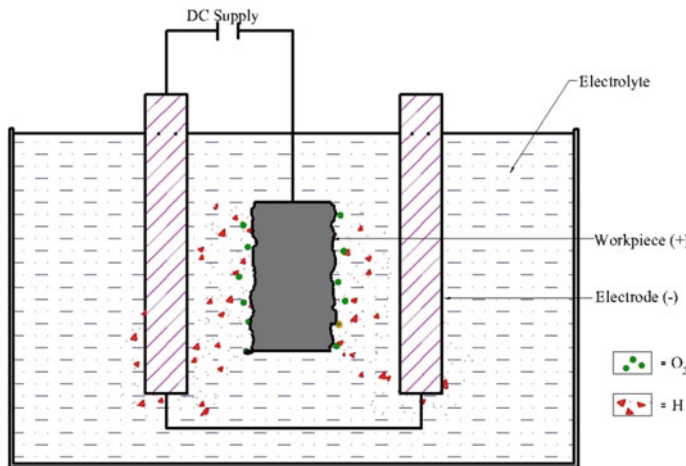


Fig. 9.13 Electrochemical polishing working setup

Electrochemical Polishing (ECP)

The application of ECP method is used to unselected finishing process adjust on freeform geometries and also the benefits of this method to get smooth surface features when adhesion particles are removed earlier [2]. The electrochemical polishing combined with some other mechanical surface treatments used in which allow to decrease the surface roughness (SR). It has the accurate finished surface and unable to detect any machining marks on the parts surface [47]. If the electrochemical solution does not remove the fused melted particles properly then the SR value increased. At that time the single electrochemical polishing stage should not eliminate the fused particles. In ECP method, the applied voltage used 12 V DC supply then the electrolyte consists majorly ethanol and less water [48, 49]. Figure 9.13 shows the principle of electrochemical polishing method working setup.

Plasma Polishing (PP)

The plasma polishing has less volatile chemicals and more finishing accuracy compared to electrochemical polishing method [2]. This process is performed at a temperature nearly 800 °C and voltage is 300 V DC supply, also the electrolyte contain majorly water with less salts of ammonium sulphate. The plasma polishing is also similar to electrochemical polishing but PP only able to decrease the required surface roughness, this lower value of SR obtained when it is combined with mechanical pre-treatment. Although this method is only possible to flat surface structures [50]. Figure 9.14 represents the diagram for plasma polishing process.

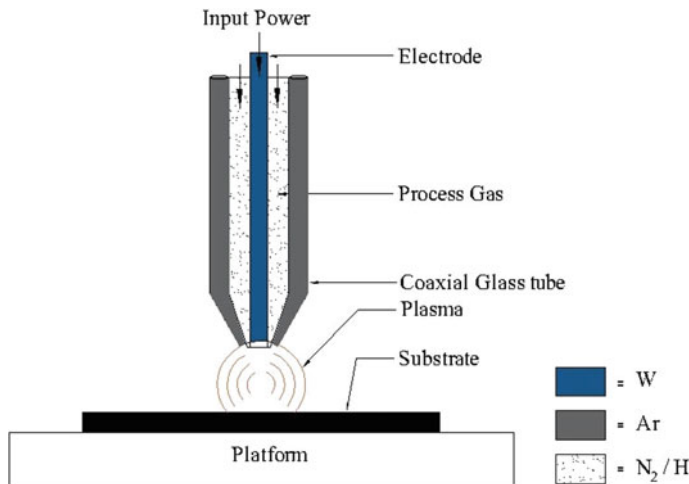


Fig. 9.14 Schematic diagram of plasma polishing

9.3.5 Thermal Methods

In thermal methods, thermal energy is the main source to create the required temperature and melt the built part surface then decrease irregularity of the part. It can achieve the low surface roughness and also get the highly smooth surface [49]. This type of method is most suitable for flat, curved and irregular surface specimens. Laser polishing and Electron beam irradiation processes are discussed in this section. Table 9.6 explains the thermal type surface modification method.

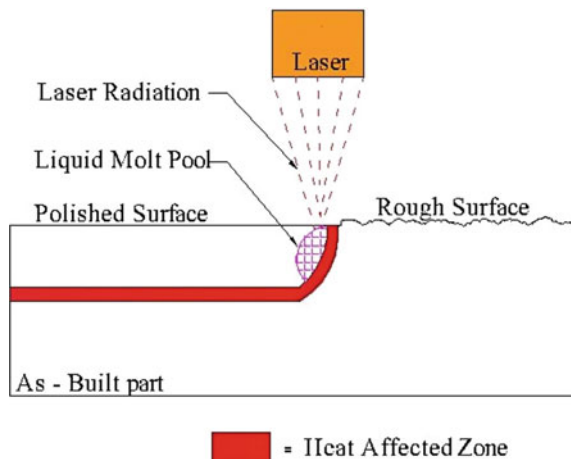
Laser Polishing (LP)

The laser polishing method is more or else same as the idea of re-melting process. Obviously the application of this method is to develop a smooth surfaces of built

Table 9.6 Thermal surface modification methods detail

Thermal methods	Advantages	Limitations	Applications	Refs.
Laser polishing	To get less surface roughness, R_a ($<2 \mu\text{m}$)	Uniform intensity profile on sloped/curved features not possible	Flat, sloped, and curved geometries	[2, 15]
Electron beam irradiation	To get good surface roughness, ($R_a = 0.7 \mu\text{m}$)	Needs line of sight, impacts surface microstructure	Simple and complex geometries	[2, 15]

Fig. 9.15 Laser polishing working principle



part by the suitable selection of material [51]. Also the benefit of this method able to achieve less surface roughness ($<2 \mu\text{m}$) with proper chosen surfaces like flat, slope and curve shape of the parts [2]. Figure 9.15 illustrate the laser polishing working principle. Avoiding ablation is the main reason to decreasing the roughness on AM part surface. The local melting from nm to μm caused by the material top surface irradiates with minimum laser pulse and power density [52, 53].

Electron Beam Irradiation (EBI)

EBI is developed to base on thermal type finishing in simple, irregular or texturing surface wide area parts. The benefits are it can create highly polished surface roughness ($0.7 \mu\text{m}$) with fixing of cracks and pores on its surface [54]. This method is most suitable in different applications like sterilization, contamination control and decomposition of biorefractory compounds. It also develops more energy by using a linear accelerator with movement of electrons, the produced energy ranges from 3 to 10 meV. EBI is not only cost effective, more yield and environment protection method, also improve hydroxyapatite (HA) dissolution compared with heavy ion irradiation [55]. Figure 9.16 shown the diagram of EBI setup.

9.3.6 *Laser Methods*

Laser surface modification methods are used to decrease the value of surface roughness in metallic built part from 3D printers with the help of laser source [56]. It does not cut any unwanted material from targeted surface, instead reconstructs the

Fig. 9.16 Schematic diagram of electron beam irradiation

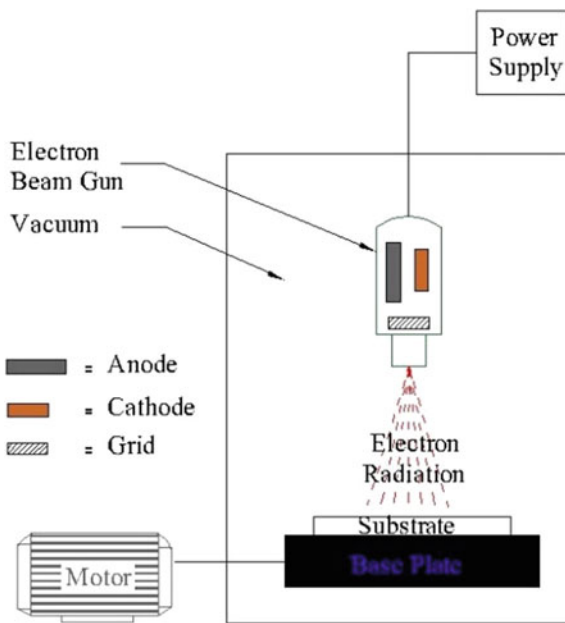


Table 9.7 Laser surface modification methods detail

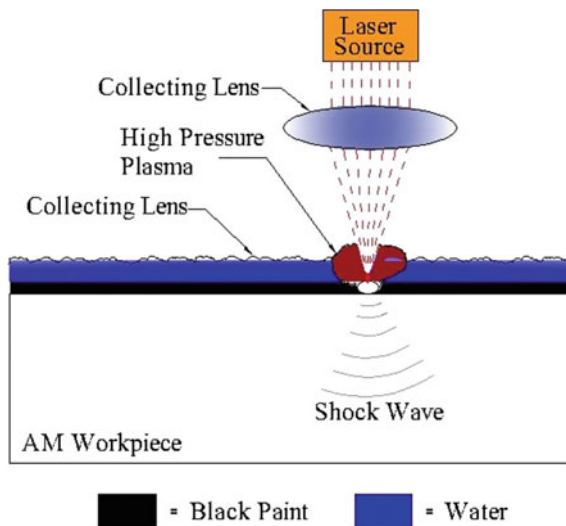
Laser methods	Advantages	Limitations	Applications	Refs.
Laser shock peening	It can develop compressive residual stress layer >1 mm deep, improve fatigue performances	More intense stress relaxation effects during cyclic loading	Simple and complex geometries with holes	[40, 57]
Laser re-melting	It decrease the surface roughness, it escape the pores on melting pools	It produce high temperature so fatigue problems may occur	Inclined or curved surfaces	[40, 57]

material over melting then re-solidify. Table 9.7 discussed about Laser type surface modifications method advantages, limitations and applications.

Laser Shock Peening

A laser beam is pulsed on metallic material surface to creating shock waves generated using laser ablation on the targeted area; the shock waves spread on entire surface layer which precipitate plastic deformation and brings about compressive residual stresses [56]. These stresses are induced neither on surface nor in-depth. However,

Fig. 9.17 Working procedure of laser shock peening



it is a repetitive method and applied in different directions [58, 59]. Figure 9.17 illustrates the working procedure of laser shock peening process.

Laser Re-melting

The laser re-melting method was applied after the part produced in which the external layer of the specific part area. The main motto of this method is reducing surface roughness and porosity [40]. Moreover, it improved some performances like current increases, scanning speed decreases and higher overlaps. This method has a laser source of second passage on the coated layer to melting partially combined powders in which before depositing a new layer [57].

9.4 Surface Modification Techniques

The surface modification techniques are commonly developed for the post processing works in AM and also increase the surface finishing of the built part come out from 3D printer. It is very essential to improve physical, mechanical, chemical and biological properties in which the finished object directly apply on its specific application [60]. The surface modification methods can be separated into six categories depends on its characteristics such as physical, chemical, electrochemical, thermal and laser [21]. The mentioned methods are already discussed in the previous chapter. Further the surface modification techniques to be explained using surface coating, surface deposition, surface oxidation and surface texturing [44]. In addition to the surface

modification effects, issues and challenges are discussed properly. These available techniques may be applied either individually or combined, also each and every method has specific advantages and disadvantages. Obviously, it is much needed to choosing the correct method for desired application due to manufacturing process [18].

9.4.1 Introduction of Surface Modification

Nowadays the surface modification mainly used is biomedical field especially medical implants for which overcome the challenges to internal corrosion in human body. The techniques were used for this objective together deposition of uniform coating, developing oxide layer and surface texturing [61]. In additive manufacturing, every finishing process has some drawbacks and complexities which affect the design of physical object. So these problems are rectified by the selection on part design, improve the surface roughness, corrosion resistance and other properties. Because these decisions are highly essential and dependent on part application and geometry [62].

9.4.2 Surface Coating and Deposition

Coatings improve the surface characteristics to achieve the surface functionalities in AM materials. It has been used to reduce the coated surface roughness, eliminate defects, and increasing surface quality [63]. In addition to raise the wear and corrosion resistance of AM finished parts. To accept the biological performance in AM materials by the use of coatings produce surface morphologies Fig. 9.18 shows the schematic diagram of laser metal deposition surface coating to apply on different materials surface. The actual surface microhardness will increased by high energy coating [64]. Similarly some other coating methods and materials are also used to improve the mechanical properties like hardness, tensile strength and corrosion [65]. For example, Inconel 625 material was fabricated by binder jetting process using electro spark deposition coating on surface to get the roughness reduction and eliminating high temperature oxidation [66]. By utilizing the laser beam, powder melts on the parts surface layer then mixed and form a coating to ensure high adhesion of coating on desired surface [67, 68].

9.4.3 Surface Oxidation

Generally oxidation occurred in nature due to the chemical reaction taking place between any metal and oxygen. The oxygen molecules consists from atmosphere

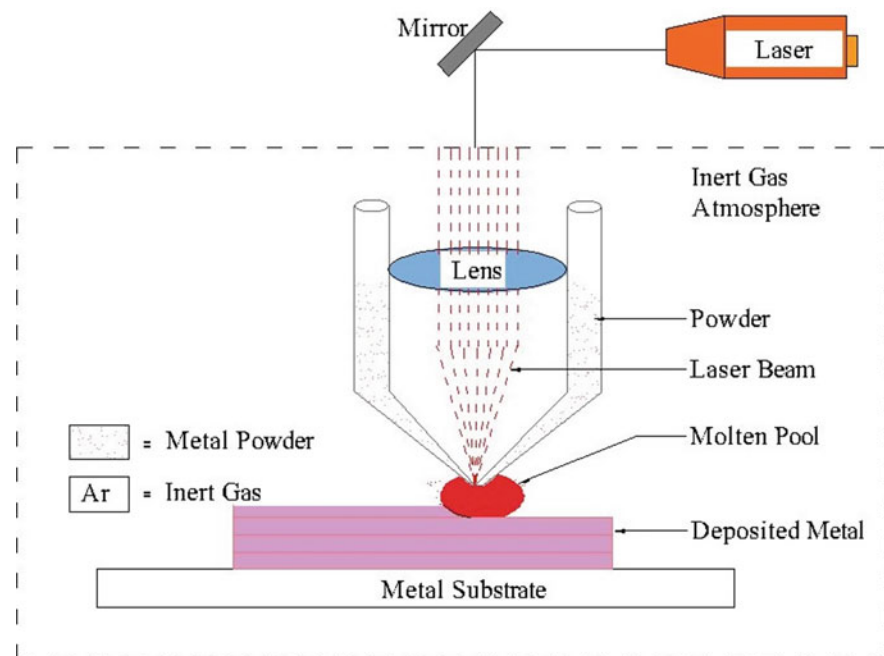
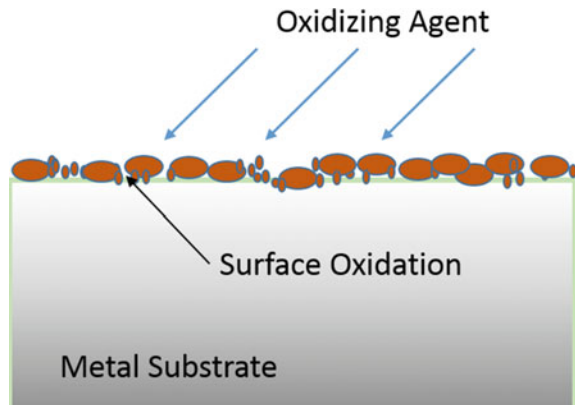


Fig. 9.18 Schematic represents of laser metal deposition

combined with metal formed a thin oxide layer on to the substrate [69]. The oxidation process started with gas adsorption on metallic surface during chemical reaction (metal and oxygen). In part surface the dissolved oxygen in metal forms either film or nuclei as an oxide [70]. Moreover, the oxide formation on part surface which split the metal and gas also acts as a barrier oxide. The oxides may be either liquid or volatile at extreme temperature and it may form continuous film or porous structure. This oxidation process conducted at room temperature but the reaction rate is slow [71]. Figure 9.19 represents the surface oxidation occurred in metallic surface.

Similarly this process also conducted at high or extreme temperature but the reaction rate is very high. The surface modification of biomedical application used some different types of oxidation such as thermal oxidation, Anodization and micro arc oxidation (MAO) [72]. The several factors are consider in this chemical reaction mechanism for the function of selected metals, they are (a) pressure and temperature (b) pre-treatment and surface preparation (c) gas composition (d) reaction time. The surface oxidation used to deliver the surface finishing of metal materials with high accuracy due to the reaction rate [73].

Fig. 9.19 Surface oxidation in metal



9.4.4 Surface Texturing

Surface texture is the nature of surface and it gives the appearance and roughness to finishing object for the functioning. It can be used to develop the properties like adherence, wettability, electrical conductivity, thermal conductivity and friction. In any manufacturing process, machining may produce a surface texture [74]. The texturing comprises of small and local alteration of surface from completely flat ideal object. At machined parts, noticed in which surfaces incorporate complicated shape made as series of crest and troughs in different heights, density and spacing. Two ways are used to measure the surface texture such as contact and non-contact methods [75]. To develop the tribological behavior of machined parts by surface texturing and it also used like a lubricant reservoir. The surface texturing lead a crucial role in practical achievement of some engineered parts like bearing, cutting tool, hydraulic motors, piston and cylinder by reducing friction and wear [76, 77].

Figure 9.20 represents the working principle of laser surface texturing and it is also one of the main method to texture on the surface of metallic substrate. The texture design is the main drawback due to microstructure evolution, tribological and mechanical properties in surface texturing. In addition, the texture wear resistance also challenging to affect the tribological properties due to worn out texture features [76].

9.5 Effects of Surface Modification

In additive manufacturing technology the surface modification is very essential to achieve better mechanical, thermal, electrochemical, metallurgical and biological properties of printed parts based on the fabrication method and materials. The surface of AM products is influenced by the porous, cavities and partially melted powder which leads to poor surface quality [78]. The surface integrities of the

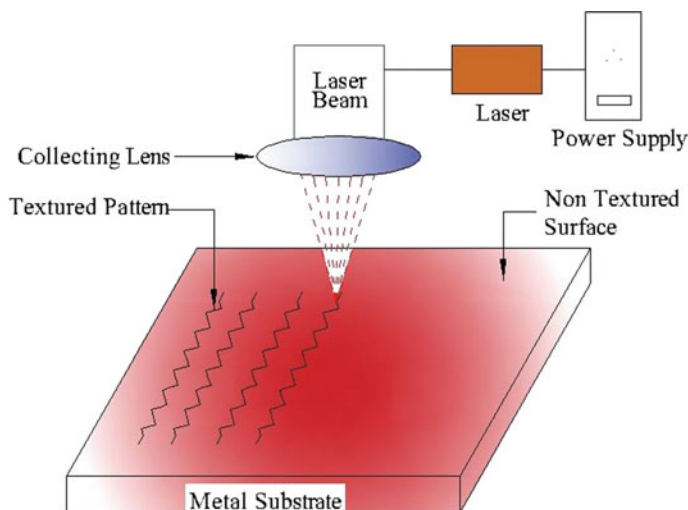


Fig. 9.20 Schematic diagram of laser surface texturing

printed components such as surface roughness, microstructure, corrosion and wear resistance, surface topography and microhardness can be modified using the post processing processes together with the AM technology. The selection of surface modification technique or process is based on the output parameters need to be modified. For example, the corrosion resistance property of the AM printed products can be improved with surface coating. The primary objective of using post processing methods in AM process is to make good surface topography. Moreover, the surface modifications can overcome the issues due to partially melted powders and undesired layer thickness.

9.6 Issues in Surface Modification Techniques

Material issue is the main drawback of AM technologies which prohibits current researches to explore in various applications. Normally, AM techniques are designed and developed to create a highly finished 3D parts with the help of any materials come under the category of metal, polymer and ceramic [17]. In the current scenario, the AM techniques are implemented in different fields with various applications. But, the commercial product development using 3D printing technique has some issues due to the manufacturing methods and materials [79]. Moreover, the AM fabricated parts have some problems when the surface modification techniques are involved. The mechanical, physical, thermal, metallurgical and biological properties of the AM developed components need to be standardized for different materials used in AM [18]. However, these critical issues can be managed by the following steps,

analyze the actual and part fabrication problems; identify the research facilities; proper training of operator; acceptance of industrial standards; research and development of material details; formulation of materials and products and distribution of project outcomes [2].

9.7 Challenges in Surface Modification Techniques

The main challenges in surface modification technique or method are the deposition rate of material, shrinkage and residual stress which influence the surface quality during the solidification of built part. The post processing treatments are used to reduce these critical issues and to increase the surface quality in demand for additive fabricated parts [80]. Moreover, the dimensional tolerances and isotropic properties are the important challenges in ongoing research of the AM technology. In metal AM, the microstructure of the printed parts, mechanical and physical properties are highly disturbed by some parameters [81]. The metallic materials should standardize and raise the reproduction when utilizing the same material in multiple machines to produce the AM parts. In recent years, low volume of large metallic parts meet the demand that means 3D printing technology is not suited to manufacture the high volume functional parts [82]. In biomedical field, the surface characteristics is a challenging possess in the corrosion analysis on metal implants. Similarly, alloyed metals have fretting corrosion and stresses are the critical issues occurring on implant failure [83]. Normally the metal implants have high surface energy that means less wettability and smooth surface. The implant mechanical properties may be affected by modifying the surface roughness [84]. The main challenges in additive manufacturing are poor repeatability, variations in part geometry and improper dimensional accuracy [33]. These problems can be rectified with suitable materials, methods and processes in due course.

9.8 Conclusions

Additive Manufacturing is used to fabricate the individual complicated functional parts as well as assembled parts using metal materials in various applications like biomedical, aerospace, automotive and other industries with less consuming cost and time. The most common metallic materials such as Stainless Steel, Titanium and its alloys, Cobalt, Chromium, Nickel based alloys are used in AM through the specific AM processes namely PBF and DED. These methods are mainly used to fabricate the 3D parts with high surface quality. In post processing stage physical, chemical, mechanical, electrochemical, thermal and laser surface modifications methods are clearly discussed. Hence, the mechanical methods are used to achieve the simple and flat surface parts with the properties such as high surface finishing and geometrical accuracy. The heat treatment is suggested to add with AM to relieve

the internal stress of the printed parts. The surface roughness of the simple and complex shaped parts was rapidly improved with the physical and chemical surface treatment methods. Moreover, the electrochemical method can be used to eliminate the residual stresses or thermal effects of the printed parts. The heat developed using both thermal and laser method on the surface of the built part enhanced the surface characteristics and eliminated the dimensional integrity. The surface modification techniques as such texturing, oxidation, coating and deposition also detailed briefly with their effects on mechanical and functional properties. Finally, the factors such as low speed of fabrication, more expensive equipment and materials, unsuitable mass production, lack of multi-material deposition and repeatability issues were identified as common challenges in the AM technology. Hence, it is suggested to select the proper post processing methods based on materials and equipment involved in AM. Thus, the better mechanical and functional properties can be obtained for additive manufactured components.

9.9 Future Prospects

The future scope of the AM techniques is the development of products using multi-material deposition where the proper surface modification technique can be attached with the specific AM equipment. The advancement of post processing techniques could be achieved the high quality surface for metallic part without compromising the limitation occurred in materials or methods. The post processing techniques can be developed by minimizing its stages which helps to reduce the time and cost of the finished components.

References

1. Wohlers, T.T.: Wohlers report 2021: 3D printing and additive manufacturing state of the industry, 26th edn. Wohlers Associates Inc., Fort Collins, CO (2021)
2. Gordon, E.R., Shokrani, A., Flynn, J.M., Goguelin, S., Barclay, J., Dhokia, V.: A surface modification decision tree to influence design in additive manufacturing. In: Smart Innovation, Systems and Technologies, vol. 52 (2016). https://doi.org/10.1007/978-3-319-32098-4_36
3. Lee, J.-Y., Nagalingam, A.P., Yeo, S.H.: A review on the state-of-the-art of surface finishing processes and related ISO/ASTM standards for metal additive manufactured components. *Virtual Phys. Prototyping* (2020). <https://doi.org/10.1080/17452759.2020.1830346>
4. Liu, W., Liu, S., Wang, L.: Surface modification of biomedical titanium alloy: micromorphology microstructure evolution and biomedical applications. *Coatings* **9**, 249 (2019). <https://doi.org/10.3390/coatings9040249>
5. Pegues, J., Shao, S., Shamsaei, N., Sanaei, N., Fatemi, A., Warner, D.H., Li, P., Phan, N.: Fatigue of additive manufactured Ti-6Al-4V, part I: the effects of powder feedstock, manufacturing, and post process conditions on the resulting microstructure and defects. *Int. J. Fatigue* (2019). <https://doi.org/10.1016/j.ijfatigue.2019.105358>

6. Chohan, J.S., Singh, R.: Pre and post processing techniques to improve surface characteristics of FDM parts: a state of art review and future applications. *RPJ* **23**(3) (2017). <https://doi.org/10.1108/RPJ-05-2015-0059>
7. Kumbhar, N.N., Mulay, A.V.: Post processing methods used to improve surface finish of products which are manufactured by additive manufacturing technologies: a review. *J. Inst. Eng. India Ser. C* **99**(4), 481–487 (2018). <https://doi.org/10.1007/s40032-016-0340-z>
8. Singh, R., Singh, S., Singh, I.P., Fabbrocino, F., Fraternali, F.: Investigation for surface finish improvement of FDM parts by vapor smoothing process. *Compos. B Eng.* **111**, 228–234 (2017). <https://doi.org/10.1016/j.compositesb.2016.11.062>
9. Singh, A.K., Saltonstall, B., Patil, B., Hoffmann, N., Doddamani, M., Gupta, N.: Additive manufacturing of syntactic foams: part 2: specimen printing and mechanical property characterization. *JOM* **70**(3), 310–314 (2018). <https://doi.org/10.1007/s11837-017-2731-x>
10. Vafadar, A., Guzzomi, F., Rassau, A., Hayward, K.: Advances in metal additive manufacturing: a review of common processes, industrial applications, and current challenges. *Appl. Sci.* **11**, 1213 (2021). <https://doi.org/10.3390/app11031213>
11. Careri, F., Imbrogno, S., Umbrello, D., Attallah, M.M., Outeiro, J., Batista, A.C.: Machining and heat treatment as post-processing strategies for Ni-superalloys structures fabricated using direct energy deposition. *J. Manufact. Process.* **61**, 236–244 (2021). <https://doi.org/10.1016/j.jmapro.2020.11.024>
12. Asensio Dominguez, L., Xu, F., Shokrani, A., Flynn, J.M., Dhokia, V., Newman, S.T.: Guidelines when considering pre and post processing of large metal additive manufactured parts. *Procedia Manufact.* **51**, 684–691 (2020). <https://doi.org/10.1016/j.promfg.2020.10.096>
13. Kapil, S., Joshi, P., Kulkarni, P.M., Negi, S., Kumar, R., Karunakaran, K.P.: Elimination of support mechanism in additive manufacturing through substrate tilting. *RPJ* **24**(7), 1155–1165 (2018). <https://doi.org/10.1108/RPJ-07-2017-0139>
14. Cunico, M.W.M., Cunico, M.M., Cavalheiro, P.M., de Carvalho, J.: Investigation of additive manufacturing surface smoothing process. *Rapid Prototyping J.* **23**(1), 201–208 (2017). <https://doi.org/10.1108/RPJ-11-2015-0176>
15. Velu, R., Calais, T., Jayakumar, A., Raspall, F.: A comprehensive review on bio-nanomaterials for medical implants and feasibility studies on fabrication of such implants by additive manufacturing technique. *Materials* **13**, 92 (2020). <https://doi.org/10.3390/ma13010092>
16. Bagherifard, S., Beretta, N., Monti, S., Riccio, M., Bandini, M., Guagliano, M.: On the fatigue strength enhancement of additive manufactured AlSi10Mg parts by mechanical and thermal post-processing. *Jmde* (2017). <https://doi.org/10.1016/j.matdes.2018.02.055>
17. Maleki, E., Bagherifard, S., Bandini, M., Guagliano, M.: Surface post-treatments for metal additive manufacturing: progress, challenges, and opportunities. *Addit. Manuf.* **37**, 101619 (2021). <https://doi.org/10.1016/j.addma.2020.101619>
18. Bose, S., Robertson, S.F., Bandyopadhyay, A.: Surface modification of biomaterials and biomedical devices using additive manufacturing. *Acta Biomater.* **66**, 6–22 (2018). <https://doi.org/10.1016/j.actbio.2017.11.003>
19. Kargupta, R., Bok, S., Darr, C.M., Crist, B.D., Gangopadhyay, K., Gangopadhyay, S., Sengupta, S.: Coatings and surface modifications imparting antimicrobial activity to orthopedic implants. *WIREs Nanomed. Nanobiotechnol.* (2014). <https://doi.org/10.1002/wnn.1273>
20. Shahali, H., Jaggesar, A., Yarlagadda, P.K.D.V.: Recent advances in manufacturing and surface modification of titanium orthopaedic applications. *Procedia Eng.* **174**, 1067–1076 (2017). <https://doi.org/10.1016/j.proeng.2017.01.259>
21. Xue, T., Attarilar, S., Liu, S., Liu, J., Song, X., Li, L., Zhao, B., Tang, Y.: Surface modification techniques of titanium and its alloys to functionally optimize their biomedical properties: thematic review. *Front. Bioeng. Biotechnol.* **8**, 603072 (2020). <https://doi.org/10.3389/fbioe.2020.603072>
22. Babtista, A., Silva, F.J.G., Porteiro, J., Miguez, J.L., Pinto, G., Fernandes, L.: On the physical vapour deposition (PVD): evolution of magnetron sputtering processes for industrial applications. *Procedia Manufact.* **17**, 746–757 (2018). <https://doi.org/10.1016/j.promfg.2018.10.125>

23. Tekdir, H., Yetim, A.F.: Additive manufacturing of multiple layered materials (Ti6Al4V/316L) and improving their tribological properties with glow discharge surface modification. *Vacuum* **184**, 109893 (2021). <https://doi.org/10.1016/j.vacuum.2020.109893>
24. Sheikhi, Z., Hosseini, S.M., Khani, M.R., Farhoodi, M., Abdolmaleki, K., Shokri, B., Shojaee-Aliabadi, S., Mirmoghadaie, L.: Treatment of starch films with a glow discharge plasma in air and O₂ at low pressure. *Food Sci. Technol. Int.* **27**(3), 1–10 (2020). <https://doi.org/10.1177/1082013220948641>
25. Scherillo, F., Manco, E., El Hassanin, A., Franchitti, S., Pirozzi, C., Borrelli, R.: Chemical surface finishing of electron beam melted Ti6Al4V using HF-HNO₃ solutions. *J. Manuf. Process.* **60**, 400–409 (2020). <https://doi.org/10.1016/j.jmapro.2020.10.033>
26. Mardali, M., SalimiJazi, H.R., Karimzadeh, F., Luthringer, B., Blawert, C., Labbaf, S.: Comparative study on microstructure and corrosion behavior of nanostructured hydroxyapatite coatings deposited by high velocity oxygen fuel and flame spraying on AZ61 magnesium based substrates. *Appl. Surf. Sci.* **465**, 614–624 (2019). <https://doi.org/10.1016/j.apsusc.2018.09.127>
27. Unabia, R., Candidato Jr, R., Pawlowski, L.: Current progress in solution precursor plasma spraying of cermets: a review. *8*, 420 (2018). <https://doi.org/10.3390/met8060420>
28. Moseke, C., Gbureck, U.: Surface treatment. In: Niinomi, M. (ed.) *Metals for Biomedical Devices* (2nd edn.), pp. 355–367. Woodhead Publishing (2019). <https://doi.org/10.1016/B978-0-08-102666-3.00013-4>
29. Xiao, J.-K., Tan, H., Wu, Y.-Q., Chen, J., Zhang, C.: Microstructure and wear behavior of FeCoNiCrMn high entropy alloy coating deposited by plasma spraying. *Surf. Coat. Technol.* **385**, 125430 (2020). <https://doi.org/10.1016/j.surfcoat.2020.125430>
30. Muvunzi, R., Dimitrov, D., Matope, S., Lameck.: Application of surface modification technologies to improve performance of hot sheet metal forming tools: a review. *Res. Gate* (2018). <https://doi.org/10.4108/eai.20-6-2017.2270182>
31. Zhang, Y., Sahasrabudhe, H., Bandyopadhyay, A.: Additive manufacturing of Ti-Si-N ceramic coatings on titanium. *Appl. Surf. Sci.* **346**, 428–437 (2015). <https://doi.org/10.1016/j.apsusc.2015.03.184>
32. Cisternas, M., Bhuyan, H., Retamal, M.J., Casanova-Morales, N., Favre, M., Volkmann, U.G., Saikia, P., Diaz-Droguett, D.E., Mändl, S., Manova, D., Moraga, N., Chandía-Cristi, A., Alvarez, A., Guzman, F.: Study of nitrogen implantation in Ti surface using plasma immersion ion implantation and deposition technique as biocompatible substrate for artificial membranes. *Mater. Sci. Eng., C* **113**, 111002 (2020). <https://doi.org/10.1016/j.msec.2020.111002>
33. Liu, Y., Rath, B., Tingart, M., Eschweiler, J.: Role of implants surface modification in osseointegration: a systematic review. *J. Biomed. Mater. Res., Part A* **108**(3), 470–484 (2020). <https://doi.org/10.1002/jbm.a.36829>
34. Yuan, S., Lin, N., Zeng, Q., Zhang, H., Liu, X., Wang, Z., Wu, Y.: Recent developments in research of double glow plasma surface alloying technology: a brief review. *J. Mater. Res. Technol.* (2020). <https://doi.org/10.1016/j.jmrt.2020.03.123>
35. Chen, L., He, D., Han, B., Guo, Z., Zhang, L., Lu, L., Wang, X., Tan, Z., Zhou, Z.: Effect of laser remelting on wear behavior of HVOF-sprayed FeCrCoNiTiAl0.6 high entropy alloy coating. *Appl. Sci.* **10**, 7211 (2020). <https://doi.org/10.3390/app10207211>
36. Ghadami, F., Sabour Roush Aghdam, A.: Improvement of high velocity oxy-fuel spray coatings by thermal post-treatments: a critical review. *Thin Solid Films* (2019). <https://doi.org/10.1016/j.tsf.2019.02.019>
37. Amanov, A.: Effect of local treatment temperature of ultrasonic nanocrystalline surface modification on tribological behavior and corrosion resistance of stainless steel 316L produced by selective laser melting. *Surf. Coat. Technol.* (2020). <https://doi.org/10.1016/j.surfcoat.2020.126080>
38. Kim, H., Lin, Y., Tseng, T.L.B.: A review on quality control in additive manufacturing. *RPJ* **24**(3), 645–669 (2018). <https://doi.org/10.1108/RPJ-03-2017-0048>
39. Liu, Y., Rath, B., Tingart, M., Eschweiler, J.: Role of implants surface modification on osseointegration: a systematic review. (2018). <https://doi.org/10.1002/jbm.a.36829>

40. Maleki, E., Bagherifard, S., Bandini, M., Guagliano, M.: Surface post-treatments for metal additive manufacturing: progress, challenges, and opportunities. *Addit. Manuf.* (2020). <https://doi.org/10.1016/j.addma.2s020.101619>
41. Mu, M., Ou, C.-Y., Wang, J., Liu, Y.: Surface modification of prototypes in fused filament fabrication using chemical vapour smoothing. *Addit. Manufact.* (2019). <https://doi.org/10.1016/j.addma.2019.100972>
42. Zhu, H., Zheng, K., Guo, D., Zang, H., Yu, S., Xu, K.: Engineering microstructure of hydroxyapatite by electron beam irradiation to induce controllable in vitro degradation. *Appl. Surf. Sci.* (2020). <https://doi.org/10.1016/j.apsusc.2020.146583>
43. Sasikumar, Y., Indira, K., Rajendran, N.: Surface modification methods for titanium and its alloys and their corrosion behavior in biological environment: a review. *J. Bio-Tribos-Corros.* **5**, 36 (2019). <https://doi.org/10.1007/s40735-019-0229-5>
44. Khan, W., Sharma, R., Saini, P.: Carbon nanotube-based polymer composites: synthesis, properties and applications. In: Carbon Nanotubes—Current Progress of their Polymer Composites, Mohamed Reda Berber and Inas Hazzaa Hafez. IntechOpen. <https://doi.org/10.5772/62497>
45. Chen, L., Richter, B., Zhang, X., Ren, X., Pfefferkorn, F.E.: Modification of surface characteristics and electrochemical corrosion behavior of laser powder bed fused stainless-steel 316L after laser polishing. *Addit. Manufact.* **32**, 101013 (2020). <https://doi.org/10.1016/j.addma.2019.101013>
46. Boschetto, A., Bottini, L., Macera, L., Veniali, F.: Post-processing of complex SLM parts by barrel finishing. *Appl. Sci.* **10**(4) (2020). <https://doi.org/10.3390/app10041382>
47. Karakurt, I., Lin, L.: 3D printing technologies: techniques, materials, and post-processing. *Curr. Opin. Chem. Eng.* **28**, 134–143 (2020). <https://doi.org/10.1016/j.coche.2020.04.001>
48. Lynch, P., Hasbrouck, C.R., Wilck, J., Kay, M., Manogharan, G.: Challenges and opportunities to integrate the oldest and newest manufacturing processes: metal casting and additive manufacturing. *RPJ* **26**(6), 1145–1154 (2020). <https://doi.org/10.1108/RPJ-10-2019-0277>
49. Kim, S.U., Park, J.W.: High-quality surface finishing of industrial three-dimensional metal additive manufacturing using electrochemical polishing. *Int. J. Precis. Eng. Manufact.-Green Technol.* (2019). <https://doi.org/10.1007/s40684-019-00019-2>
50. Nestler, K., Böttger-Hiller, F., Adamitzki, W., Glowka, G., Zeidler, H., Schubert, A.: Plasma electrolytic polishing—an overview of applied technologies and current challenges to extend the polishable material range. *Procedia CIRP* **42**, 503–507 (2016). <https://doi.org/10.1016/j.procir.2016.02.240>
51. Li, Z., Liu, C., Wang, B., Wang, C., Wang, Z., Yang, F., Gao, C., Liu, H., Qin, Y., Wang, J.: Heat treatment effect on the mechanical properties, roughness and bone ingrowth capacity of 3D printing porous titanium alloy. *Roy. Soc. Chem.* (2018). <https://doi.org/10.1039/c7ra13313h>
52. Bagehorn, S., Wehr, J., Maier, H.J.: Application of mechanical surface finishing processes for roughness reduction and fatigue improvement of additively manufactured Ti-6Al-4V parts. *Int. J. Fatigue* (2017). <https://doi.org/10.1016/j.ijfatigue.2017.05.008>
53. Nesli, S., Yilmaz, O.: Surface characteristics of laser polished Ti-6Al-4V parts produced by electron beam melting additive manufacturing process. *Int. J. Adv. Manufact. Technol.* **114**(9–10) (2021). <https://doi.org/10.1007/s00170-021-06861-6>
54. Panin, A., Kazachenok, M., Perevalova, O., Martynov, S., Panina, A., Sklyarova, E.: Continuous electron beam post-treatment of EBF3-fabricated Ti-6Al-4V parts. *Metals* **9**, 699 (2019). <https://doi.org/10.3390/met9060699>
55. Qin, L., Ya, S., Zhao, J., Zhou, C., Oates, T.W., Weir, M.D., Wu, J., Xu, H.H.K.: Review on development and dental applications of polyetheretherketone-based biomaterials and restorations. *Materials* **14**(2) (2021). <https://doi.org/10.3390/ma14020408>
56. Chen, L., Sun, Y., Li, L., Ren, X.: Improvement of high temperature oxidation resistance of additively manufactured TiC/Inconel 625 nanocomposites by laser shock peening treatment. *Addit. Manuf.* **34**, 101276 (2020). <https://doi.org/10.1016/j.addma.2020.101276>
57. Yu, W., Sing, S.L., Chua, C.K., Tian, X.: Influence of re-melting on surface roughness and porosity of AlSi10Mg parts fabricated by selective laser melting. *J. Alloys Compd.* (2019). <https://doi.org/10.1016/j.jallcom.2019.04.017>

58. Gujba, A.K., Medraj, M.: Laser peening process and its impact on materials properties in comparison with shot peening and ultrasonic impact peening. *Materials* **7**, 7925–7974 (2014). <https://doi.org/10.3390/ma7127925>
59. Wang, H., Huang, Y., Zhang, W.: The study of laser shock peening with side-water spraying and coaxial-water feeding technology. *Int. J. Lightweight Mater. Manufact.* **1**(2), 102–107 (2018). <https://doi.org/10.1016/j.ijlmm.2018.05.001>
60. Bekmurzayeva, A., Duncanson, W.J., Azevedo, H.S., Kanayeva, D.: Surface modification of stainless steel for biomedical applications: revisiting a century-old material. *MSC* (2018). <https://doi.org/10.1016/j.msec.2018.08.049>
61. Konovalov, S., Osintsev, K., Golubeva, A., Smelov, V., Ivanov, Y., Chena, X., Komissarova, I.: Surface modification of Ti-based alloy by selective laser melting of Ni-based superalloy powder. *J. Market. Res.* **9**(4), 8796–8807 (2020). <https://doi.org/10.1016/j.jmrt.2020.06.016>
62. Ginestra, P., Ceretti, E., Lobo, D., Lowther, M., Cruchley, S., Kuehne, S., Villapun, V., Cox, S., Grover, L., Shepherd, D., Attallah, M., Addison, O., Webber, M.: Post processing of 3D printed metal scaffolds: a preliminary study of antimicrobial efficiency. *Procedia Manufact.* **47**, 1106–1112 (2020). <https://doi.org/10.1016/j.promfg.2020.04.126>
63. Fang, X., Du, J., Wei, Z., Wang, X., He, P., Bai, H., Wang, B., Chen, J., Geng, R., Lu, B.: Study on metal deposit in the fused-coating based additive manufacturing. *Procedia CIRP* **55**, 115–121 (2016). <https://doi.org/10.1016/j.procir.2016.08.034>
64. Bagherifard, S., Guagliano, M.: Fatigue performance of cold spray deposits: coating, repair and additive manufacturing cases. *Int. J. Fatigue* (2020). <https://doi.org/10.1016/j.ijfatigue.2020.105744>
65. John Solomon, I., Sevvel, P., Gunasekaran, J.: A review on the various processing parameters in FDM. *Mater. Today: Proc.* (2020). <https://doi.org/10.1016/j.mtpr.2020.05.484>
66. Kovacevich, D.A., Lei, L., Han, D., Kuznetsova, C., Kooi, S.E., Lee, H., Singer, J.P.: Self-limiting electrospray deposition for the surface modification of additively manufactured parts. *ACS Appl. Mater. Interfaces* (2020). <https://doi.org/10.1021/acsami.9b23544>
67. Sagbas, B.: Post-processing effects on surface properties of direct metal laser sintered AlSi10Mg parts. *Met. Mater. Int.* (2019). <https://doi.org/10.1007/s12540-019-00375-3>
68. Mahmood, M.A., Bănică, A., Ristoscu, C., Becherescu, N., Mihăilescu, I.N.: Laser coatings via state-of-the-art additive manufacturing: a review. *Coatings* **11**, 296 (2021). <https://doi.org/10.3390/coatings11030296>
69. An, J., Chen, Y., Liu, Z., Tian, Y.: Surface oxidation behavior and wear performance of a Fe-21.3Cr-3.5Al-0.5Ti-0.4Zr steel. *Metals* **10**, 1032 (2020). <https://doi.org/10.3390/met10081032>
70. Riabov, D., Hryha, E., Rashidi, M., Bengtsson, S., Nyborg, L.: Effect of atomization on surface oxide composition in 316L stainless steel powders for additive manufacturing. *Surf. Interface Anal.* 1–13 (2020). <https://doi.org/10.1002/sia.6846>
71. Cooke, S., Ahmadi, K., Willerth, S., Herring, R.: Metal additive manufacturing: technology, metallurgy and modelling. *J. Manuf. Process.* **57**, 978–1003 (2020). <https://doi.org/10.1016/j.jmapro.2020.07.025>
72. Sames, W.J., List, F.A., Pannala, S., Dehoff, R.R., Babu, S.S.: The metallurgy and processing science of metal additive manufacturing. *Int. Mater. Rev.* (2016). <https://doi.org/10.1080/09506608.2015.1116649>
73. Guo, Y., Jia, L., Kong, B., Zhang, S., Zhang, F., Zhang, H.: Microstructure of rapidly solidified Nb-based pre-alloyed powders for additive manufacturing. *Appl. Surf. Sci.* **409**, 367–374 (2017). <https://doi.org/10.1016/j.apsusc.2017.02.221>
74. Townsend, A., Senin, N., Blunt, L., Leach, R.K., Taylor, J.S.: Surface texture metrology for metal additive manufacturing: a review. *Precis. Eng.* **46**, 34–47 (2016). <https://doi.org/10.1016/j.precisioneng.2016.06.001>
75. Kozior, T., Bochnia, J.: The influence of printing orientation on surface texture parameters in powder bed fusion technology with 316L steel. *Micromachines* **11**, 639 (2020). <https://doi.org/10.3390/mi11070639>

76. Mao, B., Siddaiah, A., Liao, Y., Menezes, P.L.: Laser surface texturing and related techniques for enhancing tribological performance of engineering materials: a review. *J. Manufact. Process.* **53**, 153–173 (2020). <https://doi.org/10.1016/j.jmapro.2020.02.009>
77. Aziz, R., Haq, M.I.U., Raina, A.: Effect of surface texturing on friction behaviour of 3D printed polylactic Acid (PLA). *Polym. Testing* (2020). <https://doi.org/10.1016/j.polymertesting.2020.106434>
78. Asri, R.I.M., Harun, W.S.W., Samykano, M., Lah, N.A.C., Ghani, S.A.C., Tarlochand, F., Raza, M.R.: Corrosion and surface modification on biocompatible metals: a review. *Mater. Sci. Eng., C* (2017). <https://doi.org/10.1016/j.msec.2017.04.102>
79. Singh, S., Ramakrishna, S., Singh, R.: Material issues in additive manufacturing: a review. *J. Manuf. Process.* **25**, 185–200 (2017). <https://doi.org/10.1016/j.jmapro.2016.11.006>
80. Tofail, S.A.M., Koumoulos, E.P., Bandyopadhyay, A., Bose, S., O'Donoghue, L., Charitidis, C.: Additive manufacturing: scientific and technological challenges, market uptake and opportunities. *Mater. Today* **21**(1), 22–37 (2018). <https://doi.org/10.1016/j.mattod.2017.07.001>
81. Michopoulos, J.G., Iliopoulos, A.P., Steuben, J.C., Birnbaum, A.J., Lambrakos, S.: On the multiphysics modeling challenges for metal additive manufacturing processes. *Addit. Manuf.* **22**, 784–799 (2018). <https://doi.org/10.1016/j.addma.2018.06.019>
82. Francois, M.M., Sun, A., King, W.E., Henson, N.J., Tourret, D., Bronkhorst, C.A., Carlson, N.N., Newman, C.K., Haut, T., Bakosi, J., Gibbs, J.W., Livescu, V., Vander Wiel, S.A., Clarke, A.J., Schraad, M.W., Blacker, T., Lim, H., Rodgers, T., Owen, S., Abdeljawad, F., Madison, J., Anderson, A.T., Fattebert, J.L., Ferencz, R.M., Hodge, N.E., Khairallah, S.A., Walton, O.: Modeling of additive manufacturing processes for metals: challenges and opportunities. *Curr. Opin. Solid State Mater. Sci.* **21**(4) Art. no. LA-UR-16-24513; SAND-2017-6832J (2017). <https://doi.org/10.1016/j.cossms.2016.12.001>
83. King, W.E., Anderson, A.T., Ferencz, R.M., Hodge, N.E., Kamath, C., Khairallah, S.A., Rubenchik, A.M.: Laser powder bed fusion additive manufacturing of metals; physics, computational, and materials challenges. *Appl. Phys. Rev.* **2**, 041304 (2015). <https://doi.org/10.1063/1.4937809>
84. Bhuvanesh Kumar, M., Sathiya, P.: Methods and materials for additive manufacturing: a critical review on advancements and challenges. *Thin-Walled Struct.* (2020). <https://doi.org/10.1016/j.tws.2020.107228>

Chapter 10

Surface Coatings and Surface Modification Techniques for Additive Manufacturing



P. Kumaravelu, S. Arulvel, and Jayakrishna Kandasamy

List of Nomenclatures

AM	Additive manufacturing
DED	Direct energy deposition
DED	Direct energy deposition
FDM	Fused deposition modelling
FSP	Friction stir processing
LOM	Laminated object manufacturing
NiP	Nickel-phosphorus
PEO	Plasma electrolytic oxidation
SLS	Selective laser sintering
SLM	Selective laser melting
SMAT	Surface mechanical attrition treatment
USR	Ultrasonic surface rolling
WLAM	Wire laser additive manufacturing
3DP	Three-dimensional printing

10.1 Introduction

Additive Manufacturing (AM) is defined as a “process of joining materials to make parts from 3D model data, usually layer upon layer”. AM technique fabricates 3D products by layering successive layers of metal on top of each other using data from 3D CAD models. Originally known as stereolithography (SLA), the technique has

P. Kumaravelu · S. Arulvel · J. Kandasamy (✉)

School of Mechanical Engineering, Vellore Institute of Technology, Vellore, Tamil Nadu 632014, India

undergone numerous improvements in methods, materials, equipment, and applications [1]. Conventional processes are considerably streamlined and AM has the potential for the replacement in the future. AM have a several advantages like; New designs will have a quicker time to market, client demand will be higher, and will be met with more speed [2].

In recent years, additive manufacturing has been used as the prototype model for end parts in variety of fields such as automobiles, medical, construction, aerospace, and food, other than the material savings and product customization. In addition, AM's advantages include extremely precise operations and design flexibility. Recent developments enable the manufacturers to produce 3D printing machines at a low cost; hence, the use of AM has been extended in many research laboratories, educational institutions, and even in homes [3]. The concept was created to assist scientists, doctors, students, professors, artists, and others in creating miniature models and prototypes for their research. Doctors could readily construct the models of diseased bones and organs, test them, and observe the results, which is extremely beneficial for the medical research. The simple availability of AM equipment allows researchers and engineers to manufacture goods by mixing different materials.

AM processes are divided into seven categories based on the deposition routes like: material extrusion, bed fusion, material jetting, binder jetting, powder, directed energy deposition, vat photopolymerization, and sheet lamination [4]. Generally, three approaches such as Solid-based, liquid-based, and powder-based approaches are in the additive manufacturing (Fig. 10.1). Among those, the common method used for the 3D printing of polymers is fused deposition modelling (FDM). For metals and ceramics, the following processes such as; selective laser sintering (SLS), selective laser melting (SLM), or liquid binding in three-dimensional printing (3DP), as well as inkjet printing, contour crafting, stereolithography, direct energy deposition (DED),

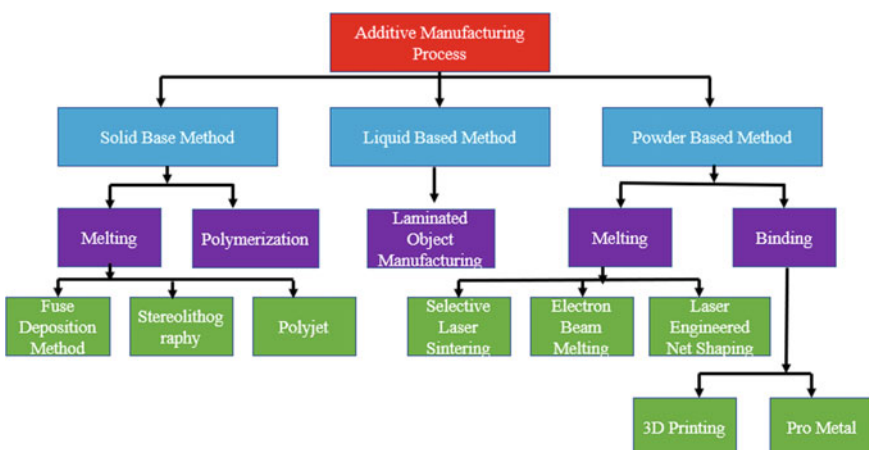


Fig. 10.1 Types of additive manufacturing method

and laminated object manufacturing (LOM) are used in the additive manufacturing [3].

Metal additive manufacturing is currently unsuitable for the mass manufacture of millions of identical simple parts due to the high processing time. However, as the systems and technology progress, the AM will become a valuable and viable choice for the production of quality and quantity components. The benefits of AM emerge from its high flexibility, which comes from the fact that the product is made directly from a CAD model without the need for tooling [3]. This also enables the AM technique to create virtually any geometry that can be imagined. Among the various industries, dental restorations have fully utilised AM's capabilities. Also, found economically reasonable to apply AM technologies to this highly customised production process, speeding up production time without inflating part costs.

AM technologies are also used to produce the aircraft components, such as the fuel nozzles for the GE LEAP engine, which indicate its capabilities in this demanding industry. It is also observed that the fuel nozzles developed through AM technologies are 25% lighter and five times more durable than the fuel nozzles produced by the other technologies. Hence, Additive Manufacturing complements the large variety of production processes, allowing designers and engineers to improve existing process chains, as well as presenting new chances for production [5]. However, there is a serious issue to use the AM component after the manufacturing. The various factors like time, particle density, solidification, etc., could play a vital role on the surface finish and build quality of the AM component. This could affect the surface properties and eventually decreases the properties like mechanical, wear, friction, and corrosion. Hence, it is important to modify the surface of the AM component after the manufacturing.

In the recent years, various coatings and treatments are carried out on the surface of the AM component to improve the properties. Each coating and treatment techniques has its own advantages and disadvantages and so, it is important to address the influence various surface treatments, coatings, and surface texturing on the surface and wear properties of AM components, which could provide a new insights, ideas, and recent innovations in this AM components. Hence, the present chapter addresses the various coatings and treatments followed after the Additive Manufacturing process.

10.1.1 Metal Additive Manufacturing

Metal additive manufacturing often referred as metal 3D printing are used to produce a precise metal with unique characteristics. The precise metal objects can be developed and built through stacking a metal powders with an energy source or a binding agent. Objects that never been constructed a few years ago may also possible now with greater strength. The variety of metal powders accessible for additive manufacturing is growing enormously, which extend its application in various industries. Stainless steel grades, nickel, cobalt-chrome, titanium alloys, and aluminium are some of the most popular metal materials used in the AM technologies. With the

ever-increasing variety of building materials available, the manufacturer can select the best material for the object's particular specifications and expectations. Selective laser sintering, selective laser melting, 3D printing, engineered net shaping laser, electron beam machining, wire and arc AM, laminated object manufacturing are the basic methods used for metal additive manufacturing processes [6]. There are no tools or moulds required for direct production of 3D CAD models, hence there are no transition expenses. Designs in the form of digital data may be freely exchanged, allowing for component and product change and customization. In the aerospace, aviation, automotive, biomedical, and defence industries, additive manufacturing of metals and alloys is mostly utilised for prototyping, research, and small-scale manufacture. Titanium and its alloys, nickel-based alloys, sterling silver, stainless and tool steel, aluminium alloys, brass, copper, gold, platinum, and bronze, among others, are used in additive manufacturing. The demand for lighter-weight materials with acceptable strength is growing rapidly in the aerospace and automotive industries (Fig. 10.2).

The focus is on hollow components that have nearly the same strength as solid components but are lighter. The cost is also reduced by using less material. The use of AM in the shipping industry is decreasing, although it is still growing [7]. The pieces of warships are made using additive manufacturing, lowering the cost and making the components lighter. AM is beneficial for medicinal applications in a variety of ways. Patients damaged bones can be scanned and exact models of their bones can be manufactured. This allows the doctors to conduct a more thorough analysis of the situation. It's also utilised for bone grafts. As people bones vary in shape and size,

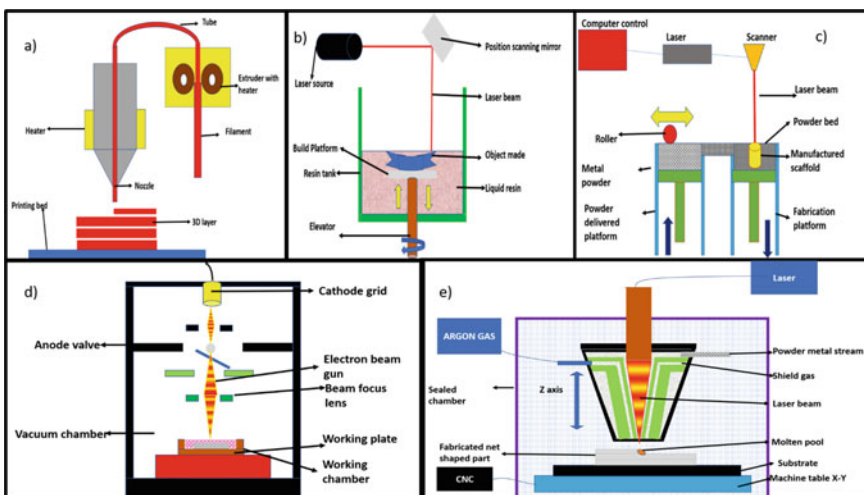


Fig. 10.2 Schematic diagram of different metal additive manufacturing process **a** fused deposition modelling, **b** stereo-lithography, **c** selective laser sintering, **d** electron beam melting, and **e** Laser engineered net shaping

AM enables the creation of bone implants that fit patient body and are also easier to implant [8] (Table 10.1)

One of the main advantages of additive manufacturing is that it can generate highly complicated geometrical shapes from light metals and light metal alloys that are difficult, uneconomical, or impossible to achieve using traditional methods. In comparison to traditional procedures, it can do it quickly and with less waste. When you require a small batch of prototypes, metal additive manufacturing can also save you money. Anything more than that, the high “per-part” prices consumes all of the early tooling cost reductions [20]. Depending on the size of the part, AM are more expensive than typical powder metal parts. Generally, two key elements cause this exorbitant cost; one is the use of technology and the other is expense of materials. In comparison to standard conventional method, the additive manufacturing powder has a low surface finish capability and layering effect, which is the inherent in AM part construction. This appears to be extremely similar to a map’s topography. A unique layering effect arises when the height of a part’s area increases gradually while the cross-section increases inward or outward. Additive manufacturing has been slow to catch on in the industrial world, and it is still regarded a specialist technology in 2021. That’s because, AM is not a cost-effective technique for producing large quantities of parts, due to slow and size limitation factors. Metal additive manufacturing materials can also play a major role for manufacturing because the available metal can be effectively used for the production. Designers should examine the preferred material for the part before committing to creating parts for metal printing. The number of metals that can be printed on the market is extremely limited due explosive, flammable nature of metal alloy [21].

10.1.2 Role of Surface Coatings (SC) and Surface Modification (SM) Techniques in AM

Additive manufacturing allows for geometric design freedom, rapid manufacture of complex geometry components with high spatial resolution, and product customisation at a reasonable cost, as well as it can generate low material waste due to the recyclability of unprocessed powder. High-value-added components that are difficult to make using the traditional manufacturing processes are in high demand today, which is credit to the rapid expansion of contemporary industry and the advent of Industry 4.0. Especially, it is seen in cutting-edge industries like aerospace, nuclear, and energy, where surface coating and modification play an important role in improving the strength and properties of AM metal components, which allows using the AM components directly. For roughness reduction and improved resistance to high temperature oxidation, electro spark deposition was employed to cover the surface of Inconel 625 samples manufactured through binder jetting [22]. The impacts of hydroxyapatite coating on LPBF Ti-6Al-4 V lattice structures to minimise surface

Table 10.1 Summary of metal additive manufacturing process, material and benefits

MAM process	Process	Material used	Benefits	References
Selective laser sintering	Powder is sintered by the use a different laser beam	Stainless steel, cobalt chromium, aluminium alloy, and titanium alloy, nickel-based alloy	High degree of accuracy, resolution and detailing in Terms of shape and design, without polymer binder	[9–11]
Electron beam melting	Computer-controlled electron gun to create fully dense 3D objects directly from metal powder	Titanium alloys cobalt chrome, steel powders, and nickel alloy 718	High strength, resistance to corrosion and top mechanical properties, which is extremely valuable in stressful applications	[12–14]
Laser engineered net shaping	A focused heat source (typically a laser or electron beam) to melt the feedstock material and build up three-dimensional objects	Stainless steel, nickel-based alloys, titanium-6 aluminum-4 vanadium, tooling steel, and copper alloys	Single crystal structures, y repairing and refurbishing defect, corrosion resistant, and wear resistant, performance and lifetime are improved	[15]
Fused Deposition Modelling (FDM)	The melt extrusion method is used to deposit filaments of metal according to a specific pattern	Low melting point alloy	Very small thickness, sharp and smooth edges, maximum used in electronic board	[16, 17]
Wire Laser Additive Manufacturing (WLAM)	3D components are built by continuously feeding a wire into a melt pool generated by a laser beam	Titanium, nickel based super alloy	The phase change is confirmed from undesirable α phase to desirable β phase. This phase change leads to decrease the plasticity of the material and increasing the hardness of the specimen	[18–20]

roughness while improving bioactivity [23]. To address the problem of implant-associated infection, a technique has been used on porous LPBF Ti-6Al-4 V structures. Antimicrobial tests and cytotoxicity assays were utilised *in vitro* and *ex vivo* to evaluate the performance of the produced implants in the biological environment, revealing that the treated AM had a strong bactericidal activity [24].

10.2 Surface Coating on Metal Additive Manufacturing

In metal additive manufacturing method, there are several defects like porosity, surface roughness, surface cavities and cracks, oxidation etc. Porosity can have a negative effect on the mechanical qualities of an additively produced object due to a variety of circumstances. For example, the porosity of powder feedstock or the atmosphere of the manufacturing process environment might be considerably influenced by its quality. Because inert gases can be trapped throughout the production process, the low-quality porous aluminium powder will be melted into porous laminations. Porosity can also diminish the component strength and lead to the component failure. The improper surface roughness can be caused because of the variety of reasons like; low process resolution and layering effects, micro surface textures from melting, binding powder feedstocks, and improper Support structures. It is important to control the surface roughness to use its application in various industries. For example, most of the AM Surface roughness exceeds 10-micron and increases the lamination thickness. This amount of thickness and roughness is limited in the aerospace applications and hence, special attention is required on the surface of AM component to increase its application. However, to processes with such laminations thickness and roughness, it takes longer duration with high cost for the manufacturing. In addition, the surface cavities and cracks in the light metal alloy tend to affect the solidification process [25]. During the AM process, most of the metal components could shrink due to the melting events [26], which could result the layer delamination [27]. Moreover, if the process is done in ambient temperature, the localised oxidation could come into picture for light metals like aluminium and magnesium So, to resist the oxidation, the manufacturing process should be carried out enclosed in a sealed container with inert gases as atmosphere. However, this can also result in delamination because the layers are unable to adhere; compromising the component strength and hence, special attention is required after the AM process. This proves that, the additive manufactured metal alloy parts are not ready for ultimate and it should undergo additional finishing process, such as machining, surface treatment, surface coating etc.

A coating is thought to be a feasible way to manage the surface characteristics of AM materials or to add additional surface capabilities. Coatings have been used to reduce roughness and hide flaws and enhance the quality of the surface. Coatings were also used as a source to adjust the AM components' tribological or corrosion resistance [28]. Coatings are also used in some circumstances to provide regulated surface morphologies that improve the biological performance of AM metallic

materials [29]. Surface coatings can be employed to solve several material processing problems like oxidation, wear corrosion, etc. Aluminium and titanium parts that have been additively produced can be shielded from corrosion and wear using the coatings. Surface coatings can also be an alternate source to the machining process to reduce the surface roughness, which eventually decreases the cost of the finishing process. The surface coating could possibly change or eliminate the porosity, depending on the applications. However, it is not mandatory for the materials produced using appropriate AM techniques. Before the coating process, pre-treatments are required for the AM components [30], especially for the spray coatings. In addition, the line-of-sight spray approaches only cover a portion of highly complicated geometric forms. As a result, the untreated portions are more prone to wear and corrosion and the porous and cracked surfaces are exposed. Some of the surfaces coating techniques are briefly discussed below.

Surface coating processes such as plasma sprayed coating, cold spray coating, plasma electrolytic oxidation, electroless Ni–P coating, chemical conversion coating, electroless coating, thermal spray coating, and others are generally used after the additive manufacturing and the schematic representation is shown in Fig. 10.3. The benefits and recommended materials for the different coating process are depicted in Table 10.2.

In plasma spray coating, different gases like argon, nitrogen, hydrogen, and helium were used to create a respective environment for the coating process. A high voltage discharge initiates the plasma, causing a localised ionisation and a conductive channel for a DC arc to form between the cathode and anode and thereby spraying the particles on the surface of the AM components [31]. It is also observed that the plasma spray

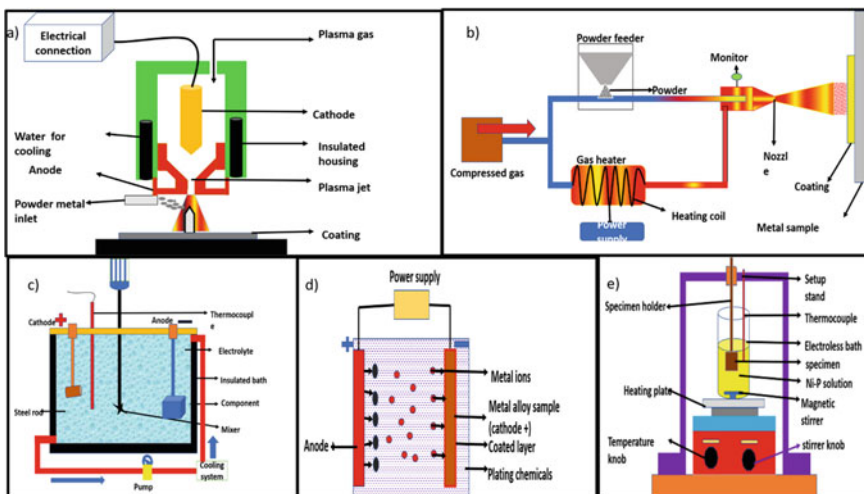


Fig. 10.3 Schematic of different surface coating processes **a** Plasma sprayed coating, **b** Cold spray coating, **c** Plasma electrolytic oxidation, **d** Chemical conversion coating, **e** Electroless Ni–P coating

Table 10.2 Summary of surface coating process, material and benefits

Surface coating process	Process	Suitable materials	Benefits	References
Plasma sprayed coating	Method of coating a metal or alloy by spraying molten or heat softened material on its surface Powder is fed into a plasma flame with a very high temperature, where it is rapidly heated and propelled to a high velocity	Stainless steel, titanium alloy, magnesium alloy. Aluminium	Enhance the hardness, corrosion and wear resistance, novel gradient surface modification system can improve osseointegration on bone implant and decrease the risk of load-bearing implant failure	[31]
Cold spray coating	Cold Spray coating accelerates powder particles (usually 10 to 40 m) to very high speeds (200 to 1200 m/s) at temperatures below their melting point using a supersonic compressed gas jet	Copper, titanium-nickel, titanium, cobalt, chromium, and nickel-base alloys	Low temperature process, no bulk particle melting Retains composition/phases of initial particles Very little oxidation High hardness Cold worked microstructure. Eliminates solidification stresses	[37, 38, 32]
Plasma electrolytic oxidation	An electrochemical surface treatment that creates an oxide coating layer on a metal surface	Titanium, zirconium, AZ91d, aluminium, zinc alloy	Significant impact on static mechanical properties such as except for maximum strength, yield stress, and energy absorption, corrosion resistance and wear resistance	[33, 34]
Electroless Ni-P coating	Chemical process that deposits a layer of nickel-phosphorus alloy on the surface of a solid substrate	Carbon steel, aluminium, magnesium,	Resistance to corrosion, improved hardness, superior strength, resistance to wear, improved ductility	[35]
Chemical conversion coating	Coating that creates a superficial layer on the parent metal using an electrochemical or chemical reaction on metal	Titanium alloy	Corrosion-resistant surface with better durability, bioactivity and biocompatibility	[33]

coating cannot be applied directly on the additive manufactured as it requires some pre-treatment process.

The advantage of plasma spray coating is that it creates a strong interfacial bonding between the parent metal and coated metal as compared to the other techniques. In cold spray coating, particles collide with the ground and undergo intense and rapid plastic deformation, breaking the thin surface oxide layers that all metals and alloys have. Also, the generation of high local pressure near the conformal contact between the exposed metal surfaces allows the effective bonding and rapid build-up of dense layers of deposited material. In addition to high temperature, the kinetic energy of the particles helps to retain the plastic strain energy from collisions [32].

Similar to plasma spray deposition, cold spray coating cannot be applied directly on the additive manufactured surface. PEO is a high-voltage electrochemical process that generates a plasma discharge at the metal-electrolyte interface, which transforms the substrate surface into a hard and dense ceramic oxide layer [33]. Plasma electrolytic oxidation improves the hardness, wear resistance, corrosion resistance and protect from the heat generation during the deposition. The application of PEO also extended in the bio-medical applications. For example, the PEO-Ca/P coatings produced an extremely viable outcome with high cell numbers as a result of cell proliferation, which indicate the cyto-compatibility.

The other coating technique, namely electroless coating was followed in recent years to improve the surface, corrosion, and wear properties of AM components. Electroless coating is an autocatalytic dip coating process, where nickel salt and reducing agent used for the deposition. Unlike electroplating, the electroless plating techniques do not need an electric current across the bath and the substrate. Rather, the reduction of metal cations from the solution to metallic is accomplished entirely through chemical methods, via redox reaction [34]. Electroless plating provides a homogeneous coating of metal, which is independent of the geometry of the surface. AISI 316L are fabricated by Laser additive manufacturing are Electrodeposited nickel and chromium then Pin-On-Rod test also reveals that electroplating with bright nickel and chromium will increase both friction force and friction coefficient is due to the very thin chromium layers [35]. additive manufacturing carbon steel are coated by electroless Nickel coating then electrochemical characterization allows evidence of a significant increase in corrosion resistance for the coated material with a noise resistance of $20 \text{ k}\Omega\text{-cm}^2$ after 576 h of evaluation [36].

10.3 Surface Modification (SM) Techniques for MAM

Surface modification is the process of altering a material's surface by adding physical, chemical, or biological features that differ from those found on the surface of the material originally. Surface modification techniques are being used in automotive, aerospace, power, electronic, biomedical, textile, petroleum, petrochemical, chemical, steel, power, cement, machine tools etc. Surface changes are mandatory for the additively manufactured metals in order to improve the mechanical, chemical,

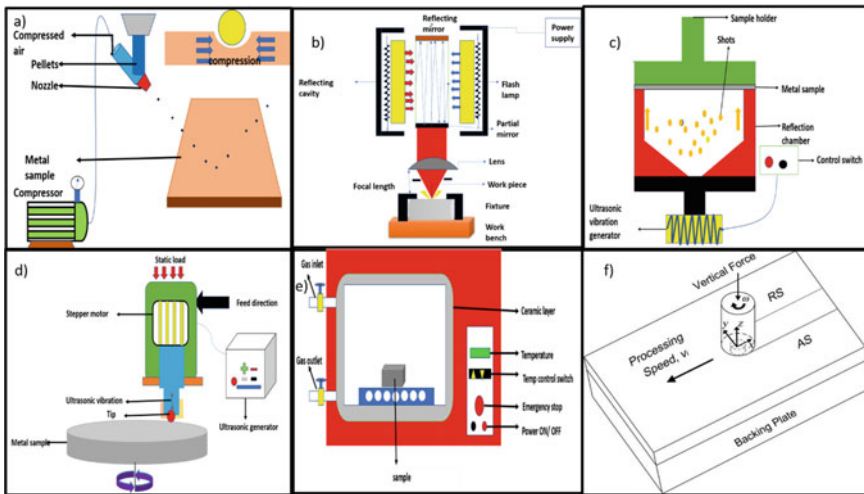


Fig. 10.4 Schematic diagram of different surface modification processes **a** Shot peening, **b** Laser surface treatment, **c** Ultrasonic surface rolling (USR), **d** Surface Mechanical Attrition treatment, **e** Heat treatment, and **f** Friction stir processing

and physical properties such as wear resistance, corrosion resistance, biocompatibility, and surface wettability. The post-treatments induces surface plastic deformation without any material removal, which increases the surface and mechanical properties of AM metallic parts. Deformation is caused due to the application of stresses or impacts, kinetic energy, thermal energy that can affect the surface layer of the entire body [39]. Apart from this, the phase composition and phase structure of the surface treated AM components determine the functional qualities of materials. Surface atoms are always distinct from their bulk counterparts for the simple reason that, unlike the bulk, where atoms are surrounded by other atoms from all sides, surface atoms are only connected to other atoms from one side. As a result, the attractive force of the surface atoms could be from the one direction of the atoms, resulting in high surface energy. Furthermore, the attractive force induced by the surface atoms could attract the gas-phase atoms or molecules. As a result, the surface of the materials is covered with foreign molecules in practise.

Most metals and alloys have an oxidised surface that is covered by a thin film of organic molecules that have produced from the surrounding air [39]. As a result, the surface composition is frequently differing from the bulk material composition. When the surface functional characteristics are lacking, the capacity to bond foreign atoms and molecules is found advantageous. These surface modifications have been grouped into many types like; mechanical, laser-based technologies, ultrasonic, thermal etc. Surface modification methods which are used for additive manufacturing of metals are shot peening, rolling sand blasting, laser surface treatment, friction stir processing, ultrasonic surface rolling heat treatment, cryogenic treatment, surface mechanical attrition treatment etc. (Fig. 10.4). Table 10.3 explains the

Table 10.3 Summary of surface modification process, material and benefits

SM process	Process	Suitable over	Benefits	References
Shot peening	SP is a cold working process that bombards the part surface with spherical beads using high pressure	Aluminium alloy, stainless steel titanium alloy	Improve surface rough, micro strain, and grain refinement, microhardness, and wear resistance compressive residual strength and mechanical properties of metal and composites	[40, 41]
Laser surface treatment	Passing a laser beam through the surface of a metal or alloy to harden the layer through metallurgical change, followed by rapid cooling and solidification	Ti6Al4V, aluminium	Surface strength, hardness, roughness, coefficient of friction, chemical resistance, and corrosion, eliminate porous, fatigue life	[42]
Ultrasonic surface rolling (USR)	Ultrasonic vibration and static force to the metal or alloy of the surface to create a nanostructured surface layer	Titanium alloy, stainless steel	Improving mechanical properties, fatigue strength, and wear resistance of various metals, slow down corrosion and prevent cracks from spreading	[43]
Surface Mechanical Attrition treatment	A small ball is placed in a reflector chamber connected to a vibration generator, and when the ball resonates, it connects with a large number of fly balls in a short period of time	Stainless steel, aluminium alloys, titanium	Surface hardness, augmentation of wear resistance, and fatigue characteristic. Corrosion resistance	[44, 45]
Heat treatment	Heating of a metal and keeping it at the same temperature for particular time, then cooling it to room temperature	Nickel alloy, low alloy steel, aluminium, magnesium, titanium	Enhance tensile strength, surface hardness, reduce porous, wear resistance	[46]

(continued)

Table 10.3 (continued)

SM process	Process	Suitable over	Benefits	References
Friction stir processing	Pressing a non-consumable tool into the workpiece and rotating it in a stirring motion as it is thrust laterally through it	Aluminium alloy, titanium, magnesium alloy	Ductility, strength, fatigue life, manipulating the microstructure, hardness	[47, 48]

various materials used in the surface modification processes and its benefits.

Shot penning (SP) is one of the effective surface treatment process used after the additive manufacturing to produce a high surface properties through the compressive residual stress. During shot penning, there is a formation of dome-shaped structures at the surface, which causes the surface expansions and plastic deformations. SP has been applied to AM composite alloys as a post-treatment for the following reasons; reducing the surface roughness, grain refinement, high compressive residual stresses, enhancing surface hardness, and improving fatigue life [41]. When compared to the as-built material, SP produces a more regular surface shape, while the treated surface remains rough. The parameters used in the SP process could have a significant role on the mechanical and wear properties of AM components.

Among the various techniques, Laser surface treatment was the effective techniques used to eliminate the surface defects like porous, cavity, etc., which majorly affects the fatigue property of the component. The lack of fatigue life could be due to the microstructure of the remelted layer or other factors. The laser surface treatment has improved the fatigue properties of AM components through the reduction of elastic stress concentration at surfaces, where fatigue cracks were developed [42]. Ultrasonic surface rolling (USRP) is another surface treatment procedure in which the USRP operator applies ultrasonic vibration and static force to the metal or alloy of the surface to create a nanostructured surface layer with greatly improved mechanical properties. USRP specimens is more homogeneous and denser (with a thinner thickness) than on untreated specimens, and the interface between corrosion products and metallic matrix is smoother. Furthermore, the USRP specimen's stress corrosion fracture is narrower than the untreated specimens [43]. This process could be used to enhance the thickness of a pore-free surface. Refined grains, dislocation walls, and deformation twins were the major advantages of USRP treatment, which increased the hardness, resistance to shear deformation, friction and wear of the modified surface.

Surface mechanical attrition is a method of surface treatment in which a small ball is placed in a reflector chamber connected to a vibration generator, and when the ball resonates, it connects with a large number of fly balls in a short period of time. The velocity of the ball is determined by the frequency of the generator. Each hit causes plastic deformation in the sample's surface layer at a high strain rate, by

inducing a grain refinement down to the nanometre scale in the top surface layer. SMAT, the additively formed alloy has a nanostructured surface layer followed by a gradient microstructure. It is observed that when the SMAT time is increased, the thickness of the SMAT-affected gradient layer increases from 20 to 40 mm in depth [44]. In heat treatment component's mechanical responsiveness is improved as a result of minimising surface contamination with high temperature treatments in vacuum condition. During the printing process, the internal stress and strains could build up in the materials. This induces various defects in the materials, which can be resolved with the help of heat treatment process [46]. In addition, heat treatment can also be used to improve the heat resistance and tensile strength.

Friction stir processing is one of the promising techniques used for altering the characteristics of AM components by severe plastic deformation [48]. The refinement is accomplished by pressing a non-consumable tool into the workpiece and rotating it in a stirring motion. FSP is an unique way to make surface composites for incorporating the microstructural changes to meet the mechanical property requirements such as ductility, strength, fatigue life, and so on [49]. This process could also effectively mix the material without changing the phase composition and generates a microstructure with fine and equiaxed grains. Figure 10.5 show how the hardness value of various material varies after surface modification process. It is clear that the mechanical properties of AM components were considerably improved after the surface modification process and surface treatments. However, the difference in the improvement was found changing with respect to the process as explained above.

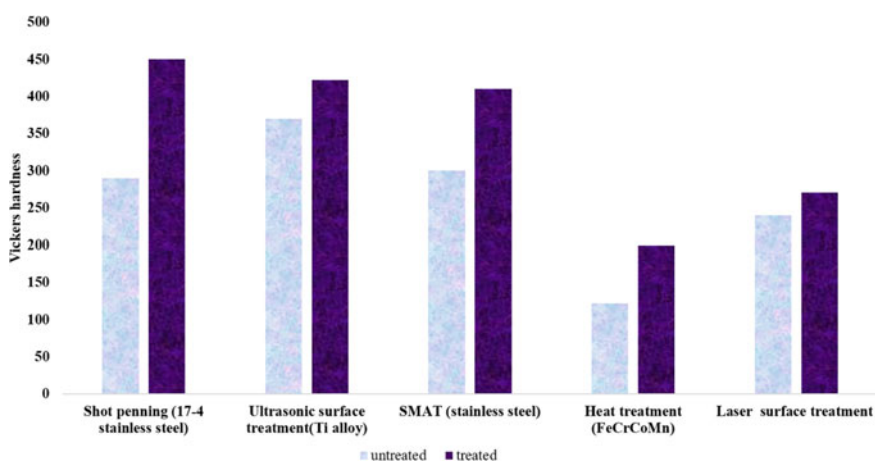


Fig. 10.5 Histogram for hardness value on different surface modification before and after treatment

10.4 Benefits of Surface Coatings and Surface Modification in AM

In terms of quality, performance, and life-cycle cost, surface coating and modification is one of the most essential ways to differentiate additive manufactured metal from traditional method. Surface properties of AM have a big impact on a component's serviceability and life; thus, they can't be overlooked in design, the engineering atmosphere is harsh. They're usually complicated, involving loading as well as chemical and physical degradation of the component's surface. Surface modification can assist in dealing with these situations in order to extend component service life and improve overall performance. Surface Engineering technique, in a nutshell, offers practical solutions to demanding applications. Surface coating could provide an extra advantage in such a way to use in the dental implant, gear application and tribological application. Chemical conversion technology is still in its early stages of development as a protective and bioactive coating on metal implants for biomedical applications.

10.5 Summary

Complex design, mass production, minimum wastage of raw material, freedom to fabricate any complex design, reduced man power, reduced time wastage and improved product quality are among the main benefits of additive manufacturing processes. These improvements and optimizations aid in the industry's transition from "rapid prototyping" to "rapid manufacturing". Substitute manufacturing is utilised for more than just prototypes, as a means of producing desired and customised products on a small scale. Despite the advantages of additive manufacturing, there are a few obstacles that would necessitate additional research and development before this technology could be adopted in numerous industries. Due to a loss in interfacial bonding between printed layers, void formation between the following layers of materials results in greater porosity throughout the production process, which can degrade mechanical performance.

Researchers are also interested in implementing surface finish processes to improve the quality of final products. Surface treatment processes like shot peening laser, heat treatment, friction stir processing have improved the surface morphology, recrystallization, hardness, tensile, wear and corrosion properties. The surface coating process covers the void that occurs during the additive manufacturing process, which helps to reduce porosity, surface roughness, cracks, and oxidation. The reduced defects after the surface coatings and treatments have improved the wear and corrosion resistance of additively manufactured components and hence, concluded to use directly to the end application. Further research into improving the surface finish of additive manufactured components can be applied to defence, bio materials, robotics, automobile parts, and other applications.

10.5.1 Future of Surface Coatings and Surface Modification (SM) Techniques in AM

The future of the technology is bright. Improvements on the high end will enable the production of higher quality AM parts, especially for the low-density metal alloys like aluminium, magnesium, and high-density alloys like titanium, nickel, zirconium, stainless stain. The properties of the AM component produced from the aforementioned materials could be further improved using the surface coating and modification. However, still there is wide research gap, especially focuses on the use of metal alloy for the biomedical applications, aviation industry etc. Another foreseeable area of research in the future that can represent a key to unlock the full potential of surface post-treatments is to design hybrid treatments that can simultaneously exploit combined beneficial effects of individual post-processes.

References

1. Hull, C.W.: Apparatus for production of three-dimensional objects by stereolithography. U.S. Patent 6,027,324, issued February 22, 2000
2. Jiménez, M., Romero, L., Domínguez, I.A., Espinosa, M.D.M., Domínguez, M.: Additive manufacturing technologies: an overview about 3D printing methods and future prospects. *Complexity* **2019** (2019)
3. Ngo, T.D., Kashani, A., Imbalzano, G., Nguyen, K.T., Hui, D.: Additive manufacturing (3D printing): a review of materials, methods, applications and challenges. *Compos. Part B Eng.* **143**, 172–196 (2018)
4. Geneva, S.: Additive manufacturing—general principles—terminology. ISO/ASTM 52900 (2015)
5. Meboldt, M., Klahn, C. (eds.): Industrializing Additive Manufacturing—Proceedings of Additive Manufacturing in Products and Applications-AMPA2017. Springer (2017)
6. Zhang, Y., Wu, L., Guo, X., Kane, S., Deng, Y., Jung, Y.G., Lee, J.H., Zhang, J.: Additive manufacturing of metallic materials: a review. *J. Mater. Eng. Perform.* **27**(1), 1–13 (2018)
7. Bergsma, J.M., van der Zalm, M., Pruyne, J.F.: 3D-Printing and the maritime construction sector. In: 10th Symposium on High-Performance Marine Vehicles, HIPER, vol. 16, pp. 428–442 (2016)
8. Shah, F.A., Snis, A., Matic, A., Thomsen, P., Palmquist, A.: 3D printed Ti6Al4V implant surface promotes bone maturation and retains a higher density of less aged osteocytes at the bone-implant interface. *Acta Biomater.* **30**, 357–367 (2016)
9. Hettesheimer, T., Hirzel, S., Roß, H.B.: Energy savings through additive manufacturing: An analysis of selective laser sintering for automotive and aircraft components. *Energy Effi.* **11**(5), 1227–1245 (2018)
10. Shahzad, K., Deckers, J., Kruth, J.-P., Vleugels, J.: Additive manufacturing of alumina parts by indirect selective laser sintering and post processing. *J. Mater. Process. Technol.* **213**(9), 1484–1494 (2013)
11. Wilkes, J., Hagedorn, Y.C., Meiners, W., Wissenbach, K.: Additive manufacturing of ZrO₂-Al₂O₃ ceramic components by selective laser melting. *Rapid Prototyping J.* (2013)
12. Murr, L.E., Gaytan, S.M., Ramirez, D.A., Martinez, E., Hernandez, J., Amato, K.N., Shindo, P.W., Medina, F.R., Wicker, R.B.: Metal fabrication by additive manufacturing using laser and electron beam melting technologies. *J. Mater. Sci. Technol.* **28**(1), 1–14 (2012)

13. Körner, C.: Additive manufacturing of metallic components by selective electron beam melting—a review. *Int. Mater. Rev.* **61**(5), 361–377 (2016)
14. Zhang, L.-C., Liu, Y., Li, S., Hao, Y.: Additive manufacturing of titanium alloys by electron beam melting: a review. *Adv. Eng. Mater.* **20**(5), 1700842 (2018)
15. Mudge, R.P., Wald, N.R.: Laser engineered net shaping advances additive manufacturing and repair. *Weld. J. New York* **86**(1), 44 (2007)
16. Mireles, J., Espalin, D., Roberson, D., Zinniel, B., Medina, F., Wicker, R.: Fused deposition modeling of metals. In: Proceedings of the Solid Freeform Fabrication Symposium, Austin, TX, USA, pp. 6–8 (2012)
17. Liu, B., Wang, Y., Lin, Z., Zhang, T.: Creating metal parts by fused deposition modeling and sintering. *Mater. Lett.* **263**, 127252 (2020)
18. Ding, D., Pan, Z., Cuiuri, D., Li, H.: Wire-feed additive manufacturing of metal components: technologies, developments and future interests. *Int. J. Adv. Manuf. Technol.* **81**(1), 465–481 (2015)
19. Dhinakaran, V., Ajith, J., Fahmidha, A.F.Y., Jagadeesha, T., Sathish, T., Stalin, B.: Wire arc additive manufacturing (WAAM) process of nickel-based superalloys—a review. *Mater. Today Proc.* **21**, 920–925 (2020)
20. Ford, S., Despeisse, M.: Additive manufacturing and sustainability: an exploratory study of the advantages and challenges. *J. Clean. Prod.* **137**, 1573–1587 (2016)
21. Enrique, P.D., Marzbanrad, E., Mahmoodkhani, Y., Jiao, Z., Toyserkani, E., Zhou, N.Y.: Surface modification of binder-jet additive manufactured Inconel 625 via electrospark deposition. *Surf. Coat. Technol.* **362**, 141–149 (2019)
22. Yan, C., Hao, L., Hussein, A., Wei, Q., Shi, Y.: Microstructural and surface modifications and hydroxyapatite coating of Ti-6Al-4V triply periodic minimal surface lattices fabricated by selective laser melting. *Mater. Sci. Eng., C* **75**, 1515–1524 (2017)
23. van Hengel, I.A., Riool, M., Fratila-Apachitei, L.E., Witte-Bouma, J., Farrell, E., Zadpoor, A.A., Zaaij, S.A., Apachitei, I.: Selective laser melting porous metallic implants with immobilized silver nanoparticles kill and prevent biofilm formation by methicillin-resistant *Staphylococcus aureus*. *Biomaterials* **140**, 1–15 (2017)
24. Gao, W., Zhang, Y., Ramanujan, D., Ramani, K., Chen, Y., Williams, C.B., Wang, C.C., Shin, Y.C., Zhang, S., Zavattieri, P.D.: The status, challenges, and future of additive manufacturing in engineering. *Comput. Aided Des.* **69**, 65–89 (2015)
25. Platl, J., Leitner, H., Turk, C., Demir, A.G., Previtali, B., Schnitzer, R.: Defects in a laser powder bed fused tool steel. *Adv. Eng. Mater.* **2000833** (2020)
26. Du Plessis, A., Yadroitseva, I., Yadroitsev, I.: Effects of defects on mechanical properties in metal additive manufacturing: A review focusing on X-ray tomography insights. *Mater. Design* **187**, 108385 (2020)
27. Ye, D., Hong, G.S., Zhang, Y., Zhu, K., Fuh, J.Y.H.: Defect detection in selective laser melting technology by acoustic signals with deep belief networks. *Int. J. Adv. Manuf. Technol.* **96**(5), 2791–2801 (2018)
28. Ralls, A.M., Kumar, P., Menezes, P.L.: Tribological properties of additive manufactured materials for energy applications: a review. *Processes* **9**(1), 31 (2021)
29. Maleki, E., Reza Kashyzadeh, K.: Effects of the hardened nickel coating on the fatigue behavior of CK45 steel: experimental, finite element method, and artificial neural network modelling. *Iran. J. Mater. Sci. Eng.* **14**(4), 81–99 (2017)
30. Fotovvati, B., Namdari, N., Dehghanhadikolaei, A.: On coating techniques for surface protection: a review. *J. Manuf. Mater. Process.* **3**(1), 28 (2019)
31. Ramesh, C.S., Kumar, R.S., Murthy, M.: Slurry erosive wear behaviour of copper plasma sprayed with titania-30wt% inconel 718. *Procedia Mater. Sci.* **5**, 1130–1135 (2014)
32. Mäkinen, M., Jauhainen, E., Matilainen, V.-P., Riihimäki, J., Ritvanen, J., Piili, H., Salminen, A.: Preliminary comparison of properties between Ni-electroplated stainless steel parts fabricated with laser additive manufacturing and conventional machining. *Phys. Procedia* **78**, 337–346 (2015)

33. Diaz, D.G.A., Pingarrón, A.B., Florez, J.J.O., Parra, J.R.G., Cabello, J.C., Moncaleano, I.A., Villar, A.C., Gallegos, M.Á.H.: Effect of a Ni-P coating on the corrosion resistance of an additive manufacturing carbon steel immersed in a 0.1 M NaCl solution. *Mater. Lett.* **275**, 128159 (2020)
34. Pathak, S., Saha, G.C.: Development of sustainable cold spray coatings and 3D additive manufacturing components for repair/manufacturing applications: A critical review. *Coatings* **7**(8), 122 (2017)
35. Garcia-Cabezón, C., Rodriguez-Mendez, M.L., Amigo Borrás, V., Raquel, B., Rodriguez Cabello, J.C., Ibañez Fonseca, A., Martin-Pedrosa, F.: Application of plasma electrolytic oxidation coating on powder metallurgy Ti-6Al-4V for dental implants. *Metals* **10**(9), 1167 (2020)
36. Rogov, A.B., Lyu, H., Matthews, A., Yerokhin, A.: AC plasma electrolytic oxidation of additively manufactured and cast AlSi12 alloys. *Surf. Coat. Technol.* **399**, 1261 (2020)
37. Cavaliere, P., Cavaliere, L., Lekhwani.: *Cold-Spray Coatings*. Springer (2018)
38. Han, Q., Jiao, Y.: Effect of heat treatment and laser surface remelting on AlSi10Mg alloy fabricated by selective laser melting. *Int. J. Adv. Manuf. Technol.* **102**(9), 3315–3324 (2019)
39. Rakoch, A.G., Khokhlov, V.V., Bautin, V.A., Lebedeva, N.A., Magurova, Y.V., Bardin, I.V.: Model concepts on the mechanism of microarc oxidation of metal materials and the control over this process. *Prot. Metals* **42**(2), 158–169 (2006)
40. Maleki, E., Bagherifard, S., Bandini, M., Guagliano, M.: Surface post-treatments for metal additive manufacturing: progress, challenges, and opportunities. *Addit. Manuf.* **101619** (2020)
41. Champaigne, J.: Shot peening overview. Metal Improvement Company (2001)
42. AlMangour, B., Yang, J.-M.: Improving the surface quality and mechanical properties by shot-peening of 17–4 stainless steel fabricated by additive manufacturing. *Mater. Des.* **110**, 914–924 (2016)
43. Zhou, C., Wang, J., Guo, C., Zhao, C., Jiang, G., Dong, T., Jiang, F.: Numerical study of the ultrasonic impact on additive manufactured parts. *Int. J. Mech. Sci.* **197**, 106334 (2021)
44. Sheng, G.: Investigation of surface self-nanocrystallization in 0Cr18Ni9Ti induced by surface mechanical attrition treatment. *Int. Sch. Res. Not.* **2011** (2011)
45. Ghosh, S., Bibhanshu, N., Suwas, S., Chatterjee, K.: Surface mechanical attrition treatment of additively manufactured 316L stainless steel yields gradient nanostructure with superior strength and ductility. *Mater. Sci. Eng. A* (2021)
46. Deirmina, F., Peghini, N., AlMangour, B., Grzesiak, D., Pellizzari, M.: Heat treatment and properties of a hot work tool steel fabricated by additive manufacturing. *Mater. Sci. Eng., A* **753**, 109–121 (2019)
47. Mondal, M., Das, H., Hong, S.T., Jeong, B.S., Han, H.N.: Local enhancement of the material properties of aluminium sheets by a combination of additive manufacturing and friction stir processing. *CIRP Annals* **68**(1), 289–292 (2019)
48. Zykova, A.P., Tarasov, S.Y., Chumaevskiy, A.V., Kolubaev, E.A.: A review of friction stir processing of structural metallic materials: process, properties, and methods. *Metals* **10**(6), 772 (2020)
49. Zhao, L., Macías, J.G.S., Dolimont, A., Simar, A., Rivière-Lorphèvre, E.: Comparison of residual stresses obtained by the crack compliance method for parts produced by different metal additive manufacturing techniques and after friction stir processing. *Addit. Manuf.* **36**, 101499 (2020)

Chapter 11

Mechanical Testing of Additive Manufacturing Materials



I. Akilan and C. Velmurugan

11.1 Introduction to Additive Manufacturing Techniques

Nowadays, additive manufacturing (AM) matters in large industries and research communities because of its speed, features, and other key features, all of which contribute to the development of superior products [92]. Charles Hull pioneered additive manufacturing methods in 1986 [61]. In 2009, one million AM products were produced by using these 3D Additive Manufacturing (AM) methods. During this time, people are paying more attention to 3D AM products. As a result, every major industry and academic scientist has been working tirelessly to develop AM products. The number of AM products sold in 2019 thus increased by (95%) by almost 5 million compared with 2009 [68]. AMs are also familiar with rapid prototyping and 3D printing technology, which both aid in the production of complex structures through layer-by-layer methods [63]. The traditional 2D method was initially used, but it could not produce sufficient items or construct strong structures. The 3D additive manufacturing process was used. The AM printing system requires the use of high-altitude materials such as polymers, metals, and ceramics [6]. According to the 2017 Wohler's Statement, 97 manufacturing companies worldwide produced and distributed AM systems in 2016 are in Fig. 11.1, with almost half of service providers investing in AM structures that produce metal parts. Because these AM substances were originally based on polymers, academic scientists and their critical effort have focused on the development and improvement of AM systems in all steel substances [76].

This enables investors to help with the development of AM metallic objects that use the net- or mesh algorithms rather than traditional machine or machine tools

I. Akilan · C. Velmurugan (✉)

Department of Mechanical Engineering, Indian Institute of Information Technology
Tiruchirappalli, Tiruchirapalli, Tamil Nadu 620012, India
e-mail: velmuruganc@iiit.ac.in

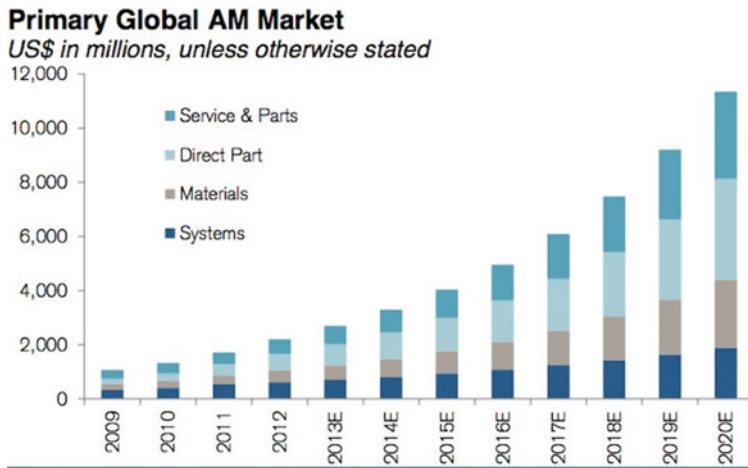


Fig. 11.1 Market growth for AM/3D printing in the future, changes in the aerospace, automotive, healthcare, and consumer markets are expected to grow at a 20–30% annual rate [132]

[92]. The structure of such metal elements is extremely solid and frightening when compared to polymer products. Because of their ability to create complex shapes in the biomedical industry and many other forms, these metal components were very useful in the aerospace industry. These metal components are made of powder or wire-based innovations that are thoroughly assimilated into the basic structure through a heat source and subsequent cooling rate [90]. The technology currently employs less space and is the most reliable in the production of 3D structures of steel, aluminum, and tungsten materials. All these materials are printers that produce rapid prototypes with a small structure and a design of the fabricated part [58]. There are many processes for additive technological methods are shown in the Fig. 11.2, such as high-quality selective laser sintering, electron beam melting, direct metal laser sintering, and selective laser melting, as well as energy deposition techniques such as (laser engineered net shaping, laser metal deposition, direct metal deposition, and so on), all of which include the usage of additive manufacturing fabrication methodologies. In commercial applications, almost all the components of this metal structure are sparingly used. The density, hardness of the surface, tensile strength [41], compressive strength, fatigue, crease, waste stress, and decomposition of printed metal materials is measured using the correct standard ASTM processes and all metal components are systematically produced using 3D fusion technology to determine how well their performance under load is determined [78]. The entire examination process examines AM's mechanical characteristics and test method, and its advantages and disadvantages that are followed by future direction are discussed in the following chapters.

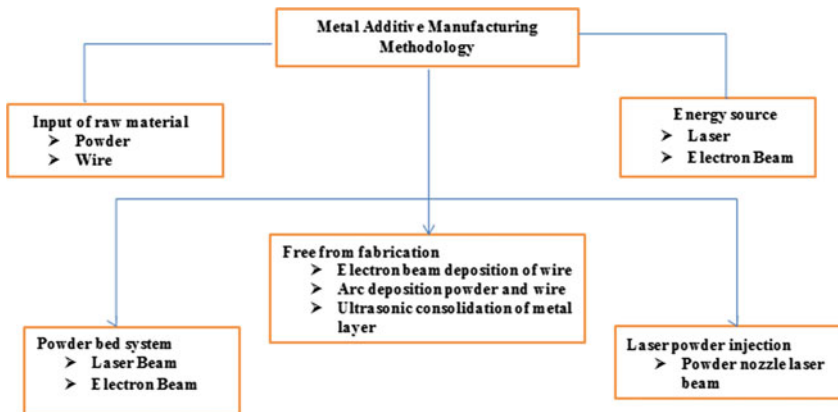


Fig. 11.2 AM processes for metal additive manufacturing

11.2 Classification of Metal Based AM Techniques

The most important characteristics are the type and complete status of the feed, as well as the connection mechanism for the classified AM metal materials. Layered by layering in AM metal, the power input of a laser or electron beam completely melts a powdered feed, or rarely a wire, and transforms it into a firm part of nearly any geometry [48]. The maximum not unusual AM steel approaches are Laser Beam Melting-LBM, Electron Beam Melting-EBM, and Laser Metal Deposition-LMD). For LBM processes, examples include Selective Laser Melting-SLM, Direct Metal Laser Sintering-DMLS, Laser Curing, Laser Metal Fusion-LMF, and business 3-D printing. These all terms are frequently used to describe the LBM process [8]. Metal AM techniques, regardless of their names, all use the same three basic methods: a three-dimensional CAD model is developed on a computer, an imaging device is used, or reverse engineering is used. However, these three procedures differ from LBM, EBM, and LMD in key characteristics, benefits, and drawbacks [20]. These designs are cut into virtually thin layers with a standard layer thickness of D_s 20 μm –1 mm, depending on the metal-based complete AM technology [112].

11.2.1 *Laser Beam Melting (LBM)*

The material and process risks inherent in each compound production process must be surveyed. The starting materials for Laser Beam Melt (LBM) are permeable and classified by their various size distributions as lung or alveolar (electron fraction or a fraction). This is true for a metal powder that is 15–60 microns larger than the standard particle size distribution [109]. These metal powders have maximum permissible and a limited concentration. Titanium, aluminum, and alloys are reacting with metal that

is of low density. A typical LBM chain is extremely flammable, carcinogenic, and dangerous to the aquatic environment. The specific risk of these hazards must be evaluated for each piece of equipment, material, or process infrastructure.

A galvanometer scanner drives across the deposited powder layer at a (Scanning Velocity-V_s) of up to 900 m/m and LBM beam (P_L) power range of 20 W–1 kW [94]. Single filament radiation beams with wavelengths ranging from 1060 to 1080 nm are released in the nearby infrastructure, which is largely in continuous wave modes in LBM. The standard laser beam interval for the X–Y nozzle jet range between 50 μm and 180 microns, according to the production processes used to produce the selected laser beam output [109]. A sequence, like a strategic structural scan, usually follows the order of each melting path and the melting paths are overlapping at a certain hatch distance. Besides melting exposed material, heat moves volumetric energy from the powder layer to the surface or next to the melting pool. Figure 11.3 depicts the solidification of various melting tracks during and beneath a hard layer. This component is attached to a supporting structure, which is an integrated blade. The support structures are ladle structures that are required to dissipate and adjust the heat in the powder bed, specifically to improve horizontal orientation and surface excess. After preventing the decay of this region, structures to support the removal of the part are added [13]. Besides the substructure, pre-heating the structure can reduce partial deformation by minimizing temperature gradients, resulting in reduced residual stresses during LBM operation. The common setting temperature for the LBM pack of Ti-6Al-4 V components is 500–200 °C. The LBM process is carried out in a closed process chamber with an inert gas atmosphere, which are maintained at less than 0.1% oxygen. The metal powder, when injected with nitrogen or argon into the room, prevents it from melting in contact with the environment. Noble gas flow around the workplace is used to remove secondary process products such as solder sparks and solder spreaders [98].

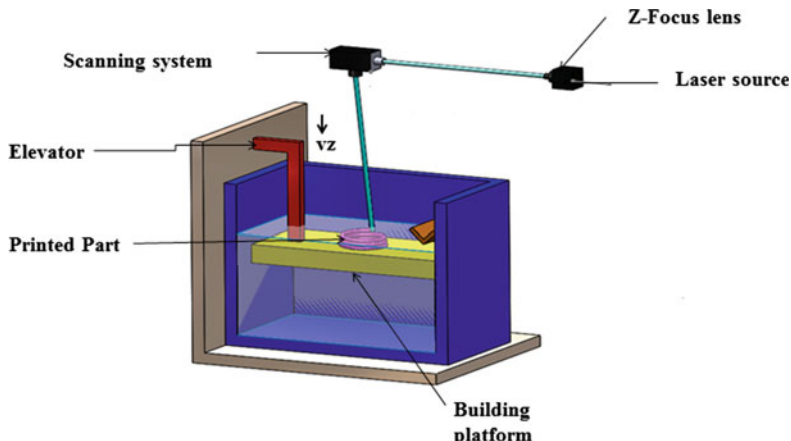
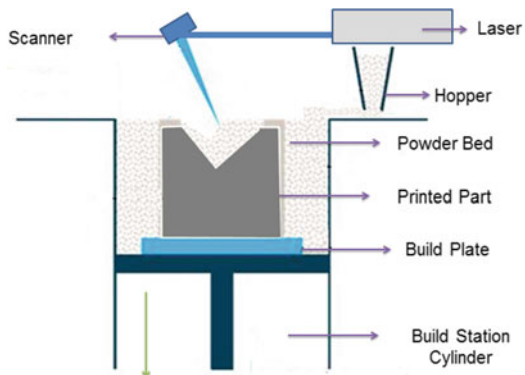


Fig. 11.3 Layer-by-Layer LBM process

Fig. 11.4 Systematic diagram laser metal fusion



11.2.2 *Laser Metal Fusion*

The LMF is also known as metal 3D printing. The know-how in metal 3D can picture the interest of designers of fabrics, but it takes more effort to print a 3D part. A 3D model, typically 20–100 microns thick and using specialist software, is “sliced” into thin layers. All components must be optimized for fusion efficiency, location density, and heat management. Finally, as shown in Fig. 11.4, the part is built layer by layer using a cultured laser fusion method. A layer of metal powder is used to connect the cross-phase geometry to the plate, which is then driven by the optical scanner using a laser beam [32]. The plate is reduced after treatment, and it adhered in the next particle layer to. It follows a series of steps until the part is finished. This can take longer depending on the size, thickness of the components, materials used, laser energy, scan velocity, spot dimension, and other variables [107]. Some post-processing steps may be required when removing a partition from the system. After heating, removal of hips and integrated panes, production of any interface layers, and final surface processing, such as bell surface processing (including high-density hips). In many industries, metal 3D printing has already affected such as dental, medical or marketing prototyping, including titanium for hip joints, cobalt chrome for dents and bridge steel, among other examples. Even though the parts are mass-produced, each one of its materials has a unique characterization [30]. In fact, the aviation industry has since shifted toward the production of 3D printed prototypes. The ability to create simple and flexible bionic structures has enabled structural geometries which were impossible to implement with traditional manufacturing methods.

11.2.3 *Electron Beam Melting (EBM)*

Electron beam melting-EBM is a method of melting powdered metal layers using electron beams. Arkham, a Swedish company, first introduced EBM in 1997, making it ideal for light, long-lasting, and dense finishing elements, including space,

medicine, and security, are the most common applications of technology. Laser Powder Bed Fusion (LPBF) combines metal particles using electron beams to create layer-by-layer, desired areas [40]. The heat source used is the primary distinction of LPBF technology. Here, EBM technology makes use of electron beams generated by an electron gun. Under vacuum, the latter removes electrons from the building tray of a 3D printer and quickly converts them into a layer of metal powder, as shown in Fig. 11.5. These electrons can then choose the powder and produce some of it (2017). The drive removes a component from the machine at the end of the manufacturing process and uses a brush to clean the blister or dust. This can remove print media and partitions from the box (if needed). After printing, working, and polishing surfaces in contact with other parts. The stress created by the manufacturing process may cause several hours of heating in the oven. For the electron beam to function properly, all production must take place in a vacuum. This prevents the powder from oxidizing when heated. Most insoluble powders can be reused after the manufacturing process is finished. Manufacturers, particularly in aeronautics, understand the appeal because from the materials purchased only 20% is used for the unalterable part, with the rest being separated and recycled [57].

Today's most common materials are titanium and chromium-cobalt alloys, limiting the range of Arcam compliant products. Users must first complete the additional training and get permission to use the machine as needed before using or testing another product. Because the powder is more granular, electron beam melting produces components faster than LPBM, but the process is less accurate and the cover quality is lower [15]. The electron beam is separated, allowing dirt to be heated in multiple locations at the same time and speed up production. When controlling heat dissipation before melting and reducing the need for reinforcement and production help [69]. At the fine powder level, the electron beam is broader than the laser beam,

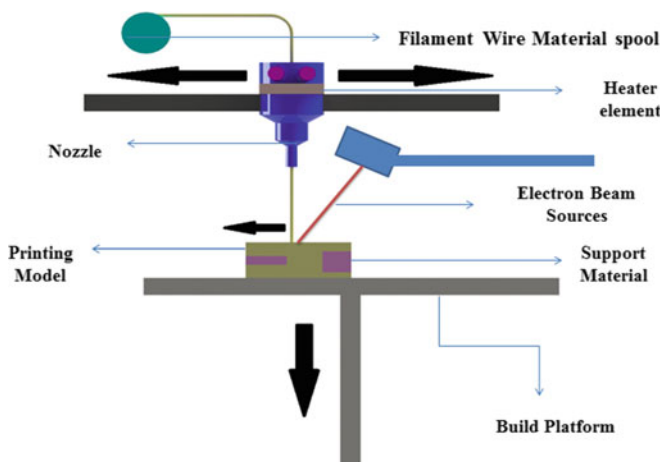


Fig. 11.5 EBM 3D printed process diagram

which affects accuracy. The EBM (Q20 Machine) has the largest construction size, with a circle of 110 cm of 38 cm.

11.2.4 *Laser Metal Deposition (LMD)*

Laser metal deposition-LMD is a type of metal production process. The term “Laser Metal Deposit,” abbreviated as LMD, is widely used throughout the universe. LMD is also known as “Direct Metal Deposition-DMD” or “Direct Energy Deposition-DED”. LMD is a new technology that combines powdered components and laser drilling to achieve greater accuracy [89]. As a result, this process continues to develop in significant applications such as aeronautical and medical regardless of performance and acceptance criteria in those industries. In terms of repairs, the low thermal input allows an automatic change of complex spaces to create a smaller thermal surface. The layer’s overall microstructures, as well as the residual stress caused by the steep thermal gradient, are anisotropic [79]. These effects have a negative impact on the machine’s component properties. Because there are so many process variables in LMD today, estimating the properties of manufactured LMD components is extremely difficult. Thermal history is a cumbersome subject that can be altered by different factors. Depending on the material structure, the process metrics can have a complex impact on the microstructure [104]. Despite the significant benefits of LMD, a thorough understanding of the process structure and asset relationships should place a special emphasis on the impact of powder properties. The geometry, structure, and grouping of sediments are critical for a variety of service applications, depending on the process variables, the metal, and the resulting mechanical properties [79].

DLMD is a quick tooling process that uses a laser to liquefy the metallic sediments into pieces and molds. In this method, which is comparable to traditional rapid prototyping, metal powder and tool steel melt faster than plastic polymers. The DLMD tool can create or reassemble genuine finishing materials such as metal materials of aluminum parts, molds, and dies. It always generates a new CAD drawing area or reconstructs an existing component. To extend the molten pool, a small stream of molten tool steel is injected into it. Layer builds the solid metal element layer by moving the laser beam back and forth under CNC control and locating the controlled form using a computerized CAD design. The components are consistent, well structured, of high quality, and well equipped. By combining several metal powders in the melting pool, the alloy can be replaced by DLMD [59].

Direct Laser Metal Sintering-DLMS and Selective Laser Melting-SLM are high-intensity laser sintering techniques that are also known as Direct Laser Metal Fusion (DLMF). A metal part is included in the computer-aided design file, and the bed is covered in metal powder. This technology improves the SLS process by layering metal powder to create true three-dimensional parts. This technology allows for the direct production of human implants from computer-aided design models with minimal processing time. The primary goal is to produce completely high-density

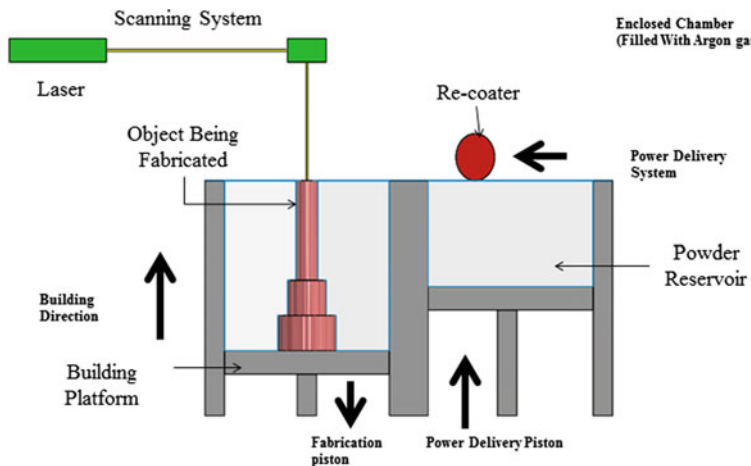


Fig. 11.6 Experimental setup of selective laser melting (SLM) process

metal parts [34]. Figure 11.6 shown traditional SLM systems use high-precision beams with a diameter of only 0.03 mm and Z-axis steps of only 0.05 mm, with no complex metal components. If the high-power laser beam is heated in layers of 20 to 40 μm without a binder or fluxing agent, bronze, steel, 316L steel, titanium, or Al-30% are possible. DLMS can improve a wide range of applications, such as aircraft, interfaces, and frames. Using costly materials with complex devices, as well as 3D metal printing, is beneficial in the medical field. Customer requirements are typically highly specialized/precise [83].

11.3 Additive Manufacturing of Metal Based Products

The success of AM powder sheet fusion is critical for high-quality metal powder and wires. Titanium and its alloys, stainless steel and alloys, aluminum alloys and different metals in the form of a powder, depending on processor requirements such as copper(cu), nickel chromium and cobalt alloys, found less alloys and highly expensive metals like gold, platinum, palladium or silver, are the focus of this section [78]. Wire feeds are also available in a variety of materials, including iron and carbon—its alloys, including pure metals substance such as Titanium-Ti, Tungsten-W, Niobium-Nb, Molybdenum-Mo, and Aluminum-Al. However, not all materials have been used in additive manufacturing, but the metal powder can be qualified for a specific purpose most times and with the right equipment.

The layer thickness and partial sphere geometry distribution of gas atom particles typically range from 10 to 50 μm . This is a common feature of metal powders suitable for AMs. Tensile strength, hardness, and lengthening are important material characteristics that are frequently used to determine the right material [48, 28].

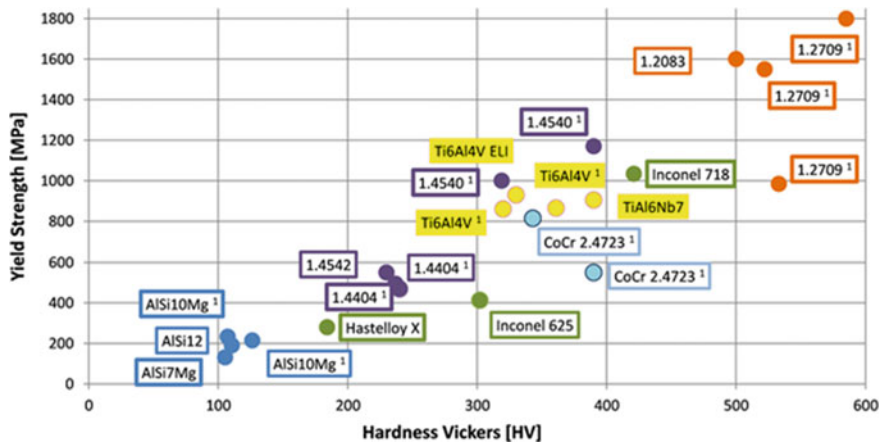


Fig. 11.7 Mechanical characteristic of metal products

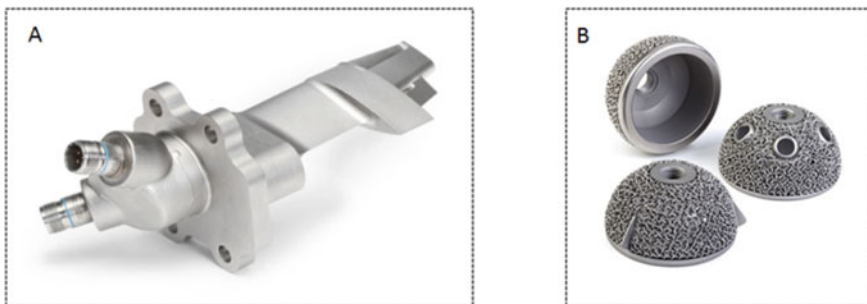


Fig. 11.8 **a** 3D Inlet sensor housing unit in jet motor **b** 3D acetabular cup [78]

The image (Fig. 11.7) depicts some of the various alloys and their detailed output yield strengths. Based on two mechanical properties, the user can select the object using this diagram. Yield strength was calculated using the best value found on the manufacturer's datasheets [96].

11.3.1 Titanium and Its Alloys

Non-workable titanium alloys are traditionally available and have a variety of manufacturing applications. It is available in one to four grade classes, depending on the quality of the application. Even though all grades have exceptional corrosion resistance, ductility, and weldability, grade one is far superior to grades II, III, and IV are powerful. Level II titanium is the best combination of design and strength [25]. Only a few industries use condenser pipes, high heat exchangers, turbojet jet

engines, aviation, and marines. Titanium grade-II is used in biomedical implants and prostheses. In precious metals such as titanium and other alloys, reducing waste is an enormous benefit. Shorter lead times and more constrained manufacturing flows are becoming more prevalent [25]. According to the well-known laser and electron beam AM methods, Boeing estimates that using fully 3D-printed titanium components could save the 787 Dreamliner \$3 million. GE has developed miniature titanium of 3D inlet sensor housing unit in Jet Motor as shown in Fig. 8a. In a NASA-tested demonstration of that engine, fluid hydrogen was extracted at 696.15 K and fuel burned at 6273.15 K [58].

The titanium ASTM grade five casting alloy is a combination of alpha–beta alloy with a Young module of 0.1–0.130 Tera pascal. Huge bone implants have such a young modulus, but the level of porosity can be reduced as well as porosity can be controlled, which are shown in Fig. 8. With the help of EBM, titanium composites are used to manufacture a variety of industrial essentials, such as turbine blades, latches, screws, rings, discs, acetabular cups, hubs, and ships [78]. High-performance engine parts like gear trains and piston rods employs Titanium alloys for its production. Metal is a viable option in medical applications because of materials with high biocompatibility, such as cobalt chromium and titanium, especially when there is direct metal contact with bone or tissue [93].

11.3.2 *Stainless Steel*

Stainless steel has many tremendous mechanical properties in additive manufacturing, including robustness, design, and tensile strength to a wide range of automobile, light industries, food production, and therapeutic diagnostic application [108]. EBM technology employs stainless steel powder to create super-strong and dense waterproofing components for aerospace applications such as jet engines, rocket motors, and nuclear power plants [36]. The 2016 review of literature looks into the use of low-carbon steel in EBM machines, such as those used to develop nuclear energy pressure vessels. Following that, 316L steel was chosen because of its softness, strength, and resistance to corrosion. Most AM's literature focuses on 316L quality austenitic stainless steel, which is a popular choice for a variety of industrial applications as shown in Fig. 11.9 [31]. However, if any successes or difficulties in various properties are reported, other types of austenite steel, such as grades 304 L, will be investigated. The most significant difference between 316 and 304L chemical composition is that 316L contains close to 2 with % Mo to improve corrosion resistance [52].

Tool steels differ significantly from structural steels in that they are used to making tools that are resistant to wear and hardness. “Tool Steel” believes such steel contains at least 0.7% carbon. However, the maraging steel compositions are Fe-65, Ni-18, and C-80%, and are established in the tool and die-making industries because of their increased unique strength, fractural hardness, and weldability. Molding, high pressurized die-casting, stomping and protrusion die-cutting, and plastic injection

Fig. 11.9 Air brackets of 316L austenitic stainless steels



are some of its tools [62]. Steel is a powder that can be used in a variety of ways in compliance with additive manufacturing solutions like SLS or DMLS. Steel is more accessible on the 3D printing market than other metals and it can be used in a broad range of alloys, making it even more attractive to specially designed through industry requirements. Steel metal has been the most frequently used material in the AM because of its high mechanical properties. According to the investigation, the number of powdered steel supplies used in industries such as aerospace and automotive increased by 48% in 2018 [43].

11.3.3 Aluminum and Its Alloys

DMLS will be used to sinter aluminium, and a Selective Laser Melting process will be used to melt it (SLM). As a result, it can be applied to walls with layer thicknesses ranging from 25 to 50 microns. As shown in Fig. 11.10, the reusable jig parts have a rough, matte finish that distinguishes them from standard milled aluminium parts. 3D-printed aluminium parts are mostly used for automobile parts and, in particular, racing



Fig. 11.10 Reusable jig for automobile car parts [18]

car components due to their good mechanical properties of lightweight, strength, and impact under load conditions [18]. They have excellent strength-to-weight ratios and are resistant to excessive wear and corrosion. The aluminum alloy powder has a significant advantage over other metal powders commonly used in PBF because it provides higher training levels. Because of the geometrically complex structures used in additive manufacturing, additional weight reduction has been frequently possible with little or no loss of strength or overall performance [18].

The strength of aluminum alloys with a thin grain microstructure and grass dimensions is like those of forged counterparts. It is ideal for 3D printing with aluminum alloys because of its excellent fusion properties. Aluminum cast alloys are often used for the AM category PBF, whilst wrought aluminum alloys should be used in DED processes, sheet, and film for SL types of processes. Although most research and development of PBF alloys of aluminum is done by melting alloys that are well suited to the conditions of heating and cooling in electron beam processing, manufactured alloys such as 6061 and 7075 have long gardeners that allow PBF processing [2, 4, 112]. HRL labs recently solved this problem by incorporating zirconium hydride nanoparticles into powders 7075 and 6061. Nanoparticles act as nucleating sites for the desired alloy microstructure during PPF processing, preventing hot cracking and resulting in high-strength aluminum alloy AM components [51].

11.4 Metallurgical Characteristics of the AM Metallic Component

The microstructures of AM-made metals are distinct because of the AM process. A column with a high grain orientation dominates the grain structure. The creative process is broken down into phases, each of which focuses on a different topic. Axial grain and grid fluctuations can occur because of the material's subsequent heat and cooling cycles. In theory, the scan method can control the microstructure, and recent research has made significant progress in this area. Porosity refers to all processes that can be handled using DED, LM, or EBM to optimize less than 1% of process parameters.

11.4.1 Microstructural Properties on AM (PBF) Components

Several studies have been conducted to investigate the relationship between PBF microstructure and process parameters. Most scanned powder melts and thickens at higher processing temperatures, but PBF manufactured components keep some porosity. Figure 11.11 depicts the Ti-6Al-4 V microstructure following SLM processing [111]. Two parameters that influence the granular microstructure of PBF regions are temperature gradient and interface velocity of solidification. Column

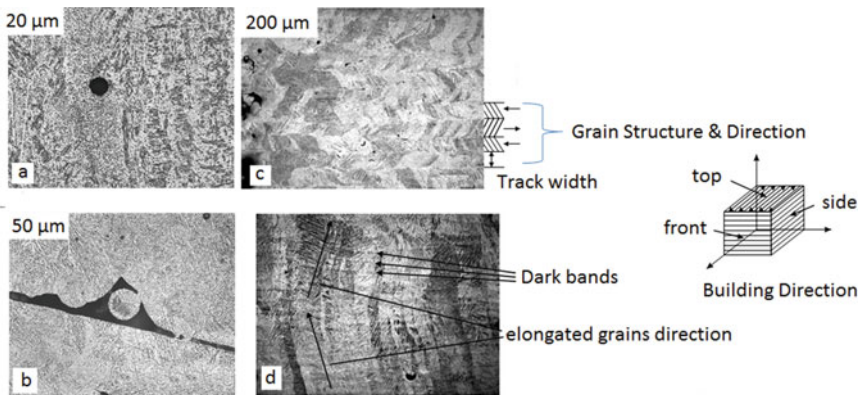


Fig. 11.11 SLM-built Ti-6Al-4 V microstructures; **(a)**-porosity caused by trapping gas), **(b)**-inadequate heating), **(c)**-top view) and **(d)**-side view) [72]

grains form when the interface speed is slow and there is a large temperature differential. In contrast, small temperature gradients and chief contact speeds result in equal grains. The grain conversion can be calculated using the Hunt dendrite growth model [40, 84]. Built their strategy around this approach, solid maps are created using a variety of nickel alloys for Inconel 718 and RS5 alloys. Sames et al. [74] have developed an EBM processing window. Their findings suggest that these two parameters can have a significant impact on the grain development of Arcam Inconel 718. The scan speed, laser, or E-beam feature may affect the temperature gradient and the speed of the interface. Several recent papers have addressed the use of process design to manage the microstructure. Later examined the processing window to determine which grains in the column were the best. Mechanical qualities of materials created by SLM or EPM are critical for their applications.

11.4.2 Microstructural Properties on AM (DED) Components

Ziętala et al. [114] we are the first to present a thorough examination of the microstructure of LENS manufactured regions. They were specifically used in their research to compare the tensile properties of the materials created. The rate of local solidification in the melt pool, the temperature differential at the solid–liquid interface, and the rate of refrigeration all influence the solidified microstructure. Changes in these values can cause one of three structural morphologies in Ti-6Al-4 V/DLD components. To create products with exceptional mechanical properties, the effect of process parameters on the microstructure must be efficiently optimized and managed. The Ti-5Al4V macrostructure is shown in the Fig. 11.12 comprises columns of prior-b grains stretched toward solidification (build) [11].

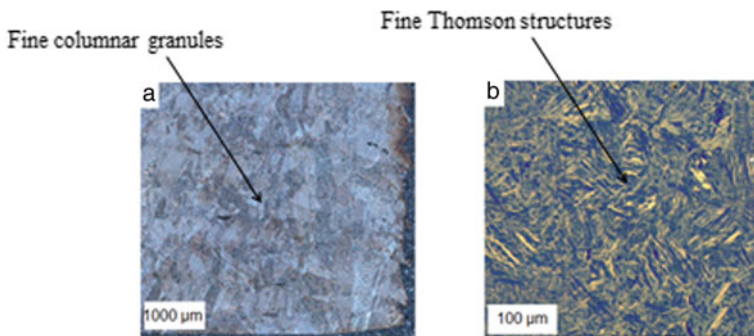


Fig. 11.12 Ti6Al-4 V generated by a LENS [11]. **a** Macrostructure. **b** Microstructure

A melt pool's border is a superstructure filled with a cellular structure and cellular spacing as small as 1 mm. Larger melting pools are found in large 100 mm 140 mm grains and a nearly mono crystalline LMD structure than in LBM [37]. According to Morrow [55] larger melt pools coarsen the microstructure and texture because of slower cooling rates.

Smaller melting pools form fine-graining microstructures that are weakly expanded by increased replacement. After AM manufacturing, austenitic steels (such as 304L and 316L) frequently exhibit entirely austenitic microstructures, particularly LBM. D-ferrite was found in as-machined 316L samples as shown in Fig. 11.13, and it converts to extent after a 2-h heat treatment at 1150 °C and cooling with air. Precipitation has been observed in stainless steel (17-4 PH), maraging steel (18-Ni300), and martensitic steel grade AISI420 (X46Cr13). Because of the changing thermos-conductivity of the gas, even minor changes in the cover gas in LBM can cause significant changes in phase composition because of the behavior's compatibility with freezing settings [10, 72].

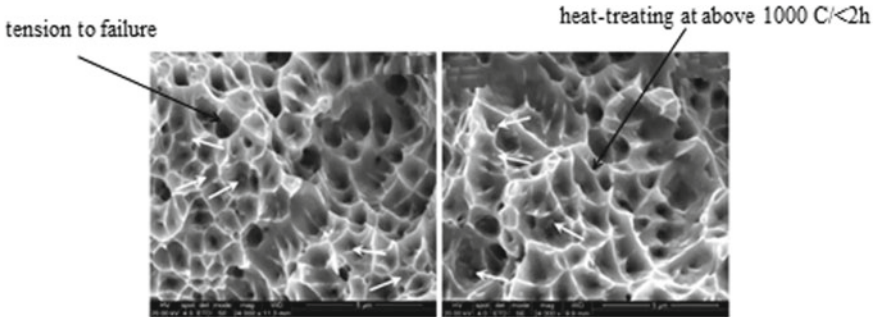


Fig. 11.13 316L stainless steel fracture surfaces [55]

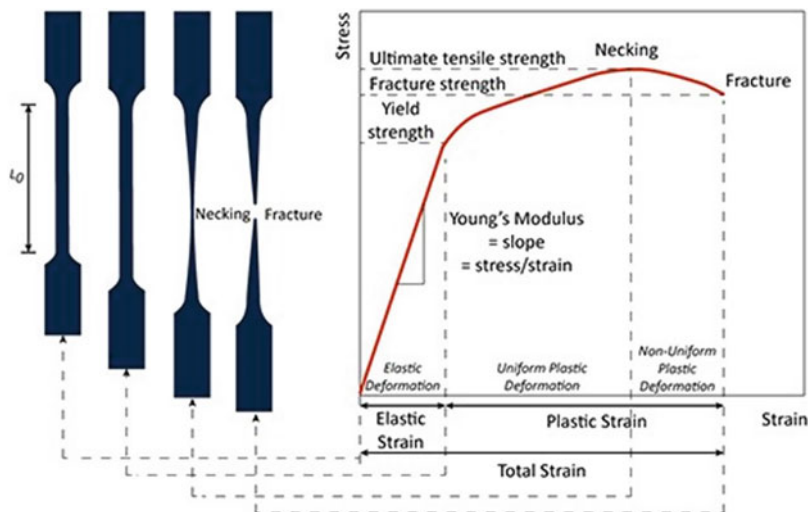


Fig. 11.14 ASTM standard testing methods for AM metallic materials

11.5 Standards of Mechanical Testing

As technology advances and enters the market, the need to comprehend technical jargon and system features grows. Metal additive manufacturing has progressed to the point of commercialization. The dental and aviation industries, for example, have moved to commercial manufacturing and now require material belongings standards, inspection methods, and other data. Added substance Manufacturing is changing ventures across the globe and a different scope of organizations are seeing the large number of noteworthy freedoms that the innovation offers. There are still numerous difficulties ahead to make this innovation a supported achievement [97].

The solid connections between the boundaries of assembly and the material properties require special consideration in contrast to the standard measuring measures for metal molding. It is also necessary to consider the impact of different machine frameworks and conditions, resulting in various characteristics as shown in Table 11.1. Most major organizations currently use AM to create end-use components in view of the lack of guidelines, make own interior arrangements of materials and operating rules. The improvement of measurement information and the development of standard specialized guidance are therefore of outrageous importance. The Plan Guidelines will help further recognize that AM does not make use of the maximum capacity of additive manufacturing in the vast majority of current CAD devices [54].

Two fundamental worldwide establishments, ISO (International Standardization Organization) and ASTM International, universally plan, create and distribute principles identifying with AM. The European Committee for Standardization (CEN) has likewise shaped normalization boards of trustees for AM on a territorial level. There are a few public exercises identified with normalization and rules. These incorporate

BSI (British Standards Institution) and France's AFNOR/UN (Union de Normalization de la Mécanique). In Germany, the public principles body DIN (Deutsches Institut für Normung) distributes guidelines identifying with AM in collaboration with VDMA (Verband deutscher Maschinen-und Anlagenbauer) and VDI (Verein Deutscher Ingenieure) [82]. ASTM International set up the F42 Committee on the

Table 11.1 Metal part mechanical testing [97]

Typical designation	Typical name	Remarks
ISO/ASTM 52,900:2015	Creates and defines phrasing for use in added substance manufacturing (AM) innovation	This applies the added substance-forming rule and along these lines constructs actual 3D calculations by the progressive option of material
ISO/ASTM 52,921:2013	Standard wording for added substance producing—Coordinate frameworks and test systems	The terms covered include definitions for machines/frameworks and their organizing frameworks, as well as the area and direction of components
ISO 17296–2:2015	Added substance producing—General standards—Part 2: Overview of cycle classes and feedstock	Shows how extraordinary cycle classes use various materials to frame the math of an item. This standard builds up the preparation for the Additive Manufacturing measure. It is anything but an outline of existing cycle classifications, which are not and cannot be finished as innovations arise
VDI 3405	Basics, definitions, and methods of additive manufacturing and fast manufacturing	Explains the monetary available additional substance manufacturing measures, Works with a superior evaluation of different additional substance generating measures, Establishes the quality limitations for different added ingredient production measures, Recommends the scope and content of testing and supply agreements
ISO 17296–4:2014	Added substance fabricating—General ideas—Part 4: Data preparing outline	Enables the determination of an appropriate arrangement for information trade It shows the most recent developments in the addition of material to 3d computations, It tracks existing document designs that are being employed as a part of contemporary occurrences, and Facilitates international standard adopters' understanding of key points for information exchange

(continued)

Table 11.1 (continued)

Typical designation	Typical name	Remarks
ISO/ASTM 52,915:2016	File Format Specification for Additive Manufacturing (AMF)	This record details Additive Manufacturing File Format (AMF), a configuration for commercial applications to satisfy the current and future needs of innovation in additional substances The need for preparation, display and forwarding for the AMF is defined in that archive. At this time, the perfect adherence to the extensible labelling language (XML)(1)2 in a structured electronic organization maintains standards for acceptable interoperability
ASTM F2924	Added substance Manufacturing Standard Specification PBF of Titanium-6 Aluminum-4 Vanadium	This standard relates to titanium-6aluminum-4vanadium (Ti-6Al-4 V) segments manufactured additively using a full-dissolve powder bed combination, such as electron bar softening and laser liquefying. It displays the segment configurations as well as the feedstock used to produce Class 1, 2, and 3 segments, as well as the component microstructure
ASTM F3001-14	Additive Manufacturing Specification ELI (Extra Low Interstitial) Titanium-6 Aluminum-4 Vanadium with PBF	The standard addresses material characterization, request data, manufacturing plan, feedstock, measurement, synthetic structure, microstructure, mechanical properties, warm handles, Hot Isostatic Pressing, measurements, and weight. These lay the groundwork for the usage of complete liquid PBF for additively manufactured titanium-6 aluminum-4vanadium with extra low rates (Ti-6Al-4 V ELI)
ASTM F3055-14a	Standard specification for PBF manufacturing additive nickel alloy (UNS N07718)	This decision applies to UNS N07718 (2.4668–NiCr19NbMo) segments produced additively utilizing a full-soften powder bed combination, such as electron bar dissolving and laser liquefying. These cycles produce products that are widely utilized in applications that need mechanical characteristics, such as machined forgings and fashioned objects

(continued)

Table 11.1 (continued)

Typical designation	Typical name	Remarks
ASTM F3056–14e1	Powder Bed Fusion Standard Specification Nickel alloy manufacturing additive (UNS N06625)	ASTM F3056–14e1 covers additively produced UNS N06625 (2, 4856–NiCr22Mo9Nb) components employing a fully dissolved mixture of powder beds such as electron pillar softening and laser liquefying
VDI 3405 Part 2.1:2015–07	Speedy creation strategies—LBM of metallic parts; Aluminum composite AlSi10Mg material information sheet	VDI 3405, Part 2-made use of the test techniques and tactics. Because this load of approaches and methods corresponds to recognized industry norms, the trade name values and customary assembly measures can be compared
ASTM F2971–13	Standard practice for the reporting of additive manufacturing data for test specimens	Test example representations and test reports standardization To help creators normalize information bases for AM materials Aid material deactivated by testing and evaluation Capturing AM examples for property limit execution to empower high-performance displays and other computational methods
ASTM F3049–14	Standard Guide for Characterizing the Properties of Metal Powders Used in Additive Processes	This document aims for the provision of current standards for metal powder for additive manufacturing for purchasers, suppliers and manufacturers. It is linked to several current standards for determining the cleanliness of new and used metal powders
ISO 17296–3:2014	Manufacturing additives—General concepts—Part 3: Principal features and appropriate testing procedures	ISO standards 17,296–3:2014 are required when testing components created using additive manufacturing techniques. It shows the components' essential quality characteristics, determines appropriate test techniques, and proposes test and supply arrangements in terms of degree and substance. The main guidelines are machine manufacturers, feedstock suppliers, machine customers, part suppliers, and customers

Additive Manufacturing Technology in 2009. Public workouts began in Germany and the United Kingdom around the same time. In 2011 and July 2013 ISO started its TC 261 exercises and the two associations, ASTM and ISO, established a Joint Improvement Plan for Guidelines. In 2018, the Standardizing Roadmap for AM was distributed under a joint effort between ANSI and America Makes, the Additive Manufacturing Standardization Collaborative [97].

Substance was added Manufacturing is a form of invention that both enables and animates growth. AM is rapidly evolving, with major investments being made all over the world. We are just looking into the many possible results of AM innovation. It is critical to acquire knowledge and benefit from teamwork in order to exploit maximal capability. It is advantageous to employ new item strategies. Item creators characterize the specific requirements of products based on demonstrated manufacturing measures. It is critical to have standards coordinated within the item improvement measure in order to meet requirements such as material characteristics and quality control difficulties. The application of principles is required for the evolution of innovation. Global collaboration is undeniably beneficial to everybody, while a conflict over values would be detrimental. The shared aim should be a collection of universally applicable ideas. A global handbook to AM principles might be a step in the right direction. Existing principles, for example, might be modified for AM to speed up this interaction. The combined endeavor of ASTM International and ISO to create and successfully communicate a first principle agreement is a prime example of collaboration. The ISO/ASTM Guidelines have the potential to shift the next phase to CEN standards.

11.6 Mechanical Properties of Metal AM Components

This section discusses the mechanical characteristics of metal AM components, such as ductility, strength, and anisotropy, with an emphasis on the relationship between construction and properties. The primary goal of AM process optimization is to produce materials with a high density, which is typically higher than 99.5% [3]. The volume energy used affects partial density. Because of the irregular vacuums caused by insufficient energy consumption, the material remains unmolten, resulting in a reduction in density. When there is a surplus of input energy, the dynamics and density of the melting pool increase [99]. Straightaway structure deformity in Ti-6Al-4 V was caused by scarce melting, according to Vilaro et al. [95] and Carlton et al. [21]. These events were typically longer (10–15 cm) than the vents discovered previously.

Qiu et al. [65] discovered that the residual porosity of LBM-produced Ti-6Al-4 V was primarily spherical. They claimed that most voids were not filled with gas because they were not reopened in subsequent heat treatments after the preceding HIP. Yasa et al. [106, 115] Proposed a collage strategy to reduce the residual porosity of 316 LBM from 0.77 to 0.036% by cooling a layer twice time before implementing the next metal powder layer. The 3D printing test determines how a 3D printed material will

withstand a load and provides information about its quality and mechanical conduct. ASTM-based testing assists manufacturers in ensuring that their processes meet industry standards. Mechanical tests can aid in the investigation and development of a new or altering material, manufacturing process, or high-quality product. The outcomes of various processes, such as DED-EB, DED-L, PBF-EB, and PBF-L, are addressed.

11.6.1 Hardness

Hardness testing is an effective method for demonstrating that metal AM components have limited mechanical strength. Table 11.2 summarizes the hardness properties of several AM metal composites. The current study found a link between Vickers micro hardness and AM titanium composite microstructural highlights, as well as a relationship with the Hall–Petch. Several studies were conducted to ascertain the effect on cross-sectional hardness estimates. A previous study discovered that metal component size AM had no effect on micro-hardness, most likely due to insufficient warm separation. A recent study evaluated the hardness attribute on a cross-sectional region. Because of microstructural coarsening, the micro-hardness decreased as the cross-sectional area increased. Because the portion with the thicker cross section has more conspicuous heated information and slower cooling rates, microstructural coarsening occurs. In addition, the study found that differences in 2D planar estimations had an impact on micro-hardness due to contrasting heat movement. Further research was carried out to assess the impact on durability of the manufactured height. However, the results of these studies were contradictory. For example, Hrabe and Quinn [39] have found that Vickers' structural micro-hardness values are contrasted with no critical contrasts of up to 25 mm from the substrate while Tan and colleagues have

Table 11.2 Hardness characteristics of different metal AM parts

Process	Material	Microhardness (Hv)	Distance measured from the substrate (mm)
EBM/Arcam [39, 88, 97]	Ti-6Al-4 V	347	2–25
	Pure Cu	57–88	NA
	AlCoCrFeNi	400–500	0–16
	SS316L	184 ± 11	2
	IN718	241 ± 12	2
	Al-8.5Fe-1.3 V-1.7Si	153 ± 2.5	NA
SLM [38, 42, 113]	Ti-6Al-4 V	360	NA
	SS316L	213–220	NA
	IN718	365	1.3–2.4
	Al-8.5Fe-1.3 V-1.7Si	135–175	NA

found that Vickers' structural micro-hardness values do not differ from any critical contrast between the substrates up to 25 mm.

Tan et al. [88] concluded that Vickers micro-hardness decreased as the tallness of EBM Ti-6Al-4 V increased. The heated conductivity increases the rate of cooling of the treated steel substrate. The microstructure of the base site was superior to that of the top site. Nonetheless, Wang et al. [97] investigated the pulley's micro-hardness. According to the study, the value of micro-hardness increased as assembly size increased. Many people claim that the variability in hardness estimates is caused by warm data from a specific stratum. Compared to a smaller transversal area, the greater transversal area would result in a warmer contribution and in a variety of final microstructures. Future improvements to change the cycle limits in the cross-sectional area could help to simplify this heterogeneity of hardness.

11.6.2 Tensile Properties of AM Developed Metal Components

In the manufactured state of the AM, the tensile strength of existing steel grades frequently meets the specific requirements for industrial applications. Grain refining increases yield and tensile strength significantly. In terms of ductility, lower porosity (0.1%) results in a malleable fault mode with lengthening values compared to the material used. High remaining porosity of 2.4%, on the other hand, results in flexible modes with significantly lower elasticity [21]. Table 11.3 compares Yield Strength-Y_S, Ultimate Elastic Resistance-U_{TS}, and Failure Elongation-E_L to the reference qualities of the materials produced for the selected grades of steel, aluminum, and titanium for the various AM technologies derived from literature [23]. Stability properties differ widely in LBM, which depends on the tensile test, which can be determined by selected parameters of processing and post-processing conditions under various loads. In the AM-microstructure/yield correlation, the tensile properties of Al alloys compare favorably to those of AM-constructed steels. AM techniques produce granular configurations that primarily or solely increase the strength of the manufactured state [28].

The actual coarsening of smooth grains during the hardening period of a manufactured additive AlSi10 Mg alloy, which counteracts the later impact and maintains a constant yield strength as the manufactured part (Table 11.3). Mg was lost during AM production for AA 2139 (Al-Cu, Mg), which reduced precipitation and thus output strength. When attempting to maintain a thin grain structure while producing an unnaturally aged precipitate, an LBM manufactured scan-based alloy produces the best results [2]. Because titanium is a great material for EBM, LMD, and LBM, the complicated interrelationships among various AM methods, specifications, and the resulting fatigue and tensile properties, particularly for Ti-6Al-4 V, are widely preferred for metals and alloys (2015).

Table 11.3 Tensile properties of different metallic materials are generated AM process

AMTechniques	Materials	Reference by	EL [%]	UTS [MPa]	YS [MPa]
LBM	Steel	Carlton et al. [21]	44 ± 7	705 ± 15	590 ± 17
LMD	Steel	Yadollahi et al. [102]	36 ± 4	640 ± 20	410 ± 5
LBM	304L Stainless	Elghany and Bourell [1]	25.9	393	182
LBM	18Ni-300 Maraging Steel	Yasa et al. [106]	1290 ± 114,	1214 ± 99	13.3 ± 1.9
LBM	AlSi ₁₂	Prashanth et al. [64]	3	380	260a
LBM	AlSi ₁₀ mg	Monteiro [53]	6.2 ± 0.4	328 ± 4	230 ± 5
LBM	AlMg ₁ sicu	Fulcher et al. [29]	E	42	E
LBM	AlMg _{4.4} Sc _{0.66} MnZr	Schmidtke et al. [75]	16	530	520
EBF	AA 2139 (AlCu, Mg)	Brice et al. [16]	E	430 ± 8	321 ± 26
EBM	Ti-6Al-4v	Yamanaka et al. [103]	28.5 ± 0.5	475 ± 15	377 ± 10
LBM	Ti-6Al-4v	Vilaro et al. [95]	8.2 ± 0.5	1140 ± 10	1040 ± 10
LBM	Cp Ti (Grade 2)	Ambrogio et al. [9]	20	345	280
LMD	Ti-6.5Al-3.5Mo-1.5 Zr-0.3Si	Zhai et al. [110]	7	1042	990
PDF	Inconel 625	Martinez et al. [50]	58	900	380
DED	Inconel 718	Blackwell [12]	38	1000	650
DED	Inconel 625	Wang et al. [96]	E	722 ± 17	42.27 ± 2.4

Table 11.3 shows that AM processes for Cp-Ti result in higher output strengths and ductility than sheet Ti processes (20%). When test conditions, such as LBM's extremely high melting temperature, produce a very thin martensitic (Alpha) microstructure, the greatest strength will be achieved. Grain refining improves ductility and yield. LMD has lower output strengths than LBM or EBM due to lower cooling rates (Table 11.3), and the resistance of tensile failure to the testing parameters varies significantly. Moisture levels have increased, but ductility has decreased [22]. Furthermore, it is related to the increased α-martensitic, remaining permeable,

and residual stresses in the flexible mode of as-made AM Ti-6Al 4 V. As shown in Table 11.3, computer imaging has been used successfully to detect material structural limitations, and additive mechanical flexible fracture software has been used to show the effect of these limitations on EBM Ti-6Al-4 V fatigue life.

Some specialized ASTM procedures for 3D-printed metal materials address the material properties expected for powder-based sintering implementations. Mechanical characteristics commonly reported include ultimate stress or maximum stress caused by stress, as well as elongation during breakage. The elastic modulus is calculated by dividing the stress by the strain. SLA materials are harder and more fragile than injection-molded counterparts are. They have such a different flexural and small elastic deformation before the dog's bone stress fractures as shown in Fig. 11.14 [133].

11.6.3 Compressive Test Properties of AM Developed Metal Components

The mechanical characteristics of metal AM components have also been evaluated using compressive testing. An investigation of the SLM-assembled tantalum amalgam found that the compressive yield strength was higher upward than evenly. The reason is that crystallographic surfaces are shifting. Despite its anisotropy stiffness, the mechanical properties of the SLM tantalum compound were found to be superior to those of an electron pillar heater or powder metallurgy. Basic design may be used to plan mechanical anisotropy in a segment [91]. During the investigation, anisotropic shifting level was observed in several cross-sectional schemes of EBM assemblies (Ti-6Al-4 V). The compressive force anisotropy was determined by the size of the cross-sectional structural unit. During compression tests in compression according to DIN 50,106, the specimens were continuously distorted until a predicted minimum height was reached [20].

The compressive elasticity module and the compressive output power R_{dp} have been calculated within the linear elasticity zone. The center of the exemplar was used to record deformation values in the specimen areas subject to uniaxial stress alone by means of a fine stretcher extensometer with a starting length of 1 cm. The compressive output strength is good at 75° and 90° (Fig. 11.15). Although porosity is a significant defect in SLM materials, it is recognized that it is only a vital factor in compressive loads. This is because, while the porosity is modest, the idea of heap shuns pores and produces flaws. Surprisingly, the pores expand, mix and distribute under folding stacking, leading to misleading [80]. When the results are checked, the influence of porosity on the direction of the stacking layer will most likely be determined. This would suggest that flaws have a wider impact when the direction of the layer corresponds to the stacking path and when the direction of the layer is animated along these lines than when the direction of the layer is reversed. The samples would have high compression yield strength at 75° and 90°. When compared

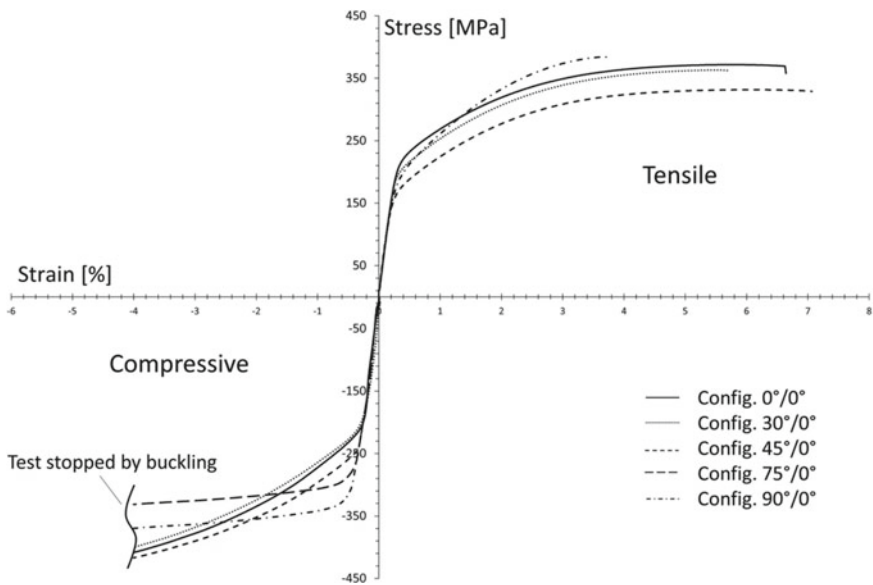
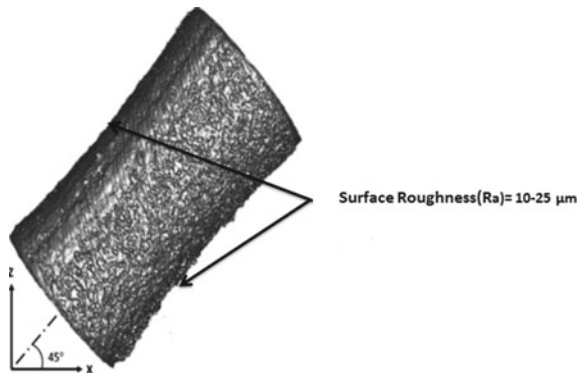


Fig. 11.15 Stress–strain curves compressive and tensile diagram [80]

Fig. 11.16 Demonstrating a larger surface roughness [101] (Down-Upward facing side)



to the results of the related study from [5], the results of the 90° cases indicate that the compressive yield strength is comparably inclined (Fig. 11.16).

11.6.4 Surface Roughness Properties of AM Developed Metal Components

A variety of inputs influences the surface characteristics of AM components, resulting in the development of various visible and quantifiable output variables that influence

performance. Input parameters include material presentation, component design, process sections, process parameters, and post-processing. Benefits range from partially fused powder granules (or beads) to improper melting because of construction, fusing, or detecting routes, such as balling Fig. 11.17a layer of fusion absence, or striation. The surface roughness of joint replacement bone interface implants, for example, may contribute to faster development, and thus periosteum—direct physical and functional contact between live tissue and the load-bearing implant surface—may be characterized as fastest and possibly most effective.

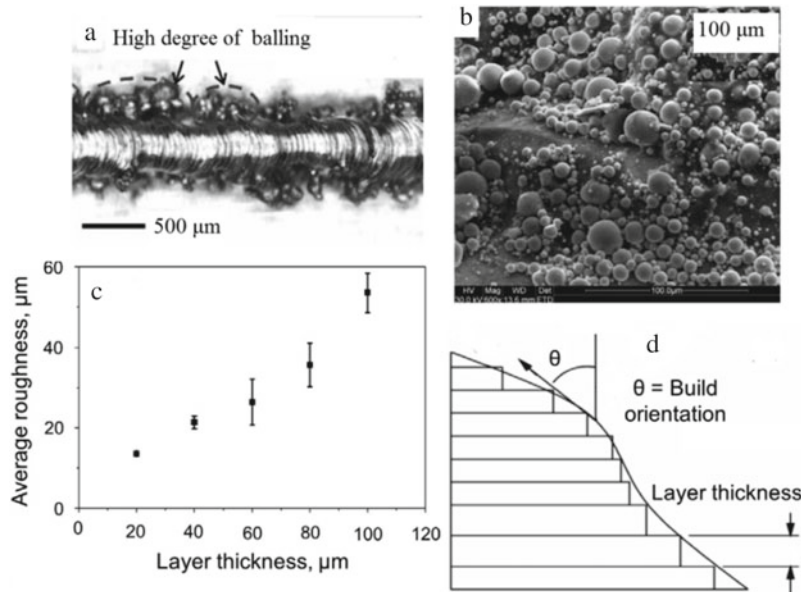


Fig. 11.17 **a** Balling effects [35] **b** solid granules on the construction surface [56] **c** surface roughness versus layer thickness [67] **d** surface roughness because of stairwell effects [66]

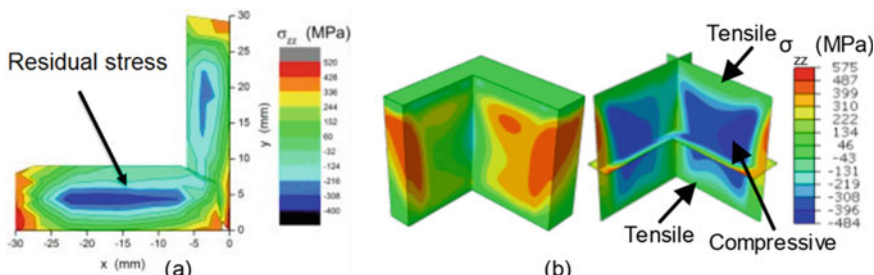


Fig. 11.18 Typical residual stress of an as-SLM item in the building direction **a** contours residual stress **b** anticipated residual stress

Surface roughness is one of the most detrimental effects on performing metal products and rotating fatigue. As a result, post-production activities are usually required to extend the life of AM components. This is difficult because many AM components, especially those with complicated geometry, want to be used as net-shaped as they were produced. As a result, after-surface treatment product loses one of AM's primary advantages: the ability to produce complex geometry that conventional manufacturing cannot [24]. Consequently, the fatigue of the components and their relationship to the surface coating must be fully known. The type of equipment used, powder size, process parameters, and orientation of the device can all affect the surface hardness of an AM surface. It is, thus, essential to fully understand fatigue. Because of the use of thicker hatches, DLD techniques typically produce the rough surfaces found in L-PBF techniques, due there is a lot of powder, pieces, and layers in this area. Increased hatching pitch, layer thickness, and/or powder size improve the surface hardness of AM components [105]. An X-ray CD image of a 45-degree Inconel 718 model created with the L-PBF method is shown here in Fig. 11.16. The excessive roughness on the face is caused by direct contact. Powder bedding is used throughout the manufacturing process, resulting in thermal decomposition pool heat/liquid fringe effects [101].

A mixture of many input parameters and processing situations determines surface hardness optimization and reduction. The type and procedure of the powder (10–60 μm powder), the powder circulation, and the material used for roller/blade spreading can all affect the hardness of the surface of the extremely low range of the PSD (Fig. 11.17c). The PBF-EB technique employs powder sizes ranging from 45 to 105 μm (Fig. 11.17b), which reduces the impact of electric charge, dissipation, powder flow ability, and diffusion disturbance on powder layer thickness (Fig. 11.17d). For example, transferring high PSDs to high surface hardness due to a process disruption results in an electrically charged PBF-EB surface that is slightly riche [75].

11.6.5 Fracture Toughness Properties of AM Developed Metal Components

The ability of a material to withstand fracture is described by its break strength. Based on various studies, Table 11.4 organizes the discovered crack strength benefits of specific metal AM components. Crack-life anisotropy was considered in both the SLM-assembled and EBM-assembled Ti-6Al-4 V. Because of break durability, anisotropy had an effect on how breaks spread.

Breaks occur across the columnar grains in evenly oriented examples, whereas breaks occur at the grain column boundaries in upwardly oriented examples [26]. The fracture force of EBM-built Ti-6Al-4 V is comparable to the specifications for Ti-6Al-4 V constructions or castings of 44–66 MPa $\text{m}^{1/2}$ and 88–110 MPa $\text{m}^{1/2}$, respectively. The reduced durability values reported in SLM-produced Ti-6Al-4 V are due to the

Table 11.4 Fracture toughness of different metallic materials are generated AM process

Process/Model	Material	Anisotropy in fracture toughness (%)	Fracture toughness (MPa \sqrt{m})	References
EBM/Arcam (A1)	Ti-6Al-4 V	7.3	110 ± 7.4	Edwards [26]
EBM/Arcam (A2)	Ti-6Al-4 V	18.8	67–80	Seifi [77]
SLM	Ti-6Al-4 V	17.9	28 ± 2	Cain [19]
LBM-MTT 250	Ti-6Al-4 V	3.1	66.9 ± 2.6	Edwards [27]
SLM	Al-12Si	18.8	46.7	Suryawanshi [87]

fine acicular alpha/beta martensitic microstructure, which is more brittle than EBM-assembled Ti-6Al-4 V / duplex microstructure. Anisotropic break strength can result from residual stresses on metal AM components [19]. The use of post-warm therapy treatments may minimize residual stresses such as HIP or stress reduction treatment. Following SLM-built Ti-6Al-4 V therapy with HIP and stress relief, fracture strength improved and anisotropy reduced, according to research utilizing SLM TI-6Al-4 V. In any case, a review on EBM-constructed Ti-6Al-4 V demonstrated a decrease in break strength after heat treatment procedures, which came from microstructure coarsening. Understandings of the as-built microstructures for the unique metal AM frameworks are critical in determining post-heat treatment approaches to provide superior fracture durability [19, 87].

11.6.6 Fatigue Strength in AM Metal

The fatigue strength of such metals is determined by the static mechanical properties of materials that are identical to the microstructure of various metals. However, the fatigue performance of AM-produced parts is poor because of inherent properties, such as surface ruggedness and material failures. AM process is used to conduct experiments for the study of monotonic tensile behavior of different metals and alloys. The wear-out characteristics of the additive Ti-6Al-4 V have been investigated (Table 11.5) because of its potential use in aviation and biomedical applications [7, 100]. Comparing the fatigue characteristics of PBF-EB and DMLS made from Ti-6Al-4 V, the lower the wear rate, the better the fatigue strength of both was found (DMLS reached 107 cycles at 550–600 MPa, EBM at 600 MPa as shown in Table 11.5). Surface modifications can help improve fatigue properties (e.g. polishing). Brandl et al. [14] the scatter of investigative data increases material failures, such as porosity and lack of adhesion on the layer, making tribological characteristics difficult to evaluate.

Using hot isostatic pressings to cure and density these defects results in higher wear-out and real data, similar to AM processes. Table 11.5 summarizes the fatigue

Table 11.5 Fatigue strength of different metallic materials are generated AM process

Am techniques	Materials	Referenced by	Surface treatment	Condition Kelvin /Celsius	σ_{Smax} at 107 [MPa]
EBM	Ti-6Al-4 V	Brandl et al. [14]	Refined	843 C/100 MPa/4 h-HIP	600
LMD	Ti-6Al-4 V	Brandl et al. [14]	Refined	ST-843 C/2 h	-700
LBM	Ti-6Al-4 V	Leuders et al. [47]	Not mentioned	920 C/100 MPa/2 h-HIP	620
LBM	AlSi ₁₂	Siddique et al. [81]	Refined	473.15 K in process b SR-240 C/6 h	80
LBM	AlSi ₁₀ Mg	Buchbinder et al. [17]	Refined	AF	45
LBM	AlMg _{4.4} Sc _{0.66} MnZ	Buchbinder et al. [17]	Refined	AA-325 C/4 h	300
LBM	316L	Riemer et al. [71]	Precision-machined	HIP-1150 C/100 MPa/4 h	317

ST Solution Treated, AF Manufacturing, SR Stress Relieved

strength got through the different surface and thermal treating conditions of AM-based metals such as aluminum alloys, Ti-6Al-4 V, and steels. The study shows that AM raw materials are comparable to standard products, such as static and fatigue strength, in terms of their physical fragmentation and mechanical properties, and that mechanical behavioral concepts can be used for the analysis of AM metals and alloys [33, 71].

11.6.7 Creep in AM Metals

Variability in the creeping properties of fatigue-related components in both AM and conventional components indicates failures as well as an improvement in the fine microstructure. Because of the complexities of creep tests, such as thermal processing ranges, stress and pressure, temperature measurement, and the scarcity of research, no consistent trends in the creepy conduct of additively manufactured metals can be identified. Creep-Fracture of IN 738LC, and added into high corrosion resistance precipitation-enforced created through PBF-L, has already been discovered to be anisotropic. The inhomogeneity of the minimal column grain was created dis part by its solid texture as an anisotropic elastic strap [70]. A detailed study on CCM composites (Co–28Cr–6Mo–0.23C–0.17 N) manufactured using Powder Bed Fusion Electron Beam (PBF-EB) process was conducted by Sun [85]. This CCM composite is made up of crystalline structure columnar morphology c-Fcc

and stabilized equiaxed morphology (e-hcp) phases in its as-built state. To prevent transformation during experiments, the substance was dramatically changed to e-hcp before cramping. Because the PBF-EB technique keeps the building chamber at a higher temperature (700 C), the granules near the center plate continue to grow longer than those near the top [86]. In that, E-grains were discovered to be larger in the as-produced lower part of the components than after heat treatment processing. The results show that the grain-boundary mechanism for flexibility creep promotes the formation and distribution of voids across the grain bounds. A two-step thermal process reflecting the temperature history in the PBF-EB method was proposed [47, 81], to increase grained area through buildings while ignoring grain failure zones.

11.6.8 Analysis of Residual Stress in AM Developed Metal Parts

Scanner methods, dwell time, and a variety of other factors all have an impact on the residual stress field of metal AM components. Previous heat transfer parameters have a significant impact. The residual surface stress of an SLM treated steel 316 L-shaped bar (off foot molecule) was studied using a digital picture contact mode and neutron differentiation, according to Ahmad et al. Compression and traction near surfaces, as well as residual stress near the area's centre, are depicted in Fig. 11.18a. The effects of the scanning method, laser energy scanning velocity, and residual stress orientation are all investigated thoroughly [7]. Lesyk et al. [46] investigated the effect of island size on residual stress and discovered a similar pattern. Even though the size of the island was shown to result in low residual stress of $2 \times 2 \text{ mm}^2$, significant fractures were discovered in the model created with this island size. As shown in (Fig. 18b), this pattern was captured by modeling and experimental research with an important residual stress forecast in the DED-treated Vaseline zone.

Evaluation of residual stress using SLM X-ray diffraction Xiao et al. [100] discovered that residual stress in the scanning trajectory is greatest at a higher tensile and constructed interface than in the perpendicular motion using small-scale models of treated steel and Ti6Al4V. Kruth et al. [44] devised a method for calculating the residual stress of the SLM segment based on bridge curvature. Other researchers developed a method for determining residual stress in SLM components quickly. The amount of residual stress in the bridge-formed component after it's removed from the foundation is determined by the curved tilt of the structure's two-base surfaces. Framework variables such as scan vector distance and scan scalar rotation grades were investigated for two consecutive layers, and it was discovered that controlling rest stress and displacement during the SLM technique necessitates a shorter scan vector length and a greater revolution inclination.

The residual stress of EBM processed elements is noticeably lower than that of SLM processed elements because the cooling fee is based on the resulting solidification capabilities of those methods, such as protoplasmic processes arm spacing. The

cooling rate in the EBM is significantly lower, and energy drainage from the EBM component takes longer, because of the Pulver surface and vacuum container being highly post-heated [45, 131]. Salem et al. [73] used nuclear diffraction to investigate the residual stress of Inconel 718 cubes treated with EBM and SLM in their as-built state. The researchers used (Electric Discharge Machining-EDM) to create stress-free samples to determine pressure-remote network spacing. Because SLM is further from homeostasis than EBM, every residual stress element generated by EBM reduces the order value of SLM.

The residual stress of SS 316L and Inconel 718 additives made with DEDs via nuclear crystallography and contour approach was investigated/ [60] the remaining stress within the sample centers was caused by uniaxial compaction. Longitudinal residual stress was detected at the edges and was found to be related to the construction method. Residual stress magnitudes in the cloth were greater than 50–60% of the nominal output electricity [49]. The effects of dwell time on residue stress and deformations in DED-processed Ti64 and Inconel 625 systems were investigated. The well-known Inconel 625 structure exhibits the inverse trend, resulting in significantly less residual stress during the deposition phase. Reducing the refresh time for Ti64 builds can result in significantly lower residual stress as the DED process progresses.

11.7 Conclusions

A detailed investigation of the status of metal additive manufacturing, with astonishing connections between process parameters, mechanical properties and metals has been carried out. According to the Hall-Patch regulation, “High sturdiness AM inclination creates fine-grain microstructures”. Unbalanced micro-sized structures, such as austenite, titanium, or titanium-based alloys with a martensite alpha phase, are exposed as a result of materials and manufacturing techniques. AM processes contain anisotropic microstructures with elongated grain due to anisotropic thermal conductivity, and the formation process in current structural layers is significant, resulting in the development of non-directional properties. Typically, reheating and treating solidified layers on the ground are part of the complicated AM’s temperature cycle. This could result in both desired and unintended consequences, such as a breakdown in ductile varieties, alloy component partitioning, and grain growth. Further ex-situ thermal processing can alter the microstructure and characteristics of the final component in different methods. In the process of fabricating the metal components, which affected its final structure and mechanical characteristics, it was subjected to preparation elements such as declaration rate, pillar power, climate and temperature. The mechanical properties of metal AM components (e.g., durability and rigidity) can frequently meet its basic needs through comparison of cast and model equivalents despite ani-ropy and variability.

Integrating a diverse set of input components and processing scenarios aids in the optimization and reduction of surface roughness. Welding terms such as loss

of sidewall fusion, undercutting, an anomalous pinnacle bead, and an increase in craters are used to describe surface roughness. The words for entering data in twine-driven systems are similar. This occurs on a much larger scale because of the large diameters of the molded pools, deposit bead widths, and later heights. In segment 5.4, the PBF-EB technique employs particle sizes ranging from 45 to 125 mm to reduce the effects of electrostatic transport. The EBM-manufactured Ti-6Al-4 V was shown to be dependent on the area in terms of durability of a crack due to microstructure and defect dispersion. Although the mechanical properties of metal AM components are anisotropic and heterogeneous, they are assumed to have the same or superior mechanical qualities as casted components.

The purpose of Sect. 5.7 is to summarize residual strain in AM metal. An excessive increase and rapid cooling exacerbate the residual strain. Pre-heating, approach training, remark strategic planning, and laser annealing are all individual methods for reducing long-term pressure. The presence of a substructure has a significant impact on the magnitude of residual stresses. According to the findings, the metallic AM processing and heating treatments are precise stress-discount strategies. Many statistics on fatigue and fracture toughness properties, as well as tensile and compressive properties, were calculated. According to the literature, various categories of steel, aluminum composites, and titanium materials designed and produced by LMD, LBM, and EBM have typical properties equivalent to cast or wrought processes. Most existing applications and innovation demonstration models are limited to non-existent or insignificant components in the face of variable loads. Recent studies on the efficacy of fatigue are about to change this. As a result, a sequential approach to AM can be used for a wide range of material process combinations.

11.8 Future Trends

AM can be used to create complex components such as jewels, dental implants, and electrical wires out of valuable metals such as gold, silver, palladium, and platinum. AM has distinct advantages for producing components of high liquefying conditioned inert composite materials, which are in high demand when manufactured using traditional methods. Powder-based AM methods have only recently become available. It is also used to improve the texture and properties of products by combining them in various ways. The research focused on the development of high-tech materials such as tantalum, molybdenum, chromium, tungsten, rhenium, niobium, and vanadium, which had unrivalled potential for future generation AM.

References

1. Abd-Elghany, K., Bourell, D.L.: Property evaluation of 304L stainless steel fabricated by selective laser melting. *Rapid Prototyp. J.* **18**, 420–428 (2012). <https://doi.org/10.1108/135>

52541211250418

2. Aboulkhair, N.: Additive manufacture of an aluminium alloy: processing, microstructure, and mechanical properties, (2015)
3. Aboulkhair, N.T., Maskery, I., Tuck, C., Ashcroft, I., Everitt, N.M.: The microstructure and mechanical properties of selectively laser melted AlSi₁₀Mg: the effect of a conventional T6-like heat treatment. *Mater. Sci. Eng. A* **667**, 139–146 (2016). <https://doi.org/10.1016/j.msea.2016.04.092>
4. Aboulkhair, N.T., Simonelli, M., Parry, L., Ashcroft, I., Tuck, C., Hague, R.: 3D printing of aluminium alloys: additive manufacturing of aluminium alloys using selective laser melting. *Prog. Mater. Sci.* **106**, 100578 (2019). <https://doi.org/10.1016/j.pmatsci.2019.100578>
5. Aboulkhair, N.T., Tuck, C., Ashcroft, I., Maskery, I., Everitt, N.M.: On the precipitation hardening of selective laser melted AlSi₁₀Mg. *Metall Mater Trans A* **46**, 3337–3341 (2015). <https://doi.org/10.1007/s11661-015-2980-7>
6. Ahangar, P., Cooke, M.E., Weber, M.H., Rosenzweig, D.H.: Current biomedical applications of 3D printing and additive manufacturing. *Appl. Sci.* **9**, 1713 (2019). <https://doi.org/10.3390/app9081713>
7. Ahmad, B., van der Veen, S.O., Fitzpatrick, M.E., Guo, H.: Residual stress evaluation in selective-laser-melting additively manufactured titanium (Ti-6Al-4V) and inconel 718 using the contour method and numerical simulation. *Addit. Manuf.* **22**, 571–582 (2018). <https://doi.org/10.1016/j.addma.2018.06.002>
8. Ahn, D.-G.: Direct metal additive manufacturing processes and their sustainable applications for green technology: a review. *Int. J. Precis. Eng. Manuf. Green Tech.* **3**, 381–395 (2016). <https://doi.org/10.1007/s40684-016-0048-9>
9. Ambrogio, G., Gagliardi, F., Bruschi, S., Filice, L.: On the high-speed single point incremental forming of titanium alloys. *CIRP Ann.* **62**, 243–246 (2013). <https://doi.org/10.1016/j.cirp.2013.03.053>
10. Bai, Y., Yang, Y., Wang, D., Zhang, M.: Influence mechanism of parameters process and mechanical properties evolution mechanism of maraging steel 300 by selective laser melting. *Mater. Sci. Eng. A* **703**, 116–123 (2017). <https://doi.org/10.1016/j.msea.2017.06.033>
11. Bian, L., Thompson, S.M., Shamsaei, N.: Mechanical properties and microstructural features of direct laser-deposited Ti-6Al-4V. *JOM* **67**, 629–638 (2015). <https://doi.org/10.1007/s11837-015-1308-9>
12. Blackwell, P.L.: The mechanical and microstructural characteristics of laser-deposited IN718. *J. Mater. Process. Technol.* **170**, 240–246 (2005). <https://doi.org/10.1016/j.jmatprotec.2005.05.005>
13. Bobbio, L., Qin, S., Dunbar, A., Michaleris, P., Beese, A.: Characterization of the strength of support structures used in powder bed fusion additive manufacturing of Ti-6Al-4V. *Addit. Manuf.* **14**, (2017). <https://doi.org/10.1016/j.addma.2017.01.002>
14. Brandl, E., Palm, F., Michailov, V., Viehweger, B., Leyens, C.: Mechanical properties of additive manufactured titanium (Ti-6Al-4V) blocks deposited by a solid-state laser and wire. *Mater. Des.* **32**, 4665–4675 (2011). <https://doi.org/10.1016/j.matdes.2011.06.062>
15. Bresser, D., Hosoi, K., Howell, D., Li, H., Zeisel, H., Amine, K., Passerini, S.: Perspectives of automotive battery R&D in China, Germany, Japan, and the USA. *J. Power Sources* **382**, 176–178 (2018). <https://doi.org/10.1016/j.jpowsour.2018.02.039>
16. Brice, C., Shenoy, R., Kral, M., Buchanan, K.: Precipitation behavior of aluminum alloy 2139 fabricated using additive manufacturing. *Mater. Sci. Eng. A* **648**, 9–14 (2015). <https://doi.org/10.1016/j.msea.2015.08.088>
17. Buchbinder, D., Meiners, W., Pirch, N., Wissenbach, K., Schrage, J.: Investigation on reducing distortion by preheating during manufacture of aluminum components using selective laser melting. *J. Laser Appl.* **26**, 012004 (2014). <https://doi.org/10.2351/1.4828755>
18. Caba, S.: Aluminum alloy for additive manufacturing in automotive production. *ATZ Worldw.* **122**, 58–61 (2020). <https://doi.org/10.1007/s38311-020-0285-y>
19. Cain, V., Thijs, L., Van Humbeeck, J., Van Hooreweder, B., Knutsen, R.: Crack propagation and fracture toughness of Ti₆Al₄V alloy produced by selective laser melting. *Addit. Manuf.* **5**, 68–76 (2015). <https://doi.org/10.1016/j.addma.2014.12.006>

20. Cansizoglu, O., Harrysson, O., Cormier, D., West, H., Mahale, T.: Properties of Ti-6Al-4V non-stochastic lattice structures fabricated via electron beam melting. *Mater. Sci. Eng. A* **492**, 468–474 (2008). <https://doi.org/10.1016/j.msea.2008.04.002>
21. Carlton, H.D., Haboub, A., Gallegos, G.F., Parkinson, D.Y., MacDowell, A.A.: Damage evolution and failure mechanisms in additively manufactured stainless steel. *Mater. Sci. Eng., A* **651**, 406–414 (2016). <https://doi.org/10.1016/j.msea.2015.10.073>
22. Chan, K.S., Koike, M., Mason, R.L., Okabe, T.: Fatigue life of titanium alloys fabricated by additive layer manufacturing techniques for dental implants. *Metall Mater Trans A* **44**, 1010–1022 (2013). <https://doi.org/10.1007/s11661-012-1470-4>
23. DebRoy, T., Wei, H.L., Zuback, J.S., Mukherjee, T., Elmer, J.W., Milewski, J.O., Beese, A.M., Wilson-Heid, A., De, A., Zhang, W.: Additive manufacturing of metallic components—process, structure and properties. *Prog. Mater Sci.* **92**, 112–224 (2018). <https://doi.org/10.1016/j.pmatsci.2017.10.001>
24. Doornewaard, R., Christiaens, V., Bruyn, H.D., Jacobsson, M., Cosyn, J., Vervaeke, S., Jacquet, W.: Long-Term effect of surface roughness and patients' factors on crestal bone loss at dental implants. A systematic review and meta-analysis. *Clin. Implant Dent. Relat Res.* **19**, 372–399 (2017). <https://doi.org/10.1111/cid.12457>
25. Dutta, B., Froes, F.H.: (Sam): The additive manufacturing (AM) of titanium alloys. *Met. Powder Rep.* **72**, 96–106 (2017). <https://doi.org/10.1016/j.mprp.2016.12.062>
26. Edwards, P., O'Conner, A., Ramulu, M.: Electron beam additive manufacturing of titanium components: properties and performance. *J. Manuf. Sci. Eng.* **135**, (2013). <https://doi.org/10.1115/1.4025773>
27. Edwards, P., Ramulu, M.: Effect of build direction on the fracture toughness and fatigue crack growth in selective laser melted Ti-6Al-4 V. *Fatigue Fract. Eng. Mater. Struct.* **38**, 1228–1236 (2015). <https://doi.org/10.1111/ffe.12303>
28. Frazier, W.E.: Metal additive manufacturing: a review. *J. Mater Eng Perform.* **23**, 1917–1928 (2014). <https://doi.org/10.1007/s11665-014-0958-z>
29. Fulcher, B.A., Leigh, D.K., Watt, T.J.: Comparison of AlSi₁₀Mg and Al 6061 processed through DMLS. **16**
30. Galati, M.: Chapter 8—Electron beam melting process: a general overview. In: Pou, J., Riveiro, A., and Davim, J.P. (eds.) *Additive Manufacturing*, pp. 277–301. Elsevier (2021)
31. Gorsse, S., Hutchinson, C., Gouné, M., Banerjee, R.: Additive manufacturing of metals: a brief review of the characteristic microstructures and properties of steels, Ti-6Al-4V and high-entropy alloys. *Sci. Technol. Adv. Mater.* **18**, 584–610 (2017). <https://doi.org/10.1080/14686996.2017.1361305>
32. Graf, B., Schuch, M., Petrat, T., Gumenuk, A., Rethmeier, M.: Combined laser additive manufacturing with powderbed and powder nozzle for turbine parts. In: Presented at the Proceedings of 6th International Conference and Additive Technologies (2016)
33. Greitemeier, D., Palm, F., Syassen, F., Melz, T.: Fatigue performance of additive manufactured TiAl₆V₄ using electron and laser beam melting. *Int. J. Fatigue* **94**, 211–217 (2017). <https://doi.org/10.1016/j.ijfatigue.2016.05.001>
34. Gu, D.: Materials creation adds new dimensions to 3D printing. *Sci. Bull.* **61**, 1718–1722 (2016). <https://doi.org/10.1007/s11434-016-1191-y>
35. Gu, D., Shen, Y.: Balling phenomena in direct laser sintering of stainless steel powder: metallurgical mechanisms and control methods. *Mater. Des.* **30**, 2903–2910 (2009). <https://doi.org/10.1016/j.matdes.2009.01.013>
36. Haghdadi, N., Laleh, M., Moyle, M., Primig, S.: Additive manufacturing of steels: a review of achievements and challenges. *J Mater Sci.* **56**, 64–107 (2021). <https://doi.org/10.1007/s10853-020-05109-0>
37. Herzog, D., Seyda, V., Wycisk, E., Emmelmann, C.: Additive manufacturing of metals. *Acta Mater.* **117**, 371–392 (2016). <https://doi.org/10.1016/j.actamat.2016.07.019>
38. Hinojos, A., Mireles, J., Reichardt, A., Frigola, P., Hosemann, P., Murr, L.E., Wicker, R.B.: Joining of inconel 718 and 316 stainless steel using electron beam melting additive manufacturing technology. *Mater. Des.* **94**, 17–27 (2016). <https://doi.org/10.1016/j.matdes.2016.01.041>

39. Hrabe, N., Quinn, T.: Effects of processing on microstructure and mechanical properties of a titanium alloy (Ti–6Al–4V) fabricated using electron beam melting (EBM), Part 2: Energy input, orientation, and location. *Mater. Sci. Eng., A* **573**, 271–277 (2013). <https://doi.org/10.1016/j.msea.2013.02.065>
40. Hunt, J.D.: Steady state columnar and equiaxed growth of dendrites and eutectic. *Mater. Sci. Eng.* **65**, 75–83 (1984). [https://doi.org/10.1016/0025-5416\(84\)90201-5](https://doi.org/10.1016/0025-5416(84)90201-5)
41. Kannan, G.B., Rajendran, D.K.: A review on status of research in metal additive manufacturing. *Adv. 3D Print. Addit. Manuf. Technol.*, 95–100 (2017). https://doi.org/10.1007/978-981-10-0812-2_8
42. Kasperovich, G., Hausmann, J.: Improvement of fatigue resistance and ductility of TiAl₆V₄ processed by selective laser melting. *J. Mater. Process. Technol.* **220**, 202–214 (2015). <https://doi.org/10.1016/j.jmatprotec.2015.01.025>
43. Ko, G., Kim, W., Kwon, K., Lee, T.-K.: The corrosion of stainless steel made by additive manufacturing: a review. *Metals.* **11**, 516 (2021). <https://doi.org/10.3390/met11030516>
44. Kruth, J., Mercelis, P., Van Vaerenbergh, J., Froyen, L., Rombouts, M.: Binding mechanisms in selective laser sintering and selective laser melting. *Rapid Prototyp. J.* **11**, 26–36 (2005). <https://doi.org/10.1108/13552540510573365>
45. Kundakcioğlu, E., Lazoglu, I., Poyraz, Ö., Yasa, E., Cizicioğlu, N.: Thermal and molten pool model in selective laser melting process of Inconel 625. *Int J Adv Manuf Technol.* **95**, 3977–3984 (2018). <https://doi.org/10.1007/s00170-017-1489-1>
46. Lesyk, D.A., Martinez, S., Mordyuk, B.N., Dzhemelinskyi, V.V., Lamikiz, A., Prokopenko, G.I.: Post-processing of the Inconel 718 alloy parts fabricated by selective laser melting: effects of mechanical surface treatments on surface topography, porosity, hardness and residual stress. *Surf. Coat. Technol.* **381**, 125136 (2020). <https://doi.org/10.1016/j.surfcoat.2019.125136>
47. Leuders, S., Thöne, M., Riemer, A., Niendorf, T., Tröster, T., Richard, H.A., Maier, H.J.: On the mechanical behaviour of titanium alloy TiAl₆V₄ manufactured by selective laser melting: fatigue resistance and crack growth performance. *Int. J. Fatigue* **48**, 300–307 (2013). <https://doi.org/10.1016/j.ijfatigue.2012.11.011>
48. Lewandowski, J.J., Seifi, M.: Metal additive manufacturing: a review of mechanical properties. *Annu. Rev. Mater. Res.* **46**, 151–186 (2016). <https://doi.org/10.1146/annurev-matsci-070115-032024>
49. Li, C., Liu, Z.Y., Fang, X.Y., Guo, Y.B.: Residual stress in metal additive manufacturing. *Procedia CIRP* **71**, 348–353 (2018). <https://doi.org/10.1016/j.procir.2018.05.039>
50. Martinez, E., Murr, L.E., Amato, K.N., Hernandez, J., Shindo, P.W., Gaytan, S.M., Ramirez, D.A., Medina, F., Wicker, R.B.: 3D microstructural architectures for metal and alloy components fabricated by 3D printing/additive manufacturing technologies. In: De Graef, M., Poulsen, H.F., Lewis, A., Simmons, J., and Spanos, G. (eds.) *Proceedings of the 1st International Conference on 3D Materials Science*, pp. 73–78. Springer International Publishing, Cham (2016)
51. Mehta, A., Zhou, L., Huynh, T., Park, S., Hyer, H., Song, S., Bai, Y., Imholte, D.D., Woolstenhulme, N.E., Wachs, D.M., Sohn, Y.: Additive manufacturing and mechanical properties of the dense and crack free Zr-modified aluminum alloy 6061 fabricated by the laser-powder bed fusion. *Addit. Manuf.* **41**, 101966 (2021). <https://doi.org/10.1016/j.addma.2021.101966>
52. Mirzababaei, S., Pasebani, S.: A review on binder jet additive manufacturing of 316L stainless steel. *J. Manuf. Mater. Process.* **3**, 82 (2019). <https://doi.org/10.3390/jmmp3030082>
53. Monteiro, W.A.: Light Metal Alloys Applications. BoD—Books on Demand (2014)
54. Monzón, M.D., Ortega, Z., Martínez, A., Ortega, F.: Standardization in additive manufacturing: activities carried out by international organizations and projects. *Int J Adv Manuf Technol.* **76**, 1111–1121 (2015). <https://doi.org/10.1007/s00170-014-6334-1>
55. Morrow, B.M., Lienert, T.J., Knapp, C.M., Sutton, J.O., Brand, M.J., Pacheco, R.M., Livescu, V., Carpenter, J.S., Gray, G.T.: Impact of defects in powder feedstock materials on microstructure of 304L and 316L stainless steel produced by additive manufacturing. *Metall Mat Trans A* **49**, 3637–3650 (2018). <https://doi.org/10.1007/s11661-018-4661-9>

56. Mumtaz, K., Hopkinson, N.: Top surface and side roughness of Inconel 625 parts processed using selective laser melting. *Rapid Prototyp. J.* **15**, 96–103 (2009). <https://doi.org/10.1108/13552540910943397>
57. Murr, L.E.: Metallurgy of additive manufacturing: examples from electron beam melting. *Addit. Manuf.* **5**, 40–53 (2015). <https://doi.org/10.1016/j.addma.2014.12.002>
58. Ngo, T.D., Kashani, A., Imbalzano, G., Nguyen, K.T.Q., Hui, D.: Additive manufacturing (3D printing): a review of materials, methods, applications and challenges. *Compos. B Eng.* **143**, 172–196 (2018). <https://doi.org/10.1016/j.compositesb.2018.02.012>
59. Patterson, A.E., Messimer, S.L., Farrington, P.A.: Overhanging features and the SLM/DMLS residual stresses problem: review and future research need. *Technologies*. **5**, 15 (2017). <https://doi.org/10.3390/technologies5020015>
60. Phan, T.Q., Strantza, M., Hill, M.R., Gnaupel-Herold, T.H., Heigel, J., D'Elia, C.R., DeWald, A.T., Clausen, B., Pagan, D.C., Peter Ko, J.Y., Brown, D.W., Levine, L.E.: Elastic residual strain and stress measurements and corresponding part deflections of 3D additive manufacturing builds of IN625 AM-bench artifacts using neutron diffraction, synchrotron X-Ray diffraction, and contour method. *Integr Mater Manuf Innov.* **8**, 318–334 (2019). <https://doi.org/10.1007/s40192-019-00149-0>
61. Pollack, S., Venkatesh, C., Neff, M., Healy, A.V., Hu, G., Fuenmayor, E.A., Lyons, J.G., Major, I., Devine, D.M.: Polymer-Based additive manufacturing: historical developments, process types and material considerations. In: Devine, D.M. (ed.) *Polymer-Based Additive Manufacturing: Biomedical Applications*, pp. 1–22. Springer International Publishing, Cham (2019)
62. Popov, V.V., Fleisher, A.: Hybrid additive manufacturing of steels and alloys. *Manuf. Rev.* **7**, 6 (2020). <https://doi.org/10.1051/mfreview/2020005>
63. Prakash, K.S., Nancharaih, T., Rao, V.V.S.: Additive manufacturing techniques in manufacturing—an overview. *Materials Today: Proceedings*. **5**, 3873–3882 (2018). <https://doi.org/10.1016/j.matpr.2017.11.642>
64. Prashanth, K.G., Scudino, S., Klauss, H.J., Surreddi, K.B., Löber, L., Wang, Z., Chaubey, A.K., Kühn, U., Eckert, J.: Microstructure and mechanical properties of Al–12Si produced by selective laser melting: effect of heat treatment. *Mater. Sci. Eng. A* **590**, 153–160 (2014). <https://doi.org/10.1016/j.msea.2013.10.023>
65. Qiu, C., Adkins, N.J.E., Attallah, M.M.: Microstructure and tensile properties of selectively laser-melted and of HIPed laser-melted Ti-6Al-4V. *Mater. Sci. Eng. A* **578**, 230–239 (2013). <https://doi.org/10.1016/j.msea.2013.04.099>
66. Qiu, C., Panwisawas, C., Ward, M., Basoalto, H.C., Brooks, J.W., Attallah, M.M.: On the role of melt flow into the surface structure and porosity development during selective laser melting. *Acta Mater.* **96**, 72–79 (2015). <https://doi.org/10.1016/j.actamat.2015.06.004>
67. Rahmati, S., Vahabli, E.: Evaluation of analytical modeling for improvement of surface roughness of FDM test part using measurement results. *Int J Adv Manuf Technol.* **79**, 823–829 (2015). <https://doi.org/10.1007/s00170-015-6879-7>
68. Reeves, P., Tuck, C., Hague, R.: Additive manufacturing for mass customization. In: Fogliatto, F.S., da Silveira, G.J.C. (eds.) *Mass Customization: Engineering and Managing Global Operations*, pp. 275–289. Springer, London (2011)
69. Revilla-León, M., Ceballos, L., Martínez-Klemm, I., Özcan, M.: Discrepancy of complete-arch titanium frameworks manufactured using selective laser melting and electron beam melting additive manufacturing technologies. *J. Prosthet. Dent.* **120**, 942–947 (2018). <https://doi.org/10.1016/j.prosdent.2018.02.010>
70. Rickenbacher, L., Etter, T., Hövel, S., Wegener, K.: High temperature material properties of IN738LC processed by selective laser melting (SLM) technology. *Rapid Prototyp. J.* **19**, 282–290 (2013). <https://doi.org/10.1108/13552541311323281>
71. Riemer, A., Leuders, S., Thöne, M., Richard, H.A., Tröster, T., Niendorf, T.: On the fatigue crack growth behavior in 316L stainless steel manufactured by selective laser melting. *Eng. Fract. Mech.* **120**, 15–25 (2014). <https://doi.org/10.1016/j.engfracmech.2014.03.008>

72. Saeidi, K., Zapata, D.L., Lofaj, F., Kvetkova, L., Olsen, J., Shen, Z., Akhtar, F.: Ultra-high strength martensitic 420 stainless steel with high ductility. *Addit. Manuf.* **29**, 100803 (2019). <https://doi.org/10.1016/j.addma.2019.100803>
73. Salem, M., Le Roux, S., Hor, A., Dour, G.: A new insight on the analysis of residual stresses related distortions in selective laser melting of Ti-6Al-4V using the improved bridge curvature method. *Addit. Manuf.* **36**, 101586 (2020). <https://doi.org/10.1016/j.addma.2020.101586>
74. Sames, W.J., Unocic, K.A., Dehoff, R.R., Lolla, T., Babu, S.S.: Thermal effects on microstructural heterogeneity of Inconel 718 materials fabricated by electron beam melting. *J. Mater. Res.* **29**, 1920–1930 (2014). <https://doi.org/10.1557/jmr.2014.140>
75. Schmidtko, K., Palm, F., Hawkins, A., Emmelmann, C.: Process and Mechanical Properties: applicability of a scandium modified Al-alloy for laser additive manufacturing. *Phys. Procedia* **12**, 369–374 (2011). <https://doi.org/10.1016/j.phpro.2011.03.047>
76. Scott, J., Gupta, N., Weber, C., Newsome, S., Wohlers, T., Associates, W., Caffrey, T., Associates, W.: Additive Manufacturing: Status and Opportunities. 36
77. Seifi, M., Dahar, M., Aman, R., Harrysson, O., Beuth, J., Lewandowski, J.J.: Evaluation of orientation dependence of fracture toughness and fatigue crack propagation behavior of as-deposited ARCAM EBM Ti-6Al-4V. *JOM*. **67**, 597–607 (2015). <https://doi.org/10.1007/s11837-015-1298-7>
78. Seifi, M., Salem, A., Beuth, J., Harrysson, O., Lewandowski, J.J.: Overview of materials qualification needs for metal additive manufacturing. *JOM*. **68**, 747–764 (2016). <https://doi.org/10.1007/s11837-015-1810-0>
79. Selcuk, C.: Laser metal deposition for powder metallurgy parts. *Powder Metall.* **54**, 94–99 (2011). <https://doi.org/10.1179/174329011X12977874589924>
80. Sert, E., Hitzler, L., Hafenstein, S., Merkel, M., Werner, E., Öchsner, A.: Tensile and compressive behaviour of additively manufactured AlSi₁₀Mg samples. *Prog. Addit. Manuf.* **5**, 305–313 (2020). <https://doi.org/10.1007/s40964-020-00131-9>
81. Siddique, S., Imran, M., Wycisk, E., Emmelmann, C., Walther, F.: Influence of process-induced microstructure and imperfections on mechanical properties of AlSi₁₂ processed by selective laser melting. *J. Mater. Process. Technol.* **221**, 205–213 (2015). <https://doi.org/10.1016/j.jmatprotec.2015.02.023>
82. Slotwinski, J., Moylan, S.: Applicability of existing materials testing standards for additive manufacturing materials. 17, (2014)
83. Spears, T.G., Gold, S.A.: In-process sensing in selective laser melting (SLM) additive manufacturing. *Integr. Mater. Manuf. Innov.* **5**, 16–40 (2016). <https://doi.org/10.1186/s40192-016-0045-4>
84. Suave, L.M., Bertheau, D., Cormier, J., Villechaise, P., Soula, A., Hervier, Z., Laigo, J.: Impact of microstructural evolutions during thermal aging of Alloy 625 on its monotonic mechanical properties. *MATEC Web of Conferences*. **14**, 21001 (2014). <https://doi.org/10.1051/matecconf/20141421001>
85. Sun, S.-H., Koizumi, Y., Kurosu, S., Li, Y.-P., Chiba, A.: Phase and grain size inhomogeneity and their influences on creep behavior of Co–Cr–Mo alloy additive manufactured by electron beam melting. *Acta Mater.* **86**, 305–318 (2015). <https://doi.org/10.1016/j.actamat.2014.11.012>
86. Sun, S.-H., Koizumi, Y., Kurosu, S., Li, Y.-P., Matsumoto, H., Chiba, A.: Build direction dependence of microstructure and high-temperature tensile property of Co–Cr–Mo alloy fabricated by electron beam melting. *Acta Mater.* **64**, 154–168 (2014). <https://doi.org/10.1016/j.actamat.2013.10.017>
87. Suryawanshi, J., Prashanth, K.G., Scudino, S., Eckert, J., Prakash, O., Ramamurti, U.: Simultaneous enhancements of strength and toughness in an Al-12Si alloy synthesized using selective laser melting. *Acta Mater.* **115**, 285–294 (2016). <https://doi.org/10.1016/j.actamat.2016.06.009>
88. Tan, X., Kok, Y., Tan, Y.J., Descoins, M., Mangelinck, D., Tor, S.B., Leong, K.F., Chua, C.K.: Graded microstructure and mechanical properties of additive manufactured Ti-6Al-4V via electron beam melting. *Acta Mater.* **97**, 1–16 (2015). <https://doi.org/10.1016/j.actamat.2015.06.036>

89. Tang, Z.-J., Liu, W., Wang, Y., Saleheen, K., Liu, Z.-C., Peng, S.-T., Zhang, Z., Zhang, H.-C.: A review on in situ monitoring technology for directed energy deposition of metals. *Int. J. Adv. Manuf. Technol.* **108**, (2020). <https://doi.org/10.1007/s00170-020-05569-3>
90. Tapia, G., Elwany, A.: A review on process monitoring and control in metal-based additive manufacturing. *J. Manuf. Sci Eng.* **136**, 060801 (2014). <https://doi.org/10.1115/1.4028540>
91. Thijs, L., Montero Sistiaga, M.L., Wauthle, R., Xie, Q., Kruth, J.-P., Van Humbeeck, J.: Strong morphological and crystallographic texture and resulting yield strength anisotropy in selective laser melted tantalum. *Acta Mater.* **61**, 4657–4668 (2013). <https://doi.org/10.1016/j.actamat.2013.04.036>
92. Tofail, S.A.M., Koumoulos, E.P., Bandyopadhyay, A., Bose, S., O'Donoghue, L., Charitidis, C.: Additive manufacturing: scientific and technological challenges, market uptake and opportunities. *Mater. Today* **21**, 22–37 (2018). <https://doi.org/10.1016/j.mattod.2017.07.001>
93. Trevisan, F., Calignano, F., Aversa, A., Marchese, G., Lombardi, M., Biamino, S., Ugues, D., Manfredi, D.: Additive manufacturing of titanium alloys in the biomedical field: processes, properties and applications. *J Appl. Biomater. Funct. Mater.* **16**, 57–67 (2018). <https://doi.org/10.5301/jabfm.5000371>
94. Vilardell, A.M., Yadroitsev, I., Yadroitseva, I., Albu, M., Takata, N., Kobashi, M., Krakhmalev, P., Kouprianoff, D., Kothleitner, G., Plessis, A. du: Manufacturing and characterization of in-situ alloyed Ti6Al4V(ELI)-3 at.% Cu by laser powder bed fusion. *Addit. Manuf.* **36**, 101436 (2020). <https://doi.org/10.1016/j.addma.2020.101436>
95. Vilaro, T., Colin, C., Bartout, J.D.: As-Fabricated and heat-treated microstructures of the Ti-6Al-4V Alloy processed by selective laser melting. *Metall. Mater. Trans. A* **42**, 3190–3199 (2011). <https://doi.org/10.1007/s11661-011-0731-y>
96. Wang, J.F., Sun, Q.J., Wang, H., Liu, J.P., Feng, J.C.: Effect of location on microstructure and mechanical properties of additive layer manufactured Inconel 625 using gas tungsten arc welding. *Mater. Sci. Eng. A* **676**, 395–405 (2016). <https://doi.org/10.1016/j.msea.2016.09.015>
97. Wang, P., Tan, X., Nai, M.L.S., Tor, S.B., Wei, J.: Spatial and geometrical-based characterization of microstructure and microhardness for an electron beam melted Ti-6Al-4V component. *Mater. Design* **95**, 287–295 (2016). <https://doi.org/10.1016/j.matdes.2016.01.093>
98. Wei, H., Wang, L., Niu, X., Zhang, J., Simeone, A.: Fabrication, experiments, and analysis of an LBM additive-manufactured flexure parallel mechanism. *Micromachines* **9**, 572 (2018). <https://doi.org/10.3390/mi9110572>
99. Weingarten, C., Buchbinder, D., Pirch, N., Meiners, W., Wissenbach, K., Poprawe, R.: Formation and reduction of hydrogen porosity during selective laser melting of AlSi₁₀Mg. *J. Mater. Process. Technol.* **221**, 112–120 (2015). <https://doi.org/10.1016/j.jmatprotec.2015.02.013>
100. Xiao, Z., Chen, C., Zhu, H., Hu, Z., Nagarajan, B., Guo, L., Zeng, X.: Study of residual stress in selective laser melting of Ti₆Al₄V. *Mater. Design* **193**, 108846 (2020). <https://doi.org/10.1016/j.matdes.2020.108846>
101. Yadollahi, A., Shamsaei, N.: Additive manufacturing of fatigue resistant materials: challenges and opportunities. *Int. J. Fatigue* **98**, 14–31 (2017). <https://doi.org/10.1016/j.ijfatigue.2017.01.001>
102. Yadollahi, A., Shamsaei, N., Thompson, S.M., Seely, D.W.: Effects of process time interval and heat treatment on the mechanical and microstructural properties of direct laser deposited 316L stainless steel. *Mater. Sci. Eng. A* **644**, 171–183 (2015). <https://doi.org/10.1016/j.msea.2015.07.056>
103. Yamanaka, K., Saito, W., Mori, M., Matsumoto, H., Chiba, A.: Preparation of weak-textured commercially pure titanium by electron beam melting. *Addit. Manuf.* **8**, 105–109 (2015). <https://doi.org/10.1016/j.addma.2015.09.007>
104. Yan, L., Chen, Y., Liou, F.: Additive manufacturing of functionally graded metallic materials using laser metal deposition. *Addit. Manuf.* **31**, 100901 (2020). <https://doi.org/10.1016/j.addma.2019.100901>
105. Yang, T., Liu, T., Liao, W., Wei, H., Zhang, C., Chen, X., Zhang, K.: Effect of processing parameters on overhanging surface roughness during laser powder bed fusion of AlSi₁₀Mg. *J. Manuf. Process.* **61**, 440–453 (2021). <https://doi.org/10.1016/j.jmapro.2020.11.030>

106. Yasa, E., Kempen, K., Kruth, J., Thijss, L., Van Humbeeck, J.: Microstructure and mechanical properties of maraging steel 300 after selective laser melting. In: Solid freeform fabrication symposium proceedings, pp. 383–396 (2010)
107. Yin, J., Yang, L., Yang, X., Zhu, H., Wang, D., Ke, L., Wang, Z., Wang, G., Zeng, X.: High-power laser-matter interaction during laser powder bed fusion. *Addit. Manuf.* **29**, 100778 (2019). <https://doi.org/10.1016/j.addma.2019.100778>
108. Zadi-Maad, A., Rohib, R., Irawan, A.: Additive manufacturing for steels: a review. *IOP Conf. Ser.: Mater. Sci. Eng.* **285**, 012028 (2018). <https://doi.org/10.1088/1757-899X/285/1/012028>
109. Zakirov, A., Belousov, S., Bogdanova, M., Korneev, B., Stepanov, A., Perepelkina, A., Levchenko, V., Meshkov, A., Potapkin, B.: Predictive modeling of laser and electron beam powder bed fusion additive manufacturing of metals at the mesoscale. *Addit. Manuf.* **35**, 101236 (2020). <https://doi.org/10.1016/j.addma.2020.101236>
110. Zhai, Y., Galarraga, H., Lados, D.A.: Microstructure evolution, tensile properties, and fatigue damage mechanisms in Ti-6Al-4V alloys fabricated by two additive manufacturing techniques. *Procedia Eng.* **114**, 658–666 (2015). <https://doi.org/10.1016/j.proeng.2015.08.007>
111. Zhai, Y., Galarraga, H., Lados, D.A.: Microstructure, static properties, and fatigue crack growth mechanisms in Ti-6Al-4V fabricated by additive manufacturing: LENS and EBM. *Eng. Fail. Anal.* **69**, 3–14 (2016). <https://doi.org/10.1016/j.englfailanal.2016.05.036>
112. Zhang, Y., Wu, L., Guo, X., Kane, S., Deng, Y., Jung, Y.-G., Lee, J.-H., Zhang, J.: Additive manufacturing of metallic materials: a review. *J. Materi Eng Perform.* **27**, 1–13 (2018). <https://doi.org/10.1007/s11665-017-2747-y>
113. Zheng, L., Liu, Y., Sun, S., Zhang, H.: Selective laser melting of Al–8.5Fe–1.3V–1.7Si alloy: investigation on the resultant microstructure and hardness. *Chinese J Aeronaut.* **28**, 564–569 (2015). <https://doi.org/10.1016/j.cja.2015.01.013>
114. Ziętala, M., Durejko, T., Polański, M., Kunce, I., Płociński, T., Zieliński, W., Łazińska, M., Stępniewski, W., Czujko, T., Kurzydłowski, K.J., Bojar, Z.: The microstructure, mechanical properties and corrosion resistance of 316L stainless steel fabricated using laser engineered net shaping. *Mater. Sci. Eng. A* **677**, 1–10 (2016). <https://doi.org/10.1016/j.msea.2016.09.028>
115. Microstructural investigation of selective laser melting 316L stainless steel parts exposed to laser re-melting. *Procedia Eng.* **19**, 389–395 (2011). <https://doi.org/10.1016/j.proeng.2011.11.130>
116. Effects of defects in laser additive manufactured Ti-6Al-4V on fatigue properties. *Phys. Procedia.* **56**, 371–378 (2014). <https://doi.org/10.1016/j.phpro.2014.08.120>
117. Additive Manufacturing of Titanium Alloy for Aircraft Components: *Procedia CIRP* **35**, 55–60 (2015). <https://doi.org/10.1016/j.procir.2015.08.061>
118. Metal powders—the raw materials, <https://www.metal-am.com/introduction-to-metal-additive-manufacturing-and-3d-printing/metal-powders-the-raw-materials/>
119. Standards for metal Additive Manufacturing: A global perspective, <https://www.metal-am.com/articles/standards-for-metal-3d-printing-a-global-perspective/>
120. Electronic Beam Melting, <https://www.whiteclouds.com/3dpedia/ebm.html>
121. ARTICLE: Additive Manufacturing of Aluminum Alloys—Light Metal Age Magazine, <https://www.lightmetalage.com/news/industry-news/3d-printing/article-additive-manufacturing-of-aluminum-alloys/>
122. Additive manufacturing: technology, applications and research needs|SpringerLink, <https://link.springer.com/article/10.1007%2Fs11465-013-0248-8>
123. A Review on Process Monitoring and Control in Metal-Based Additive Manufacturing | *J. Manuf. Sci. Eng. | ASME Digital Collection*, <https://asmedigitalcollection.asme.org/manufacturingscience/article-abstract/136/6/060801/377521/A-Review-on-Process-Monitoring-and-Control-in>
124. Using machine learning to aid in the parameter optimisation process for metal-based additive manufacturing | Emerald Insight, <https://doi.org/10.1108/RPJ-08-2019-0213/full/html>
125. 3D printing: a critical review of current development and future prospects | Emerald Insight, <https://doi.org/10.1108/RPJ-11-2018-0293/full/html>

126. Advanced Machining Processes—Prof. Vijay Kumar Jain—Google Books, https://books.google.co.in/books?hl=en&lr=&id=ufyiV6nEyd4C&oi=fnd&pg=PR9&dq=LBM,+EBM,+and+LMD+advantage+and+disadvantages&ots=vQD071htns&sig=cQAT0zIPygNPIMuE0w7NLnQokRs&redir_esc=y#v=onepage&q&f=false
127. Evaluation of Titanium Alloys Fabricated Using Rapid Prototyping Technologies—Electron Beam Melting and Laser Beam Melting, <https://www.ncbi.nlm.nih.gov/pmc/articles/PMC5448875/>
128. Electron Beam Melting—an overview | ScienceDirect Topics, <https://www.sciencedirect.com/topics/chemistry/electron-beam-melting>
129. Tensile Testing for 3D Printing Materials, <https://www.protolabs.com/resources/blog/tensile-testing-for-3d-printing-materials/>
130. On the mechanical behaviour of titanium alloy TiAl₆V₄ manufactured by selective laser melting: Fatigue resistance and crack growth performance—ScienceDirect, <https://www.sciencedirect.com/science/article/abs/pii/S014211231200343X>
131. Process optimization, microstructures and mechanical properties of a Cu-based shape memory alloy fabricated by selective laser melting—ScienceDirect, <https://www.sciencedirect.com/science/article/abs/pii/S0925838819301616>
132. ARTICLE: Additive Manufacturing of Aluminum Alloys
133. Tensile Testing for 3D Printing Materials

Chapter 12

Electrochemical Corrosion Behavior of Heat Treated Inconel 718 Superalloy Manufactured by Direct Metal Laser Sintering (DMLS) in 3.5% NaCl Solution



B. Anushraj, N. C. Brintha, D. Chella Ganesh, and A. Ajithram

12.1 Introduction

The gas turbine has become the essential reliable device used in the field of transportation, power generation and other application. The gas turbine is known for its comparative mechanical simplicity which ability to utilize expansive range of fuels. Practically, the effectiveness of gas turbine engines is lesser than the petrol and diesel engines. Also, for outstanding power-weight relation of gas turbine engines the efficiency is increased [1]. These gas turbines are used in various high power transportation applications such as helicopters, air craft and rocket propellers [2]. Gas turbine is an internal combustion engine which transfers chemical power into mechanical power which uses air as the working fluid.

The development in the additive manufacturing has been increased over the past decade due to its features in producing the sophisticated usable materials and has the capacity to produce complex geometry objects. The additive manufacturing also facilitates industry 4.0 in the form of digital transformation. The productivity and quality of the product in automobile, gas turbine and space vehicle is improved through revolutionary changes by digital technologies [3]. The additive manufacturing is a layer-by-layer built-up process. Therefore, this type of manufacturing the hybrid layer of structures can be fabricated easily and can produce the complex geometries at an easier rate [4]. Additive manufacturing is equal to the CNC machining process. Both takes the information data from the computer but in additive machining process the metal is added to build parts and in CNC machining

B. Anushraj (✉) · D. Chella Ganesh · A. Ajithram

Department of Mechanical Engineering and Centre for Surface Engineering, Kalasalingam Academy of Research and Education, Virudhunagar, Tamilnadu, India

N. C. Brintha

Department of Computer Science and Engineering, Kalasalingam Academy of Research and Education, Virudhunagar, Tamilnadu, India

the material is deduced to construct parts [5]. The additive manufacturing development proposes several benefits towards mechanical and metallurgical properties when contrasted to traditional fabrication processes [6]. Also, the design consideration of additive manufacturing is less when compared to conventional fabrication process [7]. The metallurgical bonding of the base material obtained is fine microstructure due to the deposition of material in each layer [8]. According to ASTM F2792-12a standard the additive manufacturing are classified into seven categories namely binder jetting, directed energy deposition, material extrusion, material jetting, powder bed fusion, sheet lamination and vat photo polymerization [9]. The metal additive manufacturing normally takes place by powder bed fusion process such as Selective Laser Melting (SLM), Direct Energy Deposition (DED), Direct Metal Laser Sintering (DMLS) and Electron Beam Melting (EBM) [10]. The powder fusion additive manufacturing for metals currently use sintering process instead of melting process [11]. The DMLS methods of powder bed fusion process have good surface finish and full density materials. In DMLS process, the sample is manufactured in a protective chamber to avoid oxidation [12].

In traditional manufacturing, a product is produced by formative process, subtractive process and joining process whereas in additive manufacturing technique layer by layer manufacturing is used. The additive manufacturing serves as an enabler for transformation of ideas from the designer's workstation to a finished product and removes the traditional manufacturing steps such as creating mold, machining to give the finishing, forging and joining. Therefore, additive manufacturing provides higher level of design freedom when compared to traditional manufacturing. The traditional manufacturing is focused towards mass production to reduce the cost of the product and improves the production rate, so as to improve the sustainability of the product. To improve mass production the initial investment is high due to the creation of assembly line and tooling costs. Also, for manufacturing low volume application such as satellites, air craft and ship the manufacturing cost is high when traditional manufacturing is used [13]. Thereby, the additive manufacturing improves cost-effective, mass production when compared to conventional manufacturing.

The nickel based superalloy of IN718 is a high strength alloy intended for high temperature application. In the superalloy, the alloy IN718 is used almost half tonnage of the total super alloy world-wide [14]. The alloy is precipitation-hardenable and has outstanding resistance for corrosion, fatigue and creep strength at elevated temperature. Therefore, this alloy is used in aero space, petro chemical industry, nuclear power generation, marine application and gas turbine application [15]. The important alloying elements in IN 718 nickel alloy are chromium, niobium, molybdenum, cobalt, carbon, aluminum and titanium [16]. The chromium in the alloy gives good resistance to corrosion. The molybdenum in the alloy improves the opposition to pitting corrosion. The cobalt existing in the alloy increases the creep resistance of the alloy. The accumulation of weighty metals such as molybdenum and tungsten improves the mechanical strength of superalloy [17]. The phase of the IN718 alloy are gamma (γ), gamma prime (γ'), gamma double prime (γ''), delta (δ), laves and carbide phases [18]. The γ'' phase is the combination of nickel and niobium (Ni_3Nb) in the form of Body Centre Tetragonal (BCT) crystalline structure. This phase precipitation

of the alloy increases the tensile and creep properties [19]. This phase is transformed to δ phase at higher temperature. The principal strengthening phase of the alloy is mainly derived from the solid solution hardeners. The metastable compound of gamma double prime is suppressed by the stable delta phase at higher temperatures. The γ' phase consist of nickel, Aluminum and Titanium ($Ni_3(Ti, Al)$) in the form of Face Centered Cubic (FCC) crystalline structure. This phase is one of the secondary phases of the super alloy, it also increases the mechanical strength of the alloy. This initial nucleation starts in the grain boundaries and distributed as fine particles in the γ matrix [20]. The gamma prime also increases the ductile strength and increases the fracture toughness. Also, it improves the resistance to creep at elevated temperature of the superalloy [21]. The δ phase is a combination of nickel and niobium (Ni_3Nb) in the form orthorhombic crystal structure. The δ phase is thermodynamically stable phase of γ'' phase and its precipitation begins at 900 to 1100 °C. The δ phase controls the grain growth and also controls the formation of carbides and nitrides [22]. The formation of delta (δ) phase reduces the formation of γ'' phase and delta phase formed by the intermediate γ'' phase [23]. The increase in the aluminum and titanium ratio decreases the formation of the δ phase. The δ phase precipitates in the form of needle or plate within the grain and in the grain boundaries [24]. The primary phase of gamma (γ) in the form of austenitic face centered cubic structure. When compared to BCC structure the FCC has lower diffusivity because of its closely packed structure. This structure is the key to predominant qualities and improves the stability of the alloy at higher temperature [25]. This phase usually consist of high percentage of solid-solution elements such as Co, Cr, Mo, and W [26]. The IN718 has numerous mechanical characteristics such as toughness at low temperature, strength at high temperature and extraordinary corrosion resistance in various conditions due to its FCC crystal structure [27].

The machining of Inconel 718 was poor due to its high strength, toughness, thermal resistant and work hardening properties of the alloy [28]. Machining is the process broadly used in industries to produce various size and geometries for modern applications. The machining process is time consuming, rough surface finish and costliest process. The problems in machining the Inconel 718 produce built-up-edge and high cutting force, which reduces the tool life [29]. The tool life is reduced due to the maximum temperature increase in the tool face and tip of the tool which in turn produces the built-up-edge in the tool face and chip interface. The higher cutting speed also reduces the tool life [30]. Therefore, the solution to fabricate the sophisticated structures and complex geometries of hard superalloy by additive manufacturing processes. The weld ability of the super alloy is good in age hardened and solutionized condition. The Inconel718 superalloy has good resistance to fusion zone cracking, heat affected zone and heat treatment cracking [31]. The resistance in strain cracking ability of the alloy, the superalloy is mostly in the aero space application such as gas turbine components. The additive manufacturing is layer by layer scale welding. The Inconel718 superalloy can be manufactured by additive manufacturing [32]. The microstructure and mechanical properties of the nickel based alloy is upgraded by proper heat treatment. The nickel based alloys have standard heat treatment process such as homogenization, Solutionizing and age hardening [33].

Table 12.1 The element weight % of IN718 super alloy

Element	Ni	Fe	Cr	Nb	Mo	Ti	Al	Si	C	Co	Cu	W
Weight %	52.44	19.78	17.13	4.77	3.38	1.11	0.59	0.13	0.05	0.16	0.23	0.23

The corrosion resistance of additively manufactured Inconel718 in aqueous solution is an essential problem for consideration, due to the difference in the microstructure of the additive manufactured alloy. Generally, in a corrosive atmosphere galvanic corrosion may take place. The aim of this work is to show a correlation between the commercial alloy and additive manufactured alloy. The microstructure and electrochemical behavior at 3.5% NaCl solution was discussed with the effect of heat treatment. Also, in this work the tensile and impact strength of the additively manufactured alloys are highlighted.

12.2 Materials and Method

12.2.1 Materials and Fabrication

Materials of 3-D printed samples were procured from INTECH DMLS, Pvt Ltd, Bangalore. The EOS M280 DMLS machine has been used to fabricate the DMLS samples by additive manufacturing techniques. The optimum process used to fabricate the DMLS alloy are power 285 W, hatching distance 0.15 mm, layer thickness 40 μm , scan rate 970 mm/s and beam diameter 80 μm . The supplier's quality test certifications are validated for the procured sample. The average surface roughness of the printed samples is 2 μm (Ra), with homogeneity seen over the entire surface. The chemical combination of Inconel718 used for manufacturing the sample is shown in Table 12.1.

12.2.2 Heat Treatment

Figure 12.1 shows the graphical representation of heat treatment cycle. Heat treatment was carried out at heating rate of 10 $^{\circ}\text{C}/\text{min}$. In HT 1 plan, the sample is one hour at solutionizing temperature ($980\ ^{\circ}\text{C}$). Further, samples were heated up to $720\ ^{\circ}\text{C}$ for 8 h ageing. The second ageing started continuously after a temperature dropped down to $620\ ^{\circ}\text{C}$ ($55\ ^{\circ}\text{C}/\text{h}$) after double ageing process was completed, the samples were cooled in furnace. In HT 2, the sample is homogenized temperature at $1100\ ^{\circ}\text{C}$ for 2 h. The ageing process began at $845\ ^{\circ}\text{C}$ at 24 h and then the sample is cooled in furnace.

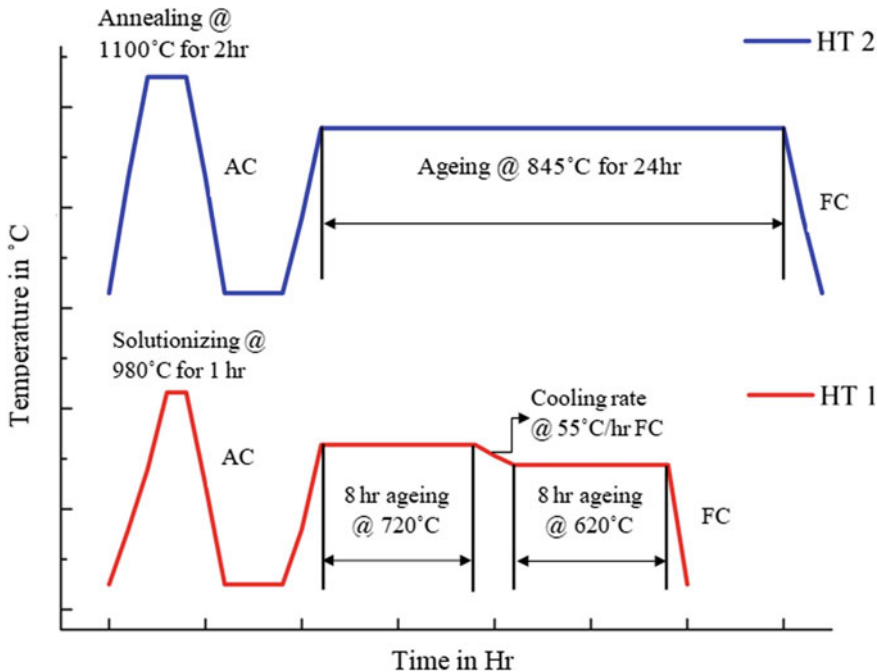


Fig. 12.1 Schematic heat treatment process for DMLS and commercial alloy

12.2.3 Mechanical Property Evaluation

The Vickers Hardness (diamond indentation) scale was used to determine the micro hardness of the samples with a load of 300 g and a dwell time of 10 s. Each hardness value was the average of six random indentations. The tensile properties of heat treated samples were examined based on the ASTM-E8 standard. The test was carried out in UTM machine with system control under the load of 100 kN and cross head speed at 1 mm/min. The ASTM E23 standard the sample size of 10 mm × 10 mm × 75 mm, impact test was carried out in Izod.

12.2.4 Electrochemical Property Evaluation

The potentiostat/galvanostat (ACM instruments GillAC, UK) electrochemical polarization identification test was conducted with the assistance of three electrode cells positioning a reference of saturated calomel electrode, counter electrode assigned as a platinum sheet and the sample was assigned as a working electrode. ASTM G3-14 standard was followed for conducting experimentation with 1 cm² on a particular room temperature on the area of exposure [34]. The 3.5% NaCl solution was used

as the medium of exposure for corrosion measurement of alloy. After a particular time, when the open circuit potential becomes constant then the sweep voltage limits were set to the -250 to $+250$ mV with 1 mV/s sweep rate. Once the electrochemical polarization measurement was finished, finally the tafel plot was obtained. Once the polarization measurement was finished the finished samples were subjected to characterization studies.

12.2.5 Surface Characterization

The samples were polished with emery paper up to 2000 grit, after that the microstructure of heated and non-heated samples were observed using optical microscope. The metallographic etching was carried out by 87 Glyceregia (ASTM E 407 STD) consisting of 15 ml HCl, 10 ml Glycerol and 5 ml HNO₃. With the help of scanning electron microscope, the corrosion morphology samples were investigated (This microscope was used to analyze (Make: Zeiss–FE SEM) the energy-dispersive spectroscopy (Make: Brukers EDS)).

12.3 Results and Discussion

12.3.1 Micro Structural and XRD Examination

Bare

The microstructure of the IN718 without heat treatment process is shown in Fig. 12.2. According to Fig. 12.2a, the layer by layer material manufacturing can be observed of alloy processed by DMLS without heat treatment. The columnar dendrites were

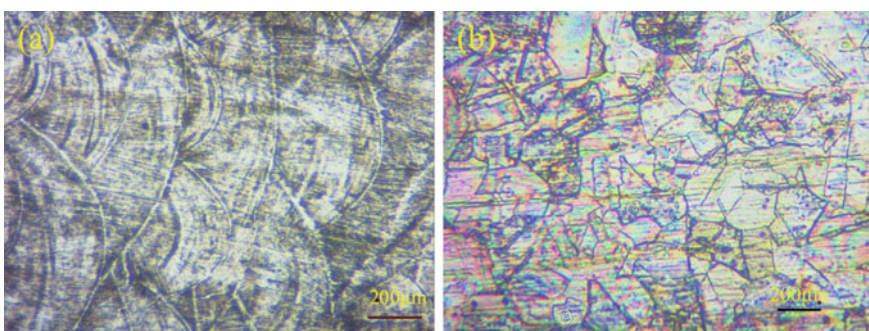


Fig. 12.2 Optical image of the bare IN718 **a**, DMLS alloy **b** commercial alloy

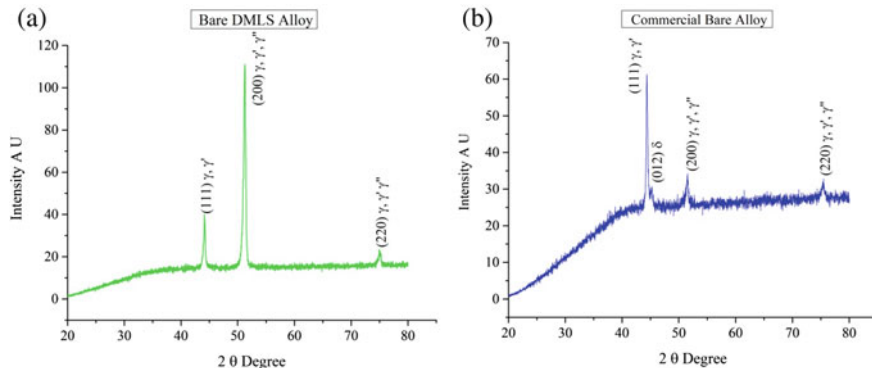


Fig. 12.3 XRD analysis of the bare IN718 **a**, DMLS alloy **b** commercial alloy

produced on the bare DMLS alloy owing to rapid cooling. Also, these dendrites are formed due to the solidification on the substrate of the each layer. These columnar dendrites microstructures are formed along the direction on the build direction of deposition. The microstructure overlapping is formed on the DMLS alloy. Figure 12.2b shows the microstructure of the bare commercial IN718 alloy. The coarse grains are formed with edge dislocations and twin boundaries.

The X-ray diffraction pattern of the bare DMLS alloy and commercial alloy are shown in Fig. 12.3. The diffraction phases are γ , γ' and γ'' intensity is high for the DMLS alloy evaluated with commercial alloy. In commercial alloy the metal is heated to molten state and solidified, therefore the δ phase is produced on the commercial alloy. The δ phase found in the alloy may reduce the strengthening phase of γ , γ' and γ'' . In DMLS alloy, the metal is sintered at 950 to 1050 °C, therefore the γ , γ' and γ'' phases is high.

HT 1

The microstructure of the HT 1 of DMLS alloy and commercial alloy is shown in Fig. 12.4. The microstructure of the DMLS alloy is shown in Fig. 12.4a, the grains are formed within the boundary of the each arc. The grains are formed as elongated columnar grains and in the arc boundary the small grains are formed. These small grains formed on the boundary due to the rapid cooling, takes place at the boundary of the arc. The microstructure of the commercial alloy is shown in Fig. 12.4b, the grains are refined to equal size on the grain boundary. Large numbers of twins were formed on the surface due to the solutionizing of the alloy.

Figure 12.5 shows the X-ray diffraction pattern of the heat treated segment of HT 1 of DMLS and commercial alloy. The precipitation of δ , γ , γ' and γ'' phase are improved by the heat treatment. The intension of strengthening phase of γ , γ' and γ'' is high for DMLS alloy when evaluated with commercial alloy. Also, for the commercial alloy the δ phase is improved when evaluated with bare commercial alloy.

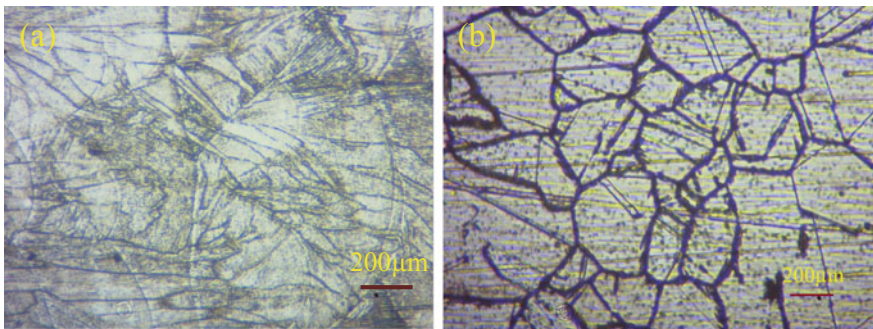


Fig. 12.4 Optical Image of the HT 1 IN718 **a**, DMLS alloy **b** commercial alloy

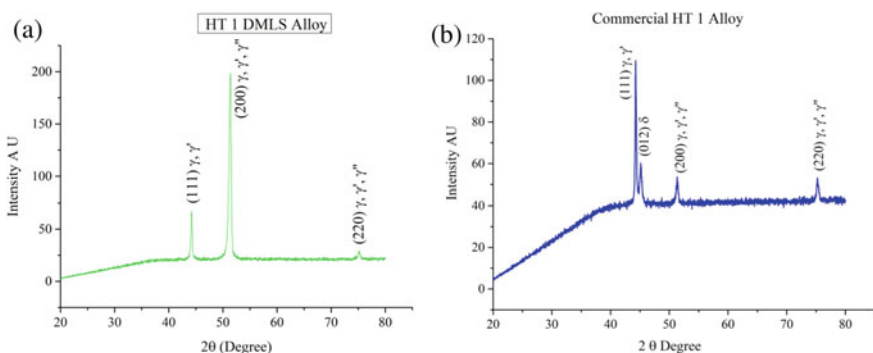


Fig. 12.5 XRD analysis of the HT 1 IN718 **a**, DMLS alloy **b** Commercial Alloy

The δ phase in the alloy improves the grain boundary strength alloy, but reduces the mechanical strength of the alloy [35]. Therefore, the DMLS alloy has high mechanical strength when compared to commercial alloy. From the TTT diagram the γ'' phase precipitation takes place at the ageing temperature at 620 and 720 °C [36].

HT 2

The microstructure of the homogenized heat treatment plan of HT 2 of DMLS alloy and commercial alloy is shown in Fig. 12.6. The HT 2 DMLS alloy is fully homogenized as shown in Fig. 12.6a. Figure 12.6b shows the commercial alloy heat treated at HT 2. The large grains are formed in the commercial alloy and elongated columnar structure is formed on the DMLS alloy.

Figure 12.7 shows the XRD pattern of the HT 2 of DMLS and commercial alloy. The δ phase is found on the both DMLS and commercial alloy. The sample is heated to 1100 °C for 2 h which induces the development of δ phases. The XRD pattern for δ phase for DMLS alloy is (211) pack and δ phase for commercial alloy is (012)

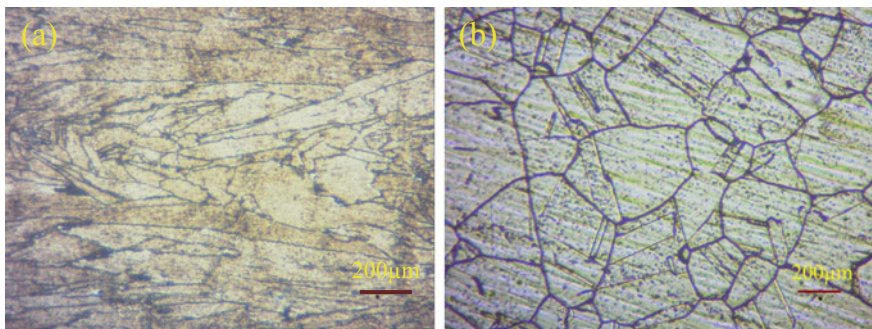


Fig. 12.6 Optical image of the HT 2 IN718 **a**, DMLS alloy **b** commercial alloy

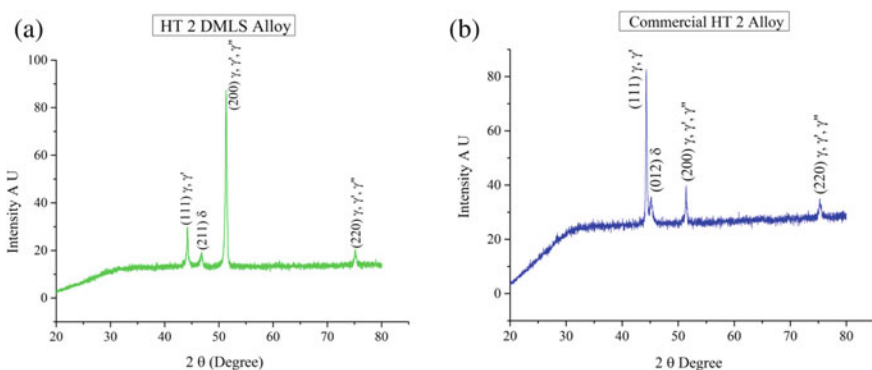


Fig. 12.7 XRD analysis of the HT 2 IN718 **a**, DMLS alloy **b** commercial alloy

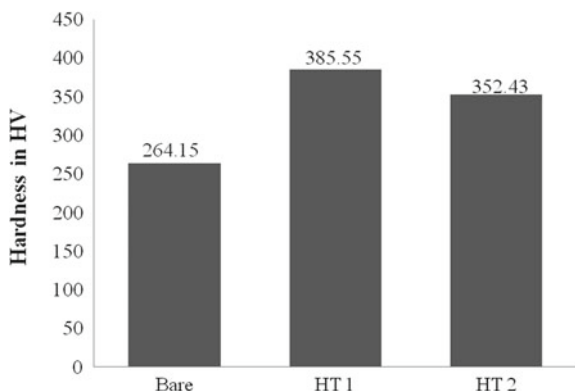
peak [37]. The δ phase formation may reduce the formation of strengthening phase γ'' which reduces the mechanical properties of the alloy. The γ'' phase formation is high for DMLS alloy when evaluated with commercial alloy. The γ and γ' formation is high for commercial alloy and the γ'' is high for DMLS alloy in HT 2 sample.

12.3.2 Mechanical Characterization

Hardness

Figure 12.8 shows the hardness value of bare and heat treated sample. When evaluating the as-built sample, the hardness value increased dramatically after heat treatment. The hardness value heat treated 1 (HT1) sample is increased up to 45% and heat treated 2 (HT2) sample is increased up to 33% at the same time hardness value of bare sample and heat treated sample value also changed respectively.

Fig. 12.8 Average Vicker hardness of DMLS alloy



Tensile Strength

The properties of tensile load, maximum displacement and maximum strain of heat treated DMLS IN718 and non-heat treated DMLS IN718 is compared in Fig. 12.9. It shows that, the properties of heat treated DMLS alloy was increased when compared with non-heat treated alloy. The tensile load of HT1 DMLS alloy was 47.34 kN and for the HT 2 DMLS alloy it is 45.2 kN, based on this it was found that, the strength of DMLS heat treated alloy has increased slightly. From the graph its shows that, DMLS HT1 has high tensile load when evaluated with bare and HT 2 DMLS alloy. In the HT1, the micro-segregation of the γ' and γ'' phases has substantially enhanced, resulting in a rise in the alloy's tensile load. The ductility property for DMLS HT 1 alloy has decreased, due to the significant precipitation of the strengthening phases. Due to presence of δ phase in the HT 2 DMLS alloy, the property of the material has decreased. Due to presence of Nb and Ti in the alloy, there is a reduction of ductile property of material [38]. Table 12.2 shows the value of tensile, impact and hardness test. After prolonged exposure of the sample, the precipitation of γ' and γ'' phase has been decreased which leads to development of δ phase which develops the tensile

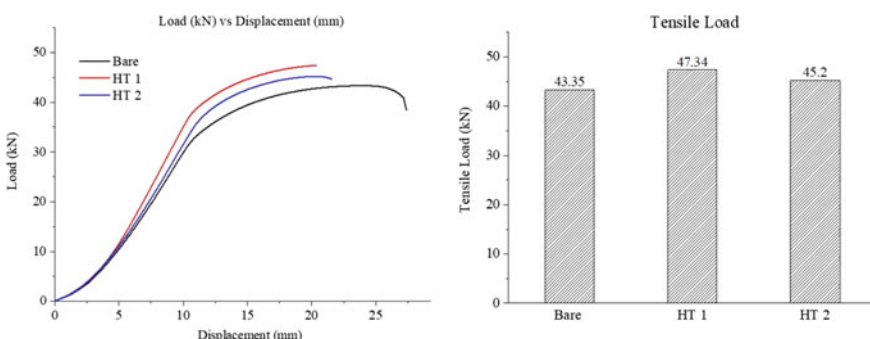


Fig. 12.9 Load versus displacement and tensile load of bare, HT 1 and HT 2

Table 12.2 Characteristics of tensile, impact and hardness test

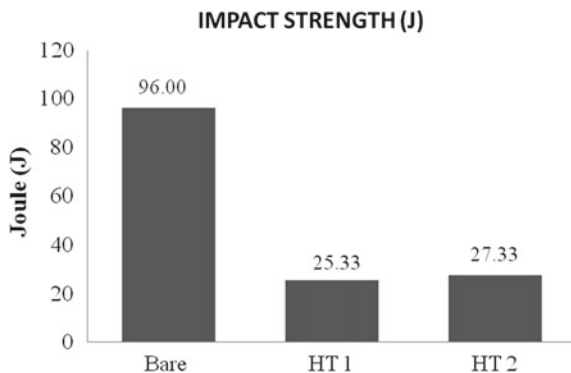
Condition	Tensile load (kN)	Max. displacement (%)	Max. strain (%)	Impact strength (J)	Hardness (HV)
Bare	43.35	27.40	91.27	96	264.15
HT 1	47.34	13.81	70.48	25.33	385.55
HT 2	45.2	18.52	72.34	27.33	352.43

property of the material and it reduces the ductile property of heat treated sample (HT 1 and HT 2). Anderson et al. has examined that, the precipitation of δ phase in IN718 and concluded that, development of δ phase enhances the tensile load, hardness and decreases the ductility of HT 2 DMLS alloy [39].

Impact Strength

Figure 12.10 shows the impact strength of the sample. The non-heat treated sample has the high impact strength of 96 J, DMLS HT 1 sample has 25.33 J and HT 2 DMLS sample has 27.33 respectively. When evaluated with heat treated DMLS alloy, bare DMLS alloy has higher impact strength. This may be due to layer by layer bonding of grains in horizontal orientation in non-heat treated sample has better tensile strength. During the heat treatment process of DMLS alloy the grain boundaries were refined and formation of brittleness were occurred which leads to reduce the impact strength of the material when compared to non-heat treated sample.

Fig. 12.10 Impact strength of bare, HT 1 and HT 2 DMLS alloy



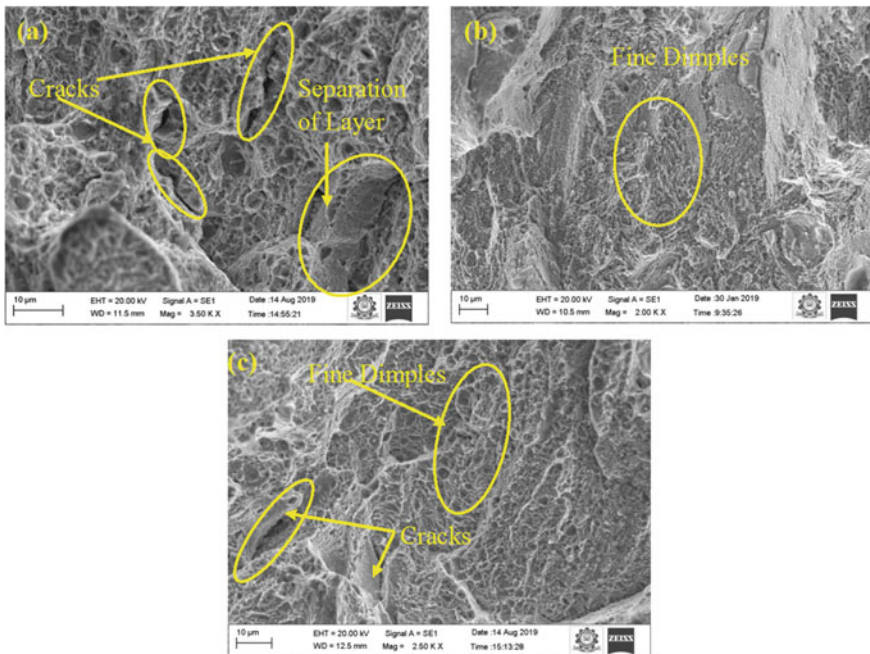


Fig. 12.11 Fracture surface of tensile test **a** bare alloy; **b** HT 1; **c** HT 2

12.3.3 Fractography

Tensile Strength

Figure 12.11 illustrates on the scanning electron microscope analysis of the fractured surface of a tensile sample at high magnifications. It was found that, micro cracks and separation of the layer was found on the non-heat treated sample, which leads to reduce the strength of the material [(12a)]. In the HT 1 [12(b)] sample fine dimples alone was found which may increase the strength of the material but in the HT 2 [12(c)] dimples and micro cracks are present which leads to reduce the strength of the material.

Impact Strength

Figure 12.12 shows the scanning electron microscope of impact test sample at the magnification. It was found that, crack formations are present in the non-heat treated sample. In HT 1 sample dimples alone were present but in HT 2 sample, fine dimples and cleavage cracks are present which leads to reduce the properties of the sample.

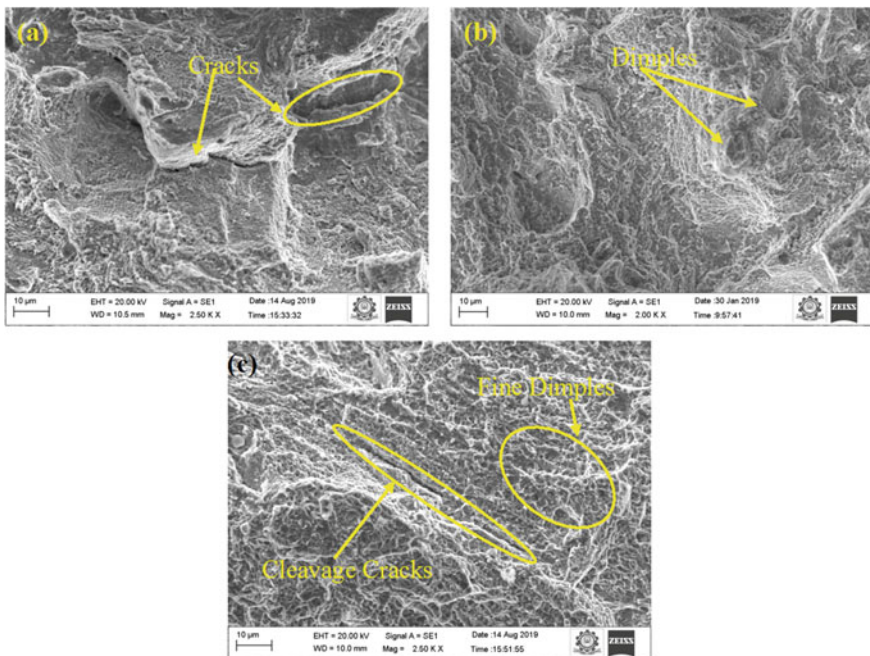


Fig. 12.12 Fracture surface of impact test **a** bare alloy; **b** HT 1; **c** HT 2

12.3.4 Electrochemical Corrosion

Potentiodynamic Polarization Analysis

The corrosion kinetics of the cathodic and anodic reaction of IN718 alloy at 3.5% NaCl solution was studied using electrochemical analysis for DMLS and commercial alloy. The polarization data and graph were obtained from the inbuilt software is shown in Table 12.3 and Fig. 12.13. The corrosion density was very low for DMLS

Table 12.3 Polarization data obtained for 3.5% NaCl solution

	Condition	Rest potential R _p (mV)	Corrosion potential E _{corr} (mV)	Corrosion density I _{corr} (mA/cm ²)	Corrosion rate C _R (mm/yr)
DMLS alloy	Bare	1.87	-132.65	2.762E-05	0.0004858
	HT 1	66.65	-127.56	2.205E-05	0.0003879
	HT 2	57.11	-117.15	1.842E-05	0.000324
Commercial alloy	Bare	-268.90	-333.57	0.002652	0.0466481
	HT 1	-218.90	-213.61	0.0019949	0.0350906
	HT 2	-218.60	-272.18	0.0019422	0.0341636

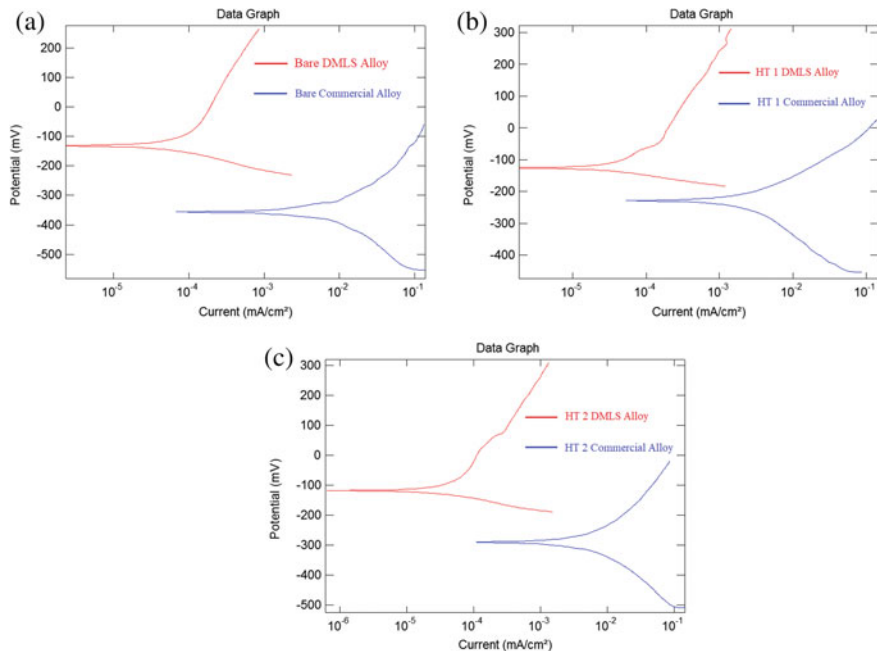


Fig. 12.13 Polarization data obtained for 3.5% NaCl solution **a** bare alloy; **b** HT 1; **c** HT 2

alloy when evaluated with commercial alloy. Therefore, the corrosion rate was low for DMLS alloy. The corrosion rate was low for HT 2 alloy for DMLS and commercial alloy. The corrosion rate of the alloy was found very small for HT 2 alloy since the corrosion density is very low and corrosion potential is high for both DMLS and commercial alloy. The corrosion resistance was very low for commercial alloy when evaluated with DMLS alloy. The higher corrosion potential and low corrosion density leads to the reduction in the corrosion rate. The corrosion resistance of the DMLS alloy and commercial alloy in descending order is HT 2 > HT 1 > Bare, which is directly influenced the corrosion density.

Corrosion Morphology

The surface analyses of the electrochemical sample were investigated through scanning electron microscope (SEM). Figure 12.14 shows, the corrosion morphology of the DMLS and commercial alloy exposed in the 3.5% of NaCl solution. The pitting corrosion mechanism has been found in the entire sample. Figure 12.14a, b shows, the surface morphologies of the bare DMLS and commercial alloy. Based on observation from Fig. 12.14b, d, f, severe galvanic corrosion takes place in the commercial alloy. Therefore, severe pitting corrosion has taken place in the commercial alloy, when compared to DMLS alloy. Also, when compared with the heat treatment plan,

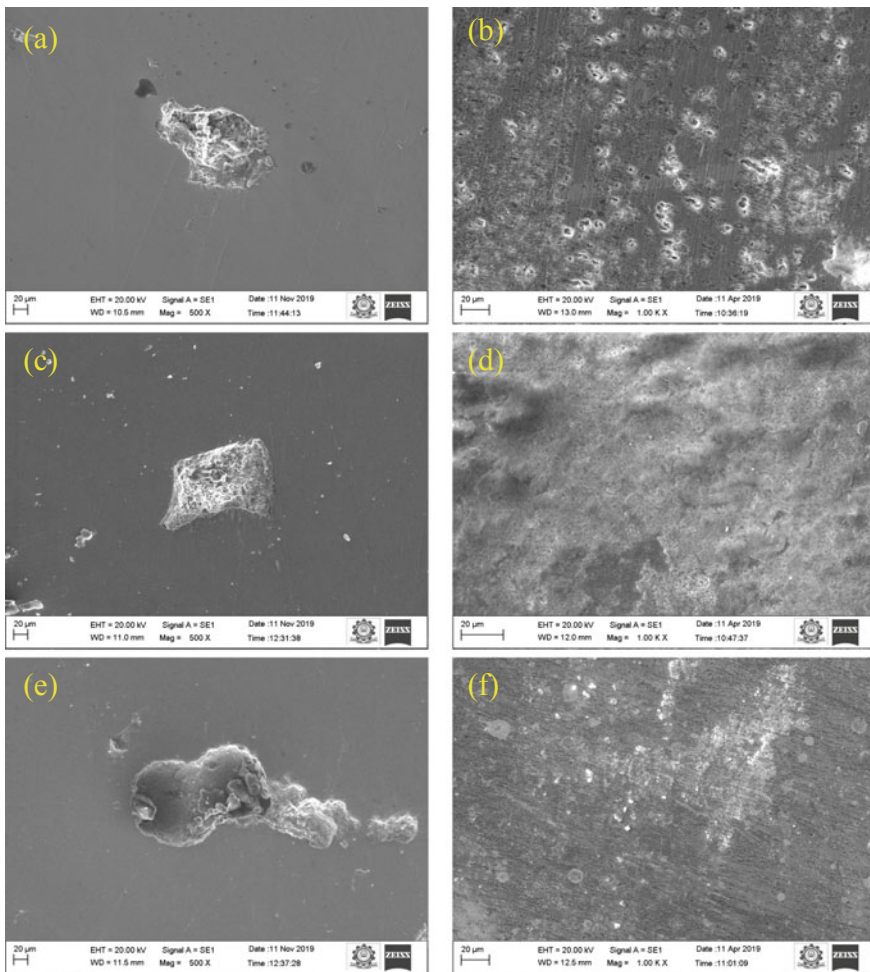


Fig. 12.14 Corrosion morphology of alloy exposed in 3.5% NaCl solution **a** bare DMLS alloy; **b** bare commercial alloy; **c** HT 1 DMLS alloy; **d** HT 1 commercial alloy; **e** HT 2 DMLS alloy; **f** HT 2 commercial alloy

the HT 2 treated alloy of DMLS and commercial alloy gives good corrosion due to the δ phase intention in the alloy. The intension of γ' and γ'' is low for the commercial alloy which also affects corrosion resistance. It was also found that, the corrosion resistance of the alloy mostly depends on the strengthening phase, but the δ phase improves the corrosion resistance.

12.4 Conclusion

In this study, the outcome of heat treatment on the microstructure, mechanical and corrosion resistance of the IN 718 superalloy manufactured by DMLS were studied and the following results can be drawn:

1. The columnar grain structures were indicated from DMLS sample on the overlapping region of every layer. Once, when the heat treatment process completes the grains are refined within the boundary of HT 1, HT 2 from fully homogenized DMLS alloy.
2. The X-ray diffraction pattern is compared with commercial alloy and found that, δ phase is found on the commercial alloy which reduces the strengthening phase of the alloy. The strengthening phase of the alloy is high for HT 1 DMLS alloy.
3. After, the heat treatment process tensile strength, and hardness parameter of DMLS fabricated IN718 alloy has increased. Considering the brittleness factor of both heat treatments 1 and 2, HT 1 alloy are more brittle compared to HT 2 alloy, because of γ' and γ'' strengthening phase present in the HT 1 DMLS alloy. In HT 2 DMLS alloy small delta (δ) phase is presented.
4. The impact strength results are replicated similar to the tensile strength results. Once when the heat treatment process is completed, the DMLS alloy impact strength is simultaneously reduced. It has been identified as very high because of horizontal orientation layer by layer fabrication method.
5. In HT 1 DMLS alloy the strengthening phase of γ' and γ'' intensity was high and the hardness value attained at 385.55 HV and with low intensity γ' , γ'' phase and additional δ phase present in the HT 2 DMLS alloy resulting the hardness is increased to 352.43 HV.
6. The corrosion resistance is high for HT 2 DMLS alloy due to the δ phase formed on the sample which strengthens the grain boundary.
7. Even though the presence of δ phase formation is high for commercial alloy the corrosion resistance of the commercial alloy is very low due to the very low intensity of strengthening phase.

References

1. Proctor, C.L.: Internal combustion engines. Encycl. Phys. Sci. Technol. 33–44 (2003). <https://doi.org/10.1016/b0-12-227410-5/00350-1>
2. Harman, R.T.C.: Applications for gas turbine engines. In: Gas Turbine Engineering. Palgrave, London (1981). https://doi.org/10.1007/978-1-349-16484-4_2
3. Craveiroa, F., Duarte, J.P., Bartoloa, H., Bartolod, P.J.: Additive manufacturing as an enabling technology for digital construction: a perspective on construction 4.0. Sustain. Dev. 4, 6 (2019). <https://doi.org/10.1016/j.autcon.2019.03.011>

4. Tofail, S.A.M., Koumoulos, E.P., Bandyopadhyay, A., Bose, S., O'Donoghue, L., Charitidis, C.: Additive manufacturing: scientific and technological challenges, market uptake and opportunities. *Mater. Today* **21**(1), 22–37 (2018). <https://doi.org/10.1016/j.mattod.2017.07.001>
5. Breaz, R.E., Bologa, O., Racz, S.G.: Selecting between CNC milling, robot milling and DMLS processes using a combined AHP and fuzzy approach. *Procedia Comput. Sci.* **122**, 796–803 (2017)
6. Prakash, K.S., Nancharaih, T., Rao, V.S.: Additive manufacturing techniques in manufacturing—an overview. *Mater. Today Proc.* **5**(2), 3873–3882 (2018)
7. Prakash, K.S., Nancharaih, T., Rao, V.V.S.: Additive manufacturing techniques in manufacturing—an overview. *Mater. Today Proc.* **5**, 3873–3882 (2018)
8. Zhong, C., Kittel, J., Gasser, A., Schleifenbaum, J.H.: Study of nickel-based super-alloys Inconel 718 and Inconel 625 in high-deposition-rate laser metal deposition. *Opt. Laser Technol.* **109**, 352–360 (2019). <https://doi.org/10.1016/j.optlastec.2018.08.003>
9. ASTM Committee F42 on additive manufacturing technologies, and ASTM committee F42 on additive manufacturing technologies. Subcommittee F42. 91 on Terminology (2012)
10. Srivatsa, S.: Additive manufacturing (AM) design and simulation tools study, p. 45433. Air Force Research Laboratory, Wright-Patterson Air Force Base, OH (2014)
11. King, W.E., Anderson, A.T., Ferencz, R.M., Hodge, N.E., Kamath, C., Khairallah, S.A., Rubenchik, A.M.: Laser powder bed fusion additive manufacturing of metals; physics, computational, and materials challenges. *Appl. Phys. Rev.* **2**(4), 041304 (2015). <https://doi.org/10.1063/1.4937809>
12. Delgado, J., Sereno, L., Ciurana, J., Hernandez, L.: Methodology for Analyzing the Depth of Sintering in the Building Platform, p. 266. CRC PressTaylor & Francis Group, Boca Raton (2012)
13. Kalpakjian, S., Schmid, S.: Manufacturing Engineering and Technology, 7th edn. Prentice Hall, Upper Saddle River, NJ (2014)
14. Kumar, S., Sudhakar Rao, G., Chattopadhyay, K., Mahobia, G.S., Santhi Srinivas, N.C., Singh, V.: Effect of surface nanostructure on tensile behavior of superalloy IN718. *Mater. Des.* **1980–2015**(62), 76–82 (2014). <https://doi.org/10.1016/j.matdes.2014.04.084>
15. Byun, T.S., Farrell, K.: Tensile properties of Inconel 718 after low temperature neutron irradiation. *J. Nucl. Mater.* **318**, 292–299 (2003). [https://doi.org/10.1016/s0022-3115\(03\)00006-0](https://doi.org/10.1016/s0022-3115(03)00006-0)
16. Special Metals Corporation: INCONEL® Alloy 718, 2007. Available from http://www.specia-lmetals.com/assets/smc/documents/inconel_alloy_718.pdf. Last accessed on 12.12.2020
17. Retima, M., Bouyegh, S., Chadli, H.: Effect of the heat treatment on the microstructural evolution of the nickel based superalloy. *Metalurgija* **17**, 71–77 (2011)
18. Silva, C., Song, M., Leonard, K., Wang, M., Was, G., Busby, J.: Characterization of alloy 718 subjected to different thermomechanical treatments. *Mater. Sci. Eng. A* **691**, 195–202 (2017)
19. Devaux, A., Nazzé, L., Molins, R., Pineau, A., Organista, A., Guédou, J.Y., Héritier, P., et al.: Gamma double prime precipitation kinetic in Alloy 718. *Mater. Sci. Eng. A* **486**(1–2), 117–122 (2008). <https://doi.org/10.1016/j.msea.2007.08.046>
20. Dong, J.X., Xie, X.S., Zhang, S.H.: Enhancements of thermal structure stability in a Ni-Base superalloy. *Scr. Metall. Mater.* **28**(12), 1477–1482 (1993). [https://doi.org/10.1016/0956-711x\(93\)90578-g](https://doi.org/10.1016/0956-711x(93)90578-g)
21. Sharpe, H.J., Saxena, A.: Effect of Microstructure on High-temperature Mechanical Behavior of Nickel-base Superalloys for Turbine Disc Applications, vol. 278, pp. 259–264. Trans Tech Publications Ltd. (2011)
22. Azadian, S., Wei, L.-Y., Warren, R.: Delta phase precipitation in Inconel 718. *Mater. Charact.* **53**(1), 7–16 (2004). <https://doi.org/10.1016/j.matchar.2004.07.004>
23. Dehmas, M., Lacaze, J., Niang, A., Viguer, B.: TEM study of high-temperature precipitation of delta phase in Inconel 718 alloy. *Adv. Mater. Sci. Eng.* **2011**, 1–9 (2011). <https://doi.org/10.1155/2011/940634>
24. Huang, Y., Langdon, T.G.: The evolution of delta-phase in a superplastic Inconel 718 alloy. *J. Mater. Sci.* **42**(2), 421–427 (2007). <https://doi.org/10.1007/s10853-006-0483-z>

25. Diltemiz, S.F., Zhang, S.: Superalloys for super jobs. In: Aerospace Material Handbook, pp. 1–76. CRC Press, London (2013)
26. Bowman, R.: Superalloys: a primer and history. In: 9th International Symposium on Superalloys, vol. 3, p. 6 (2000, May)
27. Kishawy, H.A., Hosseini, A.: Superalloys. Mach. Difficult-to-Cut Mater. 97–137 (2018). https://doi.org/10.1007/978-3-319-95966-5_4
28. Rahman, M., Seah, W.K.H., Teo, T.T.: The machinability of Inconel 718. J. Mater. Process. Technol. **63**(1–3), 199–204 (1997). [https://doi.org/10.1016/s0924-0136\(96\)02624-6](https://doi.org/10.1016/s0924-0136(96)02624-6)
29. Thakur, D.G., Ramamoorthy, B., Vijayaraghavan, L.: Machinability investigation of Inconel 718 in high-speed turning. Int. J. Adv. Manuf. Technol. **45**(5–6), 421–429 (2009). <https://doi.org/10.1007/s00170-009-1987-x>
30. Feyz, T., Safavi, S.M.: Improving machinability of Inconel 718 with a new hybrid machining technique. Int. J. Adv. Manuf. Technol. **66**(5–8), 1025–1030 (2012). <https://doi.org/10.1007/s00170-012-4386-7>
31. Tharappel, J.T., Babu, J.: Welding processes for Inconel 718—A brief review. IOP Conf. Ser. Mater. Sci. Eng. **330**(1), 012082 (2018, March). IOP Publishing
32. Sames, W.: Additive manufacturing of Inconel 718 using electron beam melting: processing, post-processing, and mechanical properties. Doctoral Dissertation (2015)
33. Thompson, R.G., Mayo, D.E., Radhakrishnan, B.: The relationship between carbon content, microstructure, and intergranular liquation cracking in cast nickel alloy 718. Metall. Trans. A **22**(2), 557–567 (1991). <https://doi.org/10.1007/bf02656823>
34. Raj, B.A., Jappes, J.T.W., Khan, M.A., Dillibabu, V., Brintha, N.C.: Studies on heat treatment and electrochemical behaviour of 3D printed DMLS processed nickel-based superalloy. Appl. Phys. A Mater. Sci. Process. **125**(10), 1–8 (2019). <https://doi.org/10.1007/s00339-019-3019-5>
35. Jambor, M., Bokuvka, O., Novy, F., Trsko, L., Belan, J.: Phase transformations in nickel base superalloy Inconel 718 during cyclic loading at high temperature. Prod. Eng. Arch. **15** (2017)
36. Yan, S., Wang, Y., Wang, Q., Zhang, C., Chen, D., Cui, G.: Enhancing mechanical properties of the spark plasma sintered Inconel 718 alloy by controlling the nano-scale precipitations. Materials **12**(20), 3336 (2019)
37. Anbarasan, N., Gupta, B.K., Prakash, S., Muthukumar, P., Oyyaravelu, R., Kumar, R.J.F., Jerome, S.: Effect of heat treatment on the microstructure and mechanical properties of Inconel 718. Mater. Today Proc. **5**(2), 7716–7724 (2018)
38. Li, X., Shi, J.J., Wang, C.H., Cao, G.H., Russell, A.M., Zhou, Z.J., Chen, G.F., et al.: Effect of heat treatment on microstructure evolution of Inconel 718 alloy fabricated by selective laser melting. J. Alloys Compounds **764**, 639–649 (2018). <https://doi.org/10.1016/j.jallcom.2018.06.112>
39. Anderson, M., Thielin, A.-L., Bridier, F., Bocher, P., Savoie, J.: δ phase precipitation in Inconel 718 and associated mechanical properties. Mater. Sci. Eng. A. <https://doi.org/10.1016/j.msea.2016.09.114>

Chapter 13

Machinability of 3D Printed Materials



Şenol Bayraktar and Erhan Şentürk

13.1 Introduction

The methods used in manufacturing and the management of the manufacturing process are changing day by day. Accordingly, manufacturing practices in the industry stand out as a field of activity that is constantly changing. In short, the evolution of industries is driven by innovative research activities related to production processes, materials and product design [1]. AM is an advanced technology that is constantly developing in accordance with the intended use of enterprises which is among the most up-to-date manufacturing processes today. AM reveals great potential for energy savings and cleaner environmental manufacturing due to the reduction in material and tooling requirements in traditional manufacturing techniques over the last decade. It is an efficient technique for the manufacturing of workpieces with high flexibility and complex geometry with waste material and time savings [2]. It also attracts a lot of attention from industrial practitioners/businesses as it enables rapid product development or product improvement in shorter timeframes [3, 4]. Smart production makes it important for production to be sustainable and effective due to the developments in production technologies in this modern age [5]. As a result of the emergence of new business models and leaner supply chains market demand for highly customized objects creates the need for AM technologies [3]. Manufacturing processes are generally divided into five categories: subtractive, additive, joining, dividing and transformative. Subtractive technology is defined as a method in which layers of material are removed to create a desired geometry. Addition technology is the addition of layers of material to create the shape of a desired

Ş. Bayraktar (✉) · E. Şentürk

Faculty of Engineering and Architecture, Department of Mechanical Engineering, Recep Tayyip Erdoğan University, 53100 Rize, Turkey
e-mail: senol.bayraktar@erdogan.edu.tr

workpiece. Joining technology refers to the physical joining of two or more workpieces to form the required shape such as the welding process. Dividing technology is used to prepare workpieces for different operations such as the sawing process. Transformative technology is preferred for changing the structural and mechanical properties of workpieces such as heat treatment and cryogenic cooling [1]. Although there are different machines for AM, the general construction of these machines is similar in that they can combine two-dimensional slices to form three-dimensional shapes. The main AM applications are Laser Melting/Laser Sintering, Fused Deposition Modeling-FDM, Stereolithography (SLA), Material Jetting, Binder Jetting and Electron Beam Melting. Each of these processes presents its own advantages and limitations in terms of the quality of the printed part, the mechanical property, the performance of the component, and the range of materials that can be manufactured. Complex industrial components which are difficult to manufacture with traditional manufacturing techniques, can be manufactured easily with AM technique [6, 7]. It is possible to produce especially lighter products using AM. Since molds are not used during manufacturing, labor and cost savings are obtained in terms of mold design and manufacturing. While a mold modification process is required due to design changes in mechanical components produced by conventional casting methods or molds, this situation is eliminated using AM. Although AM has many advantages, its applications are still limited due to its low precision and longer production times compared to the machining technique in CNC machines [1]. Similar to casting and wrought techniques workpieces manufactured using AM must have a certain tolerance range and surface quality (SQ) in order to be used as a final product in some cases. For this reason, in this book chapter, it is planned to reveal the machining characteristics of the workpieces manufactured by the AM technique in the literature and have different structural properties.

13.2 Importance of AM

AM includes processes by which complex 3D geometries can be created directly using raw materials [8]. Manufacturing can be carried out using AM without the traditional manufacturing constraints of material wastage, the difficulty of manufacturing complex shapes and the need for special tools. Engineers can increase design freedom with this technique. They can also find practical solutions for cross-sections and complex geometries [9]. Assembly time, supply chain, storage need and costs are reduced depending on the reduction in the number of parts in mechanical systems [8]. AM started out as a way for design engineers to realize design concepts without investing heavily in downstream manufacturing stage. Advances in Rapid Prototyping (RP) have contributed to the conversion of parametric CAD (computer aided design) data into physical prototypes that can be tested to check whether they ensure the design criteria. This not only saves time, but also allows more than one model to be tested [5]. Thus, AM applications began to be used in other fields such

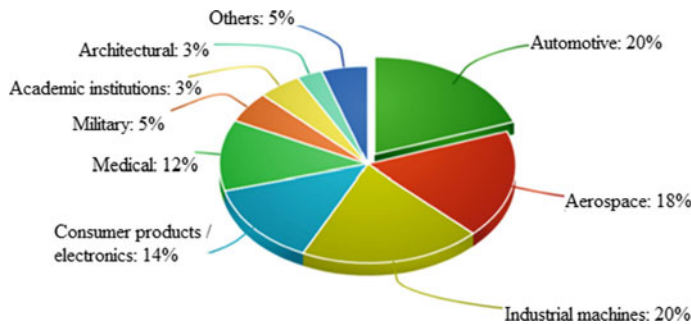


Fig. 13.1 Industrial adoption of AM [9]

as space, aviation, automotive, energy, medicine, defense industry products, and art and architectural design (Fig. 13.1).

The need for AM's use in different industries arose from extensive development and innovation in manufacturing processes. As the accuracy and versatility of the processes has been proven, the focus of industry has shifted towards the process of manufacturing complex parts with a rapid prototyping device [10]. AM applications are of great interest for the development of industrial applications in the aviation industry. Large enterprises such as Airbus, Boeing, NASA and Lockheed Martin are investing heavily in the development of this technology. One of the main factors in improving the manufacturing process in the aerospace industry is reducing the weight of components [3]. However, it is necessary to pay attention to the cost of light structural materials such as high-performance aluminum, titanium-based alloys and composite materials used in this sector. Therefore, ratio (Buy to fly-BTF) between the mass of raw materials required for a given production and the final mass of the manufactured part must be developed. Currently, the BTF ratio for aerospace components in conventional manufacturing (CM) processes is in the range of 12:1–25:1. This causes very poor material efficiency [3]. On the other hand, the use of light materials contributes to the reduction of fuel emissions and environmental impacts [9]. AM has the potential to manufacture lighter and higher-strength parts compared to traditional manufacturing methods. Acoustic applications such as sound insulation can be optimized with AM [11]. AM is used in the manufacture of components that make the most sense due to performance, time and cost. Businesses such as Boeing use three main criteria to measure the impact of AM versus conventional machining using CNC. These are workpiece performance, cost and delivery time. In the past, metal AM processes were expensive and slow to manufacture. Today, new generation AM technologies can compete with traditional metal machining methods in terms of speed and cost. This increases the importance of a more comprehensive comparison of the two manufacturing methods. Machining requires high material waste, machine cost and programming time. In addition, machining times and tool wear (TW) for hard materials such as raw titanium and tool steel are very high. Because of these limitations, businesses prefer more cost-effective processes such as casting, wrought

and molding for mass production. AM is a process-based manufacturing method that adds metal only where it is needed by building the workpiece layer by layer. Manufacturing of optimized designs using AM can be much faster than the complex programming processes in conventional CNC machining methods. There is no need for cutting tools, fixtures, stock material, experimental setup, labor or equipment changes in AM. Therefore, it is predicted that it can be an alternative to traditional subtractive manufacturing methods.

13.3 Theory of AM and Its Techniques

The ASTM F42 Technical Committee defines AM as “the process of combining materials to make objects from three-dimensional (3D) model data by adding layer upon layer as opposed to subtractive manufacturing methodologies” [5]. 3D printing (3DP), rapid prototyping (RP), direct digital manufacturing (DDM), additive layer manufacturing, layer-based manufacturing (LBM), rapid manufacturing (RM), and solid free-form manufacturing (SFF) terminologies are used to describe AM processes [1]. AM processes are based on manufacturing components using 3D computer data or Standard Tessellation Language (STL) files containing information about the geometry of the object [1]. The 3D model created in CAD software is divided into layers. Layer data in STL format is transferred to the AM machine. This machine produces material by adding layer upon layer (Fig. 13.2) to create 3D objects based on STL data [12].

The first patent on AM dates back to 1920 with Ralph Baker’s application to US Grant US1533300A entitled “Method of making decorative products”. Patents for AM processes since the late 1960s have been made possible by the invention of computers, resin polymers, and CNC machines due to the development of CAD/CAM systems [3]. MIT developed the groundbreaking 3D printing process in 1989. Other AM processes have also been developed due to increased private research study and

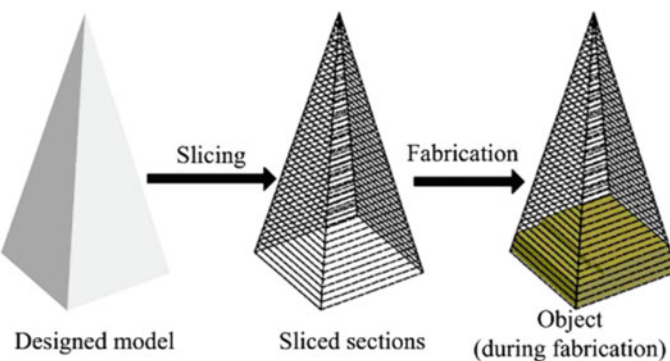


Fig. 13.2 Process of AM techniques [12]

industry interest. As professional 3D design and modeling becomes more common, the next generation of powerful computers has enabled AM technologies to be used for manufacturing purposes. Today, different AM technologies are available industrially [3]. AM technologies for metal materials are categorized by feedstock material and energy source type (Fig. 13.4). Wire feedstock and powder materials are widely used for metal AM technologies. Directed Energy Deposition (DED) and Powder Bed Fusion (PBF) techniques among the different metal AM technologies (Fig. 13.4a) are the most used methods of powder as raw material. Selective laser melting (SLM) and selective laser sintering (SLS) methods are two different PBF methods in which the laser is used as an energy source. Existing laser-based PBF systems are equipped with optical fiber lasers instead of CO₂ or Nd:YAG lasers. This increases the stability and power of the laser. Another PBF technique is electron beam melting (EBM), which uses a high-power electron beam as energy input instead of a laser. Unlike the laser-based PBF process which requires an inert gaseous printing medium for the EBM parts are produced in a vacuum chamber. The powder bed is preheated before each layer is printed with an electron beam in the EBM process. This contributes to the prevention of residual stresses in the manufactured workpiece and the formation of a martensitic phase due to rapid cooling. The latest PBF systems can achieve powder layer thicknesses as low as 20 μm and a minimum feature size of 100–150 μm. Fine resolution can greatly improve the density and quality of manufactured workpieces thanks to the surface finish. Schematic view of the PBF technique is given in Fig. 13.3. Four different stages occur in the form of solid mechanics, solid state transformation, thermal fluid and particle dynamics during the application of this technique. These consist of powder particle dynamics from gas expansion and thermal fluid dynamics that occur in solid-liquid-vapor conversion when interacting with the laser. It also includes solid mechanics to deal with the damage mechanism such as precipitation and internal heat treatment-like solid state transformation and cracking when remelted. For example, the powder interacts with all four possible states of matter such as solid, liquid, gaseous vapor and plasma when the laser comes into contact with metal. The nature of rapid and repetitive thermal cycles causes intense thermal gradients. Therefore, it triggers metallurgical defects of the material by causing metastable chemical, structural and mechanical states [13].

DED technique is metal AM technology that feeds the powder with carrier gas directly to the focus of the laser. As the laser scans the surface of the molten zone, the previous molten pool tends to solidify rapidly to form a built structure. Modern DED component includes optical fiber lasers for energy input to optimize workpiece quality and increase reliability. Another significant feature of the DED system is that the powder feed rate of each powder feeder can be individually controlled. This feature is extremely useful for the production of multi-material structures. Moreover, DED systems use a five or free axis CNC table instead of three axes. The deposition head modified by the existing coaxial powder deposition method, shows a better powder convergence, which improves the efficiency of powder use at the focal point. Recent technology also includes various monitoring devices such as melt pool sensors, laser power and layer control monitor added to the metal AM system. These provide better

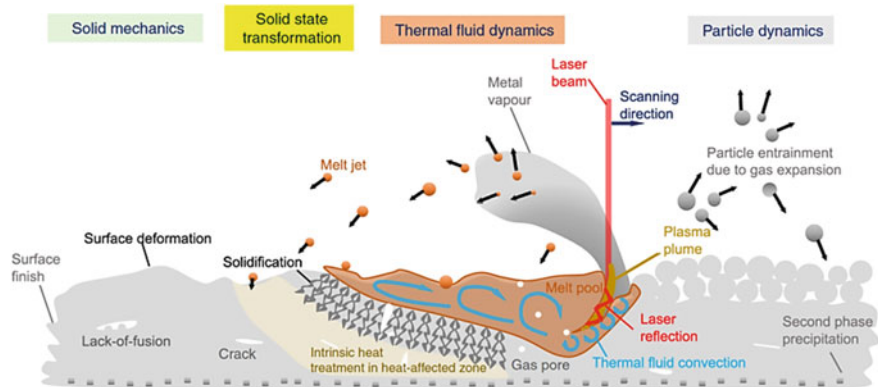


Fig. 13.3 A schematic view of PBF used in AM [13]

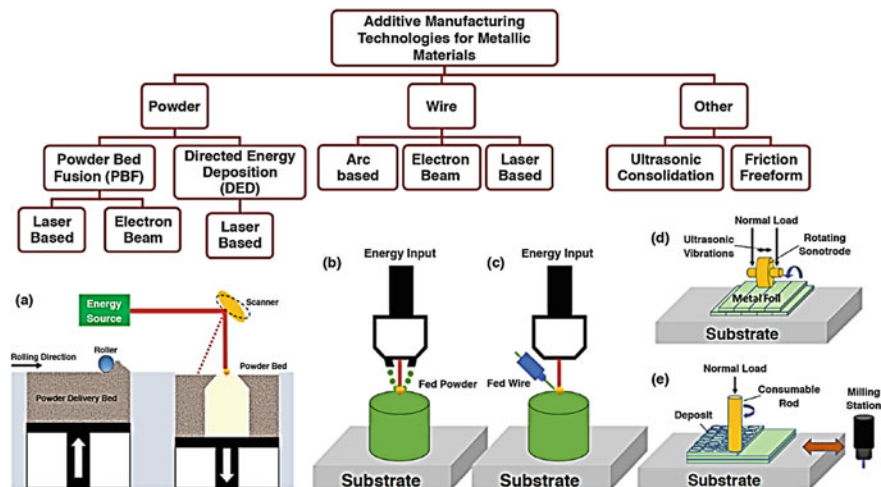


Fig. 13.4 Different AM technologies for metal materials, **a** Powder, **b** Fed powder, **c** Fed wire, **d** Ultrasonic consolidation and **e** Friction freeform [14]

control of the process and process parameters. The concept of wire-based deposition (Fig. 13.4b, c) is very similar to powder-based DED. Electron beam is an arc and laser-based energy source in AM technique applied using metal wire. There are also different techniques than AM which is perform using powder and wire. These are ultrasonic consolidation and friction freeform (Fig. 13.4d). Thin metallic foils are used as feedstock. These foils contribute to obtaining a strong binder between the layers. In addition, a certain amount of load that causes atomic diffusion between metal-metal interfaces during binder formation creates high-frequency ultrasonic vibrations. The friction freeform technique (Fig. 13.4e) with a consumable rod is very similar to traditional friction welding. In this technique, it is rotated at high

speed under a certain load in contact with the substrate surface using a consumable rod. Hereby, frictional heat arises. Thus, the accumulation of layers is provided with this heat [14].

13.4 Machining of Components Produced Using AM

Today, metal AM is among the important manufacturing techniques that have become widespread in wide sectoral applications, especially in the manufacture of components with complex geometries. However, although AM technology has some advantages compared to traditional manufacturing techniques, these components are generally not used directly in cases where the SQ is insufficient [10, 15]. The ladder effect occurs due to the layering of the additive techniques. Partially welded feedstock causes surface defects or irregular surface morphology due to spatter or insufficient fusion effects. This irregularity in the surface morphology directly affects the operating costs due to the decrease in the dimensional accuracy and service life of the manufactured parts. Therefore, a great effort has been made recently to improve the SQ of metal workpieces manufactured using AM [10]. In particular, scientists working in the field of machinability focus on this issue in order to improve the SQ of workpieces manufactured with AM technologies. This is due to two reasons. The first of these is the SQ and geometric tolerances of the workpieces produced with AM. Second, there are differences in microstructures when compared to conventionally machined materials with the same chemical composition. Surface roughness (SR) can be controlled by optimizing AM process parameters. However, in practice, some finishing operations are needed to improve the functional surfaces of almost all AM parts [16]. The differences in the microstructure of the workpieces affect the machinability properties as well as the mechanical properties [16]. Machining parts manufactured using AM is a demanding process. Because the layer orientations in the workpiece can exhibit different machinability characteristics under the same machining parameters [11]. As a result, workpieces manufactured with AMed exhibit poor surface morphology, poor SQ and out-of-tolerance dimensional stability values. These factors negatively affect the usability of the components. Therefore, secondary subtractive machining operations must be applied to achieve high SQ and dimensional stability or geometric tolerance outputs. Thus, it is ensured that workpieces produced using AM can be used as high quality products in precision engineering applications [17].

13.4.1 *Machining of Ti-6Al-4V Alloy*

Titanium (Ti) alloys are widely used in industrial areas that have critical load carrying capacity and require lightweight materials. Ti-6Al-4V is a prominent alloy in the

aerospace and medical industries due to its high specific strength, corrosion resistance and hypoallergenic features for biomedical implants among them. However, since the machinability of Ti alloys is poor, the AM method is an excellent solution for the manufacturing of titanium alloys with complex geometry [18]. Machining operations are carried out so that the Ti alloys manufactured by this method can be used as the final product. In some studies in the literature, Abdulmajeed Dabwan et al. revealed the impacts of cutting speed, feed rate and radial depth of cut on cutting force (CF), SR, microhardness, microstructure, chip and surface morphology in milling Ti-6Al-4V material manufactured by EBM method. They stated that different layer orientations according to the tool feed direction can be effective on the experimental outputs. Therefore, they investigated the cases of TILP (tool movement in a layer plane), TLP (tool movement perpendicular to layer planes) and TPLP (tool movement parallel to layers planes) (Fig. 13.5). It has been determined that various orientations have various effects on the machined surface, 29% better SQ is obtained in machining along TLP than TILP and TPLP, and the surface morphology is improved. Although ARCAM-optimized values were used on the side and top surfaces of the workpiece, it was found that the SR increased significantly. While the CFs were higher in TLP compare to other orientations, it was determined that they were lower in TILP. It has been determined that the deformation depths on the machined surfaces are measured in TLP, TPLP and TILP orientations, from highest to lowest, respectively. It was found that this situation showed a similar trend with the CF and subsurface hardness values. The highest saw-tooth chip was formed in TLP (Fig. 13.6) due to the effect of large CFs, followed by TPLP and TILP, respectively. Minimum grooves, feed marks and micro-chip accumulation occurred in TLP in terms of surface morphology [11].

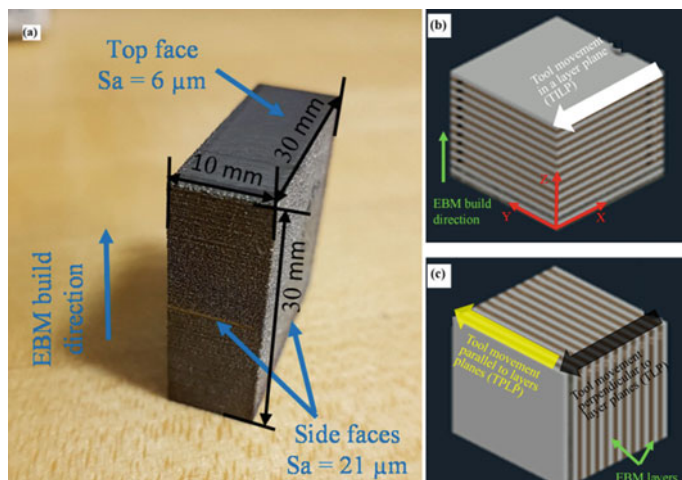


Fig. 13.5 Workpiece manufactured by EBM, **a** EBM build direction, top and side faces, **b** TILP, **c** TPLP, TLP and EBM layers [11]

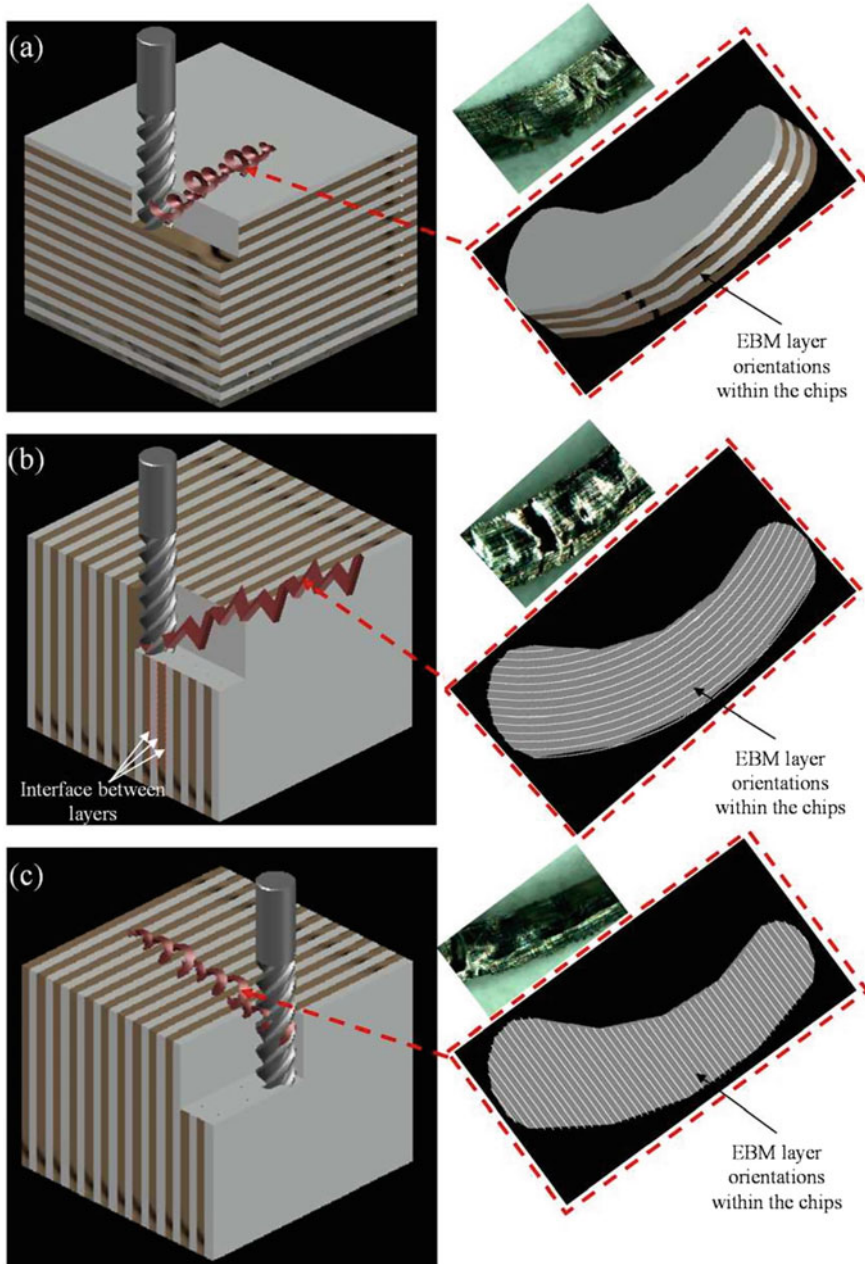


Fig. 13.6 Effect on the chip formation of layer orientations, **a** TILP, **b** TLP and **c** TPLP [11]

Chenbing et al., investigated impacts of laser scanning directions (0° , 67.5° and 90°) and machining surfaces (top and front) (Fig. 13.7) on milling performance using different cutting speed (1000–2000–3000 and 4000 rpm), feed (0.01–0.02 and 0.03 mm/tooth) and depth of cut (0.2 mm) parameters in SLMed and ASTM B235 annealed Ti-6Al-4V alloys. They stated that CF causes surface morphology and roughness on various machining surfaces due to the highly anisotropic structure of the SLMed alloy. While the machined SQ on the top surfaces of 0° and 90° SLMed Ti-6Al-4V alloys was significantly better than the front surface at low cutting speed, it was determined that the SQ on the front surface was slightly better than on the top surface in 67.5° laser scanning. It has been revealed that the SR of the top and front surfaces of SLMed Ti-6Al-4V alloys has a different growth tendency as the feed rate increases. In addition, it has been determined that the SR of these alloys is more sensitive in terms of cutting speed compare to the annealed alloy (Fig. 13.8) [17].

Lizzul et al. investigated the anisotropic effect on the SQ of Ti-6Al-4V alloy manufactured by L-PBF AM technique in both vertical and horizontal directions after milling. Tests were carried out using different cutting speed (30 and 60 m/min), feed rate (0.01 and 0.05 mm/tooth), constant depth of cut (0.2 mm) and diameter of 2 mm uncoated tungsten carbide cutting tools. In general, it was observed that the 0° orientation was comparable in SR to the 90° orientation, and higher peaks were observed in the 0° orientation samples with increasing feed per tooth (Fig. 13.9).

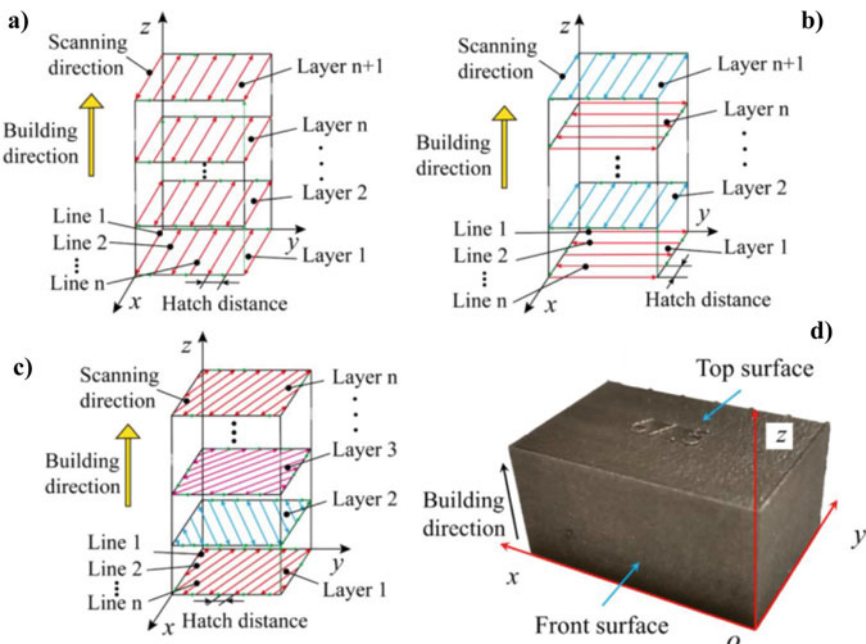


Fig. 13.7 Scanning schemes and SLMed workpiece, **a** 0° scanning view, **b** 90° rotational scanning view, **c** 67.5° rotational scanning view and **d** 67.5° SLMed workpiece [17]

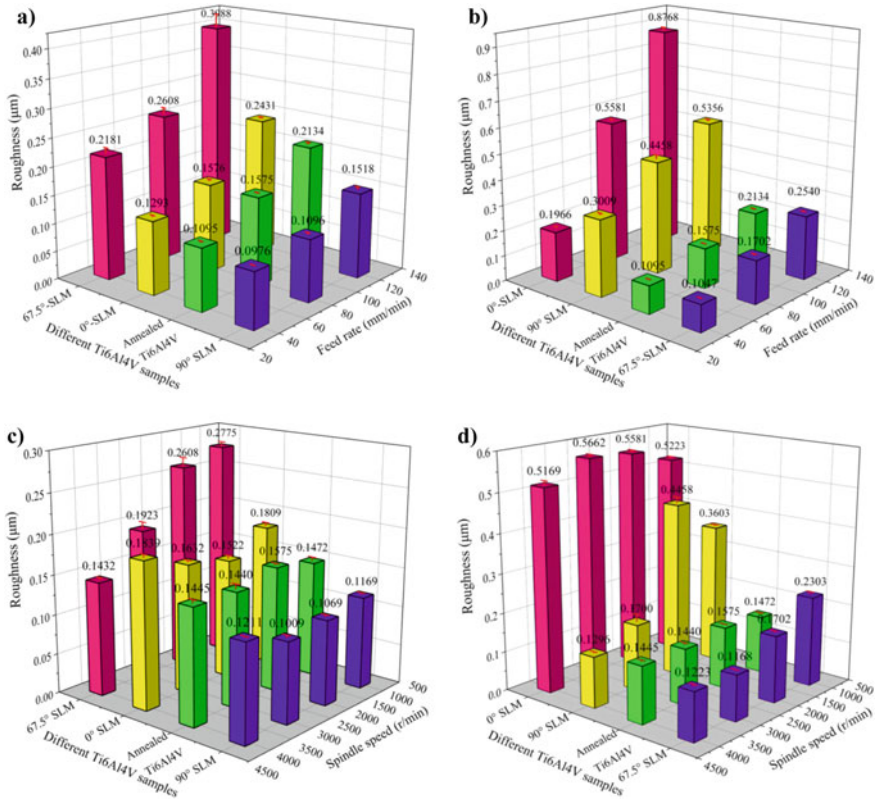


Fig. 13.8 Machined SR of various SLMed and annealed workpieces depending on spindle speed and feed rate, **a** and **c** Top surface, **b** and **d** Front surface [17]

It has been found that defects in machined surfaces are more affected by cutting parameters rather than orientations, and α GBs aid in stock removal by reducing dislocation motions that promote burr formation. According to chip morphology analysis, lower CF and cutting power were suggested for machining 0° samples instead of 90° orientation. This is underlined by the obtaining of chips with larger bend radius, which indicates the plastic flow of the material at high cutting speeds [16].

Zhang et al., examined the impacts of different cutting speed (150–200 and 250 m/min), feed (0.05–0.07 and 0.09 mm/tooth) and constant axial depth of cut (0.5 mm) conditions on CF, cutting temperature, chip morphology, SQ and TW in milling of DMLS AMed Ti-6Al-4V alloy. It has been determined that the feed rate has more effect on the CF and cutting temperature than the cutting speed. It was observed that continuous and free-broken chip structure was formed during machining. It has been stated that ideal SQ can be obtained on surfaces machined at high cutting

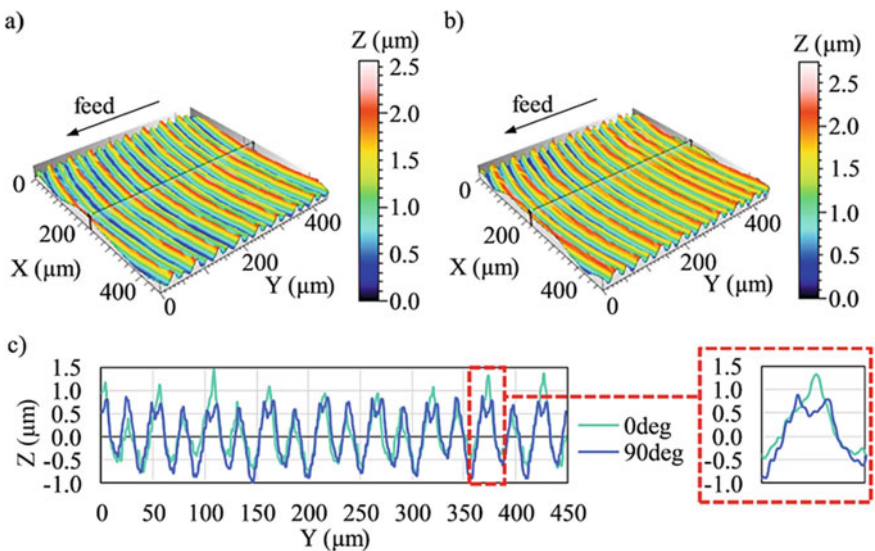


Fig. 13.9 3D SR graphs, **a** 0° orientation, **b** 90° orientation and **c** SR profiles for 0° and 90° orientations [16]

speeds, except for tool edge marks. It has been determined that micro chipping and chip adhesion wear occur due to mechanical and thermal loads [19].

13.4.2 Machining of Nickel-Based Alloys

Nickel is a versatile element that can alloy with most metals. The wide solubility ranges between iron, chromium and nickel make many alloy combinations possible. The face-centered cubic structure of the nickel matrix (γ) can be strengthened by solid solution hardening, carbide precipitation or precipitation hardening. Nickel-based alloys such as Inconel are preferred in marine, nuclear and aerospace applications where high corrosion resistance and operating temperatures are required due to their Ni and Cr content. Especially, it is preferred for IN 625 and IN 718 AM due to its good weldability [18]. Machining is required in the second step in order to meet the dimensional stability and SQ requirements of laser additive manufacturing (LAM) parts in practical applications in industrial areas [20]. The machinability index of Inconel 718 is 12 which means that it is difficult to machine compared to low carbon steel (AISI 1018) with a value of 100. Therefore, this material is defined as “difficult to cut” in the literature [21]. Current studies in the literature on the machining of nickel-based AMed alloys are still going on. Karabulut and Kaynak investigated the surface properties obtained by drilling Inconel-718 produced by wrought and

SLMed. They used different cutting speed (15 and 30 m/min), feed rate (0.025–0.05 and 0.075 mm/rev) and uncoated carbide drill diameter of 6.8 mm. It has been stated that the hole surface properties of the drilled using AMed workpieces are poor. Therefore, it is stated that these surfaces must be machined after the SLM process. It was determined that the SR values changed between 1.5 and 3 μm after drilling. Minimum feed rate and maximum cutting speed are suggested for optimum experimental outputs. It has been determined that scratches and microhardness increase on the machined surfaces at high cutting speed and feed rates. In addition, it was stated that the SR of the AMed alloy was higher than the wrought alloy under the same cutting conditions [22]. Chen et al. investigated the machinability properties of Inconel 718 superalloys manufactured using DLMS and wrought techniques in turning with cementite and coated carbide inserts. It has been observed that coated carbide tools are suitable for DLMS workpieces. In the machining of DLMS workpieces with these tools, the CF, cutting temperature and cutting vibration values were found to be 9.63%, 6.29% and 16.67% less, respectively compared to the wrought pieces. When machining DLMS workpieces with coated cutting tools, it exhibited 12.41 min longer tool life due to crater and notch wear (Fig. 13.10) and nose breakage. It has been determined that 3.28 min shorter tool life is exhibited in the machining of wrought workpieces. It has been revealed that the machined SR

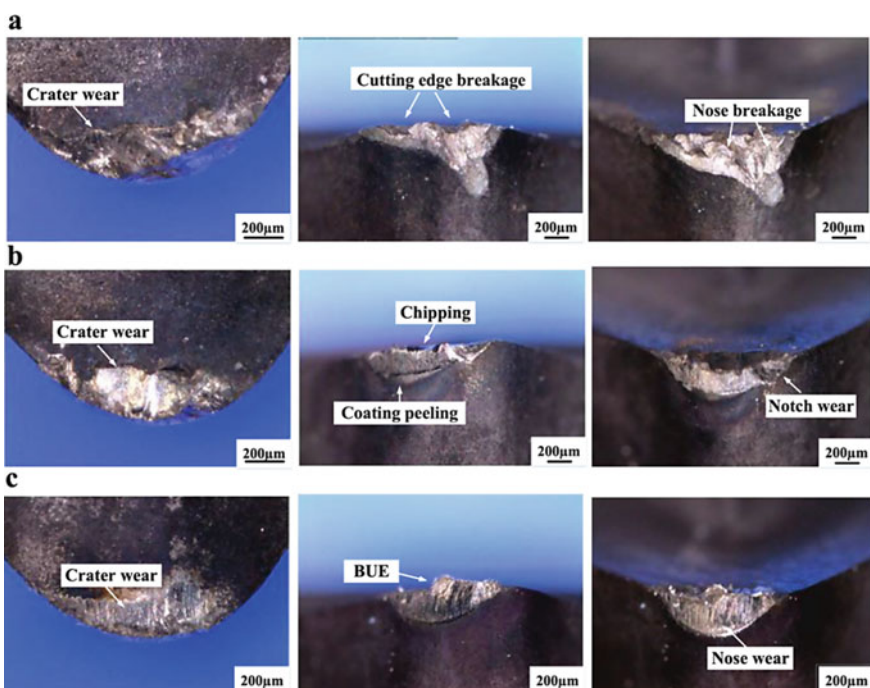


Fig. 13.10 Structure of coated carbide insert after cutting, **a** DLMS surface, **b** DLMS subsurface and **c** Wrought 718 [20]

values of the alloys manufactured with both manufacturing techniques are similar. When machining DLMS workpieces using coated carbide tools, it was observed that it performed 29.78% and 7.04% better than sintered cutting tools in terms of CF and cutting temperature, respectively [20].

Fei et al. revealed the effects of orientation direction on CF, chip formation and SQ during milling of Inconel 625 alloy manufactured using L-PBF. Therefore, they used different cutting speed (30–60 and 90 m/min) and feed rate (0.1–0.15 and 0.2 mm/rev) parameters and Ti(C,N)+Al₂O₃+TiN coated carbide insert. It has been revealed that the CF increases with the increase of cutting speed and feed rate, cutting process along the BD (build direction) or perpendicular to the BD in AMed workpieces has an effect on the CFs due to physical and microstructural properties, and the machining forces are higher if SRR=90° has been done. It has been observed that the chip has a saw-tooth structure along its inner and outer edges, and edge chipping wear type occurs on the cutting edge [23]. Jarosz et al. modeled the mechanical forces in the face milling process of Inconel 625 alloy manufactured using the L-PBF method. It has been determined that the effects of the feed per tooth value on the CF vary depending on the cutting speed and the cutting tool orientation with respect to the build direction. In addition, it was determined that the accuracy of the estimated model created for 3D CAD uncut chip models and uncut chip cross-sectional areas was high. It was stated that the error rate of the predicted model did not exceed 2.69%, and according to the experimental data it did not exceed 0.4% for the CF [24].

13.4.3 Machining of Al-Si Based Alloys

Al-Si alloys are widely used in automotive applications as well as in aerospace systems [25] to develop fuel economy by reducing vehicle weight [26]. Al-Si alloys are preferred for the manufacture of pistons and different critical equipments due to their excellent castability and wear resistance [27].

Elements are added to improve the structural, mechanical and tribological properties of these alloys. These alloys which can be produced with different casting methods can also be produced using AM technology today. Al alloys produced using AM usually consist of a combination of alloying elements such as Mg, Si or Cu. Today, while AlSi10Mg alloy is manufactured by casting technique, it is also widely manufactured using AM. It has good weldability due to its Si content close to the eutectic composition. Microstructural images of AlSi10Mg and Al 6061 alloys are given in Fig. 13.11. As a result of the conventional and AM methods have been studied the microstructural properties of these alloys in detail in the literature [18].

Considering the current studies on the machinability of Al-Si alloys manufactured using AM in the literature, Struzikiewicz et al. revealed effect of different cutting speeds (200 and 300 m/min), feed rate (0.058–0.115–0.173 and 0.249 mm/rev), depth of cut (0.5 and 1 mm) and cutting-edge radius (0.2 and 0.4 mm) values on the CF, SR and surface structure in turning of casted and DLMS AMed AlSi10Mg alloy. They

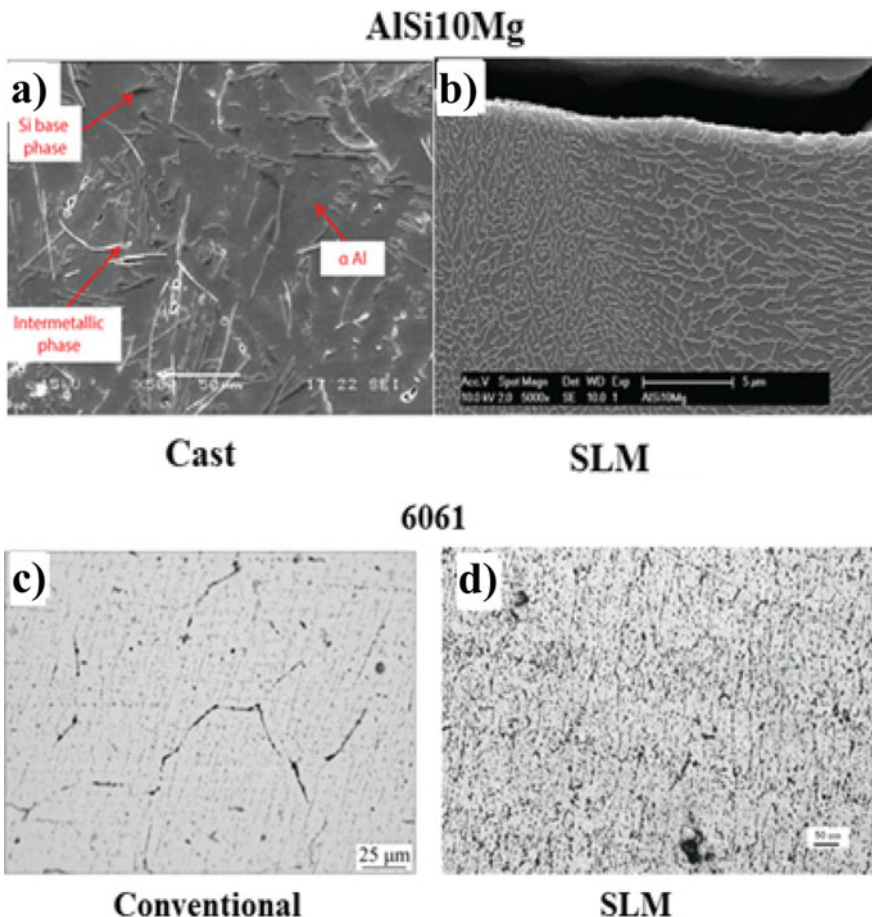


Fig. 13.11 Conventional and AMed alloys, **a** Cast AlSi10Mg, **b** SLMed AlSi10Mg, **c** Conventional Al 6061 and **d** SLM Al 6061 [18]

found that while the average SR of AMed parts increased with increasing feed rate, it decreased with increasing cutting speed (Fig. 13.12). It has been found that the CFs are higher in the cast alloy at all cutting speeds and the CFs for both alloys decrease with the increase in cutting speed. Low depth of cut and tip radius are recommended for optimum average SR, while high depth of cut and tip radius are recommended for CF in DLMS alloy [28].

Zimmermann et al., found machinability properties of two different L-PBF (L-PBF-1 and L-PBF-2) AMed processed, as-casted and T6 heat treated casted AlSi10Mg alloys using different feed per tooth (0.03–0.06 and 0.09 mm/tooth), constant cutting speed (250 m/min), depth of cut (1 mm) and diameter of 8 mm diameter cemented carbide end mill. Build up direction and cutting tool movement directions are taken into account in the cutting process (Fig. 13.13). It was observed

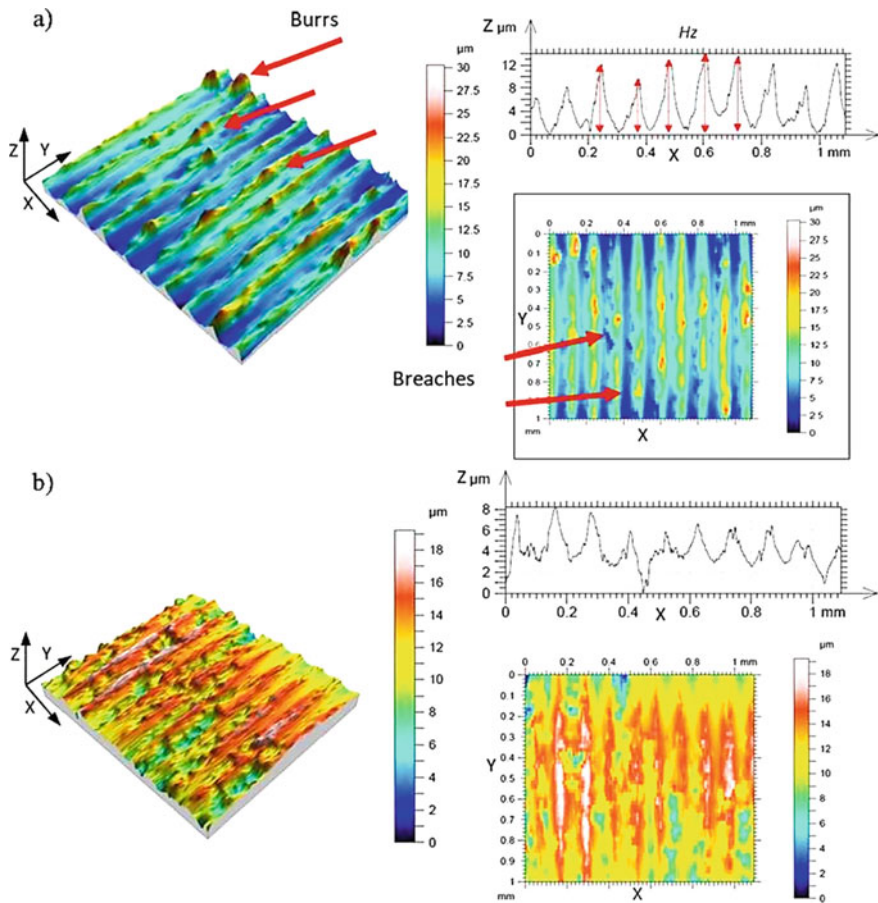


Fig. 13.12 Machined surface structures, **a** DLMS AMed workpiece and **b** Casted workpiece ($f = 0.058 \text{ mm/rev}$, $a_p = 0.5 \text{ mm}$, $V_c = 200 \text{ m/min}$) [28]

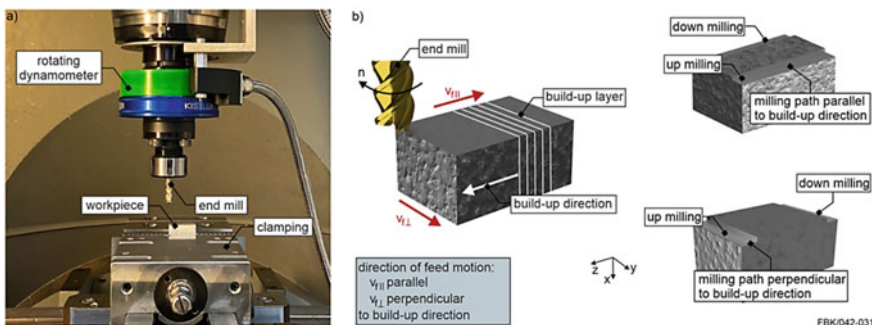


Fig. 13.13 Machining strategy of AMed workpieces, **a** Experimental mechanism and **b** Tool movement and build-up directions [29]

that there was no difference in the chip formation mechanism for all materials, however, spiral chip segments were observed for AMed workpieces, while the chip form was discontinuous in the cast alloy. Higher CFs were measured compared to AMed workpieces, despite 7% less hardness in the milling of casted alloy. They determined that this may be high degree of plastic deformation effect due to the rough microstructure of the cast alloy. While it was determined that the SR in the machining of cast alloys was less than that of AMed parts, it was observed that the material with 60 μm layer thickness (L-PBF-1) did not depend on the direction of the tool movement according to the build-up direction. It was determined that the SR increased in the case of build-up direction perpendicular to the tool movement direction in AMed workpieces with 30 μm layer thickness (L-PBF-2). In addition, it has been stated that burr formation is observed in the inlet and outlet side edges of the casted workpieces, while in no case burrs occur in machining of AMed workpieces [29].

Struzikiewicz and Sioma revealed the SR and defect formation after machining in the turning of DLMS AMed AlSi10Mg alloy using carbide inserts, different cutting speed (200 and 300 m/min), feed rate (0.06; 0.12–0.17 and 0.25 mm/rev), insert tip radius (0.2 and 0.8 mm) and depth of cut (0.5 and 1.0 mm). The optimum values for the SQ were determined as feed rate of 0.06 mm/rev, depth of cut of 1 mm and insert tip radius of 0.8 mm. It was determined that the SR decreased with the increase of cutting speed. In addition, it has been found that the cause of breaches and deformations (Fig. 13.14) on the machined surface is the layer structure of the sintered aluminum and the method and conditions of joining the material particles during sintering [30].

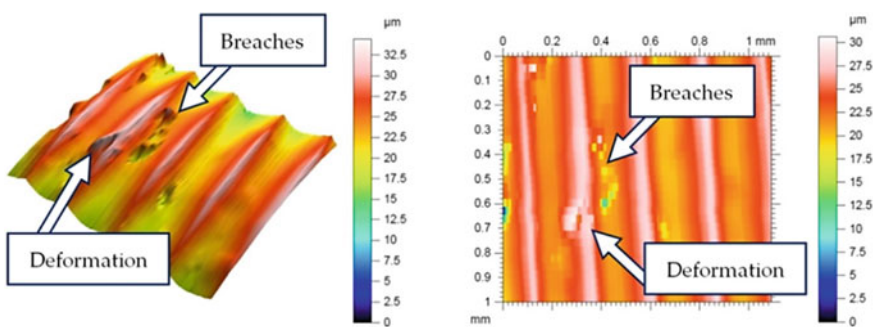


Fig. 13.14 Breaches and deformation in machining of AM workpiece ($f:0.25 \text{ mm/rev}$, $a_p:0.5 \text{ mm}$, $V_c:300 \text{ m/min}$, $r_e:0.8 \text{ mm}$) [30]

13.4.4 Machining of Other AMed Workpieces

Iron-based alloys are among the most common engineering materials used today [18]. It is widely used due to its hardness, corrosion and wear resistance as well as low price factors. Today, a large number of various steels can be manufactured using AM techniques. Various matrix structures, phases (austenite, ferrite, martensite) and precipitation stages contribute to obtain structural and mechanical properties. This also applies to steel materials manufactured using AM [31]. Hardness and mechanical properties come to the fore in the machining of steels. The change in the properties depending on microstructural changes also affects the machinability of these materials. Although there are differences in the internal structures of the materials manufacture using AM, manufacturing-related defects also occur. Therefore, it is important to shape the materials manufactured using the AM method to be used as a final product. In some studies, in the literature, Bai et al. microhardness, CF, SR, TW and chip formation in milling without heat treatment and heat-treated of maraging steels (18Ni300) manufactured using SLMed with constant cutting speed (245 m/min), feed rate (468 mm/min) and depth of cut (0.15 mm) with PVD-TiCN+TiN coated carbide inserts analyzed. As-built top (ABT) and as-built side (ABS) criteria were taken into account according to the milling direction during machining (Fig. 13.15). It was stated that the microhardness after machining increased in both as-built and heat-treated condition. It has been observed that the CF, TW and surface hardness of the ABT workpiece are higher than the ABS workpiece. While the CFs and TW increased sharply after aging treatment, it was determined that there was a small change in the workpieces subjected to as-built and solution treatment. It was found that the SR of as-built workpieces decreases after machining, and aging treatment causes adhesion on the tool surface and a high amount of chip curling (Fig. 13.16). As-built and solution treated workpieces exhibited smaller serration and continuous chip structure, while larger serrations occurred in aging treated workpieces in terms of chip morphology [15].

Tamura ve Matsumura analyzed the CF in milling of wrought and SLMed AISI 420 stainless steel workpieces using different cutting speed (20 and 50 m/min), feed rate (0.05 and 0.1 mm/tooth), constant depth of cut (1 mm), two-fluted uncoated

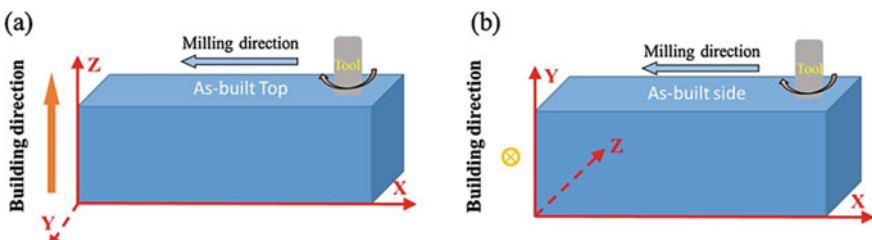


Fig. 13.15 Schematic views for the post-processing of machining: **a** Top surface and **b** Side surface of maraging steel manufactured by SLM [15]

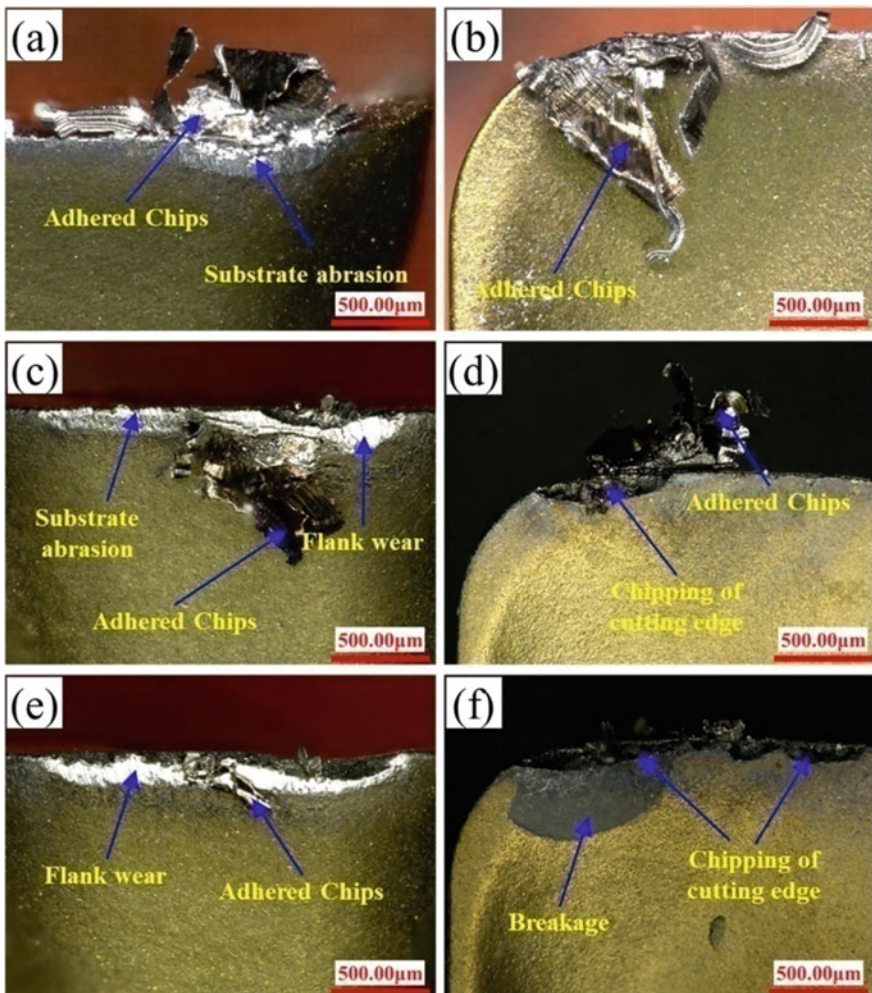


Fig. 13.16 TW formations on the cutting insert, **a** Adhere and abrasion in HT4 (520°C and 12 h) part by 5 passes, **b** Adhered chip on the rake face in HT4 part by 5 passes, **c** Adhered, abrasion and flank wear in HT4 part by 10 passes, **d** Chipping and adhered structure in HT4 sample by 10 passes, **e** Flank wear and adhered in HT6 (900°C and 1 h) sample by 10 passes and **f** Breakage and chipping in HT6 part by 10 passes [15]

straight and helical carbide end mills. As a result of the tests, it was determined that the CFs of both materials were equal and the shear angle of SLMed was greater than the orthogonal cutting [32]. Bai et al., stated machinability properties in turning of ASTM A131 steel manufactured using DED (top and side) (Fig. 13.17a, b) and hot rolled (HR) (Fig. 13.17c) with PVD TiCN+TiN coated carbide inserts at different cutting speeds (150 and 250 m/min), feed rate (286 and 477 mm/min) and constant depth of cut (0.3 mm). It was revealed that the microhardness is 30% higher than

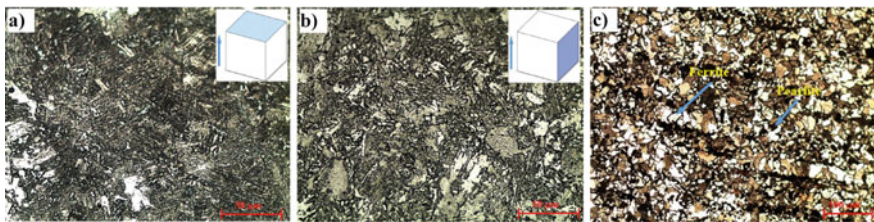


Fig. 13.17 ASTM A131 workpieces, **a** DED-top face of workpiece, **b** DED-side face of workpiece and **c** Hot rolled A131 [33]

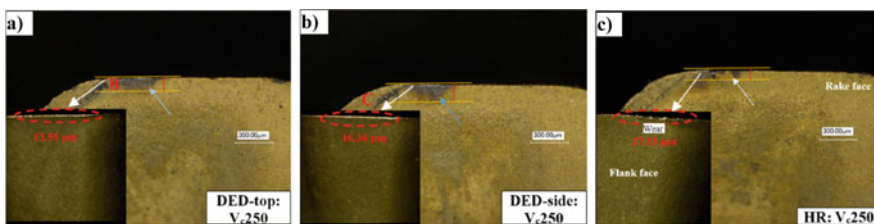


Fig. 13.18 TW on the cutting edge, **a** DED-top (V_c : 250 m/min), **b** DED-side (V_c : 250 m/min) and **c** HR (V_c : 250 m/min) [33]

HR in the machining of DED-top face, and the highest CFs are measured in DED-side workpieces due to the interaction between the cutting tool and the melt-pool boundaries that restrict the material flow. It was observed that while TW is more (Fig. 13.18) in machining of DED workpieces, burr formation is less. In addition, it was stated that high cutting speed improves SQ in all materials and $R_a = 0.41 \mu\text{m}$ was measured for DED workpieces [33].

13.4.5 Machining Quality and Its Performance

Machining covers many different manufacturing processes. These manufacturing processes are determined according to needs. The aim is to get maximum efficiency from a product in the operation environment. For this, it is extremely important to use the optimum manufacturing method for product quality. AM method is among the current manufacturing techniques. Unlike subtractive processes such as turning, milling and drilling, it is based on addition. It can also be preferred for manufacturing that is not possible with subtractive methods or for prototype-based manufacturing. In addition, it is not possible to use the product manufactured with this technique in the final systems or to obtain the desired SQ in some cases. Therefore, subtractive manufacturing techniques are used as a secondary process. AMed workpiece quality should be determined by optimizing many factors such as laser scanning speed, laser power, scanning strategy, hatch spacing, laser spot size and layer thickness. In

many studies, it has been determined that different methods are used in materials manufactured using AM. However, it has been demonstrated that the laser scanning strategy and direction affect the anisotropy of the material. It has been observed that this situation causes differences in the performance of machining outputs (such as CF, SR, TW, machined surface hardness) on different surfaces of AMed parts. It has been observed that the performance of AMed parts is compared with other manufacturing methods such as casting and wrought. As a result of machining different oriented surfaces with the effect of anisotropic properties of AMed workpieces, negative effects of machining performance are observed due to low SQ. It is necessary to evaluate in two stages; before-AMed and after-AMed. It is extremely important to optimize the AM process parameters in the before-AMed process and the machining parameters in the after-AMed process. AMed parts will be able to be used as a high performance product in mechanical systems in terms of product service life by controlling these processes.

13.5 Concluding Remarks

Thanks to AM, it is possible to create physical parts with digital data by using the innovations provided by advanced technologies. Rapid prototyping, the ability to manufacture complex geometries, freedom of design and similar geometric properties increase due to AM methods. However, this technique also includes negative effects such as undesirable microstructural defects, dimensional tolerance errors, poor SQ and morphology. Secondary machining processes such as turning, milling and drilling are required for AMed workpieces in order to achieve optimum product quality, SQ and geometric tolerance. In the literature, it has been determined that the microstructure, mechanical and machinability properties of titanium, aluminum and stainless steel materials generally manufactured using AM have been investigated. It is observed that alloys such as Ti6Al4V, Inconel 625, Inconel 718, AlSi10Mg, 18Ni300, AISI 420, AISI 316L and ASTM A131 are among them. It has been stated that the anisotropic structure of the material, the machining direction, the process parameters and AMed techniques are generally effective on the machinability properties of the applied machining methods to use these alloys as the final product mechanical systems. EBM, SLM, DED, DLMS ve L-PBF have been widely used in terms of AMed techniques. It was revealed that the SQ of the workpieces using AM was improved by machining. It was stated that 0° , 67.5° and 90° are used in terms of scanning strategies and different machinability outputs are measured in CF, SR, TW, surface morphology, burr formation and chip morphologies according to machining direction and material combinations. Literature studies have shown that combinations of high cutting speed and low feed rate improve machinability outputs. In addition, the effects of different heat treatment (T4, T5 and T6) properties on experimental outputs are also presented. The machinability properties of AMed workpieces are generally compared to workpieces manufactured by wrought and casting in terms of

manufacturing methods. Thus, alternative options are presented for mass or prototype production. Current researches on AM is still going on. According to current machinability studies, it is predicted that AMed parts can be used as mechanical components in machine systems.

References

1. Abdulhameed, O., Al-Ahmari, A., AmeenAmeen, W., Mian, W.: Additive manufacturing: challenges, trends, and applications. *Adv. Mech. Eng.* **11**(2), 1–27 (2019)
2. Didier, P., Le Coz, G., Robin, G., Lohmuller, P., Piotrowski, B., Moufki, A., Laheurte, P.: Consideration of SLM additive manufacturing supports on the stability of flexible structures in finish milling. *J. Manuf. Proc.* **62**, 213–220 (2021)
3. Gisario, A., Kazarian, M., Martina, F., Mehrpouya, M.: Metal additive manufacturing in the commercial aviation industry: a review. *J. Manuf. Syst.* **53**, 124–149 (2019)
4. Gibson, I., Rosen, D.W., Stucker, B., Khorasani, M.: *Additive Manufacturing Technologies*. Springer, New York (2014)
5. Majeed, A., Zhang, Y., Ren, S., Lv, J., Peng, T., Waqar, S., Yin, E.: A big data-driven framework for sustainable and smart additive manufacturing. *Rob. Comp. Integ. Manuf.* **67**, 102026 (2021)
6. Gong, H., Rafi, K., Gu, H., Starr, T., Stucker, B.: Analysis of defect generation in Ti-6Al-4V parts made using powder bed fusion additive manufacturing processes. *Addit. Manuf.* **1–4**, 87–98 (2014)
7. Xing, H., Zou, B., Li, S., Fu, X.: Study on surface quality, precision and mechanical properties of 3D printed ZrO₂ ceramic components by laser scanning stereolithography. *Ceram. Int.* **43**, 16340–16347 (2017)
8. Liu, S., Shin, Y.C.: Additive manufacturing of Ti6Al4V alloy: a review. *Mater. Des.* **164**, 107552 (2019)
9. Vafadar, A., Guzzomi, F., Rassau, A., Hayward, K.: Advances in metal additive manufacturing: a review of common processes, industrial applications, and current challenges. *Appl. Sci.* **11**(3), 1213 (2021)
10. Maleki, E., Bagherifard, S., Bandini, M., Guagliano, M.: Surface post-treatments for metal additive manufacturing: progress, challenges, and opportunities. *Addit. Manuf.* **37**, 101619 (2021)
11. Dabwan, A., Anwar, S., Al-Samhan, A.M., Nasr, M.M.: On the effect of electron beam melted Ti6Al4V part orientations during milling. *Metals* **10**(9), 1172 (2020)
12. Bhuvanesh Kumar, M., Sathiya, P.: Methods and materials for additive manufacturing: a critical review on advancements and challenges. *Thin-Wall. Struct.* **159**, 107228 (2021)
13. Panwisawas, C., Tang, Y.T., Reed, R.C.: Metal 3D printing as a disruptive technology for superalloys. *Nat. Com.* **11**, 2327 (2020)
14. Bandyopadhyay, A., Zhang, Y., Bose, S.: Recent developments in metal additive manufacturing. *Curr. Opin. Chem. Eng.* **28**, 96–104 (2020)
15. Bai, Y., Zhao, C., Yang, J., Hong, R., Weng, C., Wang, H.: Microstructure and machinability of selective laser melted high-strength maraging steel with heat treatment. *J. Mater. Proc. Technol.* **288**, 116906 (2021)
16. Lizzul, L., Sorgato, M., Bertolini, R., Ghiootti, A., Bruschi, S.: Anisotropy effect of additively manufactured Ti6Al4V titanium alloy on surface quality after milling. *Prec. Eng.* **67**, 301–310 (2021)
17. Ni, C., Zhu, L., Zheng, Z., Zhang, J., Yang, Y., Hong, R., Bai, Y., Lu, W.F., Wang, H.: Effects of machining surface and laser beam scanning strategy on machinability of selective laser melted Ti6Al4V alloy in milling. *Mater. Des.* **194**, 108880 (2020)
18. Cooke, S., Ahmadi, K., Willerth, S., Herring, R.: Metal additive manufacturing: technology, metallurgy and modelling. *J. Manuf. Proc.* **57**, 978–1003 (2020)

19. Zhang, H., Dang, J., Ming, W., Xu, X., Chen, M., An, Q.: Cutting responses of additive manufactured Ti6Al4V with solid ceramic tool under dry high-speed milling processes. *Ceram. Int.* **46**, 14536–14547 (2020)
20. Chen, L., Xu, Q., Liu, Y., Cai, G., Liu, J.: Machinability of the laser additively manufactured Inconel 718 superalloy in turning. *Int. J. Adv. Manuf. Technol.* **114**, 871–882 (2021)
21. Mahesh, K., Philip, J.T., Joshi, S.N., Kuriachen, B.: Machinability of Inconel 718: a critical review on the impact of cutting temperatures. *Mater. Manuf. Proc.* **36**(7), 753–791 (2021)
22. Karabulut, Y., Kaynak, Y.: Drilling process and resulting surface properties of Inconel 718 alloy fabricated by selective laser melting additive manufacturing. *Proc. CIRP.* **87**, 355–359 (2020)
23. Fei, J., Liu, G., Patel, K., Öznel, T.: Effects of machining parameters on finishing additively manufactured nickel-based alloy inconel 625. *J. Manuf. Mater. Proc.* **4**, 32 (2020)
24. Jarosz, K., Patel, K.V., Öznel, T.: Mechanistic force modeling in finish face milling of additively manufactured Inconel 625 nickel-based alloy. *Int. J. Adv. Manuf. Technol.* **111**, 1535–1551 (2020)
25. Miracle, D.B.: Metal matrix composites—from science to technological significance. *Compos. Sci. Technol.* **65**(15–16), 2526–2540 (2005)
26. Abdelaziz, M.H., Samuel, A.M., Doty, H.W., Valtierra, S., Samuel, F.H.: Effect of additives on the microstructure and tensile properties of Al–Si alloys. *J. Mater. Res. Technol.* **8**(2), 2255–2268 (2019)
27. Samuel, E., Samuel, A.M., Doty, H.W., Valtierra, S., Samuel, F.H.: Intermetallic phases in Al–Si based cast alloys: new perspective. *Int. J. Cast. Metals. Res.* **27**(2), 107–114 (2014)
28. Struzikiewicz, G., Zębala, W., Ślodziński, B.: Cutting parameters selection for sintered alloy AlSi10Mg longitudinal turning. *Measurement* **138**, 39–53 (2019)
29. Zimmermann, M., Müller, D., Kirsch, B., Greco, S., Aurich, J.C.: Analysis of the machinability when milling AlSi10Mg additively manufactured via laser-based powder bed fusion. *Int. J. Adv. Manuf. Technol.* **112**, 989–1005 (2021)
30. Struzikiewicz, G., Sioma, A.: Evaluation of surface roughness and defect formation after the machining of sintered aluminum alloy AlSi10Mg. *Materials* **13**(7), 1662 (2020)
31. Bajaj, P., Hariharan, A., Kini, A., Kürnsteiner, P., Raabe, D., Jägle, E.A.: Steels in additive manufacturing: a review of their microstructure and properties. *Mater. Sci. Eng. A* **772**, 138633 (2020)
32. Tamura, S., Matsumura, T.: Cutting force in milling of additive manufacturing AISI 420 stainless steel. Paper presented at ESAFORM 2021. In: 24th International Conference Material Forming Liège, Belgique
33. Bai, Y., Chaudhari, A., Wang, H.: Investigation on the microstructure and machinability of ASTM A131 steel manufactured by directed energy deposition. *J. Mater. Proc. Technol.* **276**, 116410 (2020)

Chapter 14

Challenges Involved in Framing Additive Manufacturing Standards



V. S. Rajashekhar and R. Ruban

14.1 Introduction

Additive Manufacturing (AM) is a bottom-up method of building 3D objects and assemblies. It is also known as three-dimensional printing. This method is commonly referred to as 3D printing. A layer by layer technique is used in this method that results in building custom parts and components using various materials like ceramics, composites, metals and polymers. In the recent years, advanced materials like biomaterials, semiconductors, smart materials [1] (like piezoelectric ceramics, shape memory alloys and magnetostrictive materials) and nano-engineered materials [2] are also being used for AM. This broadens the scope for adopting AM processes.

In the past decade, standards are being framed for AM processes which will enable the AM technology to attain mass manufacturing capabilities. The usage of computers for simulating and controlling the feedstock materials during AM processes is a common practice [3] which involves various process parameters of the AM device to be considered. When computers are being used, manufacturing systems face security challenges due to the recent developments in networking [4] for implementing Industry 4.0 [5]. The importance of cyber security for digital manufacturing has been emphasized in the recent years [6, 7] due to the highly competitive product based market. It is also due to Industry 4.0 [8], which uses modern technologies for automating traditional methods in manufacturing. With the increasing rate of industrial control systems being subjected to cyber attacks in the past decade [9], importance has to be given to detect [10, 11] and prevent them from occurring. The

V. S. Rajashekhar (✉)

Department of Aerospace Engineering, Indian Institute of Science, Bangalore, Karnataka, India

R. Ruban

Mechanical Engineering Department, National Institute of Technology, Tiruchirappalli, Tamil Nadu, India

taxonomy models [12] help in identifying the impact of threats, attack and vulnerability to industrial control systems. The AM process chain has to carefully handled to prevent theft of data at all levels [13].

In this chapter, we discuss the role of standardization for AM technologies. Further we focus on the challenges faced at various stages in the AM process chain that will help us in framing better universal standards and guidelines. This chapter is organized as follows: The Sect. 14.2 discusses about the current standards and processes being used in AM technology. In the Sect. 14.3, the challenges involved in material selection, their limitations and the Cyber-Physical security of AM devices are discussed. In Sect. 14.4, the future directions that would help in framing better standards and guidelines for a foolproof AM technology are given. The chapter ends with the concluding remarks made in Sect. 14.5.

14.2 Standardization of Additive Manufacturing Technology

14.2.1 Standards

The additive manufacturing technology is going to be used for industrial production in the near future [14]. The activities for standardization at all levels of this technology is being carried out by various international organizations [15]. By setting the standards for AM technology will be useful for several purposes like process selection, equipment design, defect identification and inspection [16]. In the year 2009, American Society for Testing and Materials (ASTM) formed Committee F42 on Additive Manufacturing Technologies to develop standards for AM technologies [17]. The roadmap for standardising the additive manufacturing process has been laid by ASTM [18]. The committee accepts ideas for new standards and is also open for modifying existing documents. The ASTM F42/ISO TC 261 standards for AM include:

1. AM process and equipment standards.
2. General standards.
3. Application specific standards.
4. Feedstock material standards.
5. Finished AM part standards.

The technical subcommittees of Committee F42 on Additive Manufacturing Technologies deal with the test methods, design specifications, materials and processes standards, terminologies, strategic planning and Technical Advisory Groups (TAGs) to International Organization for Standardization (ISO). Since the year 2011 both ISO and ASTM collaboratively work to develop International Standards for the additive manufacturing industry. These standards should be followed for the ease of implementing AM processes considering their technical and economic aspects for industries.

14.2.2 Process

Several AM processes have been developed in the past three decades [19, 20] which finds applications in the aerospace [21, 22], robotics [23, 24], medicine [25] and construction industries [26]. The AM processes approved by *ASTM—Committee F42 on Additive Manufacturing Technologies* include:

1. Binder Jetting.
2. Directed Energy Deposition.
3. Material Jetting.
4. Material Extrusion.
5. Powder Bed Fusion.
6. Sheet Lamination.
7. Vat Photo Polymerization.

It is to be noted that these processes rely on automation and computer control which leads to monitoring of several parameters in the AM system. The selection of a suitable AM process should be based on the type of material and their properties, technological limitations due to the nature of material, surface quality, post-processing requirements and tolerance levels of the part to be fabricated [27]. A study on usage of industrial robots for AM reports that robots are viable for certain AM processes [28]. In the recent past, several robot-assisted AM processes like directed energy deposition, photo polymerization and other extrusion based method have been carried out [29]. These robot assisted AM process find applications in the construction industries [30] as it is proving to be economical.

The stages involved in a particular AM process depends on several factors such as the nature of feedstocks. The general AM process chain is shown in Fig. 14.1. It starts with the preparation of CAD models in contrast to the traditional methods that involve preparation of drawings. The 3D file formats proposed for AM include STEP, X3D (VRML), PLY, SAT, OBJ, DXF, 3DS and SLC [31]. Then the CAD model is converted to a file format (mostly STL format) that contains various information about the part such as surface geometry to be produced like meshes [32]. Although the STL format contains flaws [33], it is being widely used since it is a simple and portable format. In the next stage, the STL file is sliced using a slicing software. It generates the tool path file (also known as G-Code) that can be read by the AM

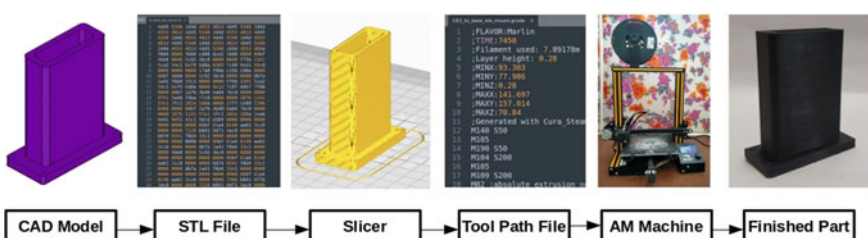


Fig. 14.1 The additive manufacturing process chain

machine. The AM machine executes the instructions given to it and produces the finished part. This part is sent for post processing and inspection. It is then tested using non-destructive methods such as ultrasonic testing [34] and Laser ultrasonic technique [35] to evaluate various properties that can ensure part quality. The process chain for AM has to be decided in the early stages of product development for better work-flow.

14.3 Challenges in Additive Manufacturing Process Chain

14.3.1 Materials Selection

The phase diagrams play an important role in understanding the correlation between various properties of an alloy. The properties of a new alloy has to be thoroughly understood by studying their phase diagrams. This will enable to understand their mechanical properties. Understanding of these properties would give knowledge about various phenomena that is important during AM process [36]. Application centred development of metal alloys for AM [37] will aid in immediate commercialisation.

The common feedstock materials for metal used in AM methods are metal powders and metal rods [3]. The challenges for metals being used for AM are their reaction to atmosphere in their powder form, their reflective and thermal behavior to heat source, and their residual stresses that lead to deformation of parts [38]. Characterization and flowability studies have to be done for metal powders in order to match their properties to a particular AM machine. This would aid in consistent production. A metal powder that is fit for AM method should have good predictable flowability properties (for layer generation) to ensure good quality products [39]. The methods and equipments used for evaluating the flowability properties of new metal powders should be emphasized rather than focusing on their nature and properties. When flowability of different metal powders were studied using different methods, they exhibited similar behavioural changes [40]. A detailed review highlighting the progress of new materials for AM [37] reports preparation methods for metals like aluminium, magnesium, titanium, steel and other inter-metallic compounds to adapt for the AM environments. Therefore the selection of metals and their alloys for different AM processes have to be dealt with at most importance.

14.3.2 Materials and Design Limitation

The materials that have smaller grain size are harder and stronger. The relation between the yield strength and grain size is given by Hall–Petch equation which

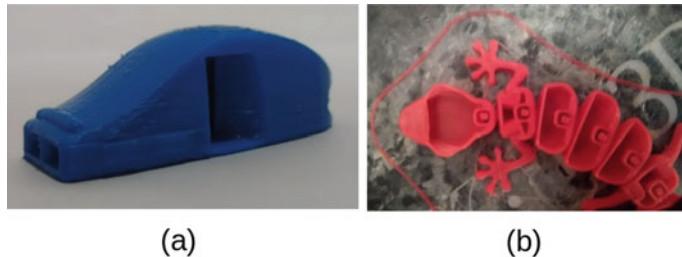


Fig. 14.2 The AMed parts without support materials: **a** An additively manufactured whistle (without any internal support material) that can be used during emergency; **b** An articulated design is being built with hollow parts on an AM machine which are light in weight and requires no assembly post printing

considers the grain diameter as a variable [36]. This relation has to be given importance while preparing metal powders. The main challenge is to obtain desired properties for AMed components by designing their raw material [37]. Although the role of AM is to give design freedom, the design standards for AM is yet to be established [41]. This causes differences in the Computer- Aided Design (CAD) and component that is produced. Therefore a mapping method has to be created which can create a relation between the CAD model, materials and the AM process to be used.

The tolerances during assembly of AMed parts should be considered during the design stages. In certain cases, the design can be AMed without any internal supports like a whistle that is shown in Fig. 14.2a. In order to make the AMed parts lighter in weight and buoyant, hollow designs can be created. The Fig. 14.2b shows an hollow part being AMed. The properties of certain metals like aluminium such as poor flow ability, high thermal conductivity and high reflectivity makes it challenging for AM [41]. The reduction of grain size enhances the strength and toughness in many alloys. The quality of the fabricated part depends on the AM device conditions, environmental conditions and the material properties. The fabricated part can suffer due to shrinkage during secondary processes which is unpredictable. This is due to non-uniform cooling and results in 0.8–2% shrinkage [39]. Therefore the limitations of materials for a particular design and vice-versa should be studied for better decision making during prototyping phases.

14.3.3 Cyber-Physical Security

The AM devices are either controlled or monitored by computer based processes. They form a cyber-physical system which are prone to attacks. With the future focusing on Industry 4.0 which would lead to digital transformation of AM, the focus should also be towards the threats that it would pose for industries. The theft of proprietary designs, intellectual property [42, 43] and the material characteristics from the AM devices would create unpredictable problems. As mentioned in [44, 45]

the AM devices could be used as weapons of destruction. Although the challenges in securing the AM devices from cyber-physical attacks is important [46], less focus is given to the related research areas.

In the recent times, the AM devices can be attacked in two aspects [47] as follows: (1) Damaging the AM related hardware and software (2) Altering the process parameters of the AM devices. The first aspect of damaging the AM device can be done by attacking the supply chain, altering the software features by auto-updating the software and firmware, and modifying the CAD models. The second aspect of altering the process parameters at different stages include.

1. Varying the scale of CAD models to cause assembly problems.
2. Modifying the G-Code properties to alter the build characteristics [48].
3. Changing the orientation of the 3D object during slicing in-order to increase the build time.
4. Altering the feed rate of wires/filament to produce poor quality parts.
5. Modifying the temperature of heating element in the AM device during critical stages of the process to alter the quality of part being produced.
6. Modifying the support material characteristics to hamper the build quality.

With Internet of Things (IoT) starting to play a role in AM [49], prevention of security breach at any level of the AM process chain is crucial. Therefore steps must be taken by framing guidelines and setting standards to ensure safety and security of AM process chain that paves way for intelligent production systems [50].

14.3.4 Standards and Guidelines

Identifying the levels of continuity and isotropy in an AMed part is crucial for setting inspection and test standards [51]. The development of standards for AM technology is primarily hampered due to the lack of testing and inspection procedures for AMed components [52]. To prevent threats for the AM devices, standards for communication protocols have to be established at all levels of the process chain to identify the causes, effects and the actions to be taken. A thorough study has to be done about the existing methods to frame the guidelines to be followed in order to prevent cyber-physical attacks. This can be done by analysing the attack descriptions using a language such as Cyber-Physical Attack Description Language (CP-ADL) [53] or using Petri net modelling to tackle coordinated attacks [54]. Attacks on AM systems during run-time to modify the control and physical parameters can be detected using Kinetic Cyber-Attack Detection (KCAD) method [10]. This method has been has been experimentally tested resulting in 77.45% accuracy.

Calibration of various AM devices and materials is a tedious task. In Fig. 14.3a, an AM key using a wrong material is made due to lack of calibration methods for the initially intended material. In Fig. 14.3b, a calibration cube is produced using a particular material to assess the status of a AM device. The same cube is place over light source in Fig. 14.3c to check the material nature. In Fig. 14.3d, the delamination

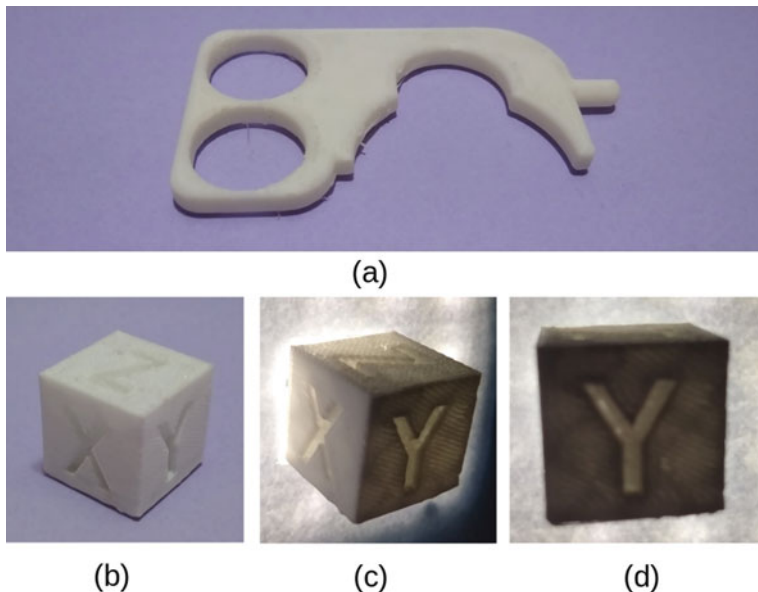


Fig. 14.3 Standards for materials selection and AM machines calibration have to be done often to reduce defects: **a** A multi-purpose additively manufactured key that can be used during pandemics made using a wrong material; **b** A calibration cube having X, Y and Z markings is printed to evaluate the alignment of AM machine axes; **c** The calibrated cube is being checked for issues related to material by placing it over bright light; **d** White light passes through the printed part indicating layer delamination due to below normal extrusion temperature

of the cube is identified. The other properties of AM processes can be considered for inspection only when standards are established.

The design standards have to be framed which would help the designers to while modelling the parts for AM. The articulated designs are fabricated using AM machines as a single part in an assembled nature. The Fig. 14.4 shows various types of failures during the initial stages of AM process. In Fig. 14.4a the failure is due to poor clearance in the part design. The slipping of the AM machine axes causes offset in prints which is as shown in Fig. 14.4b. The fabricated parts fail due to rigid joints and material shrinkage in articulated designs like the case shown in Fig. 14.4c, d respectively. The intended print is shown in Fig. 14.4e which has smooth joints.

The standards for Geometric Dimensioning and Tolerancing GD and T system has to be set in order to control the deviations in AMed components in AM devices [55]. The AMed parts fail to meet the expected standards when the CAD model is scaled. The AMed parts with scaled down designs are fragile due to thin wall structures. A case where the AMed part has broken due to this reason is shown in Fig. 14.5a. In cases where the CAD model of the part which is to be AMed is designed without considering the AM machine parameters, the parts fail due to several reasons like excessive flow of feedstock material in to the gaps in the model. The case shown in Fig. 14.5b shows such a failure of AMed part due to inappropriate CAD model. In

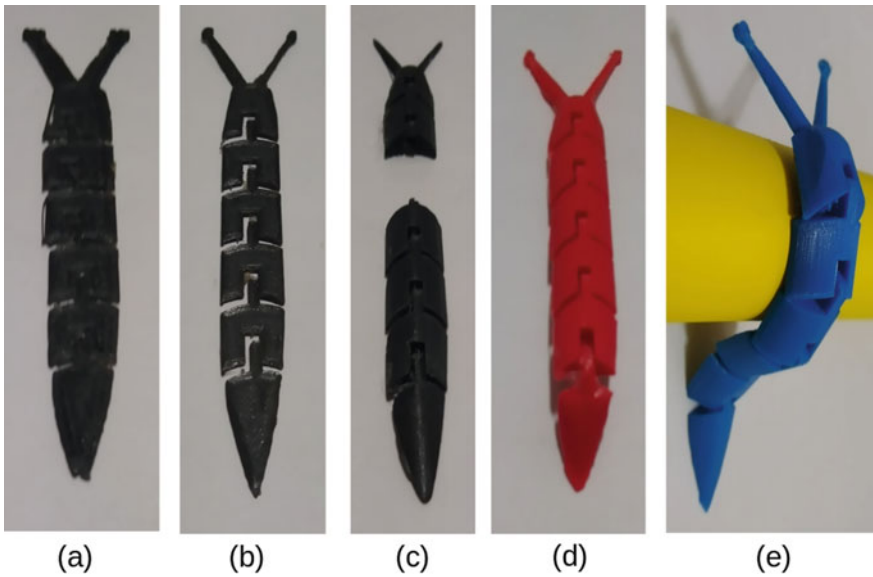


Fig. 14.4 Failure of parts that occur while printing articulated designs: **a** The series of chains start overlapping due to poor clearance in the CAD model. **b** The base layer is being offset due to slipping of an axis in the AM machine. **c** The fabricated part is broken due to rigid joints. **d** Shrink fit of joints in the printed articulated assembly causing it to be rigid. **e** The perfectly printed articulated assembly

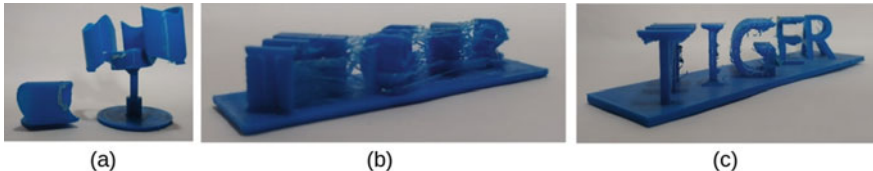


Fig. 14.5 Failure of parts related to scaling of design: **a** Broken fragile printed part due to scaling down of design. **b** Higher nozzle temperature causes the excessive material to flow in gaps during print. **c** By scaling up the design, better print quality is obtained for the same design as shown in the previous image

certain cases, this failure can be avoided by scaling up the CAD model. The Fig. 14.5c shows the same part being printed with a better quality. Failures of this kind can be prevented by setting up of design standards for a specific AM process and in some cases for a AM machine.

The STL file format, although not a standard format for AM [47], is being widely used to transfer CAD models to the slicing software. This file format is exposed to vulnerable attack since it is easily editable [56]. Guidelines for secured outsourcing models in the AM process chain have to be framed. The data needed to be transferred among design owners, manufacturing process tuning experts and AM

machine owners should be included in these outsourcing models [57]. An international standard protocol has to set for AM device owners. Many places like the United Kingdom, the AM device owners are exempted from IP constraints such as patents, trademarks and copyright if they are for non-profit and personal use [58]. Hence establishing standards and guidelines will help in sorting violations and disputes for industries that uses AM devices.

14.4 Future Directions

A lot of research works have been based on Laser based AM. In powder based AM techniques, laser source should be able to chosen properly such that the absorptivity of the powder can be increased [59]. A deeper understanding of new materials for AM process [37] is required for immediate use in various applications. The works related to electron beam melting should be focused [41] since it can be used for wide range of materials. The gaps in framing standards for AM technologies can be bridged by establishing university-industry collaboration which ensures continuous progress [60] of updating the recent advances. The combination of merits in subtractive manufacturing methods and additive manufacturing techniques can be combined in to hybrid manufacturing which can produce better products.

14.5 Conclusions

The significant contribution of additive manufacturing processes to reduce the time taken during product development stages requires focus of standardization procedures in additive manufacturing technology to face the mass production phase. The process of standardizing various elements of the AM process chain will help in creating and improving the AM technology by adopting new findings in the field of material sciences. The challenges involved in material selection and their limitations have been discussed in detail. With the Industry 4.0 playing a significant role in AM, the threats posed to cyber physical systems should be considered while setting the standards for AM technology. The other possible threats for AM technology should be identified and reported. This will help in setting the communication standards that would help in securing AM process chain. Therefore the standards for AM technology needs to be updated regularly for the additive manufacturing technology to flourish in the manufacturing sector.

References

1. Gardan, J.: Smart materials in additive manufacturing: state of the art and trends. *Virtual Phys.*

- Prototyping **14**(1), 1–18 (2019)
- 2. Velu, R., Calais, T., Jayakumar, A., Raspall, F.: A comprehensive review on bio-nanomaterials for medical implants and feasibility studies on fabrication of such implants by additive manufacturing technique. *Materials* **13**(1), 92 (2020)
 - 3. Rajashekhar, V., Pravin, T., Thiruppathi, K.: A review on droplet deposition manufacturing—a rapid prototyping technique. *Int. J. Manuf. Technol. Manage.* **33**(5), 362–383 (2019)
 - 4. Elhabashy, A.E., Wells, L.J., Camelio, J.A.: Cyber-physical security research efforts in manufacturing—a literature review. *Procedia Manuf.* **34**, 921–931 (2019)
 - 5. A. Haleem, M. Javaid, Additive manufacturing applications in industry 4.0: a review, *Journal of Industrial Integration and Management* **4** (04) (2019) 1930001.
 - 6. Wells, L.J., Camelio, J.A., Williams, C.B., White, J.: Cyber-physical security challenges in manufacturing systems. *Manuf. Lett.* **2**(2), 74–77 (2014)
 - 7. Wu, D., Ren, A., Zhang, W., Fan, F., Liu, P., Fu, X., Terpenny, J.: Cybersecurity for digital manufacturing. *J. Manuf. Syst.* **48**, 3–12 (2018)
 - 8. Bordel, B., Alcarria, R., Sánchez-de Rivera, D., Robles, T.: Protecting industry 4.0 systems against the malicious effects of cyber-physical attacks. In: *International Conference on Ubiquitous Computing and Ambient Intelligence*, pp. 161–171. Springer (2017)
 - 9. Brenner, J.F.: Eyes wide shut: The growing threat of cyber attacks on industrial control systems. *Bull. At. Scientists* **69**(5), 15–20 (2013)
 - 10. Chhetri, S.R., Canedo, A., Al Faruque, M. A.: Kcad: kinetic cyber-attack detection method for cyber-physical additive manufacturing systems. In: *2016 IEEE/ACM International Conference on Computer-Aided Design (IC-CAD)*, pp. 1–8. IEEE (2016)
 - 11. Li, G., Shen, Y., Zhao, P., Lu, X., Liu, J., Liu, Y., Hoi, S.C.: Detecting cyberattacks in industrial control systems using online learning algorithms. *Neurocomputing* **364**, 338–348 (2019)
 - 12. Drias, Z., Serhrouchni, A., Vogel, O.: Taxonomy of attacks on industrial control protocols. In: *2015 International Conference on Protocol Engineering (ICPE) and International Conference on New Technologies of Distributed Systems (NTDS)*, pp. 1–6. IEEE (2015)
 - 13. Sturm, L., Williams, C., Camelio, J., White, J., Parker, R.: Cyber-physical vulnerabilities in additive manufacturing systems. *Context* **7**(8), 951–963 (2014)
 - 14. Seifi, M., Gorelik, M., Waller, J., Hrabe, N., Shamsaei, N., Daniewicz, S., Lewandowski, J.J.: Progress towards metal additive manufacturing standardization to support qualification and certification. *Jom* **69**(3), 439–455 (2017)
 - 15. Monzón, M., Ortega, Z., Martínez, A., Ortega, F.: Standardization in additive manufacturing: activities carried out by international organizations and projects. *Int. J. Adv. Manuf. Technol.* **76**(5–8), 1111–1121 (2015)
 - 16. Vora, H. D., Sanyal, S.: A comprehensive review: metrology in additive manufacturing and 3d printing technology. *Prog. Addit. Manuf.* 1–35 (2020)
 - 17. Caffrey, T., Wohlers, T., Campbell, I.: Executive summary of the wohlers report 2016 (2016)
 - 18. Makes, A., Collaborative, A.A.M.S.: Standardization roadmap for additive manufacturing, February), Public Draft (2017)
 - 19. Wong, K.V., Hernandez, A.: A review of additive manufacturing. *Int. Sch. Res. Not* (2012)
 - 20. Turner, B.N., Strong, R., Gold, S.A.: A review of melt extrusion additive manufacturing processes: I. process design and modeling. *Rapid Prototyping J.* (2014)
 - 21. Lyons, B.: Additive manufacturing in aerospace: Examples and research outlook. *The Bridge* **44**(3)
 - 22. Liu, R., Wang, Z., Sparks, T., Liou, F., Newkirk, J.: Aerospace applications of laser additive manufacturing. In: *Laser additive manufacturing*, pp. 351–371. Elsevier (2017)
 - 23. Rajashekhar, V., Kumar, S.: A serial five-bar mechanism based robotic snake exhibiting three kinds of gait. In: *2015 IEEE International Conference on Robotics and Biomimetics (ROBIO)*, pp. 1938–1943. IEEE (2015)
 - 24. SRajashekhar, V., Vibha, M., Das, K., Ghose, D.: A robust aerial gripper for passive grasping and impulsive release using scotch yoke mechanism, arXiv preprint [arXiv:2012.06152](https://arxiv.org/abs/2012.06152)
 - 25. Haleem, A., Javaid, M., Saxena, A.: Additive manufacturing applications in cardiology: A review. *Egypt. Heart J.* **70**(4), 433–441 (2018)

26. Sartipi, F., Sartipi, A.: Brief review on advancements in construction additive manufacturing, *Journal of. Constr. Mater.* **1**, 2–4 (2020)
27. Gokuldoss, P.K., Kolla, S., Eckert, J.: Additive manufacturing processes: Selective laser melting, electron beam melting and binder jetting selection guidelines. *Materials* **10**(6), 672 (2017)
28. Zhang, G.Q., Li, X., Boca, R., Newkirk, J., Zhang, B., Fuhlbrigge, T.A., Feng, H.K., Hunt, N.J.: Use of industrial robots in additive manufacturing- a survey and feasibility study. In: ISR/Robotik 2014; 41st International Symposium on Robotics, pp. 1–6. VDE (2014)
29. Urhal, P., Weightman, A., Diver, C., Bartolo, P.: Robot assisted additive manufacturing: A review. *Robot. Comput.-Integr. Manuf.* **59**, 335–345 (2019)
30. Tankova, T., da Silva, L.S.: Robotics and additive manufacturing in the construction industry. *Curr. Robot. Rep.* **1**(1), 13–18 (2020)
31. Hiller, J.D., Lipson, H.: Stl 2.0: a proposal for a universal multi-material additive manufacturing file format. In: Proceedings of the Solid Freeform Fabrication Symposium, v1. 3, pp. 266–278. Citeseer (2009)
32. Rypl, D., Bittnar, Z.: Generation of computational surface meshes of stl models. *J. Comput. Appl. Math.* **192**(1), 148–151 (2006)
33. Petik, A.: Some aspects of using stl file format in cae systems. In: Int Workshop CA System Technol, Citeseer, pp. 80–86 (2000)
34. Aleshin, N., Murashov, V., Shchipakov, N., Krasnov, I., Lozhkova, D.: Experimental research into possibilities and peculiarities of ultrasonic testing of additive manufactured parts. *Russ. J. Nondestr. Test.* **52**(12)
35. Cerniglia, D., Scafidi, M., Pantano, A., Rudlin, J.: Inspection of additive-manufactured layered components. *Ultrasonics* **62**, 292–298 (2015)
36. Callister Jr, W.D., Rethwisch, D.G.: Callister's materials science and engineering. Wiley (2020)
37. Li, N., Huang, S., Zhang, G., Qin, R., Liu, W., Xiong, H., Shi, G., Blackburn, J.: Progress in additive manufacturing on new materials: A review. *J. Mater. Sci. Technol.* **35**(2), 242–269 (2019)
38. Bourell, D., Kruth, J.P., Leu, M., Levy, G., Rosen, D., Beese, A.M., Clare, A.: Materials for additive manufacturing. *CIRP Ann.* **66**(2), 659–681 (2017)
39. Redwood, B., Schöffer, F., Garret, B.: The 3D printing handbook: technologies, design and applications, 3D Hubs (2017)
40. Zegzulka, J., Gelnar, D., Jezerska, L., Prokes, R., Rozbroj, J.: Characterization and flowability methods for metal powders. *Sci. Rep.* **10**(1), 1–19 (2020)
41. Weinberg, M.: It will be awesome if they dont screw it up: 3D printing, intellectual property, and the fight over the next great disruptive technology, November, 2010. Retreived from <http://www.publicknowledge.org/it-will-be-awesome-if-they-dont-screw-it-up>. Accessed 20 Feb 2013
42. Barnett, M.: The next big fight: 3d printing and intellectual property (2014)
43. Sternstein, A.: Things can go kaboom when a defense contractors 3-d printer gets hacked, Nextgov, Sept 11
44. Yampolskiy, M., Skjellum, A., Kretzschmar, M., Overfelt, R.A., Sloan, K.R., Yasinsac, A.: Using 3d printers as weapons. *Int. J. Crit. Infrastruct. Prot.* **14**, 58–71 (2016)
45. Venkatachary, S.K., Prasad, J., Samikannu, R.: Cybersecurity and cyber terrorism-in energy sector—a review. *J. Cyber Secur. Technol.* **2**(3–4), 111–130 (2018)
46. Yampolskiy, M., Schutze, L., Vaidya, U., Yasinsac, A.: Security challenges of additive manufacturing with metals and alloys. In: International Conference on Critical Infrastructure Protection, pp. 169–183. Springer (2015)
47. Belikovetsky, S., Yampolskiy, M., Toh, J., Gatlin, J., Elovici, Y.: dr0wned—cyber-physical attack with additive manufacturing. In: 11th {USENIX} Workshop on Offensive Technologies ({WOOT} 17) (2017)
48. Wang, Y., Lin, Y., Zhong, R.Y., Xu, X.: IoT-enabled cloud-based additive manufacturing platform to support rapid product development. *Int. J. Prod. Res.* **57**(12), 3975–3991 (2019)
49. Suresh, A., Udendhran, R., Yamini, G.: Internet of things and additive manufacturing: Toward intelligent production systems in industry 4.0. In: Internet of Things for Industry 4.0, pp. 73–89. Springer (2020)

50. García-Domínguez, A., Claver, J., Camacho, A.M., Sebastián, M.A.: Analysis of general and specific standardization developments in additive manufacturing from a materials and technological approach. *IEEE Access* **8**, 125056–125075 (2020)
51. Vendra, L., Malkawi, A., Avagliano, A.: Standardization of additive manufacturing for oil and gas applications. In: Offshore Technology Conference, OnePetro (2020)
52. Yampolskiy, M., Horváth, P., Koutsoukos, X.D., Xue, Y., Sztipanovits, J.: A language for describing attacks on cyber-physical systems. *Int. J. Crit. Infrastruct. Prot.* **8**, 40–52 (2015)
53. Chen, T.M., Sanchez-Aarnoutse, J.C., Buford, J.: Petri net modeling of cyber-physical attacks on smart grid. *IEEE Trans. Smart Grid* **2**(4), 741–749 (2011)
54. Ameta, G., Lipman, R., Moylan, S., Witherell, P.: Investigating the role of geometric dimensioning and tolerancing in additive manufacturing. *J Mech. Des.* **137**(11)
55. Sturm, L. D., Williams, C. B., Camelio, J. A., White, J., Parker, R.: Cyber-physical vulnerabilities in additive manufacturing systems: A case study attack on the stl file with human subjects, *Journal of Manufacturing Systems* 44 (2017) 154–164.
56. Yampolskiy, M., Andel, T. R., McDonald, J. T., Glisson, W. B., Yasinsac, A.: Intellectual property protection in additive layer manufacturing: Requirements for secure outsourcing. In: Proceedings of the 4th Program Protection and Reverse Engineering Workshop, pp. 1–9 (2014)
57. Bradshaw, S., Bowyer, A., Haufe, P.: The intellectual property implications of low-cost 3d printing. *ScriptEd* **7**, 5 (2010)
58. Kumar, S., Pityana, S.: Laser-based additive manufacturing of metals. In: Advanced Materials Research, vol. 227, Trans Tech Publ, pp. 92–95 (2011)
59. Huang, Y., Leu, M.C., Mazumder, J., Donmez, A.: Additive manufacturing: current state, future potential, gaps and needs, and recommendations. *J. Manuf. Sci. Eng.* **137**(1)